SLAC-405
CONF-9203179
UC-414
(A)

PROCEEDINGS OF THE INTERNATIONAL WORKSHOP ON FINAL FOCUS AND INTERACTION REGIONS OF NEXT GENERATION LINEAR COLLIDERS

May 2-6, 1992

STANFORD LINEAR ACCELERATOR CENTER
STANFORD UNIVERSITY, STANFORD, CALIFORNIA 94309

David Burke and John Irwin
Workshop Chairmen

Kathy Asher
Workshop Administrator

Chairmen of Working Groups
W. Ash, H. Band, P. Chen, K. Oide

Prepared for the Department of Energy
under contract number DE-AC03-76SF00515

Printed in the United States of America. Available from the National Technical Information Service, U.S. Department of Commerce, 5285 Port Royal Road, Springfield, Virginia 22161

International Workshop on Final Focus and Interaction Regions of Next Generation Linear Colliders

TABLE OF CONTENTS

INTERNATIONAL WORKSHOP ON
FINAL FOCUS AND INTERACTION REGIONS
OF NEXT GENERATION LINEAR COLLIDERS

March 2-6, 1992

EXECUTIVE SUMMARY

John Irwin

Since November 1988 there have been yearly international workshops addressing the design of next-generation linear electron colliders. These have been very successful, and as designs have evolved, and specific experimental R&D programs have been defined and initiated, it has become apparent that to proceed in a timely manner to a complete design, it would be helpful to have workshops which address sub-areas.

The first such "sub-workshop," in what we hope may become a continuing series, was held March 2-6, 1992 at the Stanford Linear Accelerator Center. There were 81 participants from six countries: France, Germany, Japan, Switzerland, U.S.A., and U.S.S.R. Thirty-one of these participants came from outside the U.S.A.

The first day was devoted to four plenary "issues" talks, one for each working group: Beam-Beam Interaction, Detector, Hardware, and Optical Design. The last day was devoted to plenary talks summarizing the activities of the working groups. Each of the three remaining days there was a short morning plenary devoted to a brief summary of the preceding day and an announcement of planned working group discussions for that day. The transparencies for the "issues" and "summary" talks are included in this volume, along with some remarks from the working group chairpersons.

For an exposition of the subjects addressed in each working group, please refer to the chairperson summary. Very briefly, the beam-beam group continued to address the quantitative study of QED induced backgrounds, and attempted to better understand the nature and prevalence of QCD minijets. The detector group attempted to identify the impact on masking and detector design of the beam-beam backgrounds, the synchrotron radiation induced backgrounds from beam halos and muon backgrounds produced primarily in collimators. Nanosecond timing elements needed in conjunction with multi-bunch operation were discussed. The hardware group addressed the problem of magnet design and support, especially the final doublet magnets suspended within the detector environment, and instrumentation issues, such as high resolution beam position monitors. The optics group discussed new final focus system ideas, collimator design, and improvement of beamline tolerances.

We were gratified by the large interest in this workshop, as evidenced by the participation and the contents of the summary talks presented here. A sincere "Thank you" to all participants for your enthusiastic involvement. Thanks to the support staff at SLAC that organized an infrastructure which functioned so smoothly as to be practically invisible. And thanks to the organizing committee for their efforts in giving this workshop its shape.

If you were not here to participate, we hope that this volume will help you in your orientation to these problems, and we hope you can join us in a future workshop.

Relevant Experience with the SLC Final Focus

Nick Walker for the SLC Beam Delivery Task Force

FFIR workshop, SLAC 3/2/92

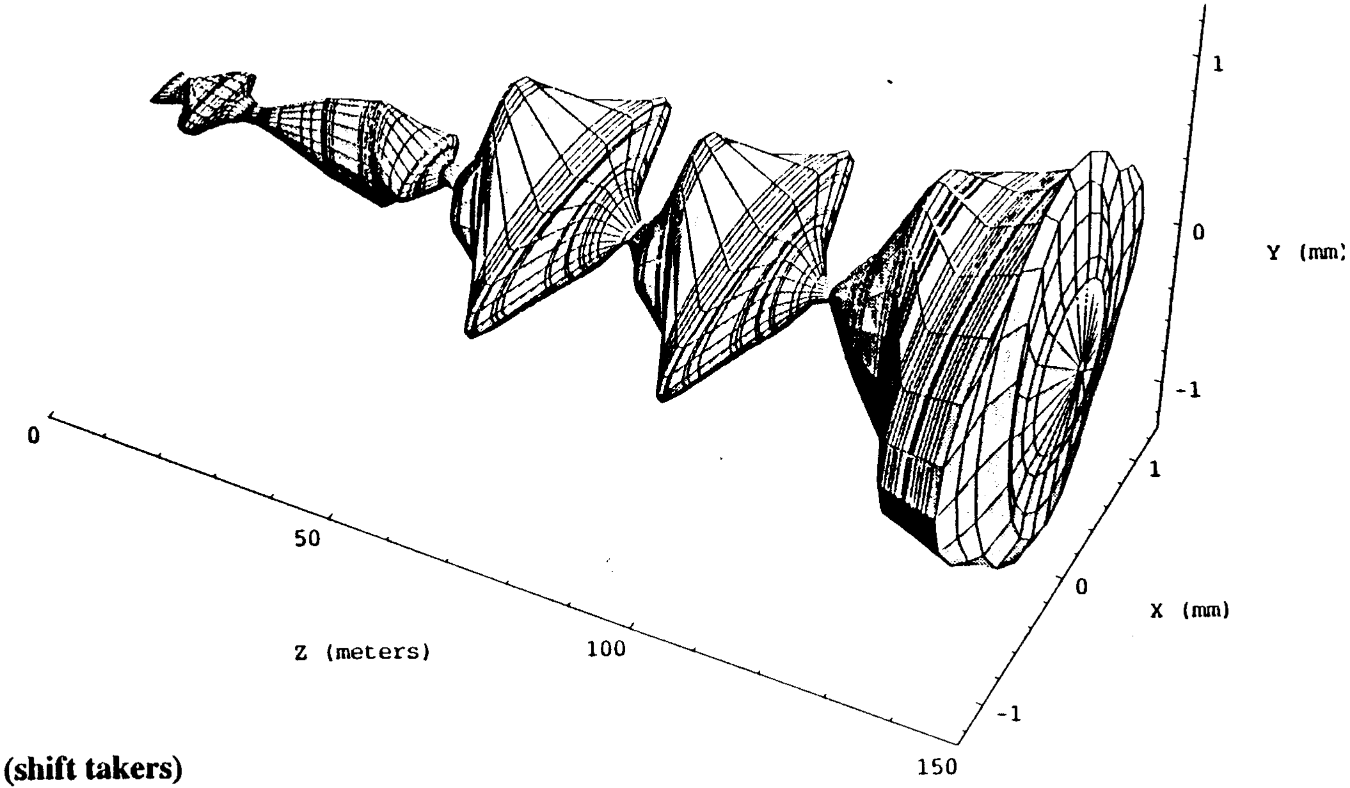

Contributors (shift takers)
Henry BAND, Tim BARKLOW, Dave BURKE, Paul EMMA,
Mike HILDRETH, John IRWIN, Patrick KREJCIK, Nan PHINNEY,
Pantaleo RAIMONDI, Nobu TOGE, Volker ZIEMANN

Circular machines have nice closed solutions

β functions are properties of lattice.

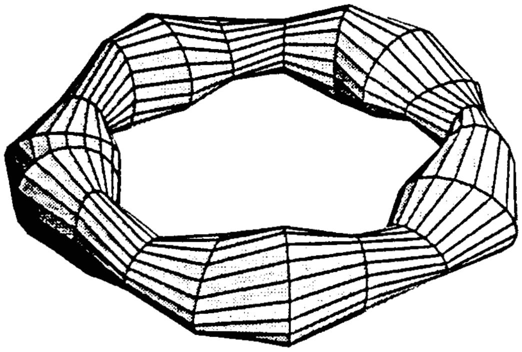

In Linear machines, β functions are properties of lattice AND initial conditions

Garbage In

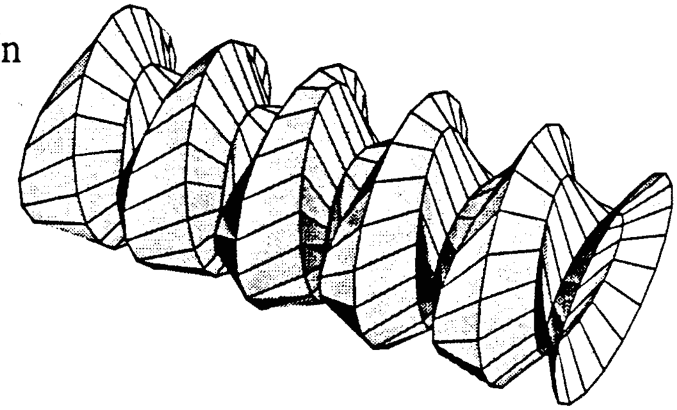

Garbage Out

In Addition, all measurements become an exersize in fitting (linear & non-linear regression) Good error analysis is essential!

Final Focus Schematics

16NOV89 NKT

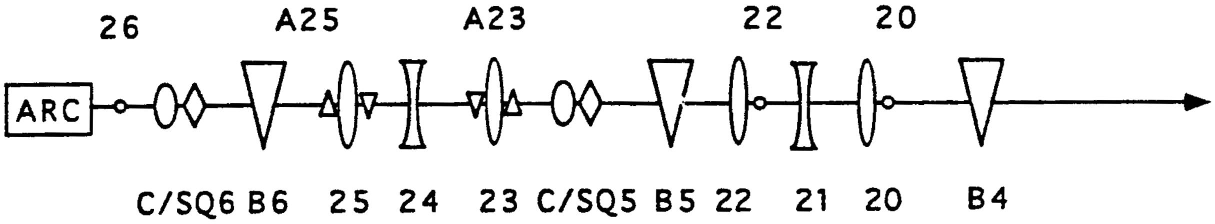

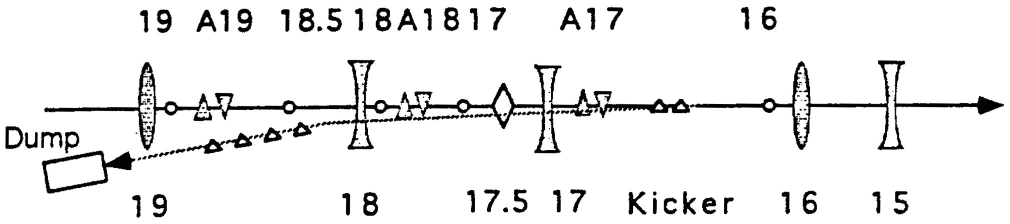

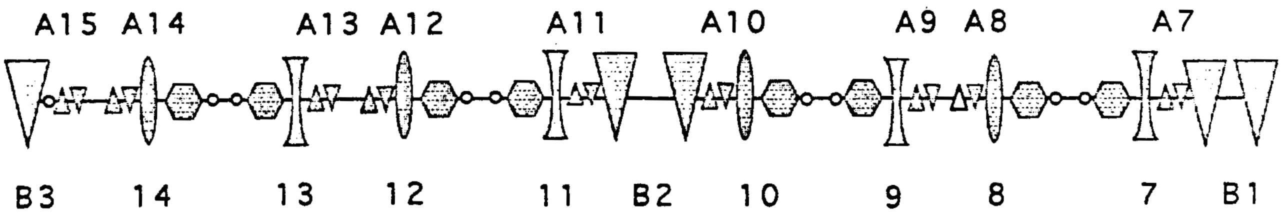

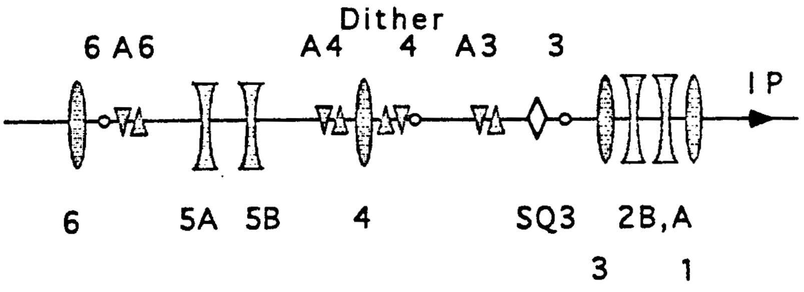

X & Y β functions

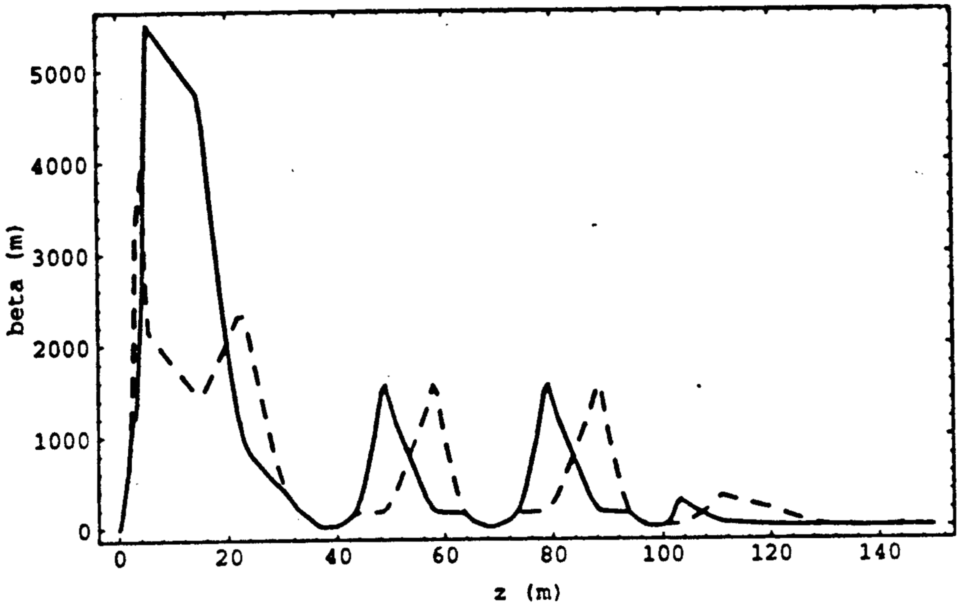

X Dispersion

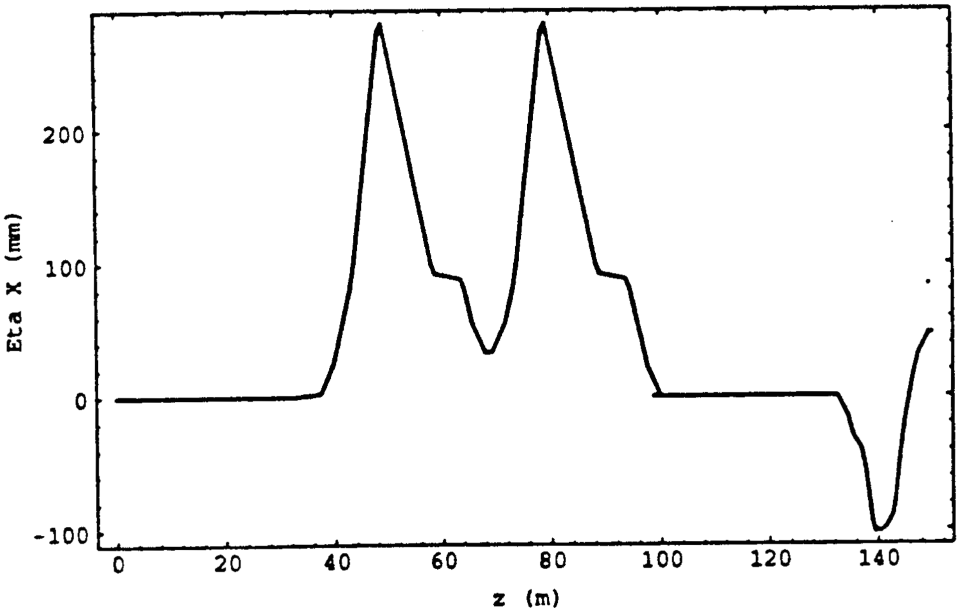

X Chromatic contribution per magnet

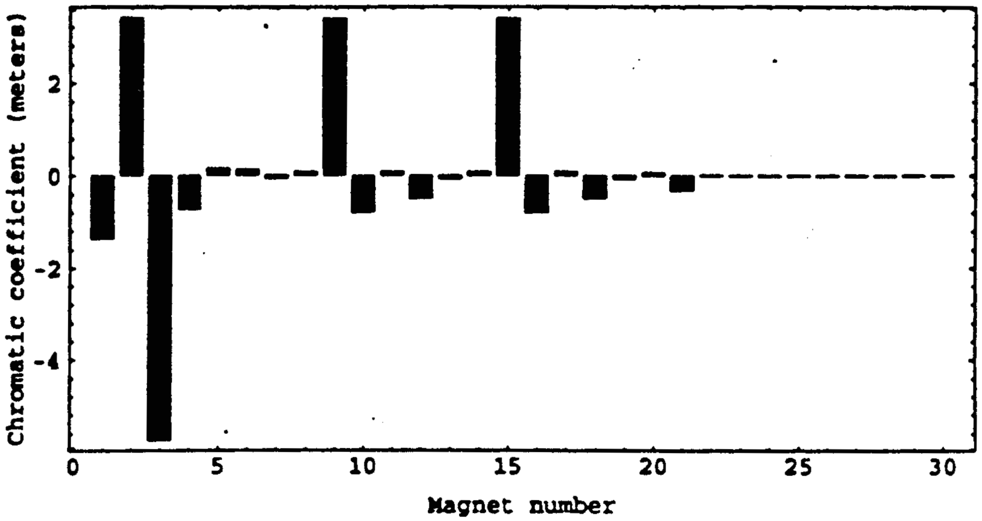

Y Chromatic contribution per magnet

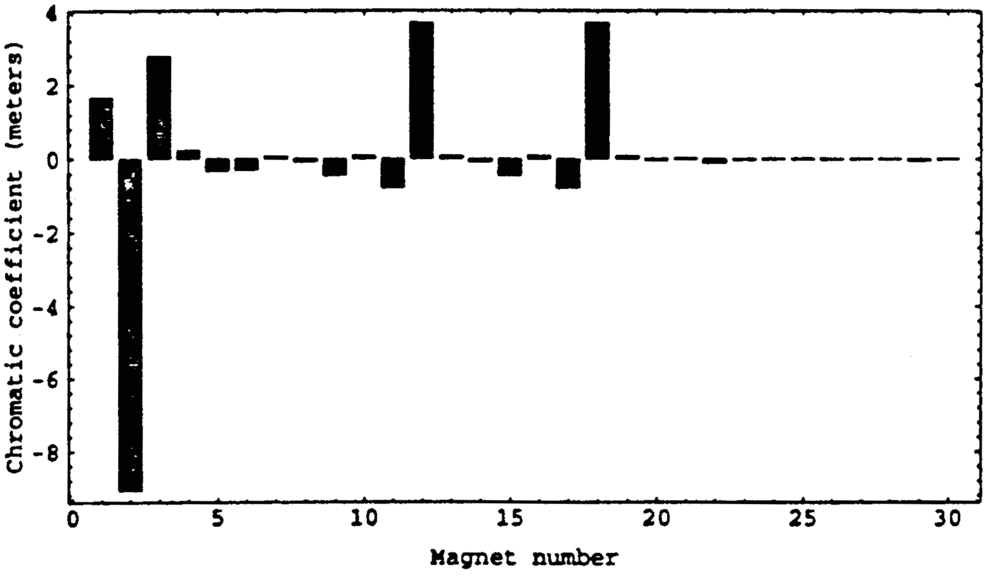

SLC FINAL FOCUS DESIGN - LIMITING ABERRATIONS

Chromaticity

- Corrected to 2nd (optical) order by CCS

  Corrected bandwidth limited to $\delta = \pm 0.5\%$
  by 3rd order aberrations.

Dominating aberrations:

- Interleaved sextupoles pairs
- Chromo-geometric

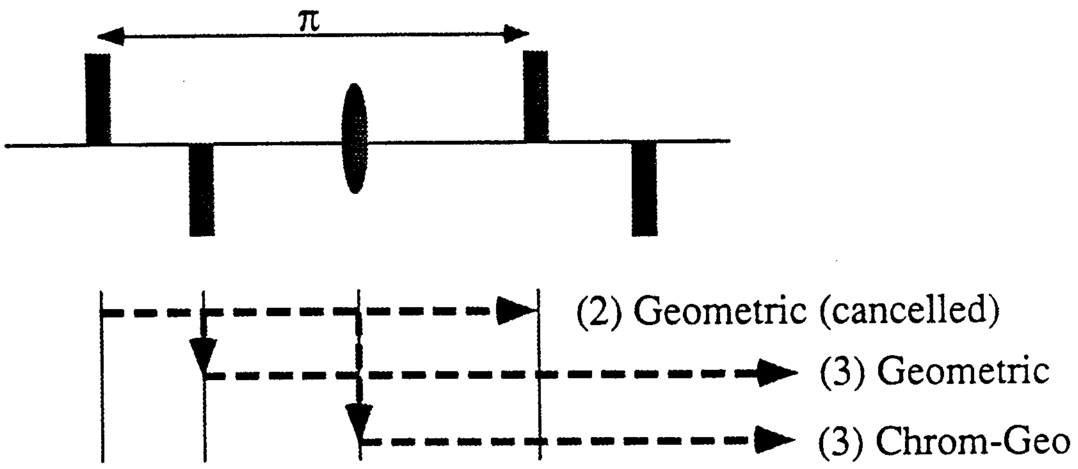

(2) Geometric (cancelled)

(3) Geometric

(3) Chrom-Geo

$\varepsilon_y = \varepsilon_x = 3.0\mathrm{x}10^{-10}$ m.r

$\delta = 0.3\%$

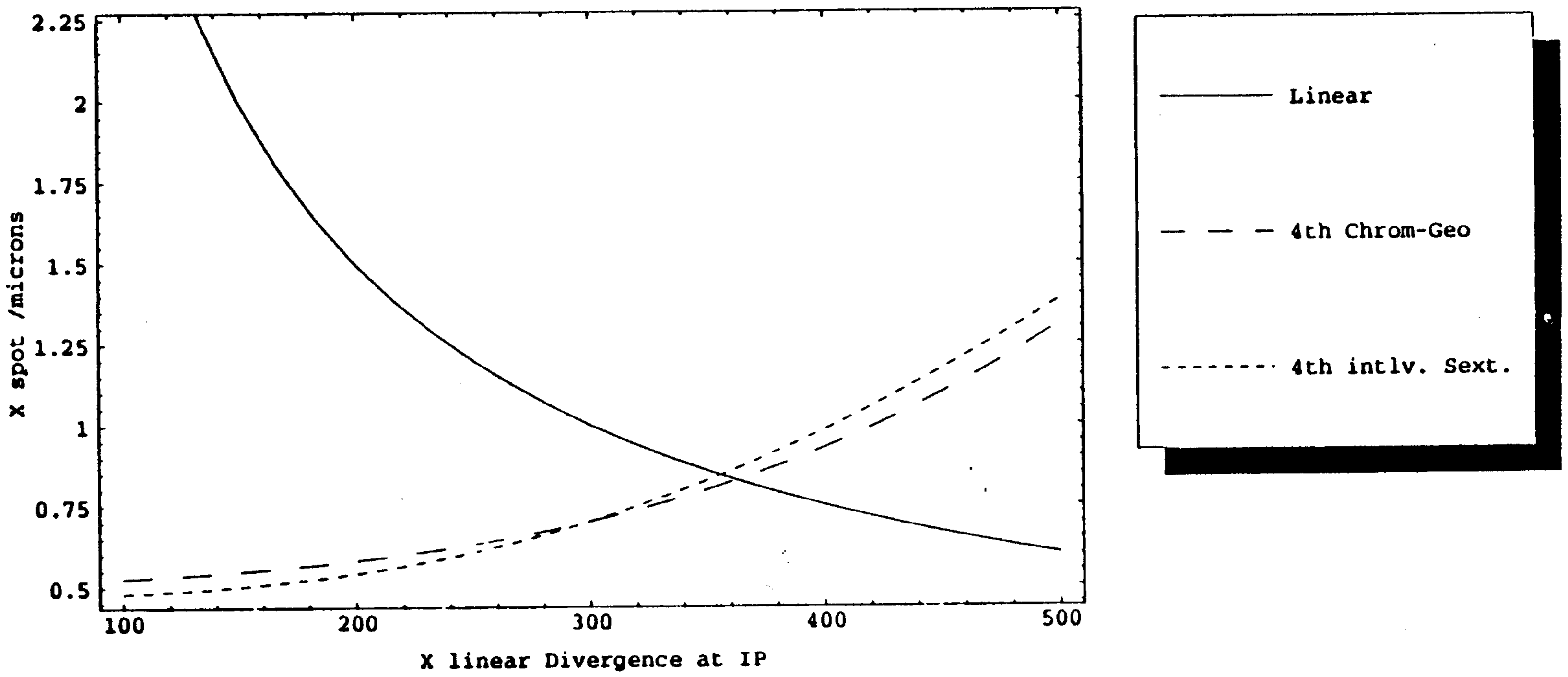

Nonlinear contributions to X spot size at IP

One Problem SLC has that FFTB/NLC will not have - ARCS

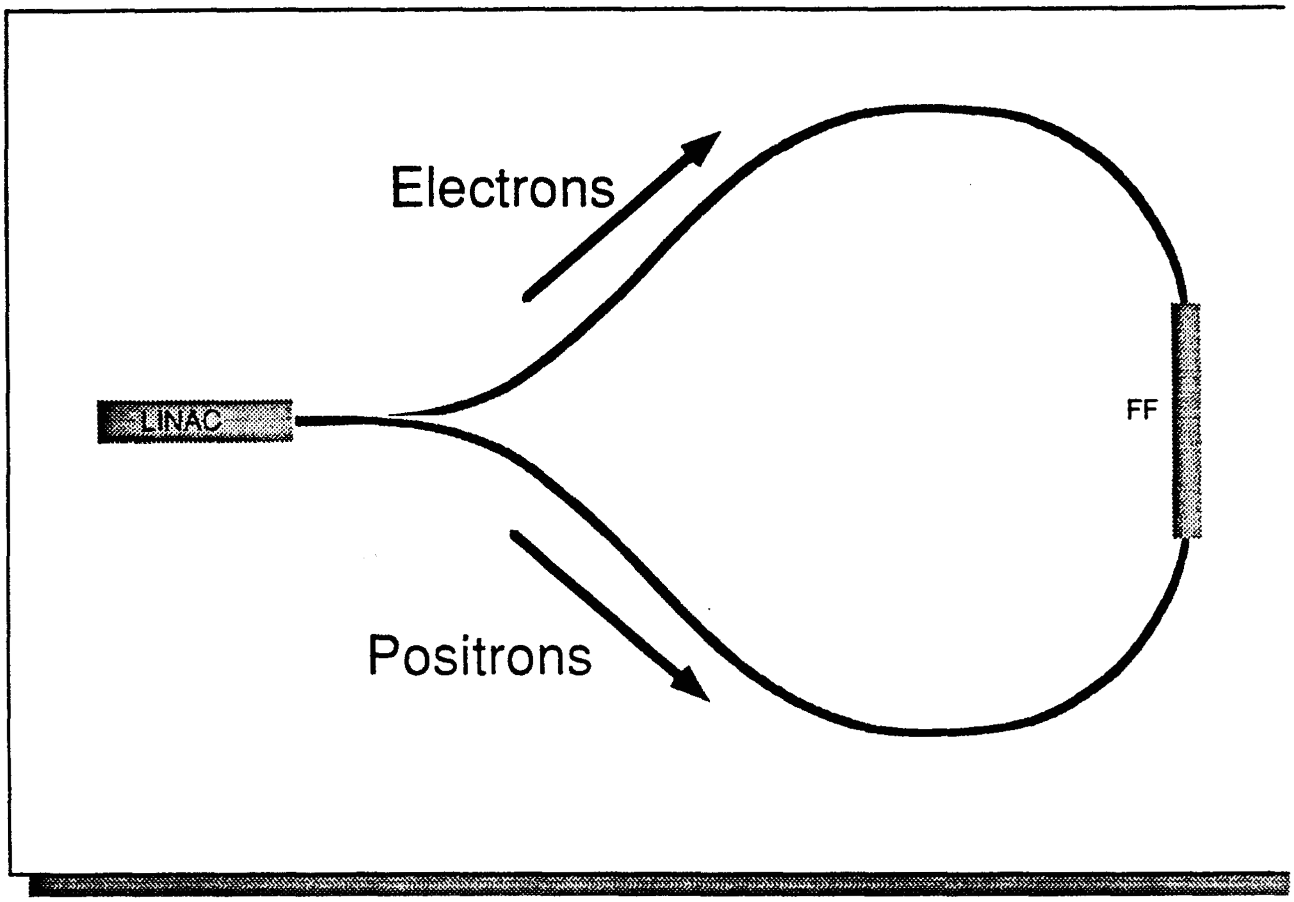

SLC Arcs cause many problems with X-Y couplin
and general phase space mismatches at entrance to FF.

Silver lining: Good Collimators

FF Tuning

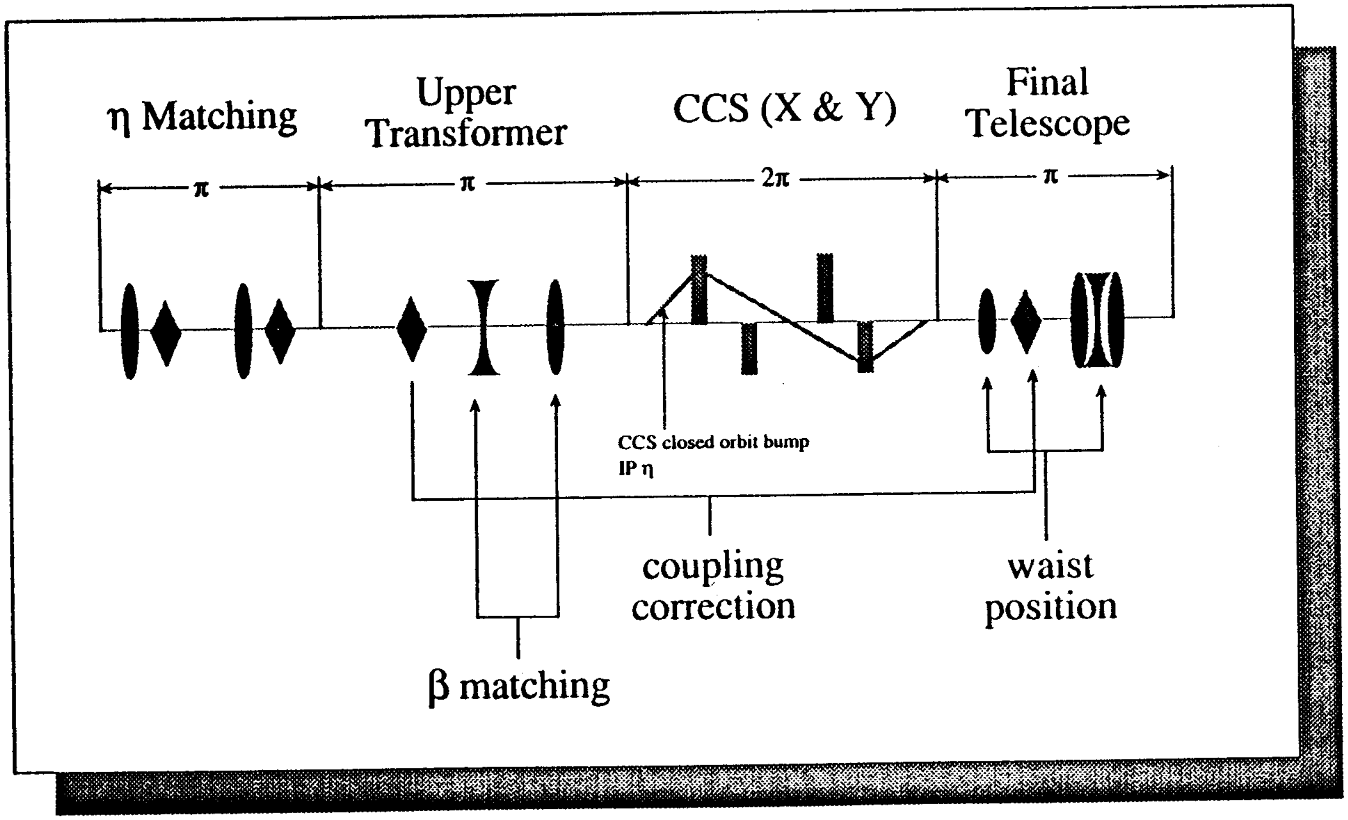

η Matching

Upper Transformer

CCS (X & Y)

Final Telescope

π

π

2π

π

CCS closed orbit bump
IP η

coupling correction

waist position

β matching

Standard Tuning Algorithm

1. η Match - uses on-line package to adjust quads.

2. No X-Y coupling at SQ17.5 (first skew quad).

   Any coupling here due to η matching quads or Arcs.
   No independent adjustment.

   Measurement technique: Wire Scanner & Florescent screen

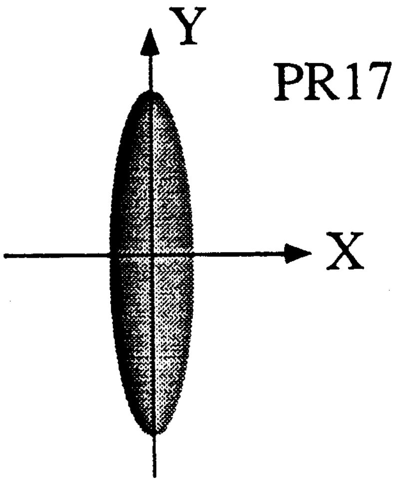

3. Beam must be "ROUND" at triplet/SQ3 (second sqew quad)

   Adjust β matching quads to obtain ~900 μm spot

   Measurement technique: Wire Scanner & Florescent screen

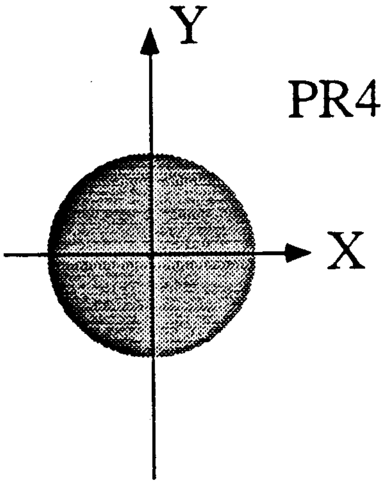

Final Adjustment
- IP spot optimization.

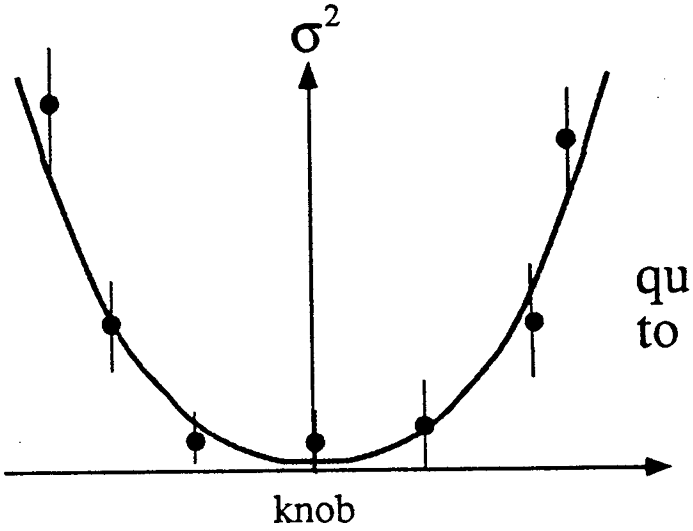

quadratic fit
to data.

Measurement of beam σ at IP using either
(a) IP wires
(b) beam-beam deflections

where "knob" can be
(a) Waist position
(b) Skew <x'y'> (second skew quad)
(c) η (CCS closed bumps)
(d) Chromaticity (sextupole strength).

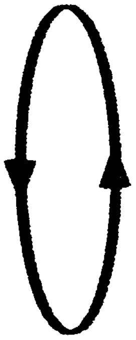

Tuning Problems #1
Optics & Orthogonality

FF tuning algorithm severely compromised by:

- Mismatch (coupling) from Arcs.
- Beam stability.
- Beam distribution (non-gaussian/tails).
- Magnet misalignments.
- Diagnostics & modeling errors.

One common theme: **Orthogonality**

Importance of Orthogonality in tuning

Tuning Goal: To tune out independent aberrations and make smallest spots possible.

Orthogonal

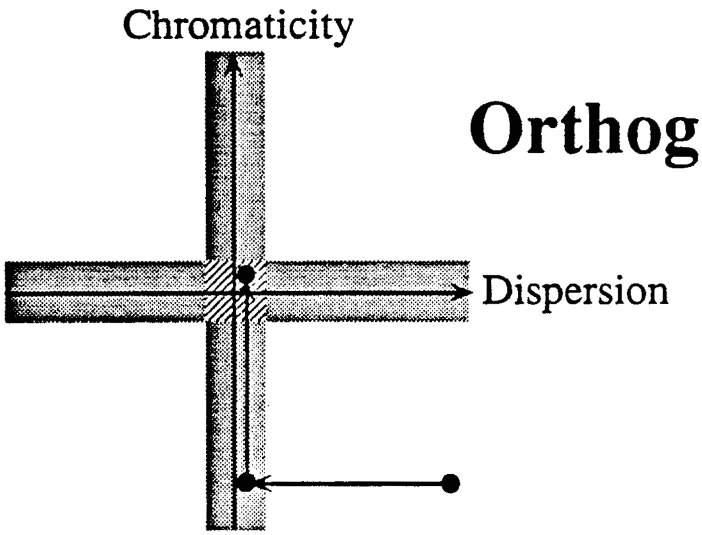

Non-orthogonal

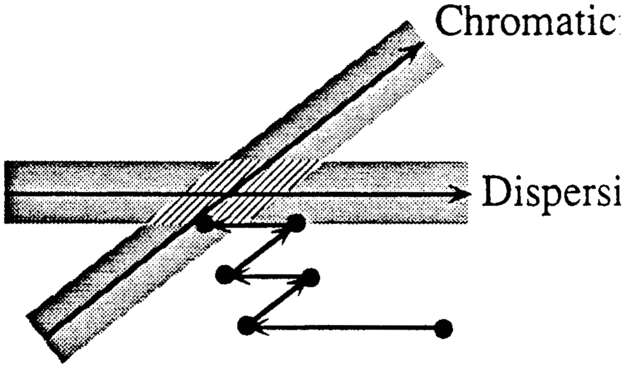

DIFFICULTIES TUNING THE FINAL FOCUS

- X-Y coupling is tuned by observing a profile monitor:
  - — Beam tails can confuse the issue
  - — Dispersion can couple the beam...

$$\sigma_{13} = \sum_{ij} R_{1i} R_{3j}\, \sigma_{ij} \;=\; R_{16} R_{36} \langle \delta^2 \rangle + \ldots$$

  - — Procedure is only valid for equal emittances
  - — Over-rotation of spot is possible

- Adjustment of IP divergence sometimes impractical because of incoming beta mismatch and/or strong X/Y coupling

ATTEMPT TUNING WITH *BEAM-DELIVERY* MODELING SOFTWARE

$$\chi^2 \equiv \left(\frac{\theta_m^* - \theta_d^*}{\delta\theta^*}\right)^2 + \left(\frac{\varphi_m^* - \varphi_d^*}{\delta\varphi^*}\right)^2 +$$

$$\left(\frac{X_{wst}}{\delta X_{wst}}\right)^2 + \left(\frac{Y_{wst}}{\delta Y_{wst}}\right)^2 +$$

$$\left(\frac{r_{13}^2 + r_{14}^2 + r_{23}^2 + r_{24}^2}{\delta r^2}\right)$$

==> SQ17.5, QD17, QF16, Q3.5, SQ3, Triplett

BEAM DELIVERY SYSTEM MODELING/TUNING

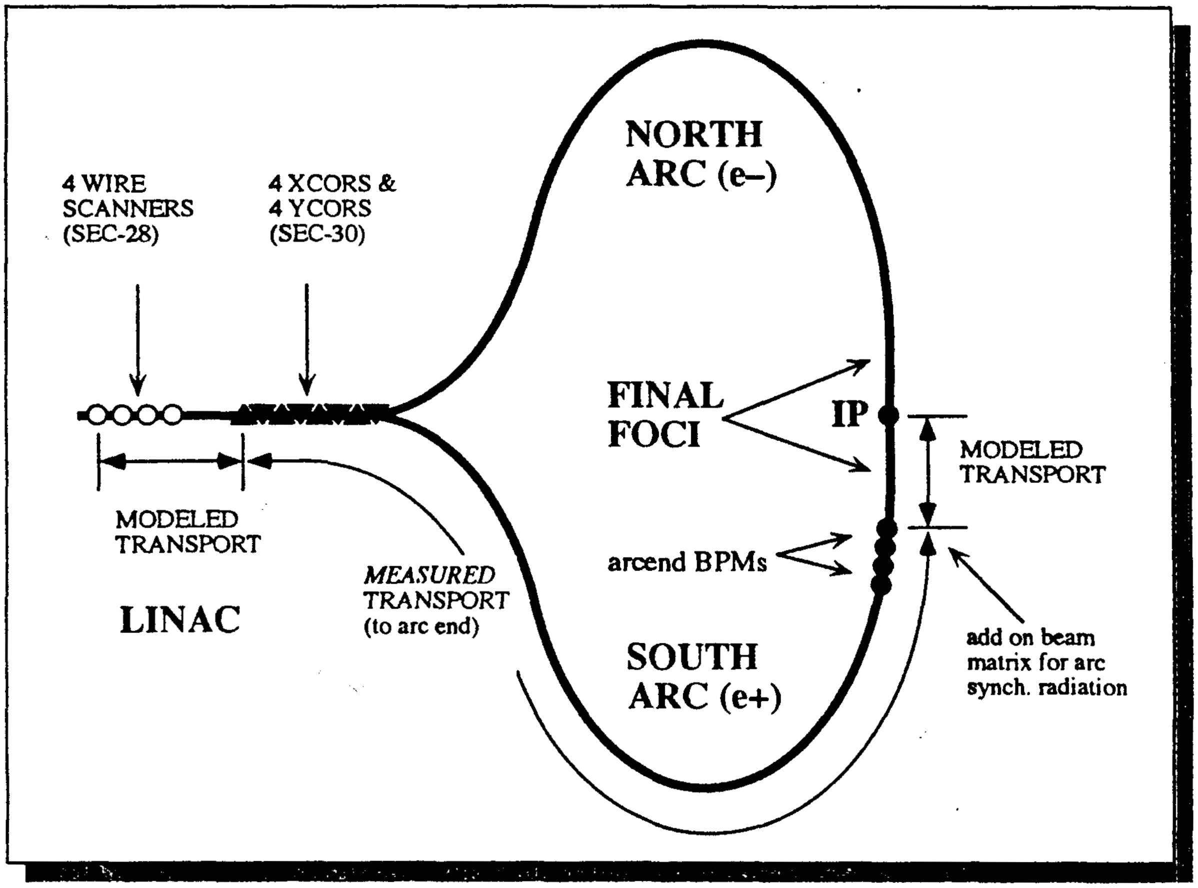

1. Measure sector-28 4x4 beam matrix with wires scanners
2. Reconstruct sector-30 to arcend 4x4 transport matrix (oscillations)
3. Model *uncoupled* transport matrix from wires to sector-30
4. Model *coupled* transport matrix from arcend to beginning of Final Focus
5. Transport measured beam matrix from wires to arcend
6. Add on arc syncrotron radiation beam matrix at arcend
7. Transport net arcend beam matrix to beginning of Final Focus
8. Fit Final Focus quads for desired IP beam given input beam

Problems with β-matching Procedure

Disagreement between observed and
calculated parameters:

- IP waist shifts
- Setting of SQ3 (2nd skew quad)
- IP angular divergence not correctly estimated.

Possible sources of error:

- Modeling problem
- Synchrotron radiation correction not good enough,
- **Sextupole magnet misalignments**

  ⇒ additional quads and skew-quads not in model

Concentrated on sextupole misalignments. Use technique proposed by **Irwin** to align sextupoles using measuremen of aberrations at IP

⇒ Orthogonalization of chromaticity adjustment w.r.t. skew (<x'y'>), η and waist adjustments.

BEAM BASED SEXTUPOLE ALIGNMENT

X-SEXTUPOLES (SX8/SX12)

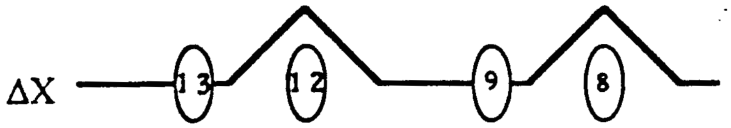

X-waist
observe: σx vs X-WAIST
set: symmetric X-bump

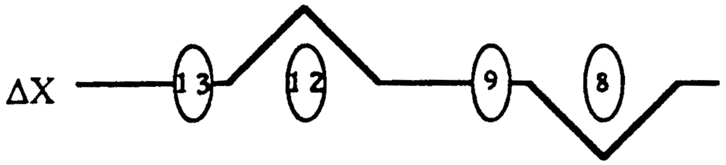

X-dispersion
observe: σx vs IP ηx
set: asymmetric X-bump

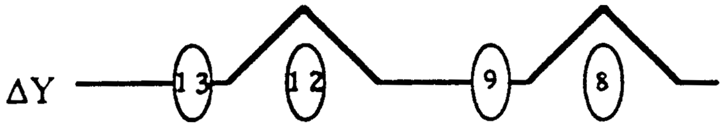

Skew
observe: σy vs skew quad
set: symmetric Y-bump

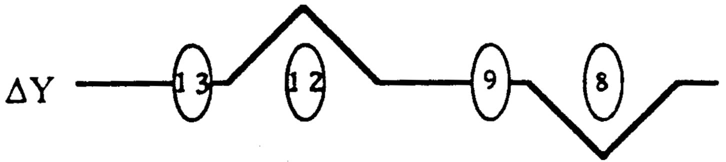

Y-dispersion
observe: σy vs IP ηy
set: asymmetric Y-bump

Y-SEXTUPOLES (SX9/SX13)

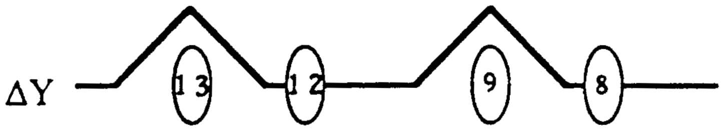

Skew
observe: σx vs skew quad
set: symmetric Y-bump

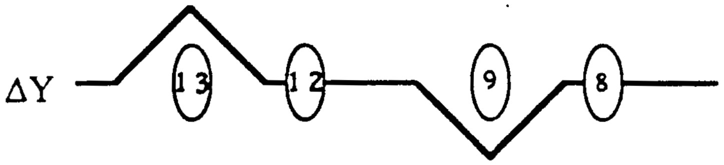

Y-dispersion
observe: σy vs IP ηy
set: asymmetric Y-bump

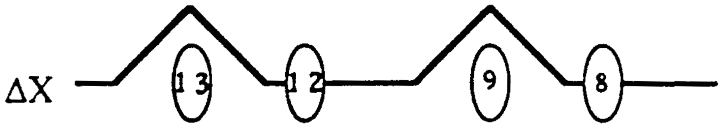

Y-Waist
observe: σy vs Y_WAIST
set: symmetric X-bump

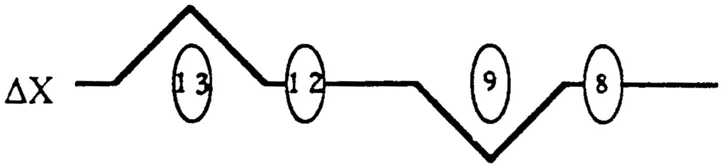

X-dispersion
observe: σx vs IP ηx
set: asymmetric X-bump

Sextupole Alignment Procedure

Example: IP Waist motion
Horizontal sextupole misalignments
⇒ additional **QUAD** (moves waist at IP)

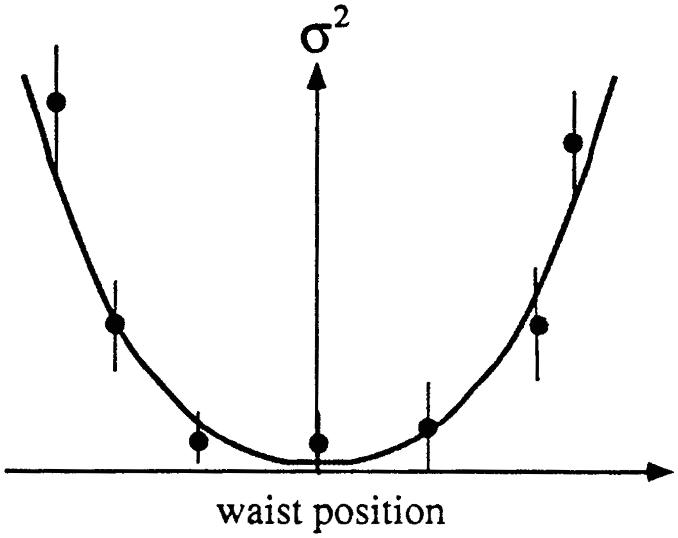

Sextupoles at nominal setting

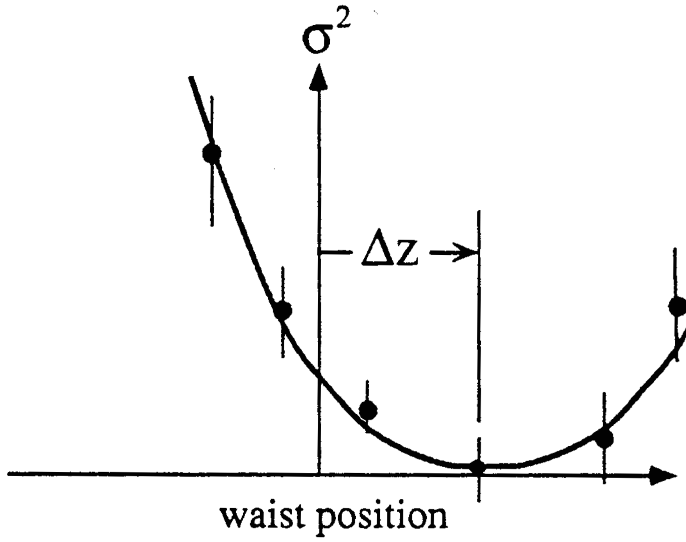

Sextupoles change by ΔK_2

$\Delta z = -2\Delta K_2 R_{12}^2 \bar{X}$

Magnet	ΔX	ΔY
SD13	175 µm to West	150 µm Up
SF12	350 µm to West	200 µm Up
SD9	175 µm to West	150 µm Down
SF8	350 µm to East	200 µm Down

Results of Electron β match after NFF sextupole alignment.

		Predicted	Achieved
	σ (μm)	1.77	1.70±0.07
X	θ^* (μr)	300	306±16
	Δz (cm)	-0.25	0.0±0.1
	σ (μm)	1.53	1.50±0.07
Y	θ^* (μr)	300	198±9
	Δz (cm)	-1.1	0.0±0.1

Still a problem

Measurements made on IP wires at low currents

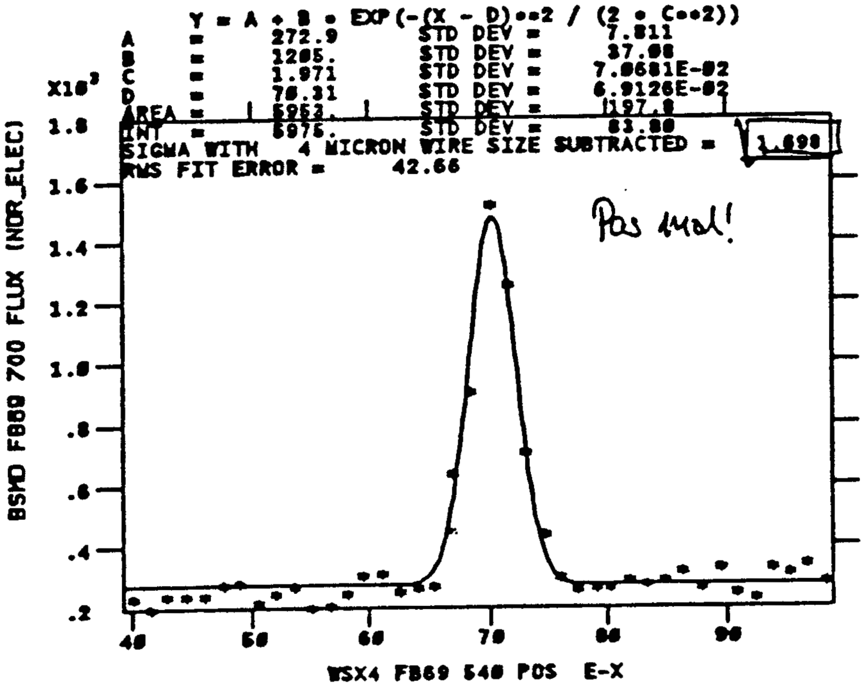

```
            Y = A + B * EXP(-(X - D)**2 / (2 * C**2))
A      =        272.9         STD DEV =      7.811
B      =        1205.         STD DEV =      37.08
C      =        1.971         STD DEV =      7.0681E-02
D      =        70.31         STD DEV =      6.9126E-02
AREA   =        5953.         STD DEV =      1197.8
INT    =        5975.         STD DEV =      83.80
SIGMA WITH   4 MICRON WIRE SIZE SUBTRACTED =   1.698
RMS FIT ERROR =         42.66
```

Pas mal!

STEP VARIABLE = ZERO

14-FEB-92 09:44:43

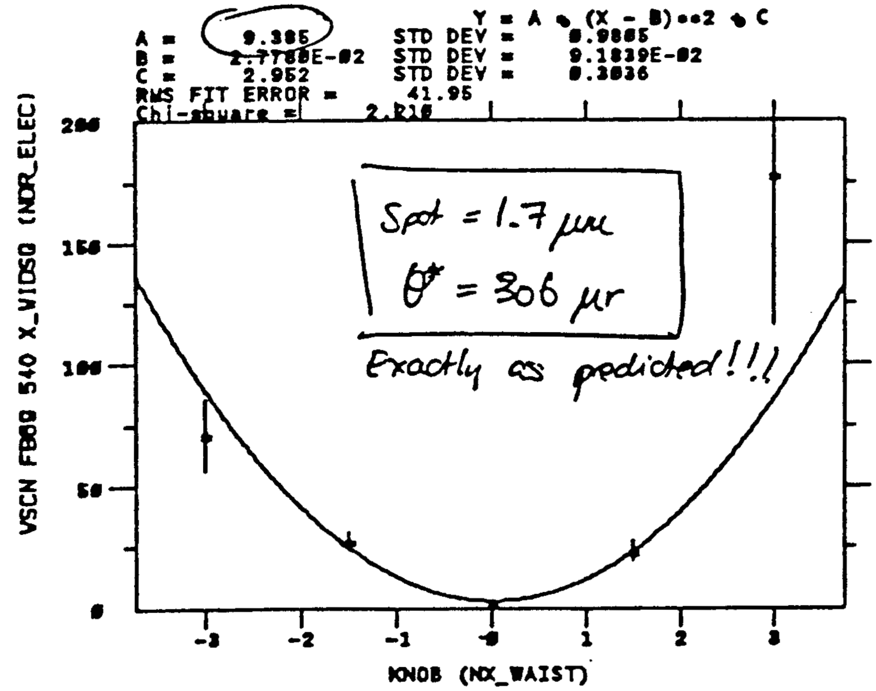

```
                         Y = A * (X - B)**2 + C
A =        9.385      STD DEV =      0.9865
B =     2.7780E-02    STD DEV =      9.1839E-02
C =        2.952      STD DEV =      0.3036
RMS FIT ERROR =        41.95
Chi-square =        2.810
```

Spot = 1.7 μm

θ* = 306 μr

Exactly as predicted!!!

KNOB (NX_WAIST) STRT=-3.000 STEPS= 5 SIZE= 1.500

14-FEB-92 09:53:04

Beam-Beam Deflections

- our bread and butter measurement!

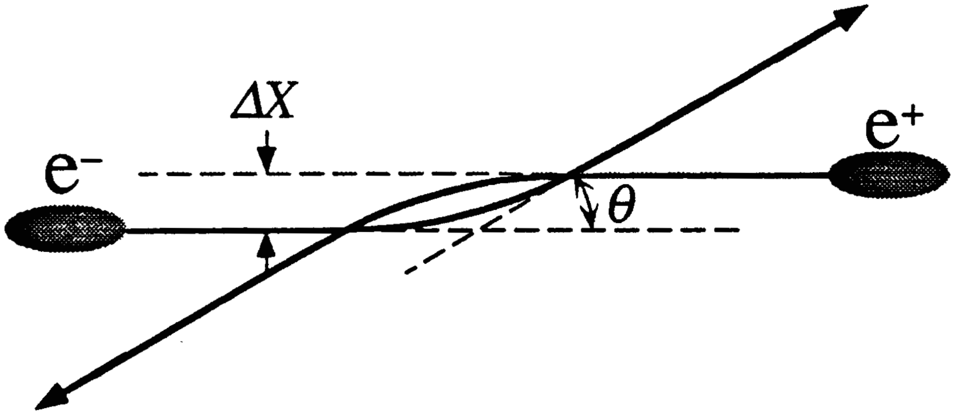

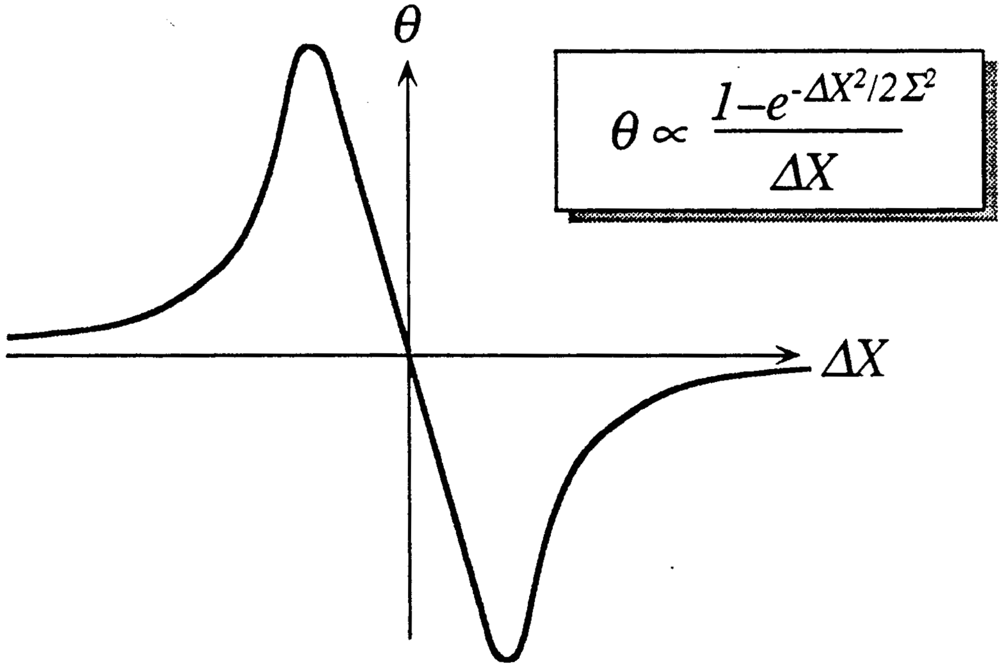

$$\theta \propto \frac{1-e^{-\Delta X^2/2\Sigma^2}}{\Delta X}$$

$$\boxed{\theta \propto \frac{1-e^{-\Delta X^2/2\Sigma^2}}{\Delta X}}$$

Non-linear fit of above function to deflection angle (θ) as we scan ΔX.

Assumptions:

- Gaussian beams
- Round beams

Fitted parameter $\Rightarrow \Sigma^2 = (\sigma_e^2 + \sigma_p^2)$

Difficult to tune one beam if other bea
is large (larger beam dominates Σ)

In addition, how do you determine θ?
Answer: Yet another least squares fit!

SLC INTERACTION REGION

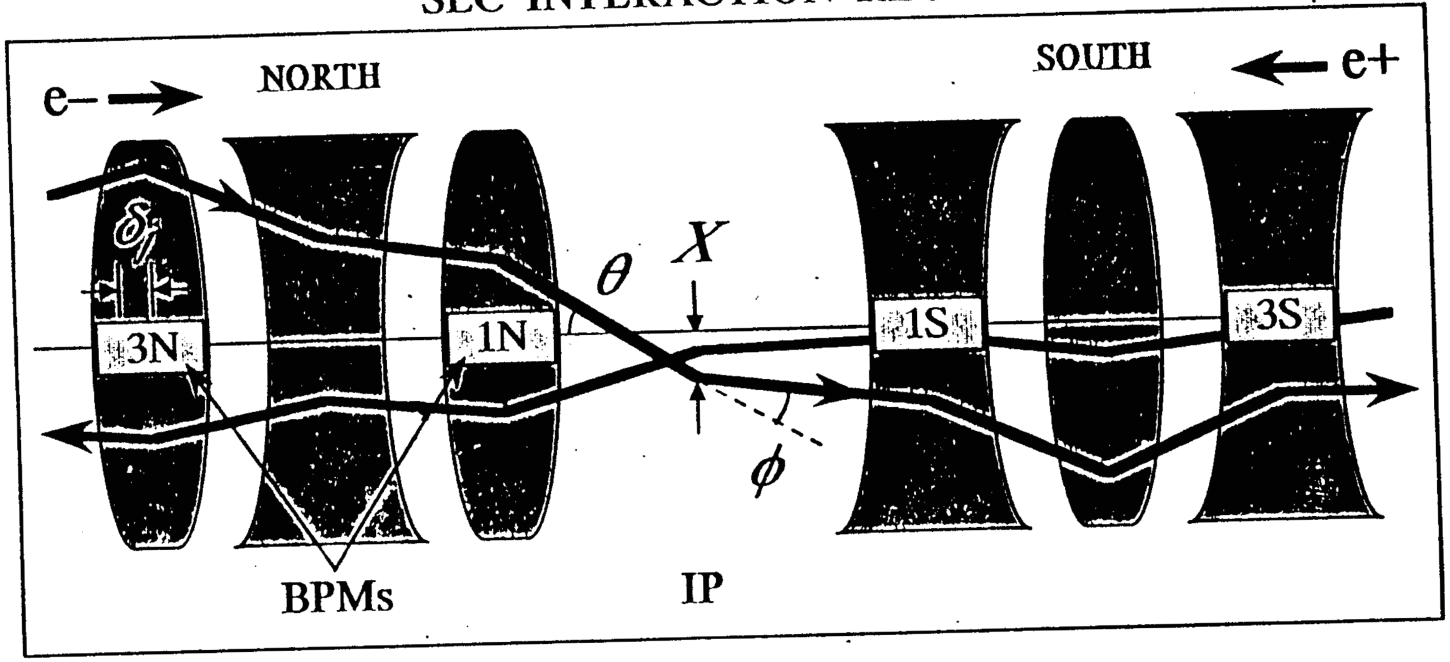

Data from 4 Beam Position Monitors (BPMs) is used in least squares fit to solve for 3 IP beam trajectory parameters:

$$\boxed{X_j = R_{11}^{(\mathrm{IP}:j)}\cdot X + R_{12}^{(\mathrm{IP}:j)}\cdot \theta + U_j R_{12}^{(\mathrm{IP}:j)}\cdot \phi}$$

$$U_j = \left\{ \begin{array}{ll} 0, & j = 1,2 \\ 1, & j = 3,4 \end{array} \right.$$

Problems with Beam-Beam scans

1. With initial deflection angle reconstruction:

   - Need to assume some model R matrix between BPMs and IP.

     ⇒ model errors give erroneous fit.

   - BPM scale errors ⇒ erroneous fit.

   - BPM offsets ⇒ bad fit χ^2

2. With deflection angle (non-linear) fit:

   - Not necessarily *gaussian* beams

   - Not necessarily *round* beams

   - Only measure Σ, not individual sizes

Round Beam Problem

Determination of angular divergence θ^*

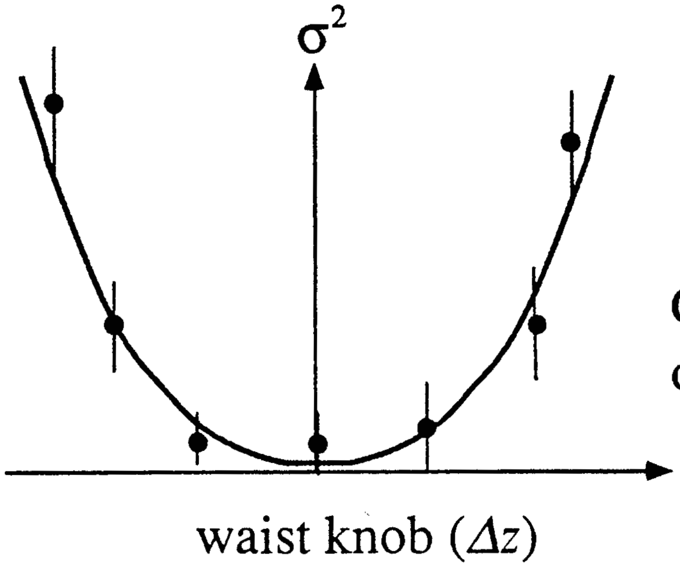

Fit $a(\Delta z - b)^2 + c$

$\uparrow$

Gives direct measurement of θ^*

However, only moving one waist gives *elliptical beam* in X-Y space

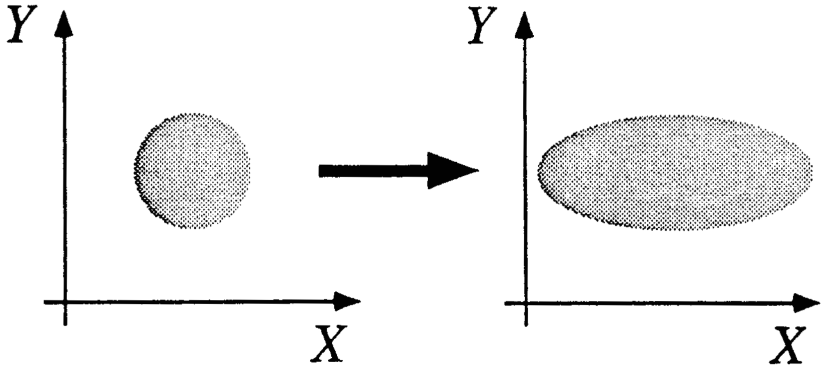

Result:
Underestimates
angular divergenc

Non-Gaussian Beam Problem

Although tuned machine probably has gaussian beams at IP, we still have *boot strap* problem of untuned machine.

Untuned FF has

- Dispersion
- Chromaticity
- higher order aberrations
- generally large spots

present at IP ⇒ NON-GAUSSIAN BEAMS

Point in case: **Dispersion.**

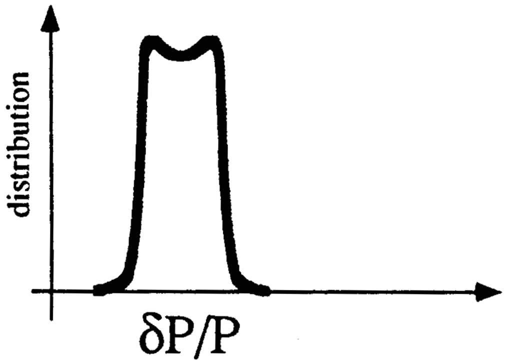

Non-Gaussian energy spread → Non-Gaussian beam at IP

Normally have very poor beam-beam scans when we begin tuning FF. Eventually scans become cleaner as aberrations are tuned out.

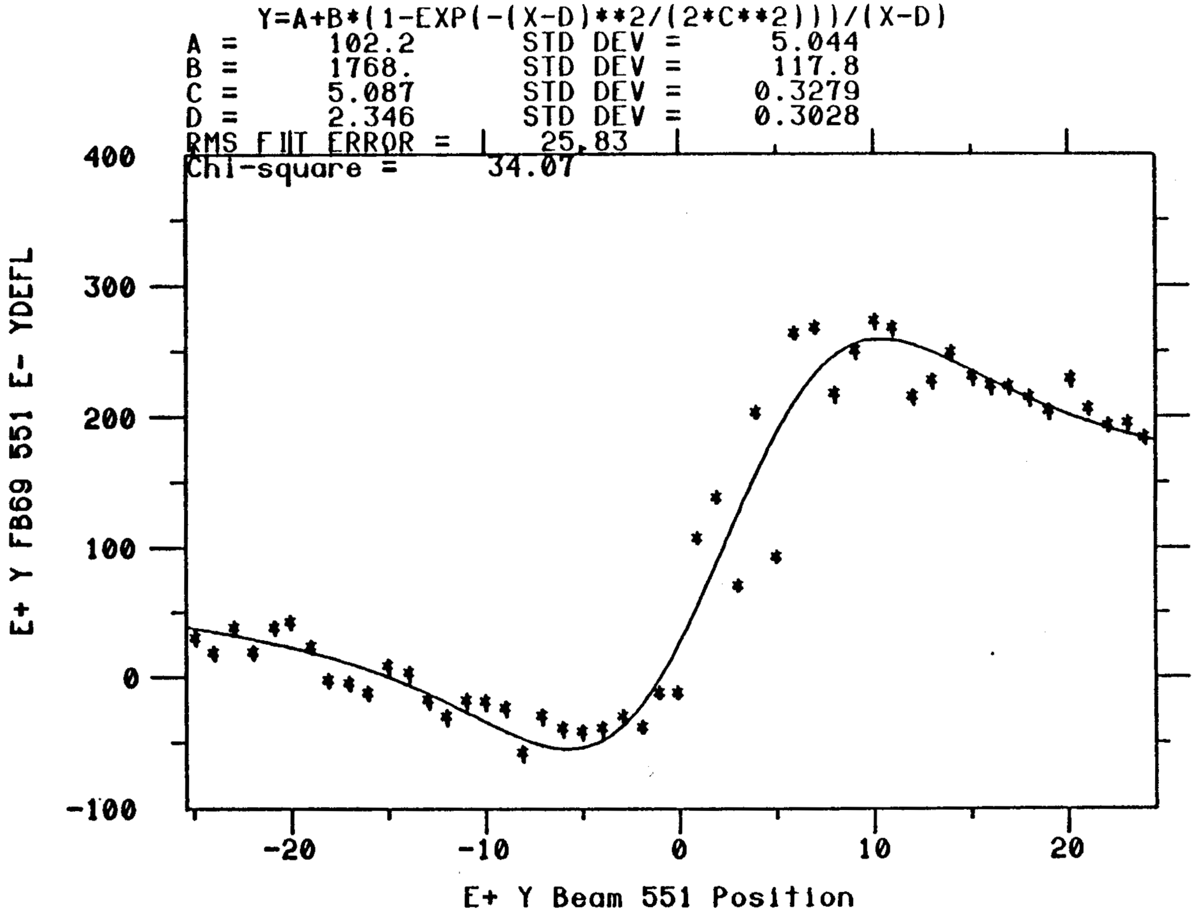

```
         Y=A+B*(1-EXP(-(X-D)**2/(2*C**2)))/(X-D)
A =        102.2        STD DEV =       5.044
B =        1768.        STD DEV =       117.8
C =        5.087        STD DEV =      0.3279
D =        2.346        STD DEV =      0.3028
RMS FIT ERROR =          25.83
Chi-square =        34.07
```

STEP VARIABLE = ZERO

29-FEB-92 19:12:31

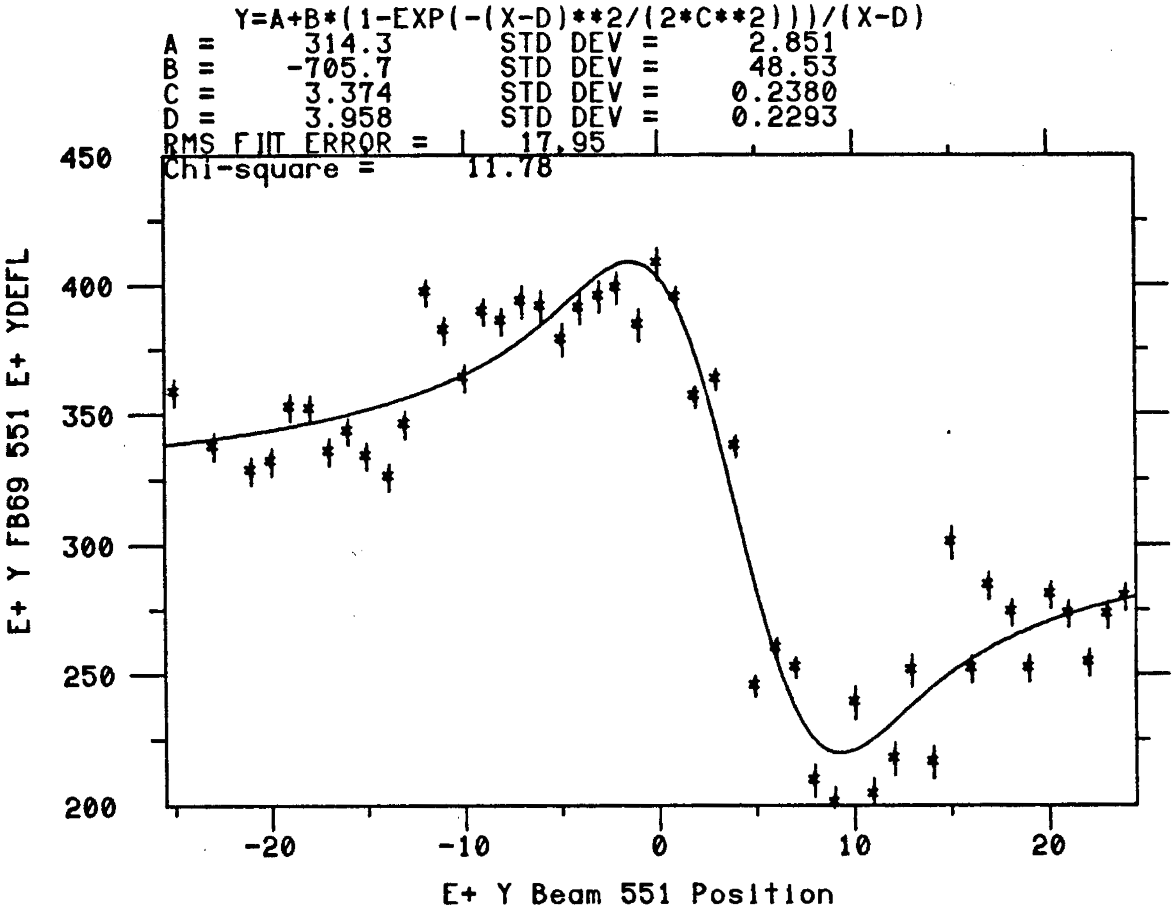

```
      Y=A+B*(1-EXP(-(X-D)**2/(2*C**2)))/(X-D)
A =        314.3        STD DEV =       2.851
B =       -705.7        STD DEV =       48.53
C =        3.374        STD DEV =      0.2380
D =        3.958        STD DEV =      0.2293
RMS FIT ERROR =         17.95
Chi-square =         11.78
```

STEP VARIABLE = ZERO

29-FEB-92 19:13:32

Tuning Problems #2
- Diagnostic & Beam Quality related Problems

3 Main problem areas:

- (fast) Beam Jitter
- Beam distribution (non-gaussians & tails)
- (slow) Drifts in beam parameters

Big problem since it generally takes many hours to tune small spots

⇒ **Important to keep entire machine stable while tuning FF.**

Defer discussion of slow drifts until later.
For now, concentrate on first two issues.

STABILITY (its impact on tuning)

Two types of stability problems

Beam jitter (energy, position, current):

- Fast random jitter (noise)
- Jitter with some time structure

Long term drifts

- Slow loss in luminosity.
- problem with identifying what has changed.

Keyword is: **FEEDBACK** future machines will be *"fly by wire"*

Question: *When to retune, and what?*

Effects of Beam Jitter on tuning

Fast Random Jitter:

Need to average measurements.
Will now tune on effective average beam.
Will degrade luminosity

Fast jitter with time structure:

example: time slot separation

SLC rep. rate = 120 Hz. Each alternate bunch (time slot) sees slightly different machine due to 60Hz mains cycle *referred to as time slot separation.*

=> systematic difference in energy, position and current between two consecutive bunches.

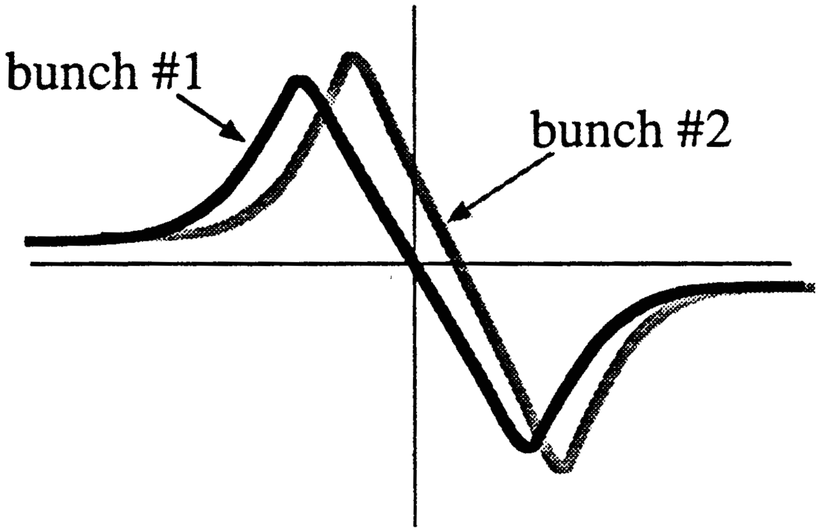

We can choose to tune on either time slot, or on the average of both.

Generalization to multibunch NLC

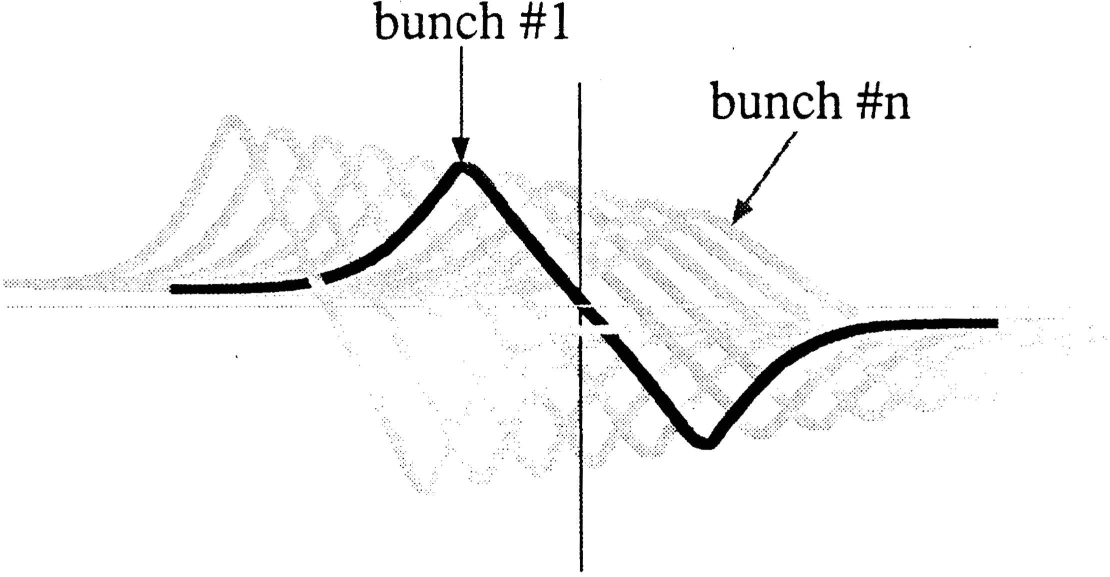

Long Term Stability - Slow Drifts

Changes in upstream system parameters (eg: DR, bunch compressor, LINAC, Arcs)

⇒ Changes in IP beam phase space

Example: Transverse phase space match at exit of LINAC.

How do changes in β & α at exit of LINAC affect IP spot?

PARAMETRIZATION OF BETA BEATS

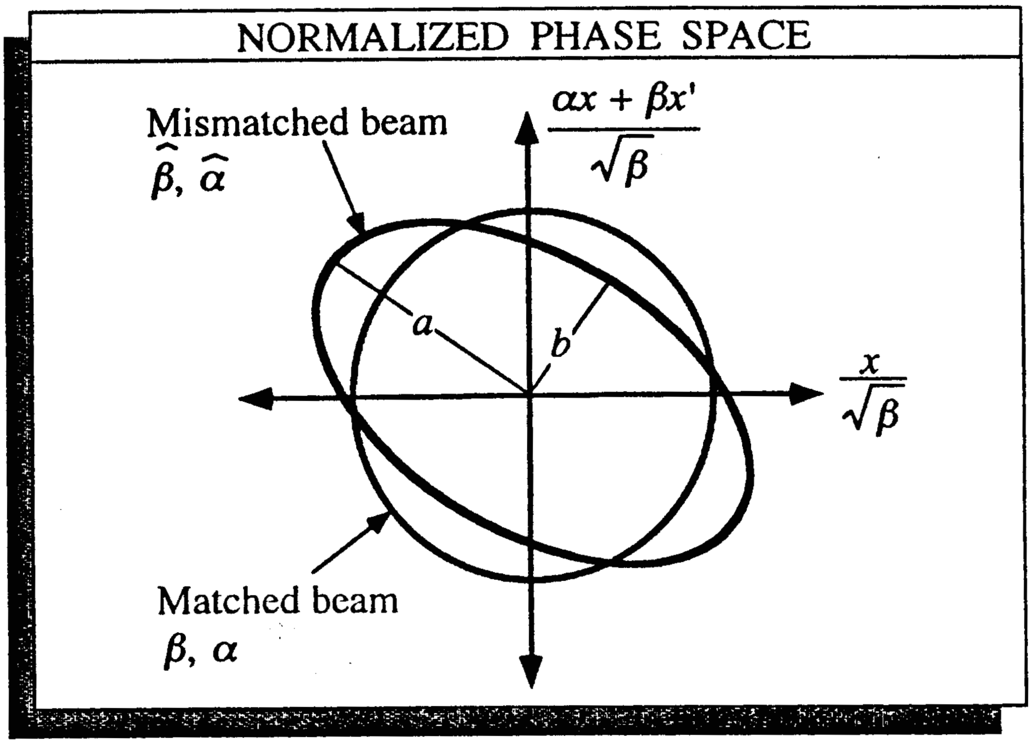

The mismatch is characterized as half the sum of squares of the major and minor axes:

$$\boxed{\frac{a^2 + b^2}{2} = \frac{1}{2}\left[\frac{\beta}{\hat{\beta}} + \frac{\hat{\beta}}{\beta} + \beta\hat{\beta}\left(\frac{\alpha}{\beta} - \frac{\hat{\alpha}}{\hat{\beta}}\right)^2\right]}$$

- Waist motion as a function of phase advance for various BMAG values (1.0 to 4.0 in steps of 0.5). A β^* of 5mm is assumed.

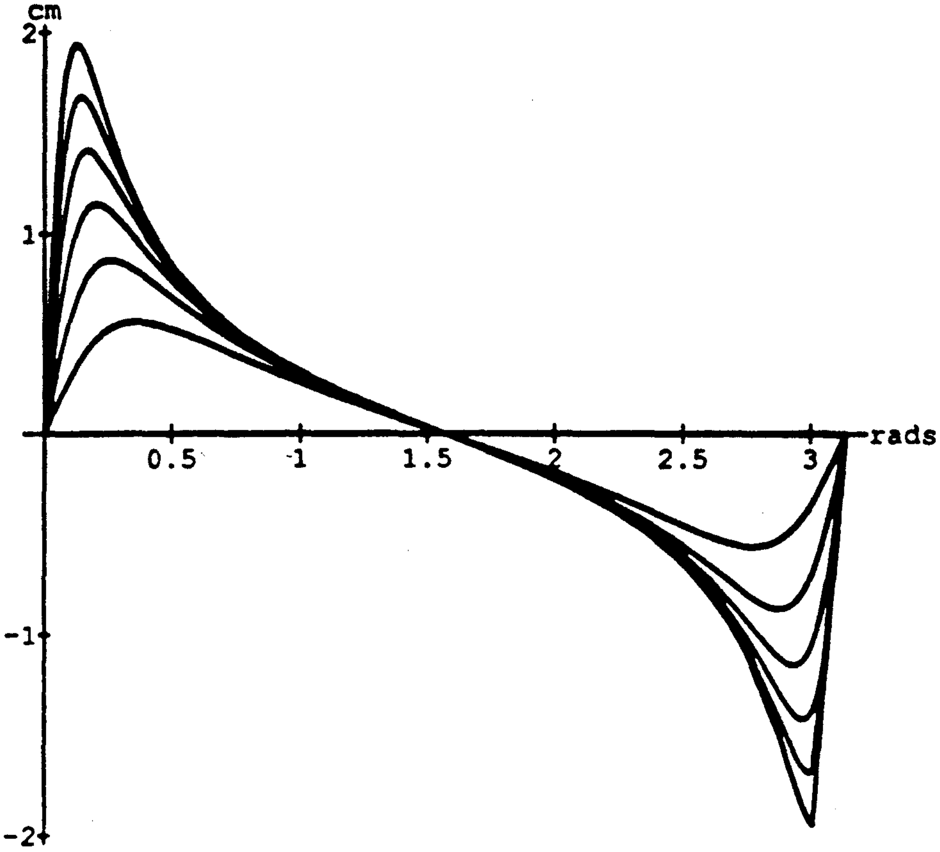

- **Angular divergence as a function of phase advance for various BMAG values (1.0 to 4.0 in steps of 0.5).
  A β^* of 5mm is assumed.**

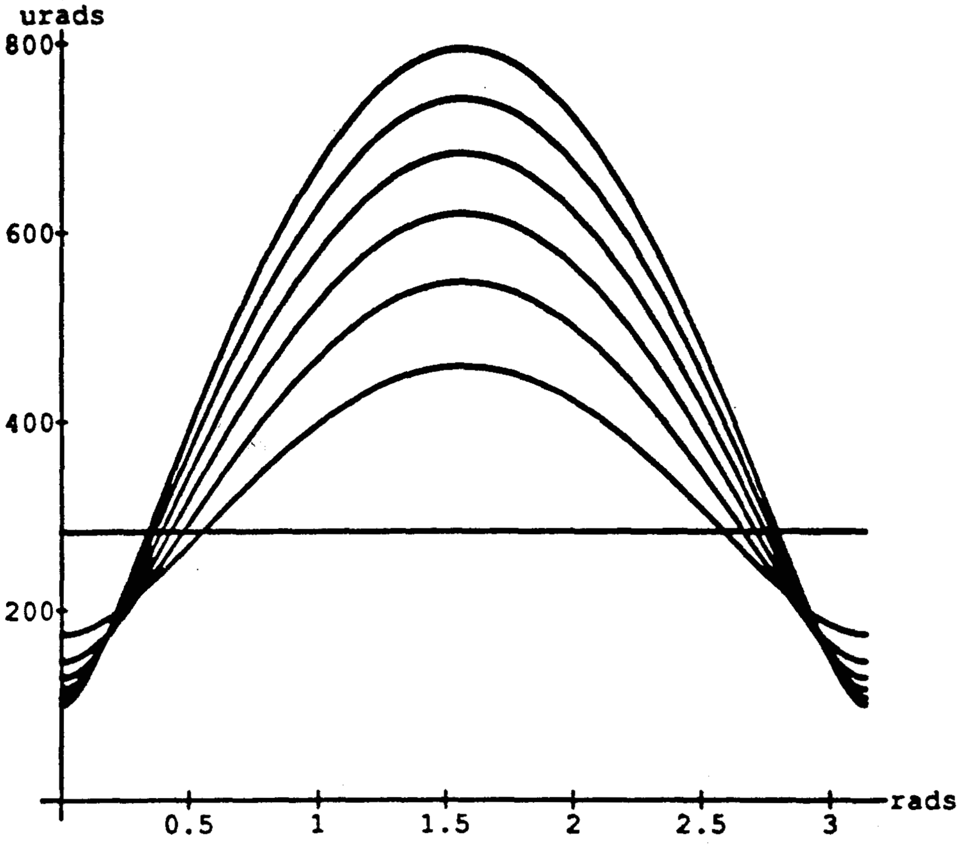

LUMINOSITY SUMMARY

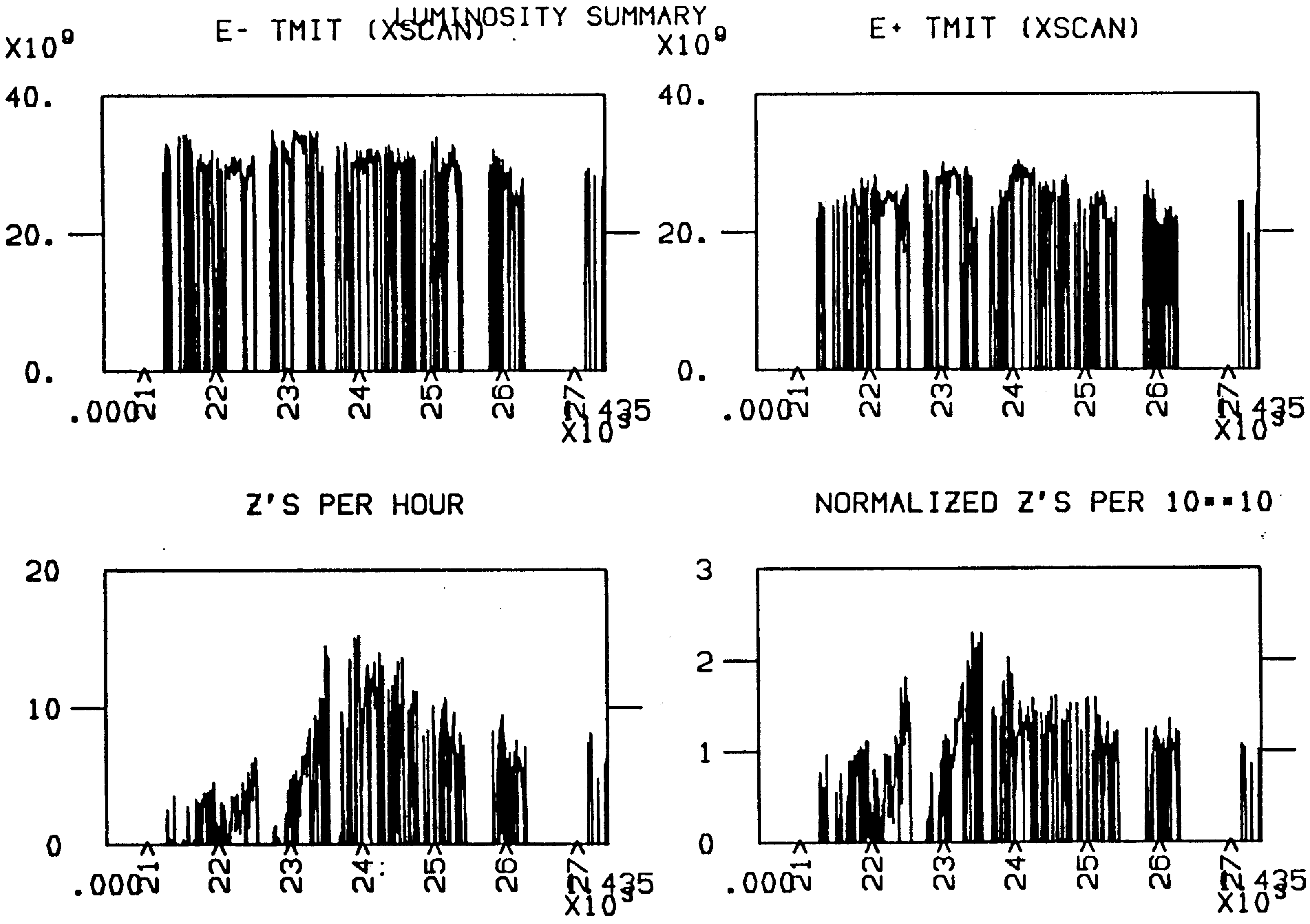

LAST DATA POINT: 27-FEB-1992 10:15:34 27-FEB-92 10:20:11

Sources of Jitter and Drift
Feedback systems

Jitter can arise from:

- Power supplies
- Klystrons
- Ground motion
- Mechanical vibration.

No matter where they occur in collider, all talk to IP spot and hence luminosity

Need **feedback systems** to stabilize beam

SLC has many feedback systems

- steering/launch feedback
- energy feedback

FF has two feedback systems

- beam launch at exit of Arcs
- IP collision feedback.

Eventual adjustment of beam parameters will be by changing setpoints of FFBK systems - FLY BY WIRE!

gain = .5 ——— 30 μm in y

FB69 DEFLECTION ANGLE

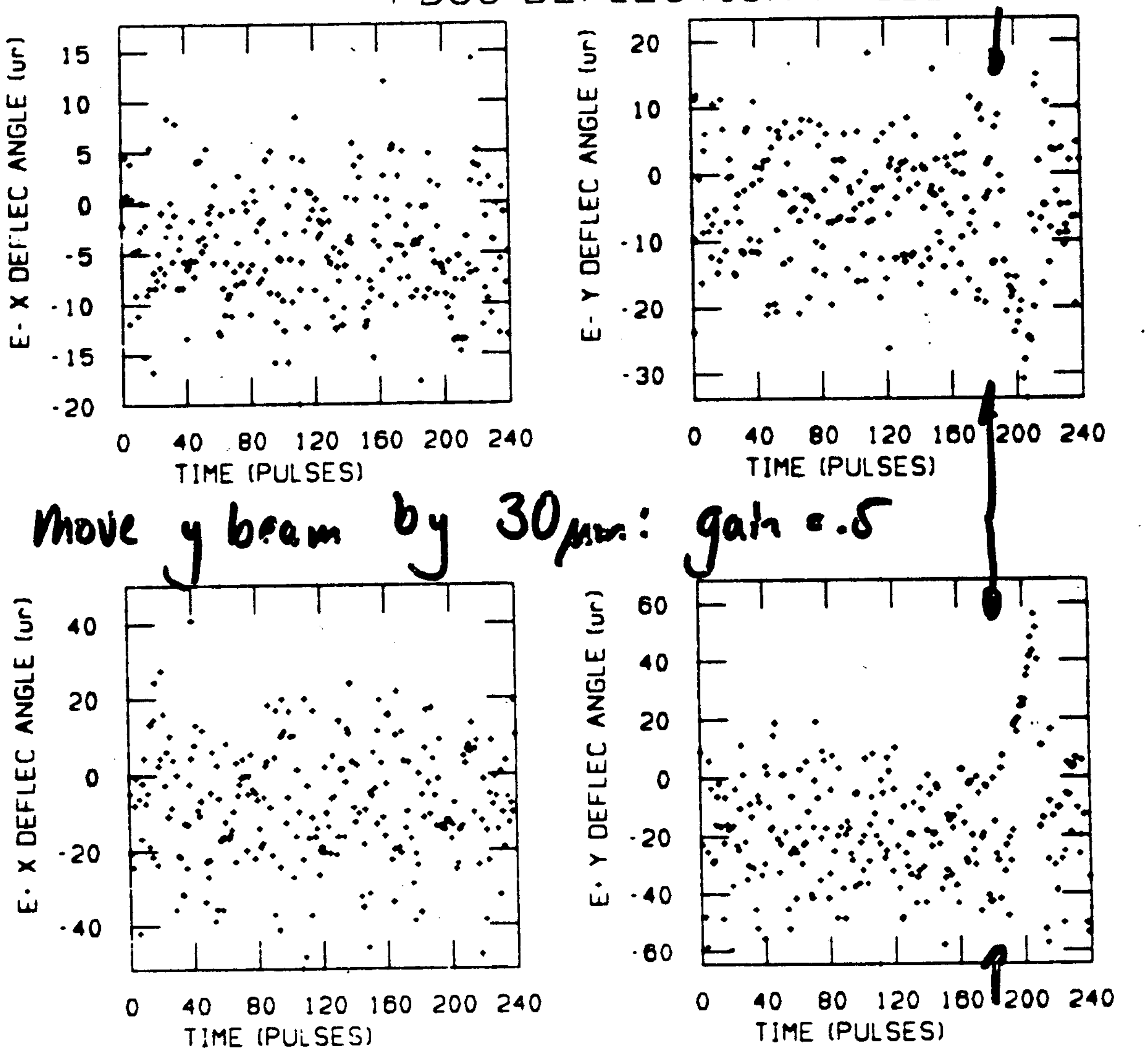

Move y beam by 30μm: gain = .5

25-JAN-90 11:58:12

Other Important Issues

Backgrounds (see talk by Hertzbach)

Important FF optics related topics:

- Steering
  FF orbit is generally arrived at through background considerations.
- IP Angular divergence
  Limited by detector, again often adjusted for background rather than luminosity tuning.

Need to design Final Focus system so the one does not trade off **BACKGROUNDS** for **LUMINOSITY**

Machine Protection System (MPS)

FF ion chambers or beam loss monitors will trigger an MPS trip.

In single pass machines, a **rate limit** is required

(*eg* 120Hz -> 10Hz)

so that problem can be diagnosed and corrected, or better still, machine can cure itself!

Trips can easily be caused by tuning since one typically:

- Changes QUADS
- adjust steering *etc*.

Particular problem with SLC extraction line (large β functions).

On-going Problems with SLC FF

Long Term Stability

- Why does luminosity "walk away".
  Machine wide problem.
  Complex multiparameter space makes problems difficult to diagnose.

Continuous monitoring of beam parameters.

- Still require more no-invasive monitoring.
  eg. Arc η
  Eventually leads to feedback systems.

Better β matching algorithms

- More robust. Need to measure phase space at entrance of FF.

Better magnet alignment.

In Conclusion
- What have we learnt from SLC?

- FF systems should be designed to be easily tunable
  - foreseen corrections should be orthogonal.
- Accurate & robust diagnostics are essential.
  - important to have the correct types and number to do the desired job.
- Magnet alignment is absolutely critical.
  - provisions for beam based alignment will be necessary.
- Include feedback systems in the design.
  Assume everything will need a feedback system.
  types of feedback systems required may have impact on lattice and types of diagnostics required.
- Detector & accelerator are one entity. Should be designe as such.
- **Luminosity is not made by FF alone**: Global approach to machine design is required.

SLAC Final Focus Workshop
March 2, 1992
O. NAPOLY

FINAL FOCUS SYSTEMS: OPTICS KEY ISSUES

SUMMARY

I) **The General Philosophy**

II) **The Perfect Machine**
- The telescope
- The chromatic correction section
- The bandwidth
- The matching section
- The residual aberrations

III) **The Imperfect Machine**
- Jitter tolerances
- Alignment tolerances
- Wake field effects

IV) **The Interaction Region**
- The crossing angle
- Collimation
- Muon protection
- The solenoid

I) The General Philosophy

- derives from the low-beta in e^+-e^- storage rings and from the final focus in the SLC:

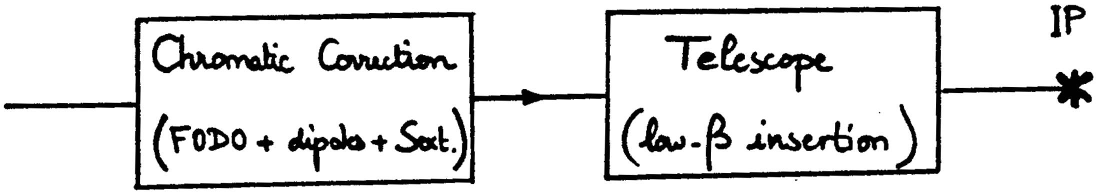

- illustrated by the one-dimensional telescope (*K. Brown*)

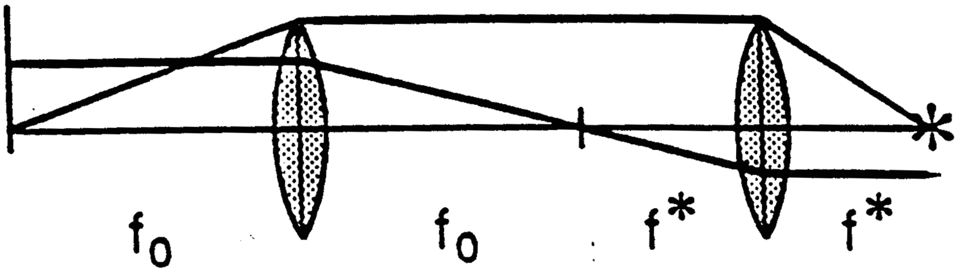

→ de-magnification $M = f_0/f^*$ $(\gg 1)$

1) sets the scale of lengths

$$1/f^* = g = K_1 l_Q = \frac{B_0}{a} \cdot \frac{l_Q}{B\rho}$$

Gradient : $B_0/a \lesssim 1.4$ T/0.5 mm (*Egawa, Taylor*)

Rigidity : $B\rho = E/ec$

Quad length : $l_Q \sim 1$ m

- Not a comparison between different parameter list

$\Longrightarrow$ $f^* \simeq 1.2\,\text{m} \cdot \text{E[TeV]}$ different designs

- 1 important difference : flat beams

$\Longrightarrow$ $L_{\text{telescope}} = 2(f_0 + f^*) = 2(M+1)f^* \sim 100's$ of meters

Very flat beams

- Review of some selected issues

2) gives the correct chromaticity and bandwidth

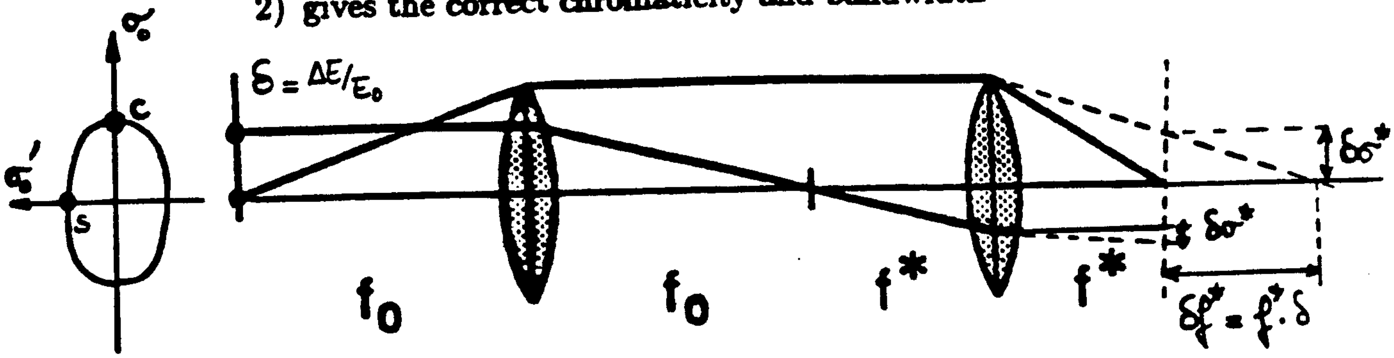

- from Thales theorem:

$$\delta\sigma^*(c) = \delta \cdot \sigma^*$$

(δ = energy spread)

$$\delta\sigma^*(s) = f^*/\beta^* \cdot \delta \cdot \sigma^*$$

- connection with TRANSPORT coefficients:

$$\delta\sigma^*(c) = T_{116}\sigma_0\delta = T_{116}M \cdot \delta \cdot \sigma^*$$

$$\Longrightarrow \quad T_{116} \sim 1/M \quad \text{negligible}$$

$$\delta\sigma^*(s) = T_{126}\sigma'_0\delta = T_{126}\frac{\epsilon}{\sigma_0}\delta = \frac{T_{126}}{M\beta^*} \cdot \delta \cdot \sigma^*$$

$$\Longrightarrow \quad T_{126} \sim Mf^* \quad \text{dominant}$$

- the bandwidth $\pm\delta_{max}$ is defined by :

$$\frac{\delta\sigma^*}{\sigma^*}(\delta_{max}) = 1 \quad \Rightarrow \quad \delta_{max} \simeq \beta^*/f^*$$

- connection with the chromaticity $\xi = \int ds\ K(s)\beta(s)$:

$$T_{126} = -c(s^*)\int ds\ K(s)\ s^2(s) \simeq \frac{\beta_0}{M}\int ds\ K\beta = M\beta^*\xi$$

$$\text{with} \quad s^2(s) = \beta_0\beta(s)\sin^2(\Delta\psi) \simeq \beta_0\beta(s)$$

$$\Longrightarrow \quad \xi = T_{126}/M\beta^* = 1/\delta_{max} \quad \text{as expected}$$

N.B.: $\delta_{max} \sim 1\%$ seems possible with $f^* \sim 1$ m and $\beta^* \sim 1$ cm

II) The Perfect Machine

1) The telescope

A 4-lens telescope = (1 weak doublet + 1 strong doublet)

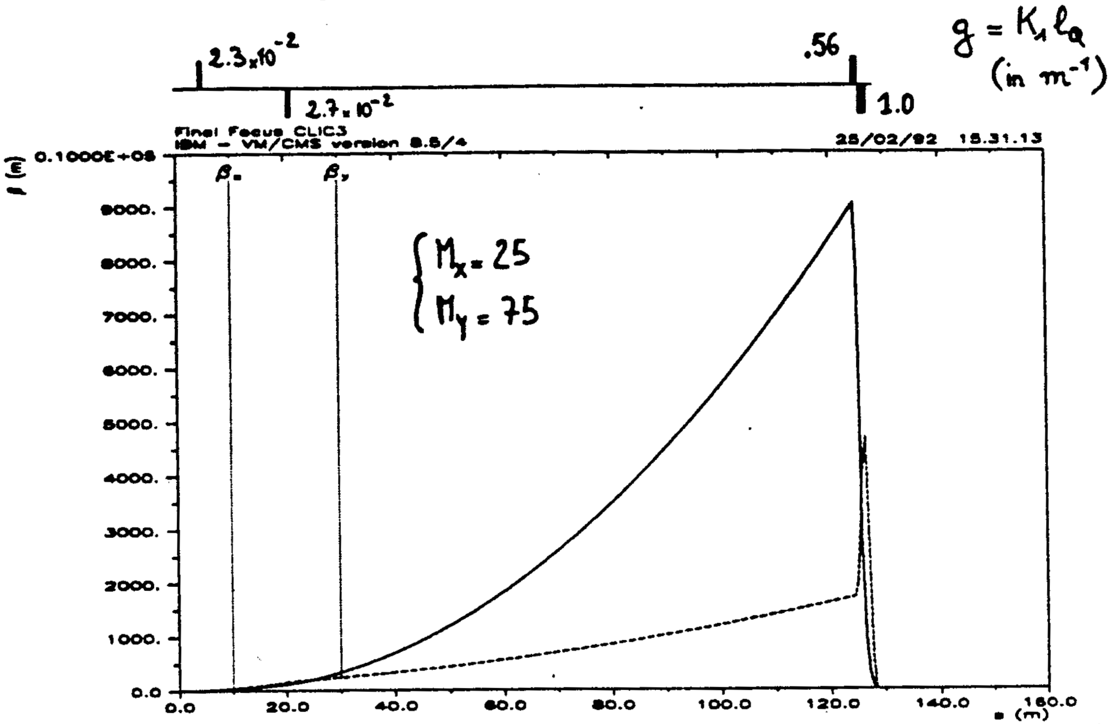

can be derived from the thin lens solution which optimizes the figure of merit ✱

$$F = 1/(l_1 + l_2 + l_3 + l_4 + l_5)(|g_1| + |g_2| + |g_3| + |g_4|)$$

(essentially 1 free parameter)

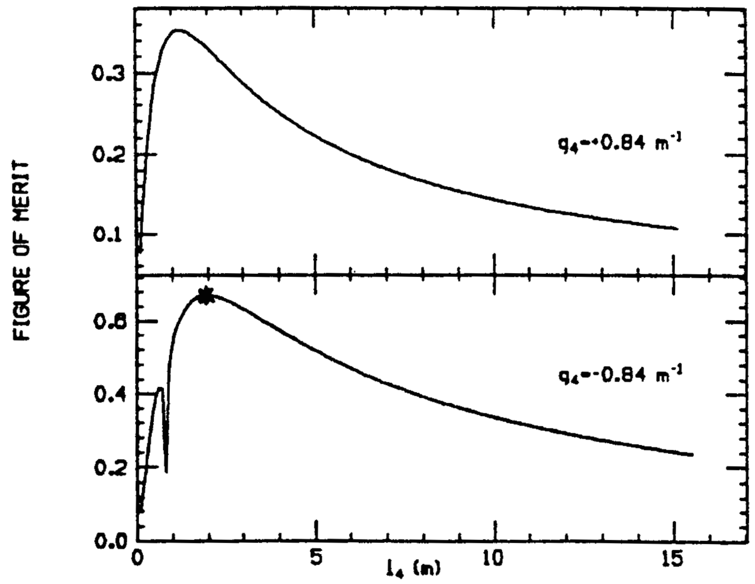

← last quad focusing horizontally

← last quad focusing vertically

vertical chromaticity

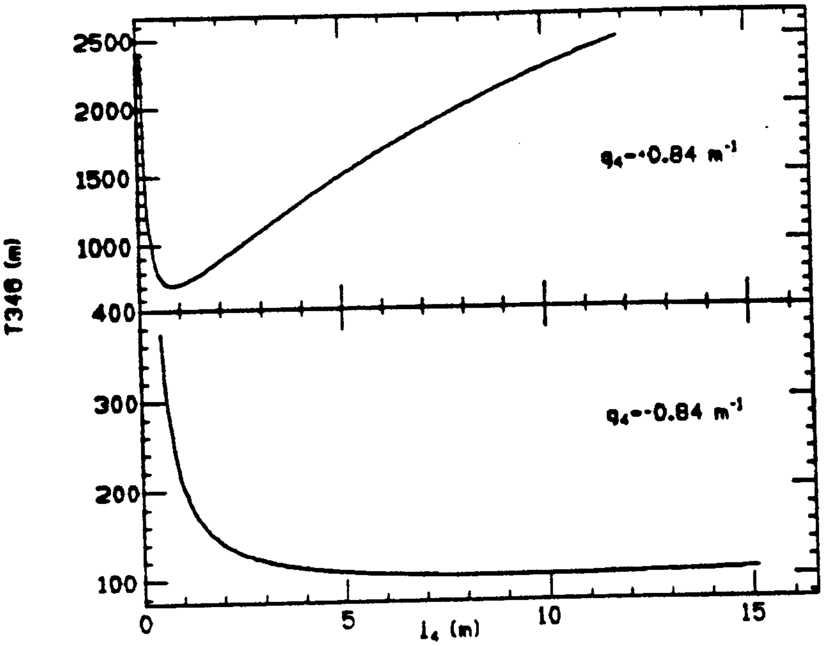

horizontal chromaticity

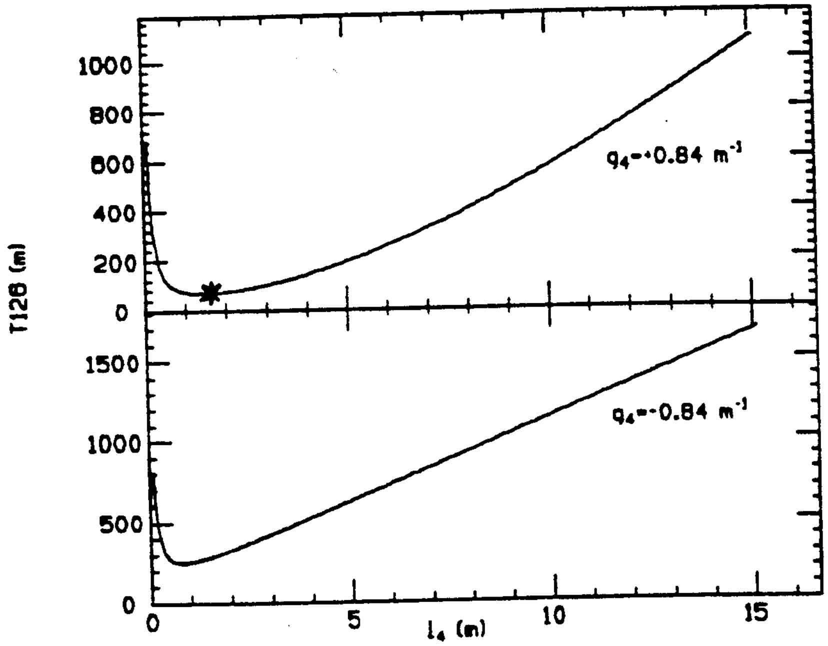

← minimum $T_{126} = 69$ m $\ast$
with last quad focusing
horizontally

$$\delta_{max} \simeq M_x \beta_x^* / T_{126} = \pm 0.7\% \quad \text{for} \quad \beta_x^* = 2 \text{ cm}$$

⟶ possibility for a flat-beam telescope with vertical correction only.

the academic design

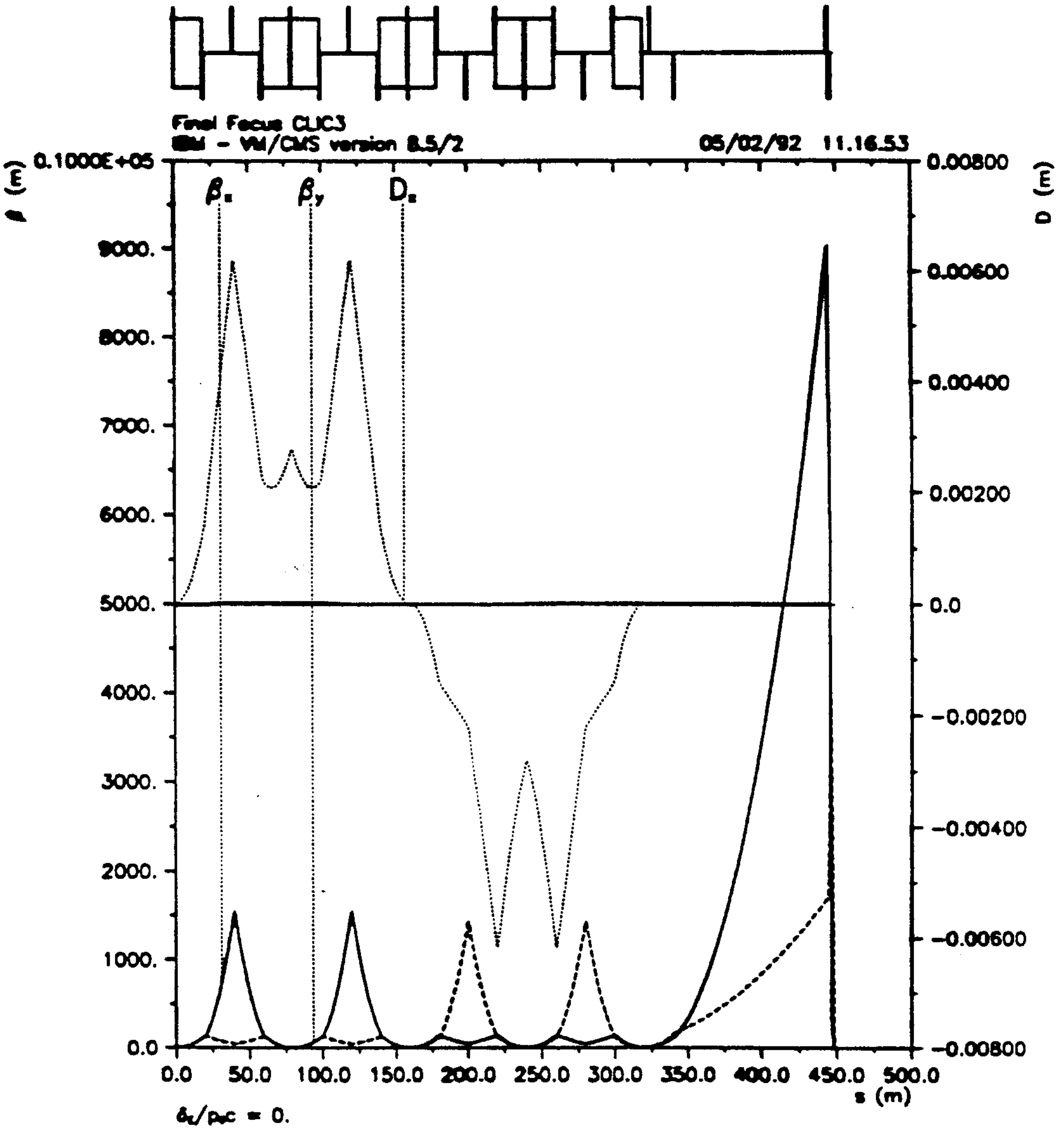

versus

the inventive design

JLC−FFS (500 GeV) $\beta_x^* = 24$ mm $\beta_y^* = 120$ μm

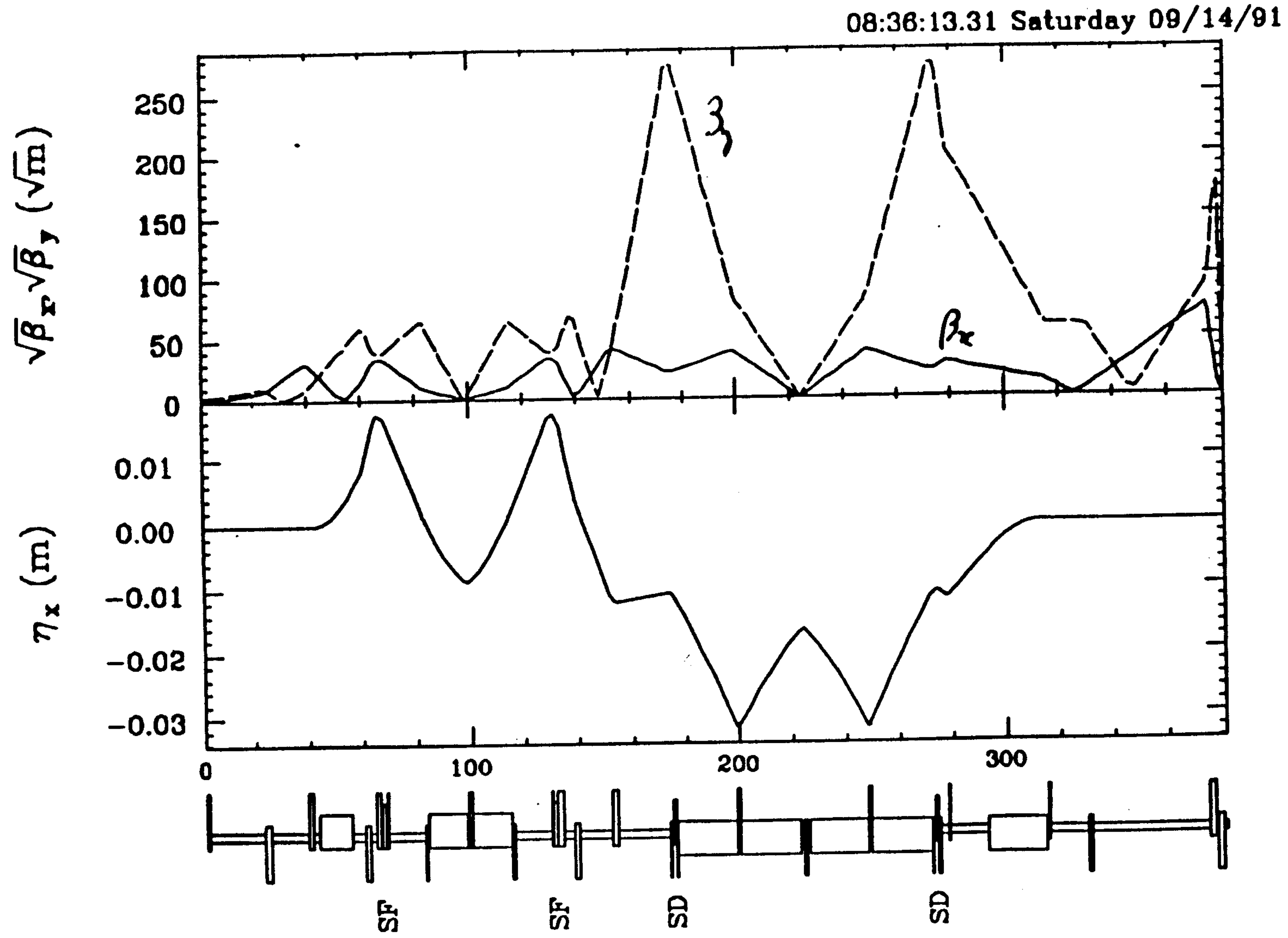

A flat beam telescope: $\beta_x^* = 2$ cm , $\beta_y^* = 100$ μm

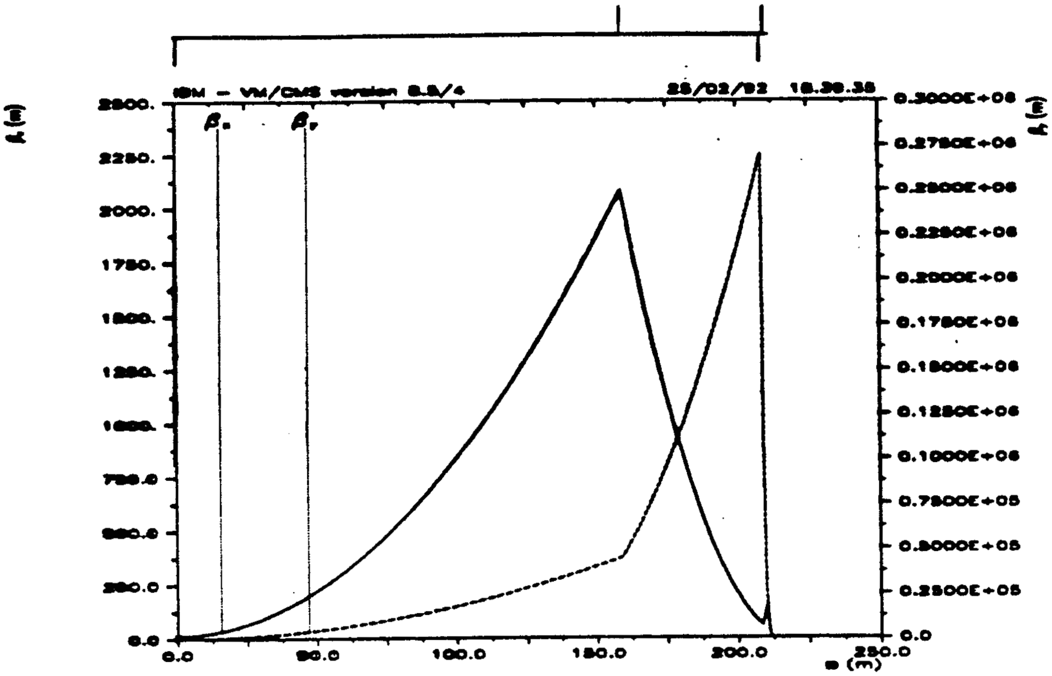

$\sqrt{\beta_y \epsilon_y} = 117$ μm for $\epsilon_{N,y} = 5 \times 10^{-8}$ @ 500 GeV

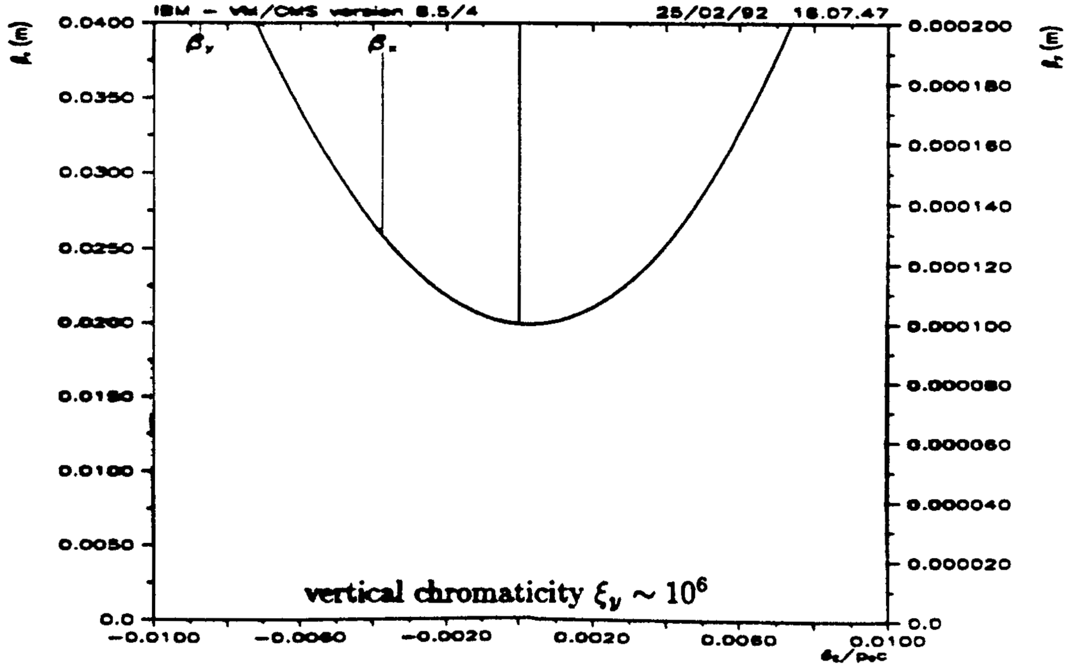

vertical chromaticity $\xi_y \sim 10^6$

Possible problems: thick lens telescope unreasonable, sextupoles too strong, *Oide* effect.

5-lens telescopes

For large de-magnifications, 4-lens telescopes are too long.

for example:

$M = 160 \times 190 \longrightarrow$ total length = 537 m for $g_4 = -0.84$ m^{-1}
(*total de-magnification for CLIC*)

→ 2 solutions:
- split in 2 telescopes (i.e. matching section + final transformer)
- use telescope with 5 or more lenses

for example:

$M = 160 \times 190 \longrightarrow$ total length $\simeq$ 60 m for g_5 or $g_6 = \pm 0.84$ m^{-1}

$\pi.(.001 - .023 - .23 — .25 - .25)$, $\Delta\phi_x = \cancel{2}\pi$

$\pi.(.008 - .043 - .30 — .75 - .75)$, $\Delta\phi_y = 2\pi$

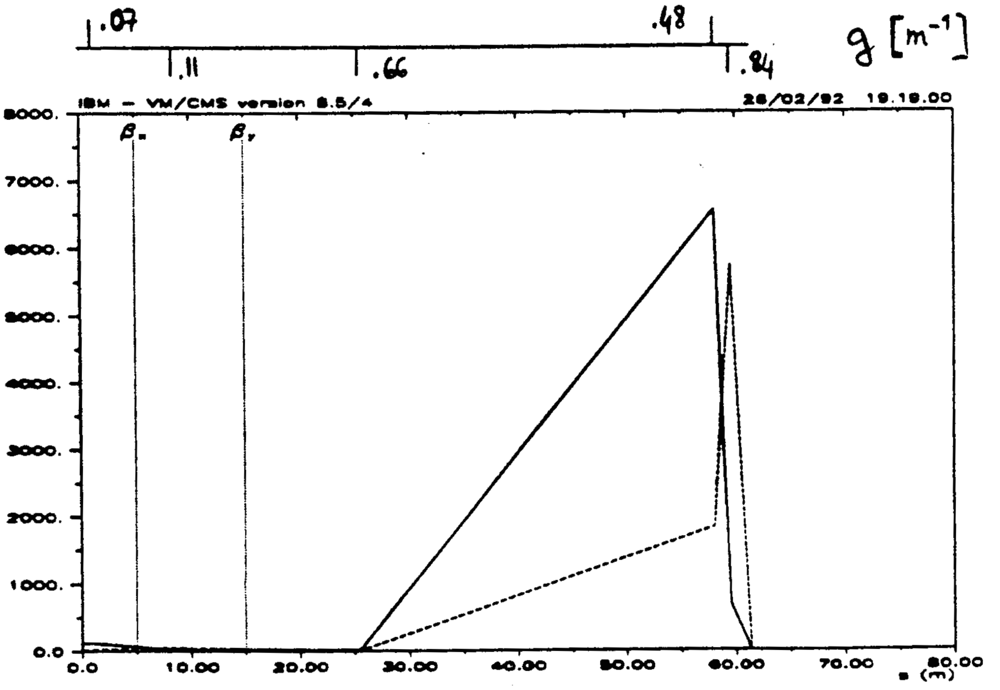

160 × 190 telescope with 5 lenses and $g_5 = -0.84$ m

2) The chromatic correction section

Obeys general principles derived from *SLC final focus*:

- sextupoles come in pair separated by π phase shift to avoid geometric aberrations

- sextupoles are separated from the IP by a multiple of $\pi/2$ (*i.e. by a multiple of π from the last doublet*) to keep T_{116}, T_{336} and T_{166} small.

- the two pairs which correct horizontal and vertical chromaticities are not interlaced to avoid third order aberrations

an alternative

vertical dispersion and skew sextupoles in CCS-V

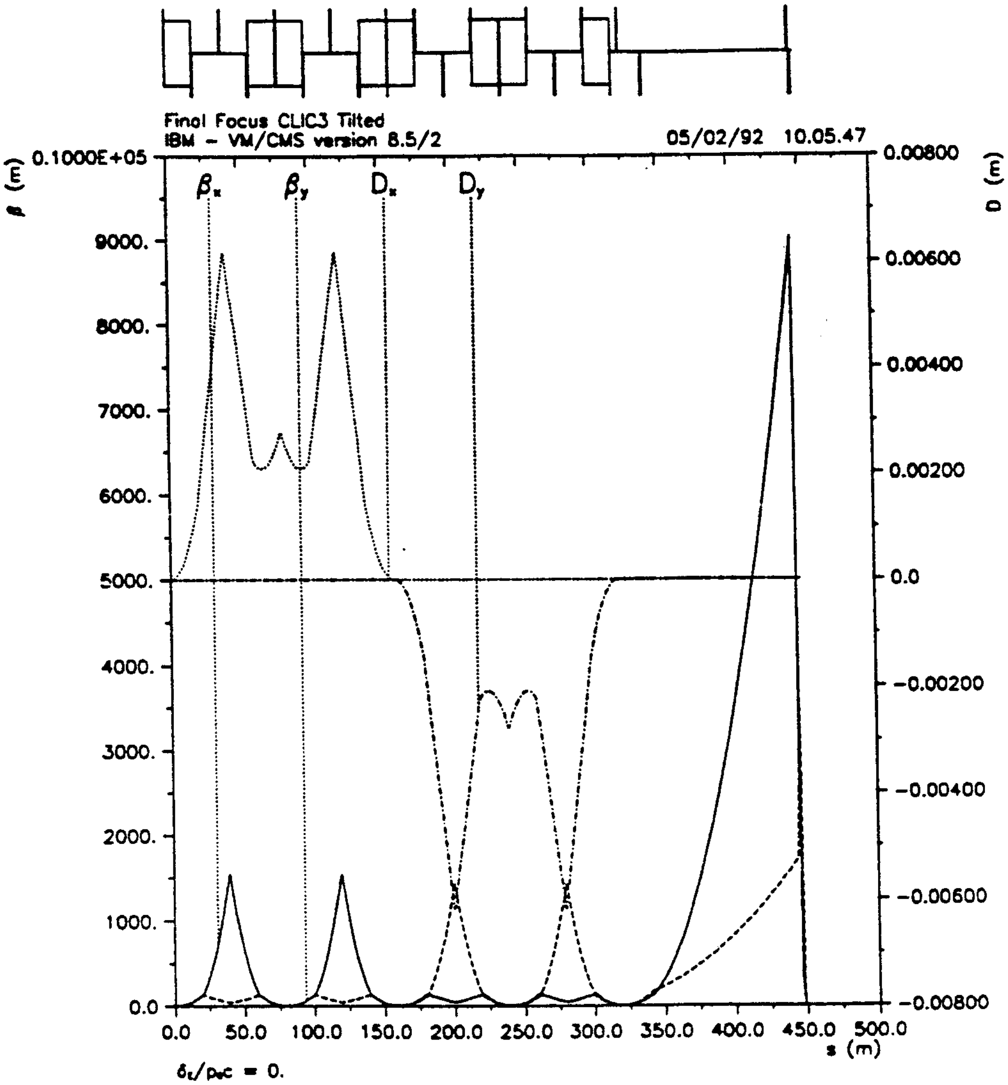

Vertical dispersion offers 2 main advantages:

- it reduces the strength of the sextupoles

$$K_2[\mathrm{MAD}]: \quad 287\ \mathrm{m}^{-2} \rightarrow 109\ \mathrm{m}^{-2}$$
$$B_0: \quad 3.01\ Tesla \rightarrow 1.15\ Tesla$$

for 2.5 mm aperture radius at 1 TeV.

- it allows to optimize the dipole strengths independently in horizontal and vertical chromatic sections.

3) The bandwidth

The energy dependence of β^* is calculated from the energy-dependent transfer matrix $R(\delta)$:

$$\beta^*(\delta) = R_{11}^2(\delta)\beta_0 + R_{12}^2(\delta)/\beta_0$$

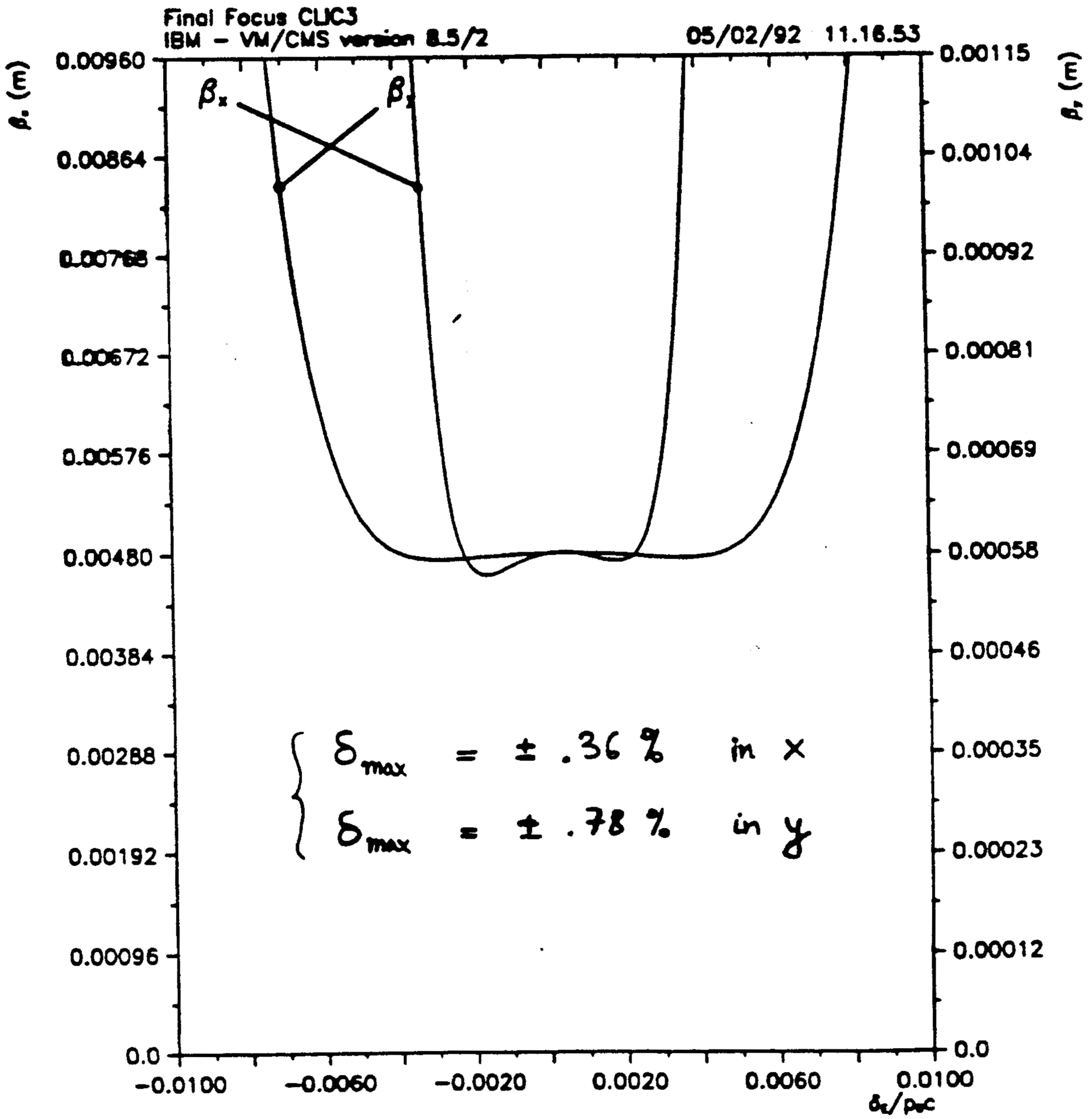

$$\begin{cases} \delta_{max} = \pm .36\ \% \quad \text{in } x \\ \delta_{max} = \pm .78\ \% \quad \text{in } y \end{cases}$$

This does not take into account synchrotron radiation in the dipoles. To optimize the strength of the dipoles, one can use **theory** and/or **tracking**.

bandwidths of 5-lens telescope

25 × 75 de-magnifications

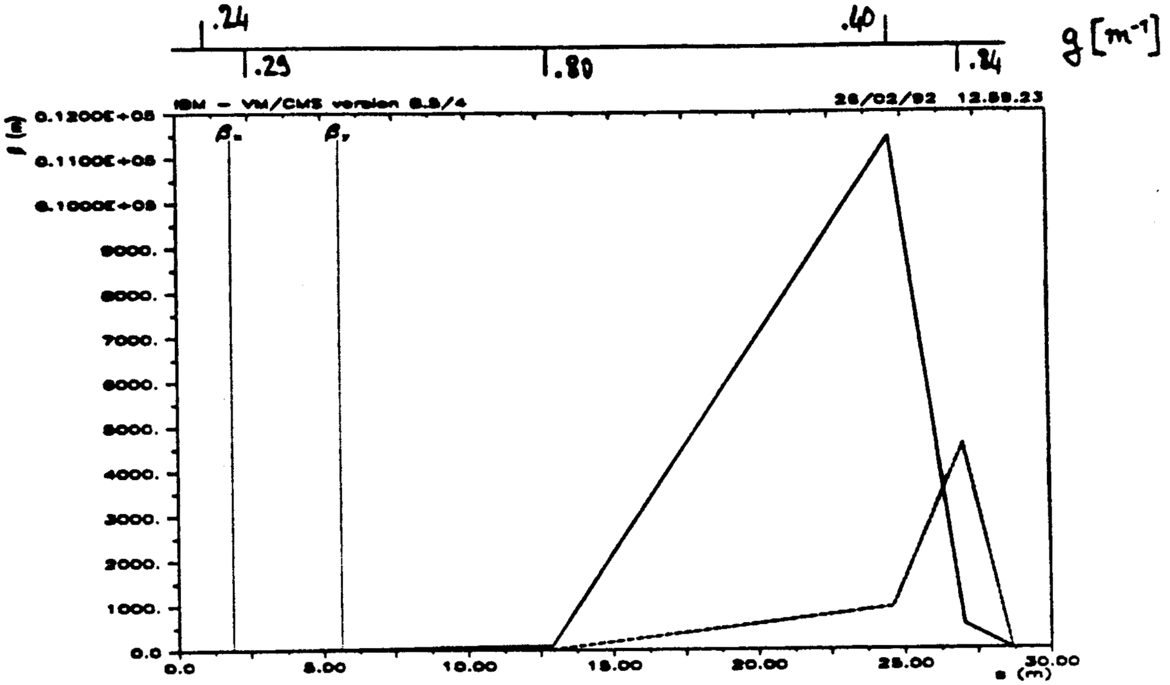

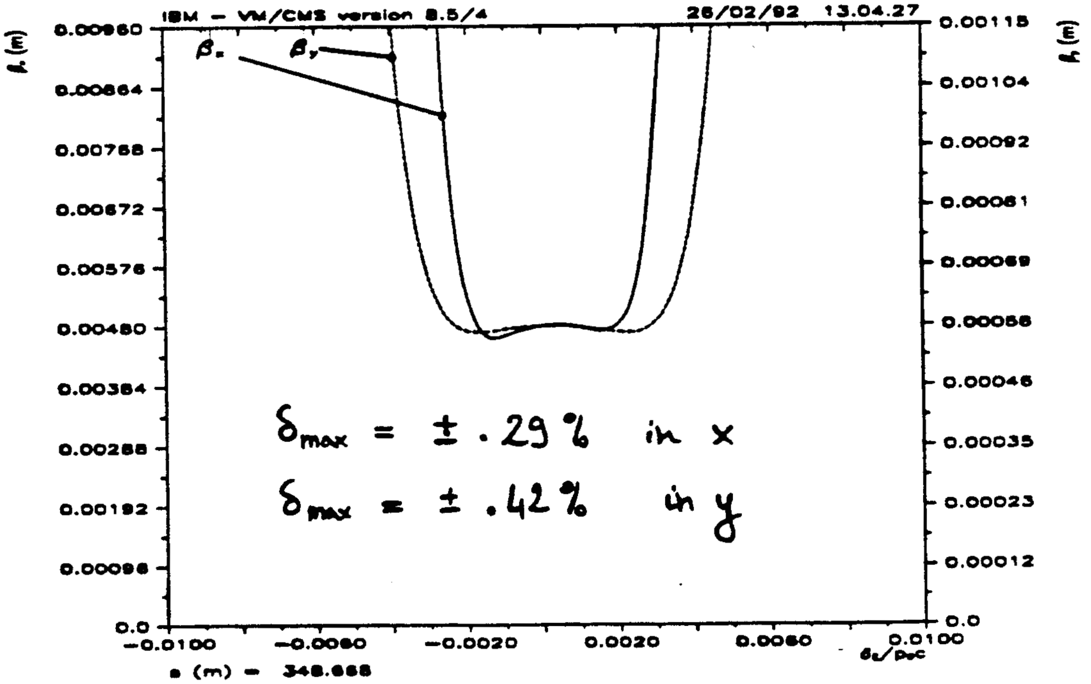

$\delta_{max} = \pm .29\%$ in x

$\delta_{max} = \pm .42\%$ in y

bandwidths of 4-lens versus 5-lens telescopes

160 × 190 de-magnifications

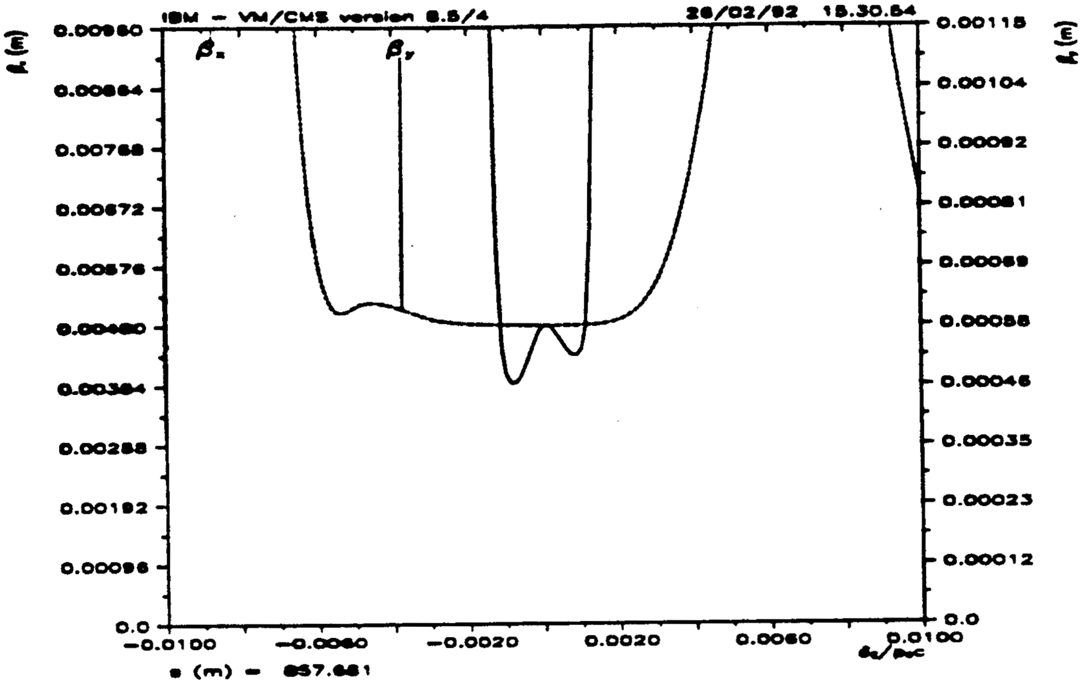

4-lens telescope

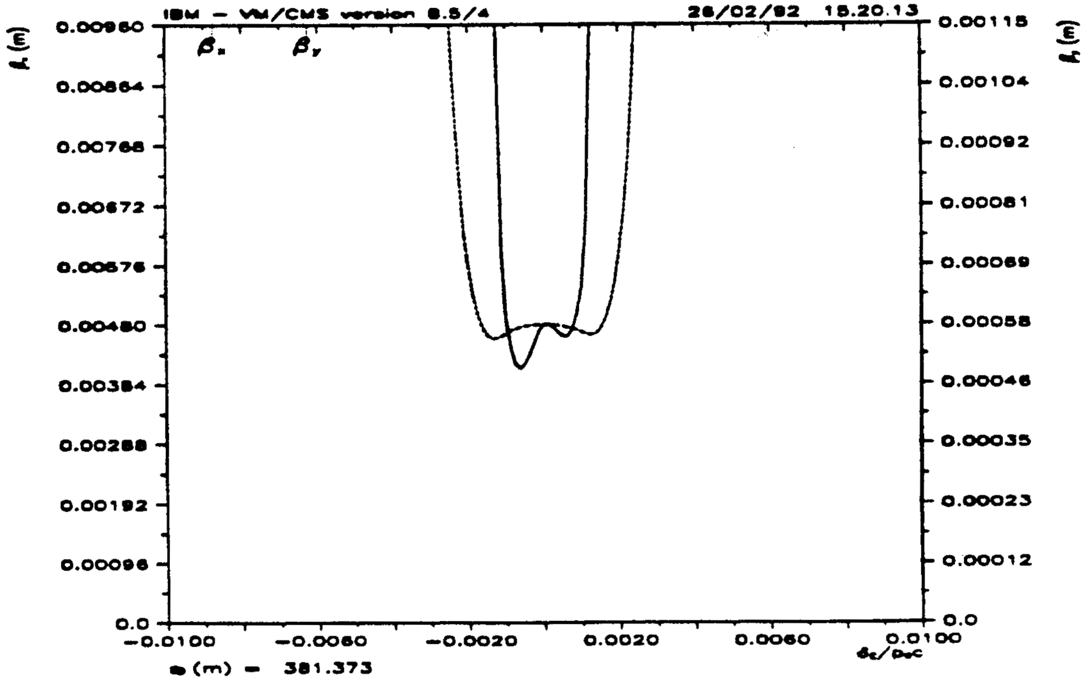

5-lens telescope

the bandwidths for the "tilted CCS"

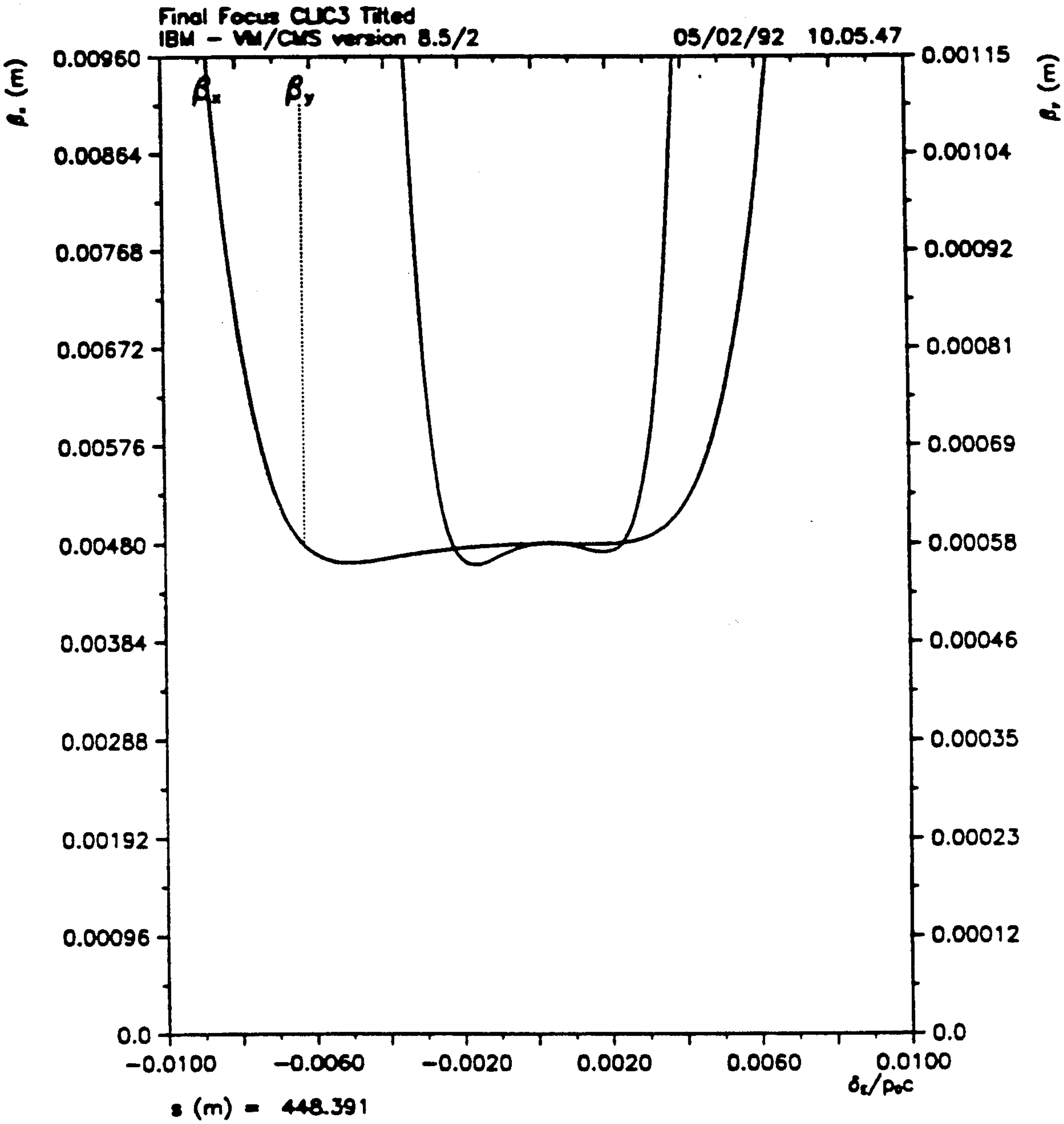

the bandwidths of the final focus system

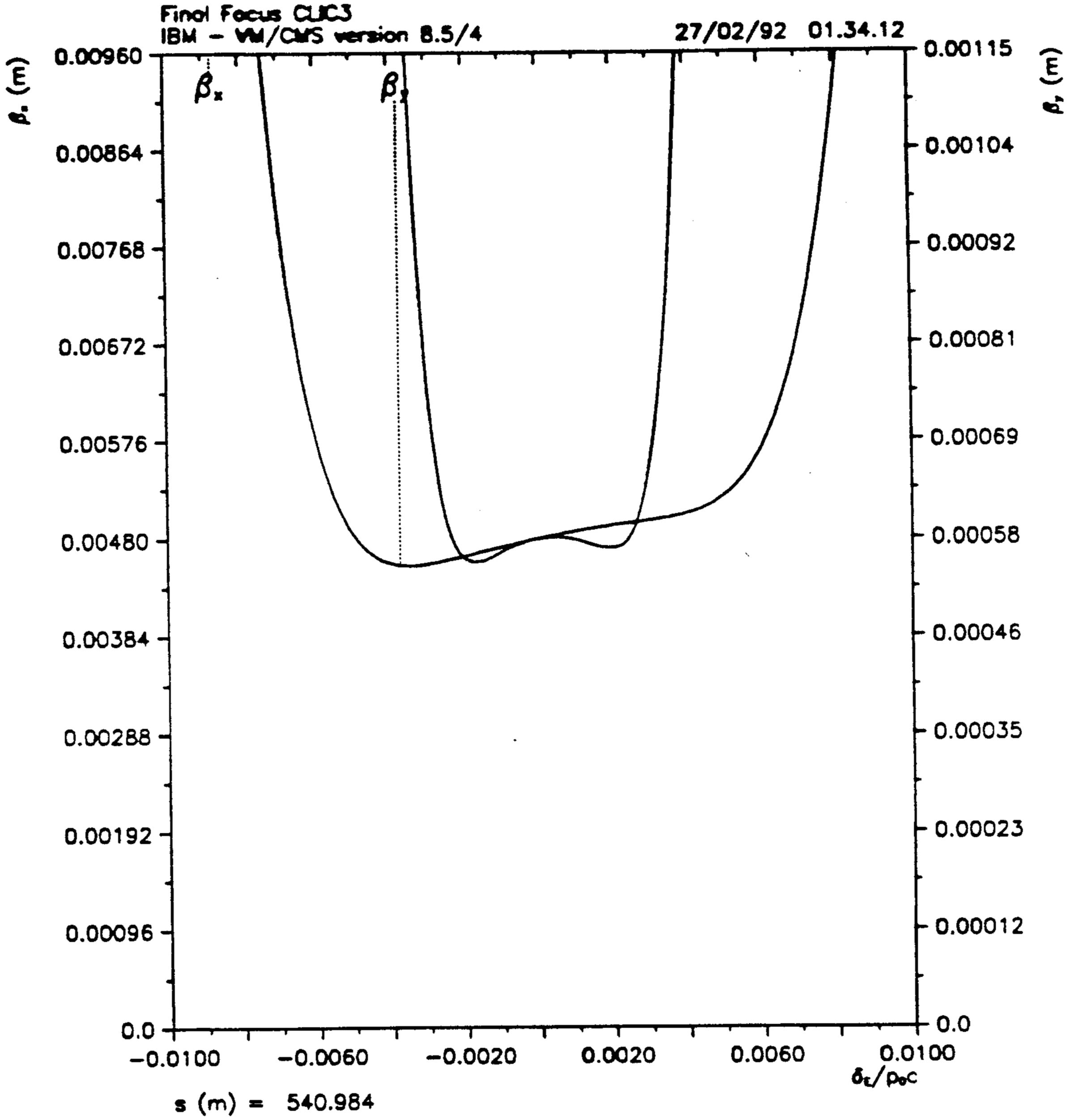

4) The matching section

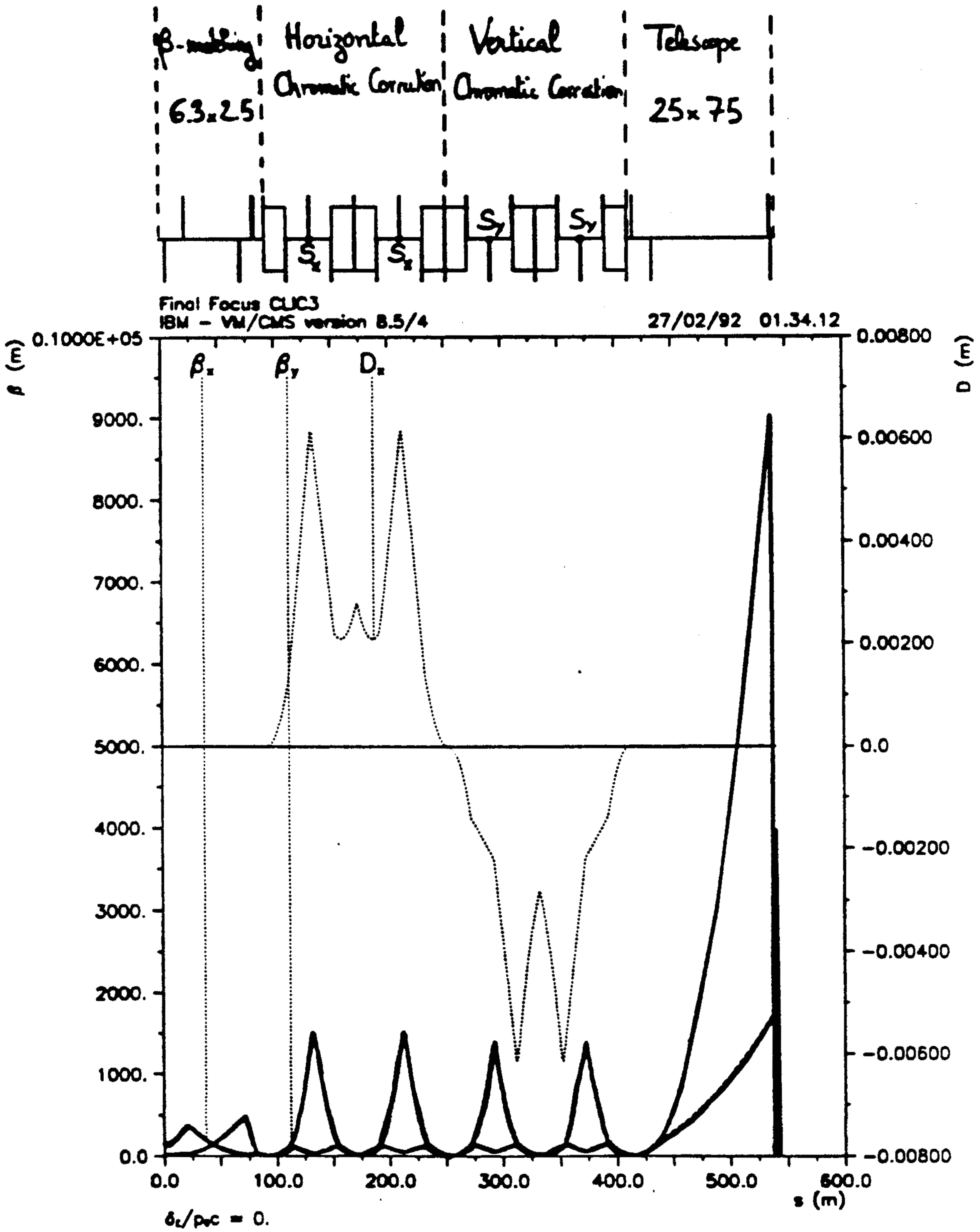

5) The residual aberrations

(K. Oide, J. Irwin, G. Roy, M.Sands ...(not me))

- **The long sextupoles**

$$\frac{\Delta\sigma_y^{*2}}{\sigma_y^{*2}} = \frac{5}{12}\, k_s^4\, l_s^2\, \beta_{y,s}^4\, \epsilon_y^2$$

with $k_s = K_2[\text{“utransport”}] \cdot l_s$

- **The synchrotron radiation in the dipoles (L, θ, ρ)**

  - effect of the energy loss

$$\frac{\Delta\sigma_y^{*2}}{\sigma_y^{*2}} = \frac{55}{24\sqrt{3}} r_e ƛ_e \xi_y^2 \gamma^5 \frac{\theta^3}{L^2} \cdot (N_1 + \frac{1}{4} N_2)$$

where

$N_1 =$ number of dipoles after the sextupole pair
$N_2 =$ number of dipoles in between the sextupole pair

  - effect of the emittance growth

The emittance is calculated from

$$\epsilon^2 = \langle x^2 \rangle \langle x'^2 \rangle - \langle xx' \rangle$$

with $\langle x^2 \rangle$ the sum in quadrature of all dipole contributions

$$\langle x^2 \rangle = \langle x^2 \rangle_0 + \sum_i \langle x^2 \rangle_i$$

$$\langle x'^2 \rangle = \langle x'^2 \rangle_0 + \sum_i \langle x'^2 \rangle_i$$

$$\langle xx' \rangle = \langle xx' \rangle_0 + \sum_i \langle xx' \rangle_i$$

The contribution of each dipole is given by

(G. Roy, M. Sands)

$$\begin{aligned}\langle x^2\rangle &= \frac{C_2E_0^5}{\rho^5}L\left[\frac{L^4R_{11}^2}{20}+\frac{L^3R_{11}R_{12}}{4}+\frac{L^2R_{12}^2}{3}+\frac{L^2R_{11}R_{16}\rho}{3}\right.\\ &\quad\left.+LR_{12}R_{16}\rho+R_{16}^2\rho^2\right]\\ \langle x'^2\rangle &= \frac{C_2E_0^5}{\rho^5}L\left[\frac{L^4R_{21}^2}{20}+\frac{L^3R_{21}R_{22}}{4}+\frac{L^2R_{22}^2}{3}+\frac{L^2R_{21}R_{26}\rho}{3}\right.\\ &\quad\left.+LR_{22}R_{26}\rho+R_{26}^2\rho^2\right]\\ \langle xx'\rangle &= \frac{C_2E_0^5}{\rho^5}L\left[\frac{L^4R_{11}R_{21}}{20}+\frac{L^3R_{12}R_{21}}{8}+\frac{L^3R_{11}R_{22}}{8}+\frac{L^2R_{12}R_{22}}{3}\right.\\ &\quad\left.+\frac{L^2R_{21}R_{16}\rho}{6}+\frac{LR_{22}R_{16}\rho}{2}+\frac{L^2R_{11}R_{26}\rho}{6}+\frac{LR_{12}R_{26}\rho}{2}+R_{16}R_{26}\rho^2\right]\end{aligned}$$

where R is the tranfer matrix from the exit of the dipole to the IP and

$$C_2=\frac{55}{24\sqrt{3}}\frac{r_e\hbar c}{(mc^2)^6}\simeq 4.13\times10^{-11}\mathrm{m}^2/\mathrm{GeV}^5$$

- **The synchrotron radiation in the last doublet** (*Oide* effect)

(K. Oide, J. Buon, K. Hirata)

$$\delta\sigma_y^{*2}=\frac{110}{3\sqrt{6\pi}}\,r_e\bar{\lambda}_eF_2\left(\frac{\gamma\epsilon_y}{\sigma_{0,y}^*}\right)^5+\frac{20}{3}\,r_e^2F_1^2\left(\frac{\gamma\epsilon_y}{\sigma_{0,y}^*}\right)^6$$

where the coefficients are given by the optics and by the program SOIL:

$$F_1=2.69\quad,\quad F_2=6.12\qquad\text{for CLIC}$$

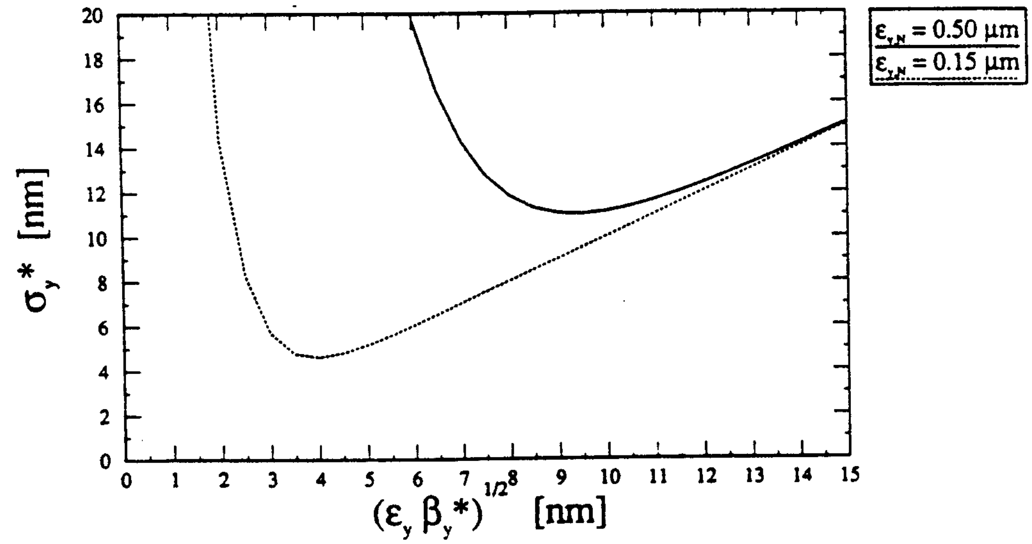

- **The badly placed quadrupoles**

(K. Oide)

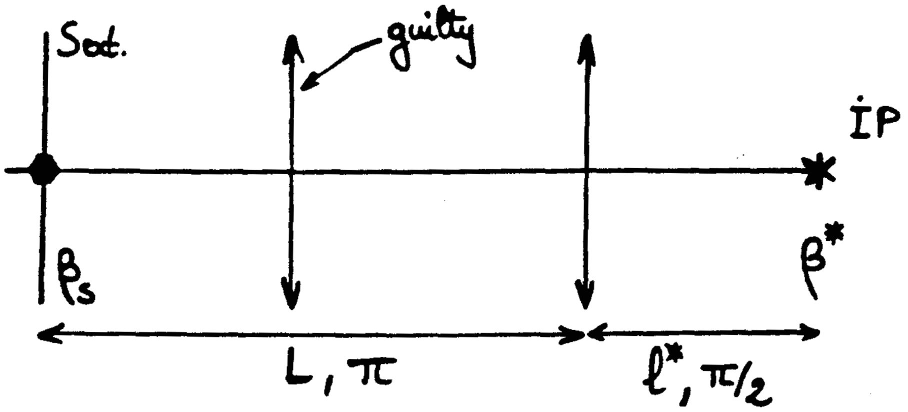

The quadrupoles which are not at a $N\pi$ phase-advance from the sextupoles (essentially the first doublet or the first quadrupoles of the telescope) generate sixth order aberrations and limit the bandwidth:

$$\frac{\Delta\sigma_y^{*2}}{\sigma_y^{*2}} = \xi_y \frac{\beta^* L^2}{\beta_S l^{*2}} \delta^6$$

where L is the distance between the sextupole pair and the final doublet.

⟹ the energy acceptance is determined by the horizontal bandwidth *(except for very flat beams)* since the CCS-V is closer to the final doublet than the CCS-H.

⟹ long telescopes are not good

⟹ increasing the bandwidth requires correcting the chromaticity of the badly placed quadrupoles, by using more sextupoles

→ final focus system with large momentum bandwidth

(R. Brinkmann, A. Sery)

Parm's "A"

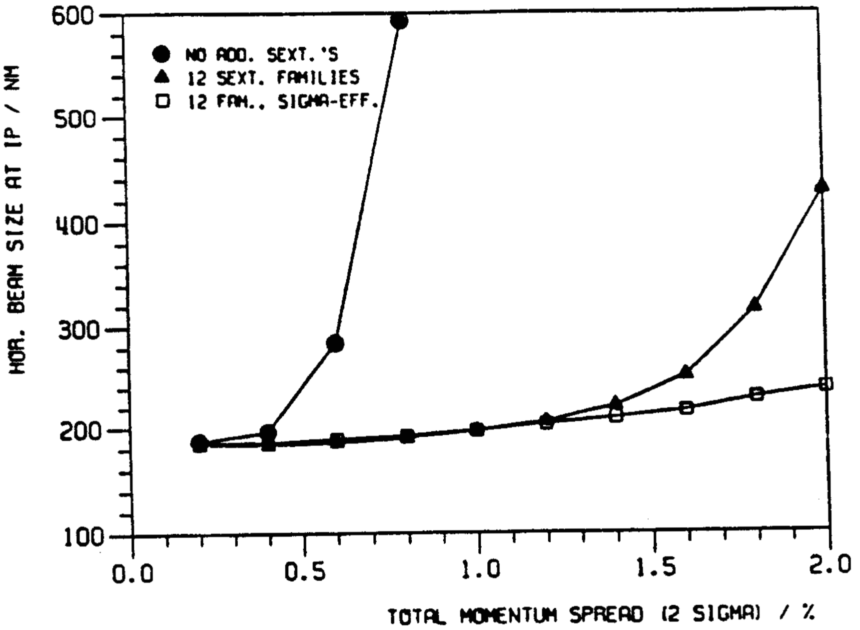

TRACKING RESULTS FOR SYSTEM FF1D WITH DX/Z=-3/.3 MM, 250 GEV
4000 PARTICLES, EPSX=1E-11, EPSY=1E-13

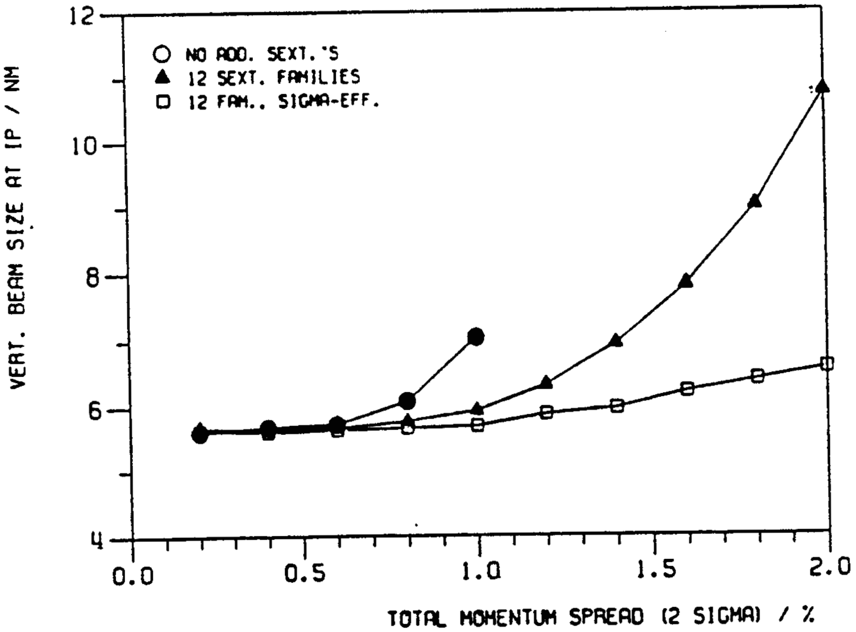

TRACKING RESULTS FOR SYSTEM FF1D WITH DX/Z=-3/.3 MM, 250 GEV
4000 PARTICLES, EPSX=1E-11, EPSY=1E-13

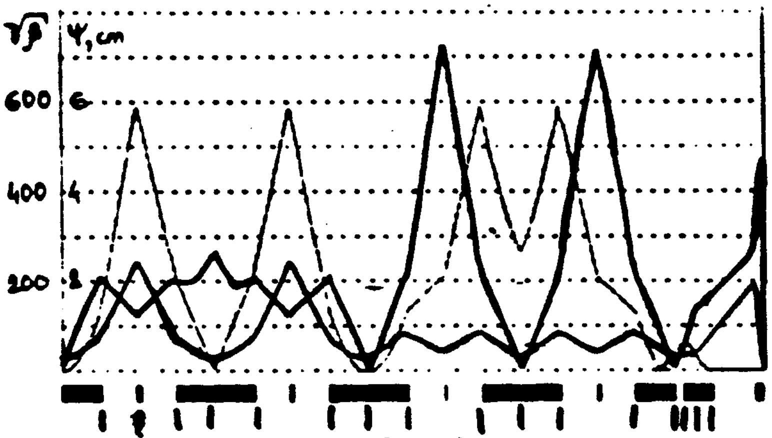

$\beta^* = 10/0.1$ cm

Add sextup. like in

* R. Brinkmann „Optimization of Final Focus System for Large Momentum Bandwidth", DESY M90-14, November 1990.

1TeV version

$B_{magnet} =$

No profit of Sadd on 1TeV confirmed (↗ ~0.1%)

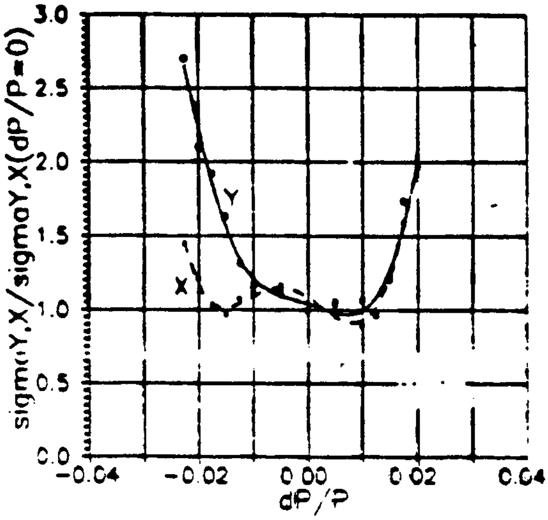

without additional sextupoles

±1.3%

$2 \cdot 10^{-4}/10^{-7}$ cm

250GeV version

$B_{magnet} \cong 0.55$ kG

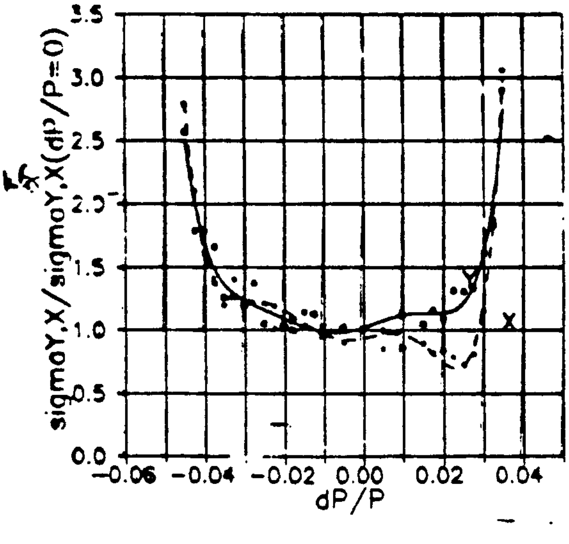

with additional sextupoles

±3%

optimized by tracking

- **Lie algebra techniques seem to provide the only *systematic* method to understand and trace the high order aberrations**

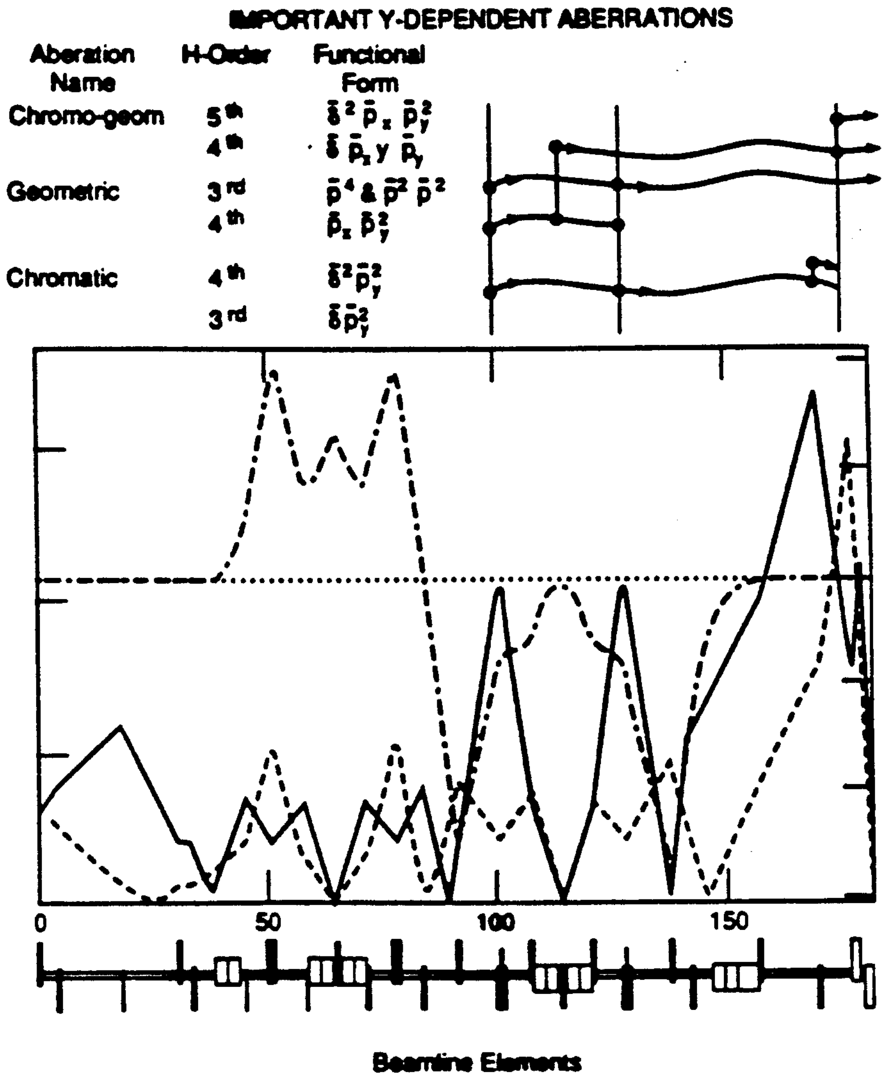

(**FFTB**, *J. Irwin*)

- **Questions to the experts:**

1. are these aberration expressions valid in both planes ?
2. how does one produce $\lambdabar_e$ in TeX?

III) The Imperfect Machine

Generalities

- Fast varying errors *(jitter)* cannot be corrected

⟶ set of tolerance limits

- Slowly varying errors must be pre-corrected and corrected

⟶ pre-alignment and tuning techniques

⟶ correction algorithm during operation

- The alignment and stability of the 2 final doublets is a special problem

δy misalignment of one doublet with respect to the other

$\Longrightarrow \delta y^* = \delta y$ offset of e^+ beam with respect to e^- beam

⟶ put the 2 doublets on the same beam to achieve $\delta y \ll \sigma_y^*$

- Much to be learnt from FFTB preparation and operation

1) Jitter tolerances

- The problem is to derive tolerances to achieve the golden criterion

$$|\frac{\delta\mathcal{L}}{\mathcal{L}_0}| < X\,\%$$

with X user supplied, depending on the efficiency of the beam-beam attraction.

- Two approaches:

1. **the analytic method** provides insight on the influence of a given type of error *(misalignment, roll, field...)* for each individual element.

For example:

$$\Delta y_Q < \frac{X}{g\ \sin\mu}\sqrt{\frac{\epsilon}{\beta_y}}$$

for vertical misalignment of a quadrupole of strength g and phase difference μ from the IP.

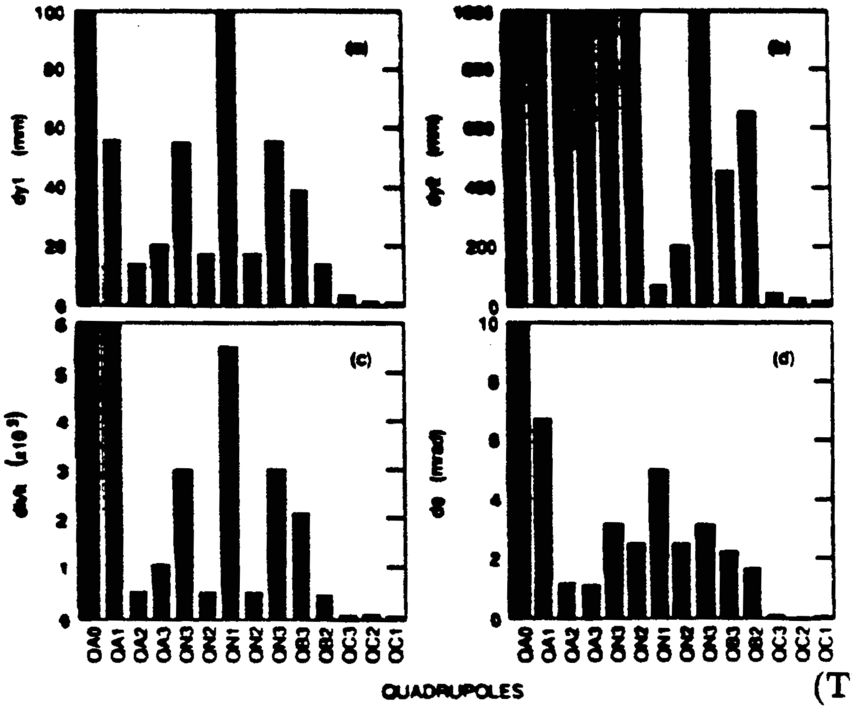

(TLC, *Oide*)

	NLC		JLC	
	H	V	H	V
CCX	3.1 μ	0.9 μ	1.0 μ	0.3 μ
CCY	0.5 μ	0.3 μ	0.1 μ	0.04 μ

Tolerances for the quadrupoles inside the CCS derived from their influence on the following sextupole:

$$\Delta y_S = g\, R^{34}_{Q \to S}\, \Delta y_Q$$

and

$$\Delta y_S < \frac{X}{g_S \sqrt{\beta_{x,S}\beta_{y,S}}} \sqrt{\frac{\epsilon_y}{\epsilon_x}}$$

(J. Irwin, G. Roy)

2. the tracking method with random errors in the line allows to study the effect of accumulation of small errors.

	SIZE-TOLERANCE LIMIT $\Delta X, Z_{rms}$ /μm		
MAGNETS	PARM'S "A"	PARM'S "B"	NLC-Like
ALL QUADS (except fin. Doubl.)	.15	.60	.25
MAIN SEXT.	2.5	10	3
ADD. SEXT.	8	40	–

Tolerances for $X = 1/2$ and $\delta E/E = \pm 1.5$ %
(S-band, *R. Brinkmann*)

A medium way

- Assume that the effect of errors is well accounted for by the zeroth order (*"closed orbit"*) and linear (*transfer matrix*) parts of the map $\mathcal{M}$ from the linac exit to the IP.
- Compute the luminosity (*integrated over one collision*) $\bar{\mathcal{L}}$ in terms of $(\rho_0, \mathcal{M})^+$ of the e$^+$ beam and $(\rho_0, \mathcal{M})^-$ of the e$^-$ beam, where

  $$\rho_0(\mathbf{X}) = \frac{\det^{1/2}\mathbf{S}}{(2\pi)^3} \exp\left[-\frac{1}{2}(\mathbf{X}-\mathbf{X}_0)^T \cdot \mathbf{S} \cdot (\mathbf{X}-\mathbf{X}_0)\right]$$

  is the "Gaussian distribution" of the beam at the entrance of the final focus line,

  $$\mathbf{X} = \begin{pmatrix} x \\ x' \\ y \\ y' \\ z \\ \delta \end{pmatrix} \quad \text{and} \quad \mathbf{X}_0 = \begin{pmatrix} x_0 \\ x'_0 \\ y_0 \\ y'_0 \\ z_0 \\ \delta_0(z) \end{pmatrix} \quad \text{is the offset at entrance,}$$

  and S is the 6 × 6 coupled beam matrix.

  $\delta_0(z)$ is given by

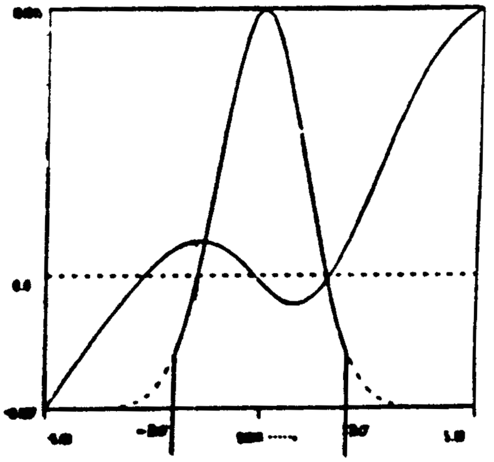

  The transfer map is approximated by

  $$\mathcal{M}(\mathbf{X}) \equiv \mathbf{X}^* \simeq \delta\mathbf{X}^* + \mathbf{R}\cdot\mathbf{X}$$

- Under the assumption that z is not coupled to the other coordinates in the matrices $\mathbf{S}$ and $\mathbf{R}$, one gets

$$\mathcal{L} = \frac{N_1\, N_2}{(2\pi)^2\, \sigma_z^+\, \sigma_z^-} \int c\, dt\, dz^+ dz^- \delta(z^+ + z^- + 2ct + z_0^+ + z_0^-)$$

$$\exp\left(\frac{-z^2}{2\sigma_z^2}\right)^+ \exp\left(\frac{-z^2}{2\sigma_z^2}\right)^- \exp\left[-\frac{1}{2}\Lambda^{\mathrm{T}}(z,t)\cdot \mathbf{A}^{-1}(t)\cdot \Lambda(z,t)\right] / \det{}^{1/2}\mathbf{A}(t)$$

where $\mathbf{A}(t)$ is the 2-dimensional square matrix

$$\mathbf{A}(t) = \mathbf{P}_{xy}\cdot \mathbf{T}_t \cdot [(\mathbf{R}\cdot \mathbf{S}^{-1}\cdot \mathbf{R}^{\mathrm{T}})^+ + (\mathbf{R}\cdot \mathbf{S}^{-1}\cdot \mathbf{R}^{\mathrm{T}})^-]\cdot \mathbf{T}_t^{\mathrm{T}}\cdot \mathbf{P}_{xy}$$

and $\Lambda(z,t)$ is the 2-dimensional vector

$$\Lambda(z,t) = \mathbf{P}_{xy}\cdot \mathbf{T}_t\, [(\mathbf{R}\cdot \mathbf{X}_0(z) + \delta\mathbf{X}^*)^+ - (\mathbf{R}\cdot \mathbf{X}_0(z) + \delta\mathbf{X}^*)^-]$$

$\mathbf{P}_{xy}$ is the projection operator on the xy-plane and $\mathbf{T}_t$ is the time translation operator.

The 2d-integral is straightforward (*for a computer*) since the integrand is exponentially decreasing for large z and ct.

- The Gaussian longitudinal distribution can be replaced by any more realistic one. Is there any ?

2) Alignment tolerances

- **Alignment algorithms have been studied in more or less details.**

1. **the most detailed one from the FFTB collaboration:**

(F. Bulos, D. Burke, R. Helm, J. Irwin, A. Odian,
G. Roy, R. Ruth, N. Yamamoto)

- mechanical pre-alignement → 100 μm *(stretched wires)*
- beam-based alignement → 10 μm and tuning *(orbit bumps)*
- global correctors

(signal from beam size monitor, beamstrahlung, ...)

NLC Tolerances

Time Scale	Generator (IP coord.)	Final Quadrupoles	Other Quadrupoles		Sextupoles	Dipoles
			Worst	RMS		
τ_0		Δx	or	Δy	n/a	n/a
	x' y'	0.06 μ 3 nm	0.32 μ 53 nm	0.24 μ 20 nm		
τ_1		Δx	or	Δy	n/a	n/a
	$x'\delta$ $y'\delta$	34 μ 268 nm	1.7 μ 71 nm	1.0 μ 47 nm		
τ_2		$\Delta k/k$	or	$\Delta\theta$	Δx or Δy	$\Delta B/B$ or $\Delta\phi$
	x'^2 y'^2 $x'y'$	4.7 10^{-4} 1.9 10^{-5} 11.3 μrad	4.5 10^{-3} 2.9 10^{-4} 129 μrad	6.2 10^{-3} 1.3 10^{-4} 80 μrad	0.30 μ 0.68 μ	1.6 10^{-5} 37 μrad
τ_3			k_s		$\Delta k/k$ or $\Delta\theta$	n/a
	$x'^2\delta, y'^2\delta$ $x'y'\delta$ $x'^3, x'y'^2$ y'^3, x'^2y'	 1.4 m^{-2} 0.40 m^{-2}	0.69 m^{-2} 1.27 m^{-2} 0.75 m^{-2} 0.50 m^{-2}	0.33 m^{-2} 0.38 m^{-2} 0.37 m^{-2} 0.23 m^{-2}	1.4 10^{-3} 15 mrad 1.6 10^{-3} 2.4 mrad	

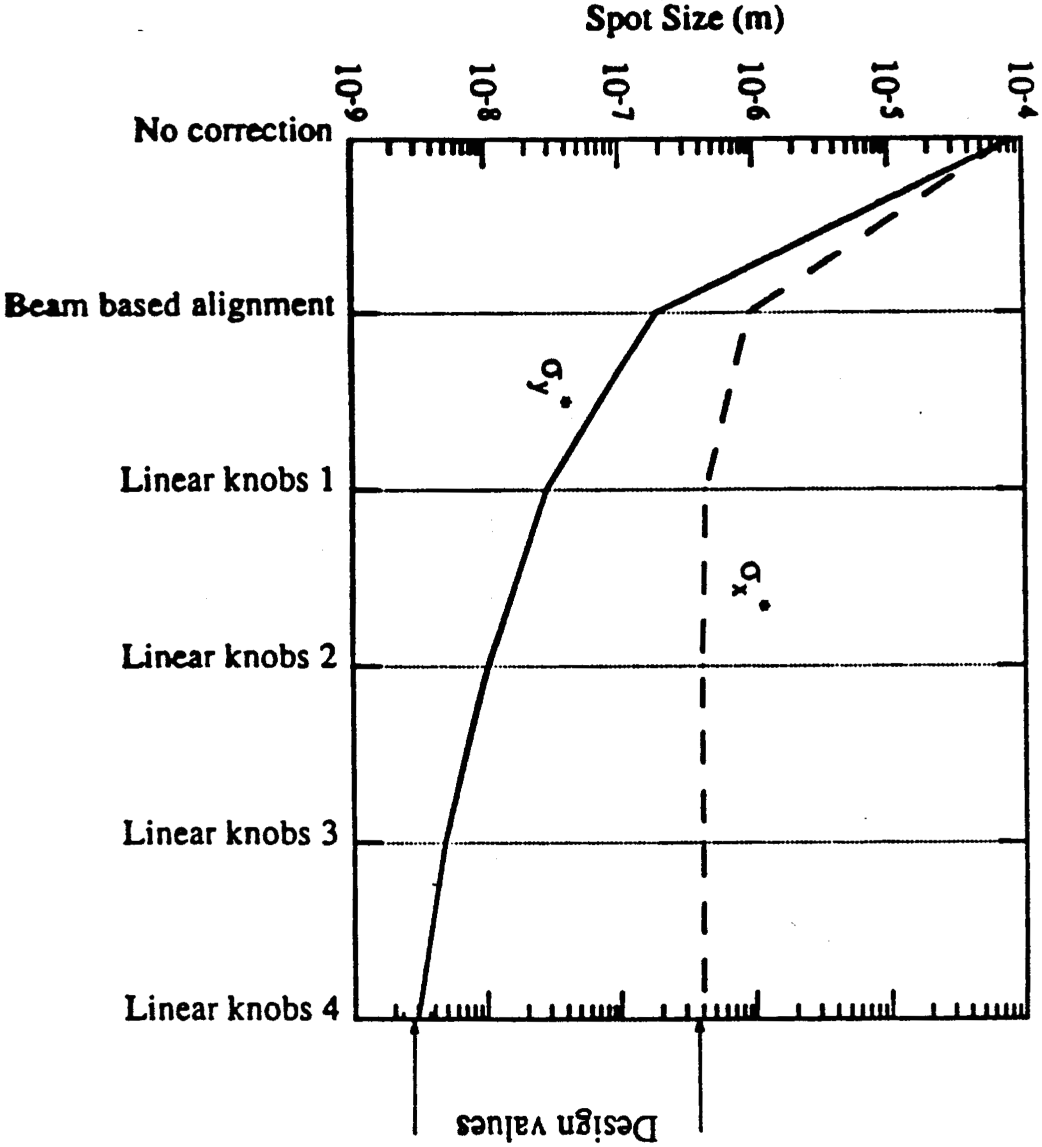
Spot Size (m)
10-9
10-8
10-7
10-6
10-5
10-4
No correction
Beam based alignment
Linear knobs 1
Linear knobs 2
Linear knobs 3
Linear knobs 4
σy*
σx*
Design values

(NLC, K.Oide)

CLIC LUMINOSITY vs TRANSVERSE OFFSET)

(T. Fieguth, B. Zotter)

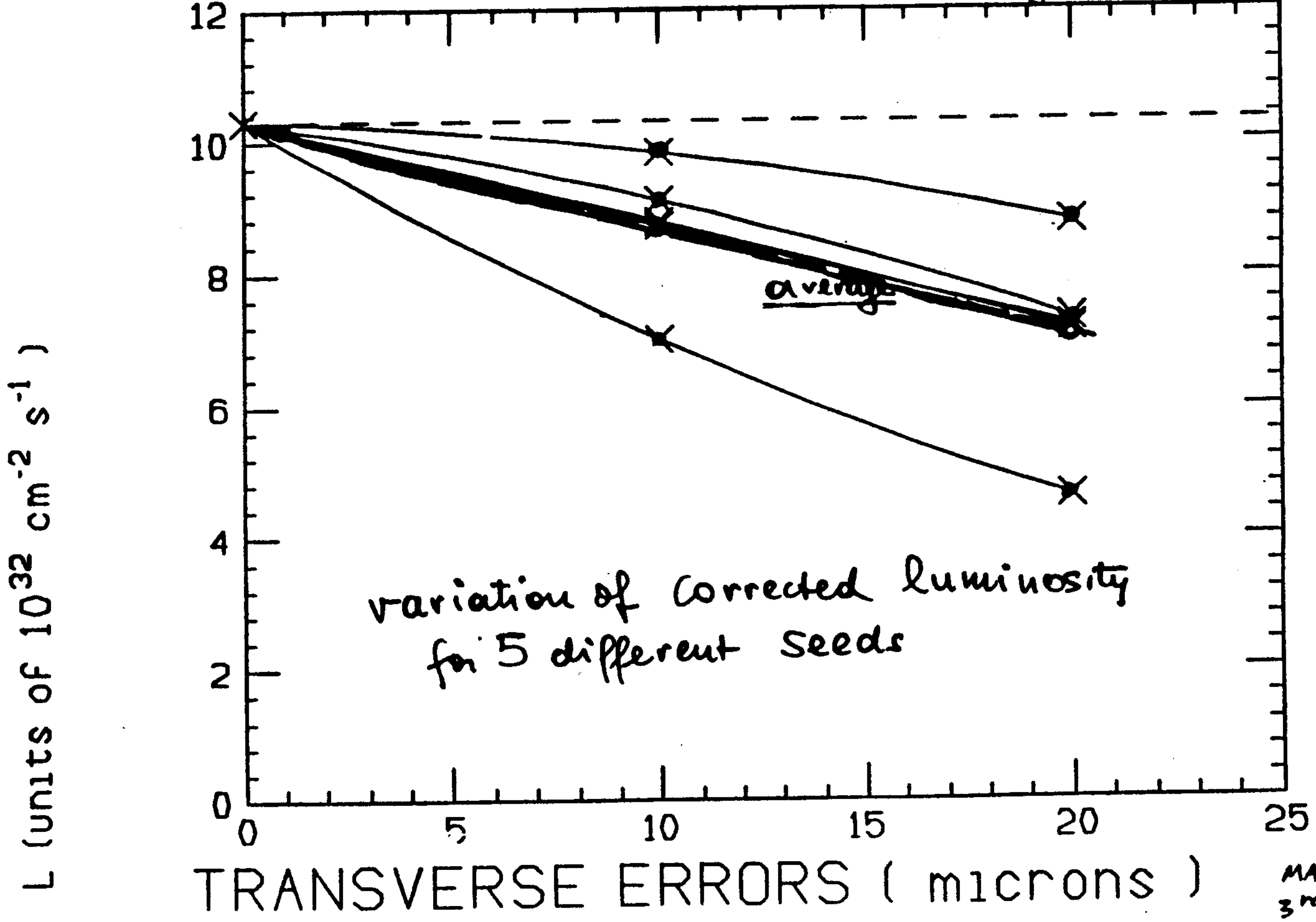

MAGNETS ALL SP.
3rd ORDER

STEERING + 7 optics correcti
1st ORDER

OTHER ERRORS: ±100 μrad roll
$\pm 10^{-4}$ field error

3) Wake field effects

- *Yokoya* observed that the resistive-wall wake fields are strong in the last quadrupoles because of the small aperture radius a.

  - the longitudinal effect is negligible:

$$\frac{\sigma_E}{E} \simeq 2.83 \times 10^{-5} \cdot \frac{N[10^{10}]\ \rho[\rho_{Cu}]^{1/2}\ l_Q[\mathrm{m}]}{\mathrm{a[mm]}\ \sigma_s[\mu\mathrm{m}]^{3/2}\ \mathrm{E[TeV]}}$$

  - the transverse effect is defocusing and s-dependent. On average, the defocusing focal length is:

$$f_Q[\mathrm{m}] \simeq 6.4 \times 10^3 \cdot \frac{\mathrm{a[mm]}^3\ \sigma_s[\mu\mathrm{m}]^{1/2}\ \mathrm{E[TeV]}}{\mathrm{N}[10^{10}]\ \rho[\rho_{\mathrm{Cu}}]^{1/2}\ \mathrm{l_Q[m]}}$$

Therefore

$$f_Q \gg f^*$$

But a beam offset in the last quadrupole induces, via the transverse wake, an offset at the IP

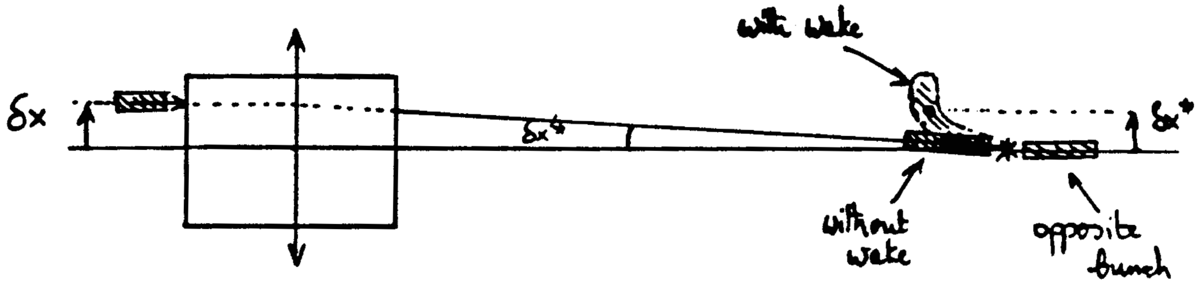

- Simplest approximation

$$\begin{pmatrix} \delta y^* \\ \delta y'^* \end{pmatrix} = \begin{pmatrix} 1 & f^* \\ 0 & 1 \end{pmatrix} \begin{pmatrix} 1 & 0 \\ -\frac{1}{f^*} + \frac{1}{f_Q} & 1 \end{pmatrix} \begin{pmatrix} \delta y \\ 0 \end{pmatrix} = \begin{pmatrix} \delta y \frac{f^*}{f_Q} \\ -\frac{\delta y}{f^*}(1 - \frac{f^*}{f_Q}) \end{pmatrix}$$

and

$$|\frac{\delta \mathcal{L}}{\mathcal{L}_0}| \simeq \frac{1}{8}\left(\frac{\delta y'^* \sigma_s}{\sigma_y^*}\right)^2 + \frac{1}{4}\left(\frac{\delta y^*}{\sigma_y^*}\right)^2$$

- Using *Yokoya*'s notations

$$\left|\frac{\delta\mathcal{L}}{\mathcal{L}_0}\right| = \frac{1}{8}\left(\frac{\delta y'^{*}\sigma_s}{\sigma_y^*}\right)^2\left(1+\frac{\Delta^2}{2}\right)$$

with the effect of the transverse wake fields contained in

$$\Delta = \frac{2.56\ Ne^2c\,l_Q f^{*2}}{\pi^2 a^3 \sigma_s^{3/2} E}\sqrt{\frac{Z_0}{\sigma}} = 1.85\,\frac{\beta_y^*}{\sigma_s}\,\Delta_{Yokoya}$$

- In practical units

$$\Delta = .304\,\frac{l_Q[\mathrm{m}]\ \mathrm{f}^*[\mathrm{m}]^2\ \mathrm{N}[10^{10}]\ \rho[\rho_{\mathrm{Cu}}]^{1/2}}{\mathrm{a}[\mathrm{mm}]^3\ \sigma_s[100\mu\mathrm{m}]^{3/2}\ \mathrm{E}[\mathrm{TeV}]}$$

It is not a small number for $a = .5$ mm.

- Questions:

1. where is the discrepancy ?
2. how big is the horizontal effect ?
3. if $a = .5$mm is really necessary, can the beam tube contain the last doublet ?
   In that case, one has to take the geometrical wake into account:

   $$k_\perp \simeq 16./a[\mathrm{mm}]\quad \mathrm{kV/pC.m}\quad \mathrm{for}\quad \sigma_s = 170\ \mu\mathrm{m}$$

   to be compared with the resistive loss factor

   $$k_\perp \simeq 7.6\ l_Q[\mathrm{m}]/\mathrm{a}[\mathrm{mm}]^3\quad \mathrm{kV/pC.m}$$

IV) The Interaction Region

(SLC final focus, FFTB collaboration)

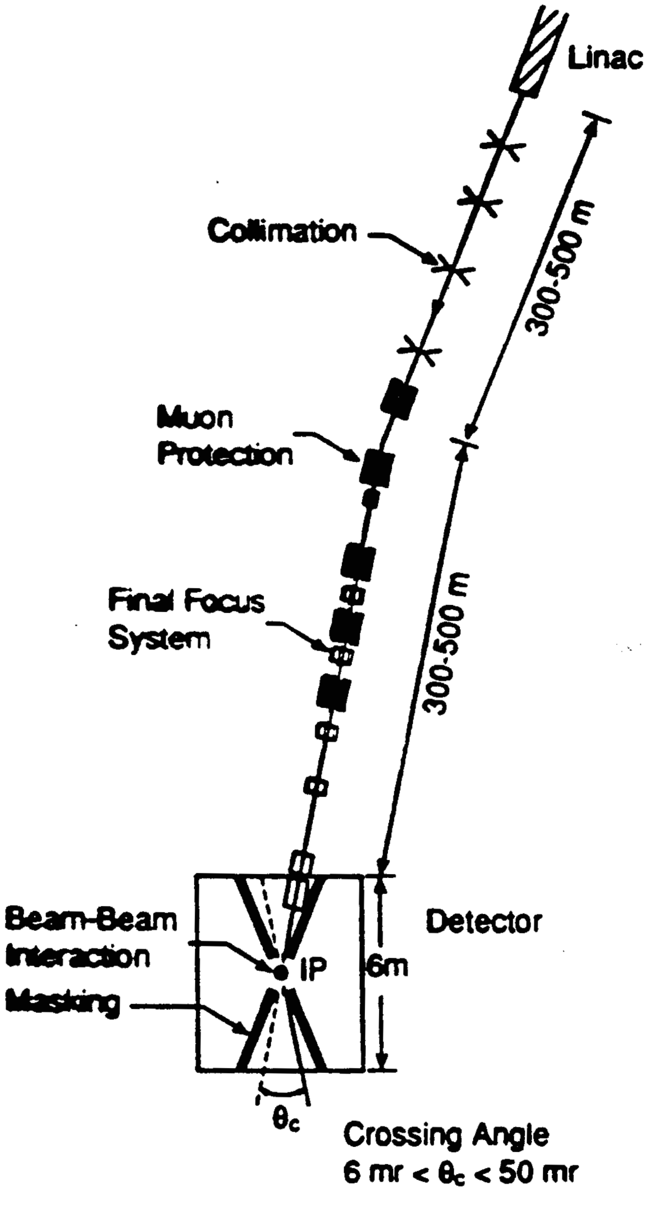

Fig. 1. End of linac to interaction point in the Next Linear Collider.

1) The crossing angle

(P. Chen, K. Yokoya, L. Wood,...)

- **The linear beam-beam effect predicts a disrupted round beam**

$$\sigma_{x,y}(s) = \theta_0 \cdot s$$

with the characteristic disruption angle

$$\theta_0 = \frac{D_{x,y}\sigma^*_{x,y}}{\sigma_s} \quad \text{for} \quad D \gg \sigma_s/\beta^*$$

for example:

$$\theta_0 = 0.24 \text{ mrad} \quad \text{and} \quad \sigma^*_r = 300\ \mu\text{m} \quad \text{for CLIC @ 1 TeV}$$

- The beam-beam simulation predicts

$$\theta_y < \theta_x < \theta_0 \quad \text{for} \quad D_y \gg 1$$

for example:

$$\begin{cases} \theta_x = 0.14 \text{ mrad} \\ \theta_y = 0.10 \text{ mrad} \end{cases} \quad \text{and} \quad \begin{cases} \sigma_x(l^*) = 170\ \mu\text{m} \\ \sigma_y(l^*) = 120\ \mu\text{m} \end{cases} \quad \begin{matrix} \text{for CLIC @ 1 TeV} \\ (D_y = 3.4) \end{matrix}$$

safe choice : x-angle $\alpha > 3a/l^*$

(cf. quadrupole design)

but

$$\frac{\delta\mathcal{L}}{\mathcal{L}_0} = \left[1 + \left(\frac{\sigma_s}{\sigma_x}\tan\frac{\alpha}{2}\right)\right]^{-1/2} \simeq -\frac{1}{8}\left(\frac{\alpha\sigma_s}{\sigma^*_x}\right)^2$$

2) Collimation

(N. Merminga, J. Irwin, R. Helm, R. Ruth)

- Collimators are necessary to scrape the transverse and low-energy tails of the beam distribution.

- Geometric and resistive wake fields preclude step and tapered scrapers in the vertical plane in a linear lattice, i.e. with $\sigma_y = \sqrt{\beta_y \epsilon_y}$.

- Introduce a skew-sextupole at maximum β_y to blow up vertical beam size + a mirror element to cancel the aberrations.

- Energy collimation is done by introducing horizontal dispersion.

- Total length of the collimation section $\simeq$ 500 m.

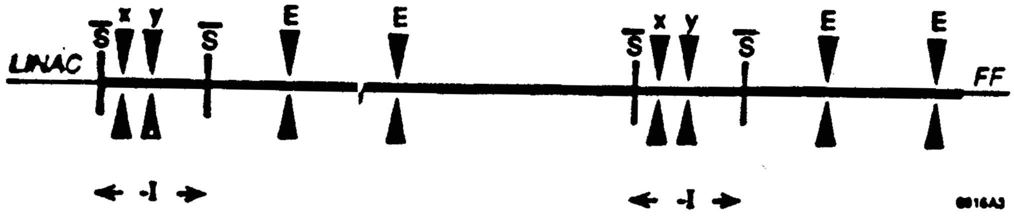

Schematic representation of the collimation systems in the NLC, located between the linac and final focus (FF). $\bar{S}$ stands for skew sextupole; x, y, E stand for horizontal, vertical and energy scraper, respectively.

- Check wake fields at sextupoles and scrapers	OK
- Check long sextupole aberrations	OK
- Check stability tolerances on sextupole and scraper offsets	OK
- Check protection of scrapers against lost beams	OK

- Non-linear collimation schemes with octupoles or decapoles induce too strong aberrations.

3) Muon protection

(L.P. Keller)

The number of muons $\mu^{\pm}$ reaching the detector per electron hitting the scapers is too large, even with an optimized configuration of toroid spoilers:

$$(N_e \text{ in scrapers})/N_e < 3.6 \times 10^7/N_e \quad \text{for} \quad N_\mu < 1$$

when ~ 10% expected.

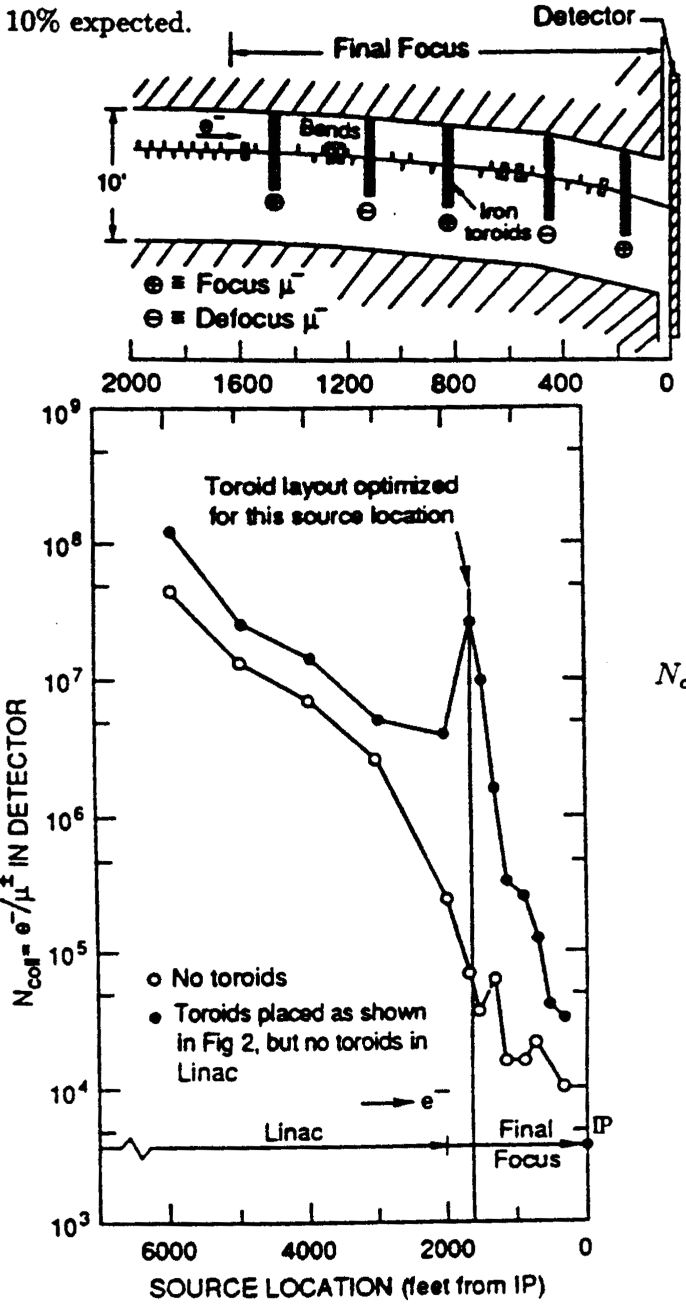

$N_{coll} = 3.6 \times 10^7$

Recommandation from previous study: increase total bend

⟶ **Big Bend design**

(R. Helm, J. Irwin)

between collimators and final focus section

$B_0 = 125$ Gauss @ 750 GeV

realized with off-centered quadrupoles of a FODO lattice

$L = 200$ m

$\alpha = 10$ mrad

⟶ **muon attenuation** $N_{cell}^{-1} < 10^{-9}$

⟶ **emittance growth** $\delta\epsilon_x/\epsilon_x = 0.04$

4) The solenoid

(SLC final focus, K. Oide)

- *Oide* considered detector solenoid with

$$B_0 = 3 \text{ T } @ \ 750 \text{ GeV}$$

$$l_S = 0.95 \text{ m} \quad \text{half length}$$

$$\alpha = 10 \text{ mrad} \quad \text{crossing angle}$$

⟶ coupling coefficients $< 10^{-3}$

$\Longrightarrow$ **no compensation is necessary**

⟶ synchrotron radiation is negligible

LINEAR COLLIDER FINAL FOCUS AND INTERACTION REGION HARDWARE

M. Ross
March 3, 1992

Impact on upstream systems

Take most technically complex final focus systems and look upstream for (partial) solutions

Use of SLC for test and development

Outline:

- Tuning methodology and related instrumentation and controls issues
- Mechanical systems
- Instrumentation
  - Position Monitors
  - Profile Monitors
  - Background / Loss Monitors
- Timing and Synchronization systems
- Protection systems

Comments on 'Long pulse' vs 'Short Pulse'
(DESY/TESLA) (J/NLC)

Tuning

Process that increases tolerances by feat <--

(Much harder to develop and verify specified performance)

Must address incoming beam conditions and data acquisition

Must not rely on global tuning except when absolutely necessary because of sensitivity to upstream systems

Even though tuning procedures are heavily used at SLC much more remains to be understood about their effectiveness.

What are the τ 's?

Proposal: Use synchronous detection techniques to provide 'continuous tuning' and remove errors introduced by changing upstream conditions

For example: use continuous 'sub-tolerance' stimulation and synchronized detection

SLC

Beam-Beam Deflections

—one beam has a tail—

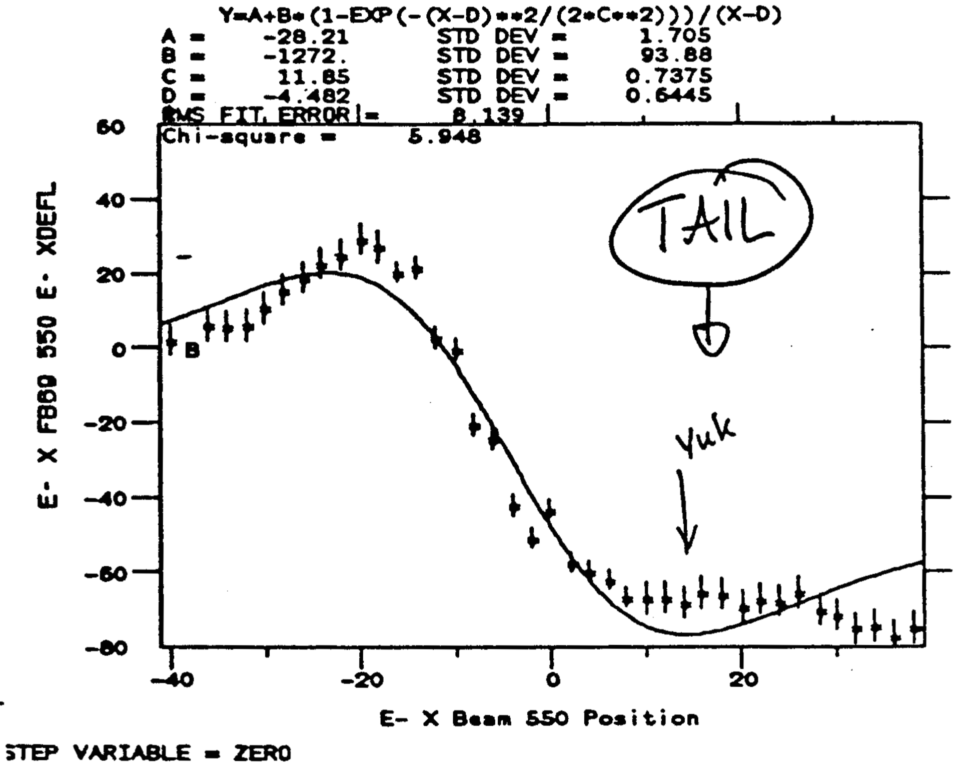

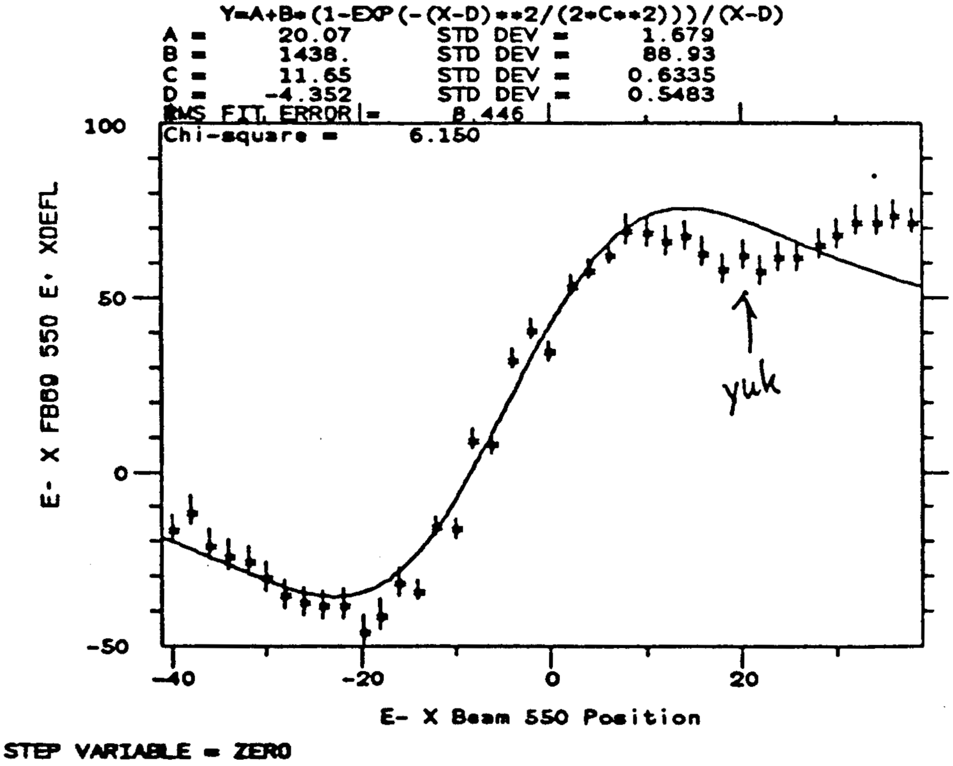

Impact:

Device controllers must have 'AC' as well as 'DC' characteristics; e.g. pulse to pulse current or pulse to pulse position control and sensing

Device tolerances reduced

Data acquisition must be synchronized; simple signal multiplexing not useful

Data taking should be done at full rate to reduce statistical error, large data bandwidth required

Single pulse beam size monitor is required to characterize phase space volume and orientation so that this can be done with more than just BPM's

Tests at SLC:

Damping Ring Extraction Kicker control

Final focus dispersion / energy sensitivity

Extraction Kicker Timing Correlation

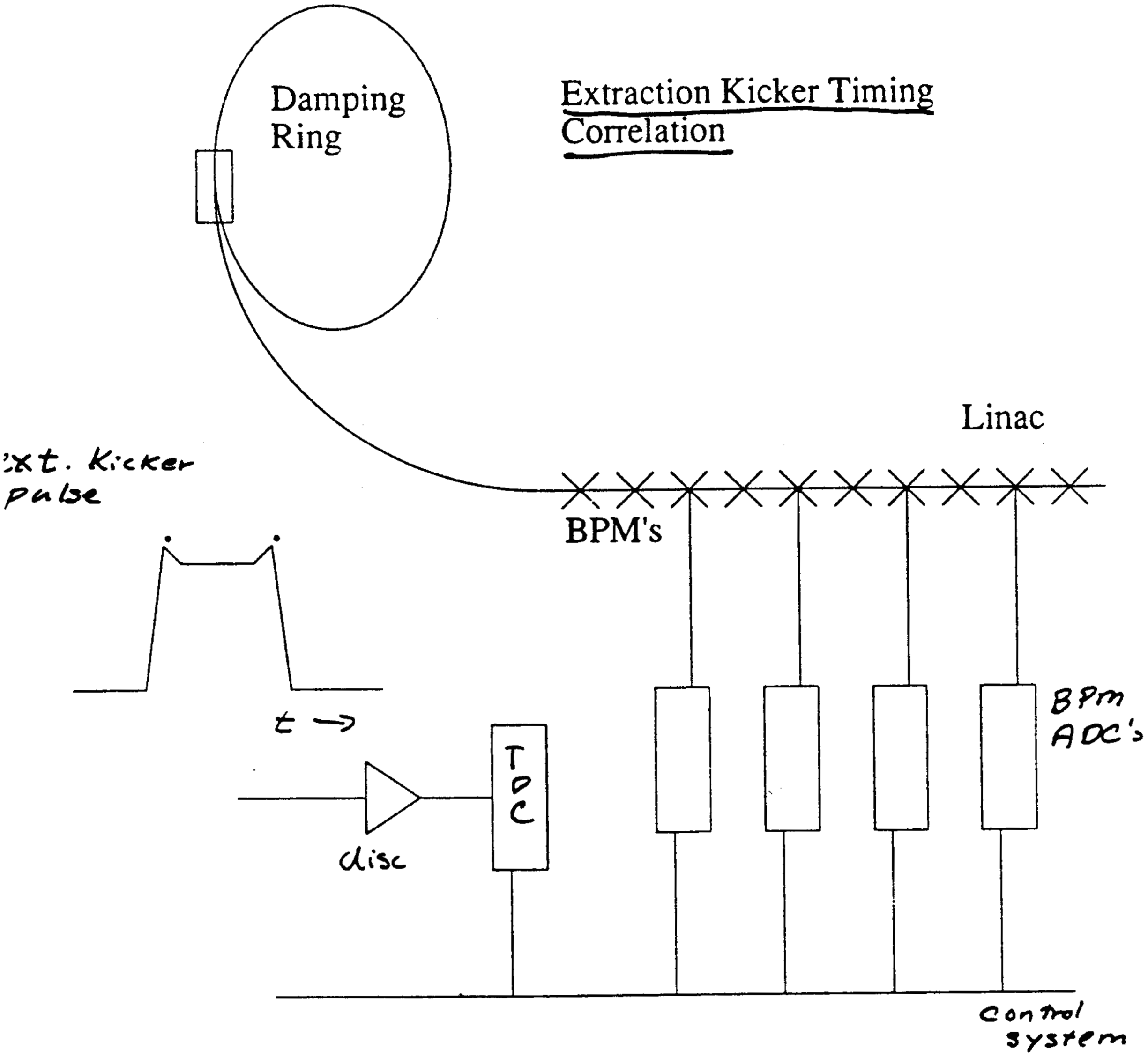

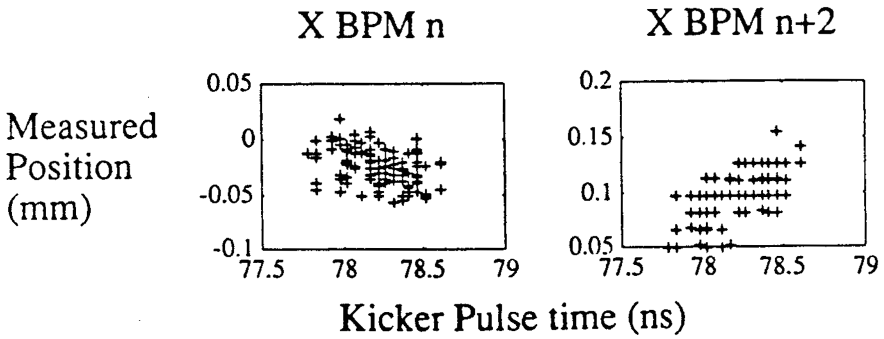

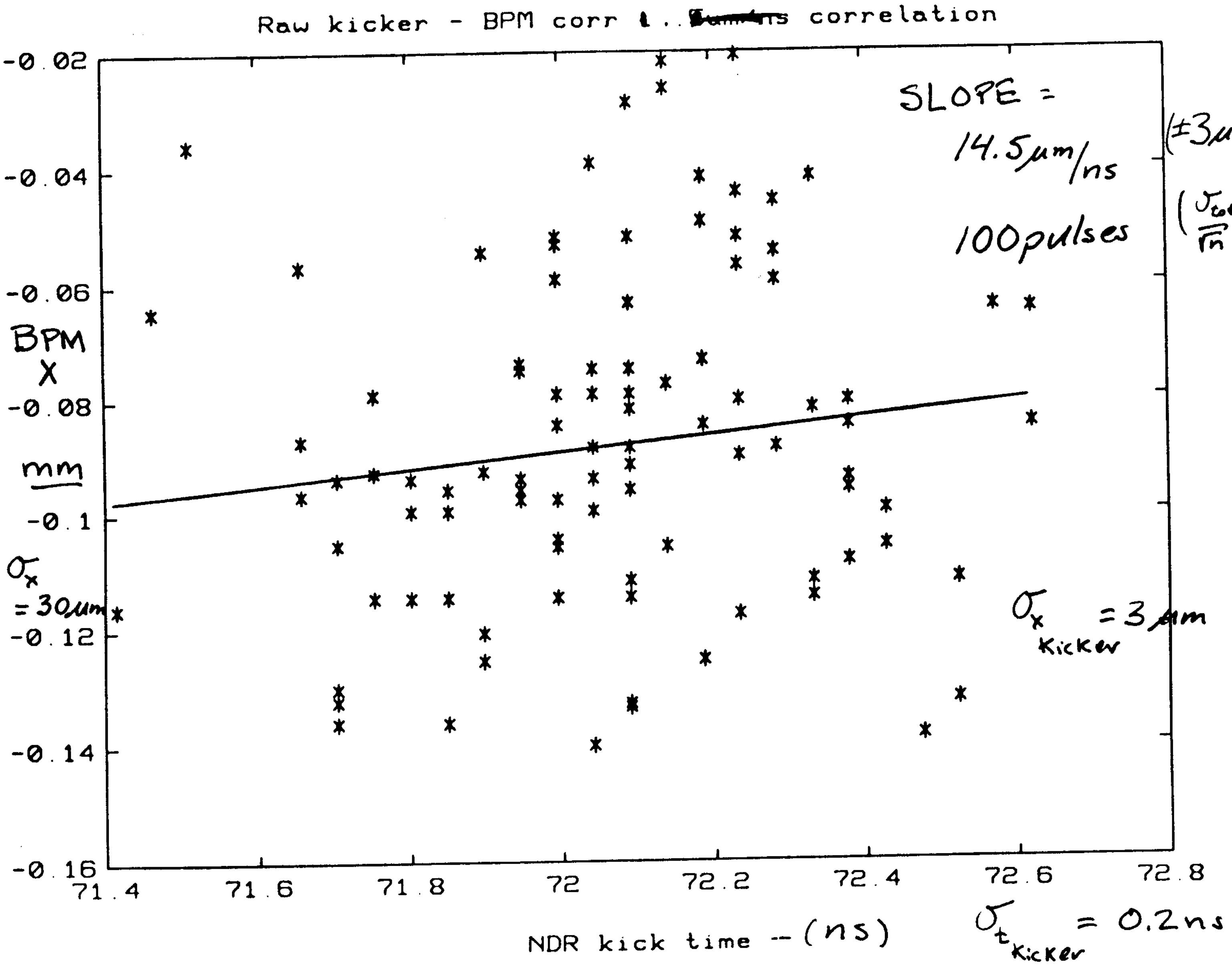
Raw kicker - BPM corr ~~1..5um/ns~~ correlation
SLOPE =
14.5µm/ns
(±3µm/ns,
(σcor/√n)
100pulses
BPM
X
mm
σx
= 30µm
σx Kicker = 3µm
σt Kicker = 0.2ns
NDR kick time -- (ns)
-0.02
-0.04
-0.06
-0.08
-0.1
-0.12
-0.14
-0.16
71.4
71.6
71.8
72
72.2
72.4
72.6
72.8

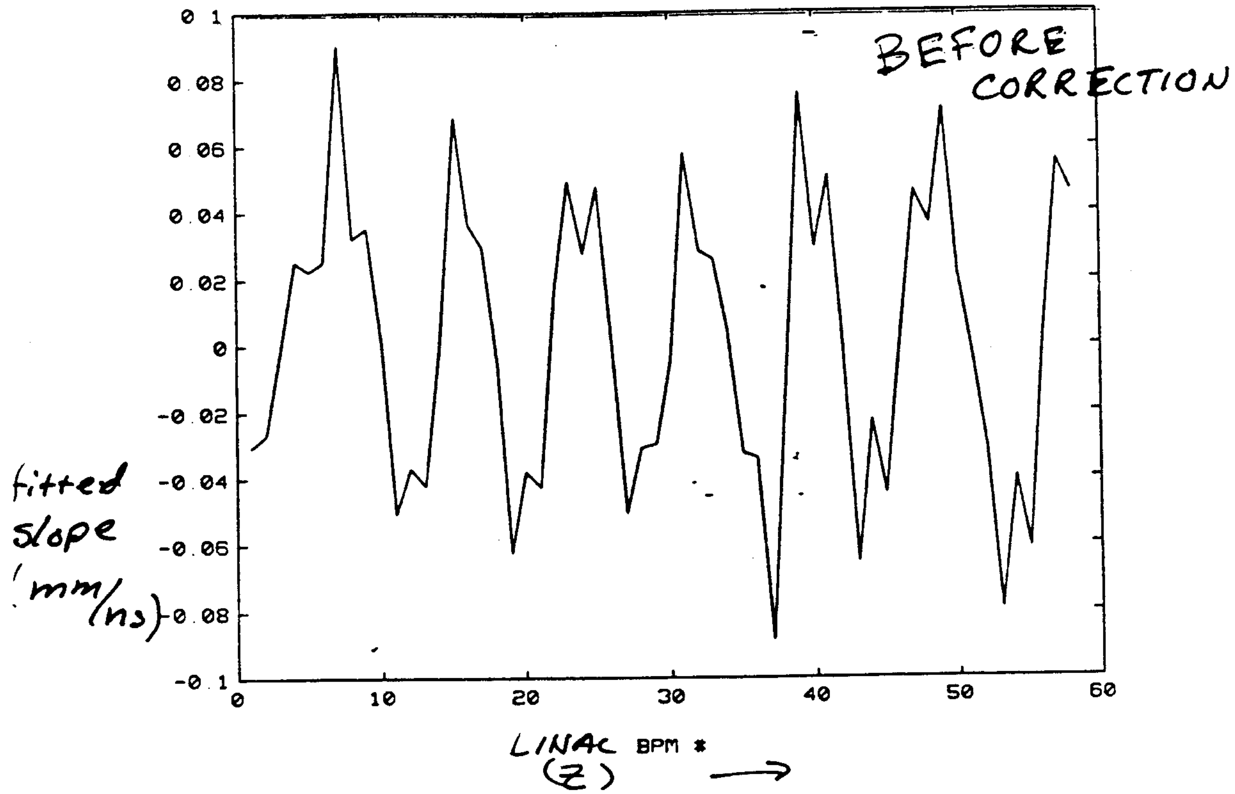

K time - BPM slope vs BPM after correction

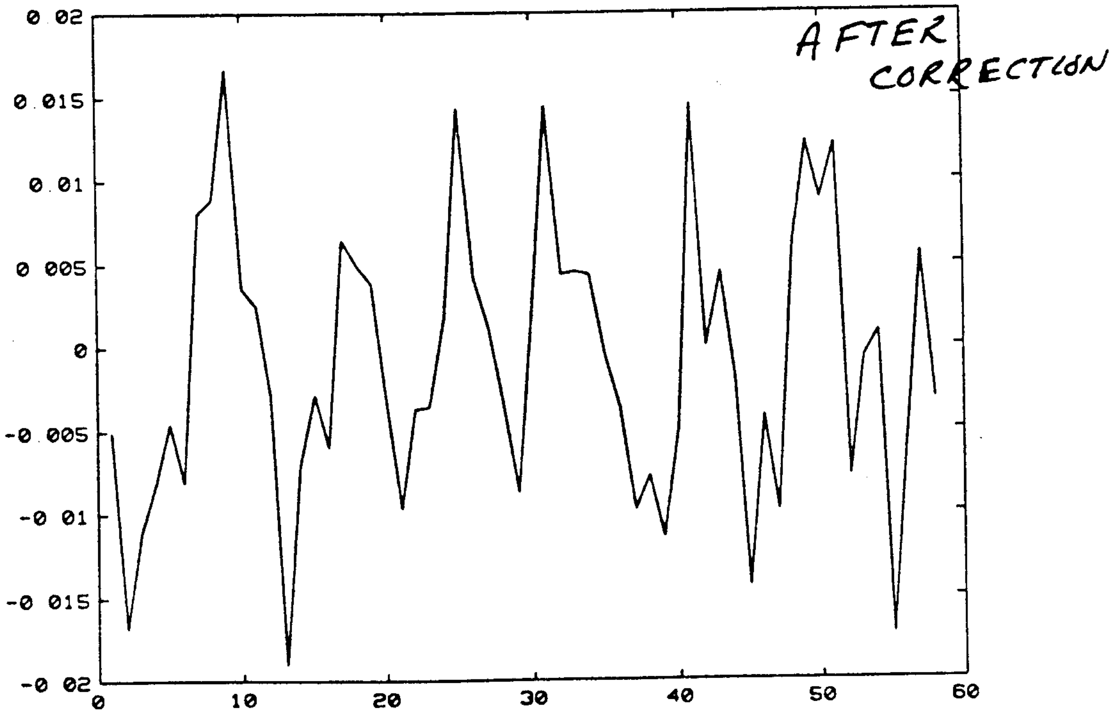

Proposal:Use redundant tuning schemes and a minimum of global 'detectors' because of :

1) Instrumentation systematics and non-linearity

Examples:

Quad - Bump technique - Are there BPM systematics that depend on beam size that would contaminate the $\Delta x/\Delta k$ tuning procedure?

Non-linear BPM systematics and BPM - BPM calibration effects on measurements of non-linear optical elements. - SLC RTL tuning

2) Upstream effects contaminating global correction

Example:

Beam - beam scans in the presence of tails

PROPOSED FFTB quad alignment tuning

$$\sigma_{ci} = S_i \sigma_{\rm bpm} = \left(2\Delta k_i \Big(\sum_{j>i} R_{12}^{ji\;2}\Big)^{1/2}\right)^{-1} \sigma_{\rm bpm} \qquad (2)$$

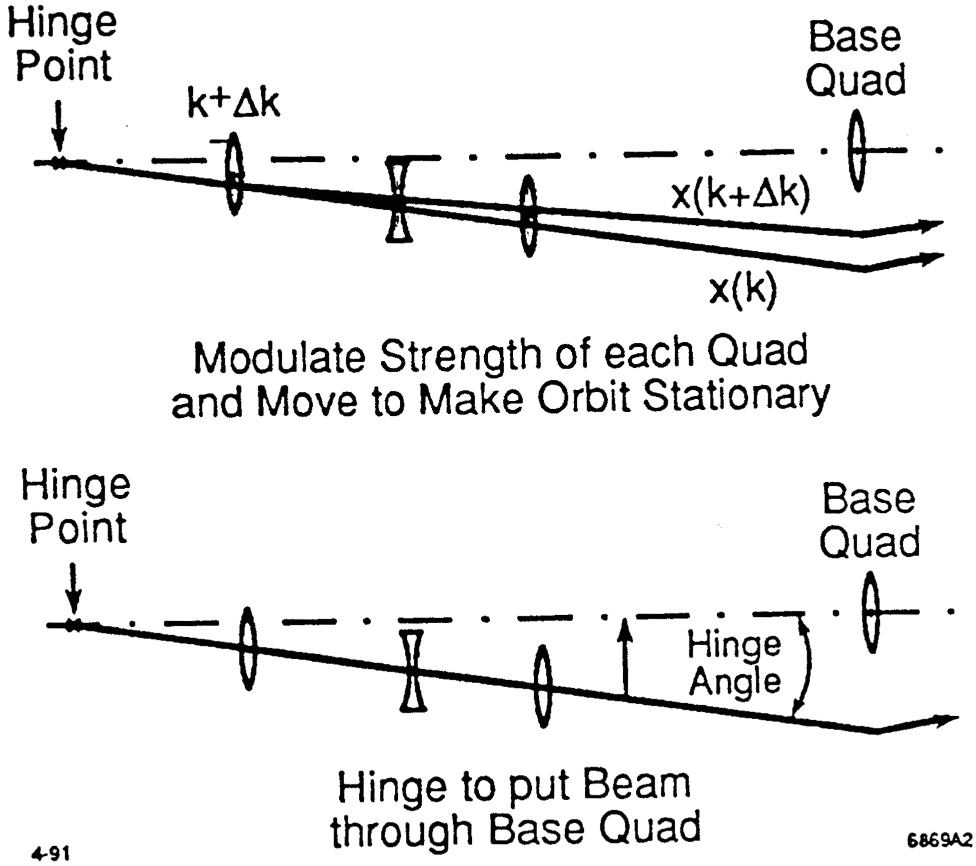

Figure 2. Quadrupole Alignment Procedure

Small beam size / tail changes may introduce (small) systematic errors → repeat tuning with different optics

PAUL EMMA
Bill SPENCE

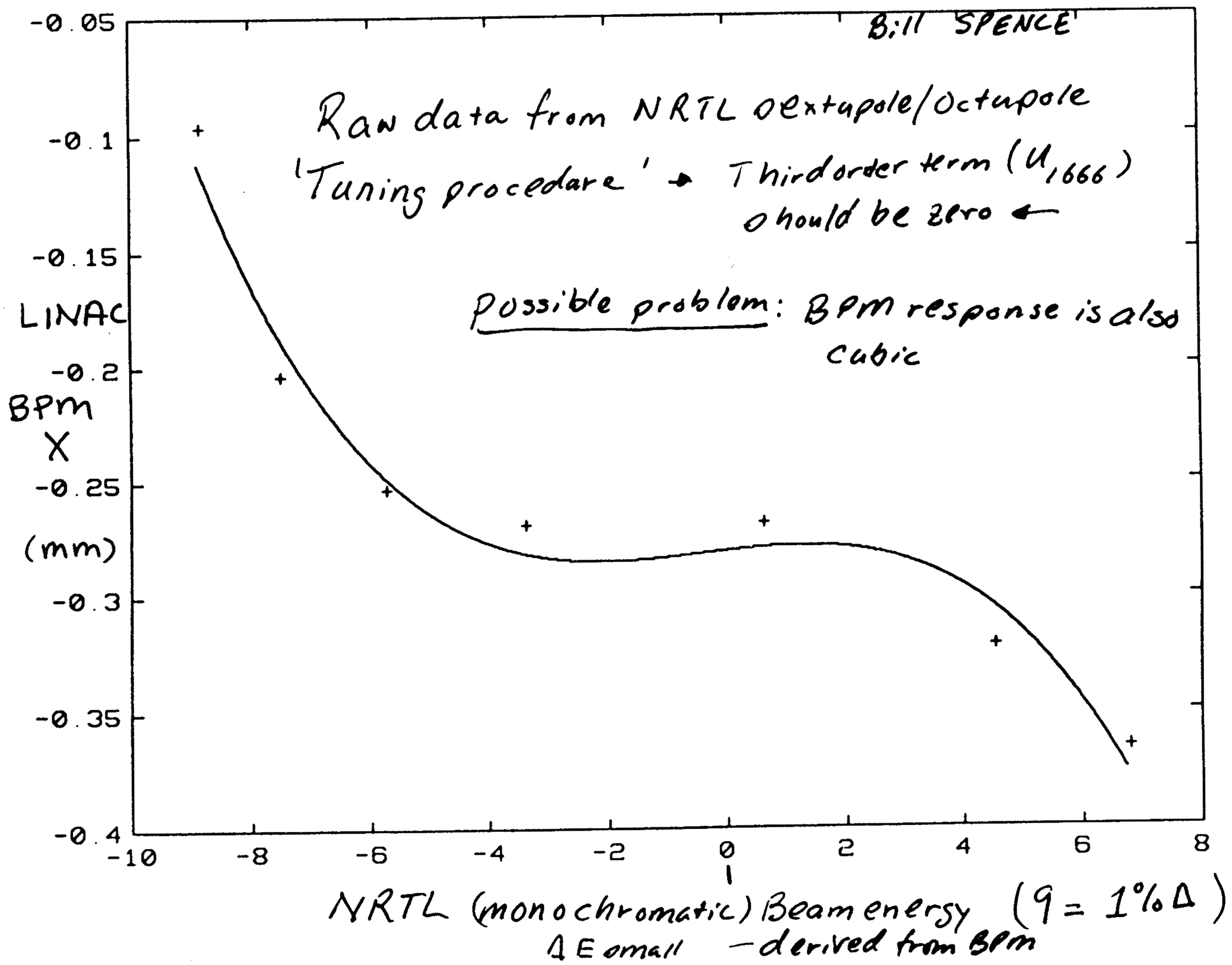

Raw data from NRTL sextupole/Octupole 'Tuning procedure' → Third order term (U_{1666}) should be zero ←

Possible problem: BPM response is also cubic

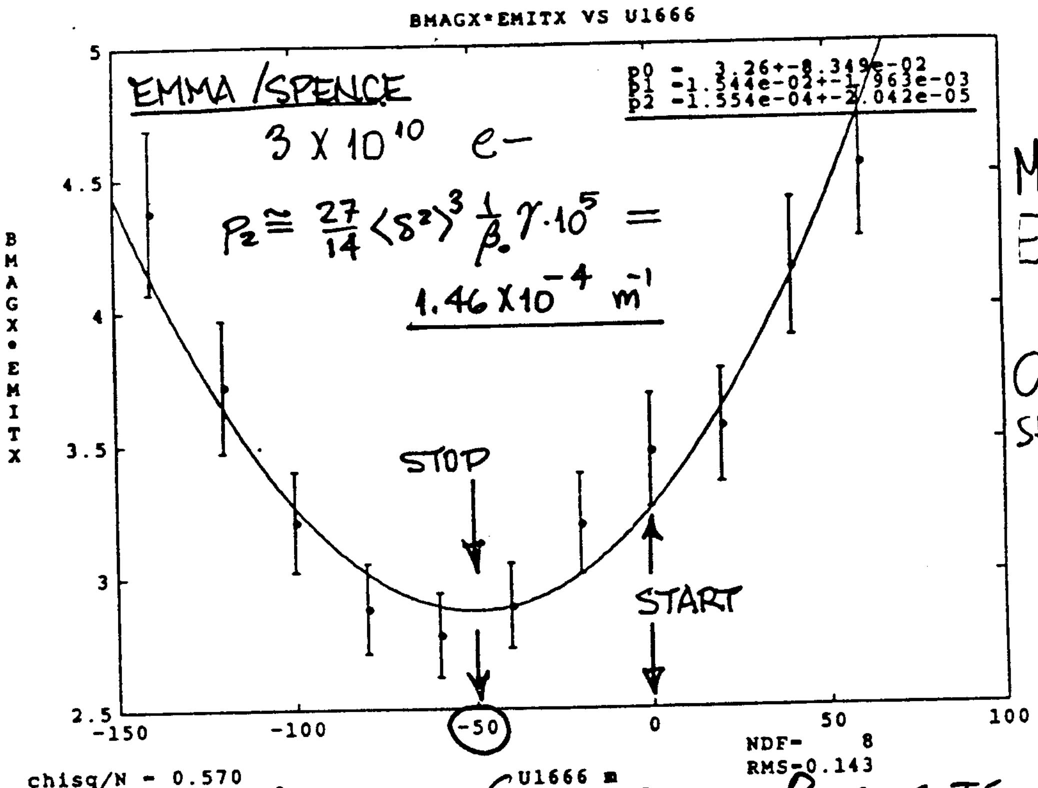

Measured Emittance vs Octupole Strength

NRTL OCTUPOLE CORRECTION RESULTS

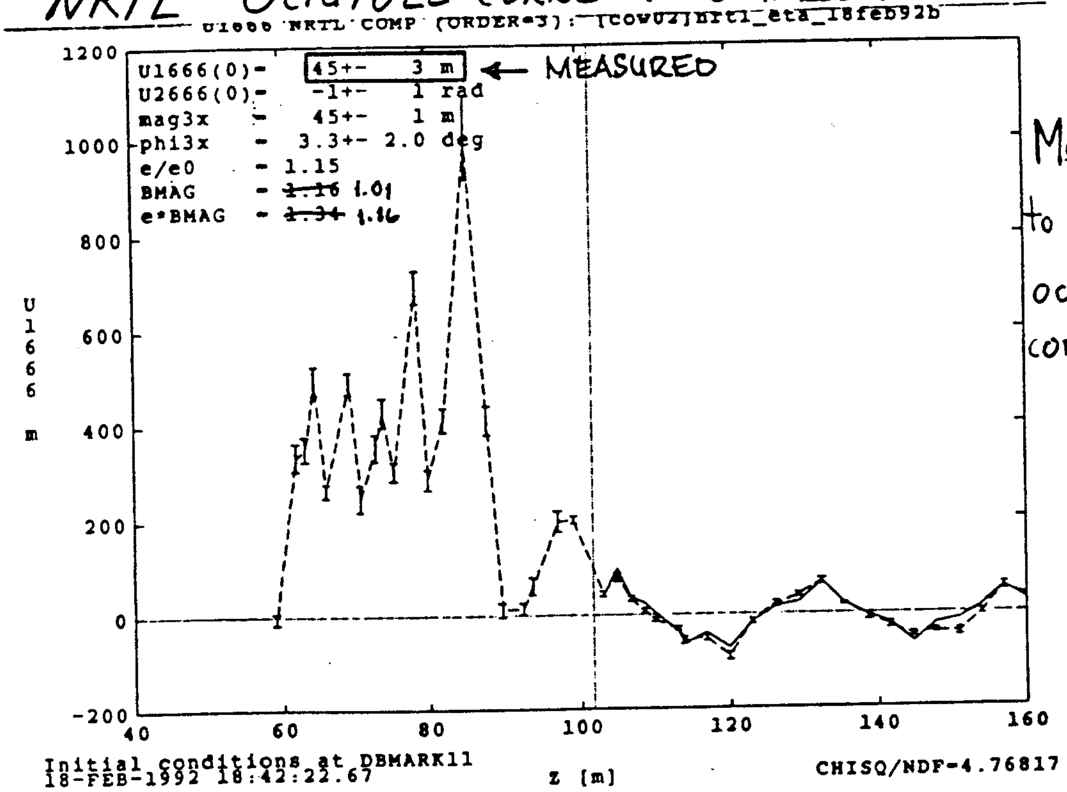

Measurement to predict octupole correction

Mechanical Systems

Focus has been on magnets, support systems and alignment schemes

Widely perceived as a significant technical challenge, e.g. final doublet relative vertical position

Proposal: Measure relative position just before collisions and correct using upstream fast steering magnets.

Feedforward

Proposal: Use precursor beam (~30ns) before luminosity bunches.

Parameters of precursor beams:

Single bunch	1E10
Energy	$0.7E_0$
IP sigma y	500nm
Deflection slope	1μrad/nm offset - 1nm offset should be detectable

Precursor beams would require separate beam lines between the end of the linac and the final doublets

Also could be used for crab cavity phase feedforward

Bill Ash

Hardware Sessions
FFIR Workshop

Magnets & Supports

Magnets:

PM, hybrid, conventional, s/c? (Spencer; Taylor/Egawa)
Any radiation or rf heating issues?
Field quality & measurement?

Supports:

Vibration (passive + active) (Bowden)
Alignment
Impact on detector (beampipe, vertex detector)
Impact on masking

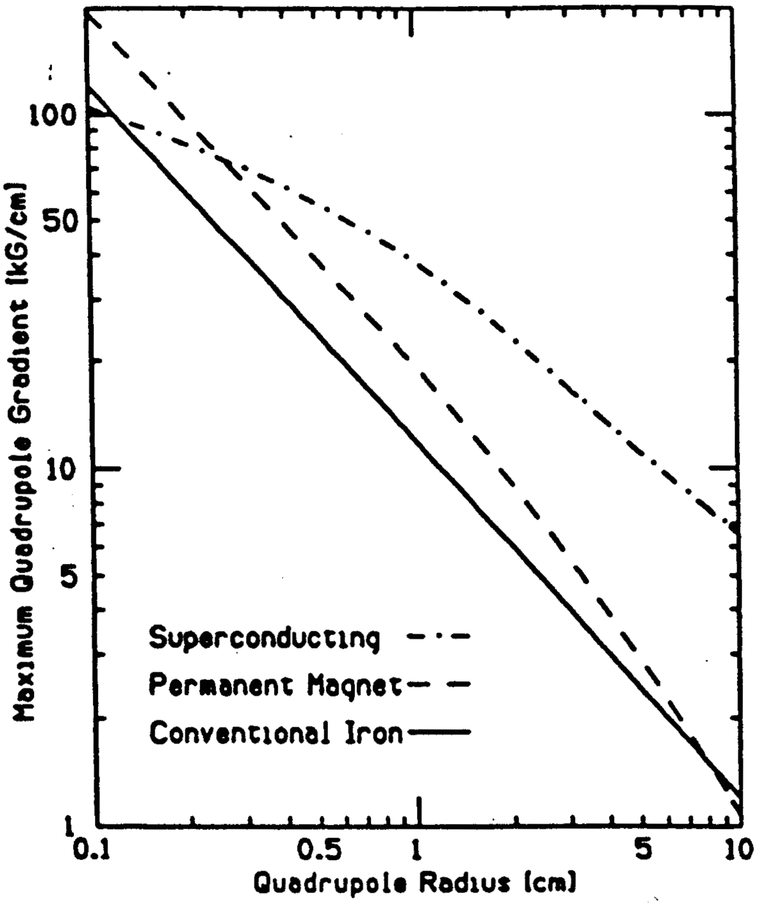

Fig. 3: Strengths obtainable for the different quad types in Fig. 2 based on a peak pole-tip field B_p=12 kG for the iron, a maximum remanent field B_r=11.5 kG for the PM material and NbTi wire with J_c=2kA/mm^2 at 5T and 4.2°K.

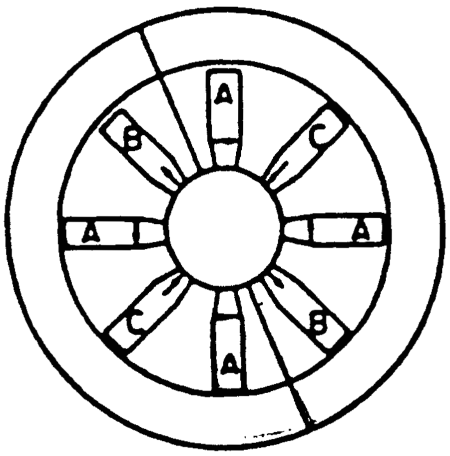

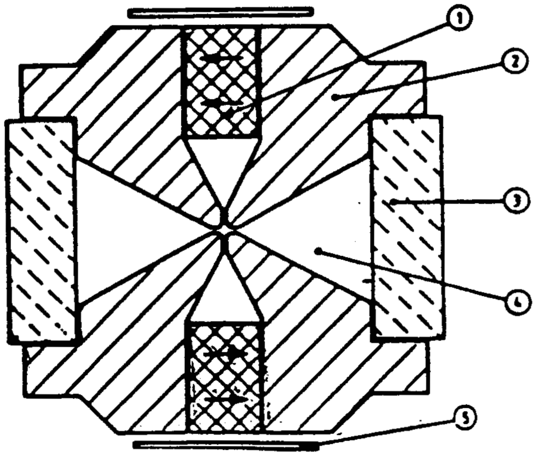

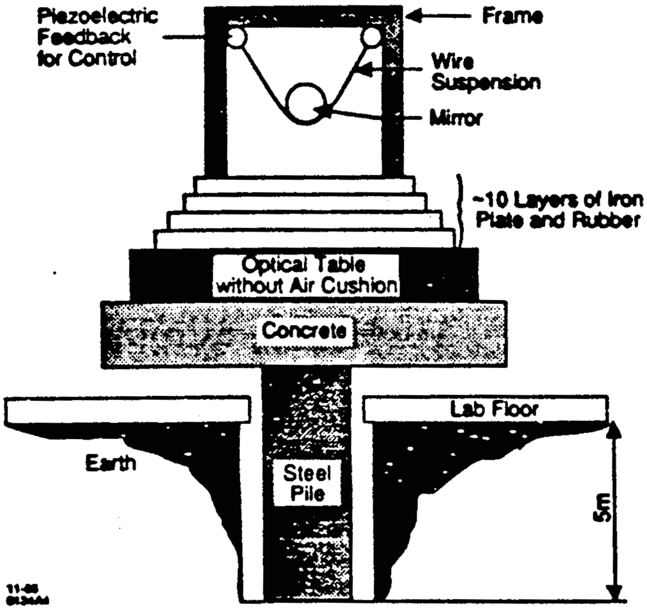

Fig. 2. Schematic layout of the passive seismic isolation for the Caltech interferometric gravity wave detector. In the application to a collider final focus, the heavy mass is the experiment's endcap, the floor might be appropriately modified, the optical table fits into the ten-degree dead region, and the final focus support beam hangs on the suspended "mirror".

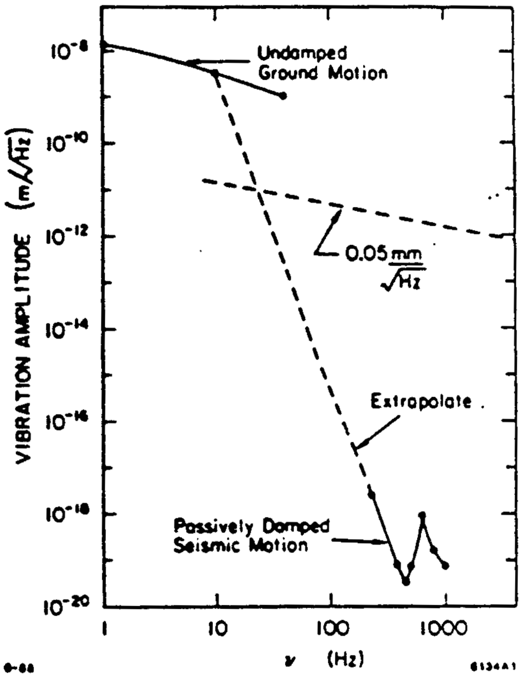

Fig. 3. This graph, adapted from the Caltech work, shows the noise measured on the kind of suspension sketched in Fig. 2. The extrapolation joins the indirect high-frequency data with undamped low-frequency seismic vibrations. The curve marked 0.05 $mm/\sqrt{Hz}$ is an estimate of the collider requirement.

SCHEMATIC VIEW OF SEISMIC SUPPORTS

VIBRATIONS AT SLD TRIPLET SUPPORT

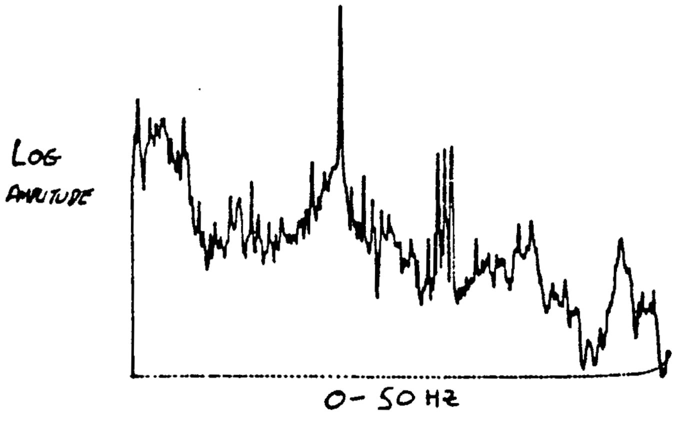

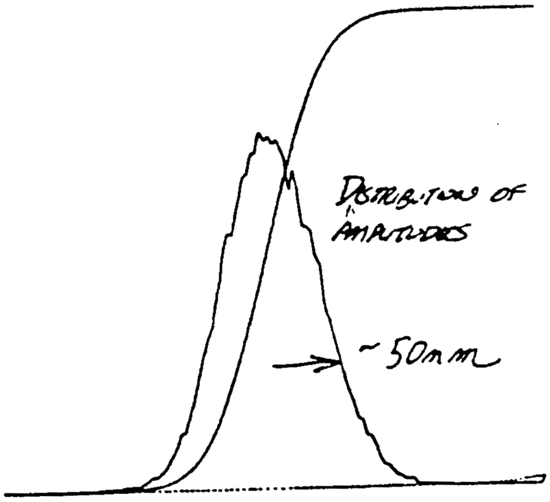

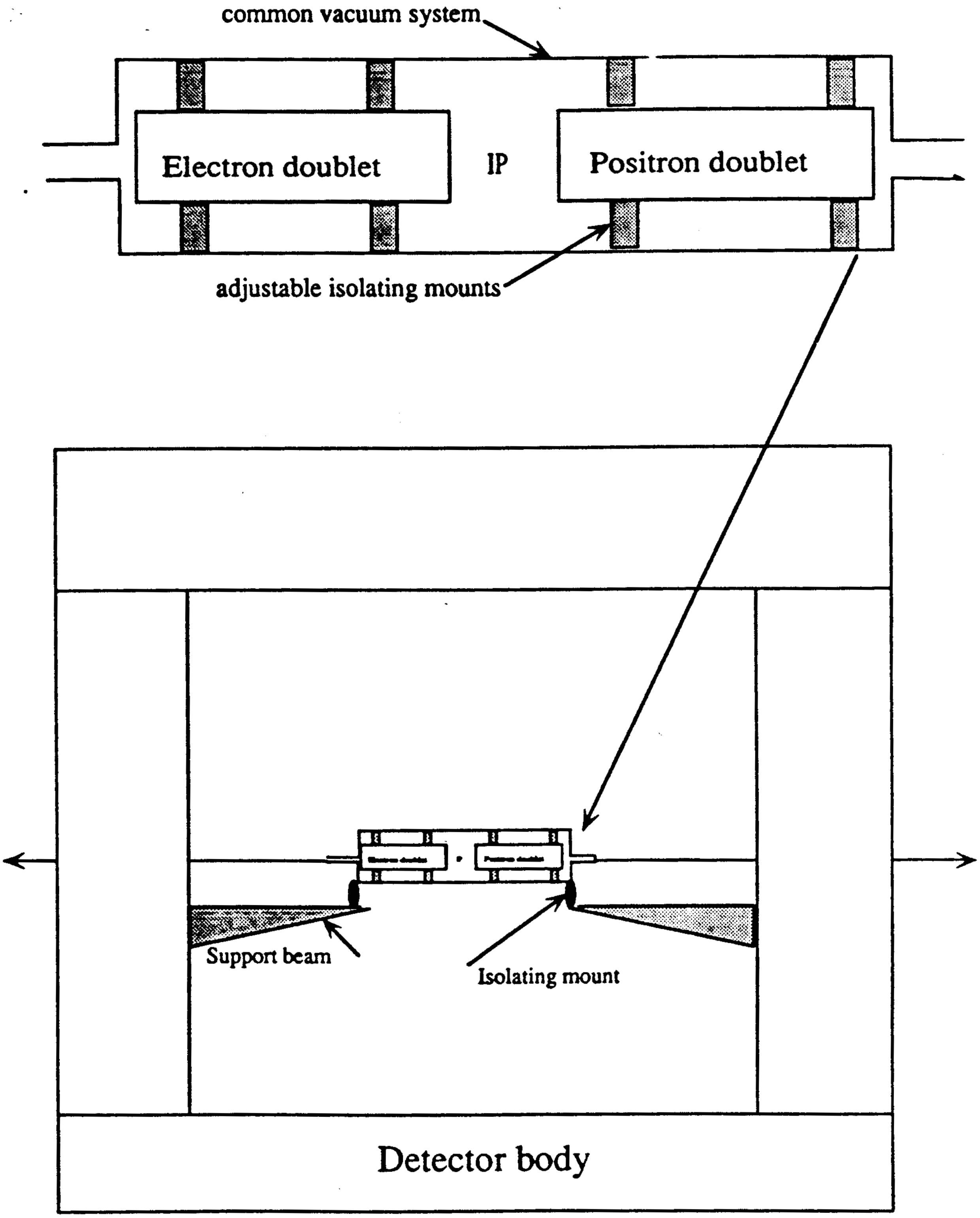
common vacuum system
Electron doublet
IP
Positron doublet
adjustable isolating mounts
Support beam
Isolating mount
Detector body

Aperture

Beam losses of about 1E9 (out of 3E10)per bunch are observed in SLC final focus

In the SLC linac (and arcs?) much smaller losses are observed (1E-5) - Determined using loss monitors

SLC:

Linac beam pipe diameter is about 70 sigma
Arc beam pipe diameter is about 16 sigma

Muon background requires losses at this level or lower

What is the impact on magnets, instrumentation etc?

Instrumentation

Beam Position Monitor Systems

A quick look seems to indicate that extensions of present technology may be adequate.

1) How large can the beam pipe be made? Is this a significant aperture restriction? Expected FFTB performance is 1μm/5000μm radius and is close to noise limit (0.7μm)

2) How can independent bunch positions be sensed in a multibunch beam? What are the requirements for single bunch position measurements?

3) How linear will these devices be? At SLC non-linear response of BPM's may interfere with attempts to control non-linear fields. How important are interdevice scale calibrations?

4) How does upstream beam loss or hard synchrotron radiation contaminate the measurement? Does every BPM require a collimator?

5) BPM systems may be required for a) same-pulse feedback and b) special purpose measurements, such as those required for CCX/Y corrections (where interdevice systematics must be minimized)

6) What are the required stability time scales? (to be tested at FFTB) Thermal / calibration question.

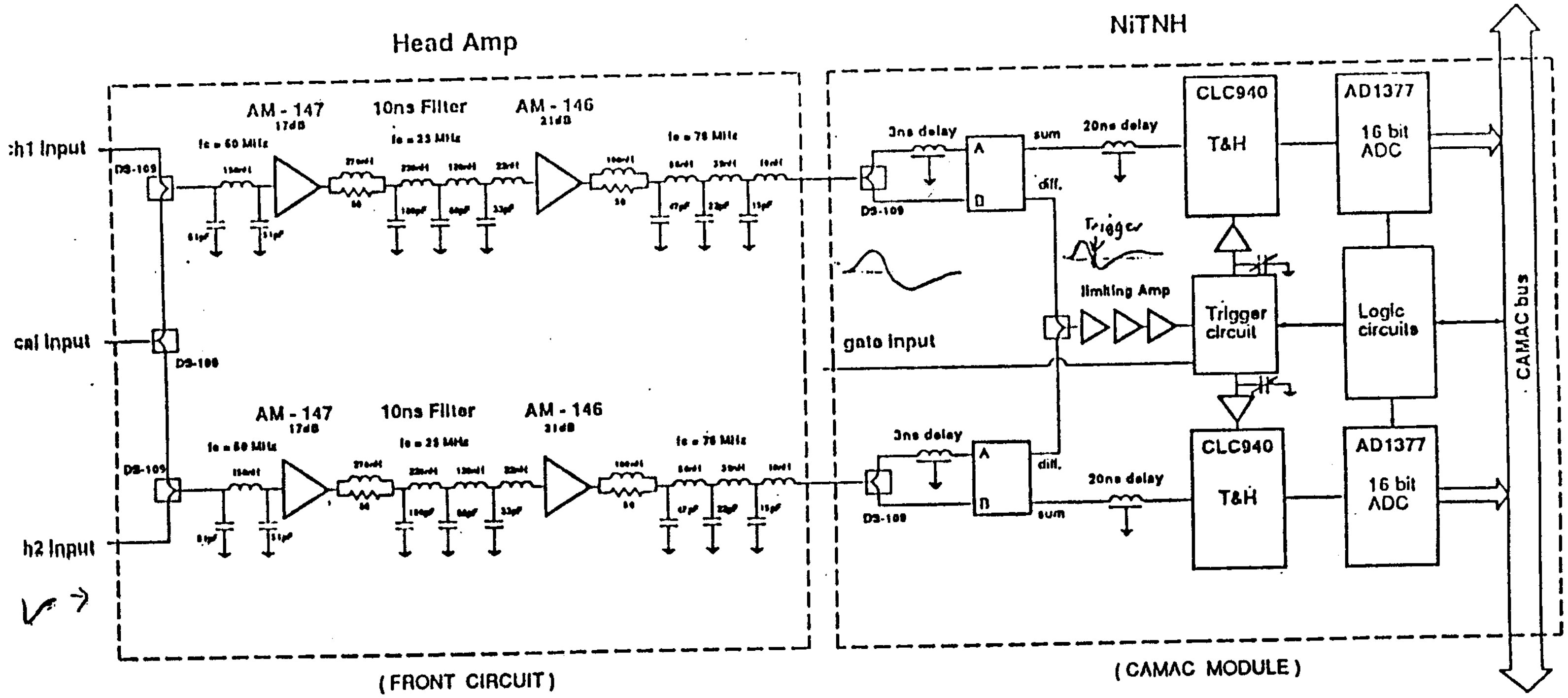

FFT3
BPM Electronics

Multi-bunch Time Domain LC BPM

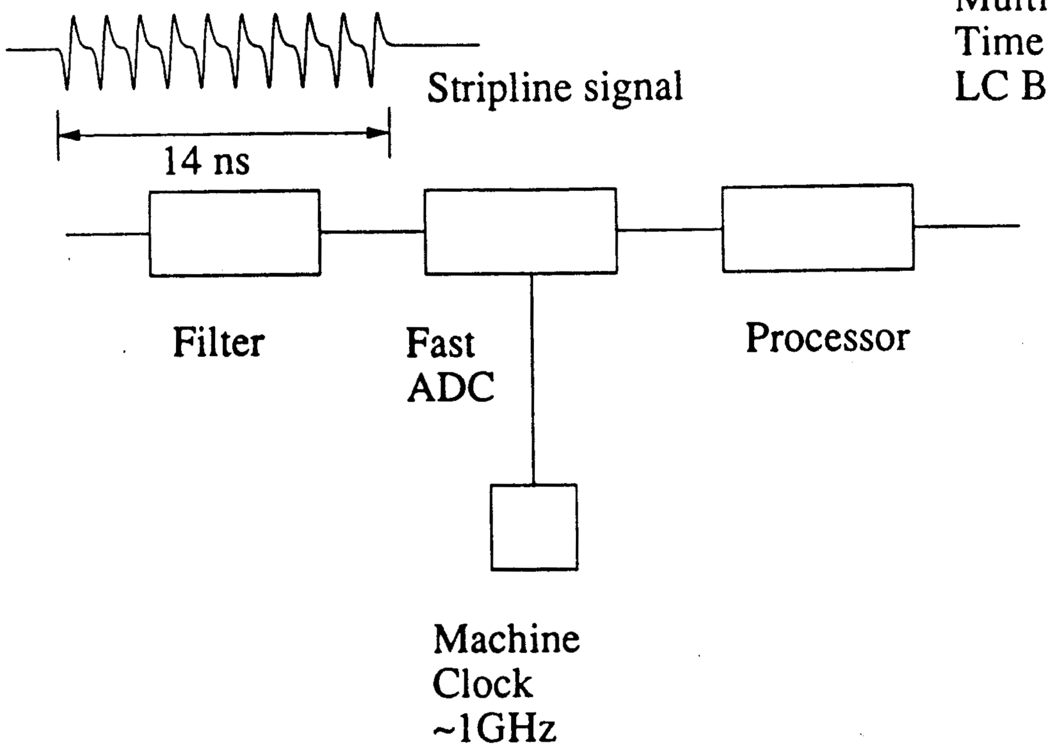

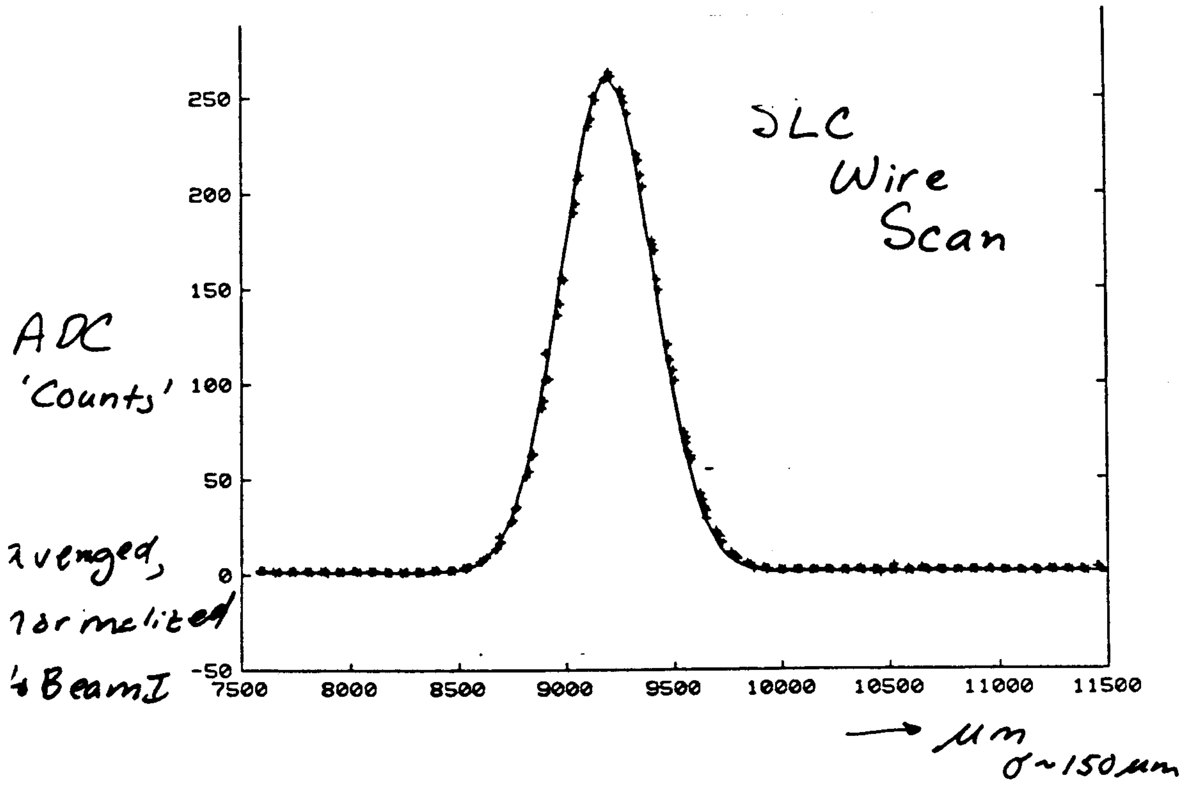

SLC Wire Scan

ADC 'Counts'

averaged, normalized to Beam I

→ μm

σ~150 μm

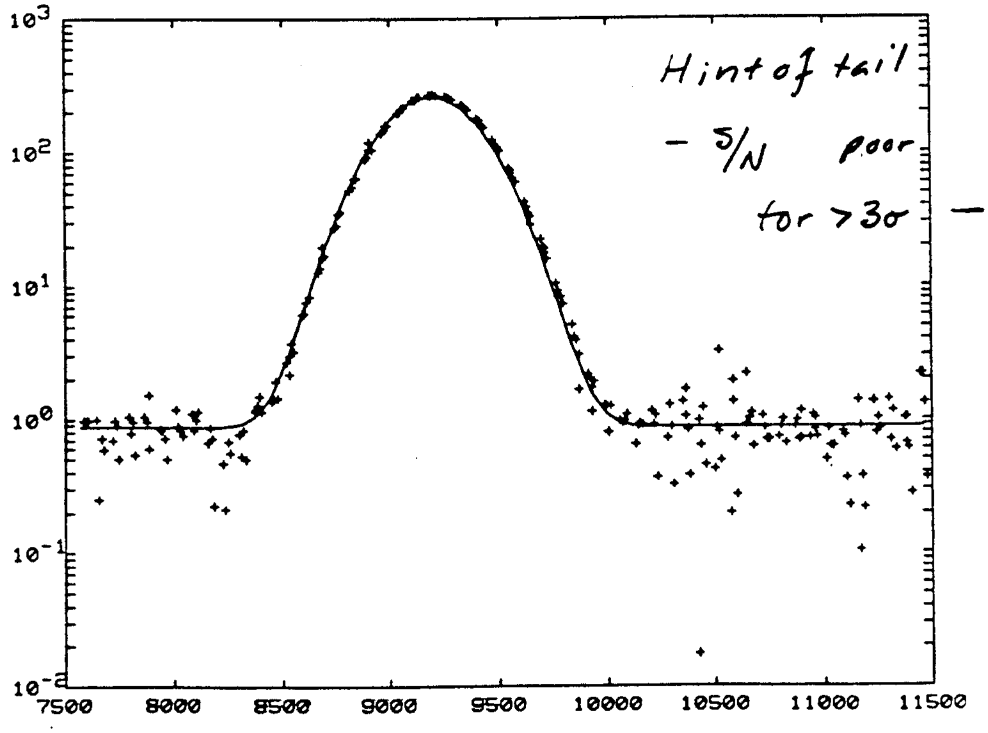

Hint of tail - S/N poor for >3σ -

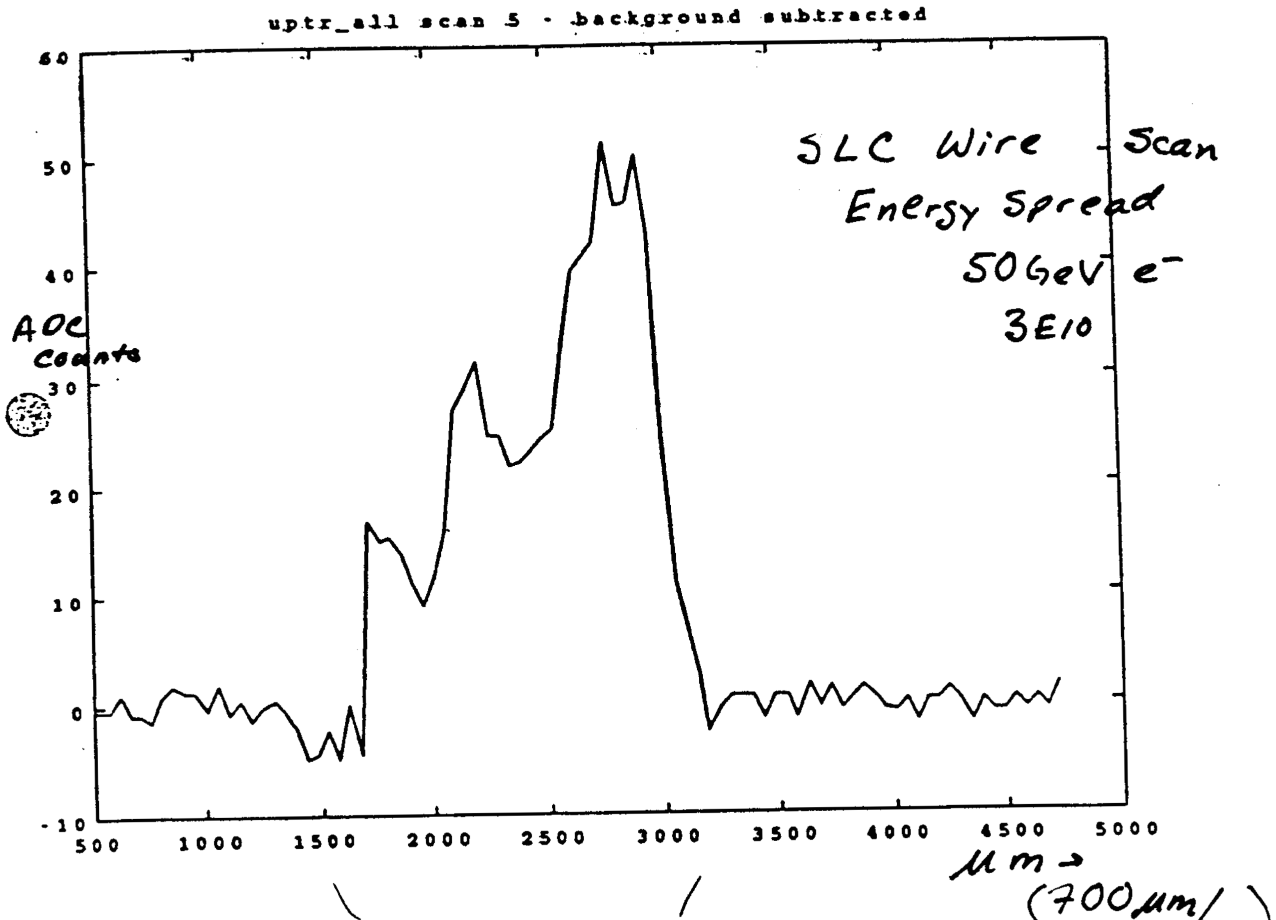

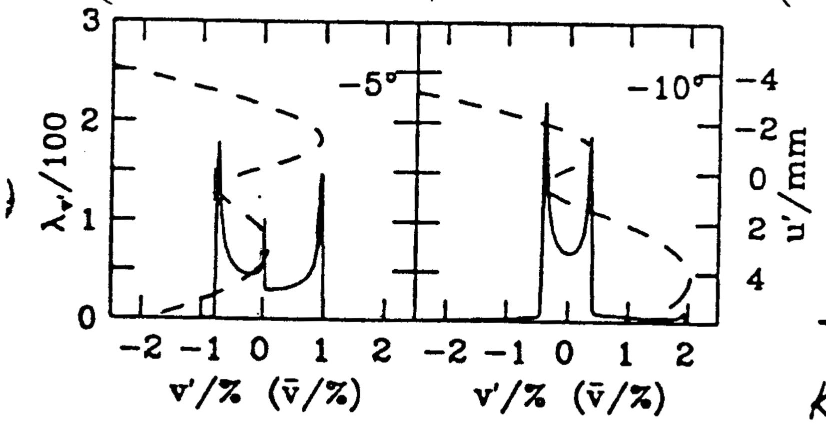

Theory

Figure 6. The bunch spectrum at the end of the linac $\lambda_{v'}$ for two values of rf phase. $N = 5 \times 10^{10}$ and $V_c = 30$ MV.

K.L. Bane

Beam Profile Monitors

What role do these devices play in tuning procedures?

Required for more than IP spot size tuning - must be included in optics design. Important for inter-system monitoring. Measure all appropriate optical parameters at each system boundary.

-> Emittance preservation <-

What are a profile monitors' desirable features?:

Non-interfering - scans should be made while the machine is any operating state, especially production operation

Single shot profiles - these can be used with synchronous detection techniques

Linearity - this is required due to emittance dilution from tails and due to the non-gaussian shapes associated with energy distribution

Extreme dynamic range - As with other machines, it would be very nice to examine the extremes of the distribution (4-5 sigma). Should be possible with FFTB/SLC wire scanners. 'Tail Monitor'

Accuracy - Several devices in sequence will be used to determine phase space parameters under non-optimum conditions. The interdevice calibration must be adequate to allow accurate phase space measurements.

Laser-Compton Spot Size Monitor

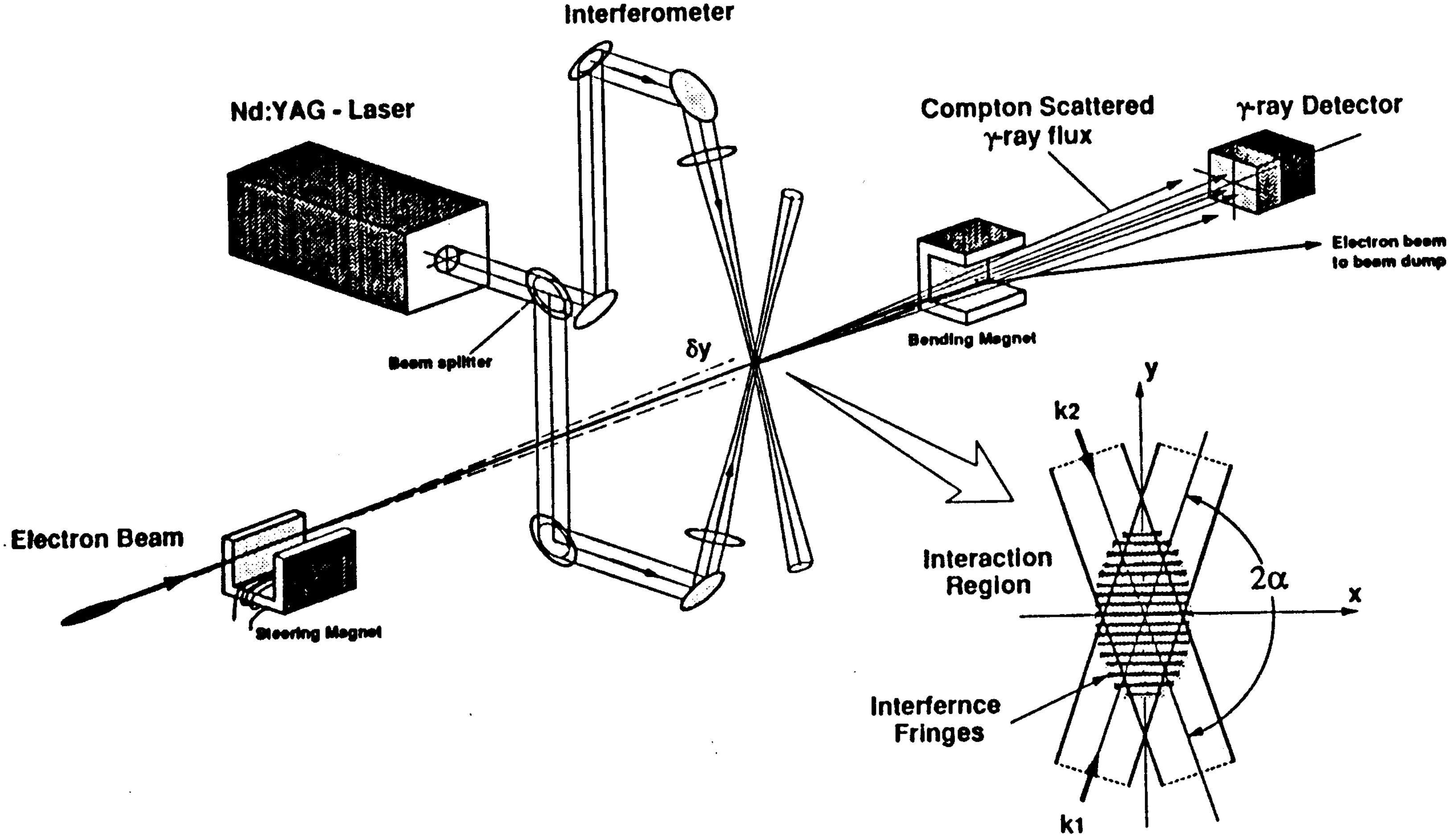

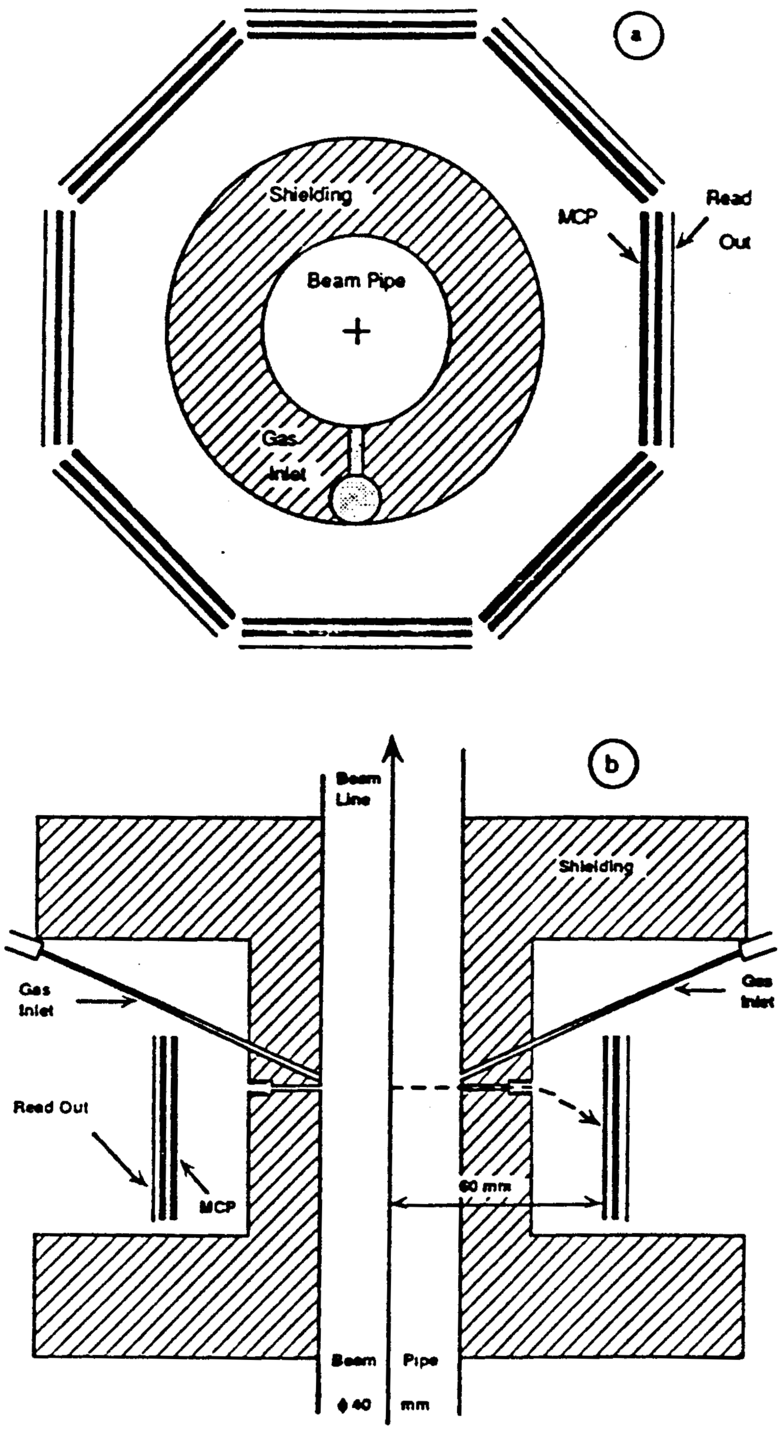

Figure 17 : Schematic view of the ion detector.
a) Transverse section at the FFTB focus.
b) Longitudinal section along the beam line.

Robustness - must be able to repeatedly provide beam size measurements for all possible beam intensities and sizes.

IP Beam profile monitors

Laser-Compton

Ion - beam 'field probe'

Liquid wire scanner ; Droplet scanner

?

Other:

Beamstrahlung

Final doublet synchrotron radiation

Single bunch ΔE/E

Bunch length (requires RF)

Correlations (ΔE/E - z, z - x,y)

Pulse stealing systems, used effectively at SLC

CASE 2
(WS.3)

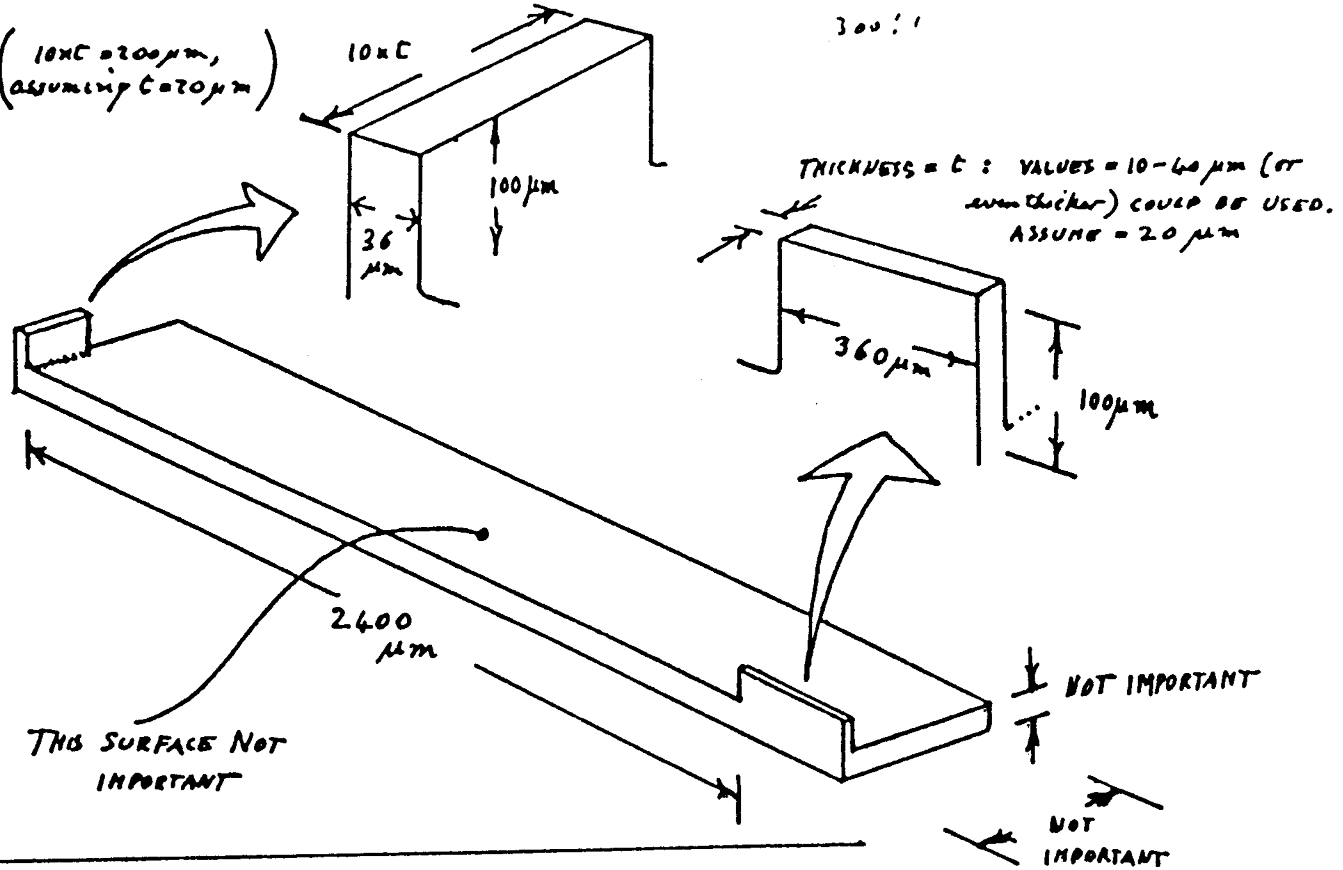

PPER SURFACES of the 2 BLADES ARE SAME PLANE WITHIN ± 0.4 µm, FLAT TO ± 0.4 µm

OTTOM SURFACE of WAFER IS PARALLEL TO TOP SURFACE of BLADES WITHIN 1 mrad.
(to assist alignment on an optical flat).

ESISTANCE of BLADE, TOP TO BASE, SHOULD BE $\lesssim 1\,M\Omega$ TO DRAIN CHARGE.

HE SHAPE OF THE BASE IS NOT IMPORTANT :—  O.K.

CROSS-SECTIONAL AREA of BLADES SHOULD BE CONSTANT ± 10% OVER (100 µm) HEIGHT INDICATED

J. T. Seeman (1986)

SLC
Xray
Synchrotron
LIGHT
PROFILE
MONITOR

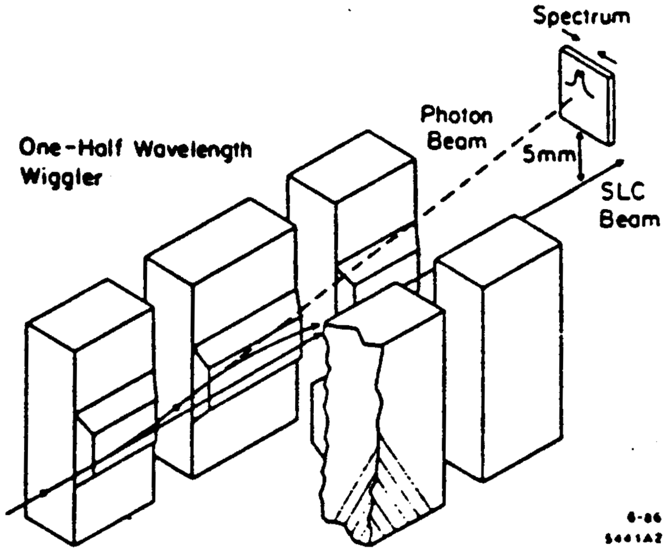

Fig. 2. SLC energy spectrum monitor using a vertical wiggler magnet and an off-axis x-ray detector.

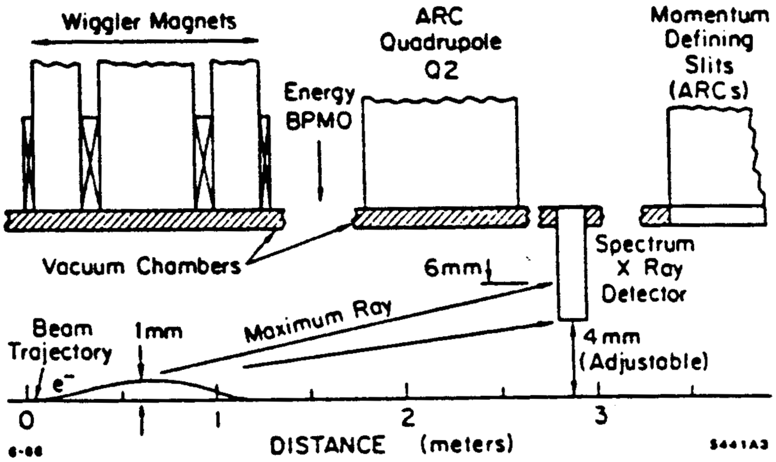

Fig. 3. Elevation view of the spectrum monitor region.

Ideas are needed for (non - IP) spot size monitors.

Measure $\sigma_{x',y'}$ using bremstrahlung with segmented detectors

- Two regimes:
  - Large $\sigma_{x',y'}$ (at IP)
  - Small $\sigma_{x',y'}$, large $\sigma_{x,y}$, Measure α, (Can test both at FFTB and SLC)

Monitor large aspect ratio beams

- 'tab' or razor edge monitors will be studied at FFTB. Ideas are needed.

Synchrotron light x-ray size monitors

- May be possible to surpass wire-breakage limit.
- μm level resolution may be possible
- Used at SLC for ΔE/E monitors

'Liquid' wire monitor - to be tested at FFTB. 'Wires' as small as 4μm have been made, sub-μm wires are probably achievable.

Profile Monitor Comparison:

Non - IP devices	Wire Scanners	Video screen	Synchrotron light
Resolution	~ < 1µm	~20µm	~1 µm
Limit to resolution	4µm smallest wire in use	5µm min grain size, optics and depth of source	L/γ
Power limits	2 x 2 µm @ 1E10 Max E dep in C	Screen burn 0.1C/mm^2	
Signal	Bremstrahlung	700nm used at SLC	FFTB E_C= 2MeV
Image	Requires about 100 pulses	Full two dimensional, single pulse profile	Single pulse, one dimension
Operation impact	Semi-invasive, requires downstream bend to separate bremstrahlung	Invasive without pulsed magnets	Non-invasive
	Divergence measurement		Divergence measurement

Beam Loss Monitors

May be important for background (e.g. muon) control

Backup for 'Tail Monitor'

What can be expected?

Questions:

- Lessons from SLC - practical items
    - Instrument masks and collimators
    - Loss monitor sensitivity
        - Can detect ~1mJ (few m-rad)using simple ion chambers (2E-9 of 400kJ DESY LC)
    - Muon monitoring

Goal is to accurately predict HEP detector response

LEP

'Instrumented Mask'

Von Holtey 1990

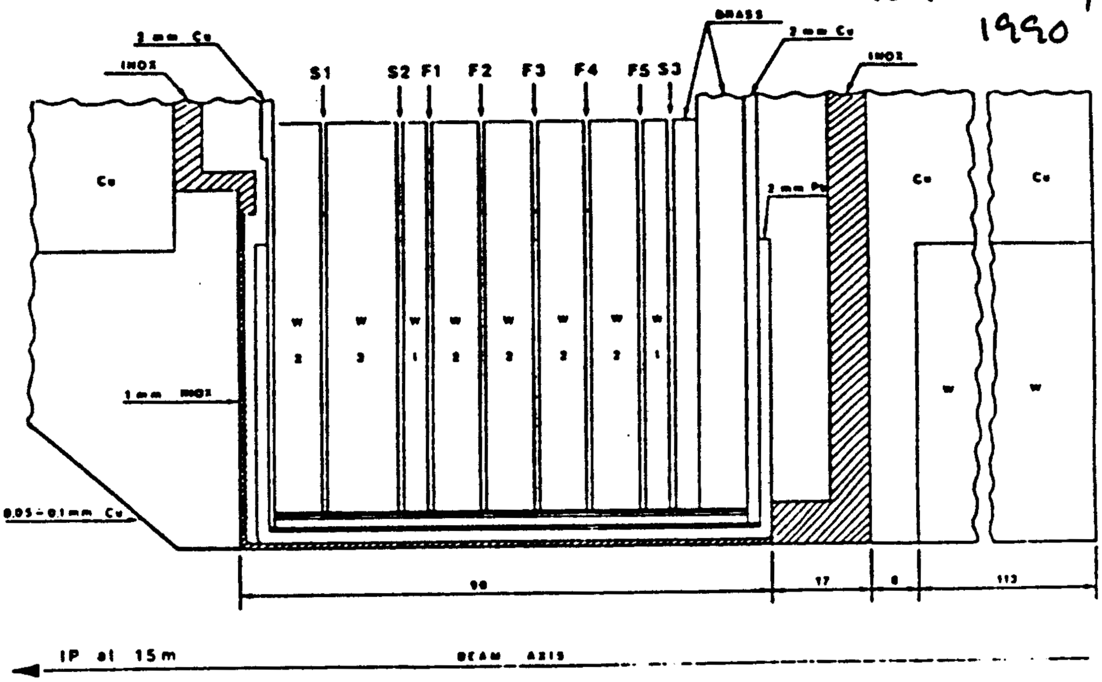

Fig.2 Cross-section of a 15 m horizontal collimator with a calorimeter embedded in its pit.

W - Si Calorimeter for : optimizing L and backgrounds

Timing / Synchronization

Must have feedback system for crab cavities

    What are the tolerances for crab?

Inter-linac synchronization? Feedback and monitoring

Laser - beam collision synchronization

(SLAC E-144 using FFTB)

This should not be a problem - 0.7ps(0.2mm) error mode lock laser timing control is commercially available. Better synchronization should be possible

Beam 'phase' or arrival time monitors are needed

Wide-band (multi bunch) and narrow-band systems are being tested at SLC. 0.1degree S-band is practical limit.

Machine Protection System

Must be able to produce low power beam, with full beam dynamics, that can do no damage to beamline components. Must be able to switch between high/low power operation instantly.

Beam diagnostic devices must function with 'appropriate' tolerances under low power conditions to allow testing, tuning etc. (e.g. mutibunch BPM's must also operate with only one bunch)

Beam power reduction control:

Repetition rate - (SLC uses a complex scheme with auxiliary beam pulses and special dumps)

Number of bunches

Other?

All high power devices must have:

Non interfering 'standby pulses' so they can remain at full rate

SLC Kickers

Thermal compensation for changes in beam power where needed.

SLC positron target

These 'baroque' details must be considered during design and R/D

General MPS philosophy

Machine protection systems (MPS)

0) Build self-protected system
    - SLC positron target extraction line

since this is not always possible... develop MPS

1) Catch all preventable events
    - Use controls to suppress all beam pulses that are 'known' to be bad.
    - Feedforward
    - SLC Veto system
    - Extend this approach for protection against single pulse faults

2) Single Pulse faults
    - Difficult, needs detailed study
    - Use spoilers

Proposed 'Controls intensive solution':

- Focus on those devices whose field can change enough in a single inter-pulse period to permit beam to cause damage.
- All other devices should generate VETO if failure can cause beam to strike a sensitive region
- Generate feedforward abort signal from BPMs etc if possible

3) Average power faults
    - Response in cases where there is no signalled device failure, yet average power limits are exceeded. (typical SLC problem)

Develop integrated, fast, beam power control for recovery and diagnosis.

Machine Protection

	SLC	NLC	DESY	SSC
Single pulse energy	400J	12KJ	400KJ	420MJ
Beam power	50KW	1.5MW	20MW	0.5MW
dE/dx energy density (1mm depth)	5J/cm^2	100,000 J/cm^2	5E6 J/cm^2	5000J/cm^2
Average/ single pulse	No single pulse failures can occur	single pulse most important	single pulse most important	single pulse damage unlikely - no pulsed devices
Abort system	Pulsed magnets, 100KW dumps (2)	?- will need more than 2	?- will need more than 2	2km with raster scan kicker to increase spot size (2)
Response time	inter-pulse	same pulse	same pulse	1 turn (300μs)
Recovery (power limit)	rate limit	rate and number bunches	rate and number bunches	intensity
Shutoff sensors	loss mon	device controller	device controller	loss mon and position mon

Radiation Hardness

All regions in next generation LC may be subject to severe radiation. (esp. 50MW long pulse machines).

SLC experience: ~10KRad / month at 1 - 2 meters from beam line.

Need radiation hard:

Position encoders

Video cameras

Optics - especially achromatic lenses

NMR electronics

Scattered radiation detectors eg Č detectors

Conclusions:

Problems:

- Further evaluation of tuning

  ↔ INTEGRATE BEAM DIAGNOSTICS and OPTICS

- Mechanics of final doublet supports
- Alignment
- Thermal
- Masking
- Beam position monitors
  - May not be fundamentally new technology, but these are clearly the most important diagnostic
- Beam size monitors
- Machine protection for multi-MW machines

BEAM-BEAM INTERACTION

Mar. 2. 1992 SLAC K. YOKOYA. KEK

Mainly. BACKGROUND PROBLEMS
related to the B-B interaction.

Physical Phenomena

- Deflection
- Beamstrahlung
- Pair Creation
- Hadron Jets

Machine Design

- Layout around the I.P.
- Constraint on the parameters

$$\left(\begin{array}{l} N \\ \sigma_x, \sigma_y, \sigma_z \\ \phi_{cross}, \quad \text{crab or not} \\ t_b, n_b, f_{rep} \end{array} \right.$$

BEAMSTRAHLUNG

$$\Upsilon_{avr} \approx \frac{5}{6} \frac{N r_e^2 \gamma}{\alpha \sigma_z (\sigma_x + \sigma_y)}$$

$$\Upsilon_{max} \approx \frac{2 N r_e^2 \gamma}{\alpha \sigma_z (\sigma_x + 1.8 \sigma_y)} \approx 2.4 \Upsilon_{avr}$$

$$(R \equiv \sigma_x / \sigma_y \gg 1)$$

Number of photons / electron

$$n_\gamma \approx 2.5 \left(\frac{\alpha \sigma_z \Upsilon_{avr}}{\lambda_e \gamma} \right) U_0(\Upsilon_{avr})$$

Average energy loss

$$\delta_{BS} \approx 1.2 \left(\frac{\alpha \sigma_z \Upsilon_{avr}}{\lambda_e \gamma} \right) \Upsilon_{avr} U_1(\Upsilon_{avr})$$

$$U_0(\Upsilon) \approx \frac{1}{\sqrt{1 + \Upsilon^{2/3}}} , \quad U_1(\Upsilon) \approx \frac{1}{\left[1 + \left(\frac{3}{2} \Upsilon \right)^{2/3} \right]^2}$$

The quantity $\left(\frac{\alpha \sigma_z \Upsilon_{avr}}{\lambda_e \gamma} \right)$ is $O(1)$ in most designs.

$n_\gamma \approx O(1)$

$$n_\gamma = \left[\frac{50}{1+R} \frac{L}{10^{30}\, \mathrm{cm}^{-2}} \right]^{1/2}$$

L: luminosity per bunch collision

$$= \frac{\mathcal{L}}{f_{rep} \cdot n_b}$$

Deflection by B-B Force

- Characteristic angle $\theta_0 \equiv \frac{D_x \sigma_x}{\sigma_z} = \frac{D_y \sigma_y}{\sigma_z}$
- Kink Instability

  Serious if $D_y \gtrsim 20$ or 30
- Deflection of full energy particles

  (assume $D_x \ll 1$)

  maximum angle

  $$\left.\begin{aligned} \theta_x &\simeq 0.76\ \theta_0 \\ \theta_y &\simeq 1.4 \frac{\theta_0}{[1+(0.5D_y)^5]^{1/6}} \end{aligned}\right\} \text{plus initial angle spread}$$

- Deflection of low energy particles

  $\epsilon \equiv E/E_0 \qquad D_x \ll 1 \ll D_y$

sign of charge (compared with primary $e^{\pm}$)

	same	opposite
$\theta_{x,\max}$	$\frac{\theta_0}{\epsilon}\min\left(1, \sqrt{\frac{1}{\sqrt{3}}\frac{1}{D_x/\epsilon}}\right)$	$\frac{\theta_0}{\epsilon}\min\left(1, \sqrt{\frac{\log 4\sqrt{3}D_x/\epsilon}{\sqrt{3}D_x/\epsilon}}\right)$
$\theta_{y,\max}$	$\frac{\theta_0}{\epsilon}\sqrt{\frac{1}{\sqrt{3}D_y/\epsilon}}$	

↑ (longitudinaly uniform bunch)

$$\theta_{y,\text{same}} \ll \theta_{x,\text{same}} < \theta_{x,\text{opp}} \lesssim \theta_{y,\text{opp}}$$

- Deflection of Center-of-Mass

$D_x \lesssim 1 \ll D_y$

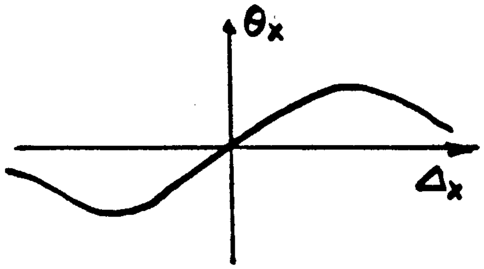

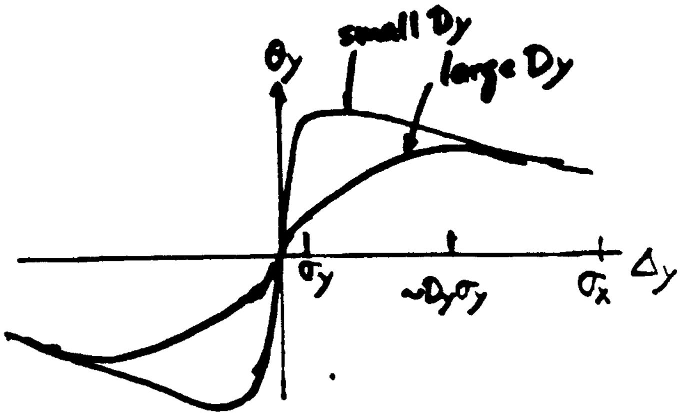

- Multibunch Crossing Instability

$$C_{MBC} \equiv D_x D_y \left[\frac{\sigma_x/\sigma_z}{\phi_{cross}} \right]^2 (m_b' - 1)$$

$$C_{MBC} \lesssim \sqrt{\frac{1}{2} + \frac{1}{3} D_y}$$

(blow up factor < 2)

COHERENT PAIR CREATION

$\gamma_{\text{beamstr.}} \longrightarrow e^+e^-$ in strong field

- number of pairs per primary electron

$$n_{\text{pair}} \approx \left(\frac{\alpha\sigma_z\Upsilon}{\gamma\lambda_e}\right)^2 \times \begin{cases} 0.05\, e^{-\frac{16}{3\Upsilon}} & (\Upsilon \lesssim 100) \\ 0.3\, \Upsilon^{-2/3} \log\frac{\Upsilon}{12} & (\Upsilon \gtrsim 100) \end{cases}$$

$$N \cdot n_{\text{pair}} \lesssim 1 \quad \text{if} \quad \Upsilon_{\max} \lesssim 0.3$$

- spectrum

$$\frac{dn_{\text{pair}}}{dx} \approx 0.2 \left(\frac{\alpha\sigma_z\Upsilon}{\gamma\lambda_e}\right)^2$$

$$\times \sqrt{\frac{1-x}{\Upsilon x}}\, \exp\left[-\frac{2}{3\Upsilon}\left(\frac{1-x}{x} + \frac{4}{1-x}\right)\right]$$

exponentially small if $x\Upsilon \ll 1$

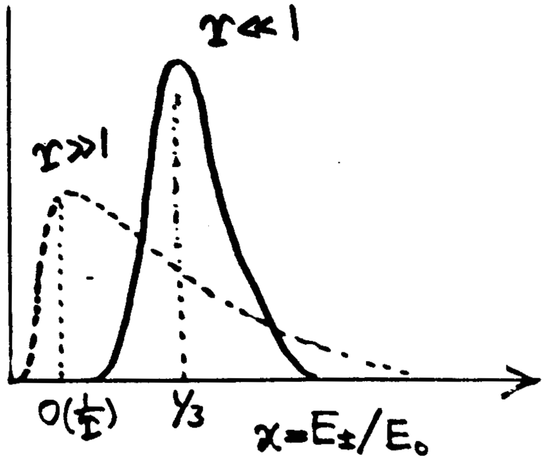

If you allow N' pairs from one bunch collision,

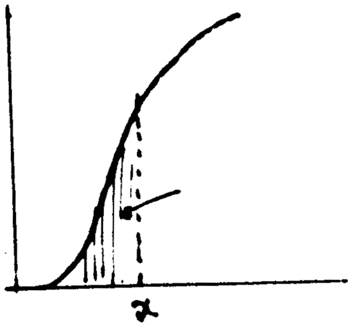

$$x \approx \frac{1}{22 + \frac{3}{2}\log\left[\frac{N}{10^{10}}\left(\frac{\alpha\sigma_z\Upsilon}{\gamma\lambda_e}\right)^2 \frac{1}{\Upsilon \cdot N'}\right]} \times \frac{1}{\Upsilon}$$

$(\Upsilon = \Upsilon_{\max})$

$N' = 1 \;\cdots\; x \approx \dfrac{1}{20\,\Upsilon_{max}}$

$N' = 10^4 \cdots\; x \approx \dfrac{1}{10\,\Upsilon_{max}}$

e.g. $E_0 = 500$ GeV. $\Upsilon_{max} = 1.25$

$\rightarrow$ 10^4 pairs in $20\text{ GeV} < E_\pm < 40\text{ GeV}$

$\uparrow$

deflection angle a few mrad.

SUMMARY SO FAR

Parameter Constraints

$D_y \lesssim 20$

$\delta_{BS} < 1\% \sim 15\%$ depending on experiments

$\Upsilon_{max} \lesssim 1.5$ $(\Upsilon_{avr} \lesssim 0.6)$

C_{MBC}

INCOHERENT PAIR CREATION

Breit-Wheeler $\gamma\gamma \to e^+e^-$

Bethe-Heitler $\gamma e^\pm \to e^\pm e^+ e^-$

Landau-Lifshitz $e^+e^- \to e^+e^-e^+e^-$

γ = real photon (beamstrahlung)

$$\sigma_{BW} \propto r_e^2 \left(\frac{\alpha\sigma_z\Upsilon}{\gamma\lambda_e}\right)^2 \frac{1}{(\gamma\Upsilon)^{2/3}} \log\gamma$$

$$\sigma_{BH} \propto \alpha r_e^2 \left(\frac{\alpha\sigma_z\Upsilon}{\gamma\lambda_e}\right) \cdot \frac{1}{\Upsilon^{1/3}} \log\gamma$$

} effective cross section seen from the primary particles

$$\sigma_{LL} \propto \alpha^2 r_e^2 (\log\gamma)^3$$

- $10^{-27} \sim 10^{-25}$ cm^2 .
- BH is dominant. LL follows.

Pair energy spectrum

$$\frac{d\sigma_{BH}}{dx_+} \sim \frac{\alpha^3 r_e \sigma_z}{\gamma} \Upsilon^{2/3} \frac{1}{x_+^{2/3}} (\log 2\gamma^2 x_+)$$

$$\frac{d\sigma_{LL}}{dx_+} \sim \frac{56}{9} \frac{\alpha^2 r_e^2}{\pi} \frac{1}{x_+} \left(\log\frac{1}{x_+}\right) (\log 4\Upsilon^2 x_+)$$

$$\left(\frac{1}{\gamma^2} \ll x_+ \ll 1\right)$$

$$\frac{LL}{BH} \sim \underbrace{\frac{\lambda_e\gamma}{\sigma_z}}_{10^{-2}} \cdot \frac{1}{\Upsilon^{2/3}} \cdot \frac{1}{x_+^{1/3}} \log\frac{1}{x_+}$$

Geometric Reduction

BH. suppression by factor 2 to 3

LL. possibility of creating pairs out side bunch

Inherent Angle

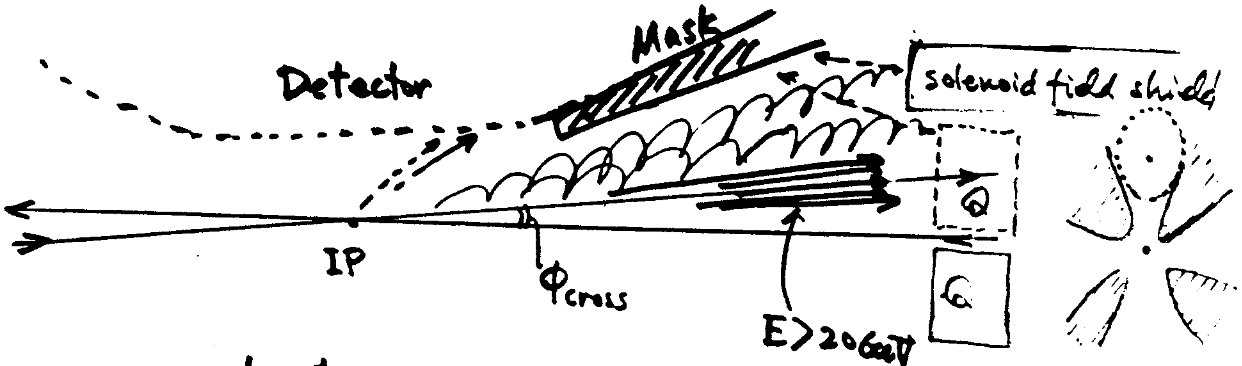

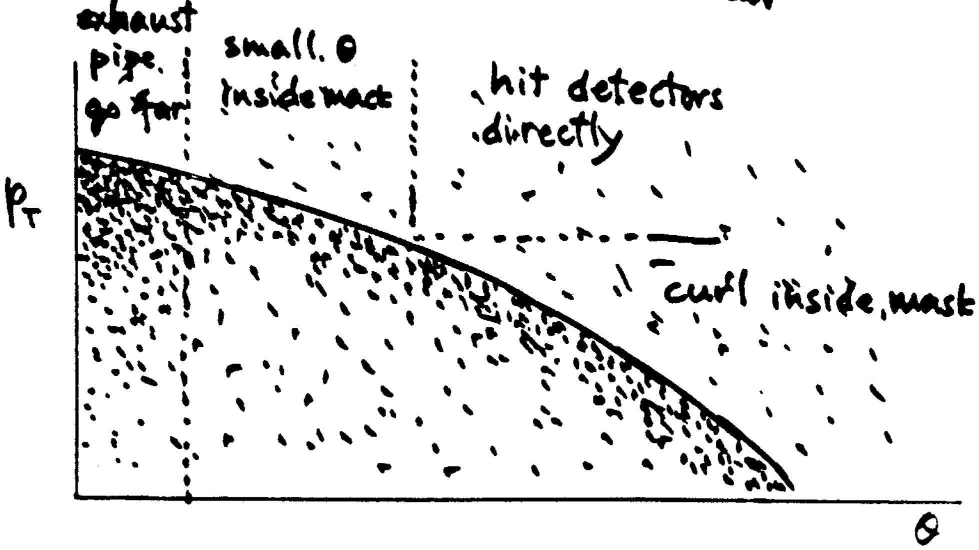

JLC 1TeV cM

@TDR.PAIR.JLC500.E5.LOCAL.PT

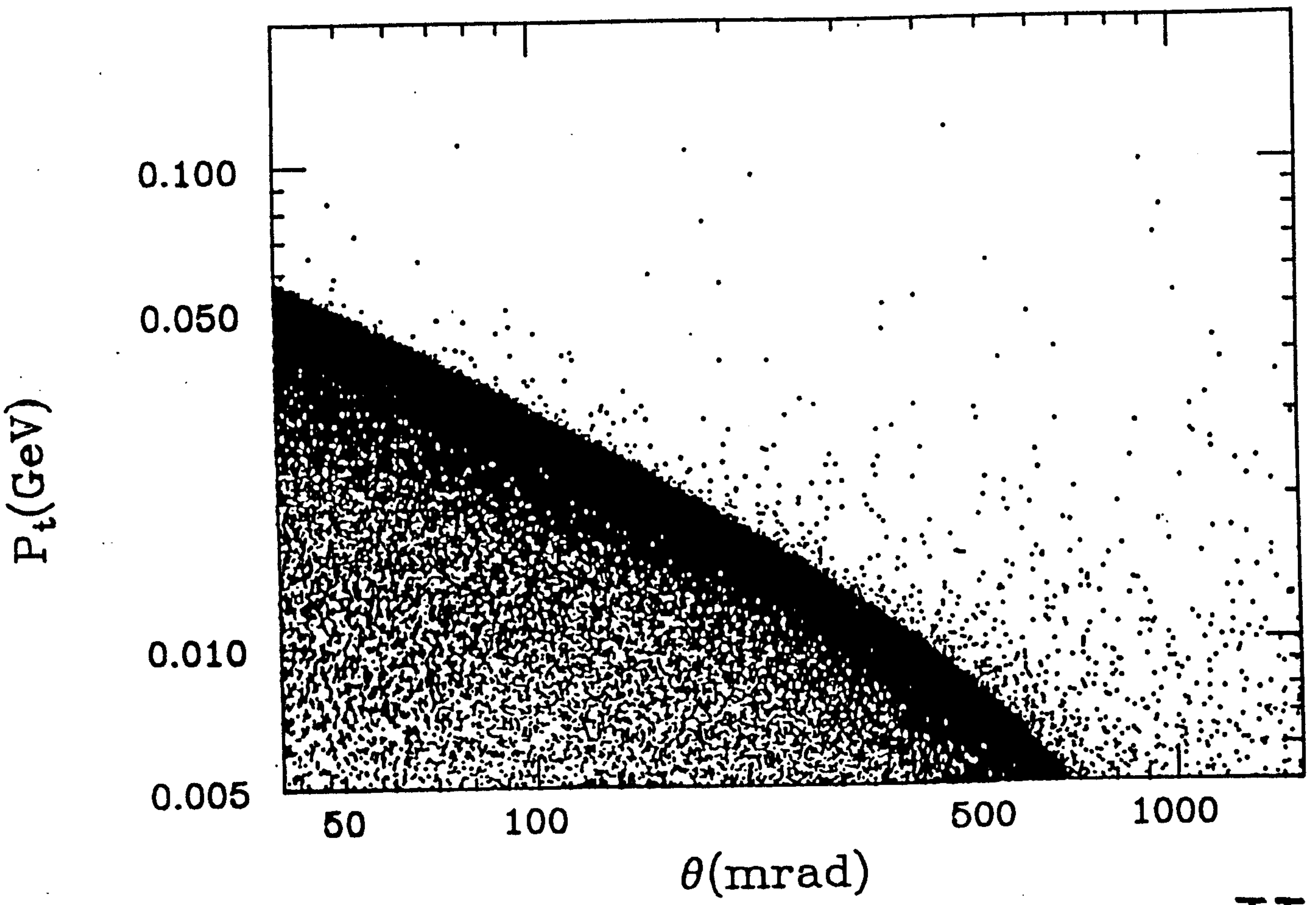

T. Tauchi

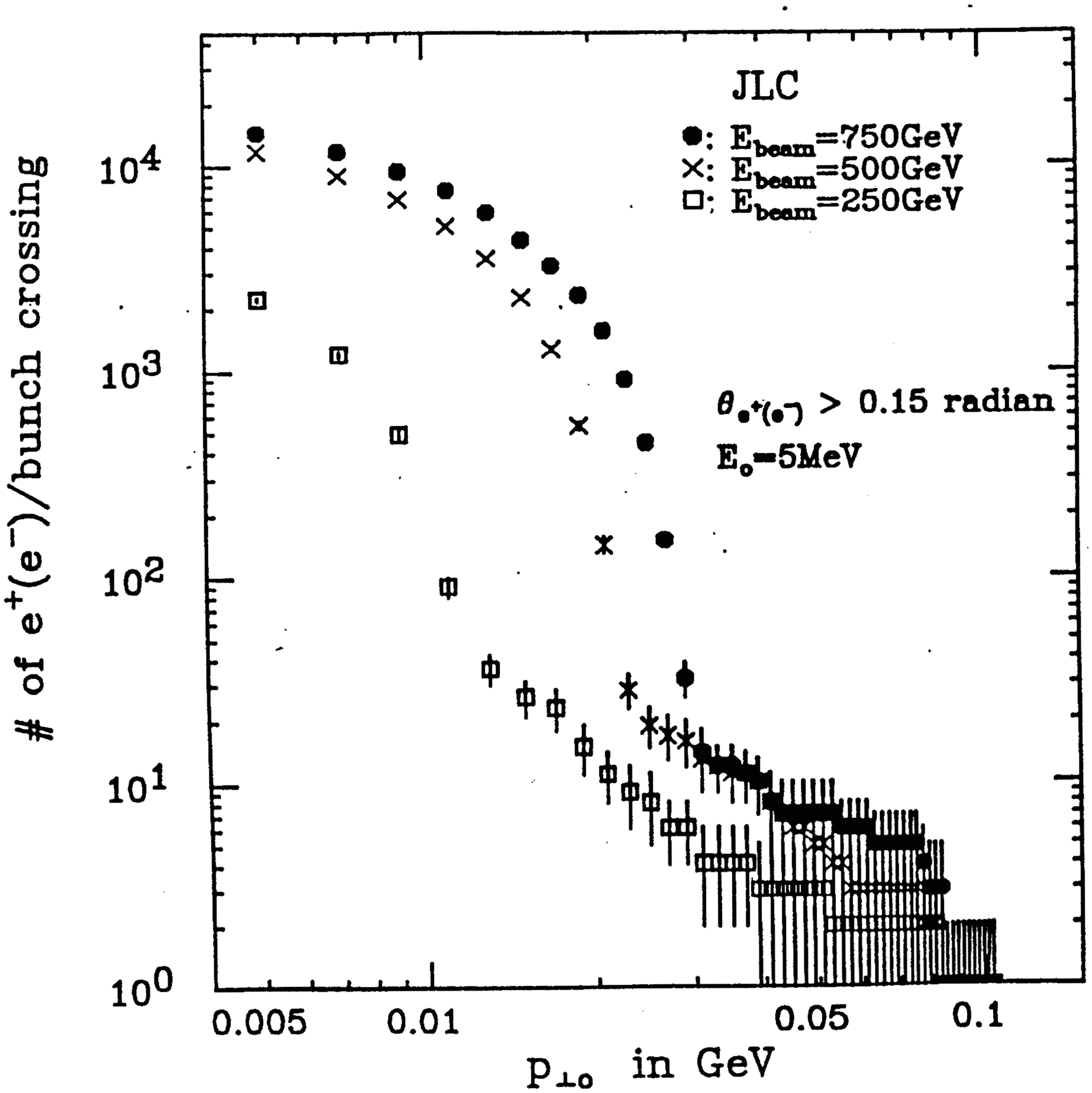
JLC
●: E_{beam}=750GeV
×: E_{beam}=500GeV
□: E_{beam}=250GeV
$\theta_{e^+(e^-)}$ > 0.15 radian
E_o=5MeV
of $e^+(e^-)$/bunch crossing
10^0
10^1
10^2
10^3
10^4
0.005
0.01
0.05
0.1
$p_{\perp o}$ in GeV

T.Tauchi

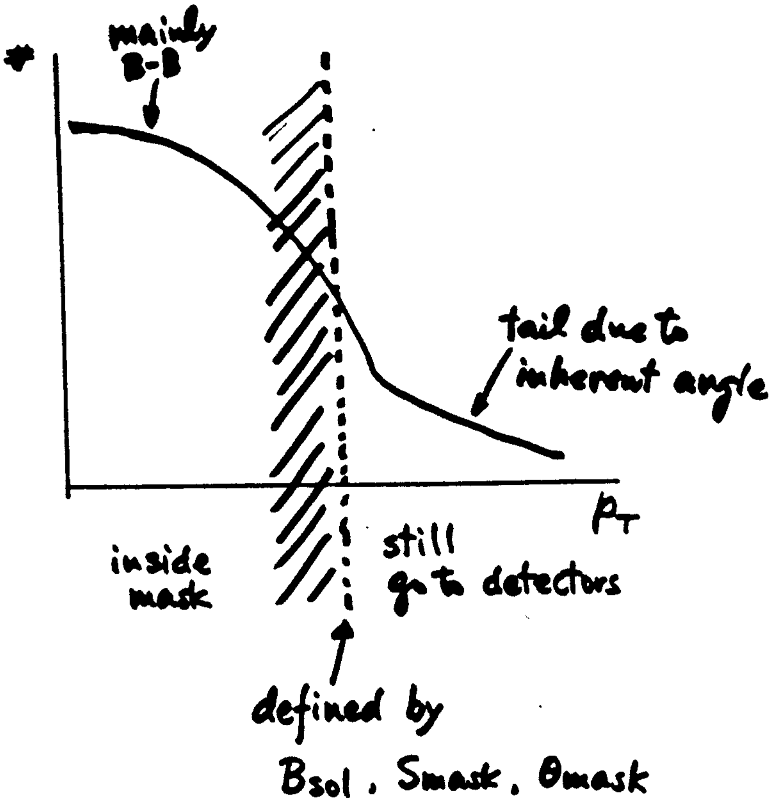

$$\theta_{mask} \propto \sqrt{\frac{N}{S_{mask} \cdot B_{sol} \cdot \sigma_z}}$$

"Mini-Jets"

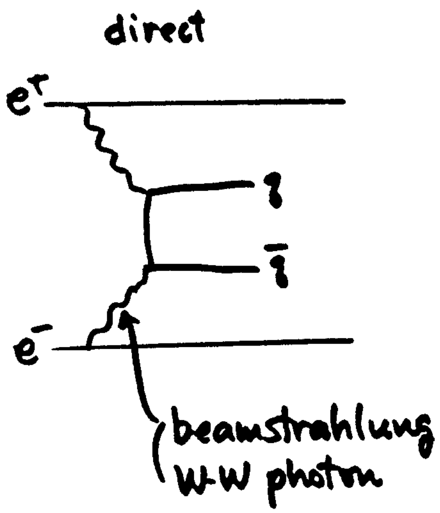

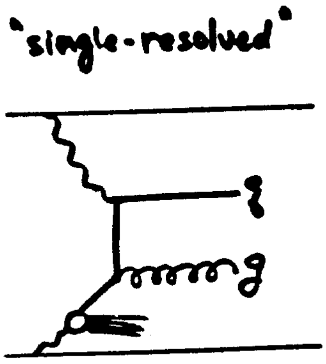

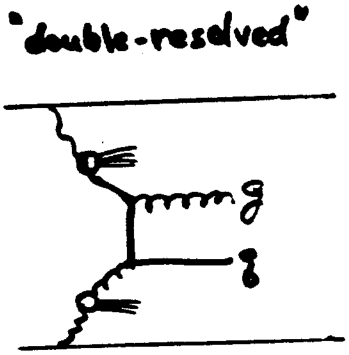

$$\sigma_{jet} = \int \underset{\text{or WW}}{F_{BS}}(x_1)\, F_{BS}(x_2) \underbrace{\left\{ \begin{array}{l} F(x_3)\, F(x_4)\ \ d\sigma_{gg,\,qq\ldots} \\ F(x_3)\, d\sigma_{\gamma q}. \\ d\sigma_{\gamma\gamma} \end{array} \right.}_{\sigma_{\gamma\gamma}}$$

↑ seen by primary e^+e^-

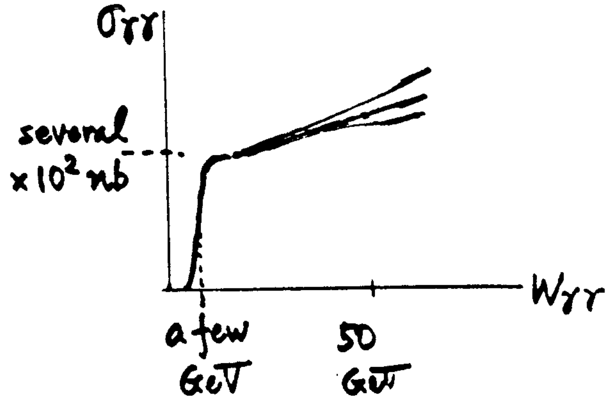

$E_{CM} = 500$ GeV

$E_{Beamstr.} \approx (20\sim40)$ GeV S band, X-band

$\gg$ a few GeV

(except TESLA)

$N_{jets} \propto n_\gamma^2$ (insensitive to Υ)

a few mini-jets / bunch train xing (JLC)

not serious at $E_{CM} \lesssim 500$ GeV

$E_{CM} \gtrsim 1$ TeV

$E_{Beamstr} \gtrsim 50$ GeV

Υ becomes important.

reduce $n_\gamma \Upsilon$

Cures

- time resolution in drift chamber
- reduce

$$\begin{pmatrix} n_\gamma^2 \\ \text{or } (n_\gamma\Upsilon)^2 \end{pmatrix} \times \frac{1}{f_{rep}} \times \frac{t_b + \Delta t_{resol}}{t_{train}}$$

DG Parameterization, No y cut.
$Q^2 = \hat{s}/4$

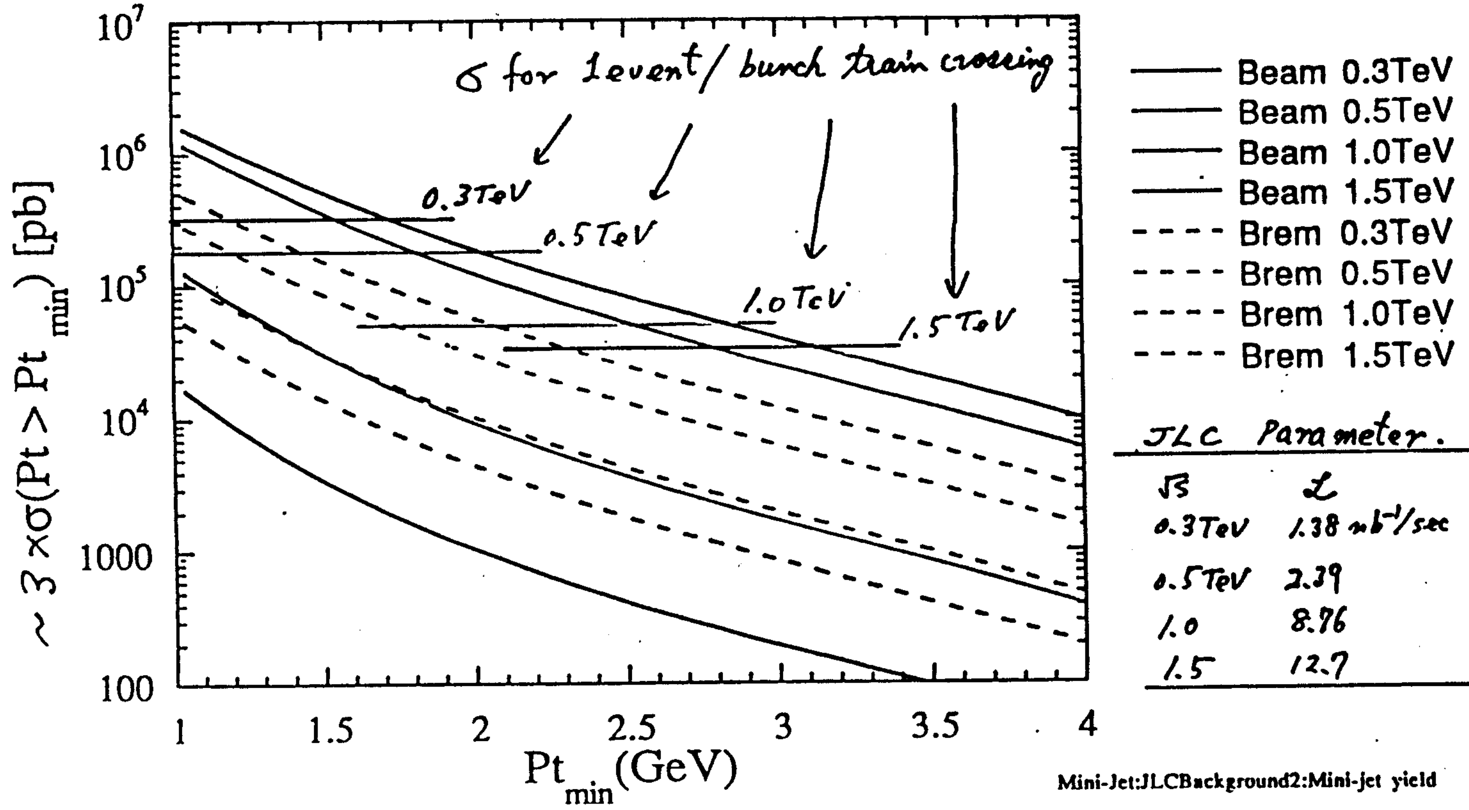

JLC Parameter.

$\sqrt{s}$	$\mathcal{L}$	σ for 1eve per train
0.3TeV	1.38 nb^{-1}/sec	109 nb
0.5TeV	2.39	63
1.0	8.76	17
1.5	12.7	12

Mini-Jet:JLCBackground2:Mini-jet yield

Miyamoto

Mini-jet yield (DG, no y cut)

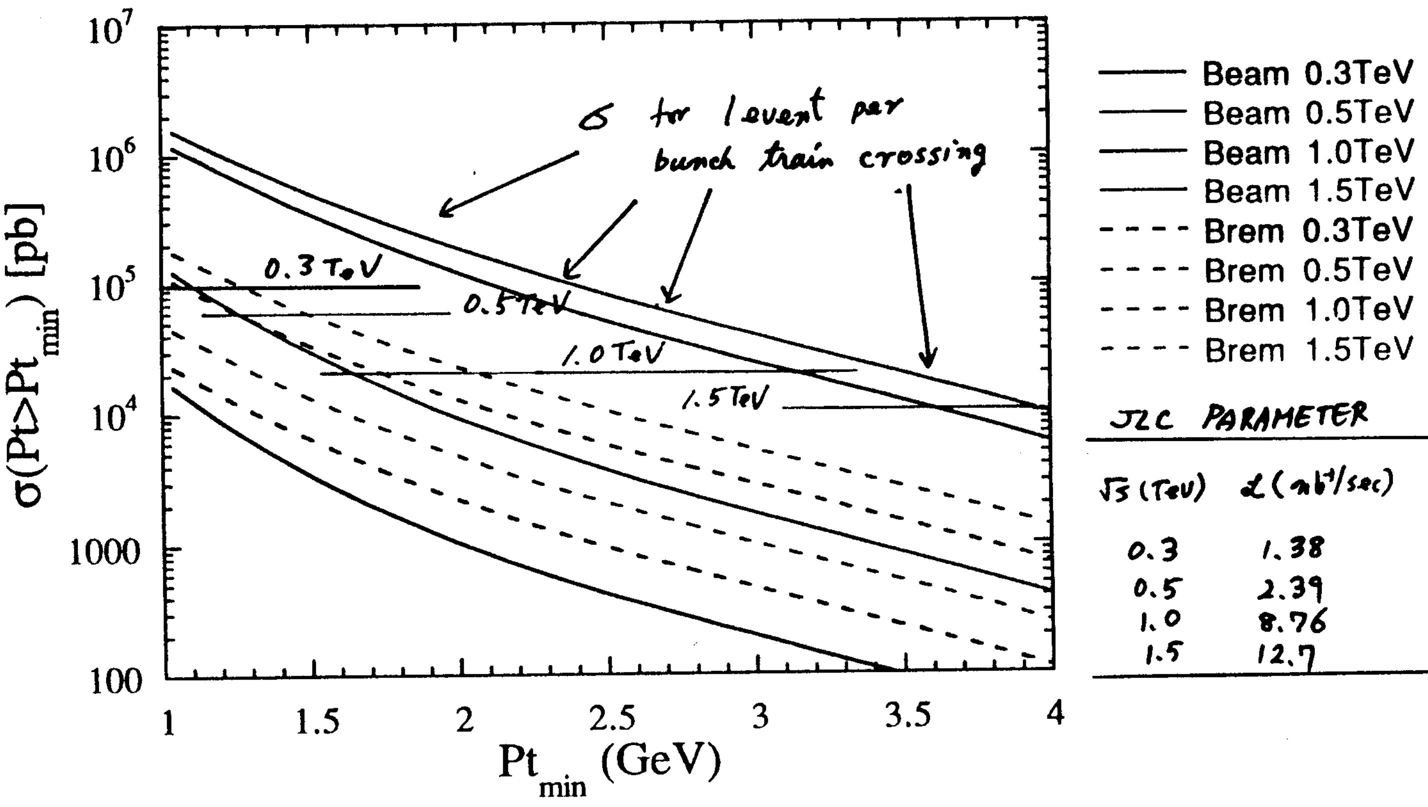

JLC PARAMETER

√s (TeV)	$\mathcal{L}$ (nb⁻¹/sec)	σ for 1 event per train
0.3	1.38	109
0.5	2.39	63
1.0	8.76	17
1.5	12.7	12

Miyamoto

IR Design Issues

FFIR 3/2/92

based on experience of
SLD & MARK II at SLC

Henry Band
T. Maruyama
S. Hertzbach
R. Kofler
+ many others
in SLD
(now that there
is data & backgrounds)

Hobey DeStaebler
Bob Jacobsen
Dave Burke

S.S. Hertzbach
Univ. of Massachusetts
3/2/92

Backgrounds → Particles in detector from sources other than the physics under study.

Sources

Accelerator
- Synchrotron Radiation
  - Bends
  - Final Quads
- Muons
  - Collimators
- Soft e^-, e^+, γ
  - Collimators
  - Detector Masks

Beam - Gas Interactions

Beam - Beam Interactions

→ All but Beam - Beam at SLC

STORAGE RING

vs.

SINGLE PASS COLLIDER

Long τ (hours) in <u>STORAGE RING</u>
⇒ few particles lost
per turn
⇒ Low Background
per beam crossing

<u>SINGLE PASS COLLIDER</u>
⇒ each pulse is "new fill"
⇒ large losses / pulse
⇒ LARGE BACKGROUND
per bunch crossing

In <u>BOTH</u> cases <u>non</u>-<u>Gaussian</u>
<u>beam</u> "<u>tails</u>" dominate
synchrotron radiation backg'd
& probably other sources also.

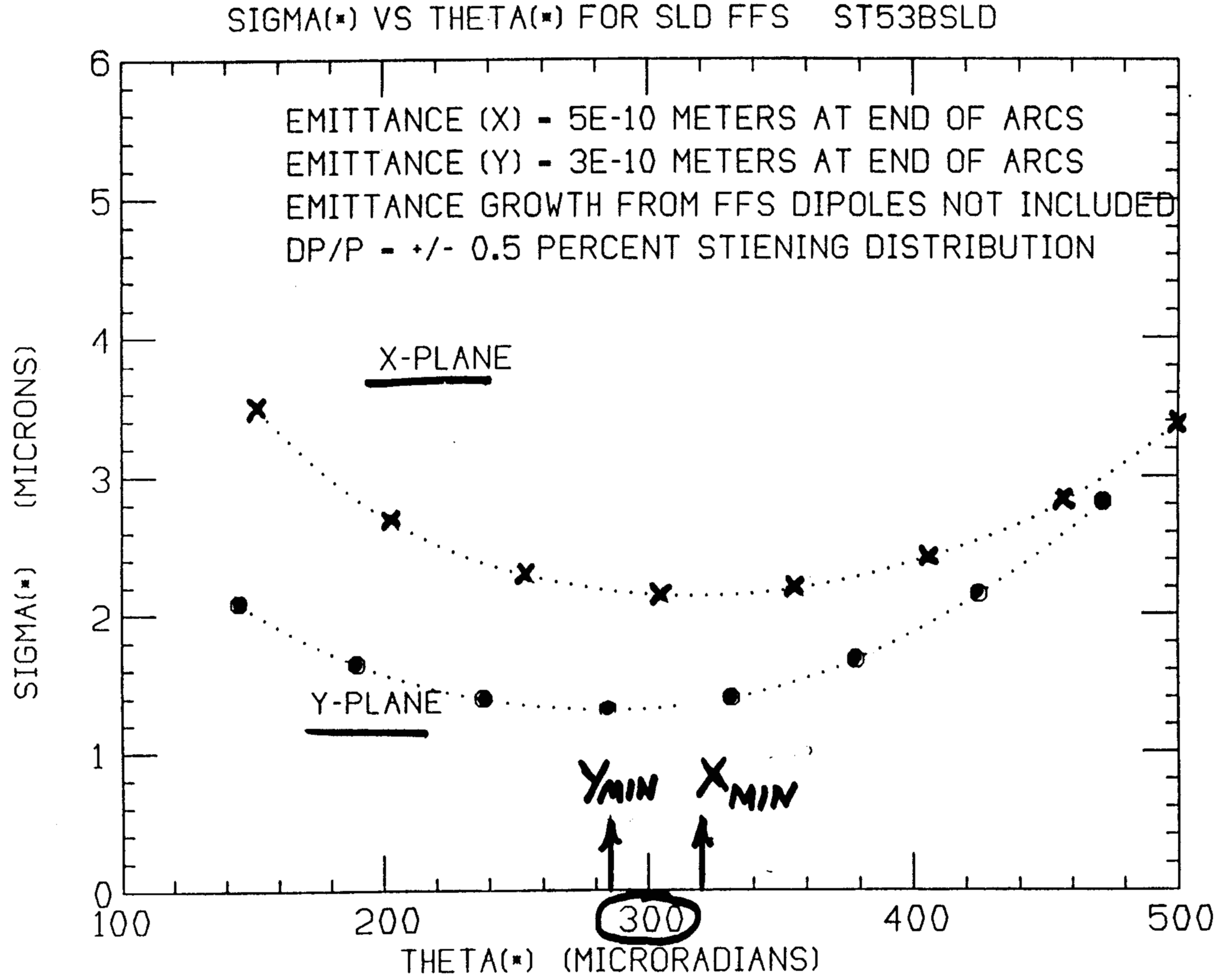

There is an optimal θ^* to minimize beam spot.

Large $\theta^* \Rightarrow$ Large beam in final triplet.

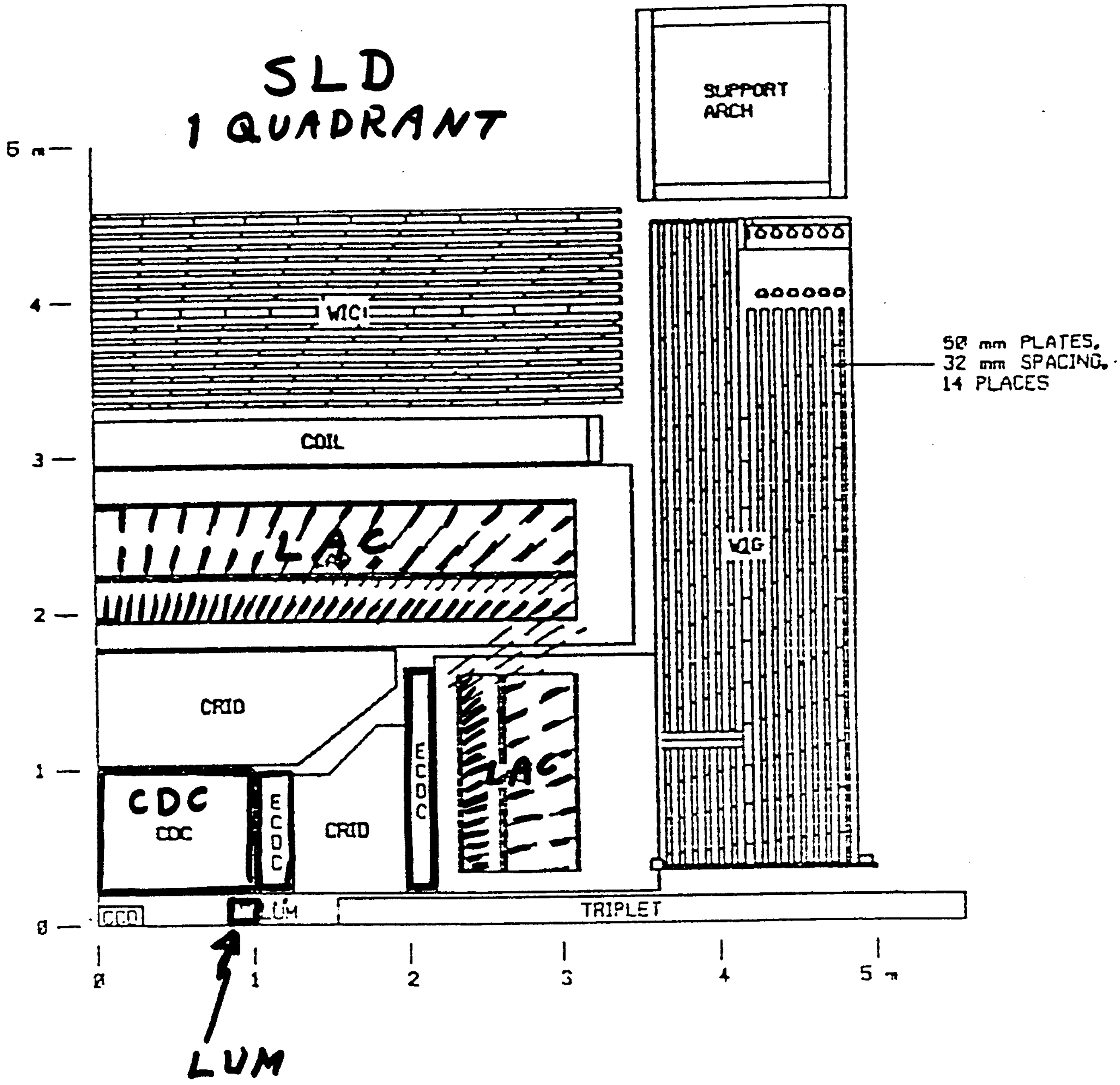
SLD
1 QUADRANT
SUPPORT ARCH
WIC
COIL
LAC
CRID
CDC
CDC
ECDC
CRID
ECDC
LAC
WIC
50 mm PLATES,
32 mm SPACING,
14 PLACES
CCD
LUM
TRIPLET
LUM
5 m
4
3
2
1
0
0
1
2
3
4
5 m

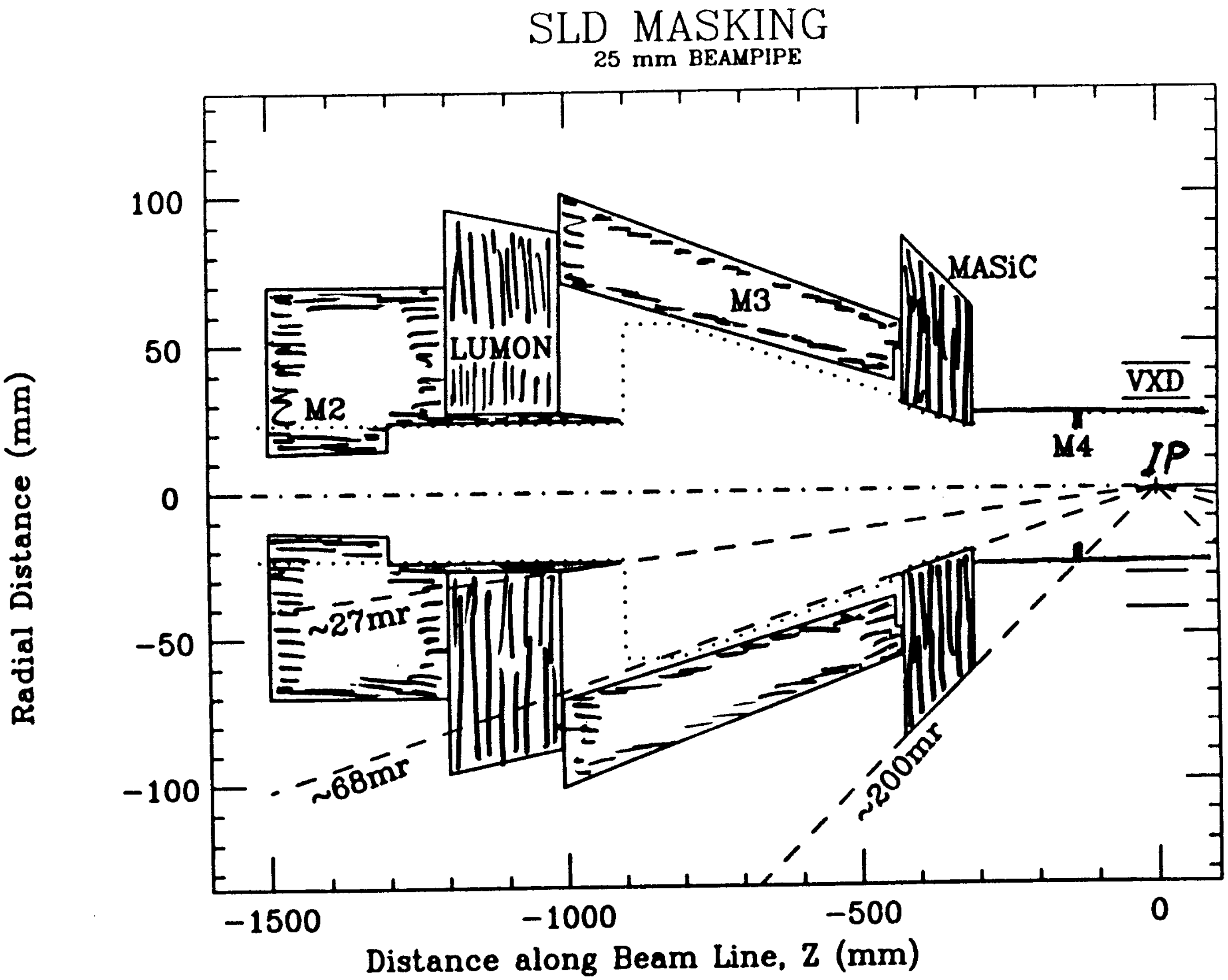
SLD MASKING
25 mm BEAMPIPE
M2
LUMON
M3
MASiC
VXD
M4
IP
~27mr
~68mr
~200mr
100
50
0
-50
-100
-1500
-1000
-500
0
Radial Distance (mm)
Distance along Beam Line, Z (mm)

SLD Backgrounds in 1991 Engineering Run

Not a problem for

Radiation Damage

Off-line analysis in

central (barrel) region

Problem for End Cap Detectors

Problem for Energy Trigger

& Dead Time

⇒ TUNING REQUIRED

All backgrounds seem to increase with θ^*.

Some indication backgrounds were related to "bad" beampulses?

Backgrounds lower for

Z & Bhabba events

& 'random' triggers than

for typical Energy Trigger.

Soft Bend Synchrotron Radiation

Calculate 0.1% CDC occ. / 10^{10} e

Observe $\lesssim$ 0.2% per 10^{10} e^+

⇒ 1 to 2% ; not a problem; calculated to facter of ~2.

Quadrupole Synchrotron Radiation

Calculations seem qualitatively OK.

Sensitive to:

- Non-Gaussian Beam Tails
- Collimation of Beam

$$\begin{array}{c} \text{Alignment} \\ \sim 250\mu\text{m} \end{array} \left\{ \begin{array}{l} \text{Detector} \\ \text{Beam Pipe} \\ \text{SCFF triplets} \end{array} \right.$$

- θ_x^*, θ_y^* (& ε_x, ε_y)

Tuning Required to control in CDC.

Muons & soft shower debris

Sensitive to

- Tails
- Collimation
- θ^*

RUN 2298, EVENT 326
BEAM CROSSING 3059170
11-AUG-1991 23:47
SOURCE: RUN DATA

ENGINEERING RUN

<u>SLD</u>

2 tracks with Background & "Chromosomes"

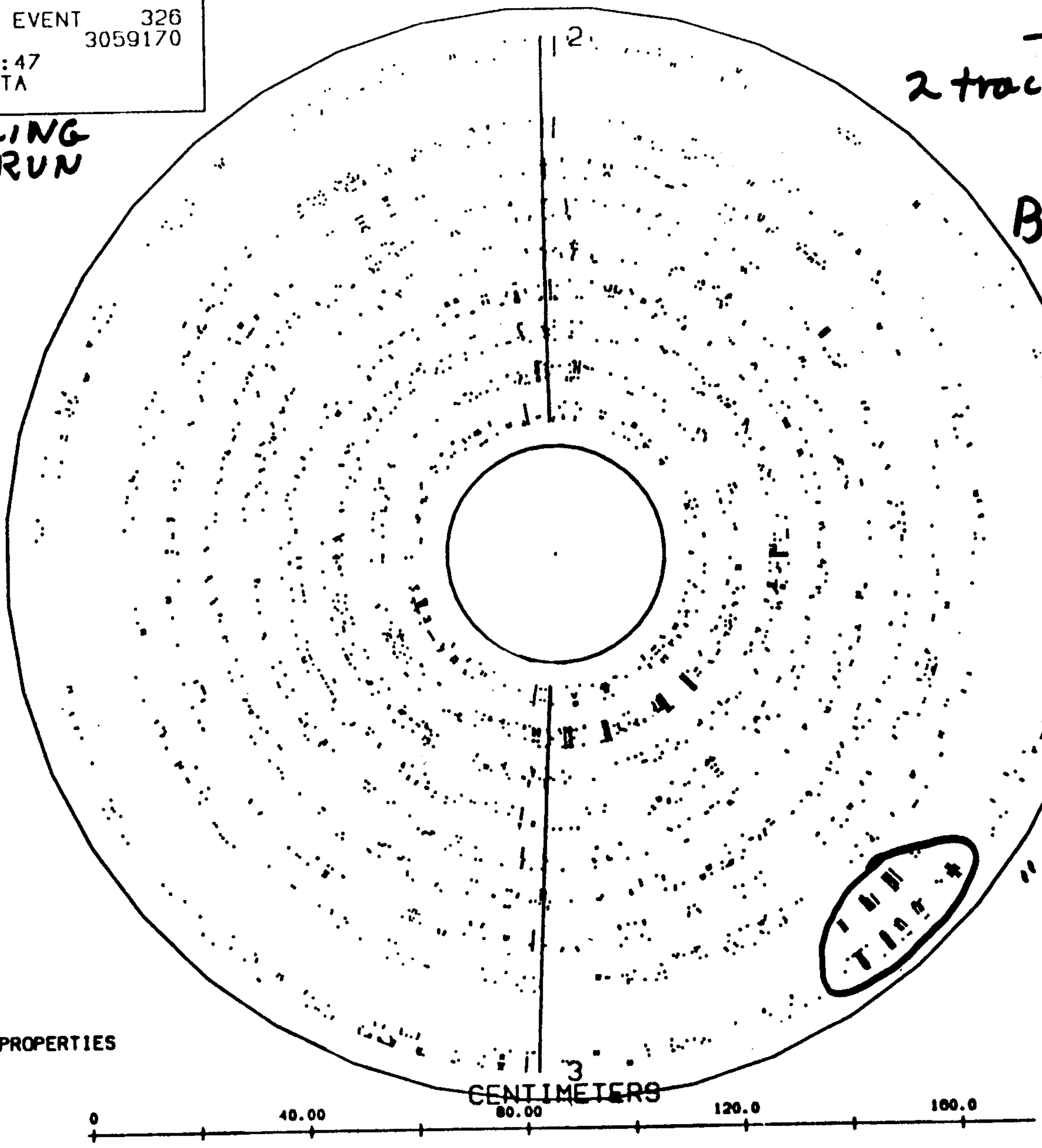

Display conditions:

MONTE CARLO TRACK PROPERTIES

P_{trk} > 2.000 GeV/c

Cos(θ_{trk}) < 1.000

ϕ_{trk} < 2.000 π

R_{origin} > 0.000 cm

RUN 2139, EVENT 1296
BEAM CROSSING 5442988
7-AUG-1991 07:33
SOURCE: RUN DATA

Cleaner 2-track event.

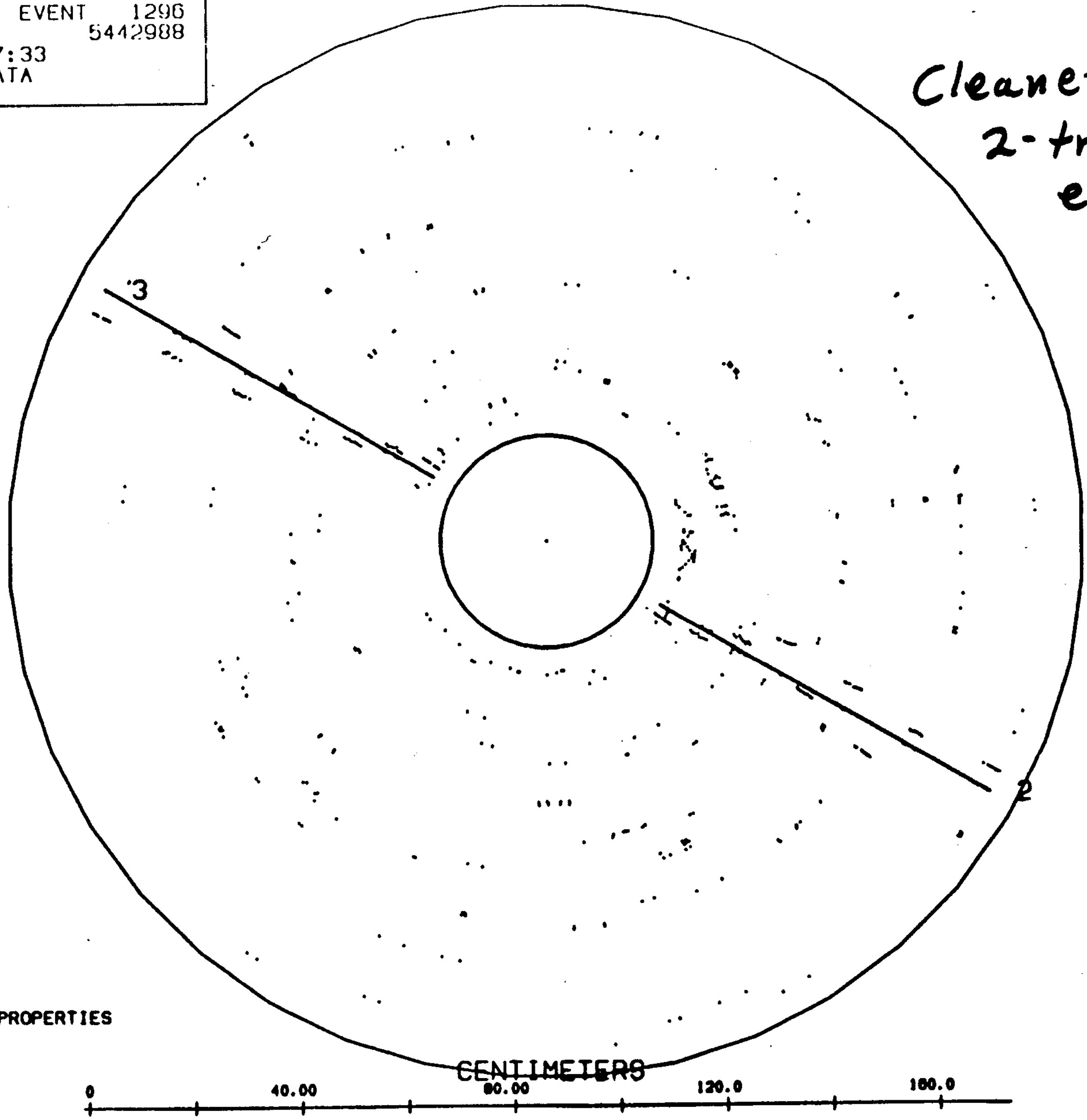

Display conditions:

MONTE CARLO TRACK PROPERTIES
P_{trk} > 2.000 GeV/c
Cos(θ_{trk}) < 1.000
ϕ_{trk} < 2.000 π
R_{origin} > 0.000 cm

RUN 2225, EVENT 85
BEAM CROSSING 306870
9-AUG-1991 17:21
SOURCE: RUN DATA

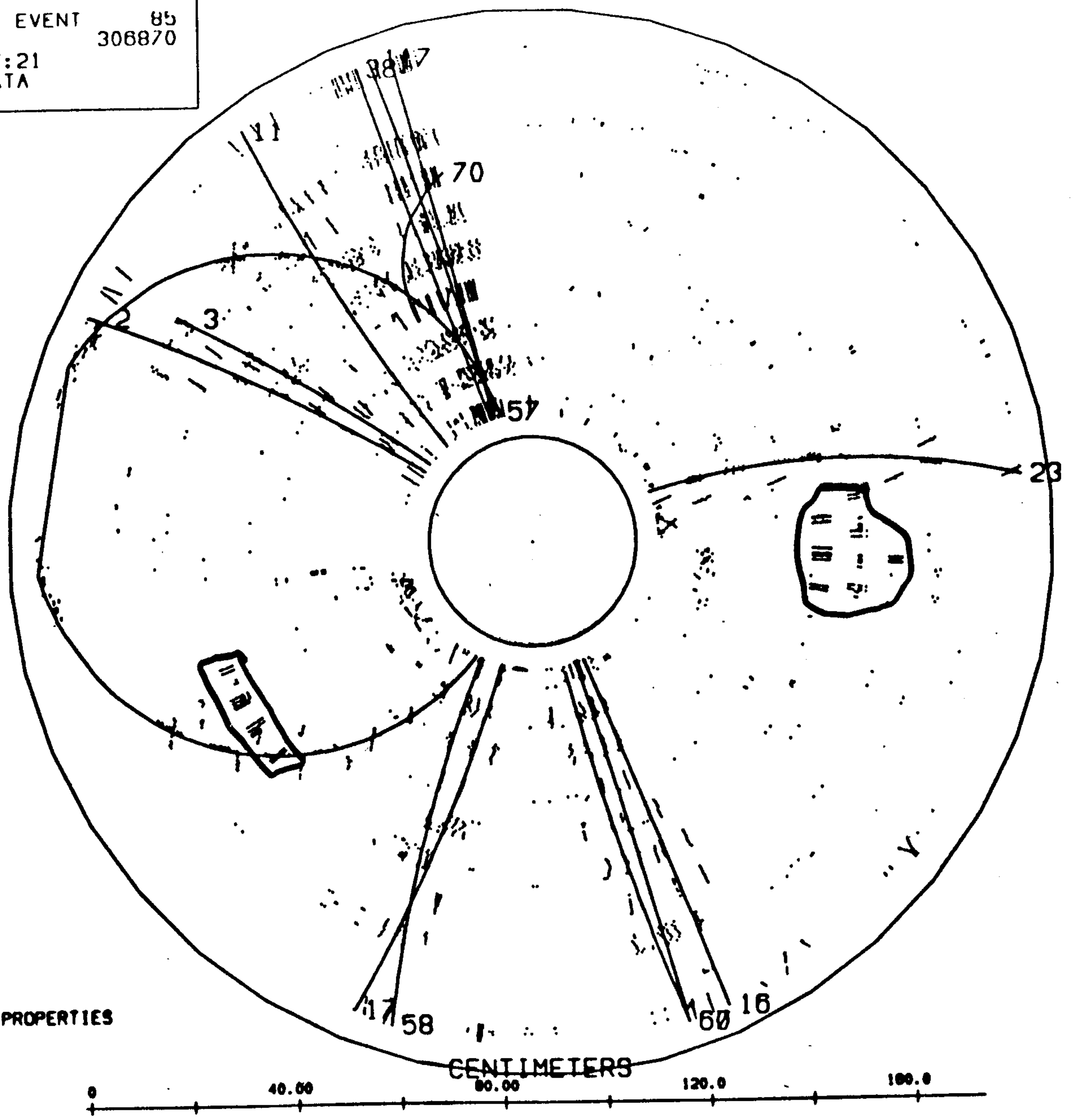

Display conditions:

MONTE CARLO TRACK PROPERTIES

p_{trk} > 2.000 GeV/c

Cos(θ_{trk}) < 1.000

ϕ_{trk} < 2.000 π

R_{origin} > 0.000 cm

Central Drift Chamber

- occupancy on typical calorimeter energy triggers > on Z's.
- occupancy on 'random' (timeout) triggers & Z's ~ 11%

Also "chromosomes" & entire layers "hit"
Cause? large local energy deposit + electronics?
?Compton e⁻ from wires?

Occupancy sensitive to
- Collimation
- θ^*
- orbits
- e⁻ energy spread

Generally under control, but required tuning.

Alignment improved for 1992 run; will study detector alignment.

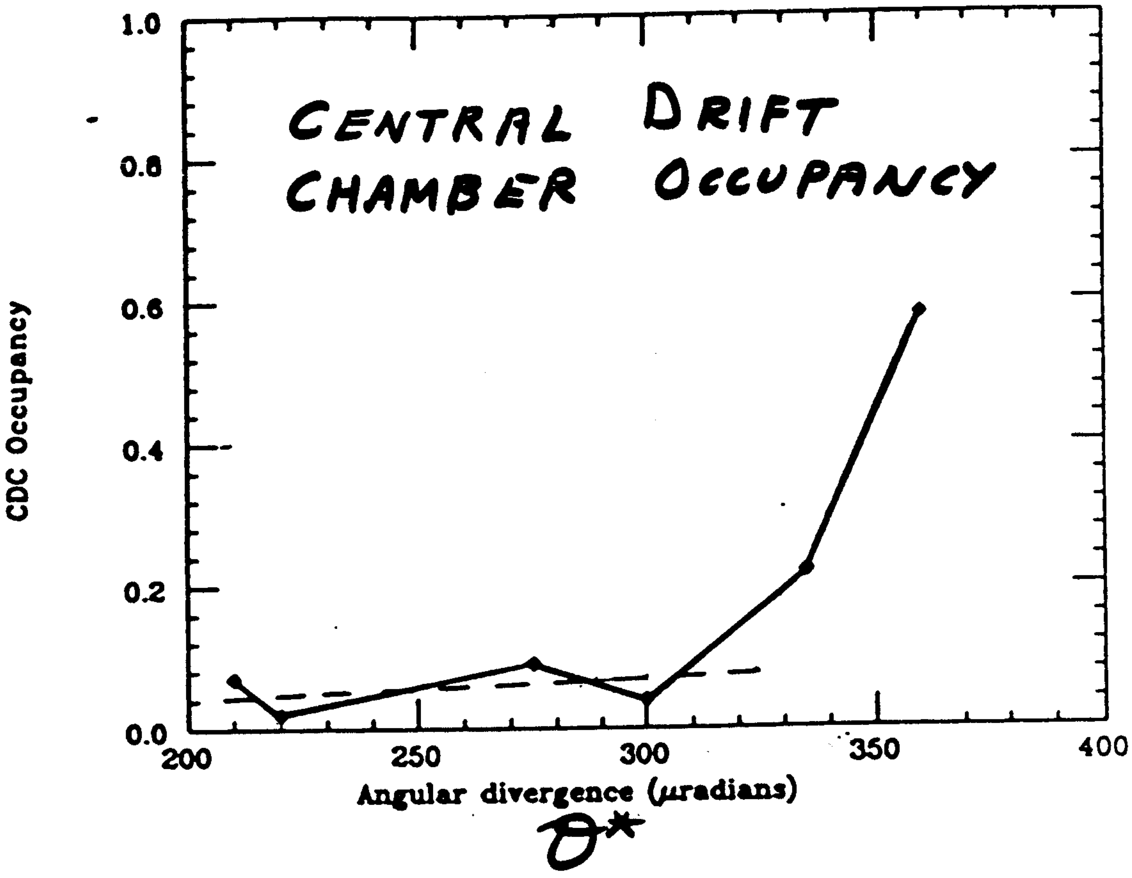

Backgrounds vs ip divergence
e^- only

Calculated CDC occupancy
Based on Quad 5 R

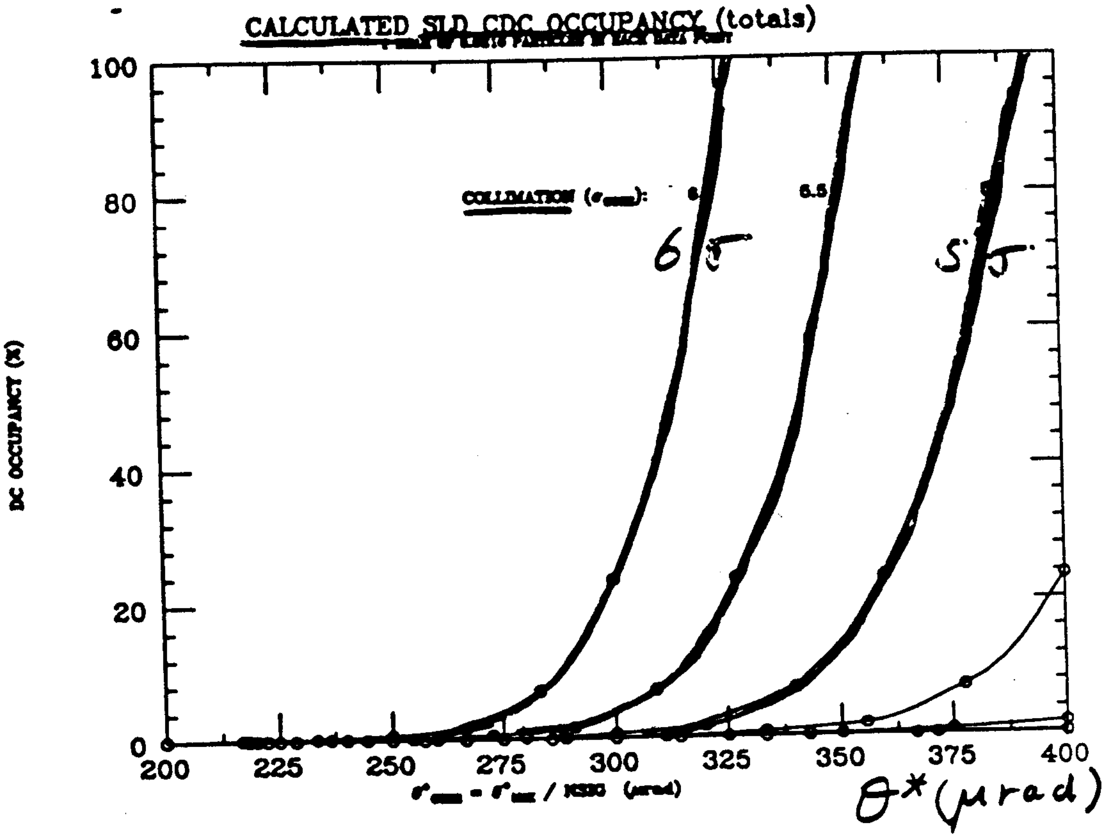

SLD BACKGROUNDS from e^-
vs IP DIVERGENCE (θ^*)

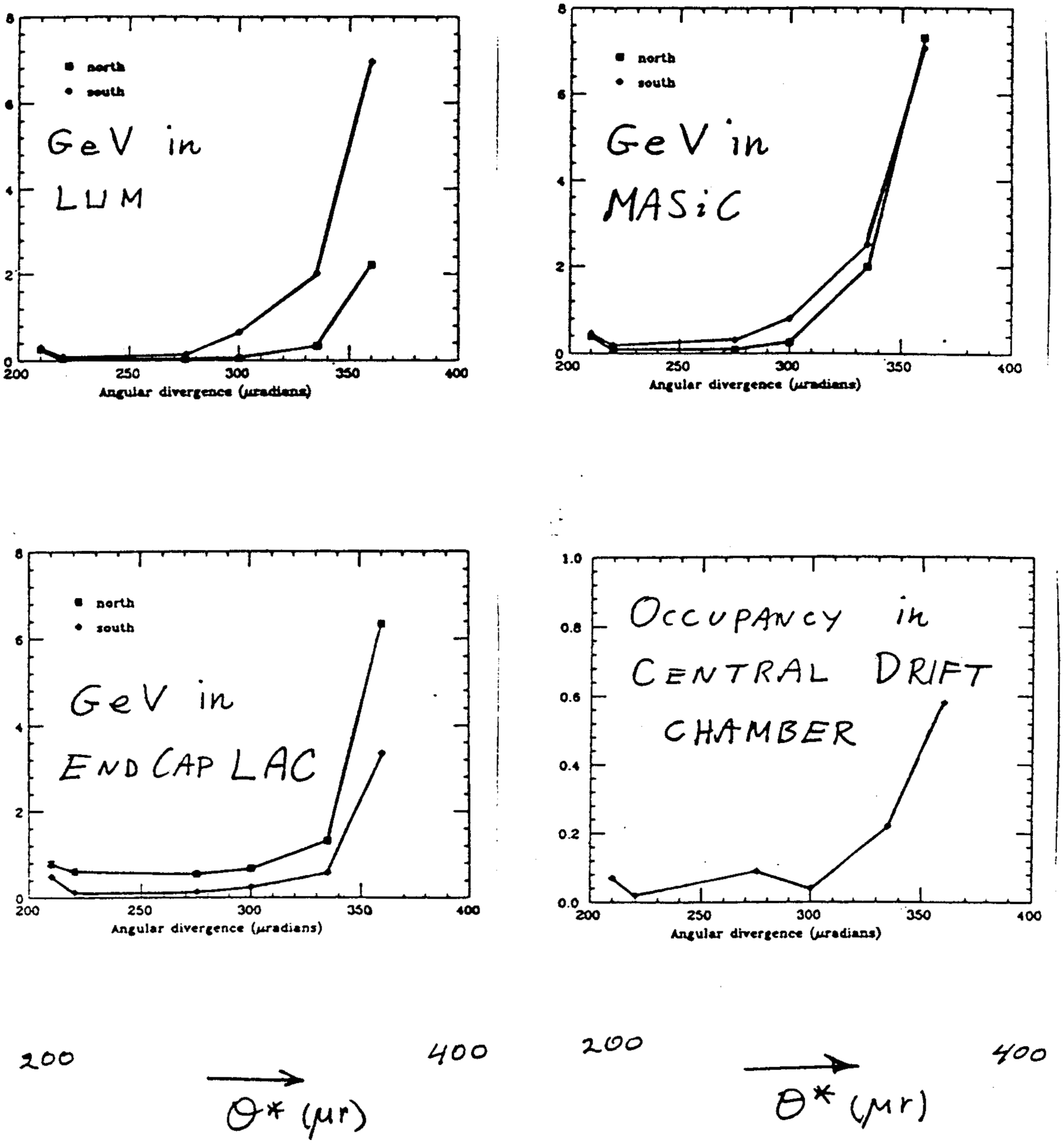

MUONS - from e^- on FF collimator(s)
- rate depends on collimator (s)
- $\sim 0.5\ \mu/m^2$ at detector per 10^8 e on C_{1X} (~100 m)

For Z events: $\langle\mu\rangle \sim 1.7$ in LAC per event
$\langle\mu\rangle \sim 14$ in WIC per event
worse in endcaps

μ's can also generate LAC Energy Trigger

Software removal of LAC μ's
→ some data loss
? ⇒ would μ filter in trigger introduce bias?

TOROIDS - modify?
Major effort required to reduce μ's by only small factors.
BEST NOT TO MAKE μ's

Also SLD small radius background
- Suspect shower debris
- Shielding improved for 1992 run.

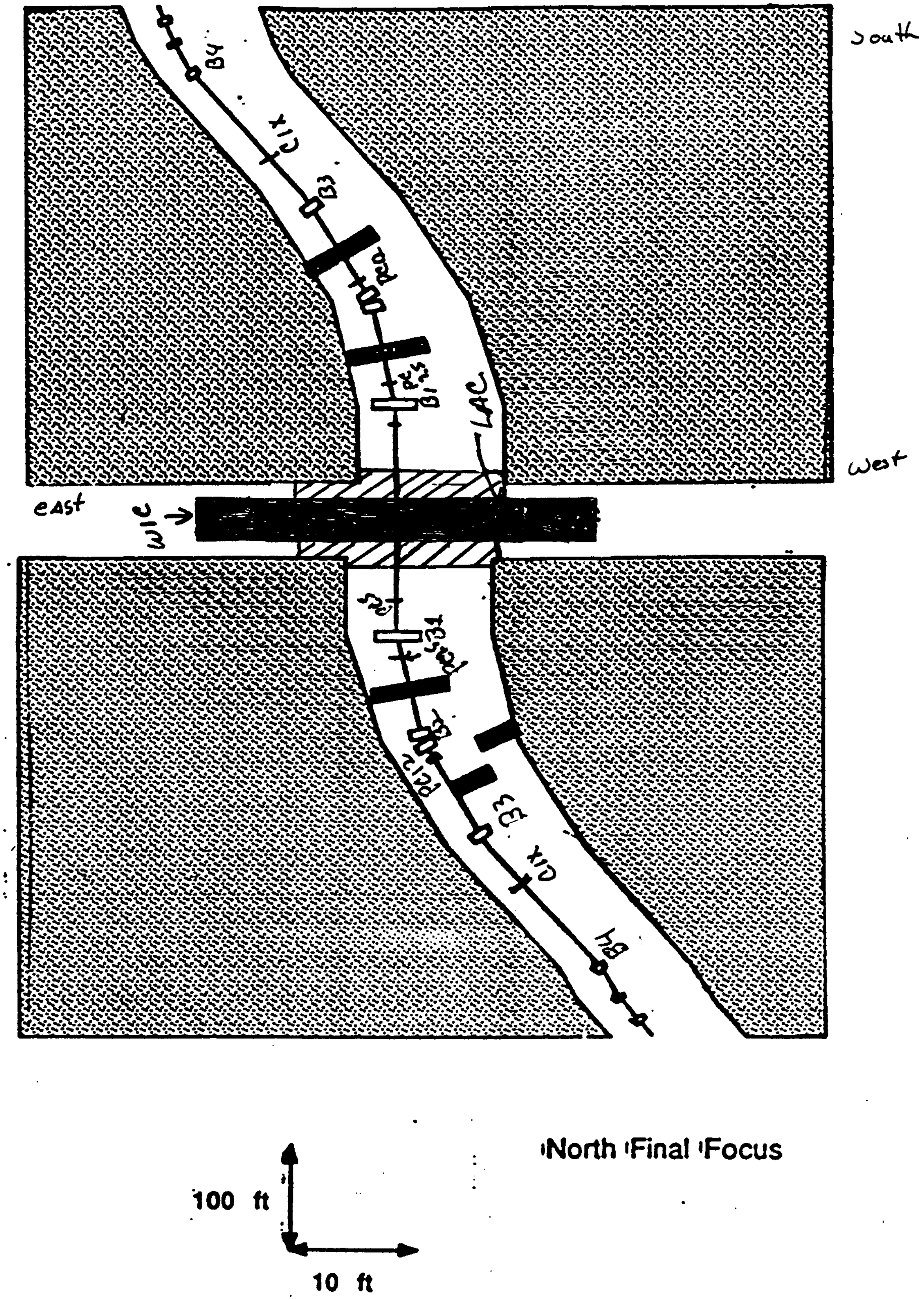

North Final Focus

RUN 2278; EVENT 525
BEAM CROSSING 3464566
11-AUG-1991 10:33
SOURCE: RUN DATA

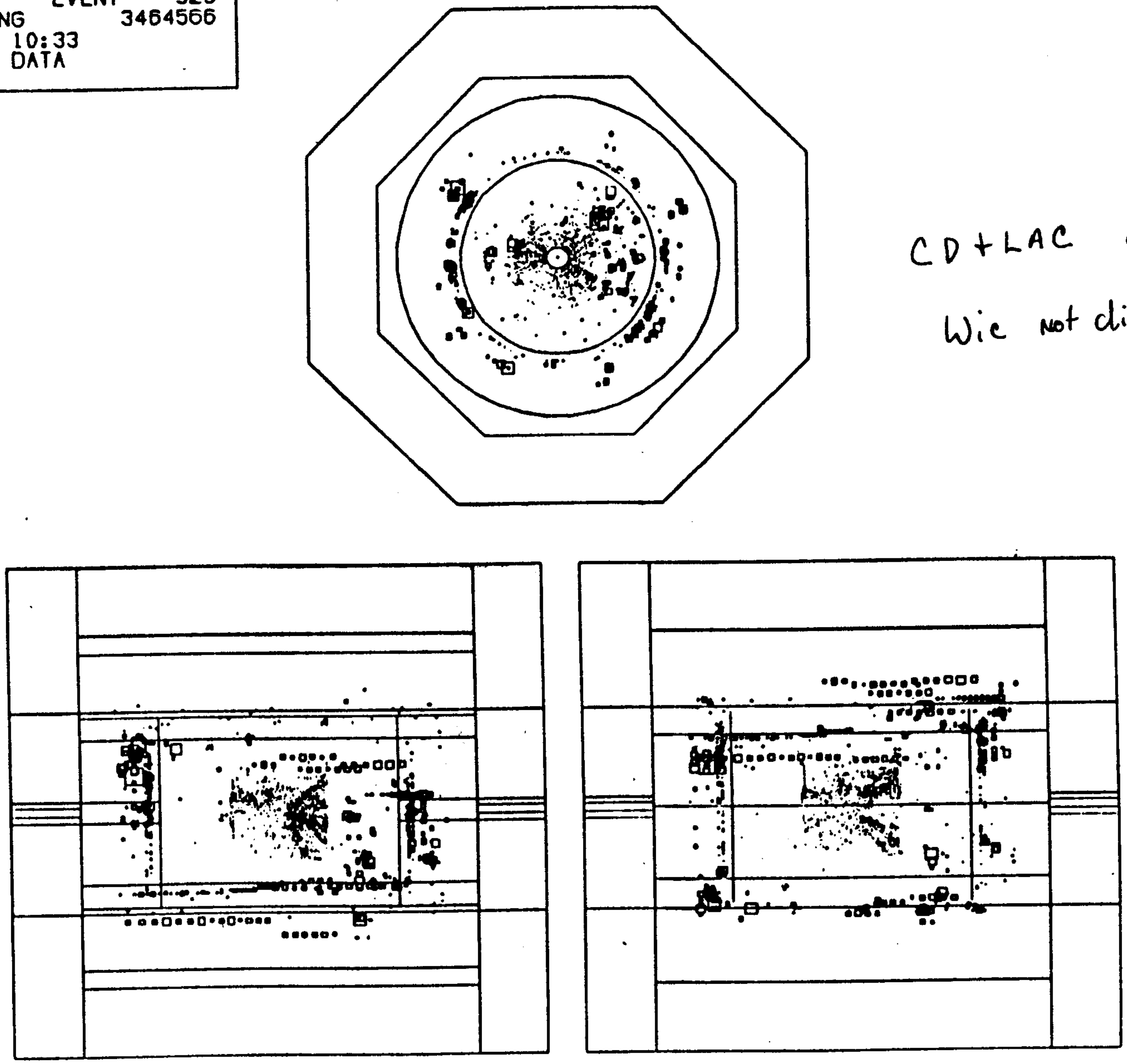

CD + LAC only

Wic not displayed

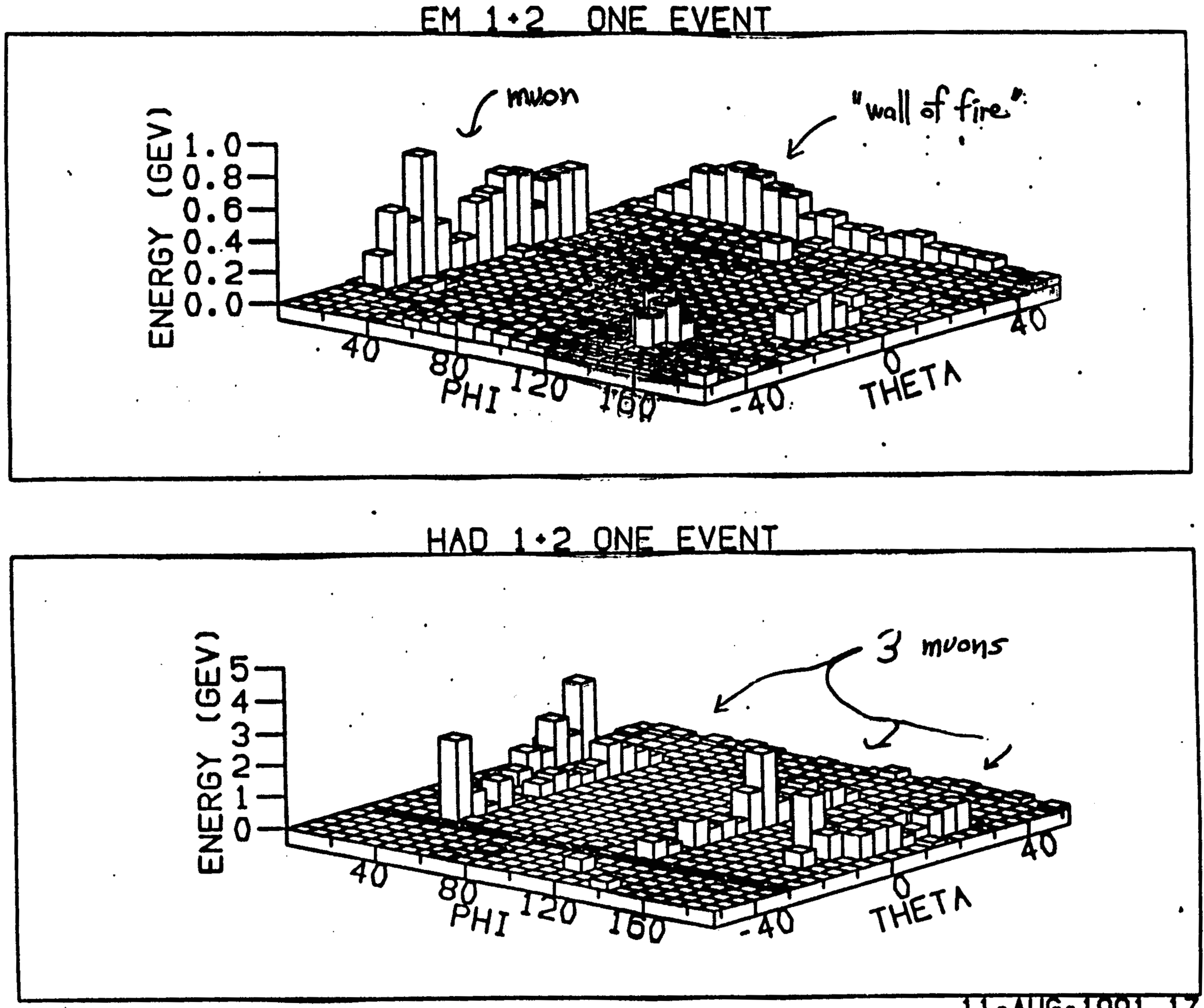

KOE: #HIT=1104 RUN -2 EVENT 311

11-AUG-1991 17:24:27

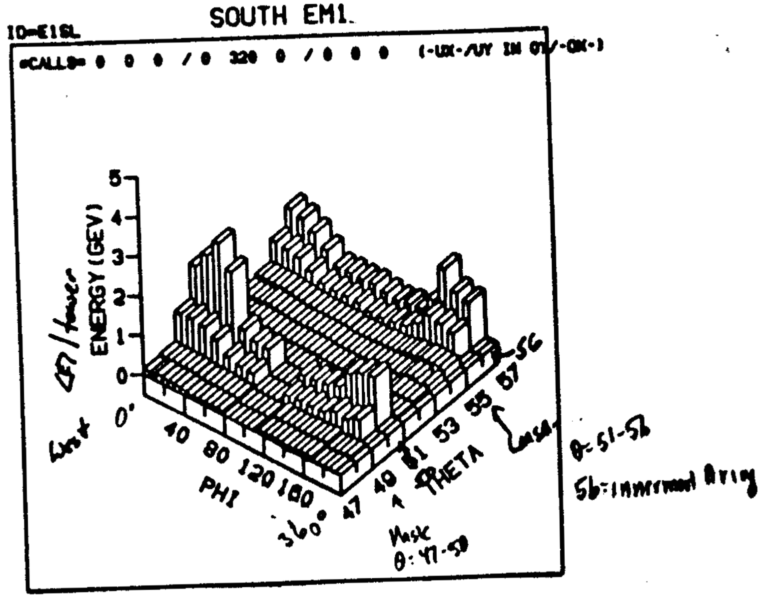

θ=51-56

56=innermost Ring

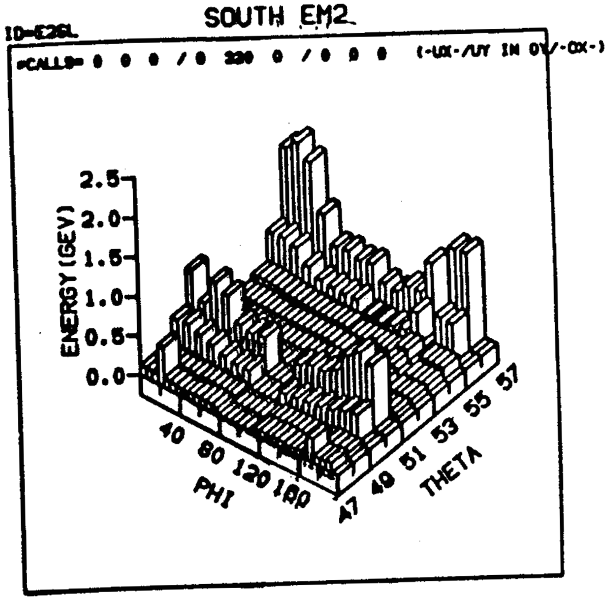

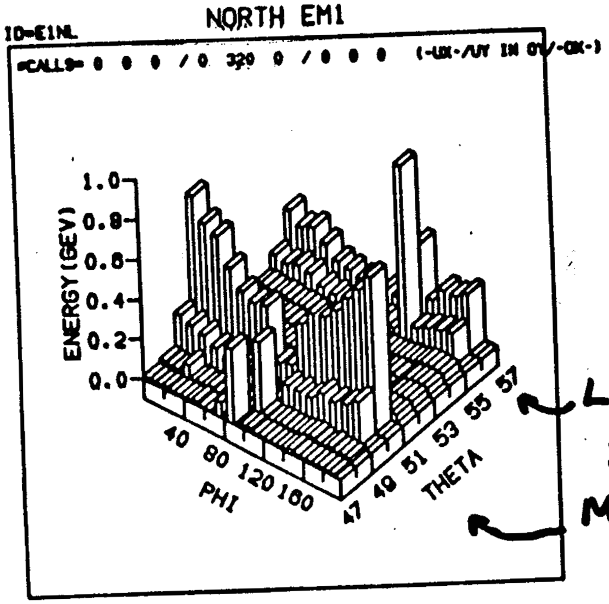

LUM
&
MASiC

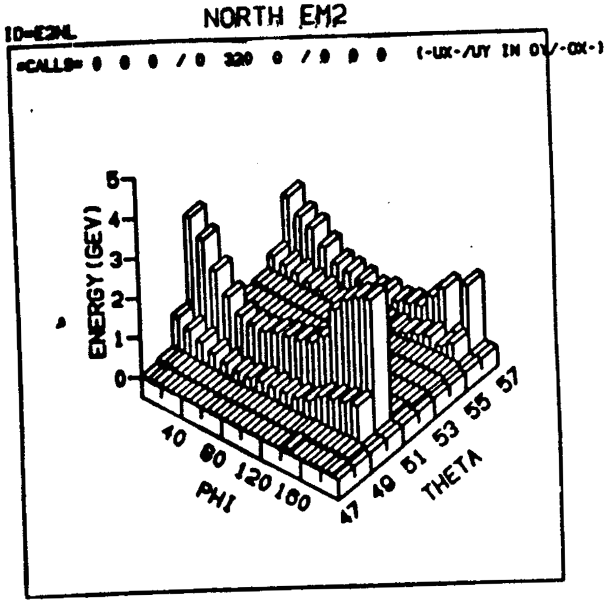

2314BKG 12SEP91

PC12 tight

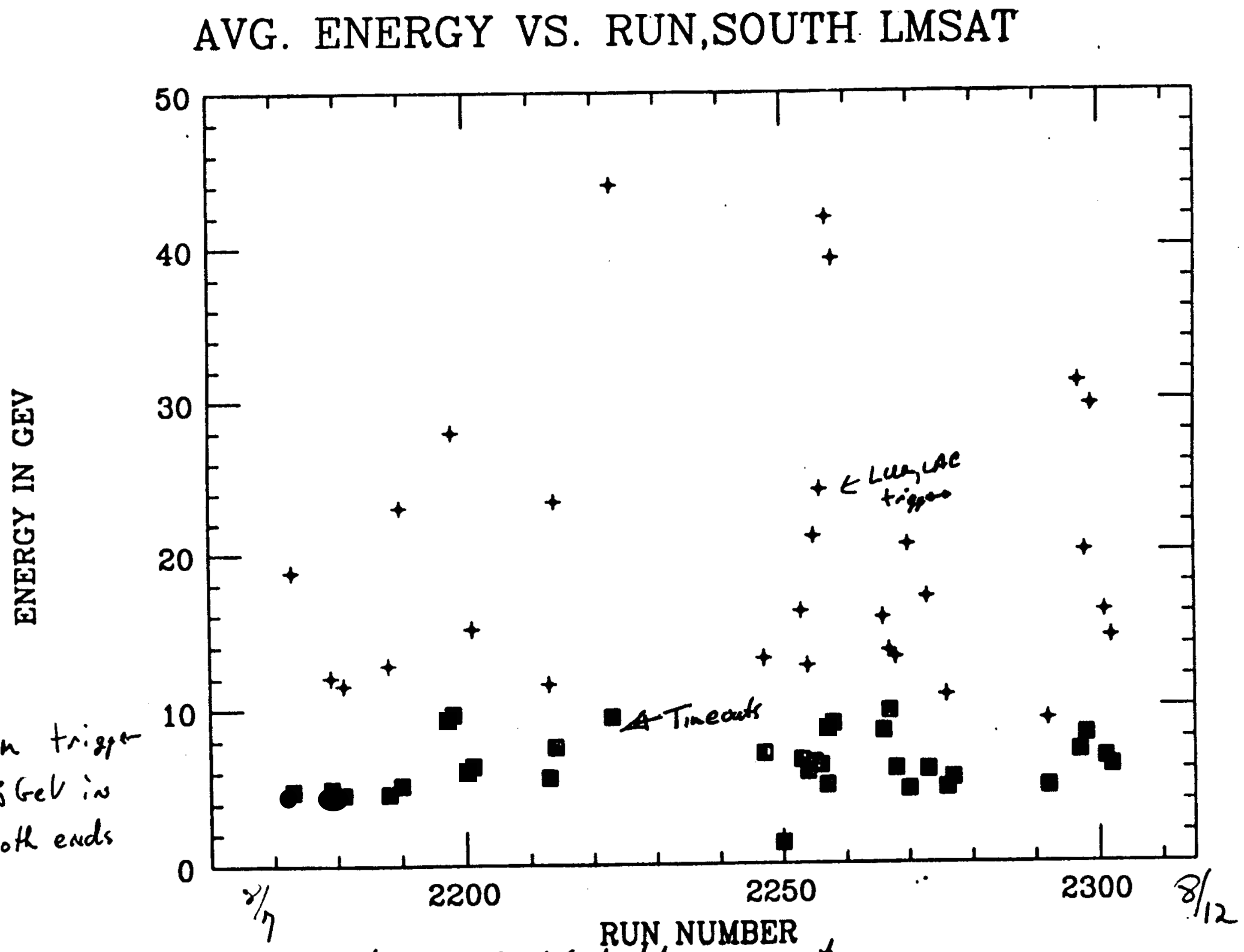

Lum trigger >7.5 GeV in both ends

Applying > 1 GeV/tower cut lowers average energy by 2 → 6

S. White

CD Occupancy North

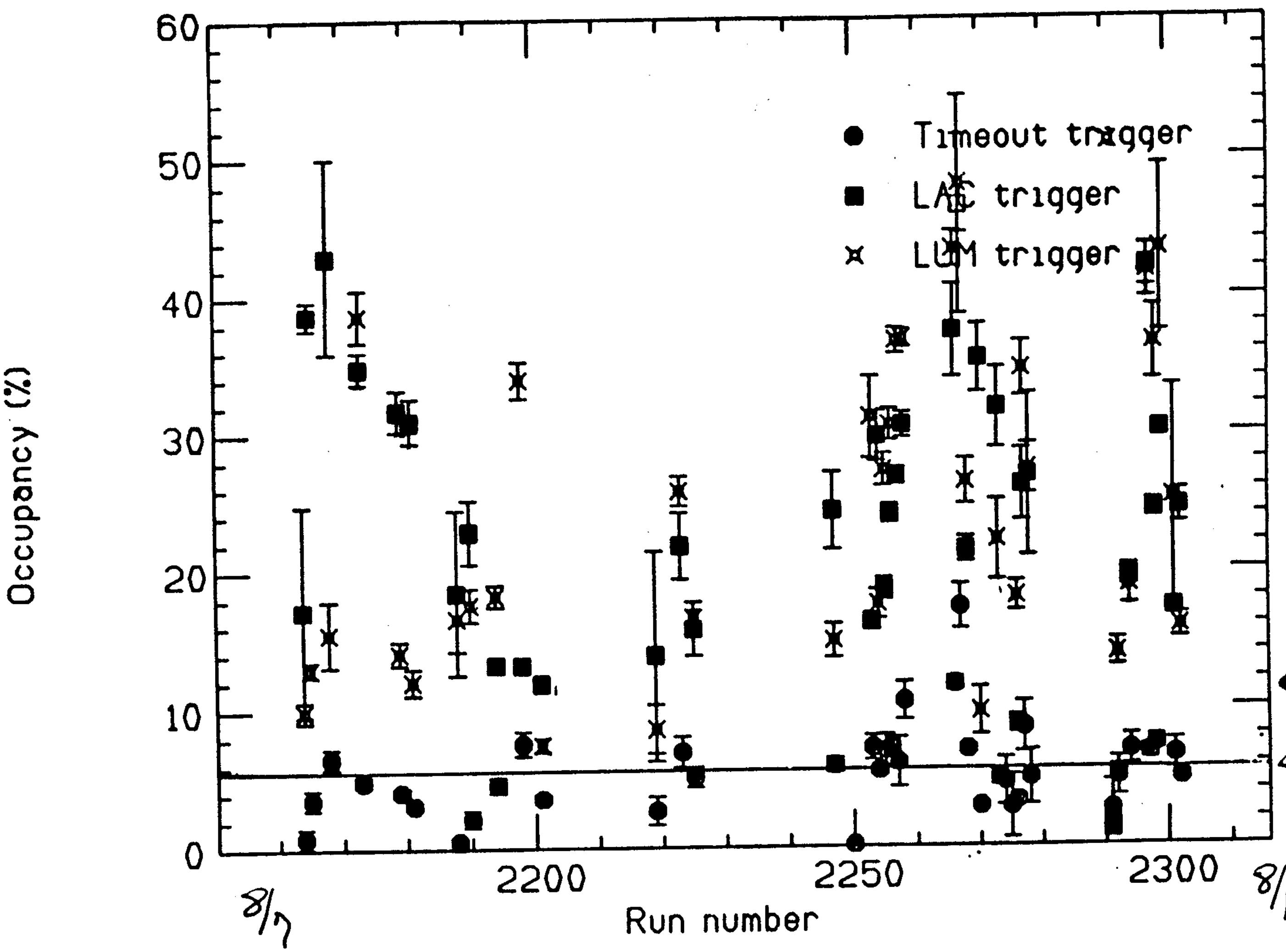

8/7

8/12

Avg. on Z's ← ~11%

<> = 5.5%
×2
= 11%

ECDC ≈ 80%

T. Takahashi

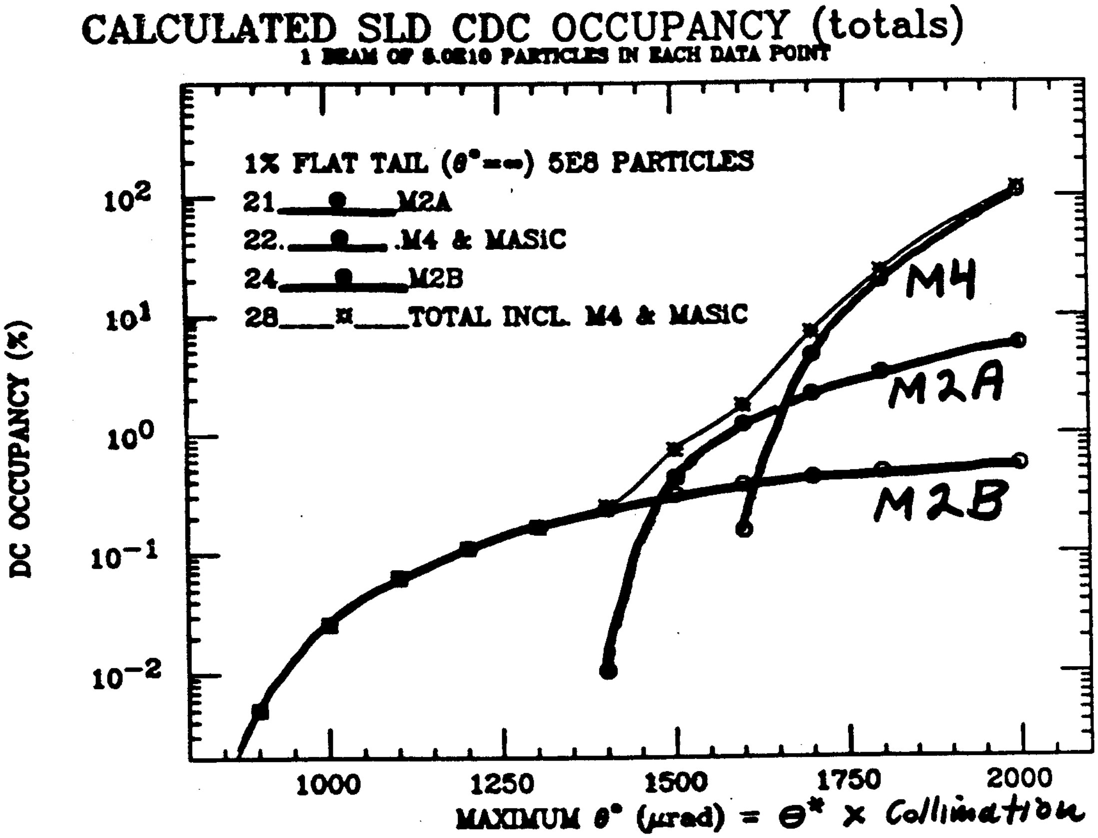

CDC OCCUPANCY DUE TO QUAD SYNCHROTRON RADIATION

LINAC COLLIMATORS at ± 600μm
⟹ 4 to 5 σ

CALCULATED SLD CDC OCCUPANCY (totals)

1 BEAM OF 5.0E10 PARTICLES IN EACH DATA POINT

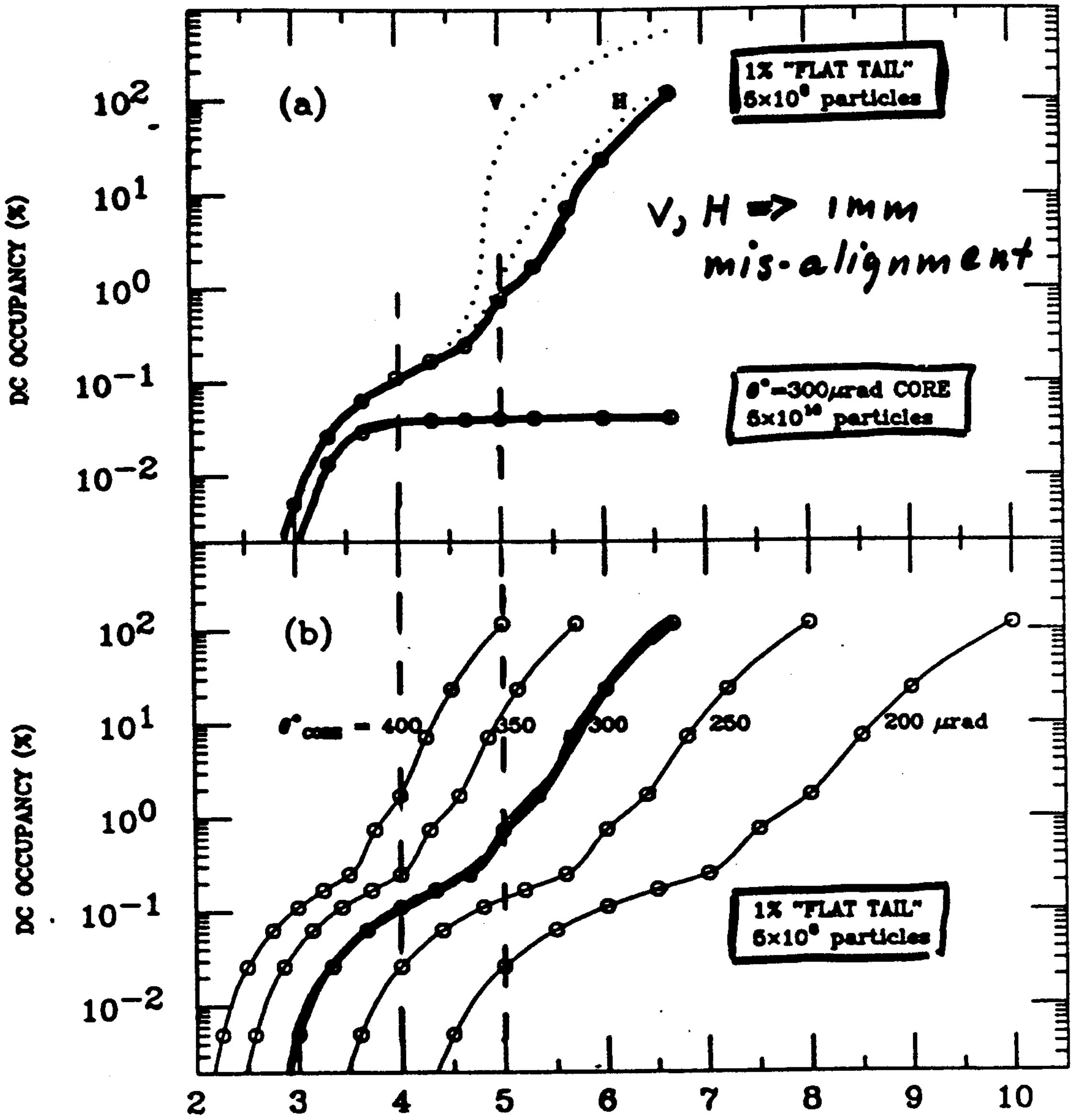

NOTE EFFECT of NON-GAUSSIAN TAIL
COLLIMATION, θ*
ALIGNMENT

PHOTON "INTERACTION" PROBABILITY IN SLD CDC

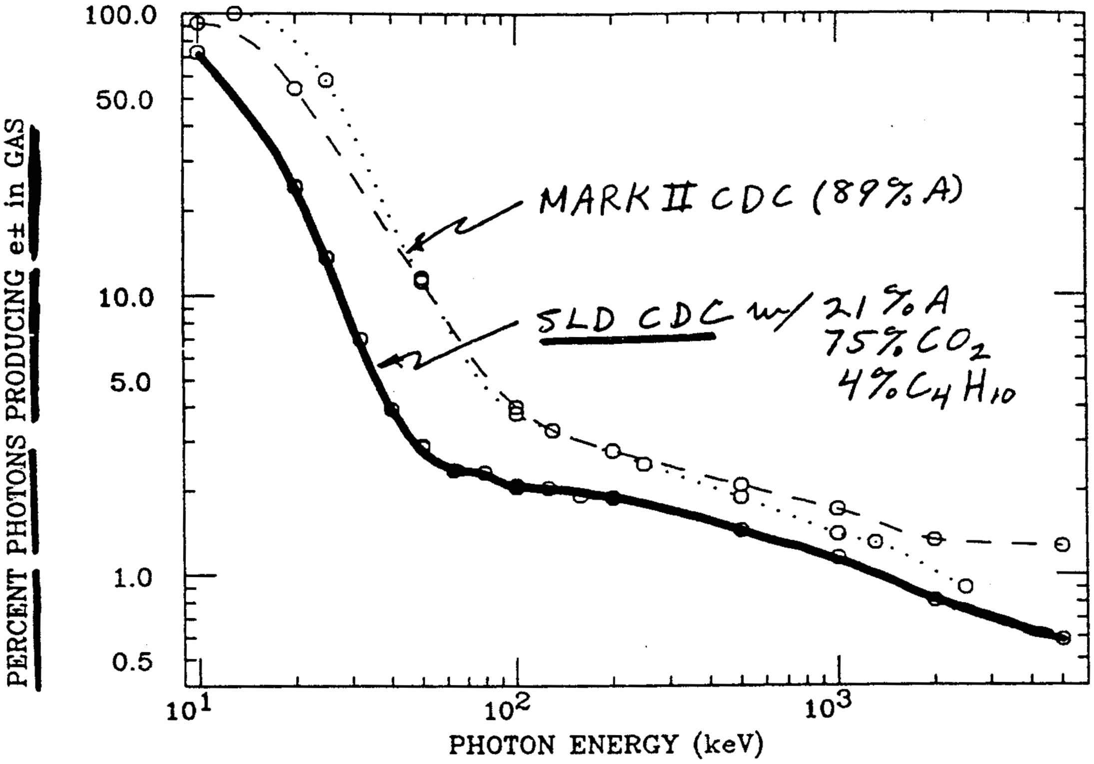

PERCENT of ELECTRONS in DC GAS COMING FROM WIRES

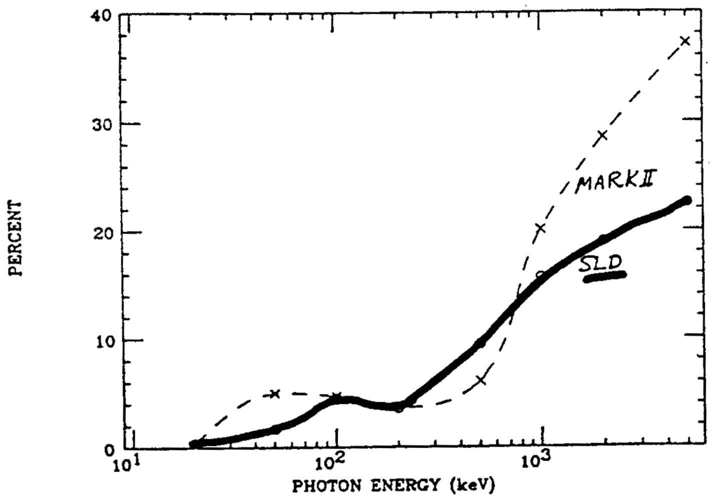

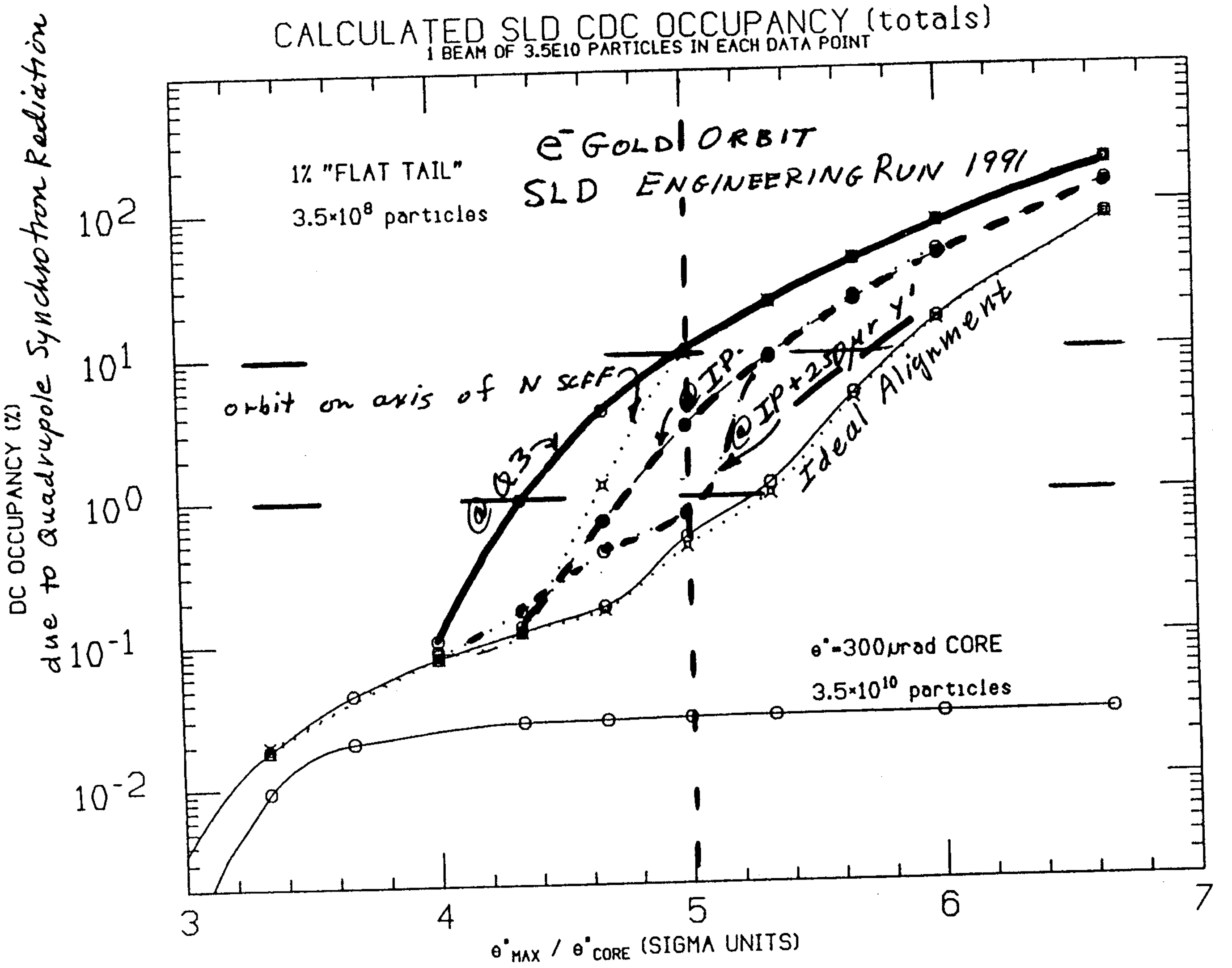

CALCULATIONS BASED ON BALLISTIC ORBIT STUDIES

Background Problems at NLC

Synchrotron Radiation should **NOT** be a major problem *if*:

- Shield IR from last hard bend.
- collimate so that QSR does not hit up-beam quads
- IR has crossing angle & quads have exit hole for outgoing disrupted beam. Synchrotron Radiation should exit with beam.

MUONS WILL be a problem.

Study of toroidal muon spoiler (L. Keller, SNOWMASS '90) found 1 μ in detector per 4×10^7 e on source 1600' from IP.

But 1 μ per 5×10^6 on Source at 2000'.

$10^7 e / 10^{11} e$ per bunch train $= 10^{-4}$

$\Rightarrow \sim 1 \mu$ at detector

Need BIG BEND?

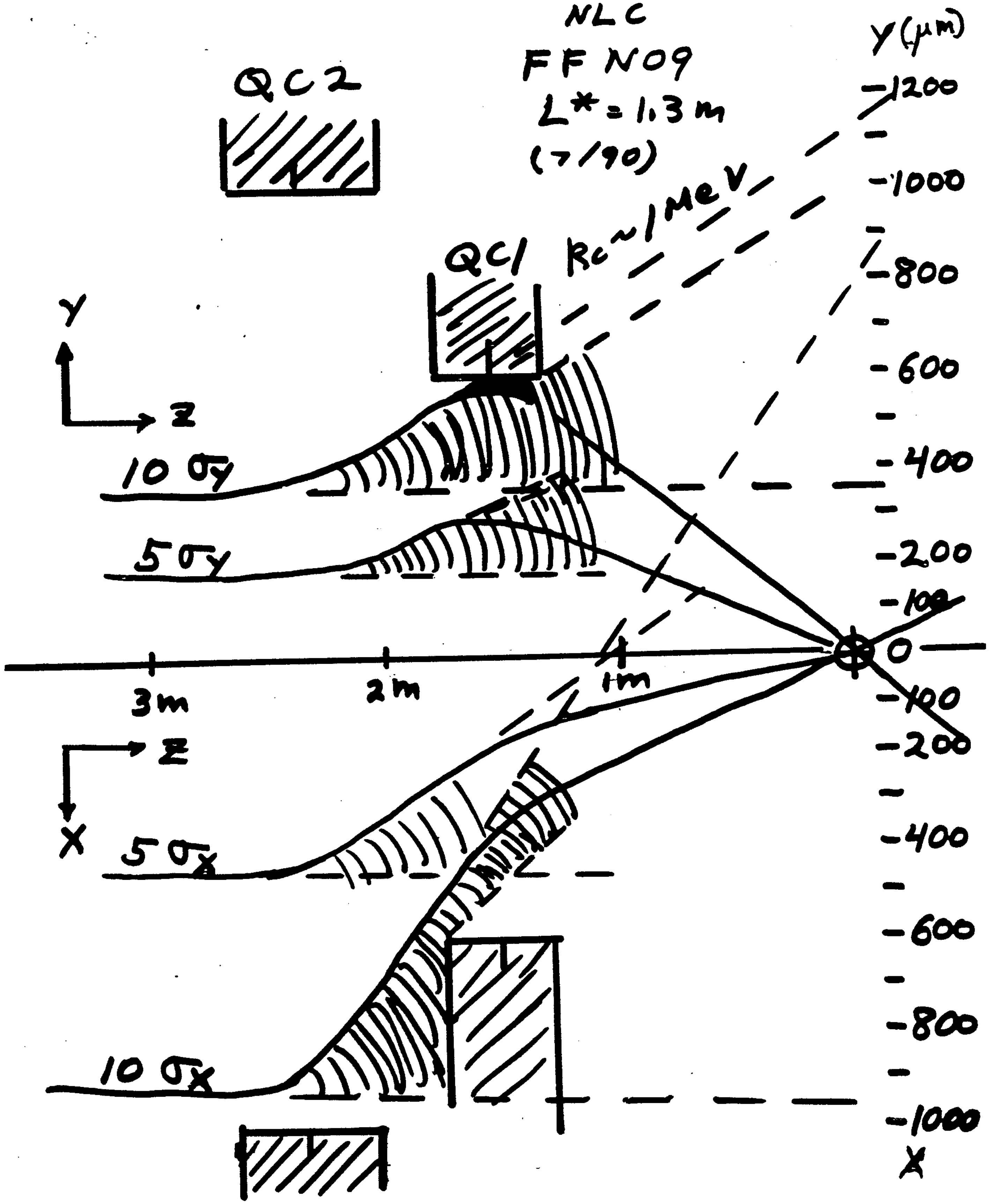
NLC
FF N09
L* = 1.3 m
(7/90)
QC2
QC1
Rc ~ 1 MeV
Y (μm)
1200
1000
800
600
400
200
100
0
100
200
400
600
800
1000
X
Y
Z
Z
X
10 σy
5 σy
5 σx
10 σx
3m
2m
1m

T. Tauchi, et. al SLAC PUB 5652
Snow-mass 1990

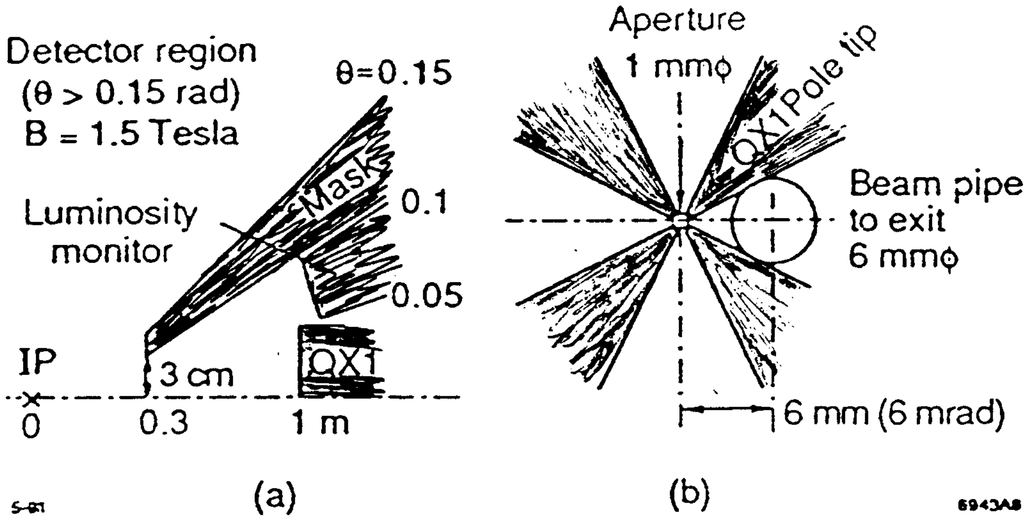

Fig. 8. Schematic view of a masking system in an IP region. Besides the finite crossing angle, the system is cylindrically symmetric around the beam axis. (b) Cross-sectional view of the beam line in front of QX1.

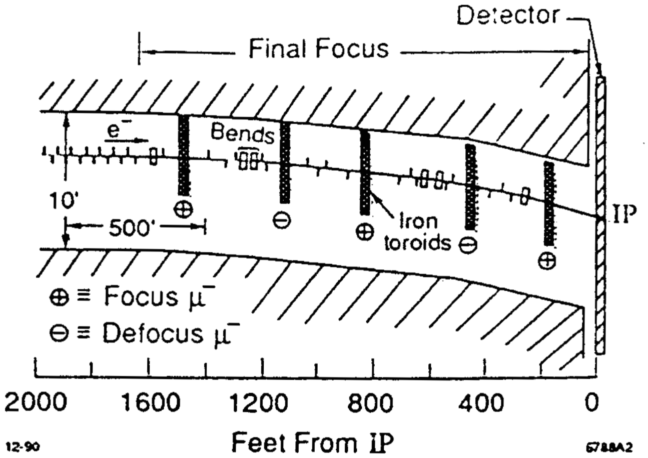

Fig. 2. Schematic of the final focus beam line used for this study. Note the different scale in the transverse and longitudinal directions.

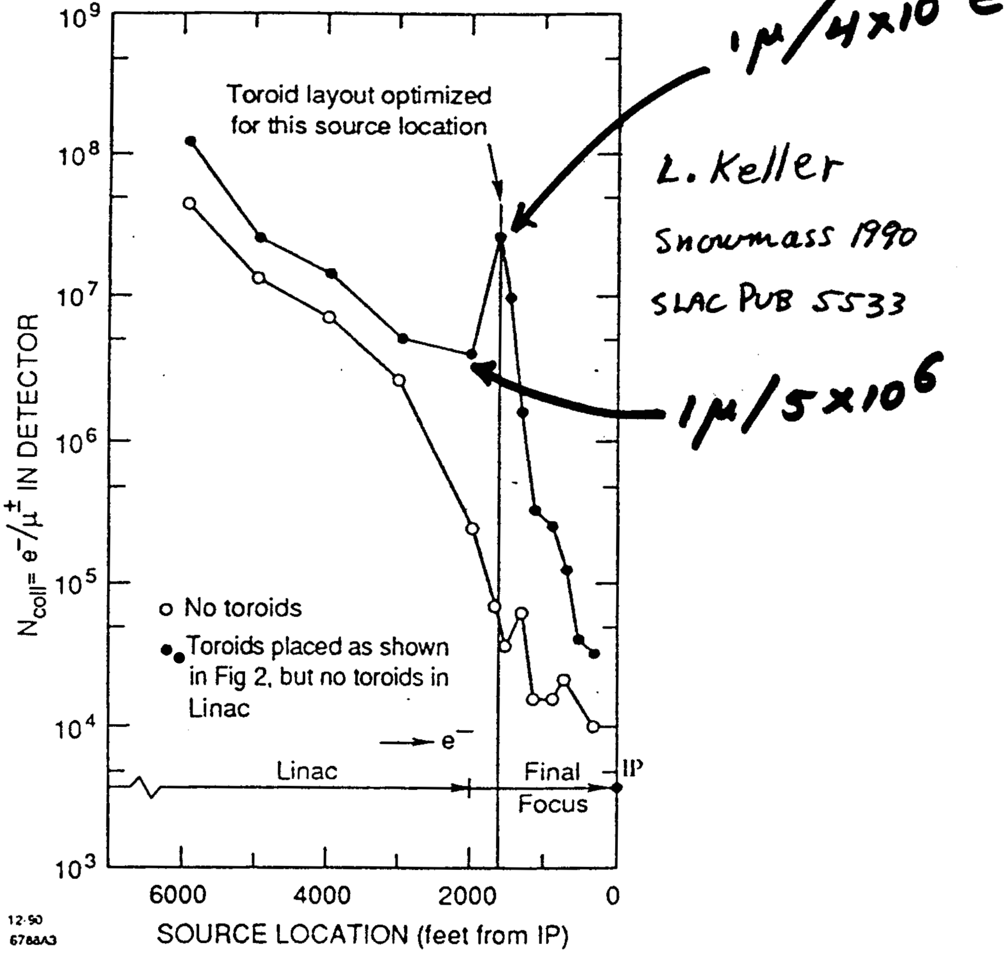

$1\mu/4\times10^7 e$

L. Keller

Snowmass 1990

SLAC PUB 5533

$1\mu/5\times10^6$

Fig. 3. Number of electrons impinging on a collimator which yield one muon in the detector (N_{coll}) as a function of source location in the linac and final focus.

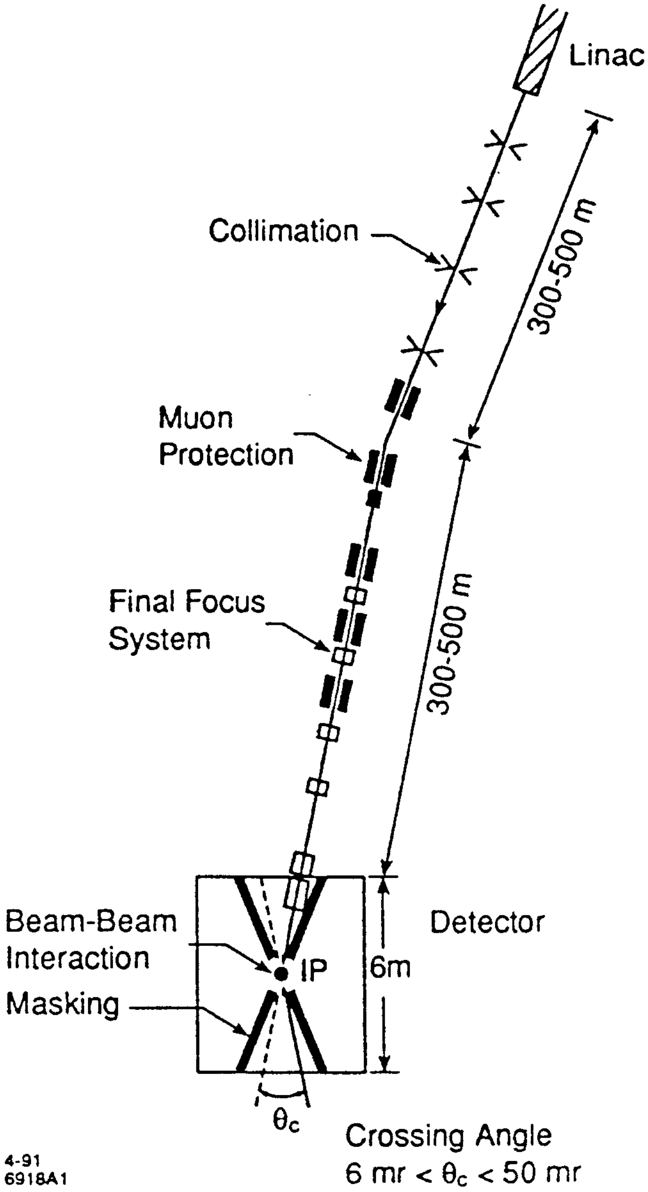

Fig. 1. End of linac to interaction point in the Next Linear Collider.

Q1 to have exit aperture for disrupted beam & synchrotron radiation.

(See T. Tauchi, et. al.)

Concluding remarks re detector

Tracking Chamber

- Minimize $\gamma \rightarrow$ charged (E_γ?)
- Electronics behaviour, e.g., with large pulses.

Calorimeters

- Projective Tower Geometry (θ-ϕ) for physics from IP.
- ? (ϕ-Z) logic for μ from machine?

Magnetic Field - Effect on background

- large-angle $e^{\pm}$ outside Tauchi mask.

All Systems:

- Time resolution - Can individual bunches be resolved to reduce trigger & background problems?
- Alignment issues (always harder than planned)

AND

- Design Detector & Machine in parallel.

- What sources & features have not been identified?

  (e.g. hadron minijets seem recent consideration)

BEAM-BEAM WORKING GROUP

Chairman: Pisin Chen

Members and Contributors

K. Berkelman	CERN	J. Rosenzweig	UCLA
M. Leenen	DESY	T. Barklow	SLAC
D. Schroeder	Grinnell	P. Chen	SLAC
V. Alexandrov	INP	S. Heifets	SLAC
E. Kushnirenko	INP	C. Ng	SLAC
S. Lepshokov	INP	R. Palmer	SLAC
A. Miyamoto	KEK	M. Peskin	SLAC
T. Tauchi	KEK	J. Spencer	SLAC
M. Ronan	LBL	K. Thompson	SLAC
R. Settles	Max Planck Inst.	V. Ziemann	SLAC
V. Telnov	Novosibirsk		

Summary of FFIR Beam-Beam Working Group Discussions

Pisin Chen

The Beam-Beam working group was charged to pin down qualitatively and quantitatively our current understanding of the beam-beam issues, including disruption, beamstrahlung, and its related background problems.

To the organizers' delight, 21 people actively participated in this working group, a number larger than originally anticipated. The first working group session started with a free-wheeled discussion on the status of the beam-beam phenomena, followed by a review of beam-beam parameters of all machines proposed by different laboratories. This set the remaining six sessions with a proper background, where one was held jointly with the Optics Group on beam-beam diagnostics, and two with the Detector Group on QED and QCD backgrounds from beamstrahlung. One session was open for free discussions. All together, there were 26 presentations, including 5 discussions on the various machine parameters. These were all nicely summarized by E. Kushnirenko on the last day.

To summarize the status in brief, at the risk of over-simplifying the situation, the group finds the issue of disruption enhancement now well understood both quantitatively and qualitatively. New ideas such as the "Traveling Focus" which intends to optimize luminosity through beam-beam disruption, has been pursued. Based on the SLC experience, beam-beam deflection and beamstrahlung signals as diagnostic tools look possible for the next generation linear colliders.

Beamstrahlung is also by now well understood. The only new development has been the analytic formula for beamstrahlung spectrum under multiphoton process. Though this spectrum can be attained from computer simulations, its general analytic form is useful for calculating other effects induced by beamstrahlung photons.

The issues of beamstrahlung induced backgrounds still occupy the center of attention. The QED backgrounds in the form of e^+e^- pair production has been studied in detail. Computer code has been developed in which all known effects, e.g., geometric reduction, external field suppression, etc., are included. The new important issue is the QCD backgrounds in the form of so-called "minijets". From the several presentations it seems clear that more work is needed before one can reach the same level of confidence as that on the e^+e^- pair production.

SUMMARY TALK

Beam-Bean Interaction Summary	E. Kushnirenko

PARALLEL SESSION TALKS

Beam-Beam Working Group Program	P. Chen
Multiphoton Beamstrahlung Spectra	P. Chen
Beamstrahlung Spectra in Next Generation Linear Colliders	T. Barklow
Theory and Simulation of Incoherent Pair Creation	P. Chen/T. Tauchi
$e^{\pm}$ Pair Background and Masking	T. Tauchi
QED Backgrounds at VLEPP	E. Kushnirenko/S. Lepshokov
The Accuracy of Beam-Beam Diagnostics at the NLC	V. Ziemann
Beamstrahlung Simulation & Beam Diagnostics	V. Ziemann
On the Scattering of e, γ Beams	S. Heifets
Conditions of "Travelling Focus" Regime	V. Balakin
Transverse Equilibrium in Linear Collider Beam-Beam Collisions	J. B. Rosenzweig
Multibunch Issues in Linacs of X-band NLC, With Longer Bunch Trains	K. Thompson
e^+ Production By e^--Laser Interaction?	R. B. Palmer/P. Chen
High Brightness $\vec{\gamma}$, $\vec{e}^{\pm}$ Sources & the E-144 Experiment	J. Spencer
$\gamma\gamma$, γe - Colliders	V. Telnov
The $\gamma\gamma$ Total Cross-section at High Energies	M. E. Peskin
An Estimation of Minijet Background at JLC	A. Miyamoto
Beamstrahlung Minijet Events in Next Generation Linear Colliders	P. Chen
Two-Photon Physics from TPC Experiments	M. Ronan
ALEPH Results on $\gamma\gamma \rightarrow$ Hadrons	R. Settles
Experimental Results on $\gamma\gamma \rightarrow$ Hadrons	K. Berkelman

Interaction Region
Workshop, SLAC,
March 2-6, 1992.

Beam - Beam Interaction
Summary

E. Kushnirenko, BINP, Protvino

Thanks for help from
Pisin Chen

Do not consider
too scrupulous
figures on the list:
all is changing, and
the accelerator's projects
parameters too.

$$E_{c.m} = 0.5\ TeV.$$

		NLC	JLC	DESY	VLEPP	TESLA	CLIC
L	$[10^{33} cm^{-2} s^{-1}]$	2	2.5	2.2	1÷3	5	0.68
N	$[10^{10}]$	1	1.3	2.1	10÷20	5.14	0.6
n_b		10	20	172	1	800	1
σ_z	$[\mu m]$	110	140	500	750	2000	170
σ_x	$[nm]$	200	340	316	1000	630	120
σ_y	$[nm]$	4	4.2	40	7	101	6
Υ		0.18	0.125	0.05	0.07	0.015	0.132
$\frac{\Delta E}{E}$	$[\%]$	8.4	5.9	3.5.	10	2	7.9
N_γ/e		1.7	1.5	1.0	3.3	3.	2.0

a) 15 jears ago – was proposed the flat beam
б) BNS, Crab crossing, Coherent pair creat.
travelling focus
TRANS 1

The beams becomes more and more flat.
Background problem
TRANS 2

Luminosity and background.

1. V.Balakin "TRAVELLING Focus"
2. V. Telnov
3. M. Peskin
Bunch trains
4. K. Tompson
5. J. Rosenzweig
6. J.E. Spencer
7. R.B Palmer
8. Analytical calculations

Multibunch issues in linacs of x-band NLC, with longer bunch trains.

K. Thompson (SLAC)

Motivation for longer pulse: Reduce minijet background, while keeping luminosity up and wall plug power down, (Palmer optimizations) for higher energy ($E_{c.m.} \sim 1$ TeV) design.

Two major multibunch problems in linacs:

1. Multibunch beam break-up
   Can the transverse wake fields be sufficiently well-controlled at these longer times ($\sim T_{fill}$) ?
2. Multibunch beam-loading compensation
   A possible method – stagger timings of a subset of rf sections, so that the transient beam loading is made approximately equal to the steady-state beam loading

Wake function
σ of Gaussian = 2.5%
Tot spread = 4σ

σ of $\frac{\Delta f}{f}$ errors = 10^{-4}
Cell-to-cell coupling neglected *

WAKE AS FUNCTION OF DISTANCE BEHIND BUNCH

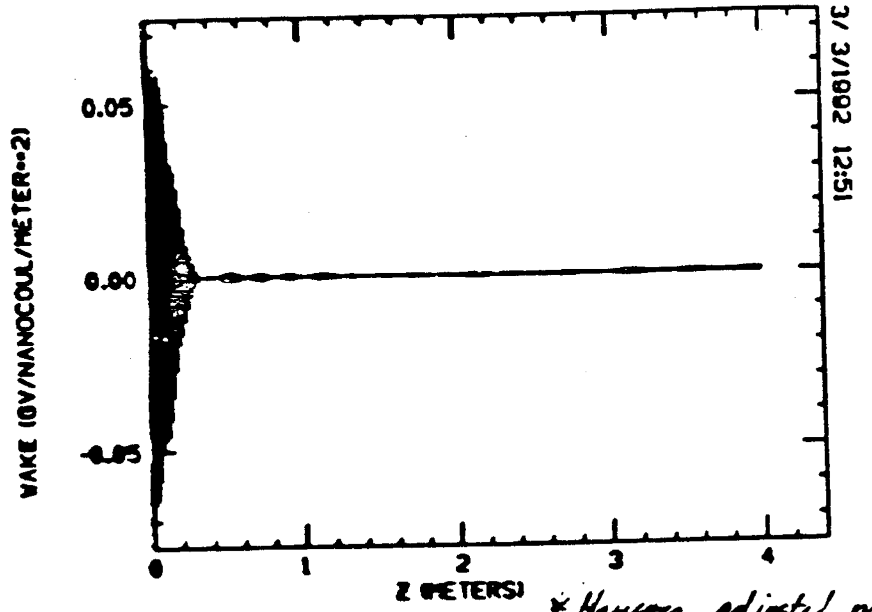

* However, adjusted parameters so as to be not very different from short & long range behavior in a coupled case calculated by K. Bane

WAKE AS FUNCTION OF DISTANCE BEHIND BUNCH

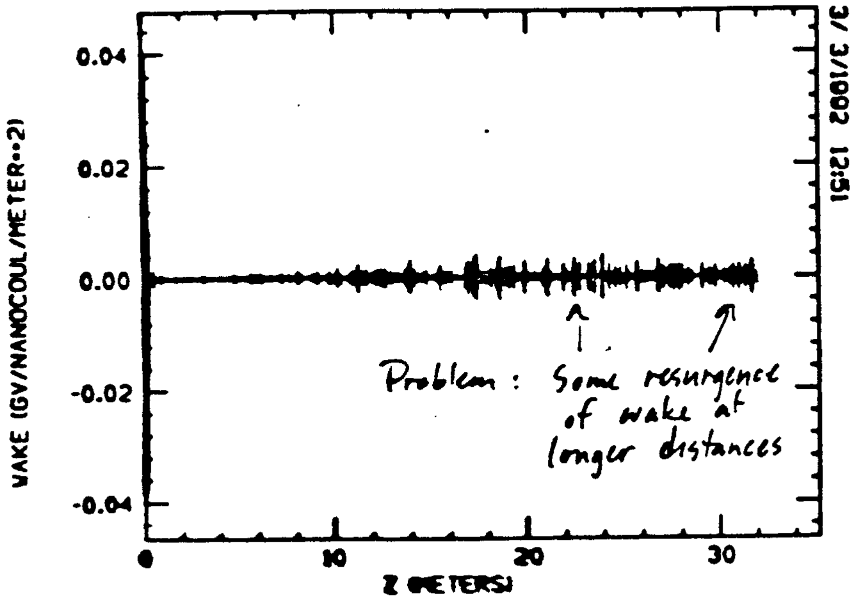

Problem: Some resurgence of wake at longer distances

Conditions „Travelling focus" regime

I. $\beta_y \longrightarrow 0.15 \cdot \sigma_z \simeq 0.1\,\mathrm{mm}$

II. „Standing focus" → "Travelling focus"

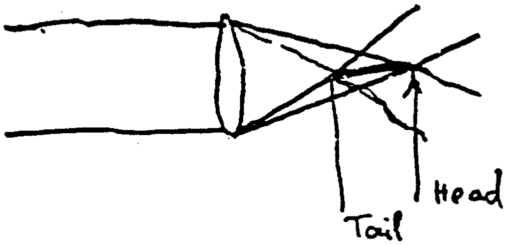

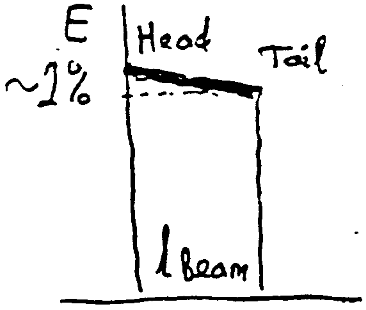

III

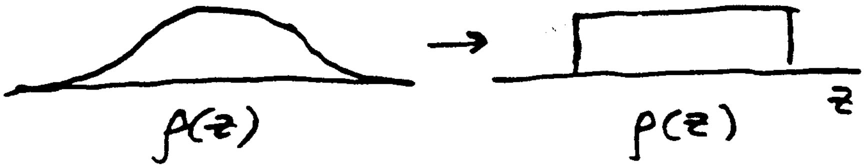

$$\varepsilon_{ny}^{T.F.} \longrightarrow \sim 5 \cdot \varepsilon_{ny}^{S.F.}$$

or

$$\mathcal{L}^{T.F.} \simeq \sqrt{5} \cdot \mathcal{L}^{S.F.}$$

$$\beta_y \simeq \sigma_z \longrightarrow \beta_y \simeq \frac{\lambda}{2\pi} \qquad \lambda = \frac{\ell}{\nu_y}$$

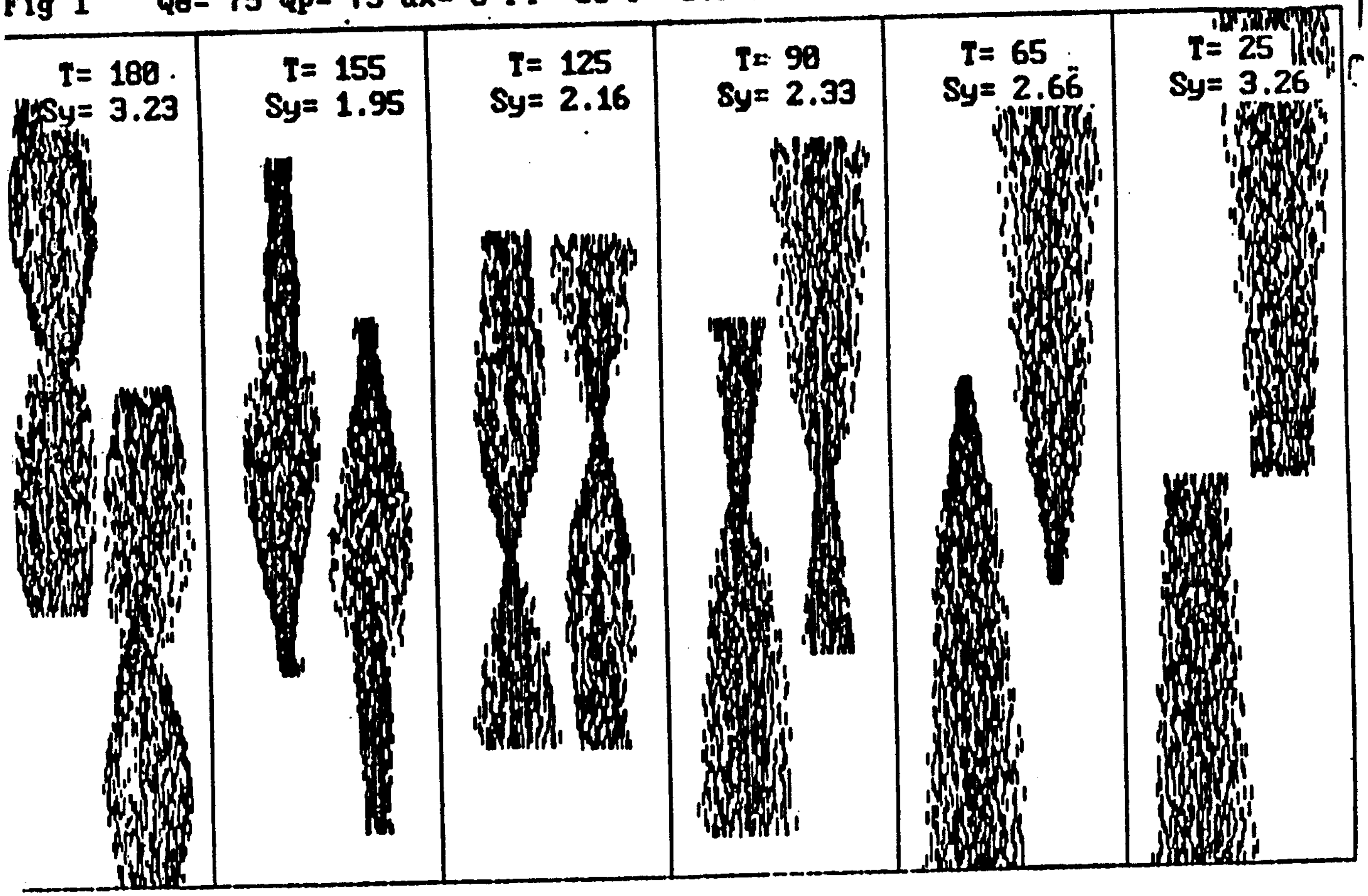

Fig 1 Qe= 75 Qp= 75 dx= 0 fi= 60 r= 6.5 n= 2000 df= 0 Standing Focus

V. Balakin

Fig 3   Qe= 75 Qp= 75 dx= 0 fi= 60 r= 20 n= 2000 df= 0   Traveling Focus

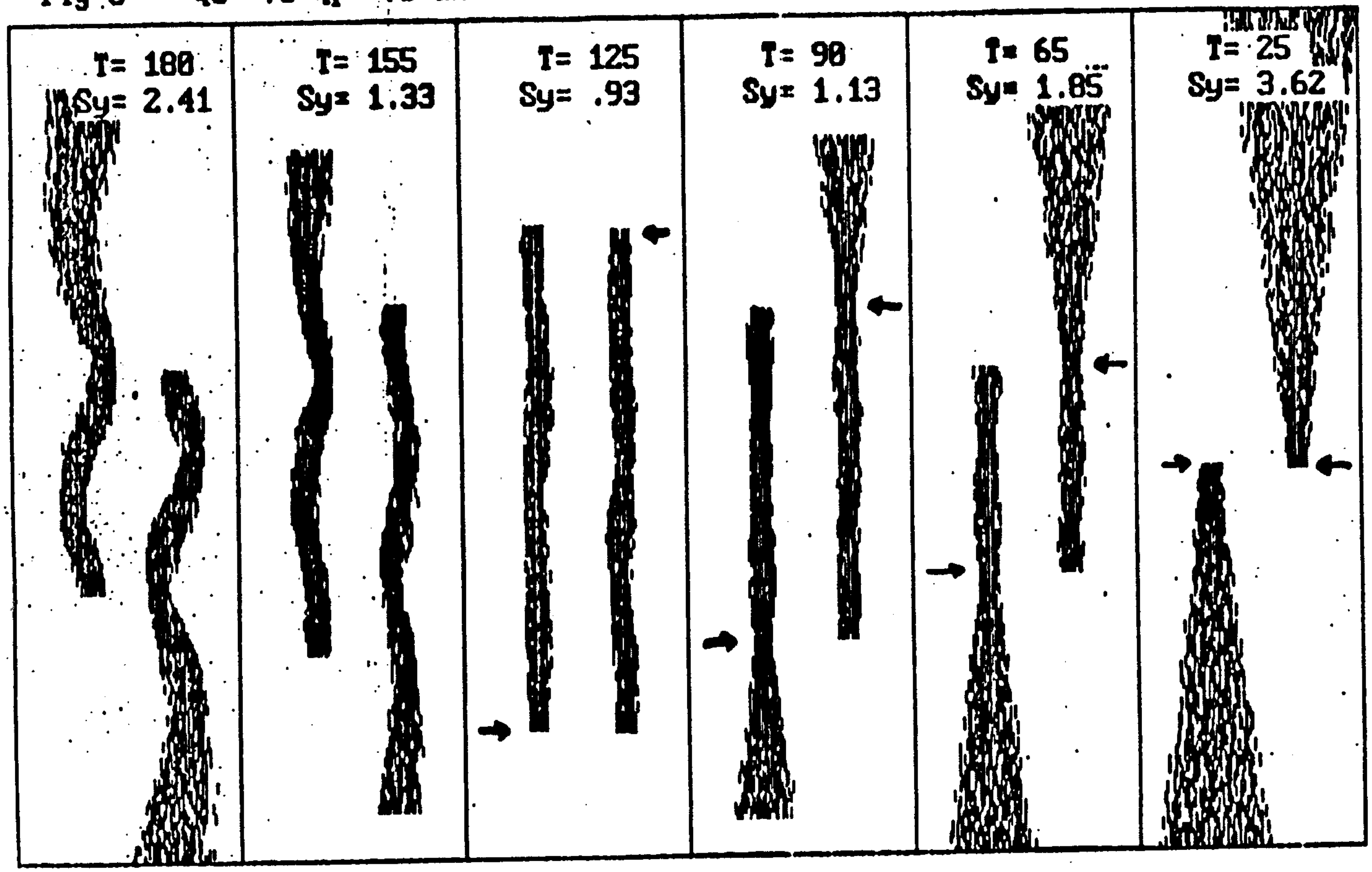

V. Balakin

Transverse Equilibrium in Linear Collider Beam-Beam Collisions

J.B. Rosenzweig
UCLA Dept. of Physics

SLAC Final Focus and Interaction Region Workshop
3/3/92

Motivation

1) Explain observation (in Chen-Yokoya simulations) of "pinch confined" near-equilibrium profiles in beam core, accompanying luminosity enhancement.

2) Explain scaling of luminosity enhancement in flat beams vs. round -

$$H_{D,\mathrm{flat}} \sim (H_{D,\mathrm{round}})^{1/3}.$$

3) Establish equilibrium profiles for use in differential luminosity and beamstrahlung calculations.

4) Better understanding and possible control of kink instability, emittance growth (angle distribution) during collision.

Luminosity Enhancement

Taking ratios of the luminosity integral, we have

$$H_D(D,A) = \frac{2}{3}\left[\frac{\sqrt{2\pi}\left(\frac{D}{A^2}\right)}{1+\sqrt{\frac{2D}{A^2}}}\right]^{1/3}$$

for D >> 1 ($k_\beta\sigma_z > 1$), A > 0.5. Note the dependence is only on

$$\frac{D}{A^2} = 1.1 k_\beta \beta^* .$$

The condition $k_\beta\beta^*=1$ is a *matched beam*; the focusing balances the thermal forces due to the emittance.

This result compares very well with the simulation findings - lets compare the asymptotic scaling:

$$H_D(D,A) \sim 0.8 \left[\frac{D}{A^2}\right]^{1/6}$$

for $k_\beta\beta^*>1$.

Emittance growth process should be examined with ABEL. Simplified computational model verifies result qualitatively.

Emittance growth is limited if $k_\beta\beta^* < 1$.

S. Hänssgen, E. Kushnirenko, T. Tajursky

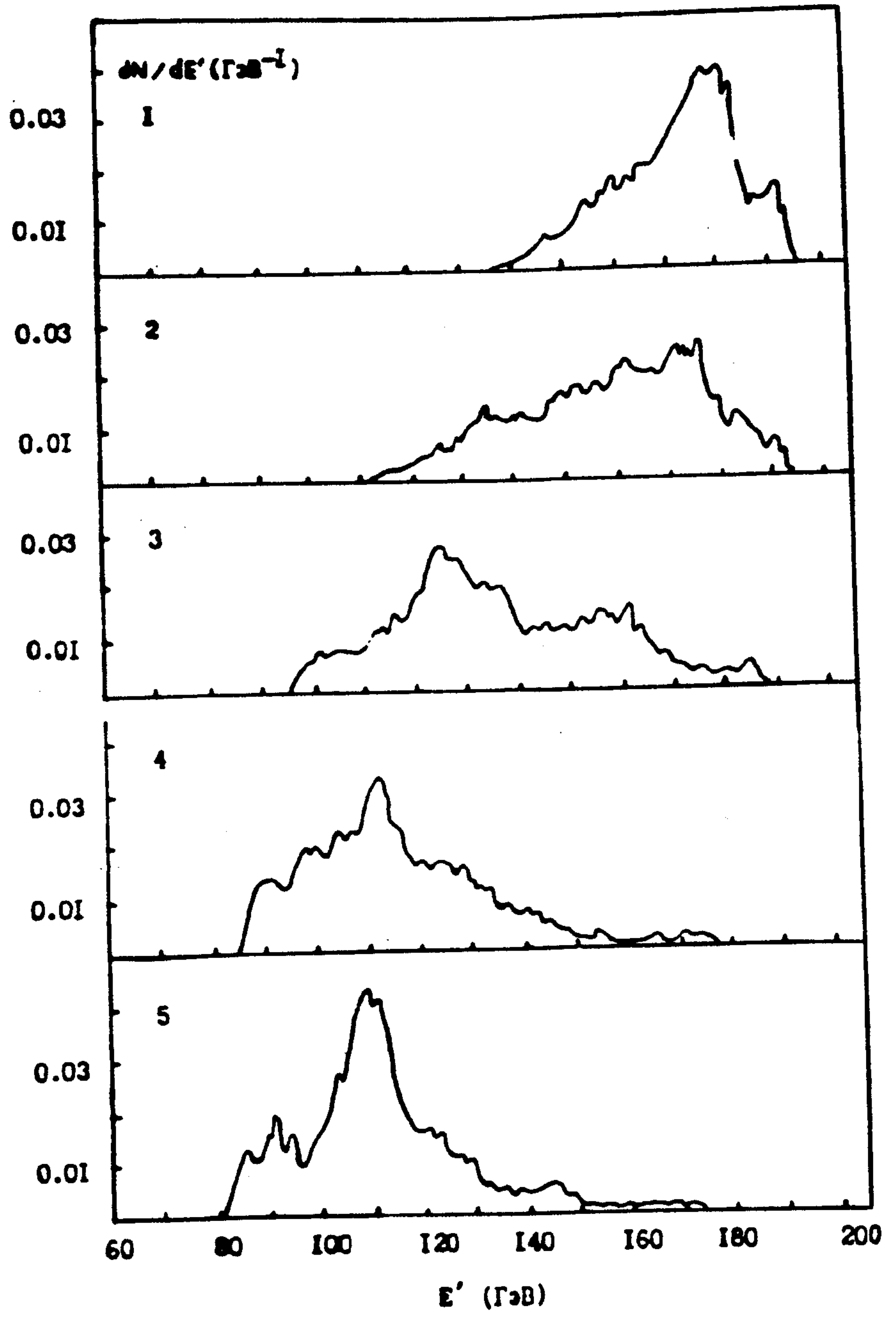

Рис. 7. Энергетические спектры электронов пучка после столкновения для различных вариантов расчета. $E_b=200$ ГэВ.

1: $R=\sigma_x/\sigma_y=30$; *2*: $R=20$; *3*: $R=10$; *4*: $R=3.3$; *5*: $R=1$.

E. Kushnirenko
S. Lepshokov
VLEPP Protvino

QED Backgrounds at VLEPP

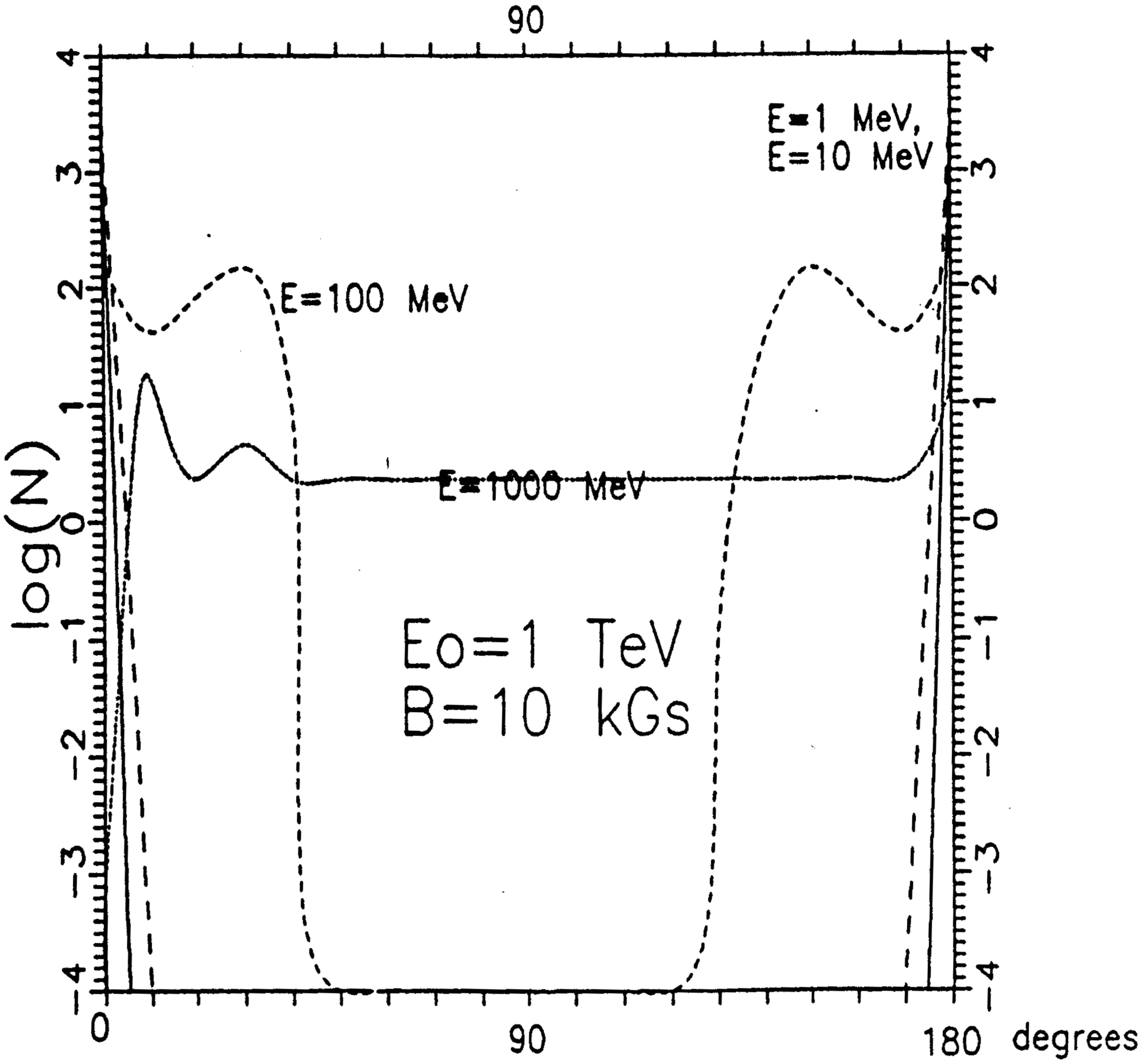

Fig.11 The distr. of electrons in magnetic field of detector in $\gamma\gamma \Rightarrow$ ee process; N – particles per 10 degrees of polar angle.

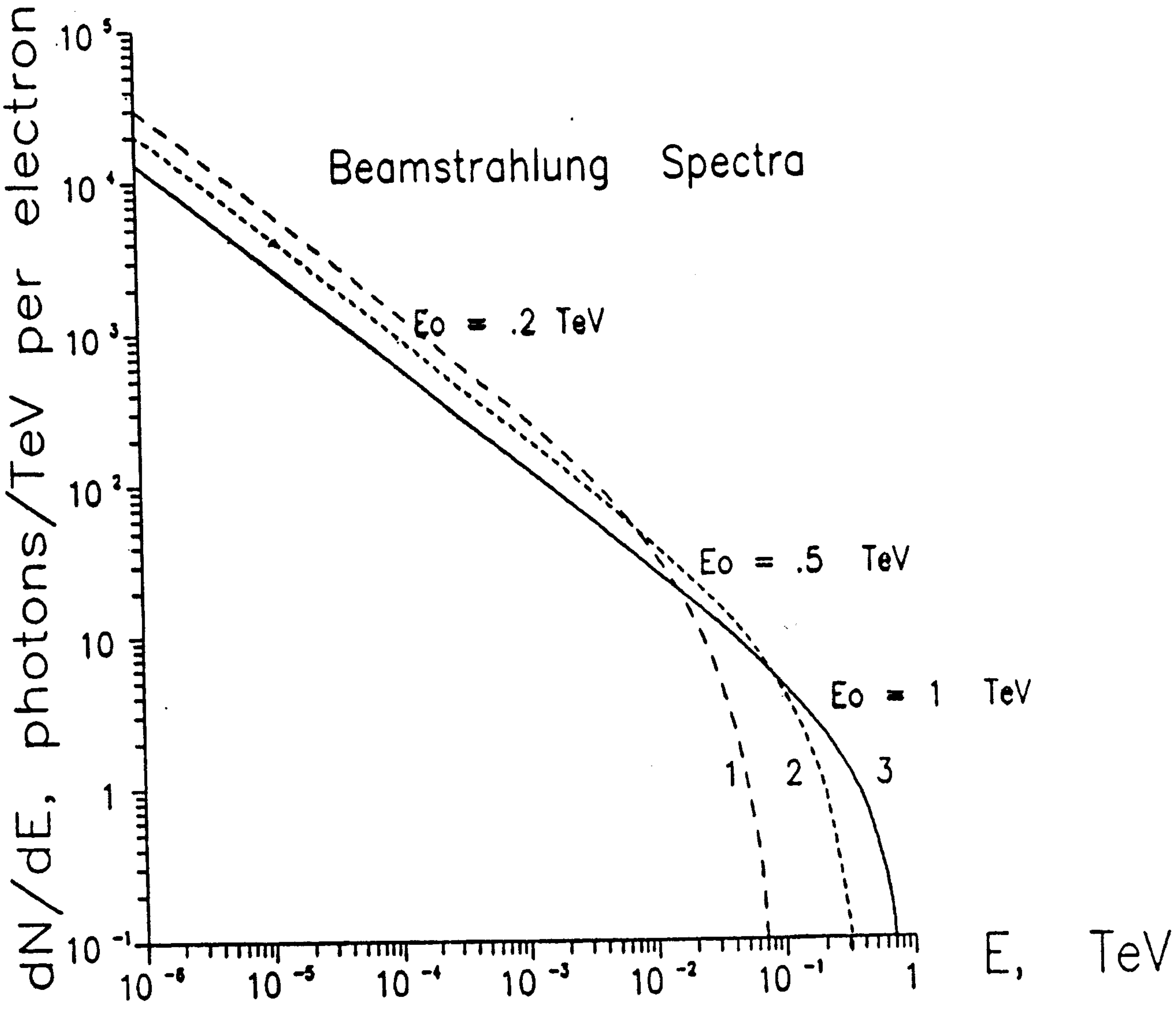
Beamstrahlung Spectra
dN/dE, photons/TeV per electron
10^5
10^4
10^3
10^2
10
1
10^-1
10^-6
10^-5
10^-4
10^-3
10^-2
10^-1
1
E, TeV
Eo = .2 TeV
Eo = .5 TeV
Eo = 1 TeV
1
2
3

Fig. 1

SLAC–PUB–5615
December 1991
(T/E/A)

DIFFERENTIAL LUMINOSITY UNDER MULTIPHOTON BEAMSTRAHLUNG*

Pisin Chen

Stanford Linear Accelerator Center
Stanford University, Stanford, Ca 94309

ABSTRACT

For the next generation of e^+e^- linear colliders in the TeV range, the energy loss due to *beamstrahlung* during the collision of the e^+e^- beams is expected to be substantial. One consequence is that the center-of-mass energy between the colliding particles can be largely degraded from the designed value. The knowledge on the differential luminosity as a function of the center-of-mass energy is essential for particle physics analysis on the interesting events. On the other hand, the beamstrahlung photon spectrum provides useful information on the low energy backgrounds and high energy $\gamma\gamma$ luminosity. In this paper, we derive analytic formulas for the e^+e^- and γ energy spectra under multiple beamstrahlung process, and the e^+e^- and $\gamma\gamma$ differential luminosities. Major characteristics of these formulas are discussed.

Submitted to *Physical Review D1*.

⋆ Work supported by Department of Energy contract DE–AC03–76SF00515.

In principle, one could then express $I(y,t')$ in terms of the Whittaker function. But if one wishes to further simplify $I(y,t')$ through the asymptotic expansion of Equation (28), then it is necessary that the correction term $w_{\mu,\nu}(z)$ be retained. In the n-photon process, the leading order $n = 1$ dominates, which gives $\mu = -1/6$ and $\nu = 1/3$. Ignoring the y-dependence in z, we find, empirically, that

$$w_{\mu,\nu}(\frac{\kappa}{1-y}) \approx w = \frac{1}{6\sqrt{\kappa}} \quad , \qquad \Upsilon \lesssim 5 \quad , \tag{35}$$

We then have

$$\phi(y,t) = \frac{\kappa^{1/3}}{\Gamma(1/3)} y^{-2/3}(1-y)^{-1/3} e^{-\kappa y/(1-y)} \tilde{G}(y) \quad , \qquad \Upsilon \lesssim 5 \quad , \tag{36}$$

where

$$\begin{aligned} \tilde{G}(y) &= \frac{1-w}{\tilde{g}(y)}\Big[1 - e^{-\tilde{g}(y)\nu_\gamma t}\Big] + w\Big[1 - e^{-\nu_\gamma t}\Big] \quad , \\ \tilde{g}(y) &= 1 - \frac{\langle\bar{\nu}\rangle}{\nu_\gamma}(1-y)^{2/3} \quad . \end{aligned} \tag{37}$$

5. CENTER-OF-MASS $\gamma\gamma$ LUMINOSITY

The $\gamma\gamma$ center-of-mass luminosity can be obtained in the same way we did in Section 3. It amounts to looking for integration of $\phi(y,t)$ over the e^+e^- collision time. We find, for $\Upsilon \ll 1$,

$$\begin{aligned} \phi(y) &= \frac{2}{l}\int_0^{l/2} dt \phi(y,t) \\ &= \frac{\kappa^{1/3}}{\Gamma(1/3)} y^{-2/3}(1-y)^{-1/3} e^{-\kappa y/(1-y)} \tilde{G}(y) \quad , \end{aligned} \tag{38}$$

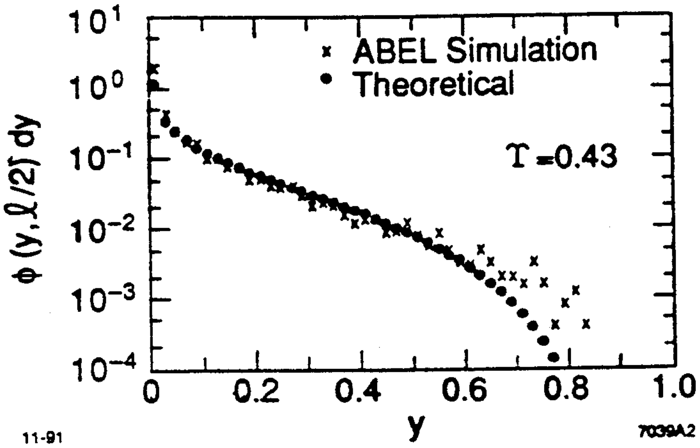

× ABEL Simulation
● Theoretical
Τ =0.43
10^1
10^0
10^{-1}
10^{-2}
10^{-3}
10^{-4}
φ (y,ℓ/2) dy
0
0.2
0.4
0.6
0.8
1.0
y
11-91
7039A2

Fig. 1

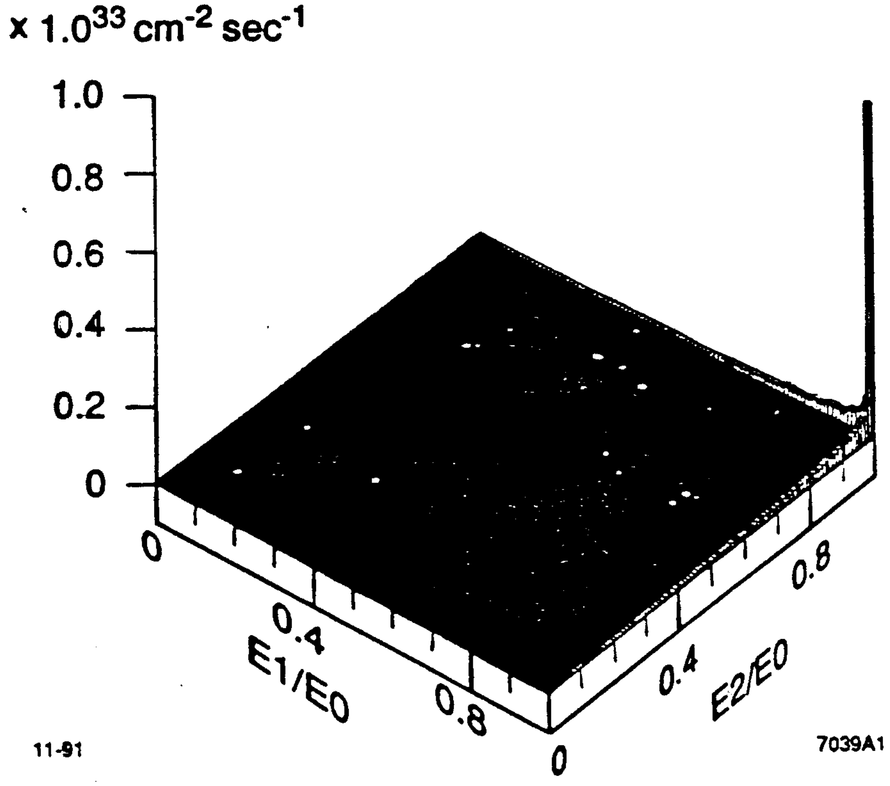

x 1.0^33 cm^-2 sec^-1
1.0
0.8
0.6
0.4
0.2
0
0
0.4
E1/E0
0.8
0
0.4
E2/E0
0.8
11-91
7039A1

Fig. 2

FIGURE CAPTIONS

Figure 1: Final beamstrahlung photon spectrum calculated by computer simulation, and by the analytic formula, Equation (36). Parameters from Palmer's G-machine, where $\Upsilon = 0.43$, were used.

Figure 2: Two dimensional plot of the center-of-mass e^+e^- luminosity as a function of the e^+e^- fractional energies, x_1, x_2, from computer simulation.

Beamstrahlung Spectra in Next Generation Linear Colliders

T. Barklow, P. Chen, and W. Kozanecki
Stanford Linear Accelerator Center
Stanford University, Stanford, Ca 94309
and DAPNIA-SPP, CEN-Saclay
91191 Gif-sur-Yvette (France)

Abstract: For the next generation of linear colliders, the energy loss due to *beamstrahlung* during the collision of the e^+e^- beams is expected to substantially influence the effective center-of-mass energy distribution of the colliding particles, thereby mandating a prediction of the e^+e^- or $\gamma\gamma$ differential luminosity as a function of the effective center-of-mass energy. In this paper, we first derive analytical formulae for the electron and photon energy spectra under multiple beamstrahlung processes, and for the e^+e^- and $\gamma\gamma$ differential luminosities. We then apply our formalism to various classes of 500 GeV e^+e^- linear colliders designs currently under study.

1 Introduction

In future Linear Colliders, contrarily to what happens in storage rings such as LEP, the e^+e^- center-of-mass (c.m.) energy is no longer confined to twice the primary beam energy, but instead gets spread over a relatively wide distribution, due to the onset of *beamstrahlung* [1], the synchrotron radiation emitted by one of the colliding bunches in the field of the opposing one. The energy so radiated by the beam particles spans a range that extends, depending on the accelerator design, from a few per mil to several tens of percent of the nominal electron energy E_0. Realistic simulation of physics processes whose cross-section or kinematics are energy-dependent (such as the top threshold scan), therefore mandates an accurate description of the differential luminosity as a function of the effective c.m. energy. In addition, the low energy end of the e^{+-} and γ spectra are also important to understand the implications of accelerator-induced backgrounds and of high energy photon-photon scattering processes.

When the average number of beamstrahlung photons radiated per beam particle is much less than unity, the energy spectrum for the final e^+ or e^- beam is simply the well-known Sokolov-Ternov spectrum [2] for the radiated photons, with the fractional photon energy, $y(\equiv E_\gamma/E_0)$, replaced by the corresponding final electron (or positron) energy, $x = 1 - y$. When conditions are such that the average number of photons radiated is not much less than unity, the effect of successive radiation processes becomes important. Previously, the multiphoton beamstrahlung process has been studied by Blankenbecler

Table 2: Effect of beamstrahlung alone on e^- and γ energy spectra

Design Class	1 Palmer G	2 Palmer F	3 D-D wide bd	4 D-D nrrw bd	5 TESLA nrrw bd
Beamstrahlung parameter Υ	.440	.111	.075	.015	.010
Mean e^- energy loss (%)	17	2.3	4.3	0.5	0.4
e^- energy spread (%)	17	5.2	6.1	1.1	0.9
Number of radiated γ's/e^-	1.5	.46	1.2	.60	.76
Mean photon energy (%)	11	4.9	3.7	0.9	0.6
Photon energy spread (%)	13	6.3	4.7	1.2	0.8

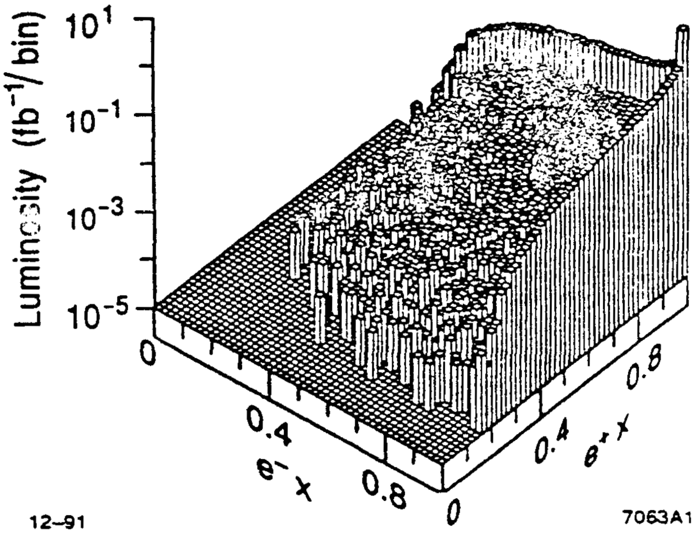

Figure 1: e^+e^- luminosity spectrum as a function of the fractional electron energy (e^- x) and the fractional positron energy (e^+ x), for the strong beamstrahlung X-band design (design 1). Linac energy spread is neglected. The total luminosity is 10 fb^{-1}. The bin size is $.02 \times .02$.

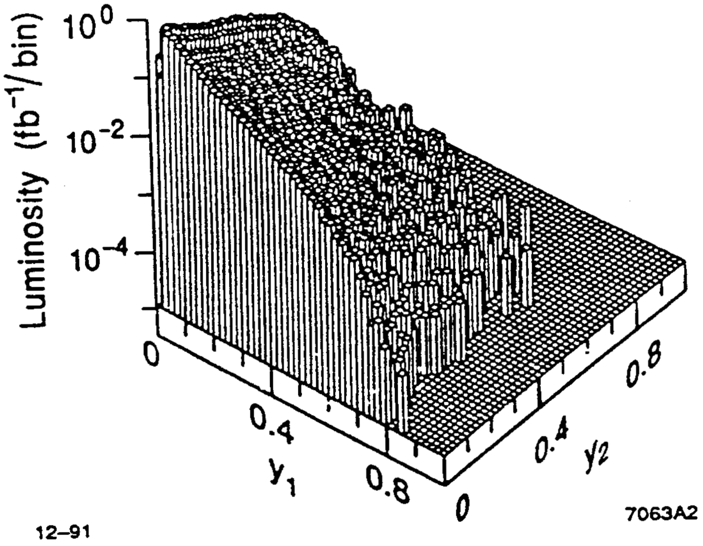

Figure 2: $\gamma\gamma$ luminosity spectrum as a function of the fractional photon energies y_1 and y_2, with a minimum $\gamma\gamma$ center–of–mass energy of 10 GeV. The figure corresponds to accelerator Design 1. Only the luminosity due to the collisions of beamstrahlung photons is shown. Luminosity from the collisions of two virtual (Weizsäcker–Williams) photons or of beamstrahlung photons with virtual photons is not included. The total e^+e^- luminosity is 10 fb^{-1}. The bin size is .02 x .02.

parameter, the larger the mean electron energy loss. In addition, because each electron radiates, on the average, several photons, the photon energy is typically smaller than the electron energy loss. Fig. 1 displays, for the design with the highest beamstrahlung flux, the distribution of electron energies (normalized to the nominal beam energy E_0), vs the corresponding positron energy. For most events, only either the electron, or the positron, actually radiates a significant amount of energy, as evidenced by the edge bands. Fig. 2 contains the corresponding plot for the photon energies.

Let us now turn to the actual luminosity spectra for e^+e^- collisions. We display separately the dependence of beamstrahlung on the linear collider design (Fig. 3), and the relative importance, for two extreme cases of strong and quasi-classical beamstrahlung, of the three electron energy loss mechanisms (Fig. 4). Some of the salient features of the effective e^+e^- energy distributions are summarized in Table 3: the average c.m. energy loss, the effective c.m. energy spread, and the fraction of the luminosity produced within a given energy interval of the nominal c.m. energy. For this last variable, we consider both a very narrow energy window (0.5 GeV), comparable to the r.m.s intrinsic Linac energy spread, and a relatively wide one (2.5 GeV), comparable to the total width of the top threshold excitation curve. The effects of beamstrahlung, Linac energy spread and initial state radiation are again first evaluated separately, and then combined.

γγ, γe - colliders

V. Telnov

SLAC, March 5, 92.

①

Principles are known: (see Proc. of Work. on Phys. and Exp. at Lin. Coll., Saariselka, Finland, 91, and ref. there

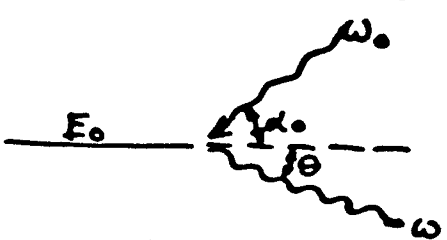

$$\omega_{max} = \frac{x}{x+1} E_0$$

$$x = \frac{4 E_0 \omega_0}{m^2 c^4}$$

Energy spectrum

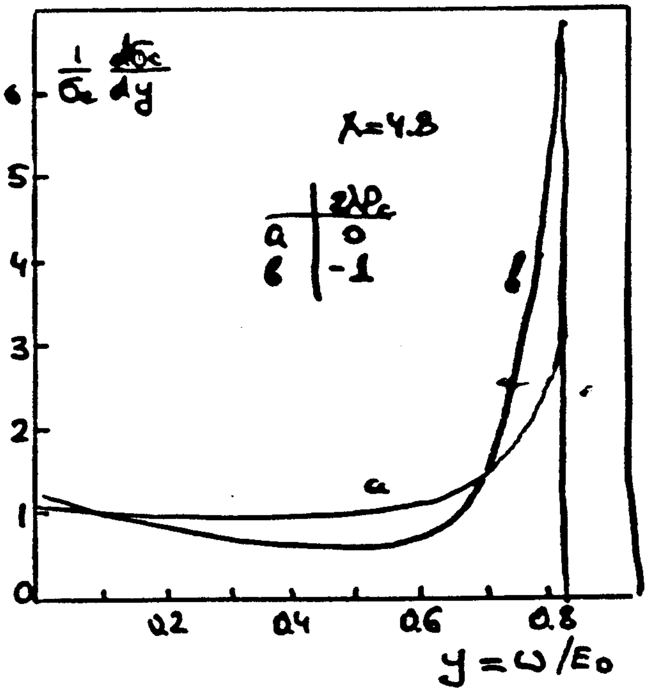

Requirements for lasers

$\xi = \frac{eB\hbar}{m\omega_0 c}$; $\Delta y_m = 5$
at $\xi^2 =$

$(\kappa \sim 0.65\,(A = A_0),\ \chi = 4.8)$

Flash energy: $A_0 = \max(\underline{25\, l_e[\mathrm{cm}]},\ 4E_0[\mathrm{TeV}])$, J

diffraction

nonlinear ef

Duration: $c\tau = \max(l_e,\ 0.17\, E_0[\mathrm{TeV}])$, cm

Wave length: $\lambda = 4.2\, E_0(\mathrm{TeV}), \mu m$ $(\omega_0 = 0.3/E_0(\mathrm{TeV}), eV)$

For example: $E_0 = 0.25$ TeV, $l_e = 200\,\mu m$

$\Rightarrow A_0 \sim 1$ J, $l_\gamma \sim 400\,\mu m$, $\lambda \sim 1\,\mu m$.

Lasers

a) Solid state lasers with chirped pulse technique give A_0 and τ, but rep. rate must be incr.

b) FEL + chirped pulse techn. ?

Scheme of γe, γγ-collision

Ⓐ

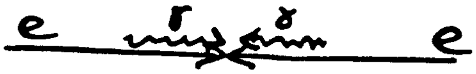

without deflection

Ⓑ

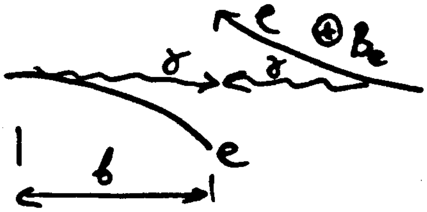

with deflection

γe

a) beamstrahlung
b) coher. pair creation
c) beam-beam instabilities

Ⓐ if $\delta = \frac{\Delta E}{E}$ is small, then $P_{e^+e^-}$ also small

$$\Rightarrow \boxed{L_{\gamma e,max} \sim \kappa L_{ee,max}}$$

flat beams

Ⓑ Ultimate $L_{\gamma e}$ (scheme B) due to
a) beamstrahlung and pair creation
b) beam displacement
c) optimum

				$E_0=0.25$ TeV			$E_0=1$ TeV
	$N(10^{10})$	σ_y (nm)	f(kHz)	$L_{\gamma e}(10^{33})$			$L_{\gamma e}(10^{33})$
SLAC	1.5	0.1	1.2	a) 0.7	b) 2.7	c) 0.7	0.35
DESY/THD	2	0.5	8.5	20	4.2	9.	10
VLEPP	20	0.75	0.1	1.1	0.95	1.	0.67

flat beams

Screening effect in $\gamma\gamma$-collisions in presence of pair creation.

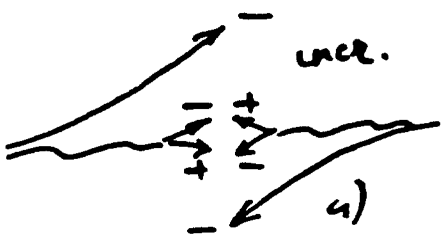

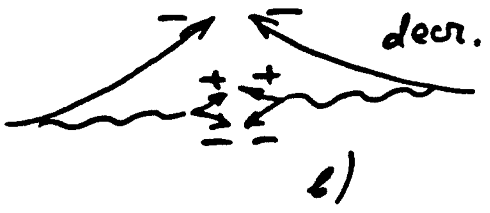

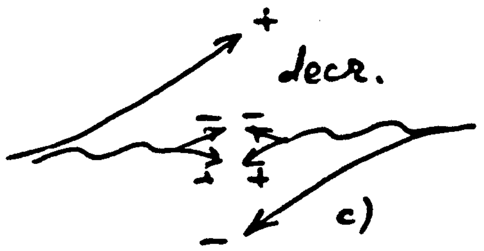

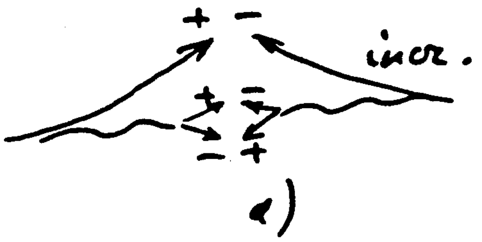

Produced e^+e^--pairs increase (a), d)) or decrease (b), c)) the field from deflected particles.

Effect of total screening take place at

$N\sigma_z \gtrsim 1.5\cdot 10^7/E_0[\text{TeV}]$, cm (at $\kappa=0.65$, $\rho_{e^+e^-}=0.05$) OK

Then $b_{min} \sim \frac{e(1-0.5\kappa)}{2e\kappa\rho B_e} \xRightarrow[\rho=0.05]{B=3\cdot10^4\text{H},\ \kappa=0.65} \Rightarrow 1.2\text{cm}$

$$L_{\gamma\gamma} \sim \left(\frac{N}{10^{10}}\right)^2 \frac{\kappa^4\rho^2 f E^2[\text{TeV}]}{(1-0.5\kappa)^2}\cdot 10^{34}\text{cm}^{-2}\text{s}^{-1} \propto E^2 \,!$$

HIGH-Brightness $\vec{\gamma}, \vec{e}^{\pm}$ Sources & E144

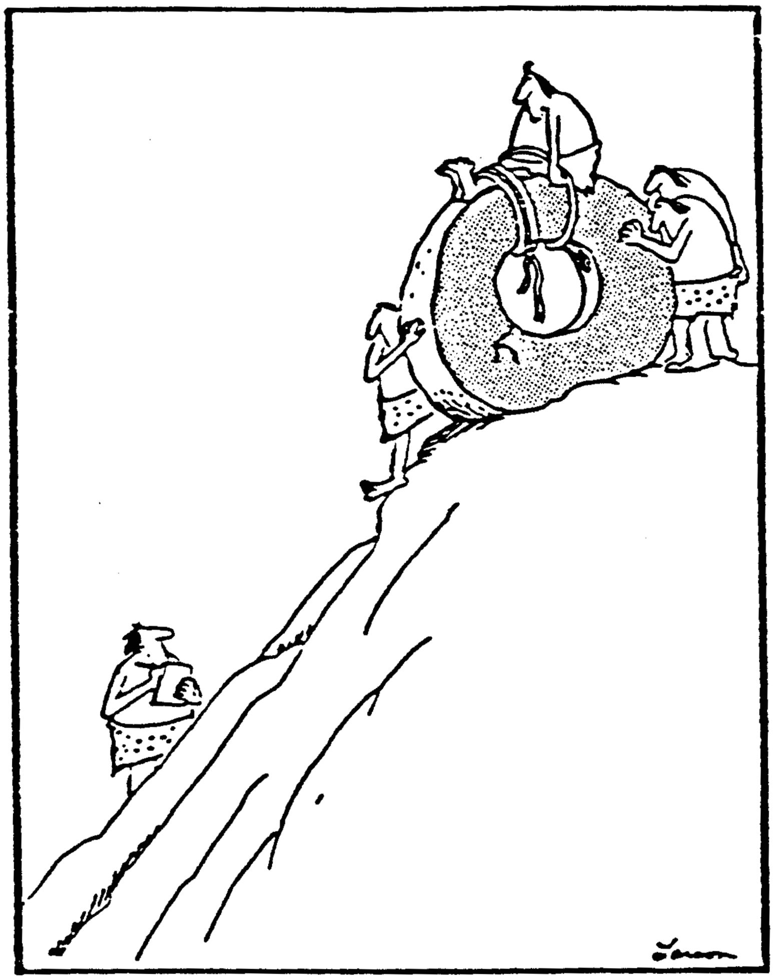

Early experiments in transportation

The current status of Linear Colliders. So what's your hobby-horse?

E144

Proposal for a

STUDY OF QED AT CRITICAL FIELD STRENGTH IN INTENSE LASER–HIGH ENERGY ELECTRON COLLISIONS AT THE STANFORD LINEAR ACCELERATOR

October 20, 1991

J. G. Heinrich, C. Lu, K. T. McDonald,
Joseph Henry Laboratories, Princeton University, Princeton, NJ 08544

C. Bamber(1), A. C. Melissinos(1), D. Meyerhofer(2) and Y. Semertzidis(1)
Department of Physics(1), Department of Mechanical Engineering(2),
University of Rochester, Rochester, NY 14627

P. Chen and J. E. Spencer
Stanford Linear Accelerator Center, Stanford University, Stanford, CA 94309

R. B. Palmer
Stanford Linear Accelerator Center, Stanford, CA 94309
and Brookhaven National Laboratory, Upton, NY 11973

Dave Burke, Tim Barklow, Clive Field, Al Odian

EXPERIMENTS

1. NONLINEAR COMPTON SCATTERING

$$n\omega_0 + e \to e' + \gamma$$

Use either IR or UV.

2. BEAMSTRAHLUNG

$$n\omega_0 + e \to e' + e^+e^- \qquad \text{(Bethe-Heitler, Landau-Lifschitz ...)}$$

$$\to e' + \gamma$$

$$\hookrightarrow \gamma + n\omega_0 \to e^+e^-$$

3. MULTIPHOTON BREIT–WHEELER EFFECT

$$n\omega_0 + \gamma \to e^+e^-$$

Need UV at second interaction.

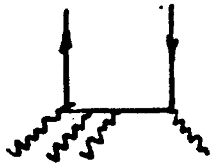

4. MEASURE MASS–SPECTRUM OF e^+e^-

5. HIGH BRIGHTNESS POSITRON SOURCE

e^+ prod by e^- - Laser interaction ?

R B Palmer 3/6/92
with Psin Chen

Motivations

- e^- may be possible from guns without damping ring!
  Can we elliminate e^+ damping ?
- Can we get polarized e^+, e^- without fancy cathodes ?
- Can be elliminate heating / melting problems in e^+ production targets ?

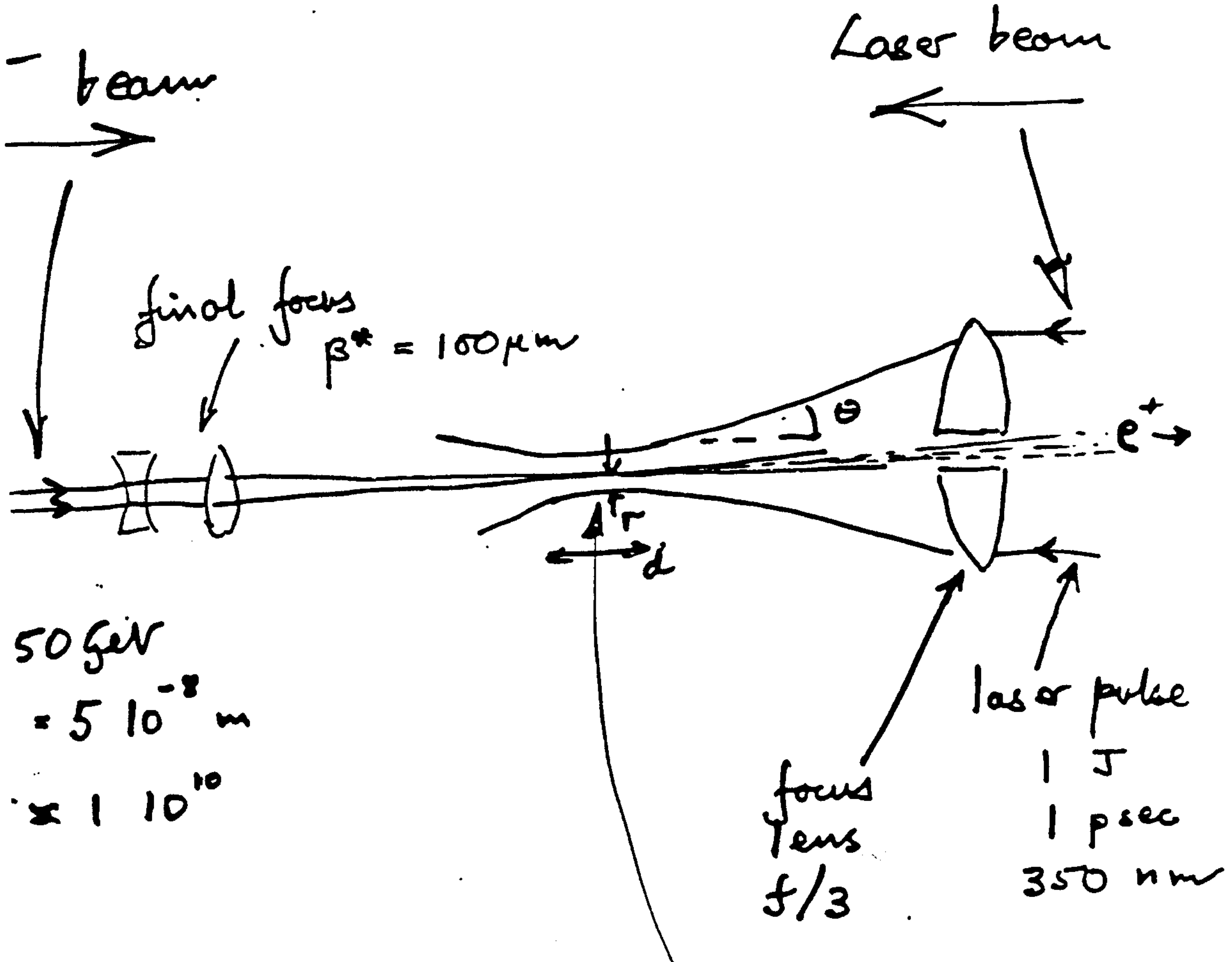

beam

$\sigma_y = 3.2$ nm
$d(\beta^*) = \pm 100\mu$
$\theta = 3.2\ 10^{-5}$ rad
$\sigma_z = 100\mu$

light.

$r \approx 1\mu$
$d \approx \pm 9\mu$
$\theta \approx .16$ rad
$\sigma_z \approx 300\mu$
!

What is emittance of e^+ out ?

β^* of collector ≈ 100μ

$$\epsilon_n = \beta^* \gamma \langle\theta\rangle^2$$

γ out ≈ 10^4

Contributions to $\langle\theta\rangle$

≥9 Initial $\theta = \sqrt{\frac{\beta \epsilon_{in}}{\gamma \beta^*}} = \underline{\underline{.32}} \quad 10^{-4}$

prod of γ at 250 GeV $\langle p_\perp \rangle \approx m_e c$

$$\Delta\theta \approx \frac{.5}{250{,}000} = \underline{\underline{.02}} \quad 10^{-4}$$

pair prod at ~ 50 GeV

$$\Delta\theta \approx \frac{.5}{50{,}000} = \underline{\underline{.1}} \quad 10^{-4}$$

2nd γ at 25 GeV

$$\Delta\theta = \underline{\underline{.2}} \quad 10^{-4}$$

Conversion at 12

$$\Delta\theta = \underline{\underline{.4}} \quad 10^{-4}$$

The $\gamma\gamma$ total cross-section at high energies

M.E. Peskin

w. thanks to Pisin Chen, Bj.

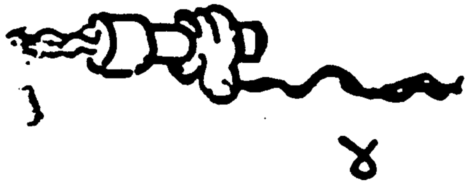

refs:

Drees + Godbole
PRL $\underline{67}$ 1181 (1991)

Drees + Halzen
PRL $\underline{61}$, 275 (1988)

Collins + Ladinsky
PRD $\underline{43}$, 2847 (1991)

Forshaw + Storrow
Manchester preprint
M/C.TH91/31

March 1992

The $\gamma\gamma$ total cross-section at high energies.

M.E. Peskin

2 theories of $\sigma(\gamma\gamma \to \text{hadrons})$:

1) Vector dominance

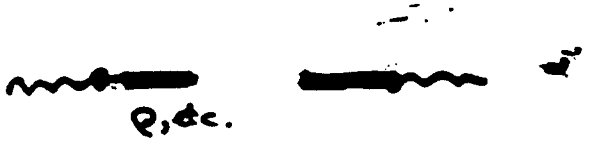

$$\sigma(\gamma\gamma) = \frac{(\sigma(\gamma p))^2}{\sigma(pp)} \approx 300 \text{ nb}$$

NB: $10^{33}/\text{cm}^2\text{sec} \cdot 10^{-2}\text{ sec/train} \cdot 300 \text{ nb} = 3/\text{train}$

2) Twice-resolved gluons (Drees-Godbole)

$$\sigma_{DG} = \int dx_1\, f_{g\leftarrow\gamma}(x_1) \int dx_2\, f_{g\leftarrow\gamma}(x_2) \int_{p_\perp > p_\perp^{\min}} dp_\perp \frac{d\sigma}{dp_\perp}(gg \to gg)$$

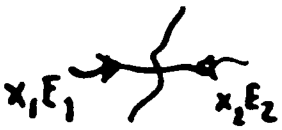

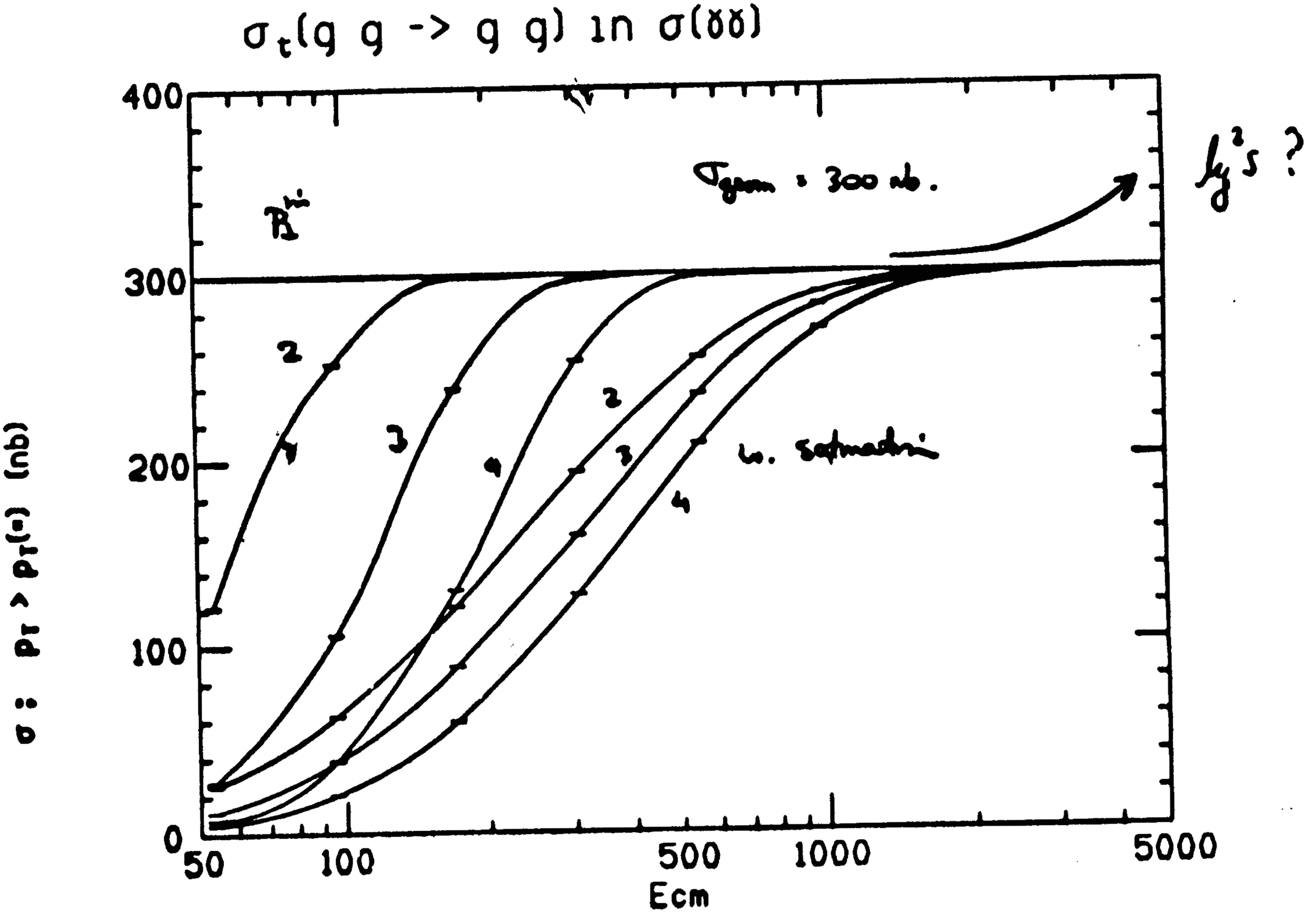

σ_t(g g -> g g) in $\sigma(\gamma\gamma)$
σ : $p_T > p_T(*)$ (nb)
Ecm
0
100
200
300
400
50
100
500
1000
5000
R^{mi}
σ_{geom} = 300 nb.
$l_g^2 s$?
2
1
3
4
2
3
4
w. softmodes

Conclusion:

1.) I do not expect large cross sections for $\gamma\gamma \to$ hadrons

$\sigma(\gamma\gamma \to \text{had}) < \sim 400\,\text{nb}$

even with Drees - Godbole

2.) The average no. of minijets per $\gamma\gamma \to$ hadron event should rise steeply w. s

	1 TeV	5 TeV	
$\langle n_{\text{minijets pairs}} \rangle \sim$	3	15	$p_\perp \sim 2$
	$\frac{1}{2}$	10	$p_\perp \sim 10$

so at 1 TeV:

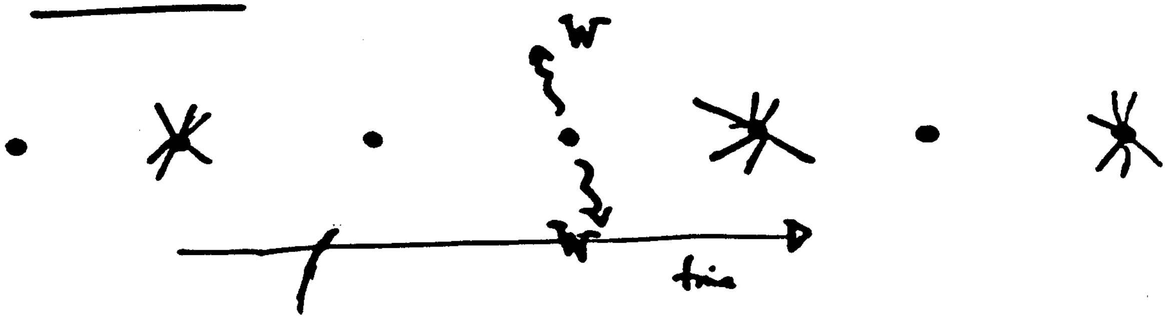

BEAMSTRAHLUNG MINIJET EVENTS

IN

NEXT GENERATION LINEAR COLLIDER

Pisin Chen

(in discussion with M. Peskin, J. Bjorken, & S. Brodsky)

March 6, 1992.

These calculations are still priliminary!

* M. Drees & Godbole first pointed out the importance of minijet events from beamstrahlung. (1991)

$N_{jet} \sim N_\gamma^2$

With cross section

$$\sigma_{\gamma\gamma\to \text{jets}}(s) = \begin{cases} \frac{1}{300}\cdot 110\,\mu b\,, \\ \frac{1}{300}\left[110 + 1200\frac{\sqrt{s}}{1\,\text{TeV}}\right]\mu b\,, \end{cases}$$

and a simplified beamstrahlung spectrum:

$$\phi(y) \simeq \frac{N_\gamma}{2}\,\frac{1}{\Gamma(1/3)}\left(\frac{2}{3\Upsilon}\right)^{1/3} y^{-2/3}\,,$$

we can calculate, with cut-off energy $\sqrt{s_0}$,

$$N_{jet}(s_0) = \mathcal{L}\int_{s_0}^{(3\Upsilon/2)^2} ds \int_s^1 \int_0^1 dy_1\,dy_2\;\delta(s - y_1 y_2)\,\phi(y_1)\,\phi(y_2)\,\sigma_{\gamma\gamma}$$

For constant cross section, we find

$$\boxed{\begin{aligned} N_{jet}(s_0) = {} & \frac{3}{4}\frac{N_\gamma^2}{\Gamma^2(1/3)}\left(\frac{2}{3\Upsilon}\right)^{2/3}\cdot\left\{\left(\frac{3\Upsilon}{2}\right)^{2/3}\left[3 - 2\ln(3\Upsilon/2)\right] + 9\left[\left(\frac{3\Upsilon}{2}\right)^{2/3} - s_0^{1/3}\right]\right\} \\ & \times\frac{1}{300}\cdot 110\,\mu b\cdot\mathcal{L}\,, \qquad \text{for } \frac{3\Upsilon}{2} < 1. \end{aligned}}$$

where $\Gamma(1/3) \simeq 2.6789$.

This formula agrees reasonably well with the numerical calculation.

CLIC 250 + 250 GeV
Log of beam spectra

$\delta_E = .26$

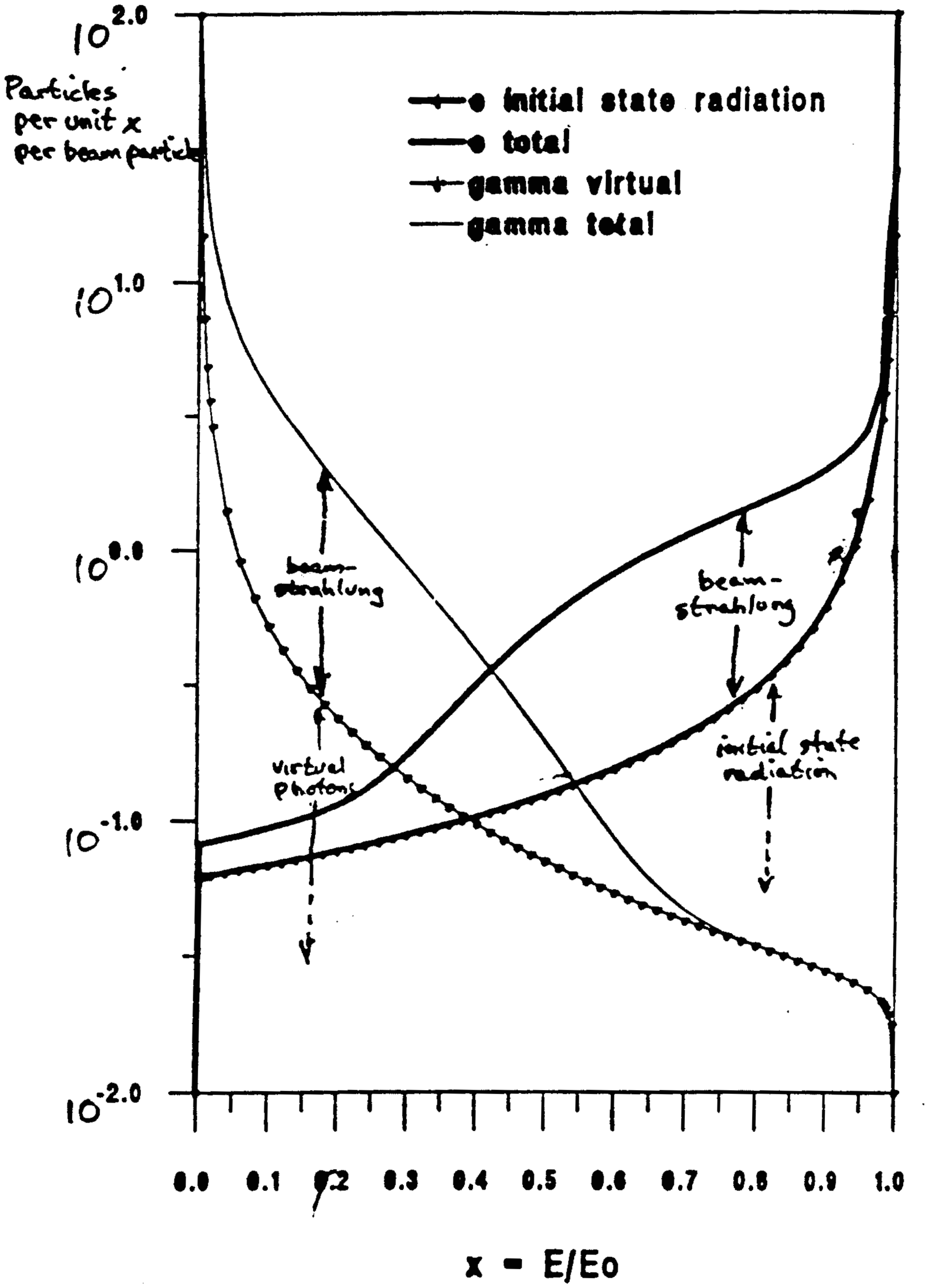

K Berkelman

MODEL FOR $\gamma\gamma$ INTERACTIONS

Single-photon spectrum

$\frac{dn_\gamma}{dx}$ = Weiszäcker-Williams virtual photon spectrum
+ Chen's formula for multiple emission of beamstrahlung photons

$\gamma\gamma$ cross section

$$\sigma_{\gamma\gamma}(s) = \sigma_0 \left[1 + C \left(\ln s - \ln s_0 \right)^2 \right]$$

σ_0: 250 nb = $\frac{\sigma_{\gamma p}^2}{\sigma_{pp}}$ C: .01 s_0: 100 GeV^2 $\underbrace{\quad}_{\text{pp data}}$

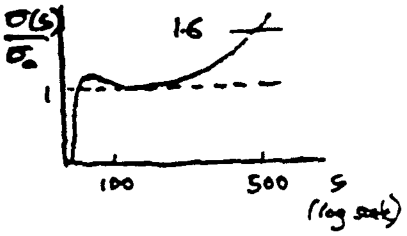

Average multiplicity

$$\bar{n} = a + b \ln s + c \ln^2 s$$

a: 4 b: −.4 c: .34   from pp data

Multiplicity spectrum

Universal KNO scaling form

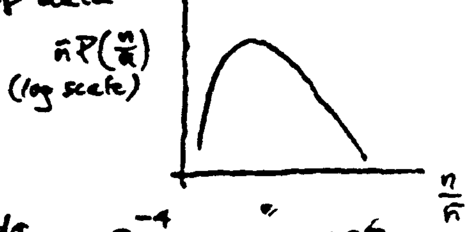

Transverse momenta

Drees prediction (twice resolved)
Constituent interchange } $\frac{d\sigma}{dp_T} \propto p_T^{-4}$ $< 3\%$

Low p_T behavior ($p_T \lesssim 1$ GeV/c) $\propto e^{-b\sqrt{p_T^2+m^2}}$

Longitudinal momenta (in $\gamma\gamma$ c.m.s.)

Flat in rapidity $y = \ln \frac{E+p_L}{E-p_L}$

kinematic limit depends on s, p_T

NOTE: Angles θ tend to be small, because

- p_T usually $\ll p_L$ in $\gamma\gamma$ c.m.s.
- boost to lab

Jet structure is <u>not</u> modeled

MODEL FOR e^+e^- ANNIHILATION CROSS SECTION

Single electron spectrum

$\frac{dn_e}{dx}$ = CONVOLUTION { Weiszäcker-Williams virtual electron spectrum
Chen's formula for beamstrahlung-degraded spectrum

e^+e^- cross section

$$\sigma_{ee} = \frac{\alpha^2}{s} \cdot \underbrace{3 \sum q_i^2}_{\sim 5}$$

(ignoring resonances, ...)

Drees (Saariselkä)

DG-para, $Q^2 = \hat{s}/4$, $p_{T,min} = 1.6$ GeV (AMY value)
(Uncetain to factor ~2!)

machine	$\sigma_{minijet}$ [nb]	σ_{VMD} [nb] ⊛	$\frac{\text{\# minijet-events}}{\text{bunch train}}$ ⊛
älmer G	480	324	22
ılmer F	42	34	0.45
ESY-Dmst	75	85	3.2
ESLA 500	17	14	3.6/800 ≃ 0.0045
γγ- ollider	2000	250	> 20; $\mathcal{L} \gtrsim 10^{31} \frac{cm^{-2}}{b.cr.}$ 85 @ D-D

) for $W_{\gamma\gamma} > 10$ GeV; assumes $\sigma_{VMD} = 250$ nb

) Assumes micro-bunches within same bunch train re not resolved

> Good time resolution can reduce this ckground! Easy for TESLA 500: $\Delta t \simeq 1$ μsec thers: $\Delta t \sim 10$ nsec)

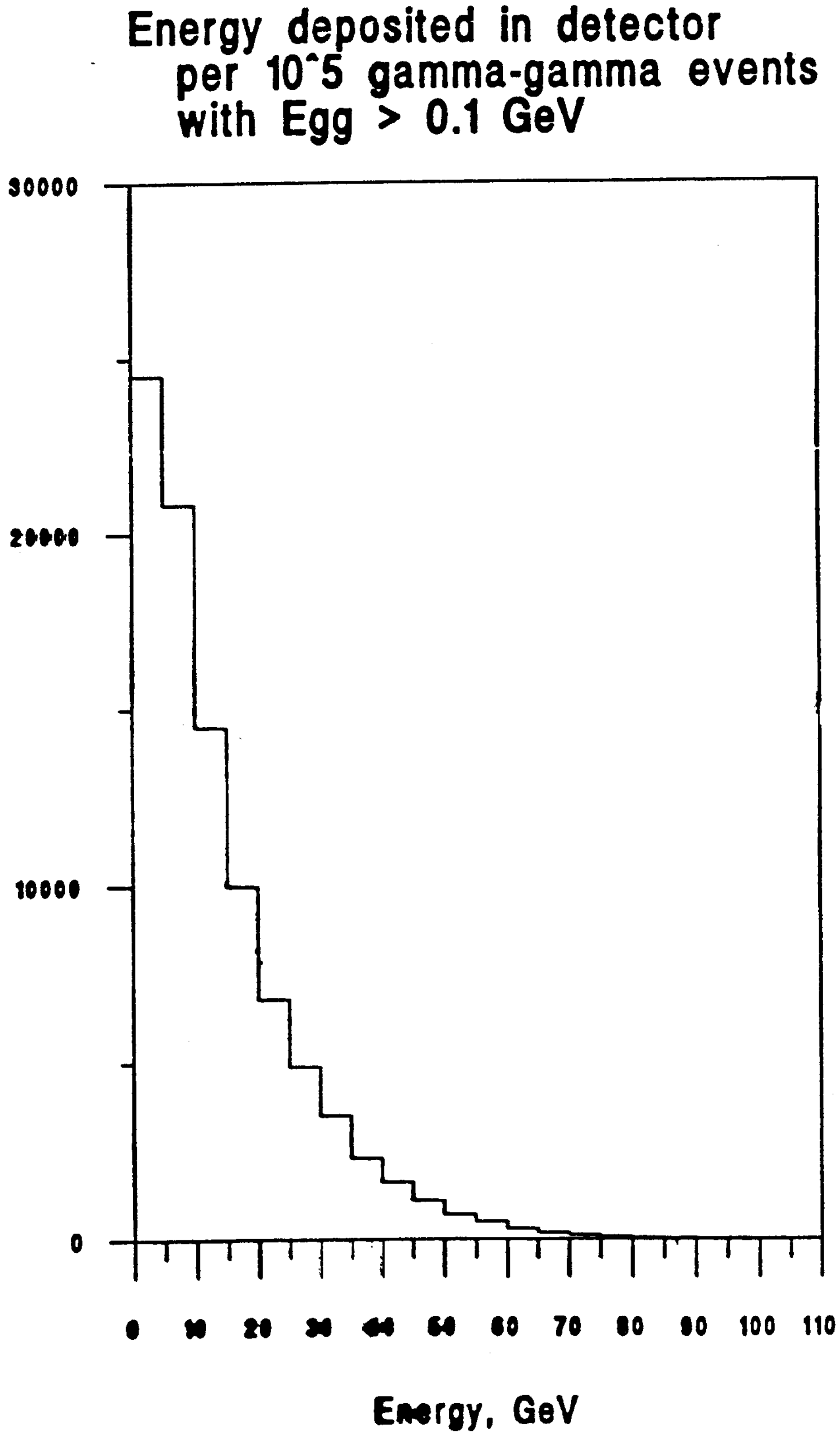

Energy deposited in detector per 10^5 gamma-gamma events with Egg > 0.1 GeV

DETECTOR WORKING GROUP

Chairman: Henry Band

Members and Contributors

K. Floettmann	DESY	V. Telnov	Novosibirsk
M. Leenen	DESY	S. Hertzbach	Univ. of Mass.
E. Kushnirenko	INP	H. Band	Univ. of Wisconsin
A. Miyamoto	KEK	C. Adolphsen	SLAC
Y. Namito	KEK	P. Chen	SLAC
K. Oide	KEK	J. Irwin	SLAC
T. Tauchi	KEK	L. Keller	SLAC
M. Ronan	LBL	R. Nelson	SLAC
R. Settles	Max Planck Inst.	S. Rokni	SLAC

Summary of FFIR Detector Working Group Discussions

Henry Band

The goal of the detector working group was to identify and quantify backgrounds which would impact the design or operation of a detector at a 500 – 1000 GeV e^+e^- collider. Some backgrounds, beam halo and muons produced by beam lost on collimators, are already significant at the lower energy SLC collider. Other, potentially more troublesome backgrounds such as low energy e^+e^- from beamstrahlung photons and minijet hadronic events from $\gamma\gamma$ collisions will only become important at the higher energy and luminosity/bunch of the new collider designs.

A talk on the background experience of SLC/SLD by Stan Hertzbach formed a valuable introduction to the workshop activities. Over eighteen people participated in the ensuing subgroup discussions. Two joint sessions were held with the Beam-Beam group and one joint session was held with the Hardware subgroup, emphasizing the interdependence of the detector and accelerator design. The talks were summarized in a thorough and comprehensive review by Toshiaki Tauchi on the final day. The introductory and review talks are included in these proceedings.

A personal summary of the sessions follow.

The potentially dominant backgrounds arise from the numerous e^+e^- produced from the beamstrahlung photons. Strong solenoidal fields are required to contain these electrons as close to the beam line as possible. Unavoidably, many electrons impact on downstream masks and quadrupoles producing backscattered γ's. Thick conical masks around the beam line are needed to shield the central drift chamber from these back scattered γ's. Suppressions of 10^{-3} can be achieved with 5 cm of tungsten. Studies to date suggest that careful masking designs can control the backscattered γ's.

Although the majority of the e^+e^- are produced at very low energy, the P_T spectrum has a tail extending out to P_T of 100-500 MeV/c. Even in a solenoidal field of 2 Tesla hundreds of electrons will spiral out to radii of 2-4 cm. Pixel vertex detectors will be necessary to obtain the required noise immunity. Subgroup discussions on the appropriate inner radius of the vertex detector yielded no consensus. Although the smallest possible radii ($\approx$ 1 cm) are desirable to obtain the best impact parameter and B tagging efficiency, examples from LEP and design studies show that Vertex chambers with inner radii of 6 - 8 cm still have excellent physics capability. Further study will be required to chose between the options.

Significant differences in the rate and hardness of the electron spectrum were seen between the various collider designs studied. Further optimization of the design parameters may decrease the expected e^+e^- production and ease the detector background constraints.

The other new background associated with high energy, high luminosity colliders are $\gamma\gamma \rightarrow$ minijets. The high energy behavior of this cross section is the object of considerable theoretical debate. For $E_{beam} = 250$ GeV, most models predict < 1 visible minijet hadronic event per bunch crossing. Tracks from minijets can be suppressed if timing information can separate the bunch crossings within a bunch train. One nanosecond track timing resolutions have been achieved in existing central drift trackers. These trackers or other specialized timing devices should aid in the rejection of tracks from minijets and are probably necessary at the higher energy colliders.

Of the remaining backgrounds studied, muons produced by collimated beam particles will be the most difficult to control. The muon production mechanisms are well studied. Tracking of the muons through the accelerator housing and beamline requires detailed Monte Carlo simulation. Even with muon spoiling toroids, studies for the NLC predict that less than 0.1% of the beam can be collimated within the last 500 meters from the detector if the muon flux in the detector is to be kept below 2–3 muons per pulse. Designs with larger bends between the collimation region and the detector are needed and require study.

SUMMARY TALK

Summary of Detector Subgroup	T. Tauchi

PARALLEL SESSION TALKS

Geometry of IP Region	J. Irwin
Estimation of Beam Induced Muon Background	Y. Namito
Lithium "Particles Guide" and Possible Layout of the Interaction Region	E. Kushnirenko
Muon Attenuation	E. Kushnirenko
Muon Background	L. Keller
Theory and Simulation of Incoherent Pair Creation	P. Chen/T. Tauchi
Drift Chamber Time Resolution	C. Adolphsen
Two-Photon Physics from TPC Experiments	M. Ronan
Der Siliziumstreifen Vertex Detektor von ALEPH	R. Settles
"Conservative" NLC Vertex Detector Design	C. Adolphsen
Physics and Background for Vertex Detector	Y. Sugimoto/T. Tauchi
Tracking of $e^{\pm}$ From Beamstrahlung at NLC	H. Band

Summary of Detector subgroup

3/6 '92 FF and IR worksho

T. Tauchi at SLAC

Paticipants Chair : H. Band

1. R. Nelson
2. V. Telnov
3. S. Rokni
4. T. Tauchi
5. S. Hertzbach
6. H. Band
7. A. Miyamoto
8. K. Flœmnann
9. M. Leenen
10. L. Keller
11. Y. Namito
12. D. Burke
13. C. Adolphsen
14. Chis Damell
15. R. Settles
16. E. Kushnirenko
17. J. Irwin
18. M. Ronan

others

Subjects (talks)

I. Backgrounds

I-1) Muons

L. keller	NLC
Y. Namito	Estimation of μ yields (JLC)
E. kushnirenko H. Band	Muon attenuation experience in SLD .

I-2) QED , $e^{\pm}$ pairs

S. Lepshokov	QED backgrounds at VLEPP
P. Chen	Theory of incoherent pairs
T. Tauchi	Simulation and masking (JLC,NLC
J. Irwin	Non-mask IR design for large crossing angle
E. kushnirenko	Li channeling for $e^{\pm}$ pairs
H. Band	NLC tracking of $e^{\pm}$ pairs

I-3) QCD , mini jets

A. Miyamoto	JLC - DG mini jets
R. Settles	ALEPH "mini" jets
M. Ronan	TPC/2γ "mini" jets
C. Adolphsen	Timing chamber (bunch separation)

II. Vertex Detectors

C. Adolphsen	'conservative' NLC vertex detector design
Chris Damerell	SLD vertex detector
R. Settles	ALEPH vertex detector
T. Tauchi	Physics and background for vertex detector at JLC

III. Others

Two detector option ?

· (e^+e^- collision
  $\gamma\gamma$, γe collision

· two experimental groups for multi-billion \$ project .

Muons

Y. Namito

1. $\mu^\pm$ pair creation.

MUON PRODUCTION FROM EACH CHANNEL

$\boxed{\mu/e}$

MUON 89 - code
by W.R. Nelson and
Y. Namito

$E_e = 750$ GeV

1 θ = 0. 10. 20. 30 mRad

	0 mRad	10 mRad	20 mRad	30 mRad (arb.unit)
Coh (IWW)	2.66e-4	2.52e-6	1.02e-6	3.54e-7
Inc (IWW)	2.68e-7	1.97e-8		
J/Ψ	2.47e-7	2.31e-8		
D	1.14e-6	1.62e-7	4.47e-8	1.93e-8
Inelastic	6.24e-6	2.92e-8		
Coh(Born)	2.46e-4	2.38e-6		
Inc(Born)	1.15e-6	2.30e-8		

π, K

2. $\int_0^{100\,\mathrm{mRad}} d\theta$

[μ-on/e]

	$E_\mu > 0$	$E_\mu > 10$ GeV
Coh	1.63e-3	4.77e-4
Inc	2.14e-5	4.01e-6
J/ψ	1.63e-5	1.62e-5

"Direct e^+ annihilation" should be included.

$$\underset{\text{shower}}{\widetilde{e^+}}\ \underset{\text{atom}}{\widetilde{e^-}} \longrightarrow \mu^+\mu^- \qquad \sim 10\% \text{ of coherent (?)}$$

$$E_{e^+} > \frac{2m_\mu^2}{m_e} = 40\ \mathrm{GeV} \sim E_{\mu^\pm}$$

2. MUON ATTENUATION – (L. KELLER) L. Keller.

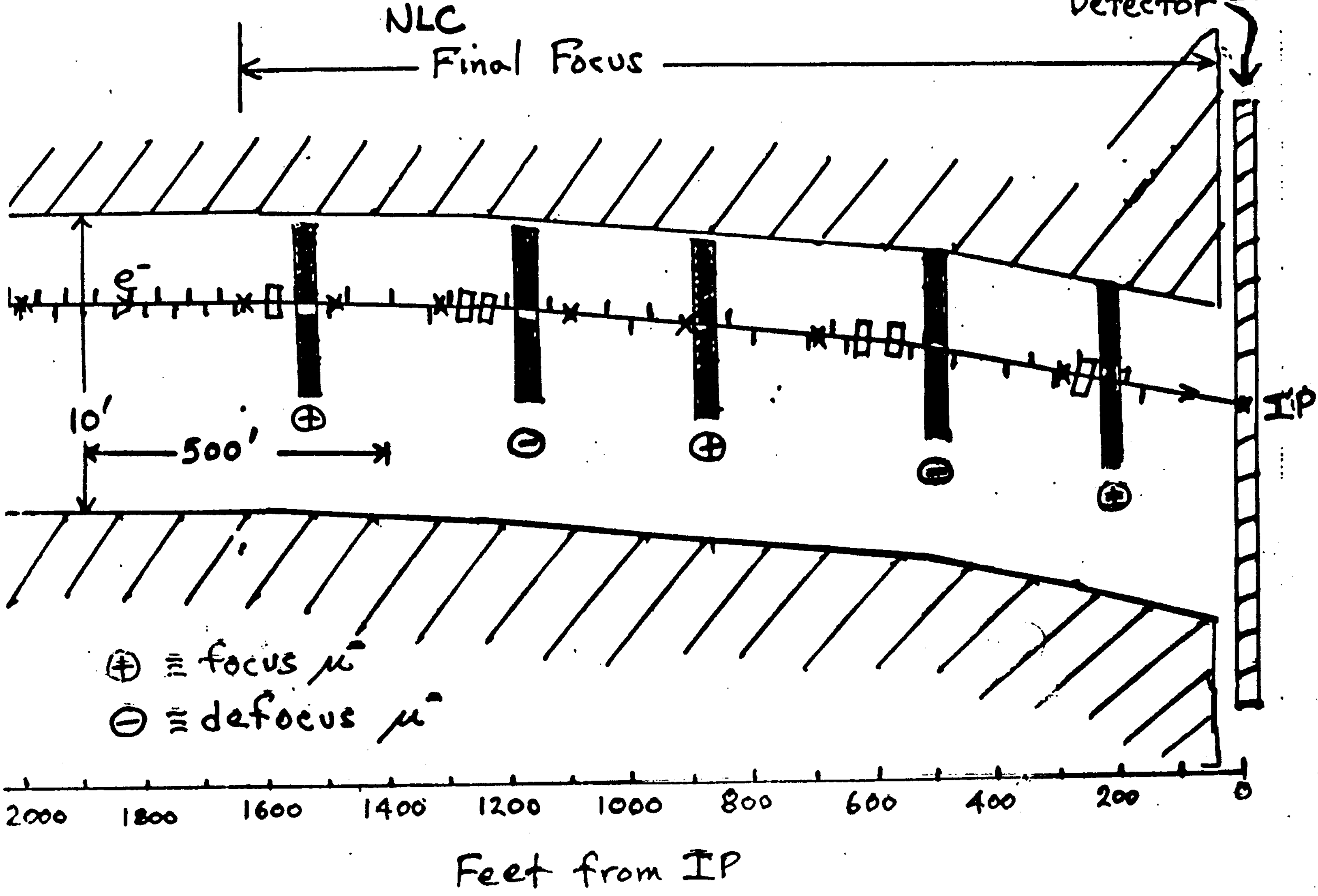

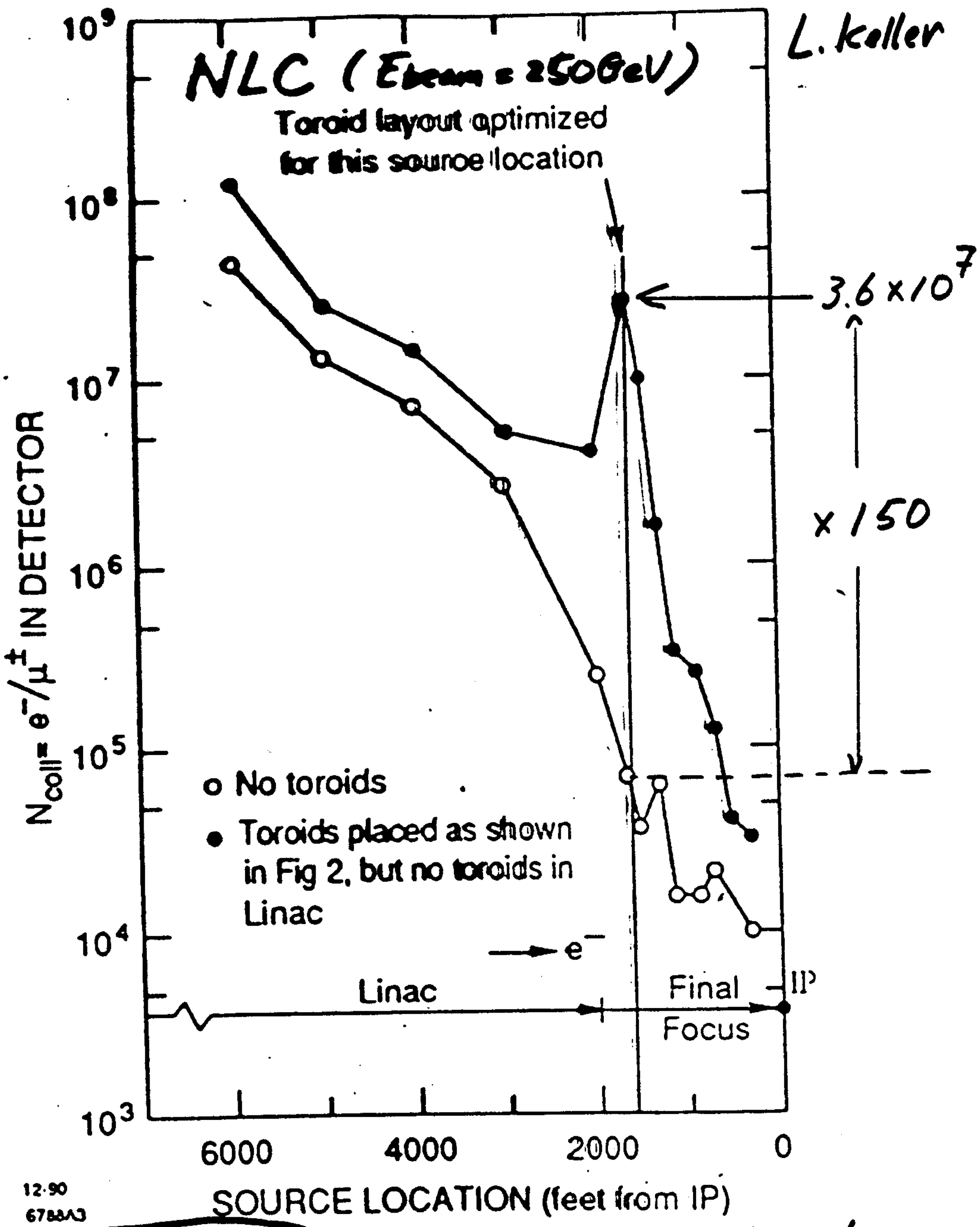

$N_{coll} = 3.6 \times 10^7$
⇑
present limit
at the end of LINAC.

μs rescattered in tunnel are dominant source. ⇐ Detail tracking is very important.

3. New Idea of muon attenuation

by E. Kushnirenko

High energy muons ($P_\mu > P_\mu^{min}$) are guided by magnetized iron pipes.

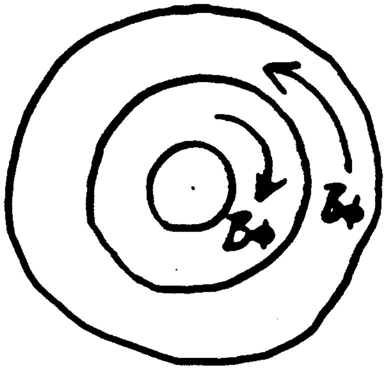

$B_\phi \sim 1.5$ Tesla

e.g. inner focus μ^- ($\sim 5\,\mathrm{cm}^t$)

outer focus μ^+ ($\sim 10\,\mathrm{cm}^t$)

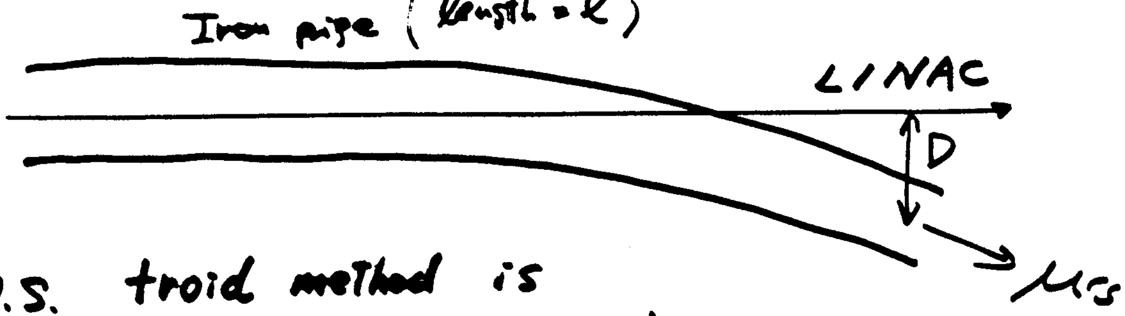

V.S. troid method is sweeping out μ's.

$$R = \frac{P_\mu}{0.3\, B_\phi}$$

$$\theta_b \simeq \frac{\ell}{R} \quad : \text{bend angle}$$

e.g. $P_\mu = 250\,\mathrm{GeV}$

$R = 556\,m$

$\ell = 56\,m$ for $\theta_b \sim 0.1$

$D = \frac{\ell^2}{2R} \sim 2.8\,m$

Summary of mask system

purpose : Shield against the backscattered γs created in collisions between high energy $e^{\pm}$ pairs and FF magnet.

require : $\eta_{escape} \lesssim 10^{-3}$

for 10^7 backscattered γs

and

enough thickness $(< 10^{-5})$

5 cm^t W for 0.5 MeV γ

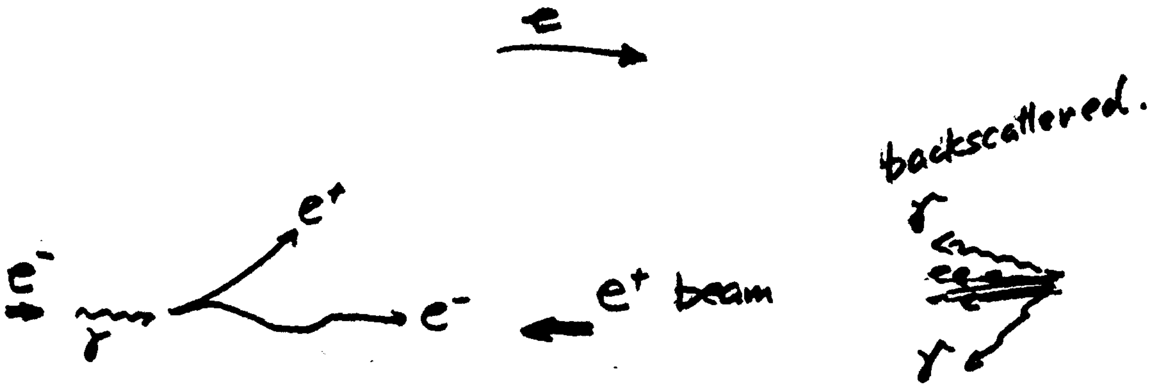
e
e⁻
γ
e⁺
e⁻
e⁺ beam
backscattered.
γ
γ

REVISED GEOMETRY

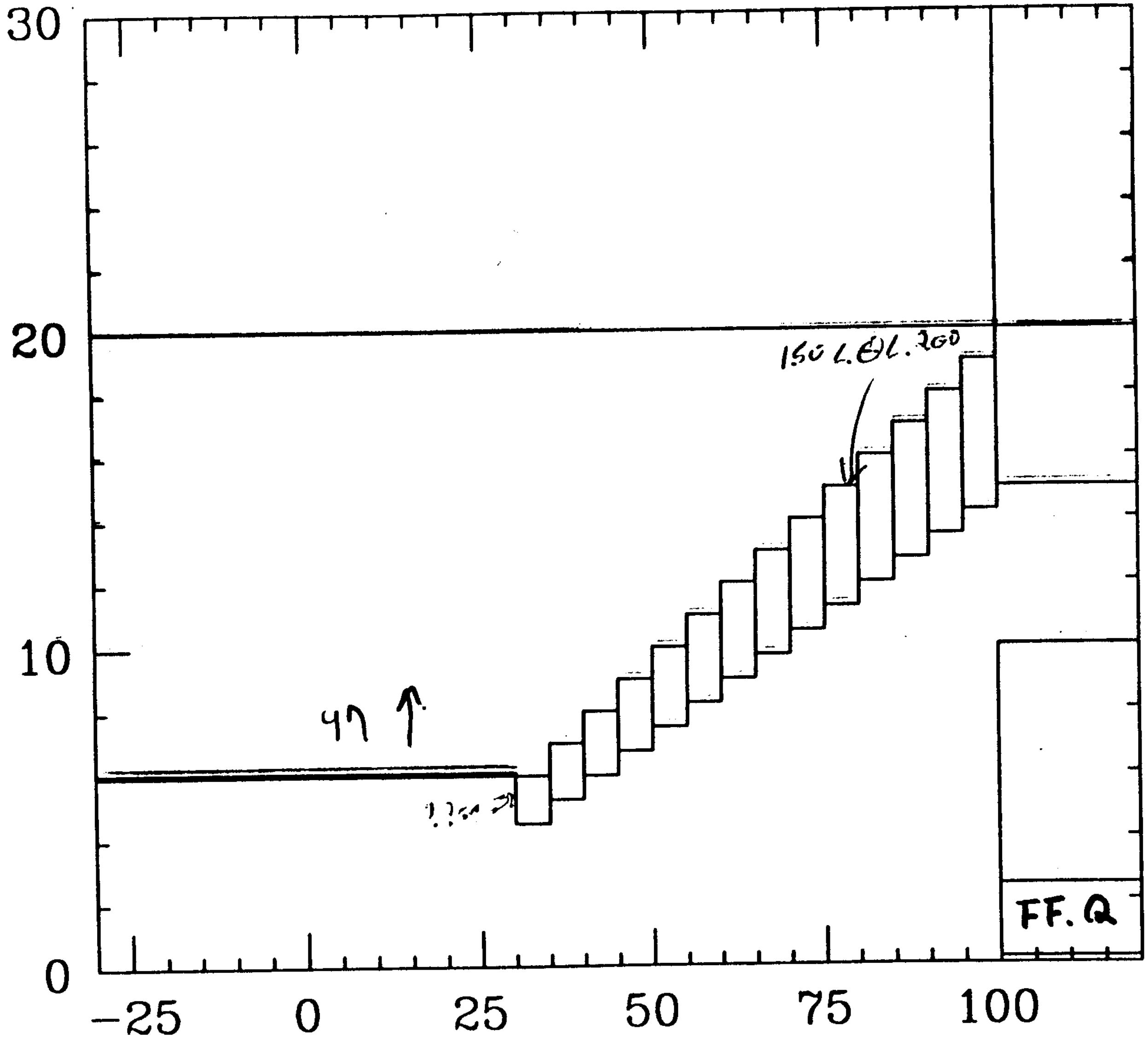

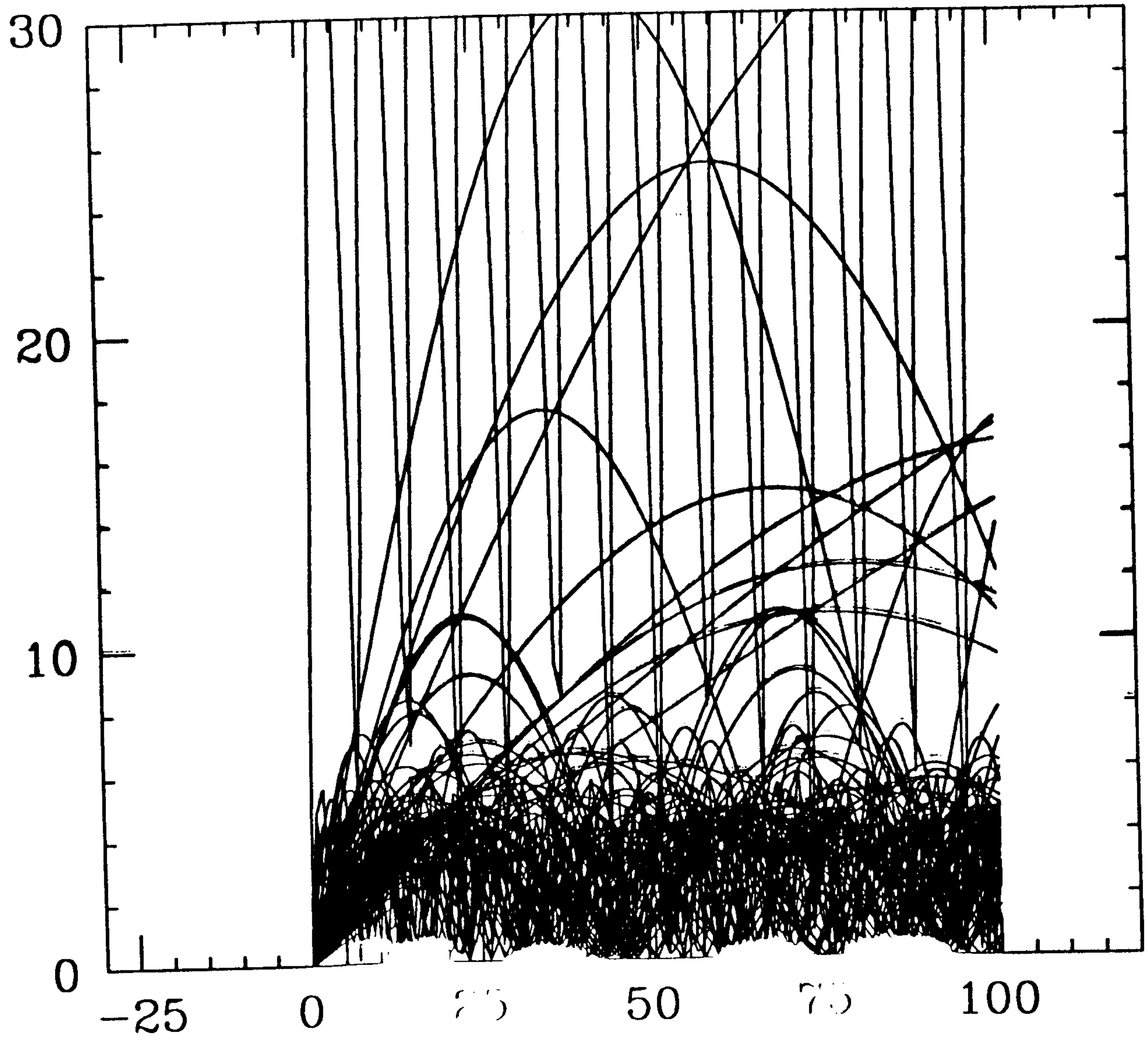
ABEL – PALMER F E>5 MEV THETA> 100 RHO>2CM

H. Band

ABEL – PALMER F E>5 MEV WEIGHT 100

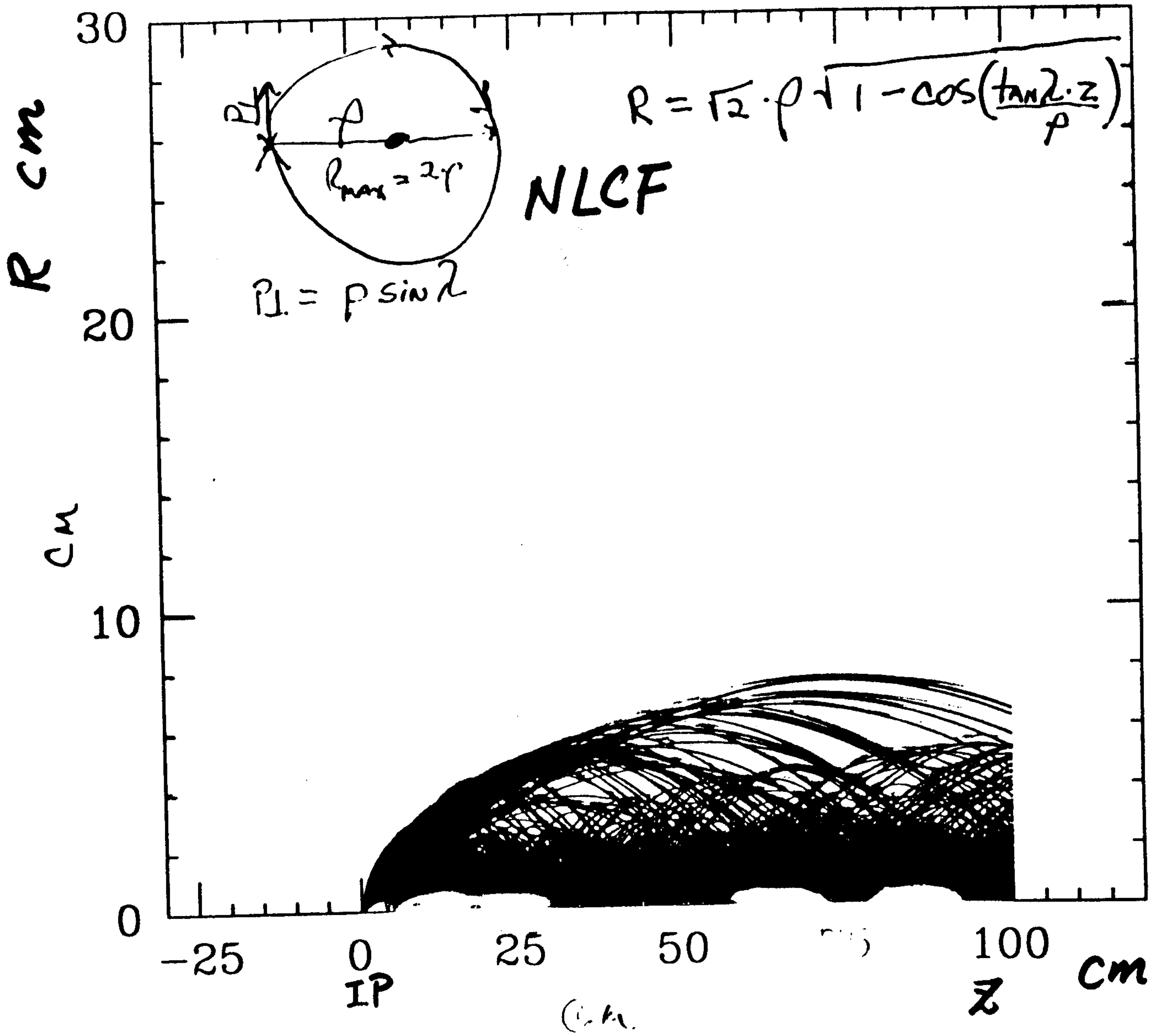

$$R = \sqrt{2}\cdot\rho\sqrt{1-\cos\left(\frac{\tan\lambda\cdot z}{\rho}\right)}$$

$R_{max} = 2\rho$

$P_\perp = \rho\sin\lambda$

Mask system proposed at LC '91.

Detector region

$B = 1.5 \sim \underline{\underline{2}}$ Tesla

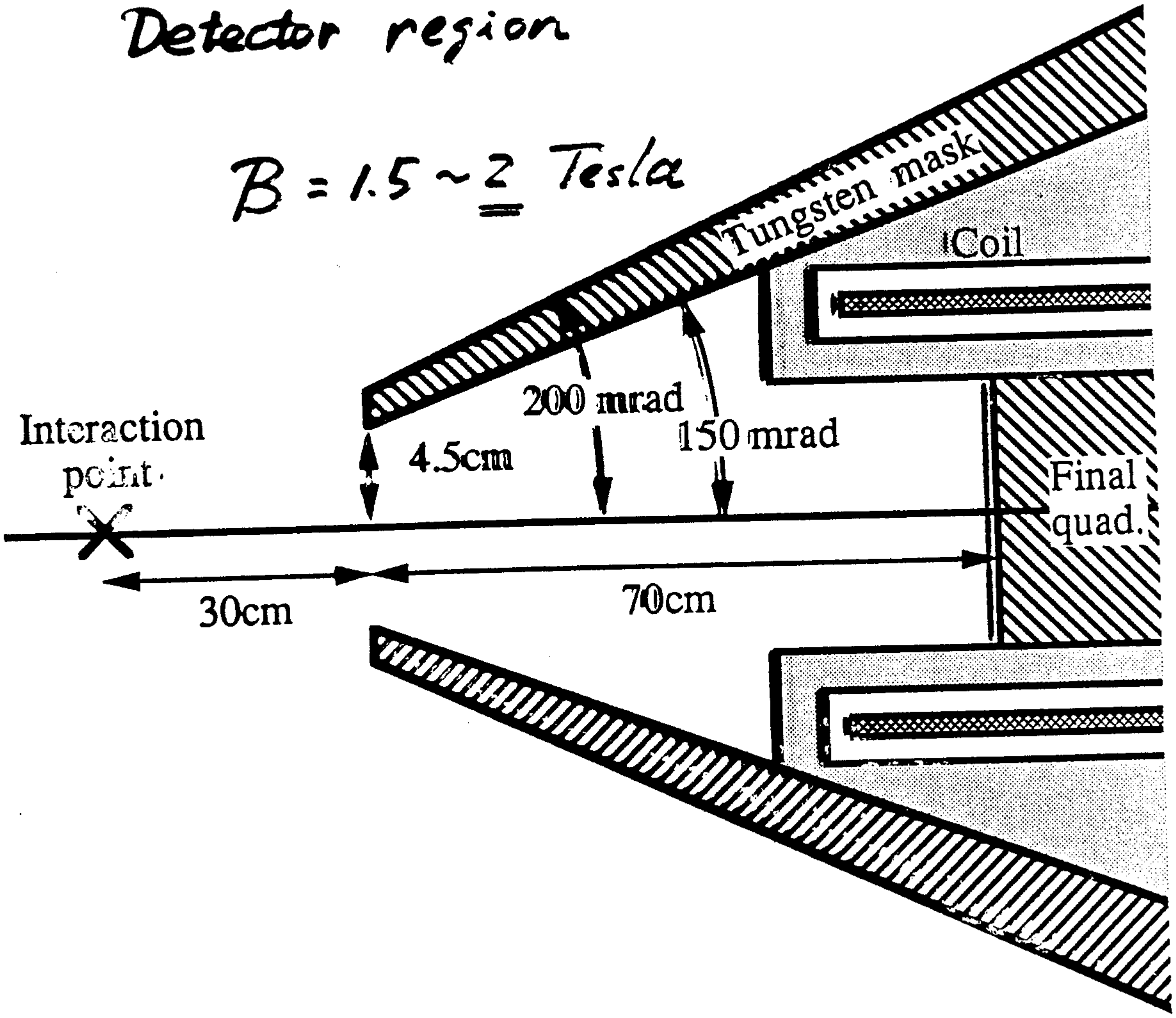

QED $e^{\pm}$ pairs

Incoherent pair creation by virtual and beamstrahlung photons.

$e^+e^- \longrightarrow e^+e^-e^+e^-$: LL

$\gamma e^{\pm} \longrightarrow e^+e^-e^{\pm}$: BH

$\gamma\gamma \longrightarrow e^+e^-$: BW.

Typical scattering angles $\sim \frac{m_e}{E_{e^{\pm}}}$: small

however the pairs are kicked by the strong magnetic field produced by comming beam. $\Rightarrow$ Background

Estimation of pairs with their angular distribution

use real photon approximation

$$n(y) = \frac{2\alpha}{\pi}\frac{1}{y}\ln\frac{1}{y}$$ energy spectrum of virtual photon.

$$y \equiv \frac{E_\gamma}{E_{beam}}$$

$$\sigma = g\int_{-c_0}^{c_0}\int_{y_-}^{1}\int_{y_b}^{1} dc\, dy_2\, dy_1\; n_b(y_1)\, n_b(y_2)\; \sigma_{\gamma\gamma}(y_1, y_2, c)$$

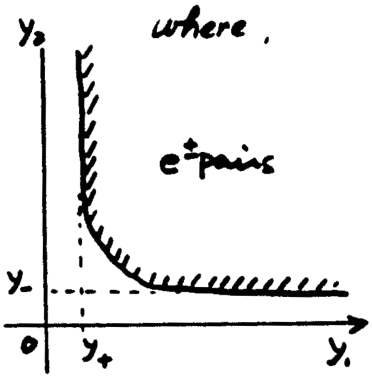

where,

$$y_\pm = \frac{x_0}{2}(1 \pm c) = \frac{x_{0\perp}}{2}\sqrt{\frac{1 \pm c}{1 \mp c}}$$

$$c = \cos\theta$$

$$y_b = \frac{y_2\, y_+}{y_2 - y_-}$$

$$x = \frac{2 y_1 y_2}{y_1(1-c) + y_2(1+c)} = \frac{\varepsilon}{E_{beam}}$$

$$\sigma_{\gamma\gamma} = \frac{\pi r_e^2}{\gamma^2 y_1 y_2}\,\frac{1}{1-c^2}\left[\underbrace{\frac{y_1^2(1-c)^2 + y_2^2(1+c)^2}{(y_1(1-c) + y_2(1+c))^2}}_{\text{Q5a}}\right]$$

Q5a : set 1 for analytic formula

$$g = \begin{cases} 1 & \text{for LL} \\ 1 & \text{BH} \\ 1/4 & \text{BW} \end{cases}$$

note : $n_b(y) = A\, y^{-2/3}$

Analytic Formula

P. Chen
T. Tauchi
K. Yokoya
D.V. Schroeder

For background estimation,

$a(\chi_{L0}, \theta_0)$ is very usufull.

e.g. $\chi_{L0} \cdot E_{beam} = 10\,\mathrm{MeV} \left(\frac{B}{1.5\,\mathrm{Tesla}}\right)$

$\theta_0 = 0.15$

with no beam deflection.

assume $\sigma_{\gamma\gamma} = \frac{\pi r_e^2}{\gamma^2} \frac{1}{[illegible]} \frac{1}{1-c^2}$ "

$$a_{LL} = 1.27 \frac{\alpha^2 r_e^2}{\gamma^2} \left(\frac{2}{\chi_{L0}}\right)^2 \ln\frac{1}{\tau_0} \left(\ln\frac{\chi_{L0}}{2\tau_0} \ln\frac{\chi_{L0}\tau_0}{2} + 3\ln\frac{\chi_{L0}}{2} + 4.44\right)$$

$$a_{BH} = 4.1 \frac{\alpha r_e^2}{\gamma^2} A \left(\frac{2}{\chi_{L0}}\right)^{5/3} (\tau_0^{-1/3} - \tau_0^{1/3}) \left(-0.94 \ln\frac{\chi_{L0}}{2} - 0.2\right)$$

$$a_{BW} = 2.42 \frac{r_e^2}{\gamma^2} A^2 \left(\frac{2}{\chi_{L0}}\right)^{4/3} \ln\frac{1}{\tau_0}$$

$$\tau_0 \equiv \tan\frac{\theta_0}{2} \sim \frac{\theta_0}{2}$$

$$a_{LL} \propto \chi_{L0}^{-2}$$

$$a_{BH} \propto \chi_{L0}^{-5/3}$$

$$a_{BW} \propto \chi_{L0}^{-4/3}$$

ABEL simulation

beam-beam interaction

a) Correct $\sigma_{\gamma\gamma}$

b) geometric reduction

$\times 0.7$ in total

c) external field effect — small effect compared to (b)
(e.m.)

$$\ell_{incoherent} < \ell_{coherent}$$

d) deflection by comming beam

$$\left(\begin{aligned} \theta_{max} &= \sqrt{\frac{\ln \frac{4\sqrt{3} D_x}{\varepsilon}}{\sqrt{3}\,\varepsilon D_x}}\;\theta_0 \\ \theta_0 &\equiv \frac{D_{x(y)}\,\sigma_{x(y)}}{\sigma_z} \\ \varepsilon &\equiv \frac{\varepsilon_c}{E_{beam}}. \end{aligned} \right)$$

Geometric Reduction

virtual photon energy spectrum

$$n(y) = \frac{2\alpha}{\pi} \frac{1}{y} \ln \frac{1}{y}$$

or

$$n(\omega, k_\perp) = \frac{\alpha}{2\omega} \frac{k_\perp^3}{\left(k_\perp^2 + \frac{\omega^2}{\gamma^2}\right)^2}$$

$$\frac{\omega}{\gamma^2} \le k_\perp \le m$$

$$\omega \equiv y \cdot E_{beam}$$

n_{max} at $k_\perp^{max} = \sqrt{3}\,\frac{\omega}{\gamma}$

e.g. $\gamma = 10^6$

$\omega = 10^{-4} \cdot 5 \cdot 10^5 = 50$ MeV

$k_\perp^{max} = 87$ eV

$1/k_\perp$ corresponds To impact parameter $\rho_\perp$.

$$\rho_\perp = 2.3 \text{ nm} \approx \sigma_y$$

analytically $\underset{\sim\sim}{\frac{\hbar c}{\sigma_y}} \le k_\perp \le m$

expects reduction of pair creation in small $k_\perp$, and pair creation outside "beam".

"Two beams interact non-locally."

L.L process

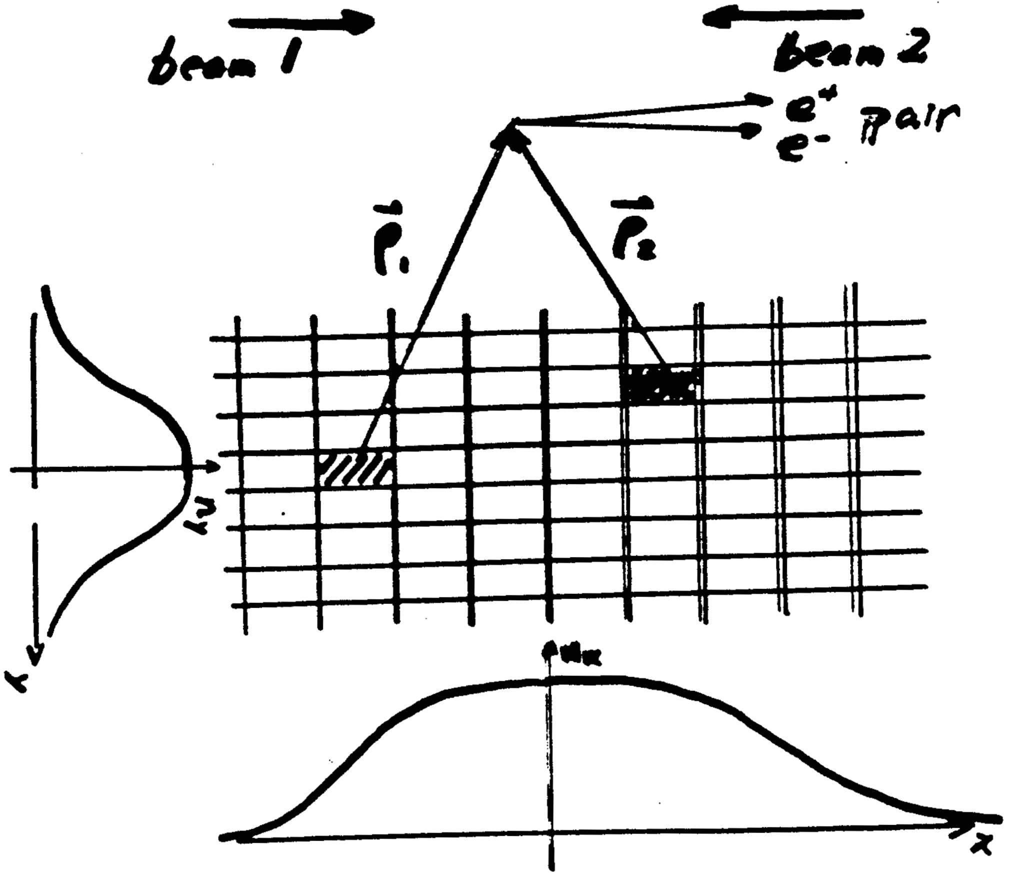

$$\text{geometric reduction factor} = \frac{n_1(x_1,y_1)\cdot n_2(x_2,y_2)}{n_1(x_1,y_1)\cdot n_2(x_1,y_1)}$$

$$x_2 = x_1 + \rho_{1x} + \rho_{2x}$$

$$y_2 = y_1 + \rho_{1y} + \rho_{2y}$$

$$\rho \equiv \frac{\hbar c}{\gamma_2 \gamma m}$$

JLC parameters at LC '91

E_{beam} GeV	250	500	750
$\mathcal{L}$/bunch $cm^{-2}s^{-1}$	1.1×10^{30}	4.0×10^{30}	5.7×10^{30}
σ_x nm	335.3	372.0	561.3
σ_y nm	4.5	3.1	2.7
σ_z μm	151.5	112.8	94.6
N/bunch	1.26×10^{10}	2.02×10^{10}	2.67×10^{10}
Υ	0.085	0.43	0.66
A	1.01	1.11	0.83
$e^{\pm}$pair yields			
N_{LL}	4.94×10^4	2.09×10^5	3.29×10^5
N_{BH}	2.68×10^5	1.13×10^6	1.24×10^6
N_{BW}	2.60×10^3	7.48×10^3	4.67×10^3
Beam deflection			
D_x	0.17	0.085	0.028
D_y	12.8	9.96	5.39
θ_0	3.8×10^{-4}	2.8×10^{-4}	1.6×10^{-4}
$\theta_{max}(E=0.1GeV)$	0.099	0.15	0.18

note : 20 bunches/pulse
150 pulses/sec.

$$\theta_0 = \frac{D_{x(y)}\,\sigma_{x(y)}}{\sigma_z}$$

$$\theta_{max} = \sqrt{\frac{\ln\frac{4\sqrt{3}D_x}{\varepsilon}}{\sqrt{3}\,\varepsilon\,D_x}}\;\theta_0 \;\propto\; \frac{N}{\sqrt{\ }}$$

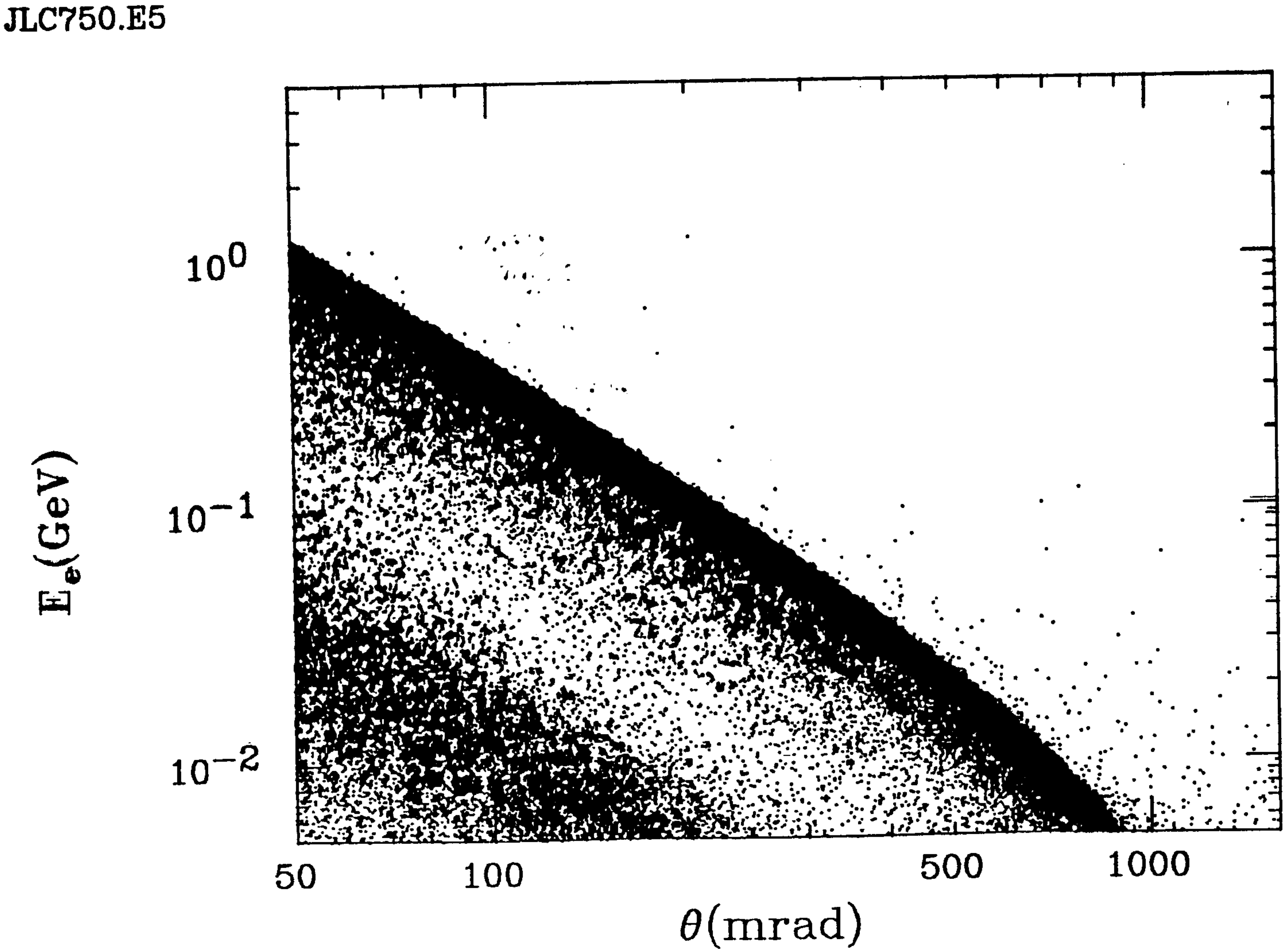
JLC750.E5
10^0
10^{-1}
10^{-2}
E_e(GeV)
50
100
500
1000
θ(mrad)

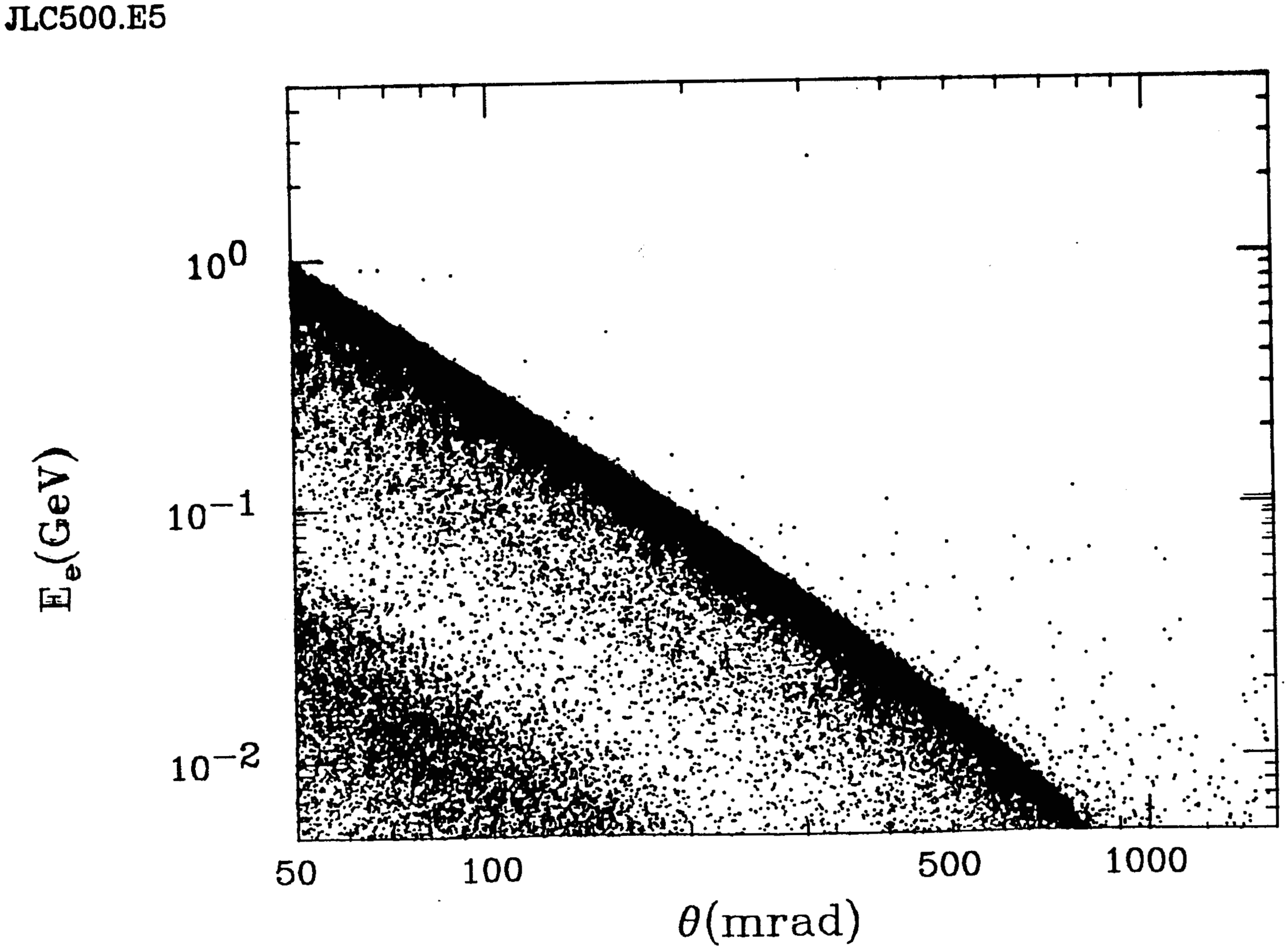
JLC500.E5
10^0
10^{-1}
10^{-2}
E_e(GeV)
50
100
500
1000
θ(mrad)

JLC250.E5

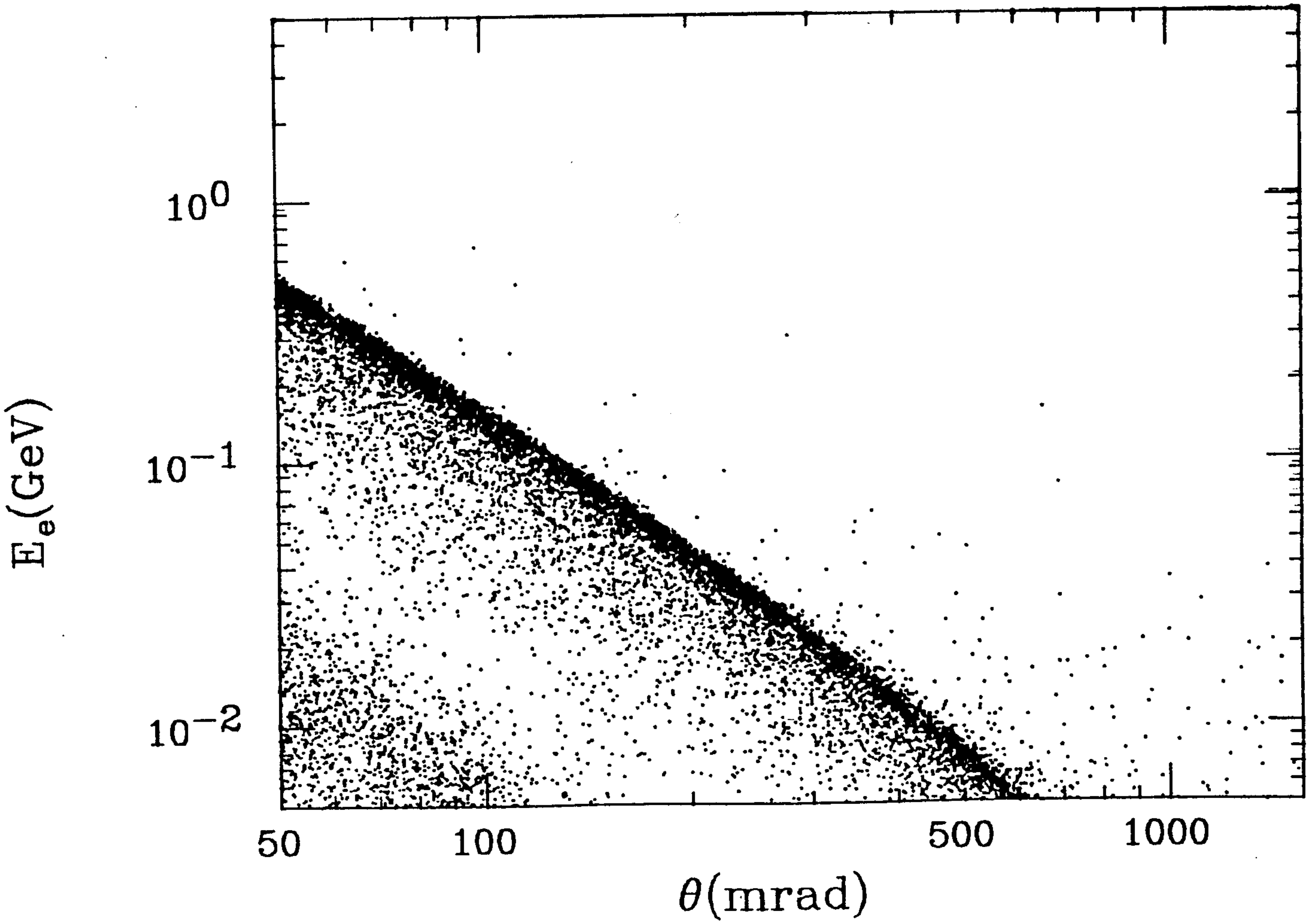

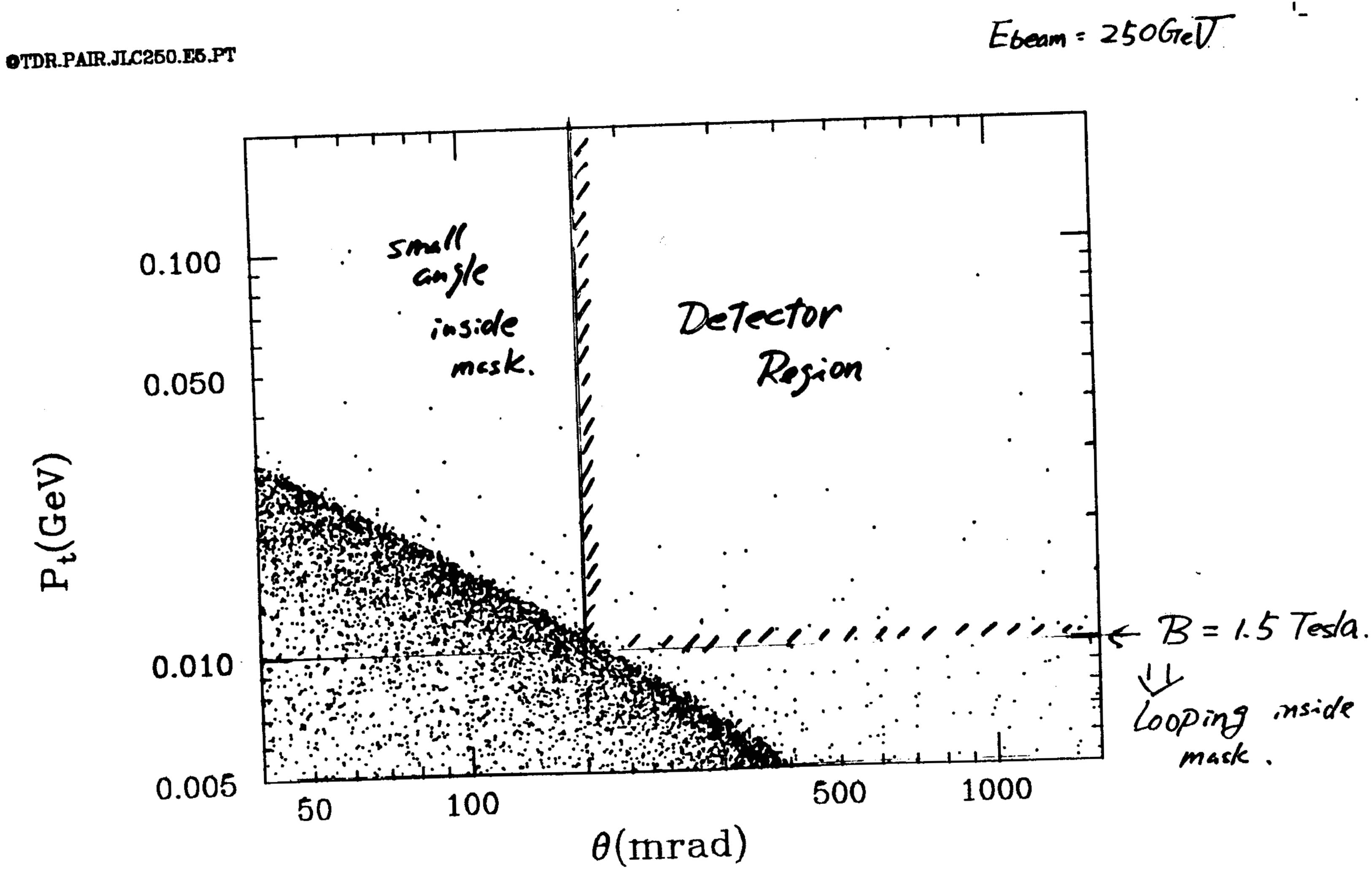
@TDR.PAIR.JLC250.E5.PT
Ebeam = 250GeV
small angle inside mask.
Detector Region
B = 1.5 Tesla.
Looping inside mask.
0.100
0.050
0.010
0.005
Pt(GeV)
50
100
500
1000
θ(mrad)

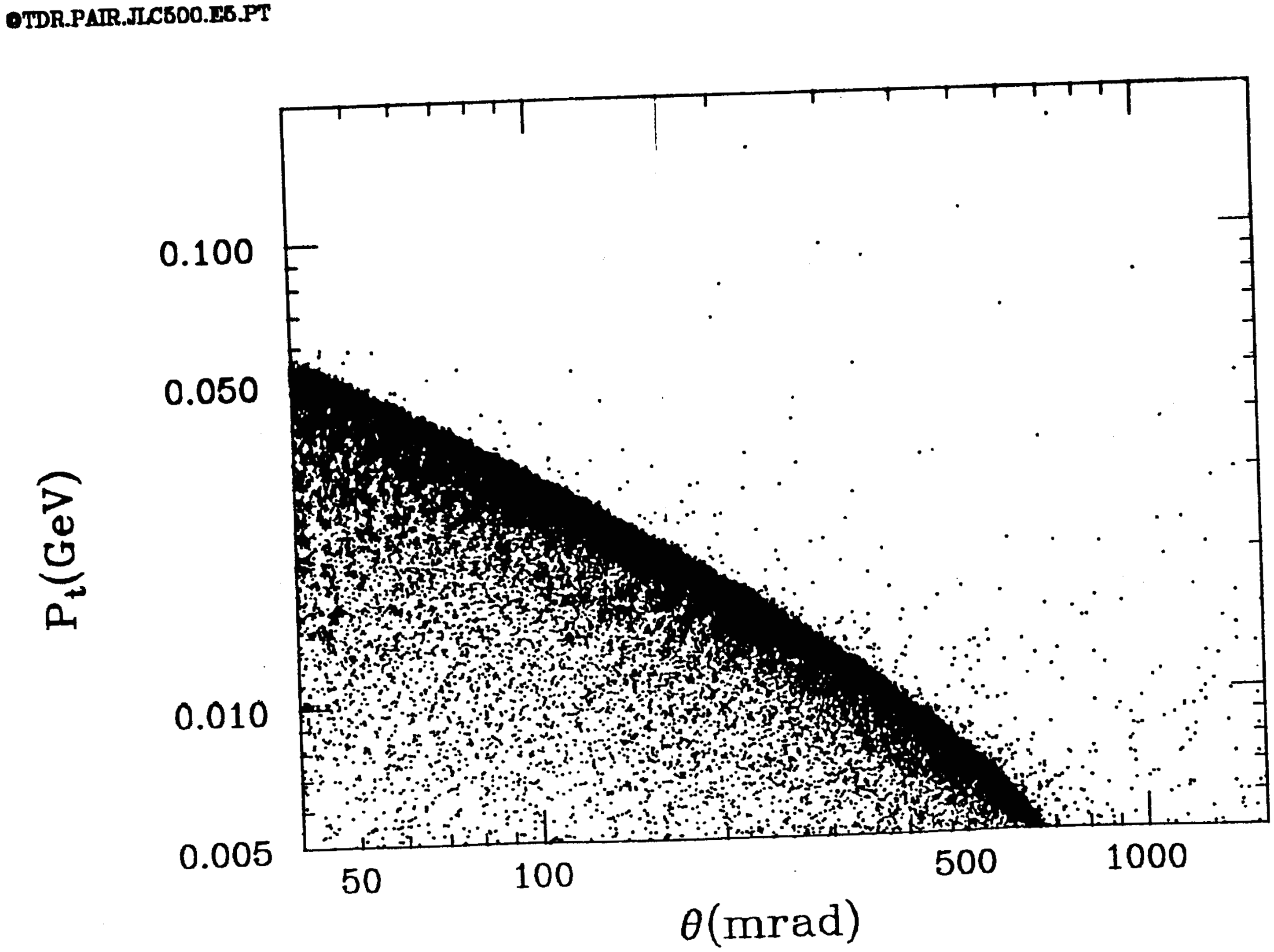
@TDR.PAIR.JLC500.E5.PT
0.100
0.050
0.010
0.005
P_t(GeV)
50
100
500
1000
θ(mrad)

@TDR.PAIR.JLC750.E5.PT

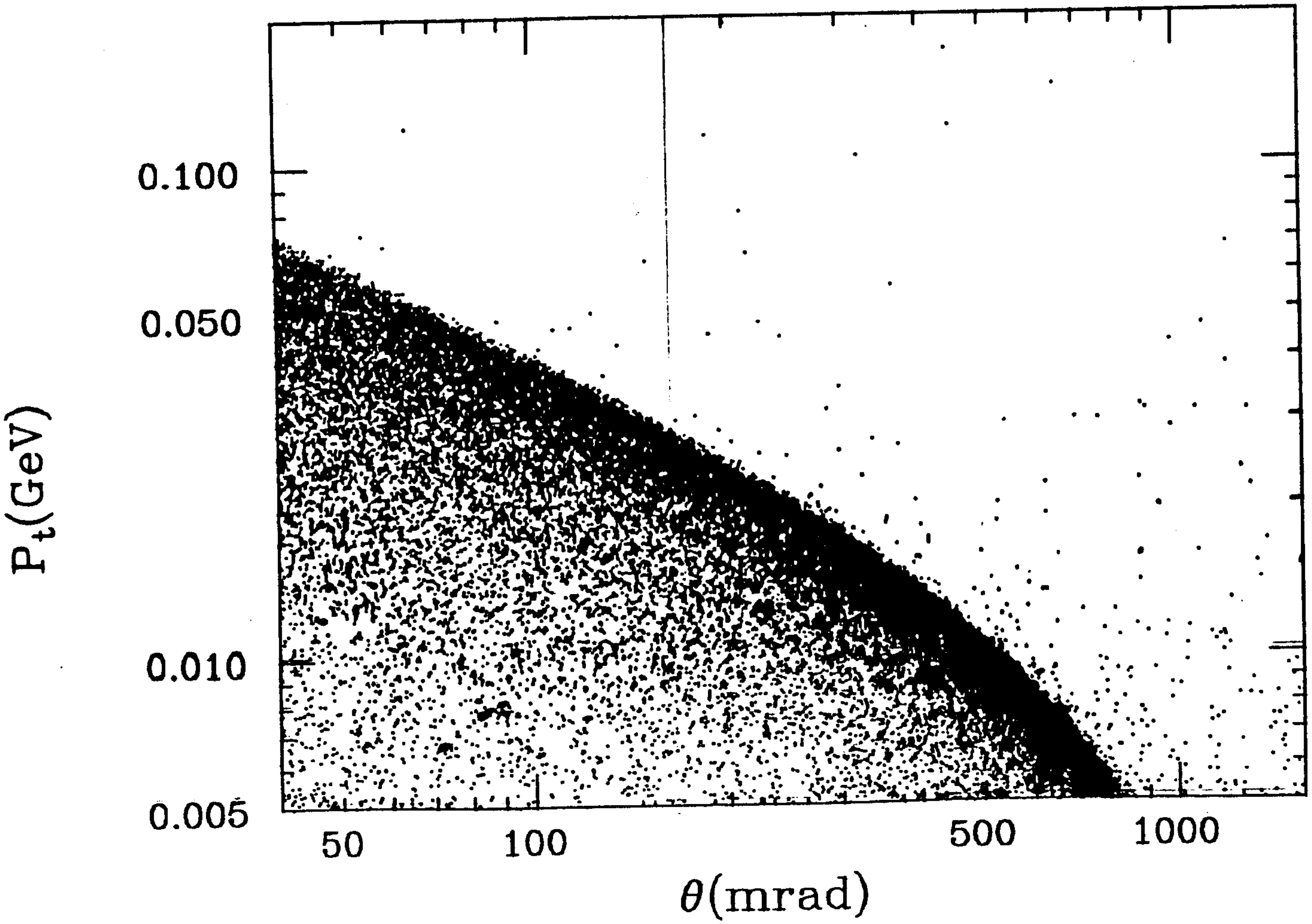

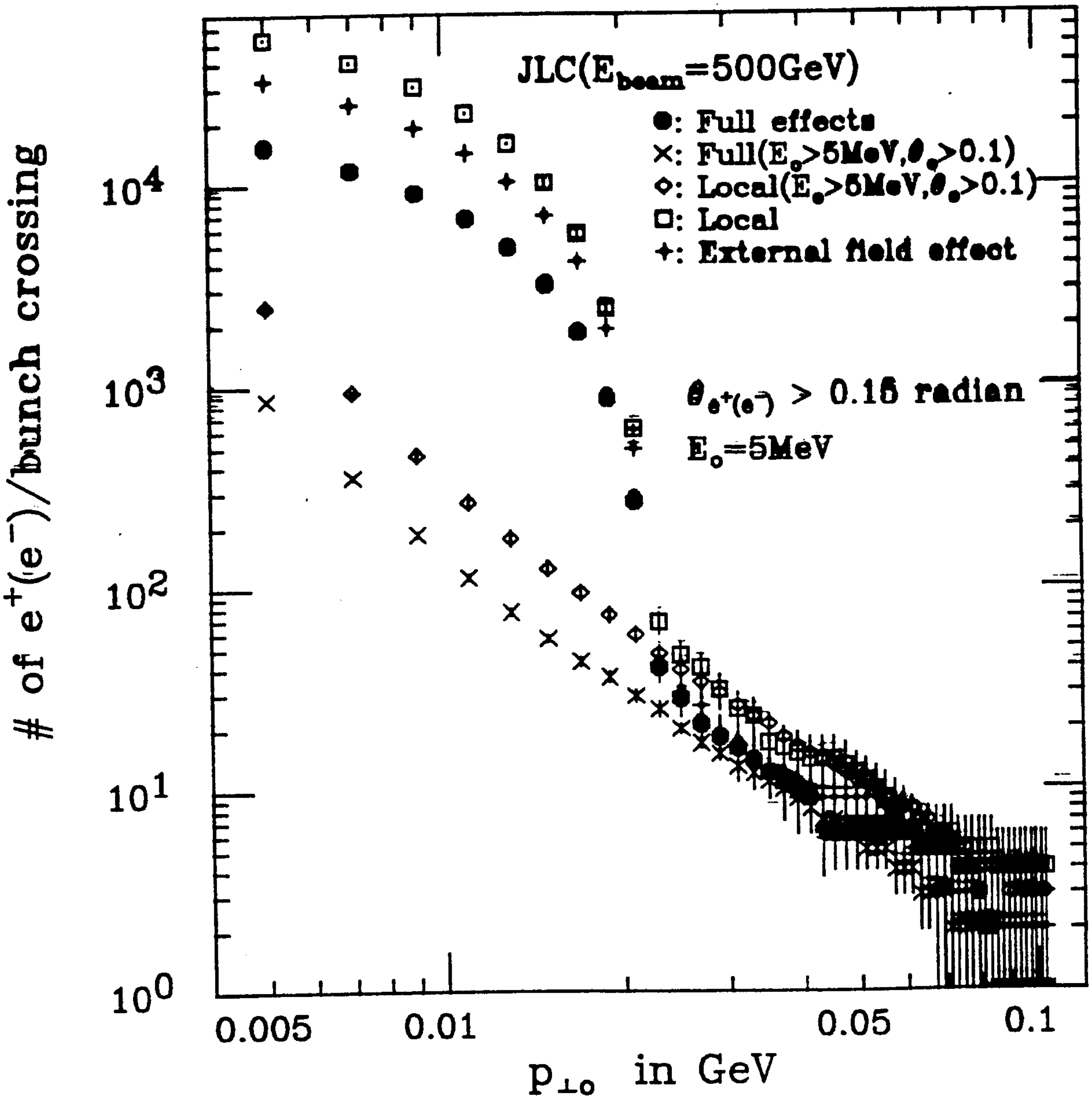
JLC(E_{beam}=500GeV)
●: Full effects
×: Full(E_o>5MeV,θ_e>0.1)
◇: Local(E_o>5MeV,θ_e>0.1)
□: Local
+: External field effect
$\theta_{e^+(e^-)}$ > 0.15 radian
E_o=5MeV
of $e^+(e^-)$/bunch crossing
10^4
10^3
10^2
10^1
10^0
0.005
0.01
0.05
0.1
$p_{\perp o}$ in GeV

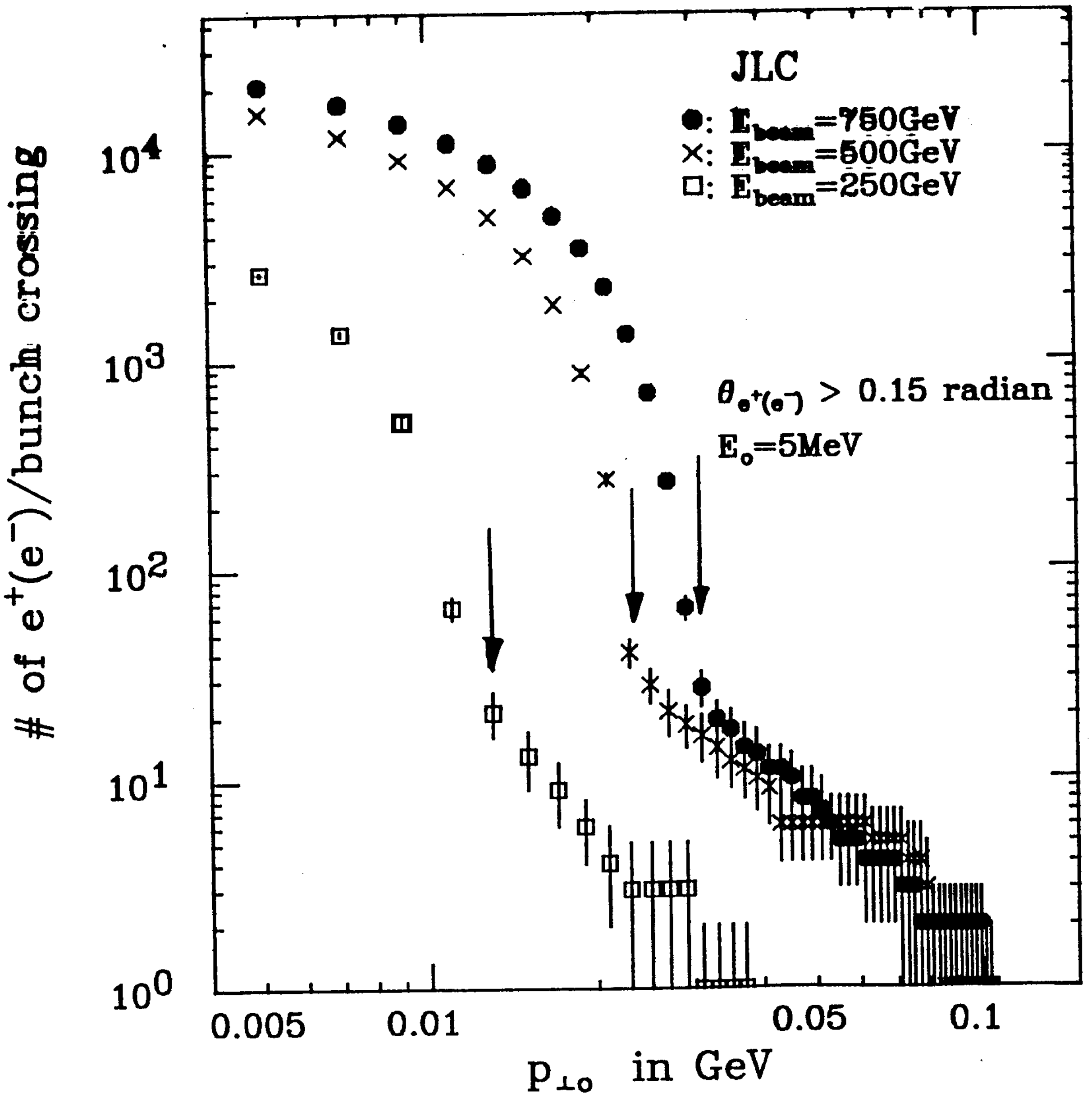
JLC
●: E_{beam}=750GeV
×: E_{beam}=500GeV
□: E_{beam}=250GeV
$\theta_{e^+(e^-)}$ > 0.15 radian
E_o=5MeV
of $e^+(e^-)$/bunch crossing
10^0
10^1
10^2
10^3
10^4
0.005
0.01
0.05
0.1
$p_{\perp o}$ in GeV

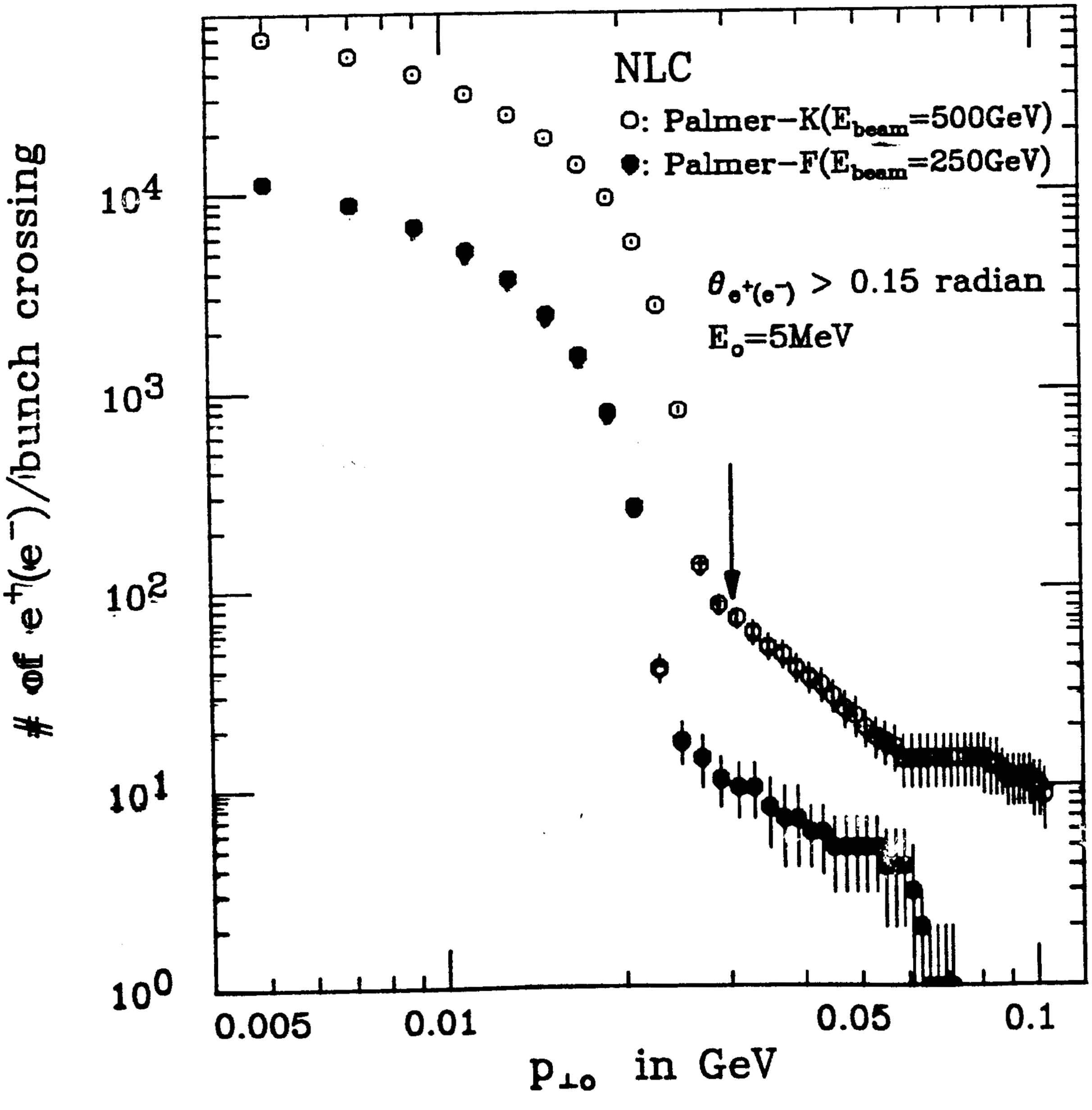

NLC
○: Palmer-K(E_{beam}=500GeV)
●: Palmer-F(E_{beam}=250GeV)
$\theta_{e^+(e^-)} > 0.15$ radian
E_o=5MeV
of $e^+(e^-)$/bunch crossing
10^4
10^3
10^2
10^1
10^0
0.005
0.01
0.05
0.1
$p_{\perp o}$ in GeV

Run 10022, EVENT 6
29-FEB-1992 18:32
Source: Run Data
Trigger: Timeout
Beam Crossing 2883161

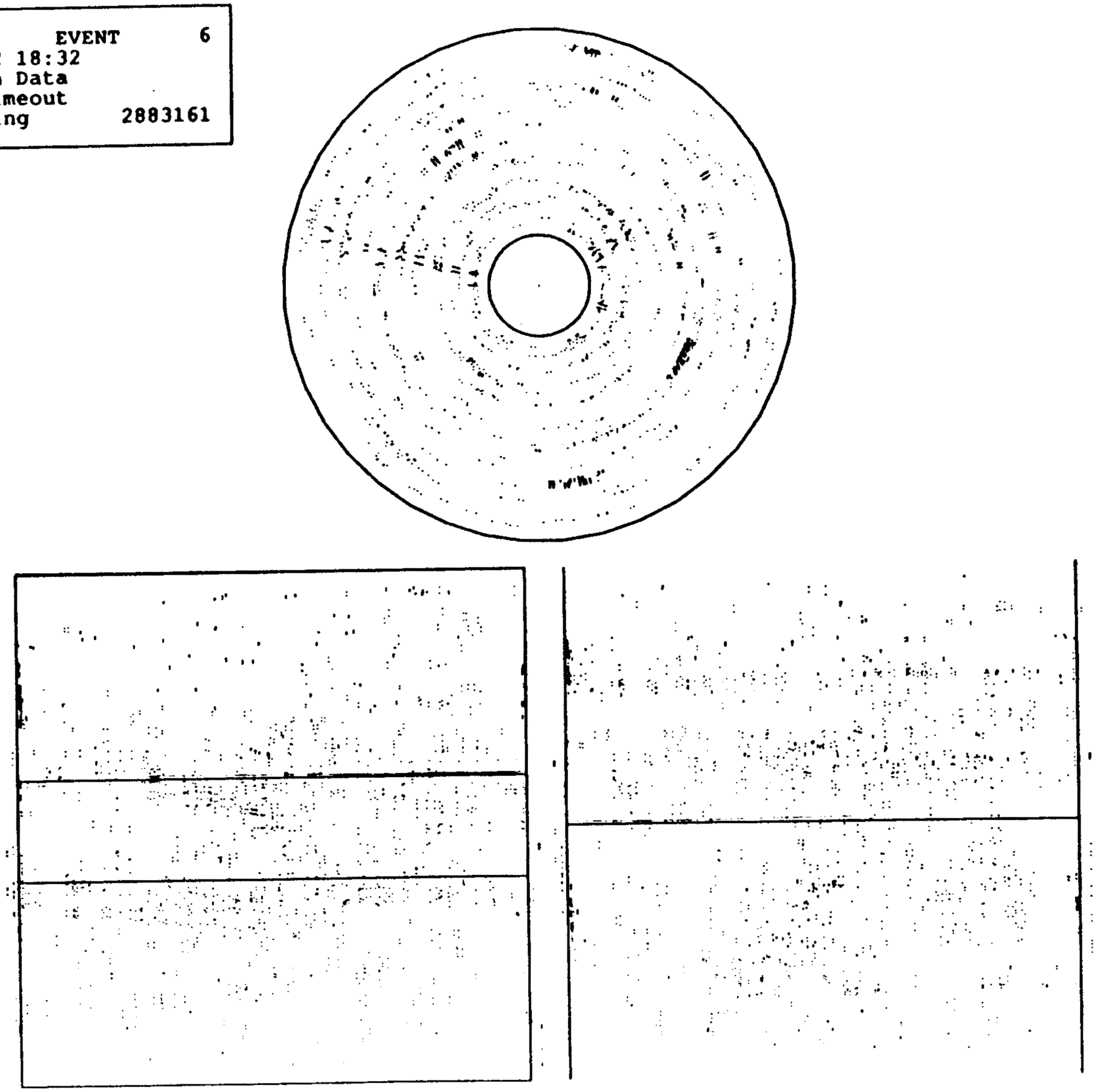

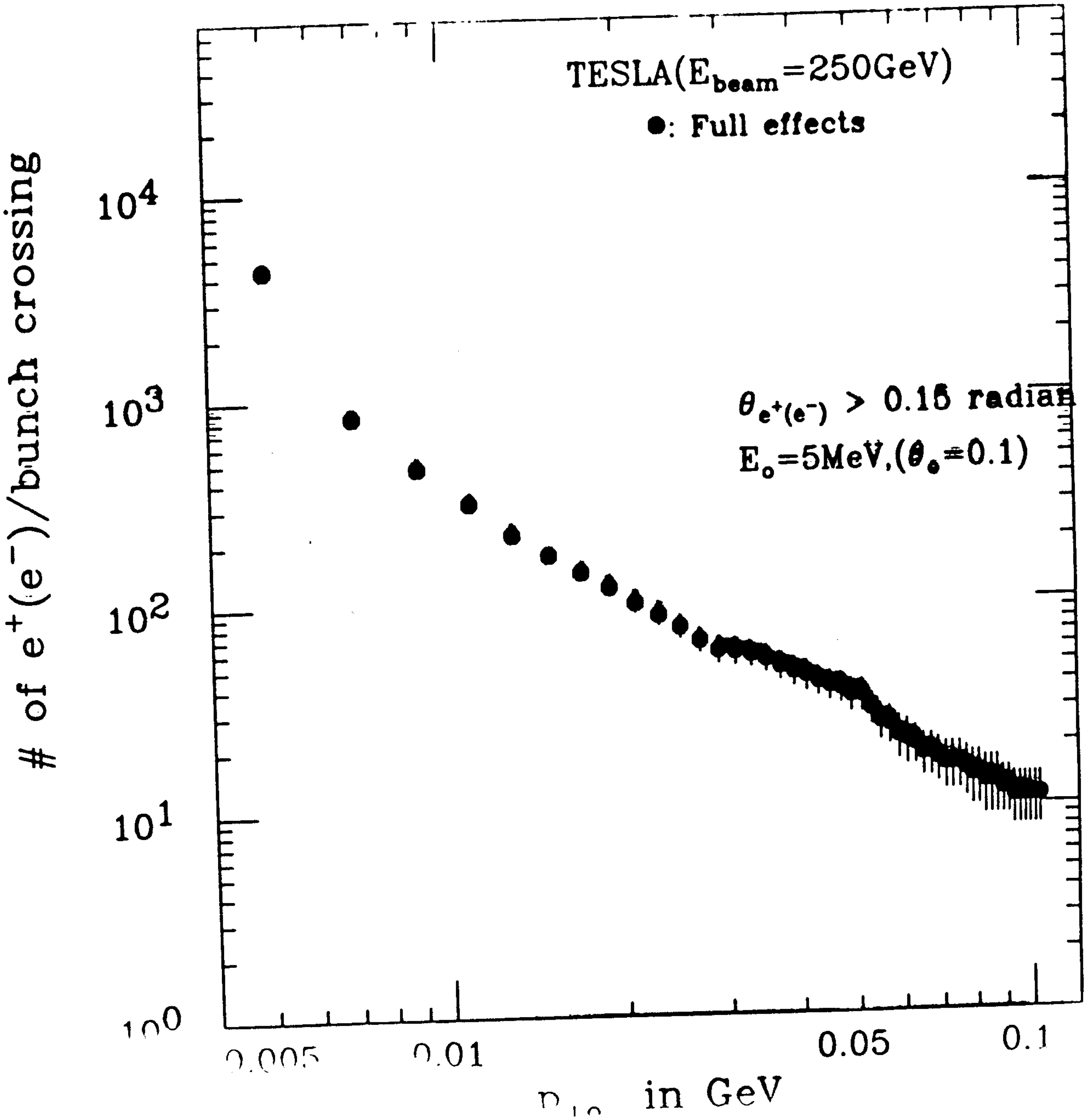
TESLA(E_{beam}=250GeV)
●: Full effects
$\theta_{e^+(e^-)}$ > 0.15 radian
E_o=5MeV,(θ_o=0.1)
of $e^+(e^-)$/bunch crossing
10^0
10^1
10^2
10^3
10^4
0.005
0.01
0.05
0.1
in GeV

Optimization of mask.

with η_{acc} = const.

B

r

ℓ

L

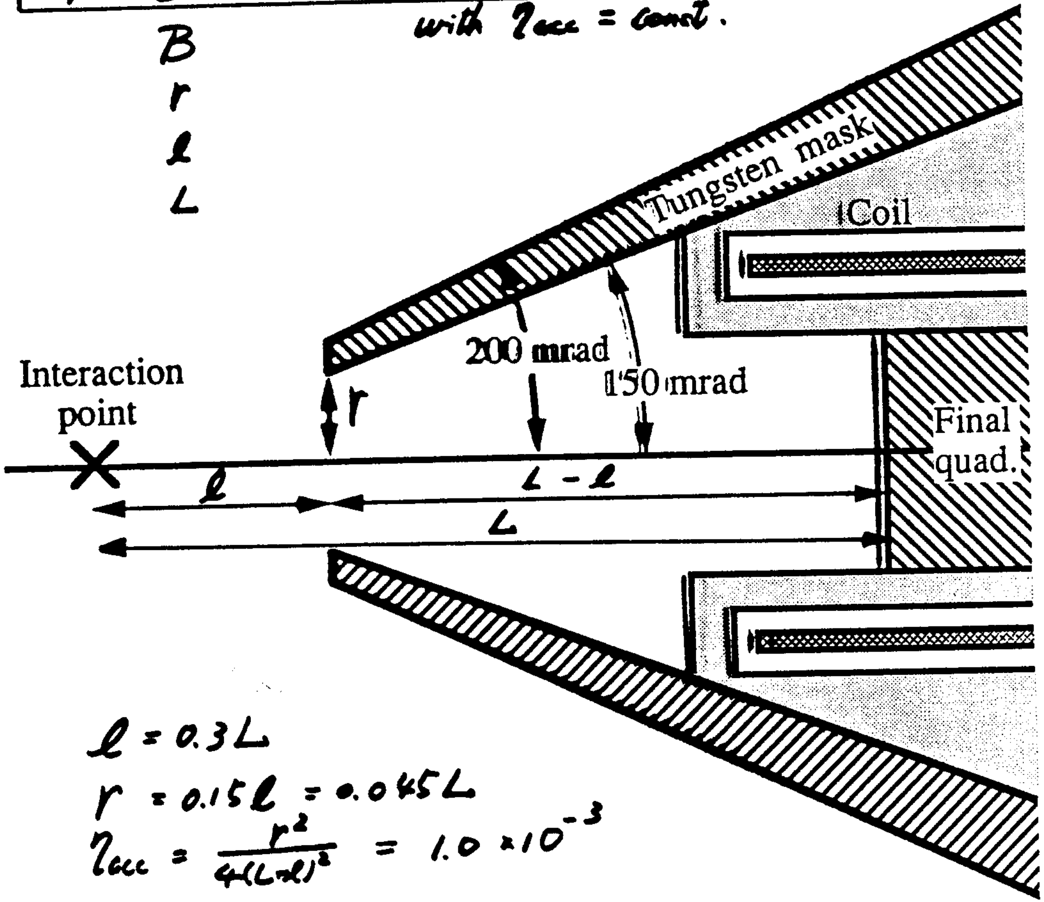

$\ell = 0.3L$

$r = 0.15\ell = 0.045L$

$\eta_{acc} = \frac{r^2}{4(L-\ell)^2} = 1.0 \times 10^{-3}$

Assume B = $\underline{2}$ Tesla

TLC beam GeV	P_t max MeV	ℓ m	r cm	η_{acc}	L m	
250	13	0.3	4.5	1.0×10^{-3}	1.0	fixed η_{acc}
500	23	0.51	7.7	"	1.7	
750	30	0.67	10.0	"	2.2	

$$L = \frac{P_t}{0.3 \cdot 0.15^2 B} \qquad [m] = \left[\frac{GeV}{Tesla}\right].$$

note : $r = \frac{2P_t}{0.3B}$

$e^{\pm}$ pairs / train crossing

outside of mask ($L = 1$ m)

$P_t > 13$ MeV, $B = 2$ Tesla

Ebeam GeV	JLC	N/TLC	TESLA
250	400	4×10^4	200
500	1×10^5	2×10^5	—
750	1.8×10^5	—	—

($L = 2.2$ m)

$P_t > 30$ MeV

Ebeam GeV	JLC	N/TLC	TESLA
250	20	100	60
500	300	1190	—
750	400	—	—

QCD mini jets

Drees.

a) "Direct." (QPM)

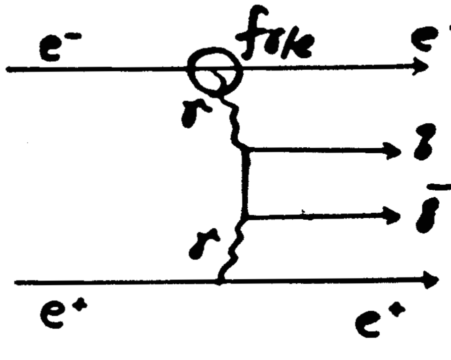

γ : virtual
or
beamstrahlung.

$f_{\gamma/e}$: well known.

$D_{\gamma/g}$: ? not known.

b) "once resolved"

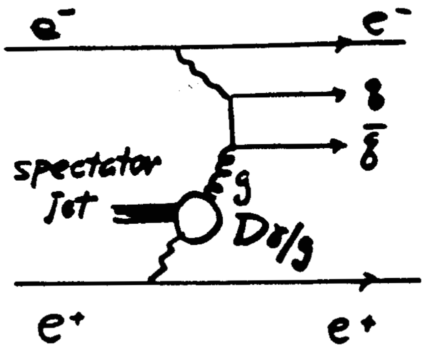

c) "twice resolved"

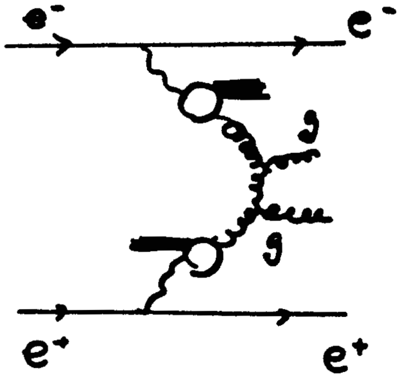

↔ VDM ($Q^2 = P_t^2$)

Any reason for
b) & c) ?

↓

2γ exp.
(AMY)
2γ/TPC
ALEPH

spectator jet can not be neglected.

M. Ronan 3/5/92

TPC/2γ

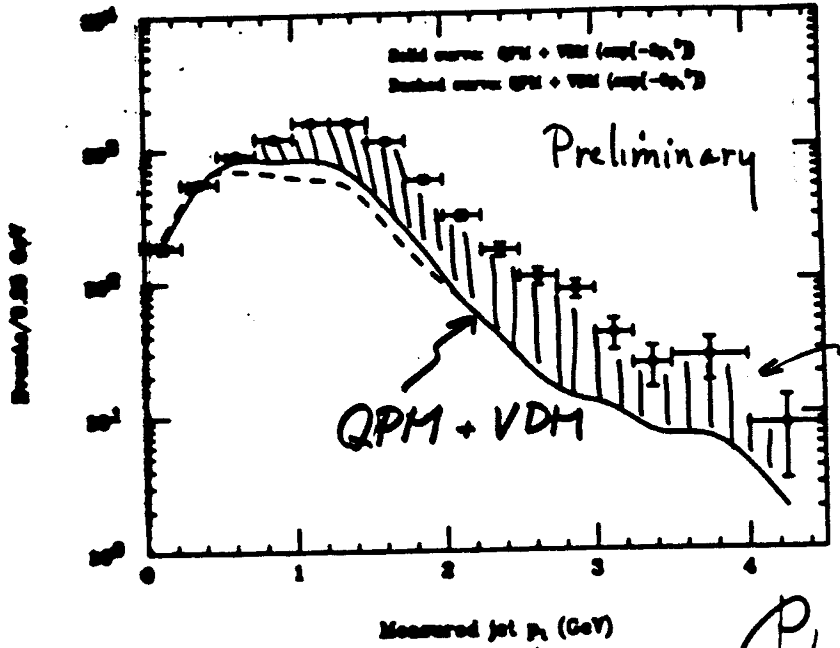

Preliminary

QPM + VDM

b) & c) ?

P_t - jet

$P^{\perp}$ jet

AMY.

ALEPH is also consistent with AMY.
R. Settles.

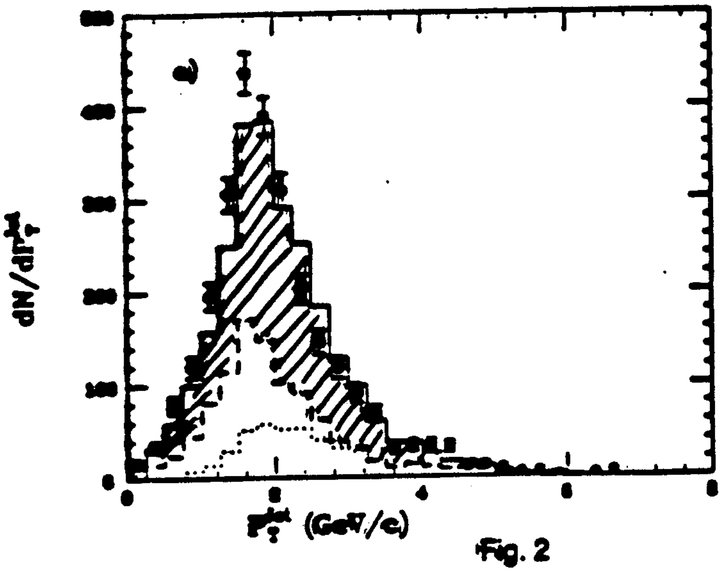

Fig. 2

HOW TO CALCULATE MINI-JET ? A. Miyamoto

$$d\sigma = f_{e/\gamma}(x_1)dx_1 \cdot f_{e/\gamma}(x_2)dx_2 \cdot D_{\gamma/p}(Q^2, x_3)dx_3 \cdot D_{\gamma/p}(Q^2, x_4)dx_4 \cdot d\hat{\sigma}$$

x_1, x_2 ; PHOTON ENERGY / ELECTRON ENERGY
x_3, x_4 ; PARTON ENERGY / PHOTON ENERGY
$\hat{s} = x_1 x_2 x_3 x_4 s$, $s = 4E_{BEAM}^2$
$Q^2 = \hat{s}/4$

$f_{e/\gamma}$: PHOTON INTENSITY FUNCTION

BREMSTRAHLUNG : EPA FORMULA

$$f_{\gamma/e}(x) = \underline{0.85}\frac{\alpha}{2\pi}\frac{1+(1-x)^2}{x}\ln\left(\frac{\overline{Q^2}}{m_e^2}\right)$$

BEAMSTRAHLUNG : ACCORDING TO YOKOYA.

$D_{\gamma/p}$: PARTON (g/q) DENSITY INSIDE γ

- DUKE & OWENS (DO)
- DREES AND GRASSIE (DG)
- ABRAMOWICZ, CHARCHULA, LEVY (LAC)

$d\hat{\sigma}$: SUBPROCESS CROSS SECTION

DIRECT $\gamma\gamma \to q\bar{q}$

1 RESOLVED $\gamma q \to g q$
$\gamma g \to q\bar{q}$

2 RESOLVED
$q_i q_i \to q_i q_i$
$q_i \bar{q}_i \to q_i \bar{q}_i$
$q_i \bar{q}_j \to q_i \bar{q}_j$
$q g \to q g$
$g g \to g g$

$q_i q_j \to q_i q_j$
$q_i \bar{q}_i \to q_j \bar{q}_j$
$q \bar{q} \to g g$
$g g \to q \bar{q}$

$i, j = u, d, s, c, b$

A. Miyamoto

Mini-jet yield (DG, no y cut)

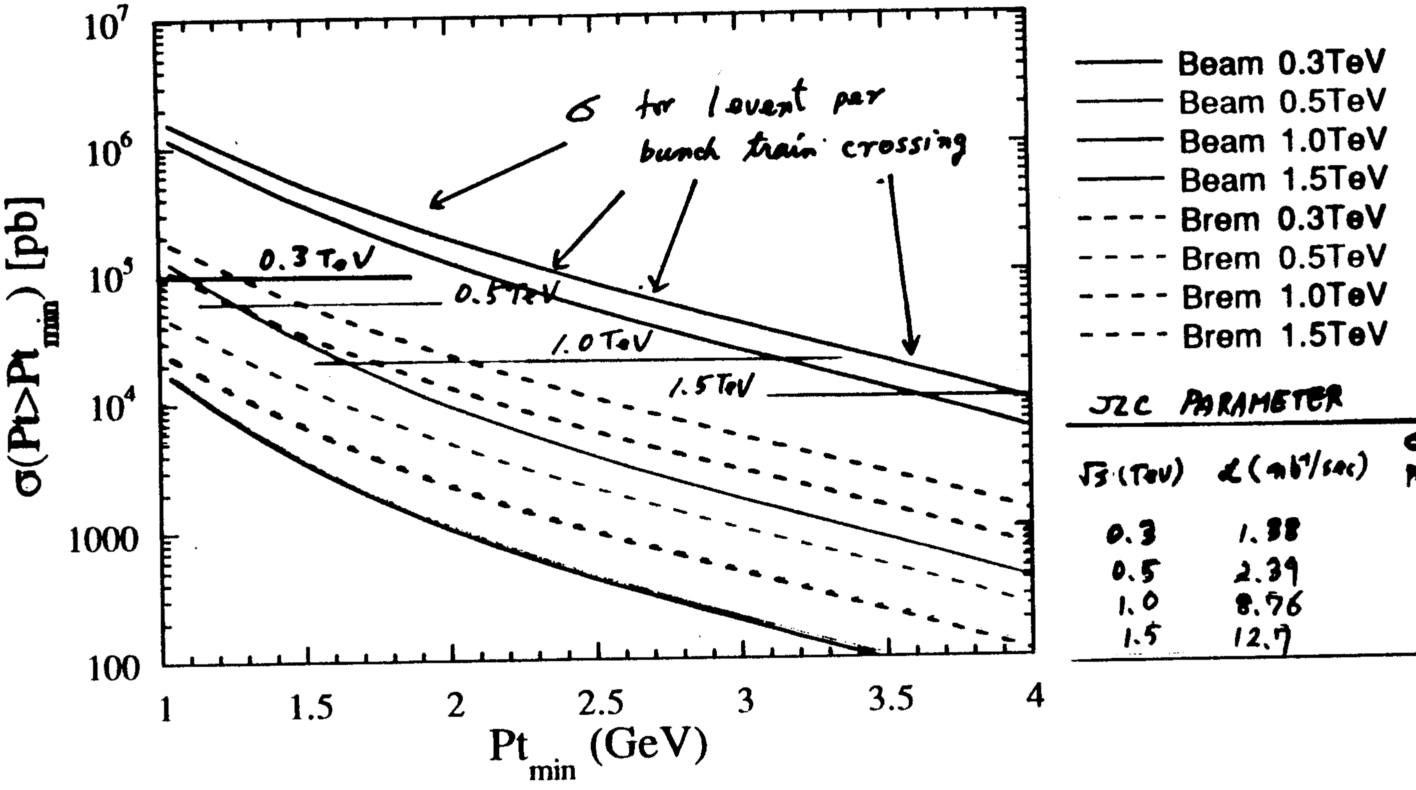

σ for 1 event per bunch train crossing

JLC PARAMETER

$\sqrt{s}$ (TeV)	$\mathcal{L}$ (nb^{-1}/sec)	σ for 1 event per train
0.3	1.88	109
0.5	2.39	63
1.0	8.76	17
1.5	12.7	12

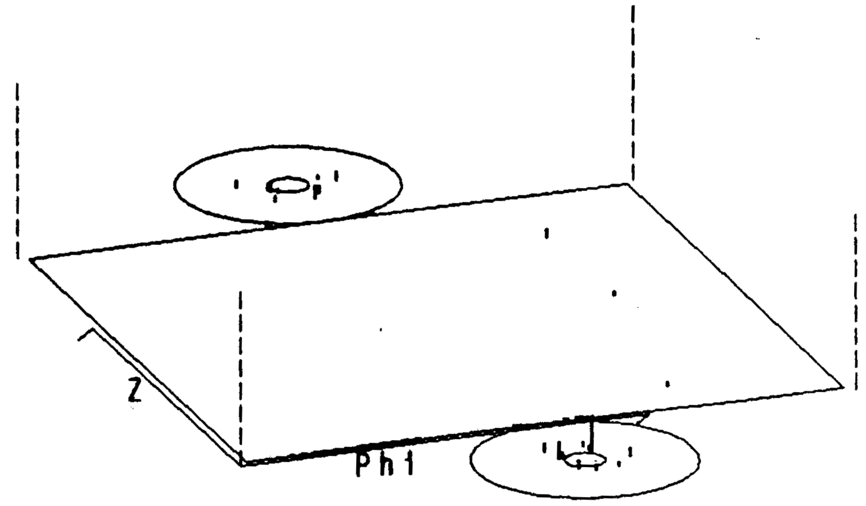

DATE=920219 E_beam= 250 EVENT= 3

W pair

A. Miyamoto

$e^+e^- \to W^+W^-$
$\hookrightarrow q\bar{q}$
$\hookrightarrow q\bar{q}$

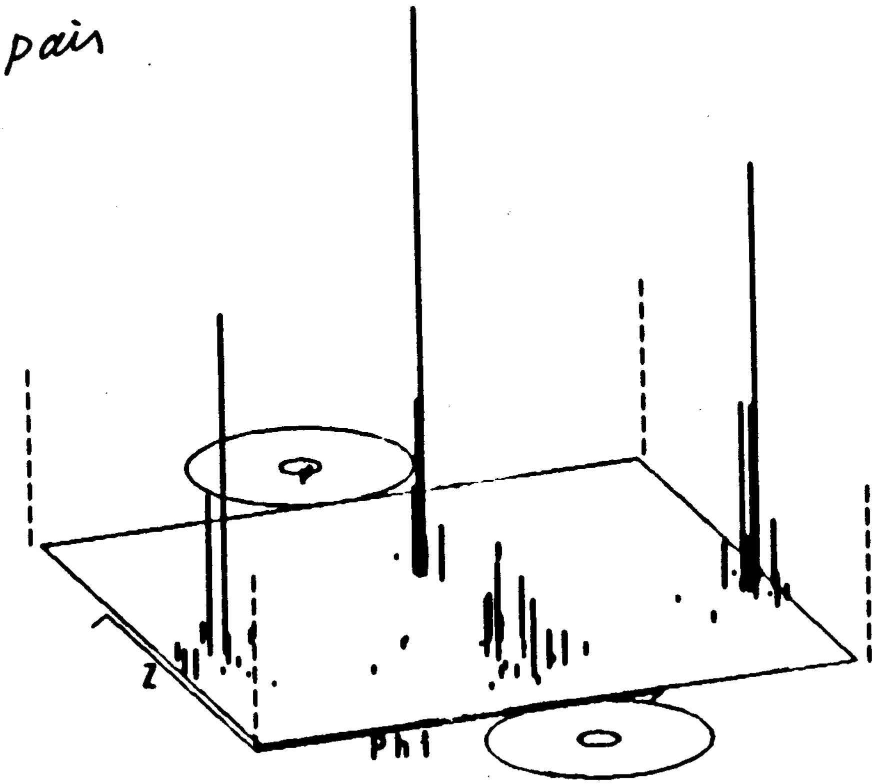

DATE=910903 E_beam= 250 EVENT= 477

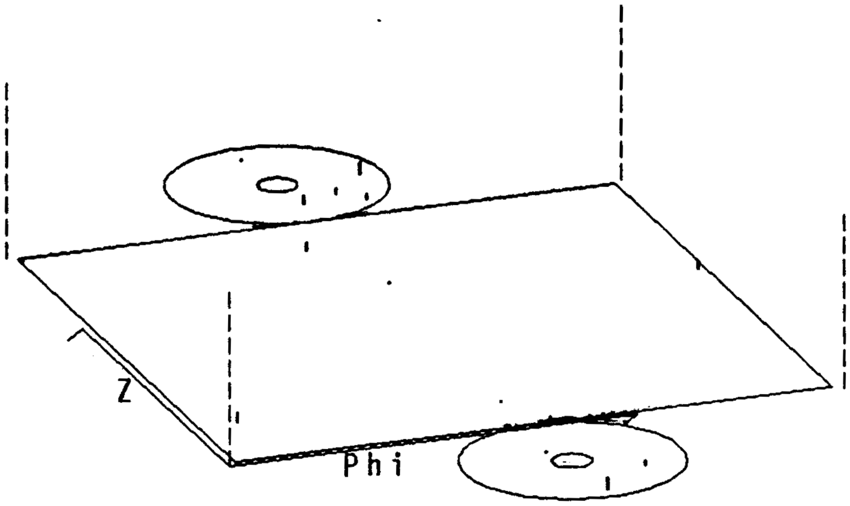

DATE=920219 E_beam= 250 EVENT= 2

CONCLUSION.

A. Miyamoto

ACCORDING TO THE MODEL BY DREES AND GODBOLE,

1. AT 1 TEV, DOMINANT SUB PROCESS OF MINI-JET EVENT ARE, $gg \to gg$ AND $qg \to qg$
2. PHOTON AT ALL ENERGY RANGE CONTRIBUTES THE PRODUCTION OF LOW P_T MINIJET EVENTS, BUT, HIGH ENERGY γ PRODUCES MORE MINIJET.
3. IF WE USE DG PARAMETRIZATION, # of MINIJET WITH $P_T > 1$ GEV PER BUNCH TRAIN CROSSING AT JLC IS.

   ~1 at Ebeam = 250 GeV
   ~50 at = 500
   ~150 at = 750

   DUE TO BEAMSTRAHLUNG PHOTON.
4. LAC PARAMETRIZATION PREDICTS 3 TO 10 TIMES LARGER RATE.
5. MINIJETS BACKGROUND FOR EBEAM = 150 AND 250 GEV WILL NOT BE A PROBLEM. AT EBEAM = 500 GEV, ABOUT 60 GEV ENERGY DEPOSIT PER PHYSICS SIGNAL IS EXPECTED, ACCORDING TO THE SIMULATION USED IN THIS STUDY, IF DG PARAMETRIZATION IS USED. A SPECIAL DETECTOR TO DISTINGUISH EVENTS WITHIN A BUNCH TRIN IS REQUIRED, IF THIS MODEL IS TRUE.
6. EXPERIMENTAL CONFIRMATION OF THE MODEL FOR HADRON PRODUCTION BY TWO PHOTON PROCESS IS NECESSARY FOR RELIABLE ESTIMATE OF MINIJET RATE.

C Adolphsen

③ The Mark II Central Drift Chamber at the SLC

- $N = 72$ $M = 6$ $F \simeq 2$
- $\langle \sigma_\omega \rangle = 175\ \mu m$ $V_d \simeq 50\ \mu m/ns$
- $S = 7.5/P_s\ (\mathrm{MeV/c})$

$$\Rightarrow \sigma_{\Delta t} \simeq .41 \left(1 + \frac{47}{P_s\,(\mathrm{MeV/c})} \right)\ \mathrm{ns}$$

However, for $P_s > 1$ GeV/c + more than 50 hits

$$\left\langle \frac{\sigma_{\Delta T}\ (\mathrm{exact})}{\sigma_{\Delta T}\ (\mathrm{approx})} \right\rangle = 1.3$$

due to the fact that the charge collection does not necessarily alternate between layers

④ Comments

- $\frac{\sigma_\omega}{V_d} \simeq$ constant
- For good ΔT resolution, want
  - At least 12 super-layers where the direction of charge collection alternates
  - Small S, M, F if measuring low P tracks
  - Large N

TRACK AND EVENT TIMES from the MARK II CDC AT THE SLC

P > 0.5 GeV/c

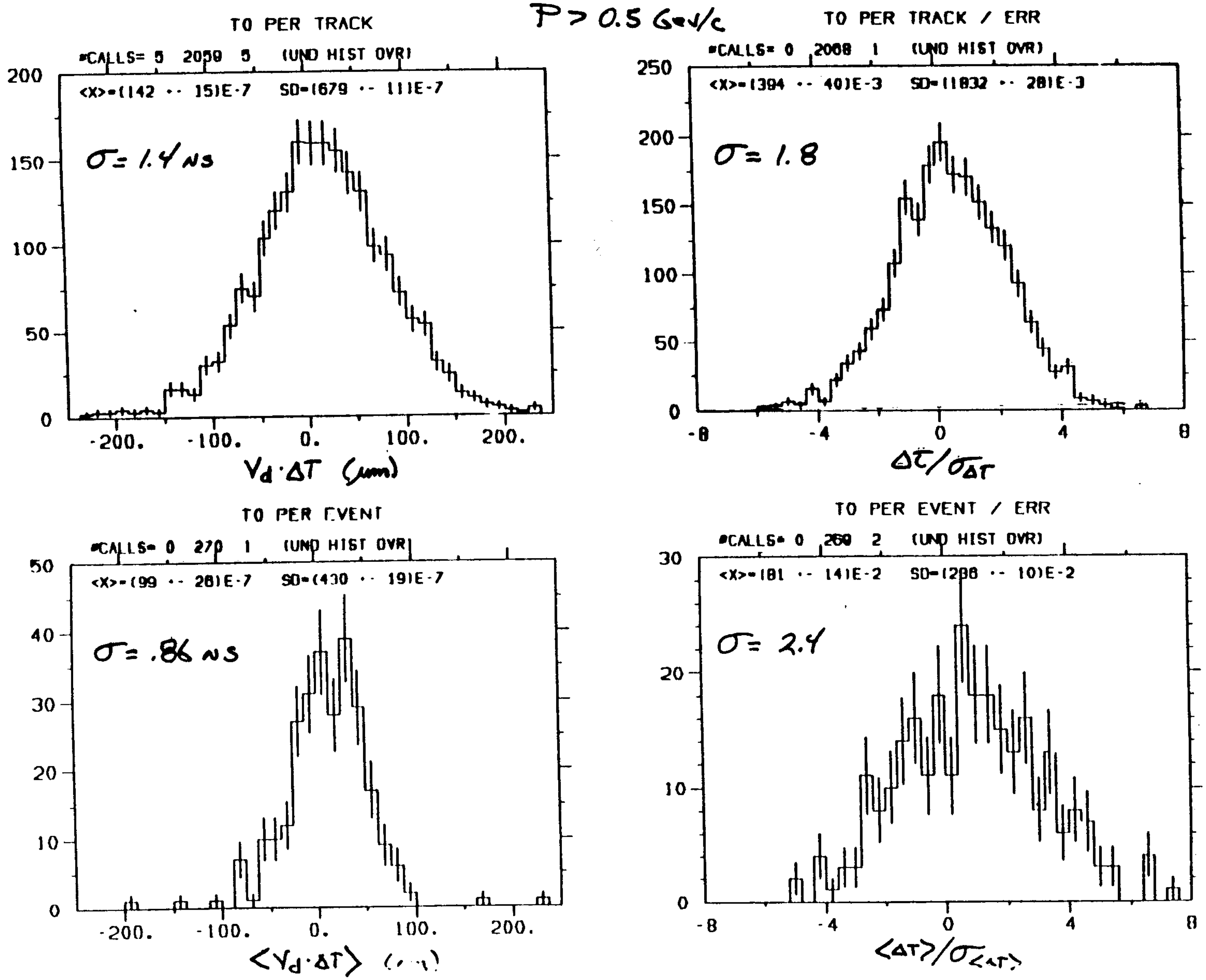

VERTEX Detectors

Physics

e.g. $\sqrt{s} \sim 400\,\text{GeV}$

$e^+e^- \longrightarrow Z H$

$m_Z < m_H < 2m_W$: intermidiate Higgs

$H \rightarrow b\bar{b}$

$$S/N = \frac{\sigma_{ZH}}{\sigma_{WW}} \sim \frac{40\,\text{fb}}{10\,\text{pb}} \sim 4 \times 10^{-3}$$

$$\Big\downarrow \times 2500$$

$S/N = 10$ can be achieved with vertex detector.

• Heavy Flavor Tagging

Y. Sugimoto

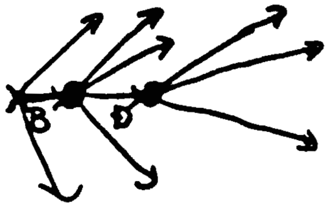

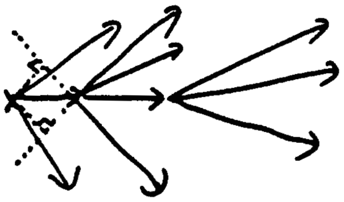

b - Tagging

⇓

Hard

Heavy-Flavor Tagging

⇓

Easy

but

c-jet remains

- Measurement of b (impact parameter) $\left(\begin{matrix}2\text{ layers}\\ R_{in}, R_{out}\end{matrix}\right)$

∵) We know precisely primary vertex position.

$$\delta^2 = \sigma^2 \left\{ \left(\frac{R_{out}}{R_{out} - R_{in}} \right)^2 + \left(\frac{R_{in}}{R_{out} - R_{in}} \right)^2 \right\} \quad \text{.... measurement}$$

$$+ \left(\frac{0.014\, R_{in}}{p} \right)^2 \cdot \frac{x_r}{\sin^3\theta} \quad \text{--- multiple scattering}$$

σ: Resolution of V. D. = 7.2 μm, $a_z = \frac{\sigma}{\sin\theta}$ (25 μm pixel)

p: momentum in GeV

x_r: thickness of inner layer in radiation length.

θ: Polar angle of the particle

Y. Sugimoto

θ

R_{in} = 2.5, 5. 7.5 cm

R_{in}=2.5 cm

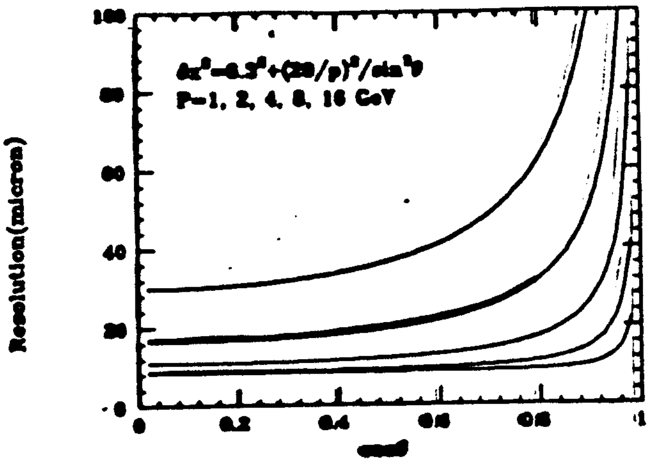

- R_{out} = 20cm
- X_r = 6.76 × 10^{-3}
  (500μ Be + 500μ Si.
- σ = 7.2 μ
  (25μ/$\sqrt{12}$)

R_{in}=5 cm

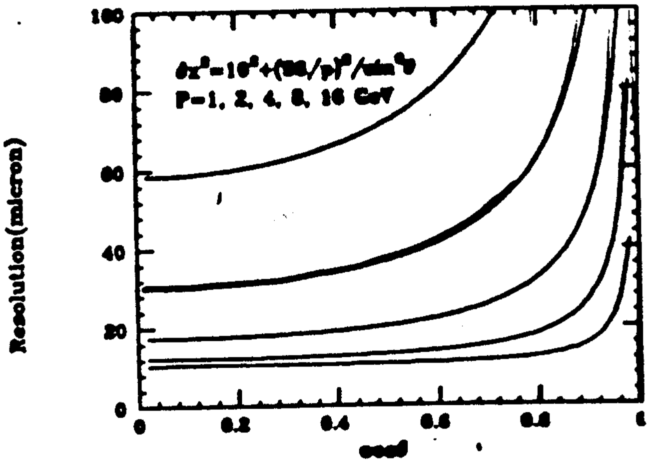

P = 2 GeV, θ = 90°

R cm	σ_b μm
2.5	[redacted]. 16.
5.	[redacted]. 30.
7.5	44.

R_{in}=7.5 cm

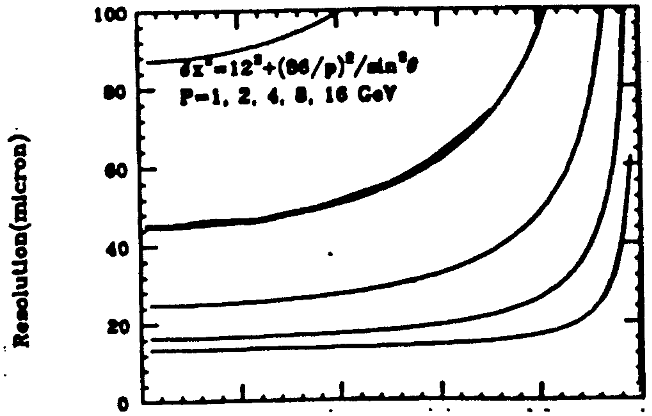

2/28 '92

Y. Sugimoto

Background ($e^+e^- \to W^+W^-$) Suppression

Y. Sugimoto.

1) ≧2 track double tag.

$u\bar{d}$: $(4\times10^{-3})^2 = 1.6\times10^{-5}$ $\times BR$ ≒ 0.5×10^{-5}

$u\bar{s}$: 〃 0.3×10^{-6}

$c\bar{d}$: $0.3 \times 4\times10^{-3} = 1.2\times10^{-3}$ 0.2×10^{-4}

$c\bar{s}$: 〃 0.38×10^{-3}

$c\bar{b}$: $0.3\times 0.73 = 0.22$ 0.19×10^{-3}

計 $\sim 0.6\times10^{-3}$

$b\bar{b}$ efficiency $\sim(0.73)^2$ ≒ 50%

⓶ ≧3 track double tag

$u\bar{d}$: $(2\times10^{-3})^2 = 0.4\times10^{-5}$ $\times BR$ ≒ 0.13×10^{-5}

$u\bar{s}$: 〃 0.7×10^{-7}

$c\bar{d}$: $0.1 \times 2\times10^{-3} = 0.2\times10^{-3}$ 0.3×10^{-5}

$c\bar{s}$: 〃 0.6×10^{-4}

$c\bar{b}$: $0.1\times0.55 = 0.055$ 0.5×10^{-4}

計 $\sim 1.2\times10^{-4}$

$b\bar{b}$ eff: $\sim (0.55)^2$ ≒ 30%

S/N : $\frac{\sigma_{ZH}}{\sigma_{WW}} \sim 4\times10^{-3}$ with no VTX

$\sim \frac{\sigma_{ZH}\times0.55^2}{\sigma_{WW}\times1.2\times10^{-4}} \sim 10.$ with VTX. $\Big\}$!

σ_{V-X} :

σ_{VTX} : $\frac{7.2}{\sin\theta}$ μm.

ALEPH vertex ch. 48 "modules" w/ 2 doublesided silicon strip detectors each R. Settles.
24 VLSI amplifier chips @ 64 channels

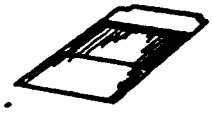

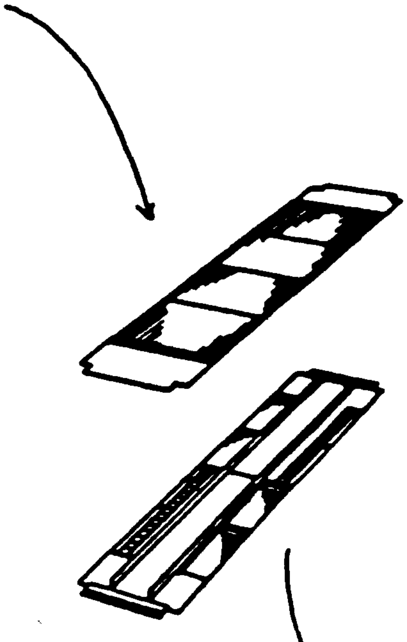

24 "faces"

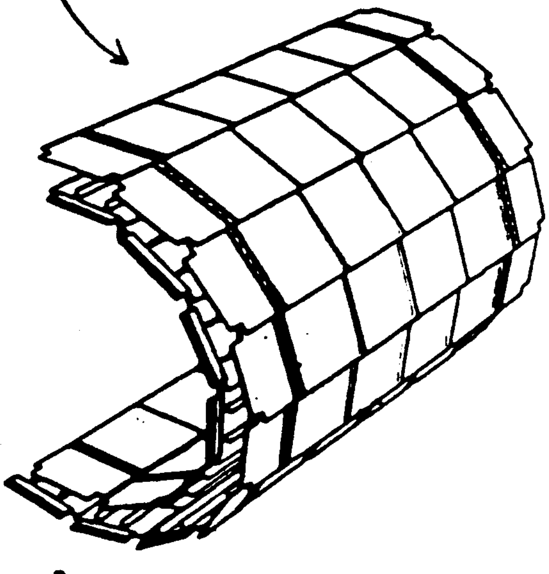

2 sectors
$r_i \sim 6.5$ cm
$r_o \sim 11.5$ cm

# of silicon detectors : 96
analog channels : 73,728
total power dissipation : ~70 W
material @ 90° incidence : ~4.2% X^0
solid angle : 87% layer 1
70% layer 1 and layer 2

ALEPH by R. Settles PRELIMINARY

$D^+ \to K^- \pi^+ \pi^+$ ff.

Require vertex displaced by ≥ 1mm

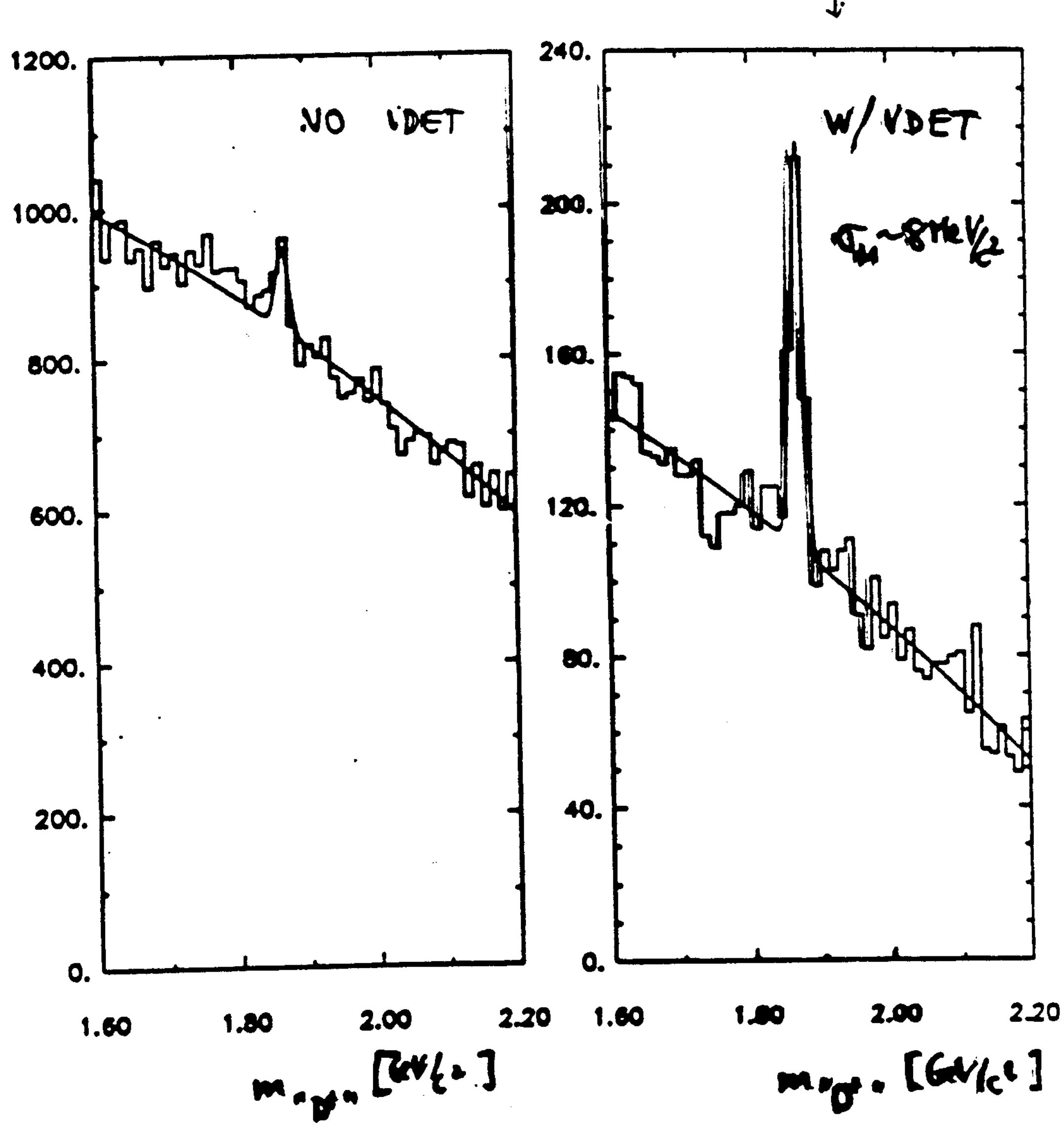

NLC vertex detector. C. Adolphsen.

Chris Monpres

'CONSERVATIVE' NLC VERTEX DETECTOR DESIGN

LAYOUT: $\underline{50\,\mu m \times 50\,\mu m \ \boxed{\text{PIXELS}}}$ ($300\,\mu m$ THICK SILICON)
8 LAYER CYLINDRICAL DESIGN : $R_1 = 6$ cm $R_8 = 16$ cm
$\cos(\theta) < .8$ coverage $\Rightarrow l_{max} = 35$ cm

RESOLUTION: $S/N > 50 \Rightarrow \sigma_{r\phi} \sim \sigma_z \lesssim 5\,\mu m$
NO bunch-to-bunch DISCRIMINATION ($T_{\text{COLLECTION}} \gtrsim 10$ nsec)

$\sigma_b \sim 10\,\mu m + 84\,\mu m/P(\text{GeV})$
$\sigma(p) \sim .007\ \text{GeV}^{-2}$
} VERTEX DETECTOR ONLY! USE CDC for MASS, Time meas. + PATTERN RECOGNITION

$\Rightarrow$ >20% B-TAG Efficiency

ELECTRONICS: $\underline{\text{RAD-HARD TO} > 100\ \text{K-rad ?} \quad \text{(few M-rad for SSC)}}$
Pulsed-Powered
Power DISSIPATION:
SAMPLE + READOUT : < 1 W/cm^2
DUTY CYCLE: $5\,\mu s \times 120$ Hz = 6×10^{-4}
AREA : ~ 3200 cm^2
$\Rightarrow$ 2 W (2 KW $\rightarrow$ 40 KW for SSC!)

Mechanics: STABILITY / ALIGNMENT < $5\,\mu m$
ΔT over volume < .2 °C

Design Issues: $\cos(\theta)$ Coverage required
σ_b required (AT LOW P, $\sigma_b \propto R$)
BACKGROUND RATE -VS- R

Background ($e^\pm$ pairs)

Y. Sugimoto
KEK.

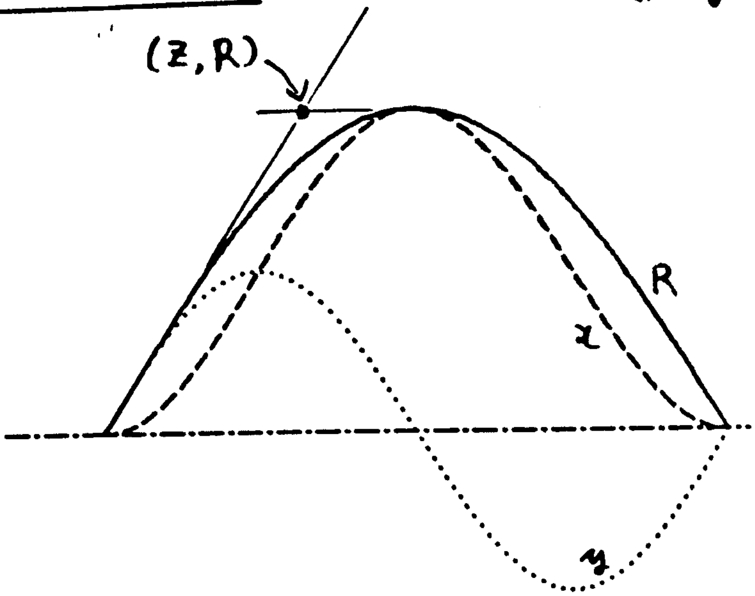

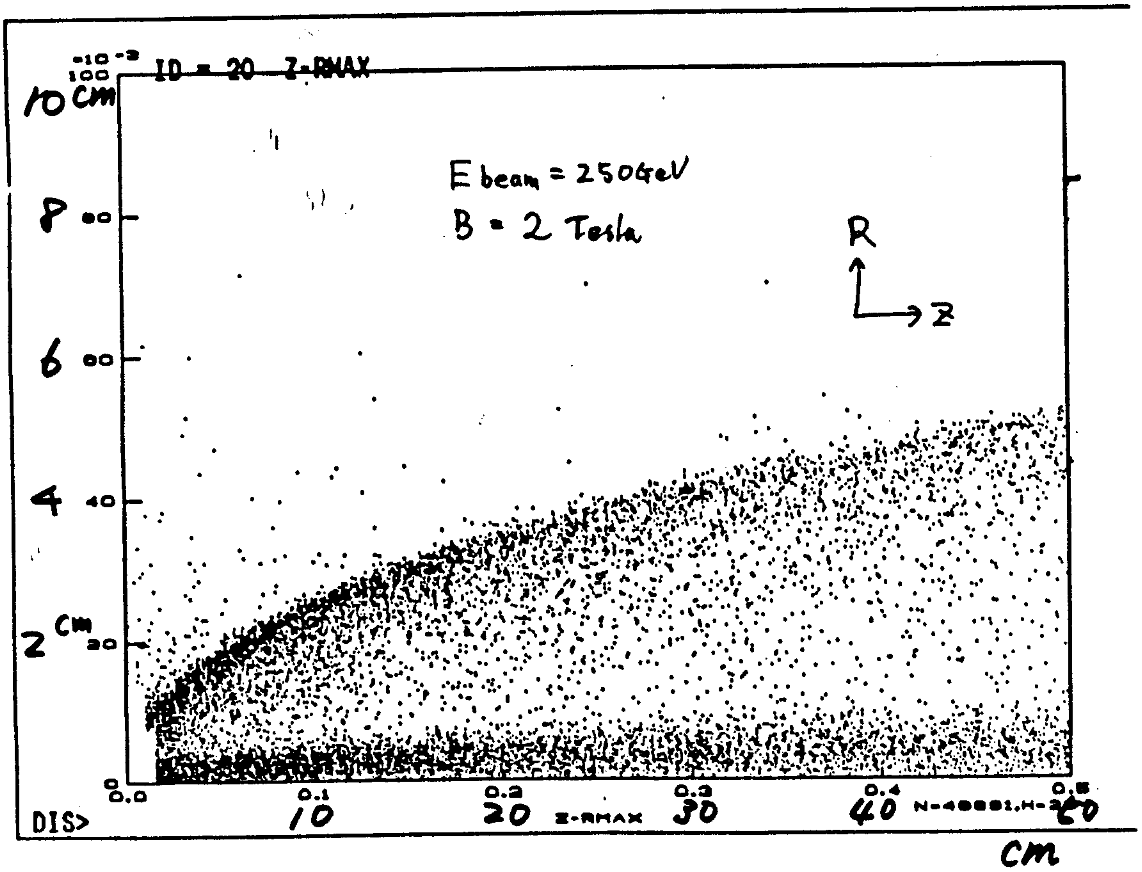

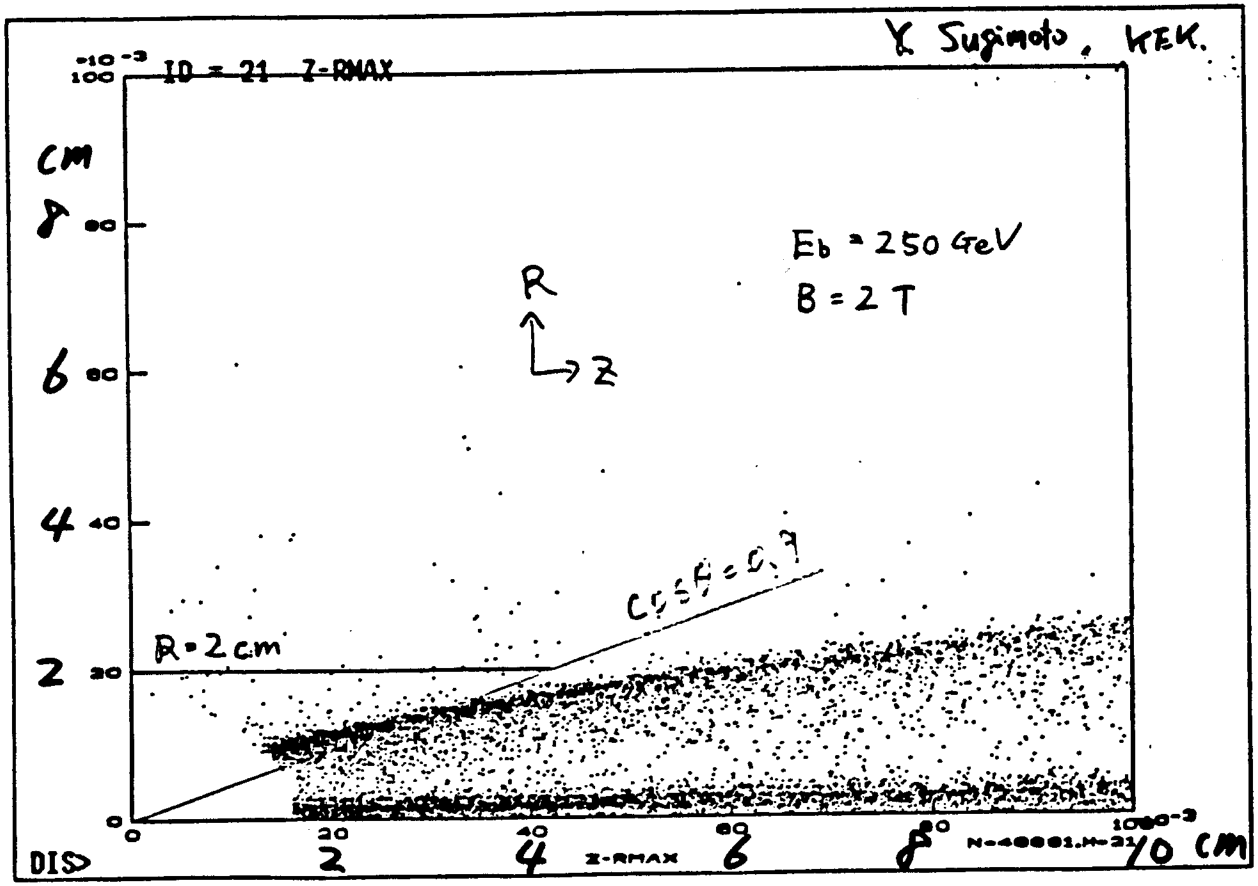

$R_{in} = 2$ cm ⇒ $\underset{\text{double}}{\text{b-tag}}$ eff. > 60%

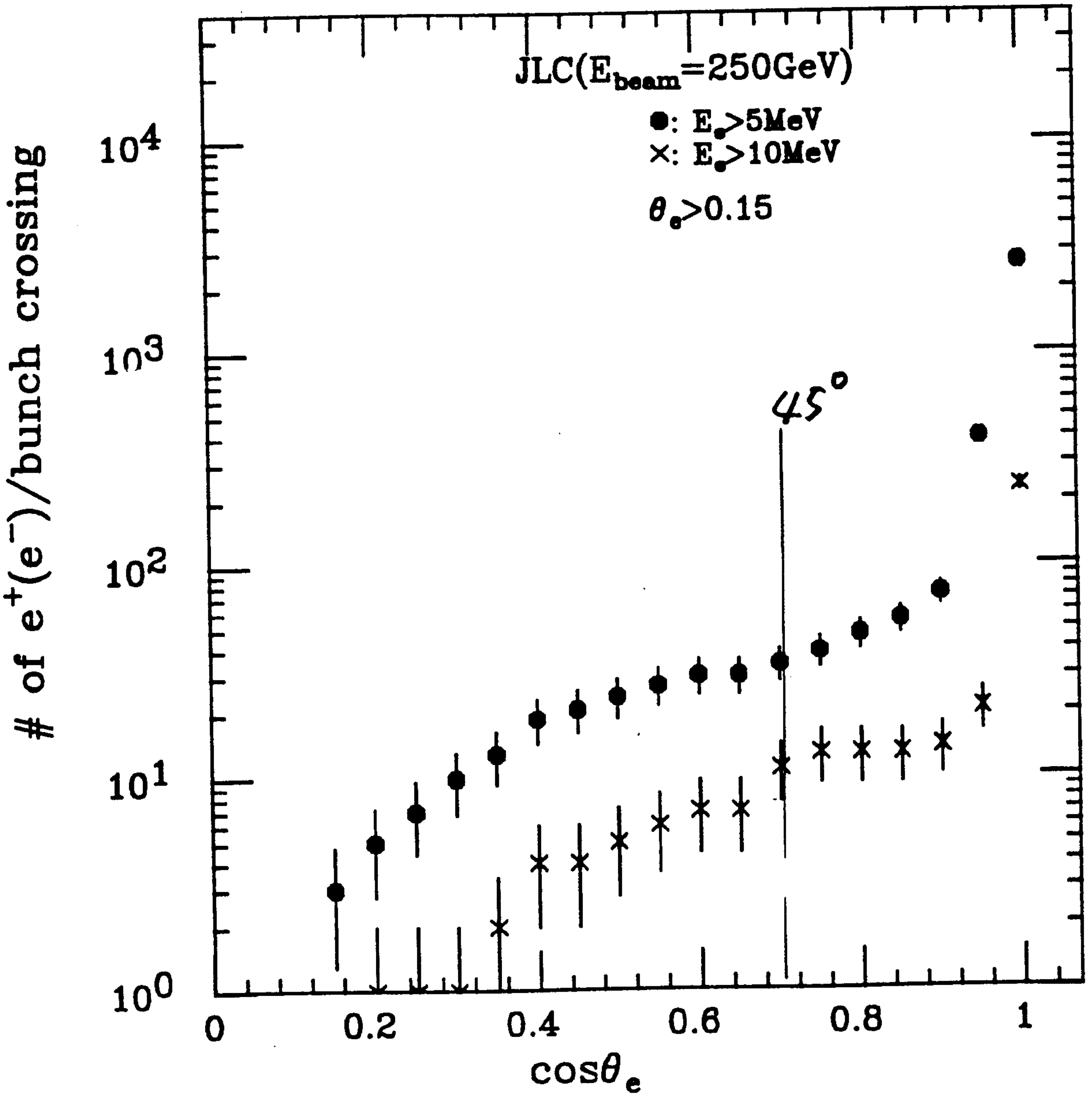
JLC(E_{beam}=250GeV)
●: E_e>5MeV
×: E_e>10MeV
θ_e>0.15
45°
of $e^+(e^-)$/bunch crossing
10^4
10^3
10^2
10^1
10^0
0
0.2
0.4
0.6
0.8
1
cosθ_e

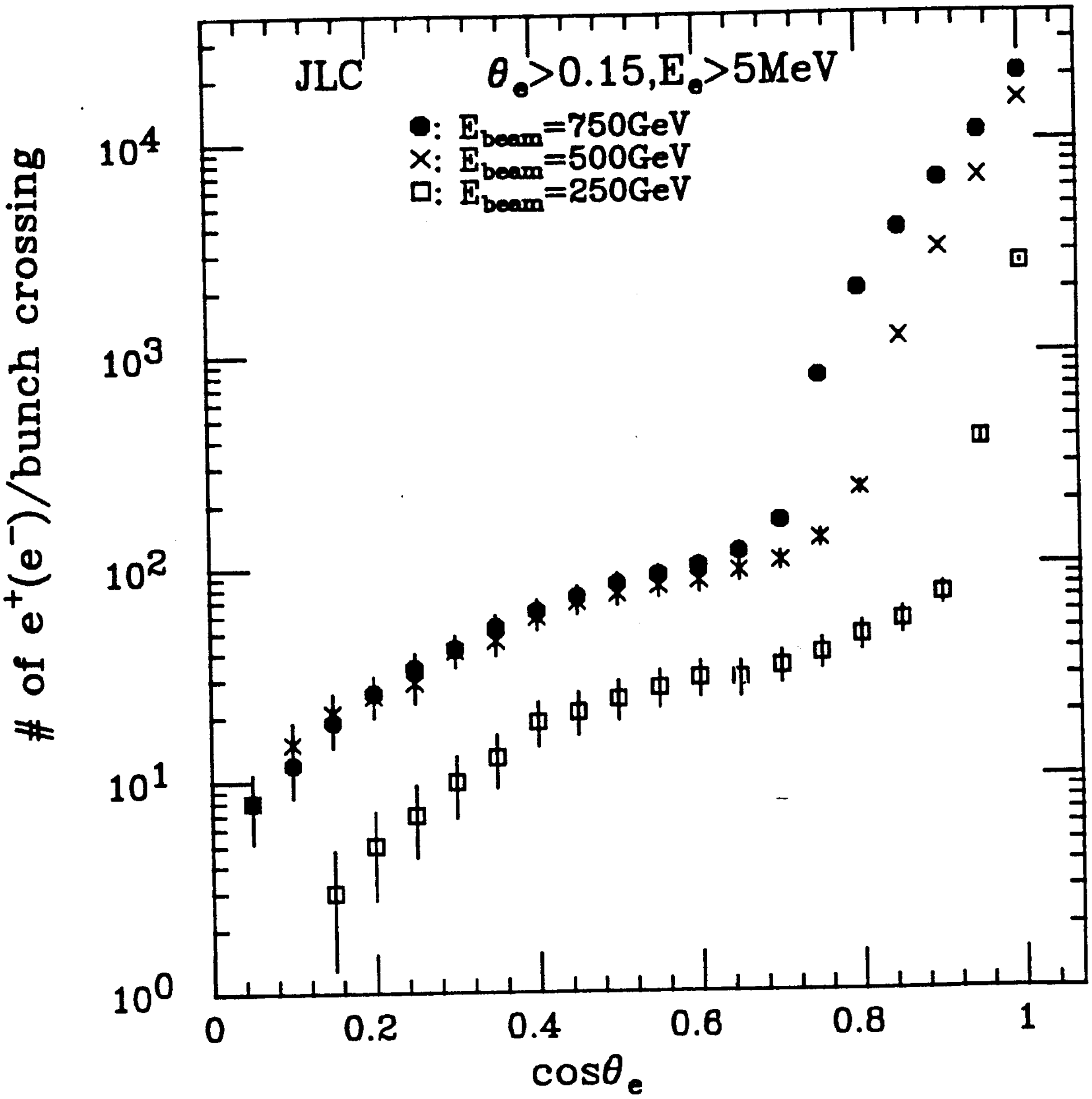
JLC
θ_e>0.15,E_e>5MeV
●: E_{beam}=750GeV
×: E_{beam}=500GeV
□: E_{beam}=250GeV
of $e^+(e^-)$/bunch crossing
10^0
10^1
10^2
10^3
10^4
0
0.2
0.4
0.6
0.8
1
$\cos\theta_e$

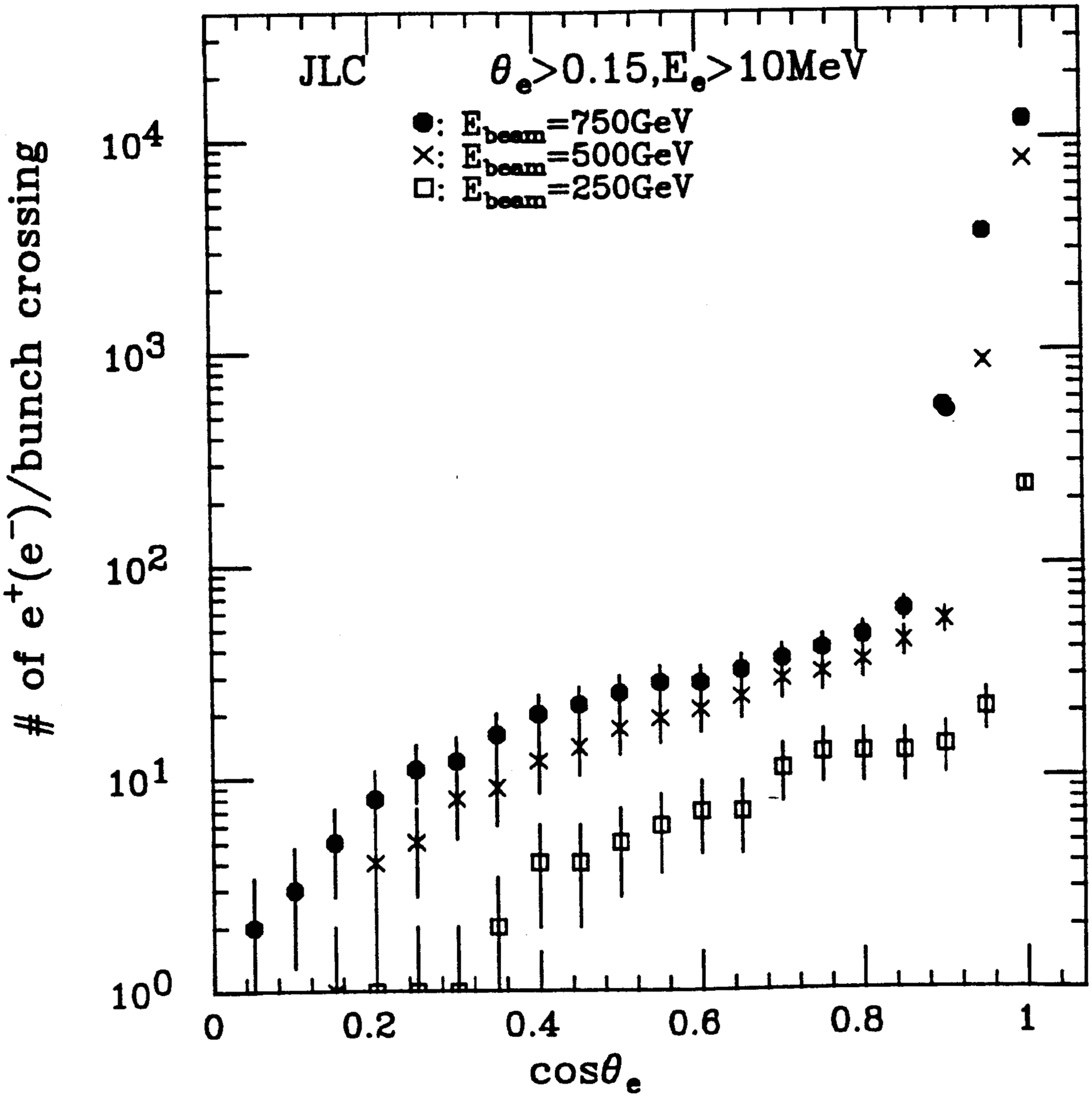
JLC
θ_e>0.15,E_e>10MeV
●: E_{beam}=750GeV
×: E_{beam}=500GeV
□: E_{beam}=250GeV
of $e^+(e^-)$/bunch crossing
10^4
10^3
10^2
10^1
10^0
0
0.2
0.4
0.6
0.8
1
$\cos\theta_e$

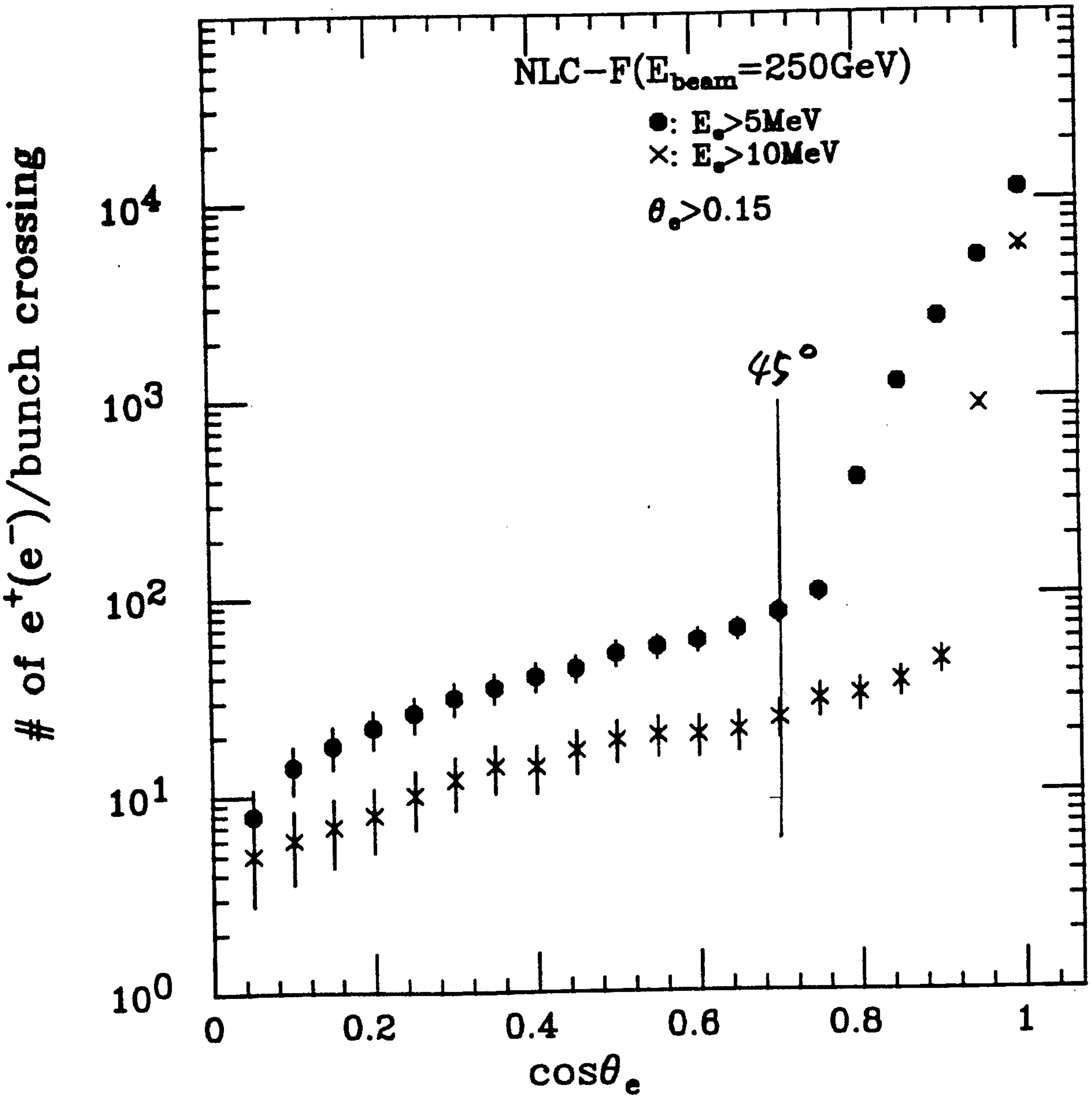
NLC−F(E_beam=250GeV)
●: E_e>5MeV
×: E_e>10MeV
θ_e>0.15
45°
# of e+(e−)/bunch crossing
10^0
10^1
10^2
10^3
10^4
0
0.2
0.4
0.6
0.8
1
cosθ_e

H. Band

ABEL – PALMER F E>5 MEV THETA> 100 RHO>2CM

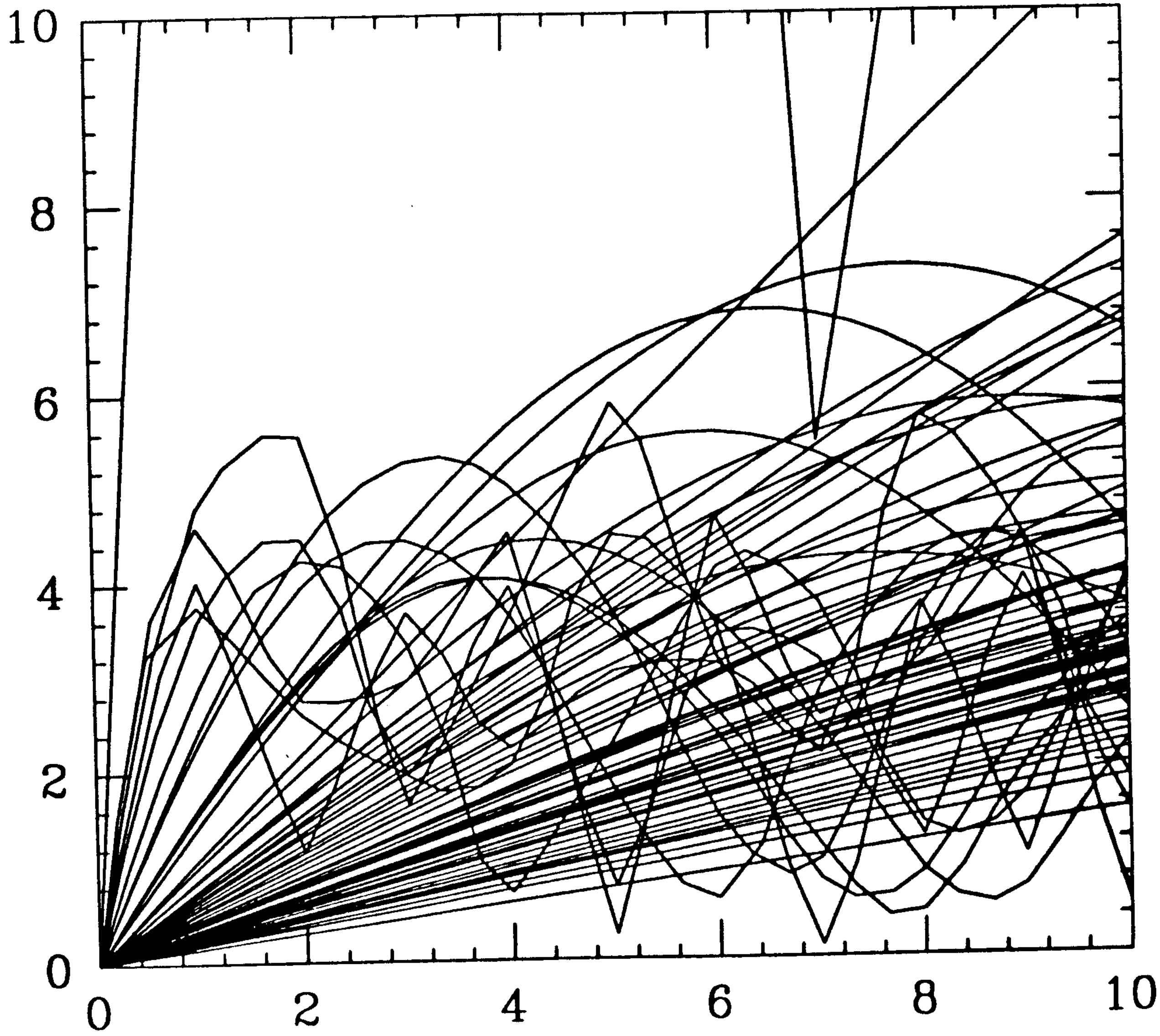

H. Band

ABEL – PALMER F E>5 MEV WEIGHT 100

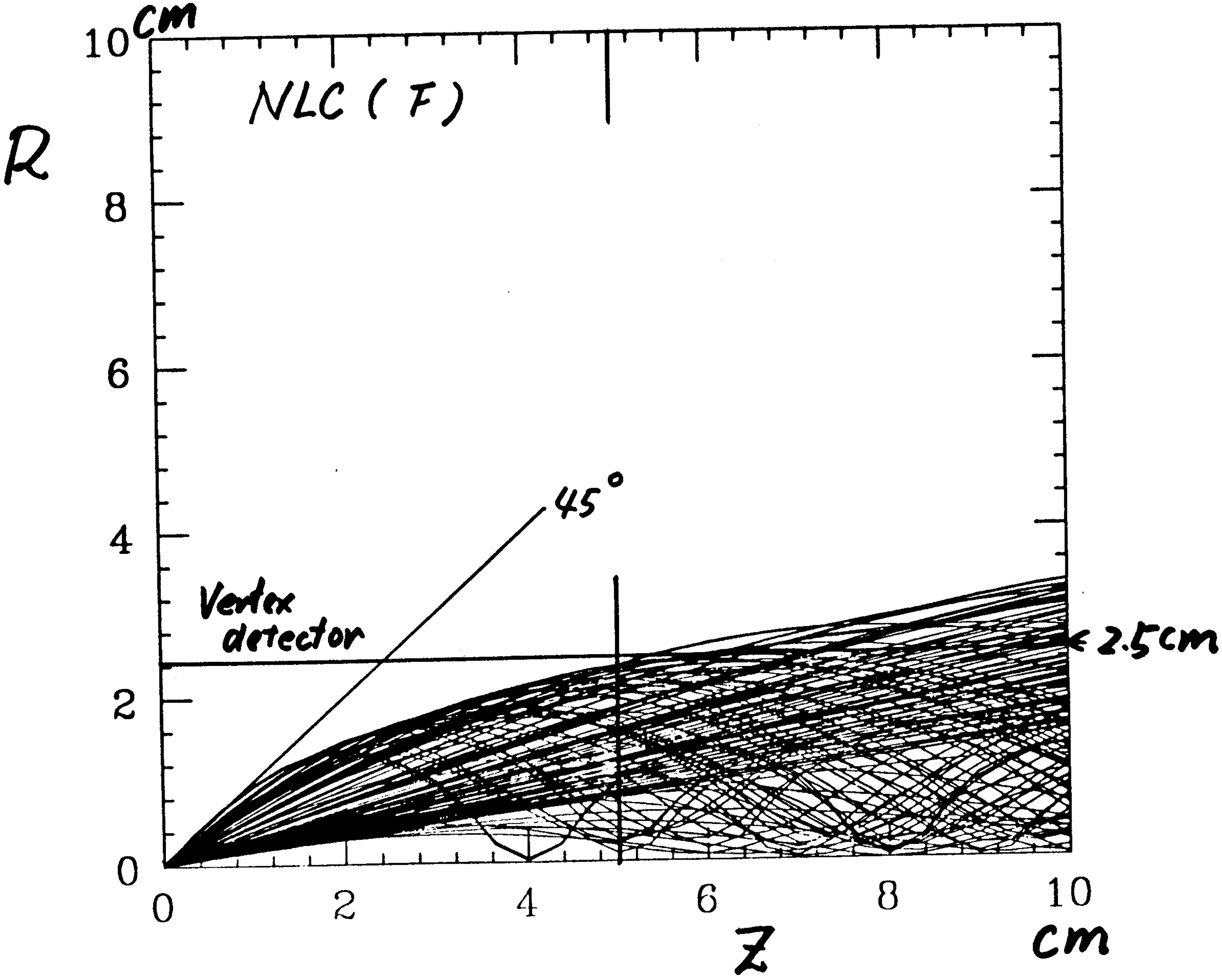

ID= 10

MAX RADIUS AT OR BEFORE Z=10cm H. Band

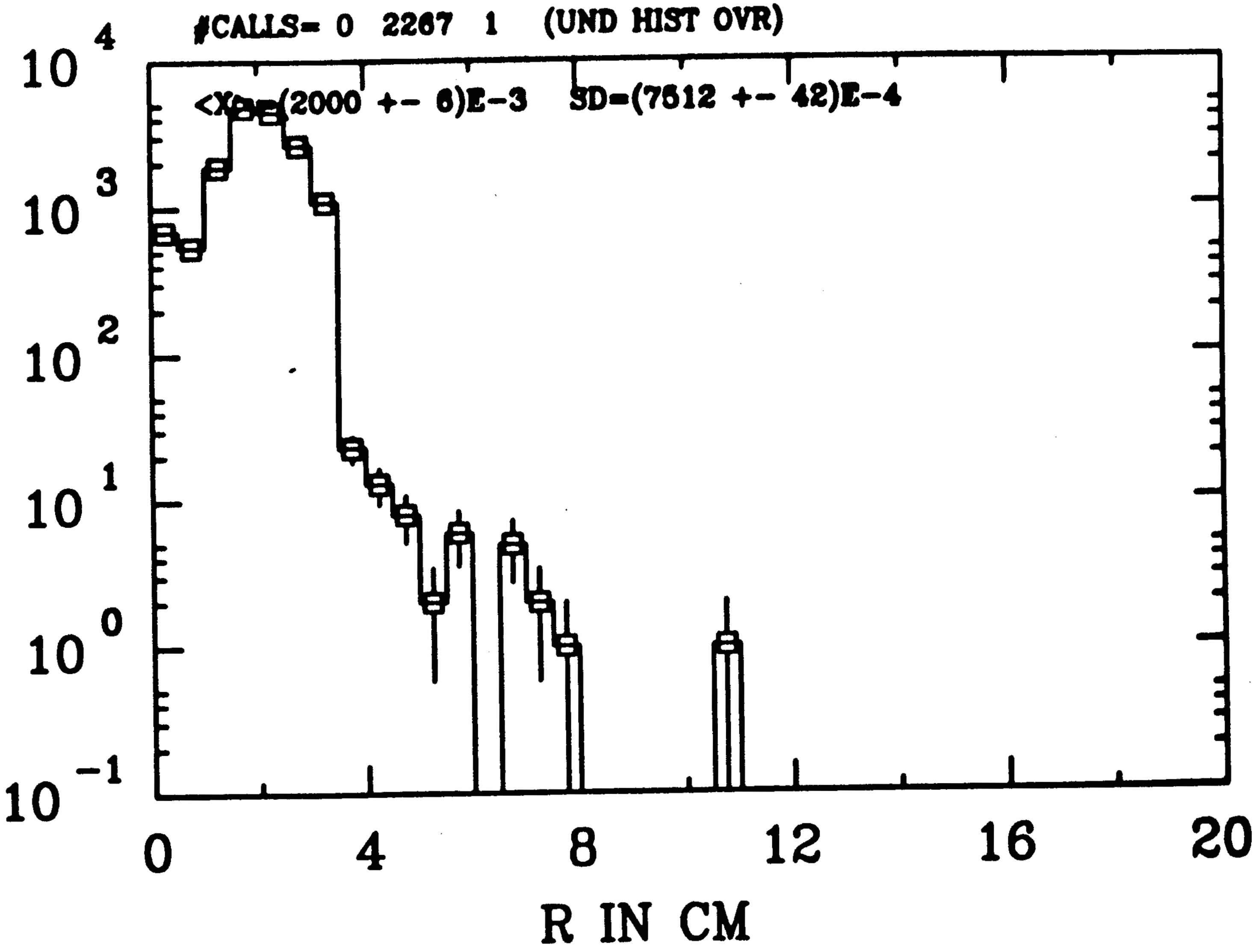

HANDYPAK [illegible] [illegible]

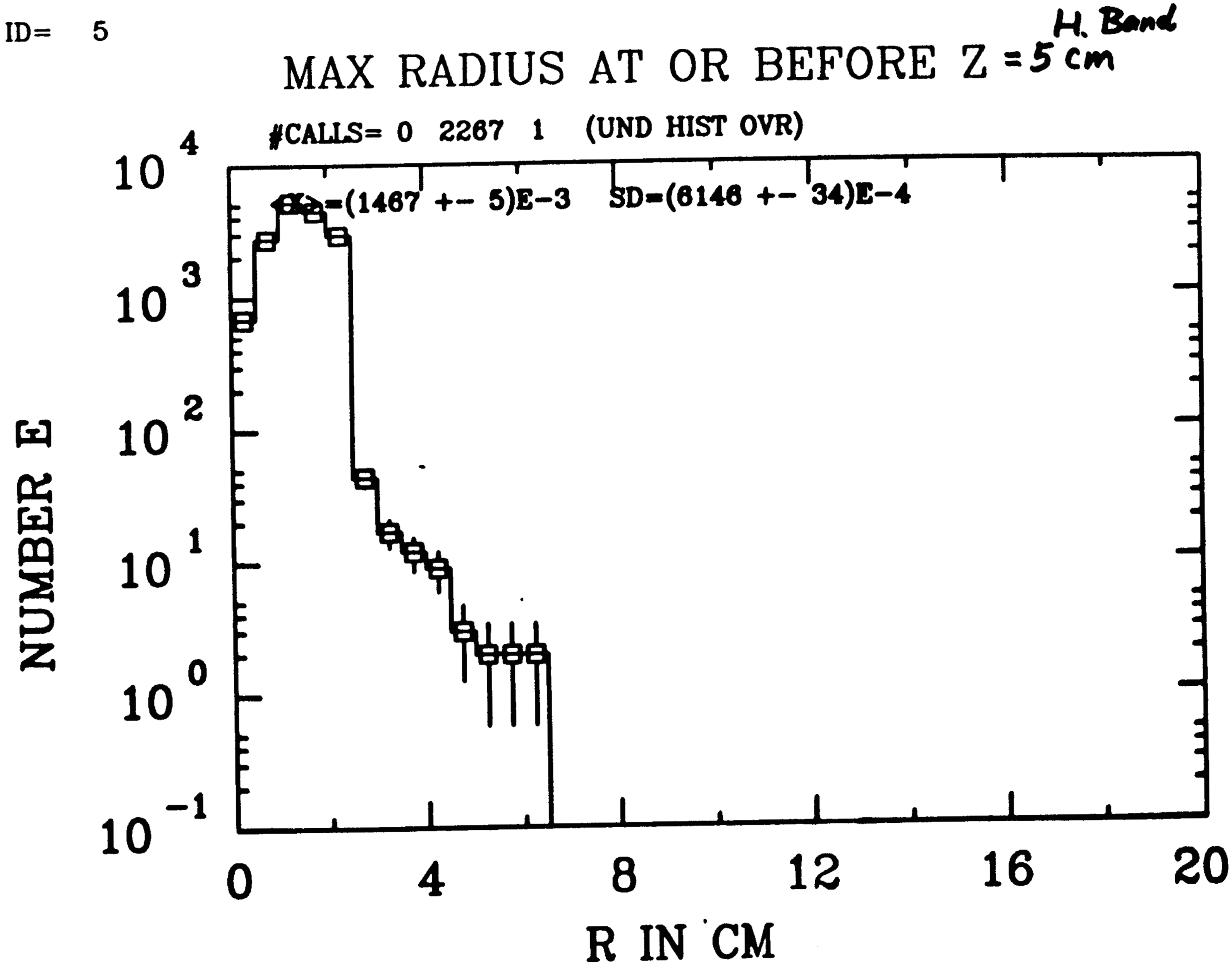
ID= 5
H. Band
MAX RADIUS AT OR BEFORE Z = 5 cm
#CALLS= 0 2267 1 (UND HIST OVR)
<X>=(1467 +- 5)E-3 SD=(6146 +- 34)E-4
NUMBER E
10^{4}
10^{3}
10^{2}
10^{1}
10^{0}
10^{-1}
0
4
8
12
16
20
R IN CM

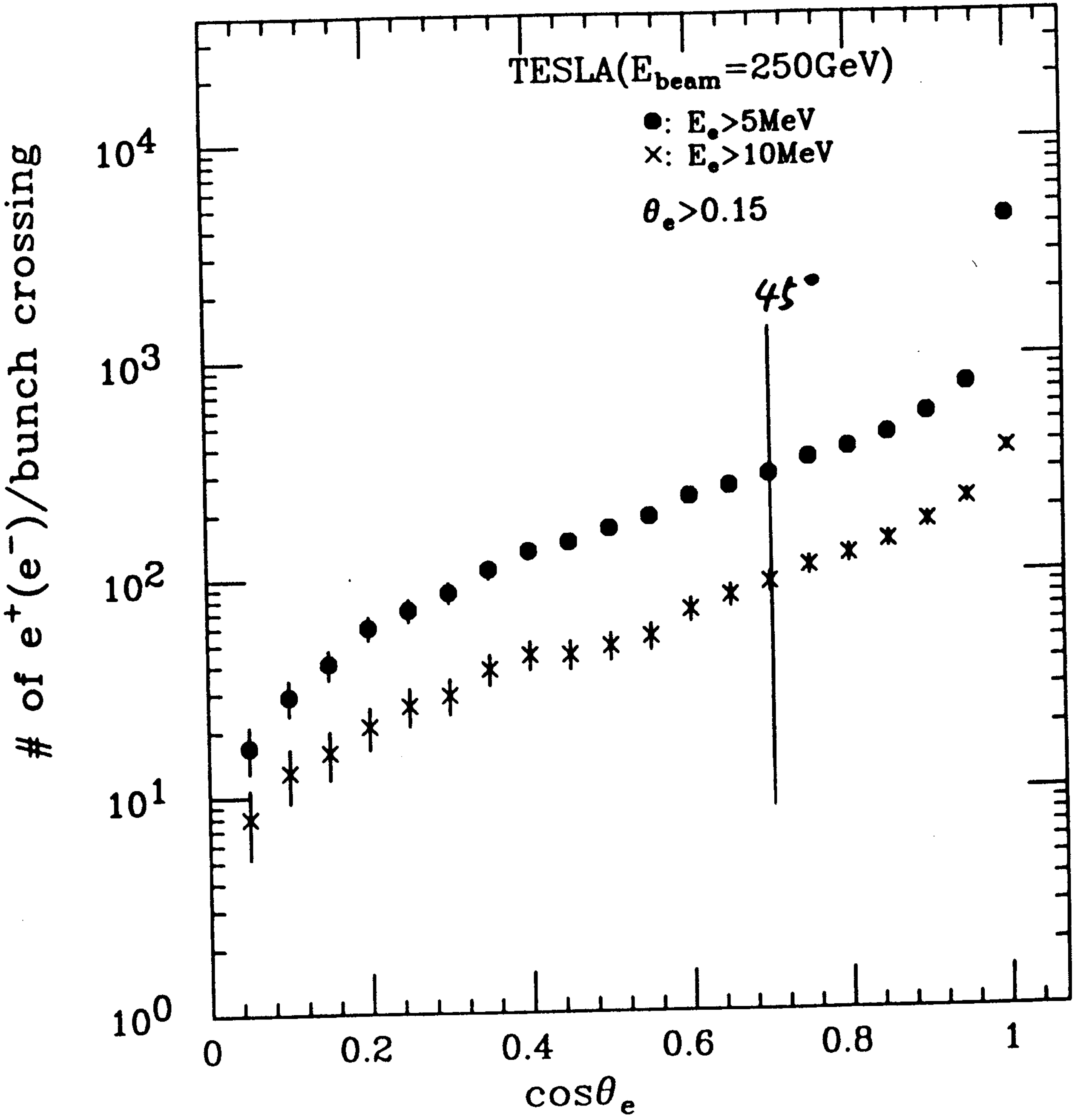
TESLA(E_beam=250GeV)
●: E_e>5MeV
×: E_e>10MeV
θ_e>0.15
45°
# of e+(e−)/bunch crossing
10^4
10^3
10^2
10^1
10^0
0
0.2
0.4
0.6
0.8
1
cosθ_e

$e^{\pm}$ pairs at Vertex detector/train.

$E_{beam} = 250$ GeV

$|\cos\theta| < 0.7$ ($|\theta| > 45°$) sensitive area

R	2.5 cm ($P_t > 5$ MeV)	5.0 cm ($P_t > 10$ MeV)	
JLC	600	200	
NLC (F)	800	200	
TESLA	300	90	/bunch

Summary

1. Muons

Detailed M.C. simulation is necessary to Take account of realistic tunnel structure and FF system.

At present, $N_{coll} \sim 3.6 \times 10^7$ for no μ in $3 \times 3\ m^2$ detector (NLC).

If one μ / m^2 is acceptable from the experience of MARK II/SLD, it still 36×10^8.

1% beam loss at the end of LINAC ⇒ $\underline{\times 10^{-3}}$

2. QED : $e^{\pm}$ pairs

Optics of $L = 2.2m$ is much more better for masking together with $B_{out} = 2$ Tesla, especially for $E_{beam} > 500$ GeV.

# of pairs on the mask $\lesssim 500$.

3. QCD : mini jets

mini jet event rate at $E_{beam} = 250$ GeV is $O(1)$.

⇐ small enough.

Although the event topology of mini jet is very different, physics study should be necessary to get tolerable mini jet events for $E_{beam} \geq 500$ GeV.

Bunch separation is very usufull to resolve overlapping. Time resolution of 1 ns is already achieved.

4. Vertex detectors

Minimum radius of vertex detector depends strongly on the QED background. As # of pairs traversing the detector is $O(10^3)$, pixel device has to be used. For $E_{beam} = 250$ GeV, $R_{min} = 2.5$ cm seems to be possible, but more detail study is necessary because of small mergin for backgrounds.

HARDWARE WORKING GROUP

Chairman: Bill Ash

Members and Contributors

J. Norem	ANL	W. Atwood	SLAC
M. Placidi	CERN	G. Bowden	SLAC
M. Tigner	Cornell	F.-J. Decker	SLAC
G. Voss	DESY	J. Ferrie	SLAC
G. Jackson	FNAL	C. Field	SLAC
E. Kushnirenko	INP	G. Fischer	SLAC
T. Matsui	KEK	A. Hutton	SLAC
T. Omori	KEK	M. Ross	SLAC
R. Sugahara	KEK	J. Seeman	SLAC
R. Shafer	LANL	S. Smith	SLAC
J. Buon	Orsay	J. Spencer	SLAC
P. Puzo	Orsay	F. Villa	SLAC
W. Ash	SLAC	D. Walz	SLAC

Summary of FFIR Hardware Working Group Discussions

Bill Ash

The task of the Hardware Working Group was to review the technical solutions for focusing and monitoring the beams at the interaction point, while keeping in mind the existence of the detector components and backgrounds.

The 26 participants, listed on the previous page, met for seven sessions during the week. The process began in all cases with prepared talks, nineteen in all. The topics are listed on the following page. Much of the progress, however, was in the questions and discussion between talks and outside the sessions.

All this was very well summarized by Maury Tigner, addressing issues related to the magnets, supports and the detector, and by Bob Shafer, covering the final focus instrumentation. Their transparencies are included here. At risk of missing their insights I offer the following précis.

What might have seemed to be the hardest problem — miniature quadrupoles for the final focus beams — may in fact have three solutions. A coil-driven, iron-alloy quadrupole and a permanent-magnet quadrupole have both been built and measured, while a conceptual design for a superconducting quadrupole based on four single-rod conductors looks feasible.

The group made significant progress in developing a conceptual scheme for mounting these magnets, a process helped by a joint meeting with the detector group. A support tube of roughly one-meter diameter spanning the detector contains the masking, vertex detector, and an internally supported set of final focus quadrupoles. This 'inner tube' must also contain built-in, straight-across ports for alignment schemes such as wires and lasers. A free-wheeling discussion of seismic isolation confronted the issue of passive versus active supports; more work is needed.

The instrumentation section mainly covered monitors for beam profile and beam position. Novel profile monitor techniques based on laser Compton scattering, gas ionization, and bremsstrahlung have been tested in part and are scheduled for direct measurements in the Final Focus Test Beam within a year or so. An R & D effort using 'liquid wires' may have application in other areas of the machine as well.

A stripline position monitor for the FFTB may be workable for a next generation collider, but there are questions on resolving individual bunches. Microwave cavity position monitors and button-electrode devices should be revisited.

The compatibility of this instrumentation with a detector-friendly support system is an open question and some thinking of retractable devices and the like has begun.

And finally, almost literally, are the beam dumps and primary collimators. The new frontiers of power density are pushing practical limits of materials.

In all, this group had a productive week and has set the stage for further collaboration.

SUMMARY TALKS

Detector, Magnets, and Supports	M.Tigner
Instrumentation in the Final Focus	R. Shafer

PARALLEL SESSION TALKS

Iron FF Quads from JLC Studies	T. Matsui
Permanent Magnet Quads	J. Spencer
Superconducting FF Quads	E. Kushnirenko
Conceptual Designs for a Detector	T. Matsui
Some Parameters for S-Band & L-Band	M. Tigner
Some Parameters for X-Band	J. Seeman
S/C Low-beta Quads at LEP	M. Placidi
S/C Triplets at SLC	W. Ash
Conceptual Support Scheme	J. Seeman
Support Tube Ideas	G. Bowden
Seismic Instrumentation	J. Norem
A Laser-QPD System	R. Sugahara
Liquid Wire Monitor R&D	F. Villa
Ionization Beam Size Monitor	P. Puzo
Shintake Laser-Compton Monitor	T. Omori
Beam Polarization Monitor	T. Omori
Beam Position Monitors	S. Smith
Bremsstrahlung-based Profile Monitor	J. Norem
FF Collimation and Dumping	D. Walz

Linear Collider Final Focus Workshop

Instrumentation Summary.

R. Shafer 3/6/92

S. Smith	Linear Collider FF Beam Position Mon.
V. Balakin	R.F. Cavity Beam Position Monitors
T. Omori	Laser Compton Scattering Beam Profile Mon.
"	" " " Polarization Mon.
P. Puzo	Residual Gas Beam Size Monitor
F. Villa	Liquid Jet Beam Profile Monitor
J. Norem	Bremsstrahlung Beam Profile Monitor

Title:

Linear Collider
Interaction Point
Beam Position Monitors

(LCIPBPM®)

Subtitle:

How far can you push stripline BPM's without stretching existing technology (too far)

Steve Smith

LCFFIR Workshop
March 5, 1992

Approach:

1. Inductive pickups
2. Low frequency linear electronics
   - a. filter out all unmanageable high frequencies
   - b. sample
   - c. digitize
   - d. $Y = \frac{R}{2} \frac{Up - Down}{Up + Down}$

Linear Collider Requirements

1. Extreme precision requirement: 20nm for JLC?
   100nm for NLC
2. Number of bunches awkward for some designs
   $1 < N <$ many
3. Must live in IP environment

FFTB

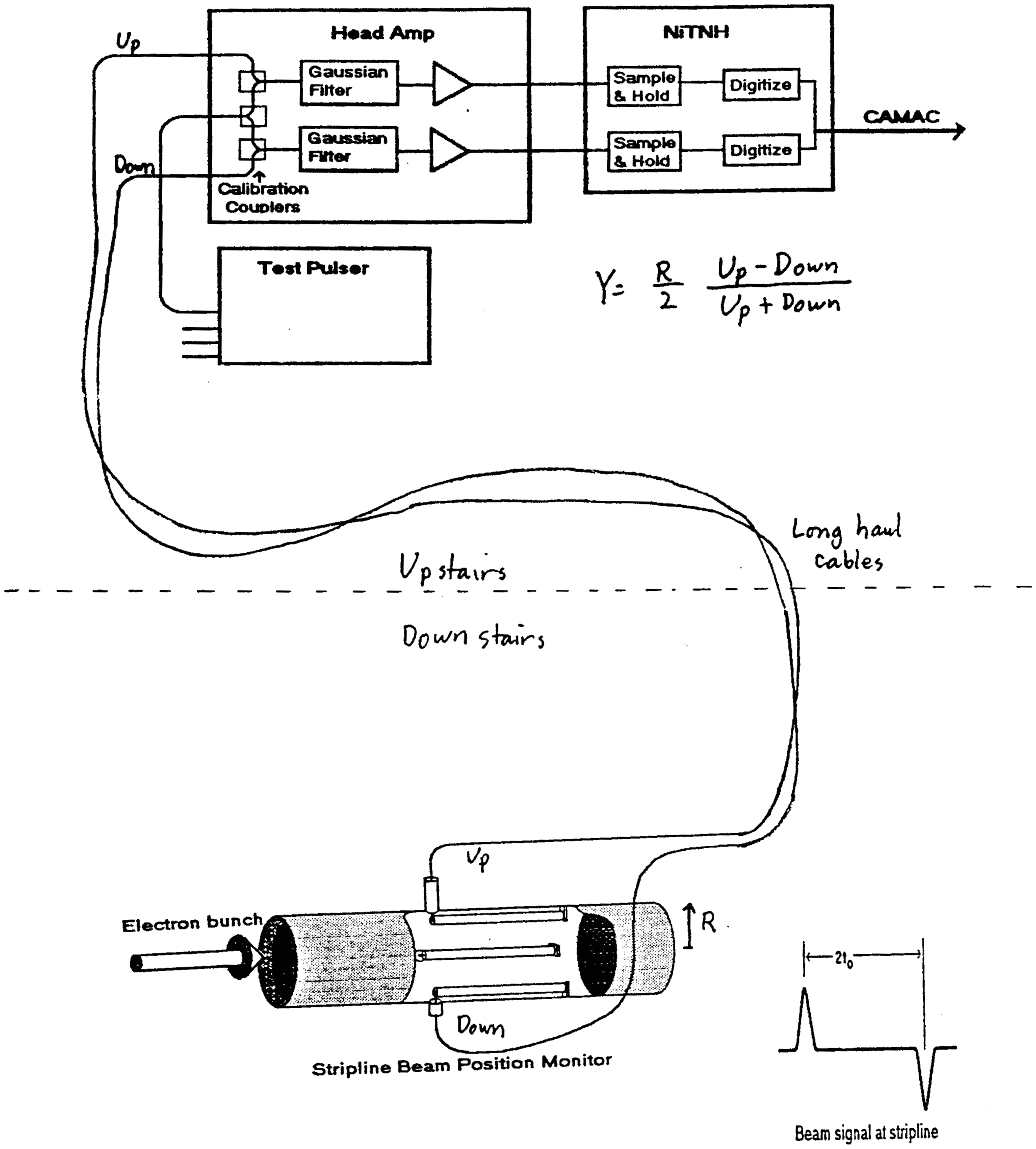

$$Y = \frac{R}{2}\,\frac{Up - Down}{Up + Down}$$

SLC IP electronics

(not FFTB electronics)

Y = AX + B

A = 0.9989 STD DEV = 1.8493E-02

B = 0.9944 STD DEV = 7.9038E-03

RMS FIT ERROR = ~~1.5927E-02~~ 8μm

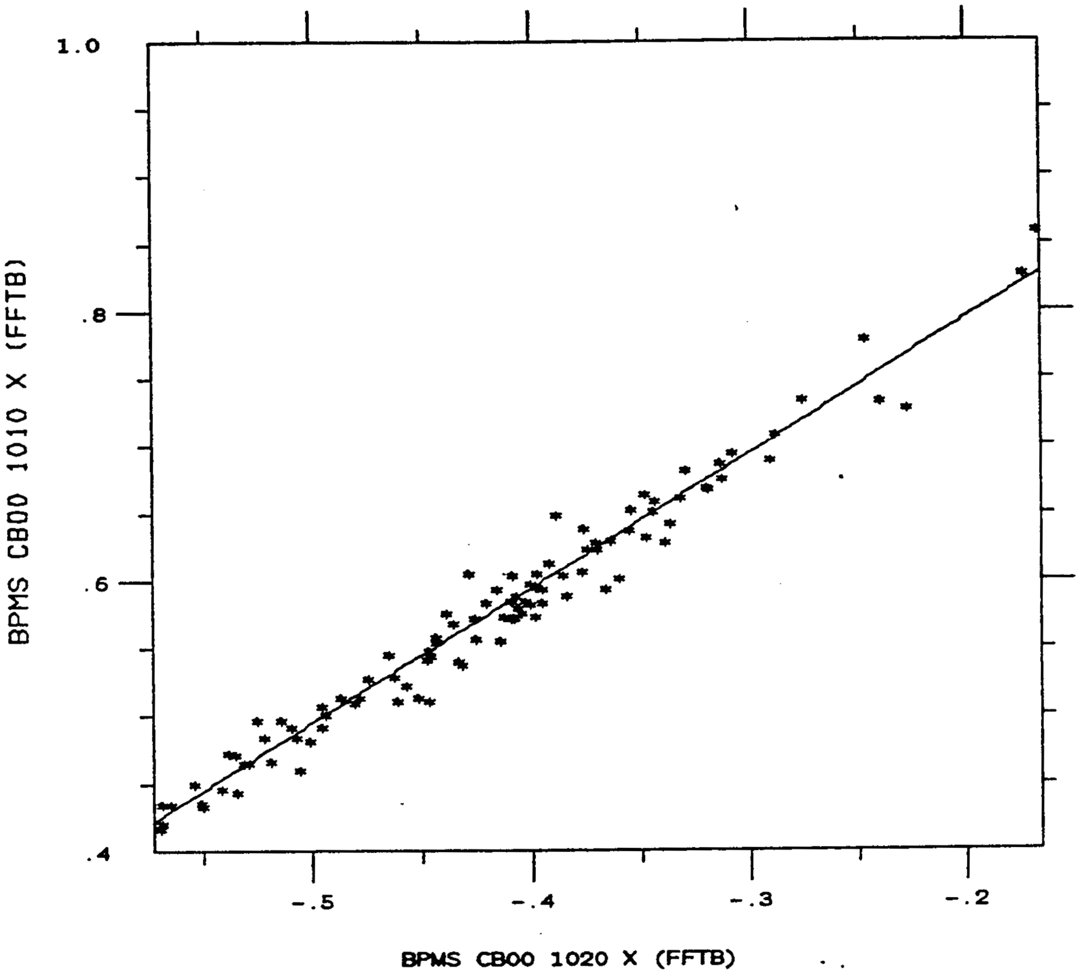

STEP VARIABLE = ZERO

4-FEB-92 02:00:31

BPM resolution ~ $\frac{8\mu m}{\sqrt{2}} = 5\mu m$

in a single pulse

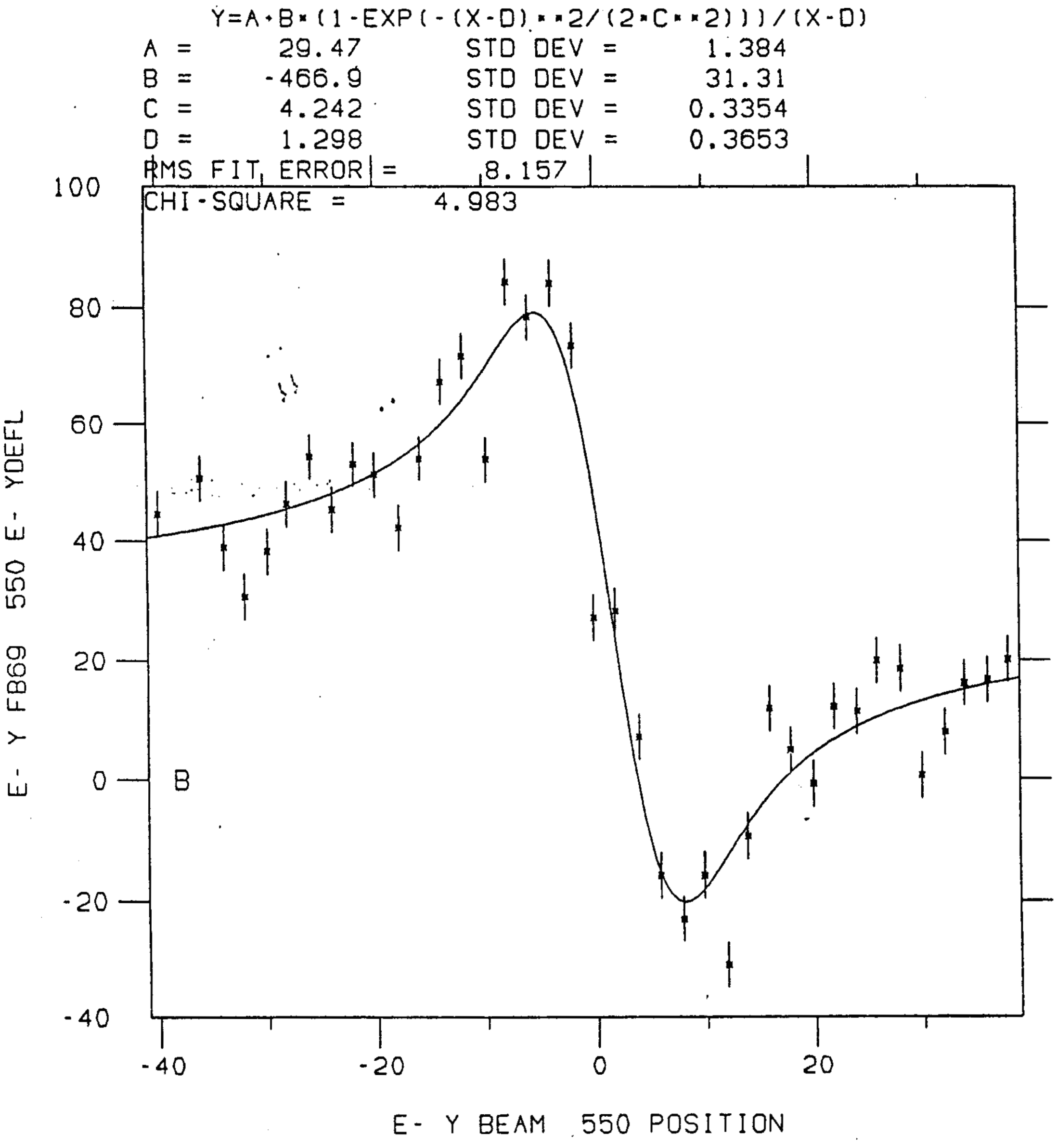

```
    Y=A+B*(1-EXP(-(X-D)**2/(2*C**2)))/(X-D)
A =       29.47       STD DEV =      1.384
B =      -466.9       STD DEV =      31.31
C =       4.242       STD DEV =     0.3354
D =       1.298       STD DEV =     0.3653
RMS FIT ERROR =       8.157
CHI-SQUARE =      4.983
```

STEP VARIABLE = ZERO

5-JUN-89 11:51:58

Summary

1 Sub micron resolution is achievable

2 High resolution and individual bunch resolution may be mutually exclusive

3. Tails, synchrotron radiation, and spray may be problem.

RF Cavity BPM's (á lá Balakin)

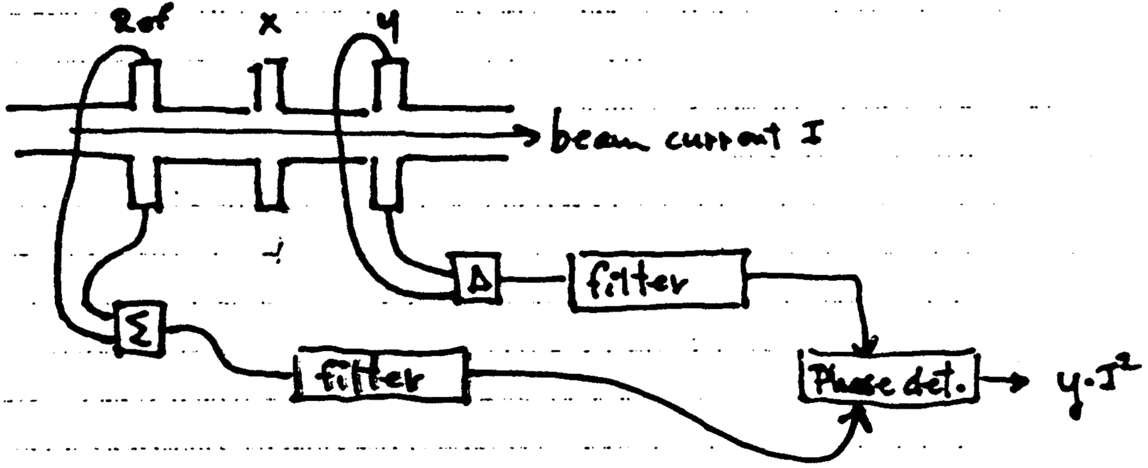

Very sensitive - good position resolution (few 10's of nm)

Output proportional to I^2 - need to normalize

Need to maintain phase coherence - very close tolerance on cavity resonant frequencies.

Requires significant beamline space unless very high frequencies are used.

Good signal format: Σ and Δ signals vs L & R: systematics create gain drift, not offset drift.

Is there a problem with wakefields (coupling impedance)?

Protvino/LEP design: 15 GHz, temp compensated cavities under development.

Possible Development Areas in BPM's

Button electrodes - very high accuracy
good for short bunches
used around new synchrotron
light sources.

Slot-coupled pickups - very high accuracy
extrapolatable to very small size

Reduction of Systematic errors

Better signal processing techniques.

Beam Profile Monitor
by
Laser-Compton Scattering

T. Shintake's New Idea

Presented by T.Omori
at FF&IR Workshop
5-Mar-1992

Shintake's Beam Profile Monitor

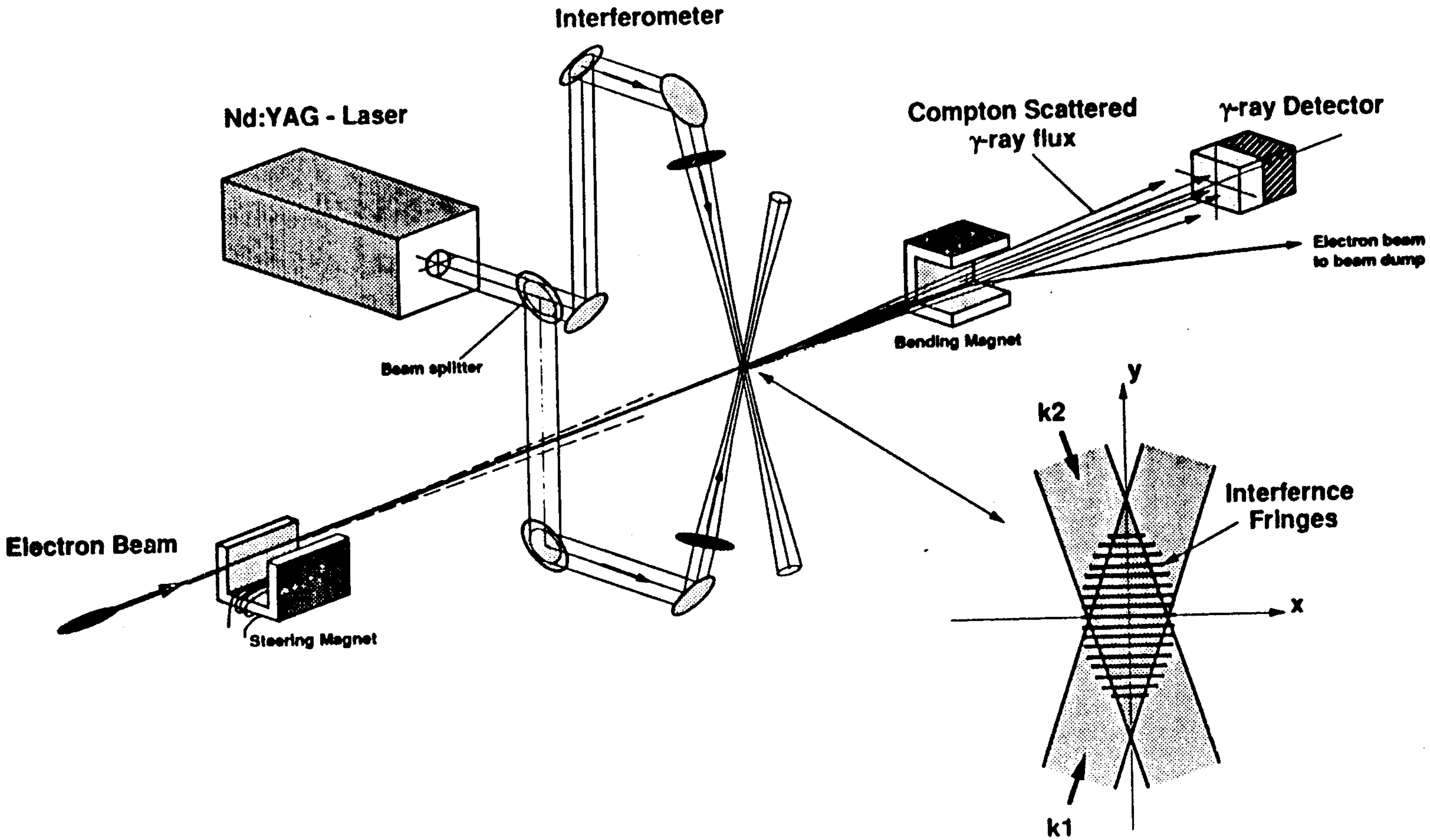

T. Shintake

Modulation

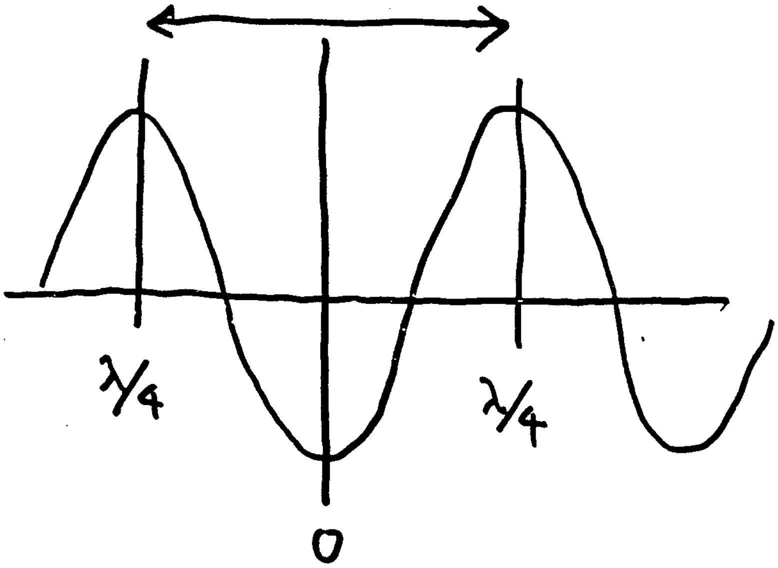

Laser Nd:YAG

2nd $\lambda = 532\,\text{nm}$ $2 \times \frac{\lambda}{4} = 266\,\text{nm}$

4th $\lambda = 266\,\text{nm}$ $2 \times \frac{\lambda}{4} = 133\,\text{nm}$

Assum $\Delta(\text{modulation}) = 10\%$ Can Measure

2nd $\sigma = 26\,\text{nm}$ } Can Measure
4th $\sigma = 13\,\text{nm}$ }

T. Shintake

σ_y Measurement

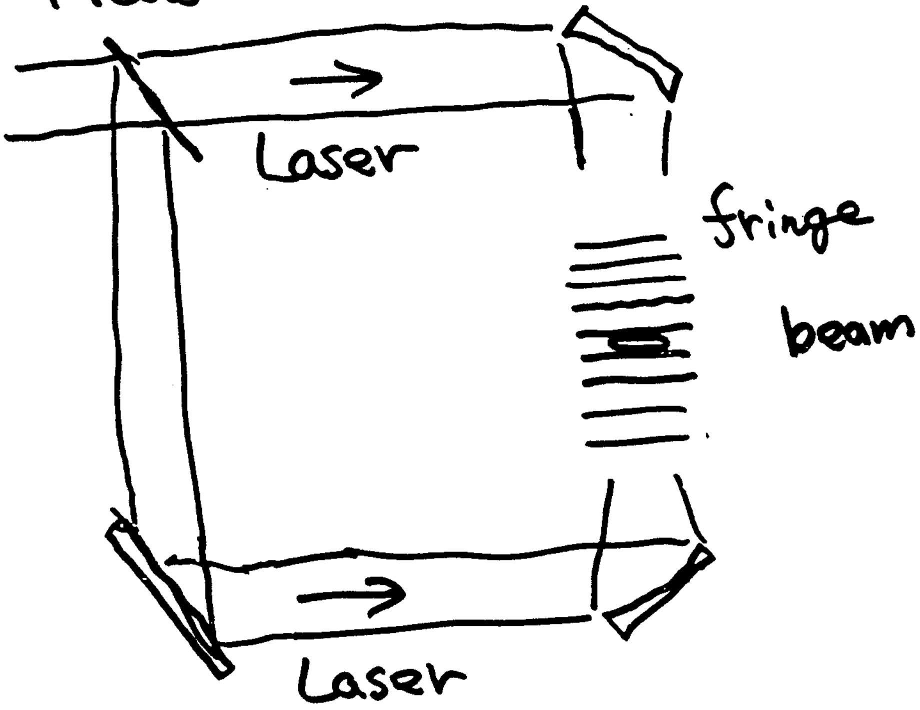

σ_x Measurement

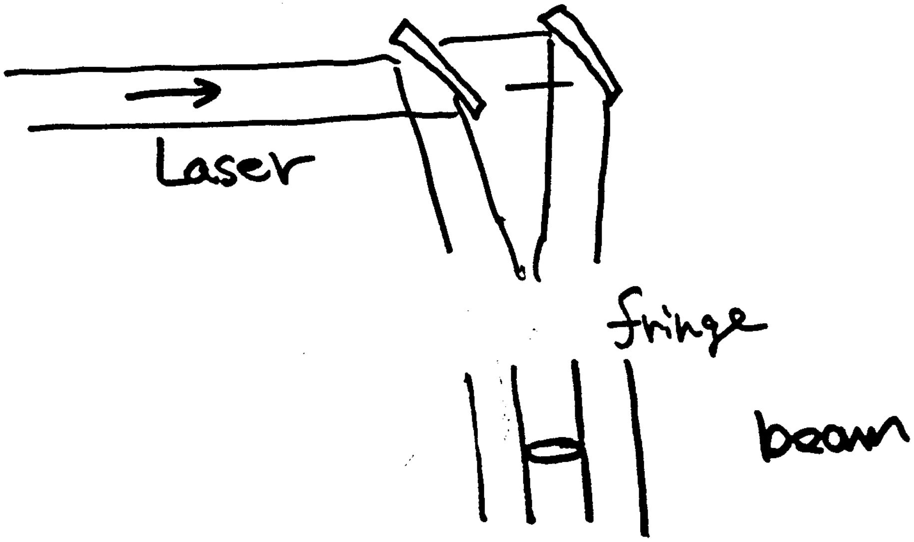

Can Measure Both σ_x and σ_y

Beam Polarization Monitor
by
Laser-Compton Scattering

5-Mar-1992 T.Omori (KEK)
at FF&IR Workshop (SLAC)

Measure the Beam Polarization by
Laser-Compton Scattering

⇨ Old Idea
  Many Experimet in Ring Accelerators
    SLAC, DESY, and KEK
  Linear Collider (under preparation)
    SLC (M.Fero etal)

My Proposal
  Measure Polarization at IP (not near)
  Combine { Polarization Monitor
          Profile Monitor (Shintake)

Basic Idea

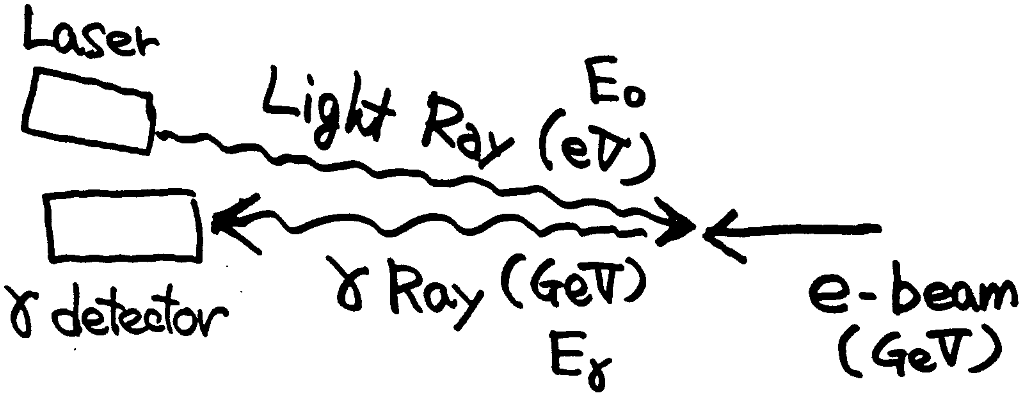

Total Cross Section & Angular Distribution } depends on the Combination of photon spin & electron spin

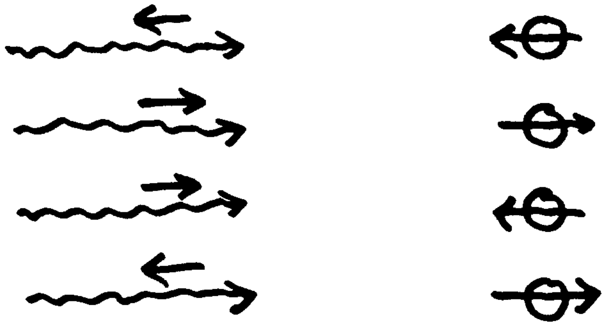

→ in Lab. frame

Energy distribution of Scattered Photon

Head-on-Collision

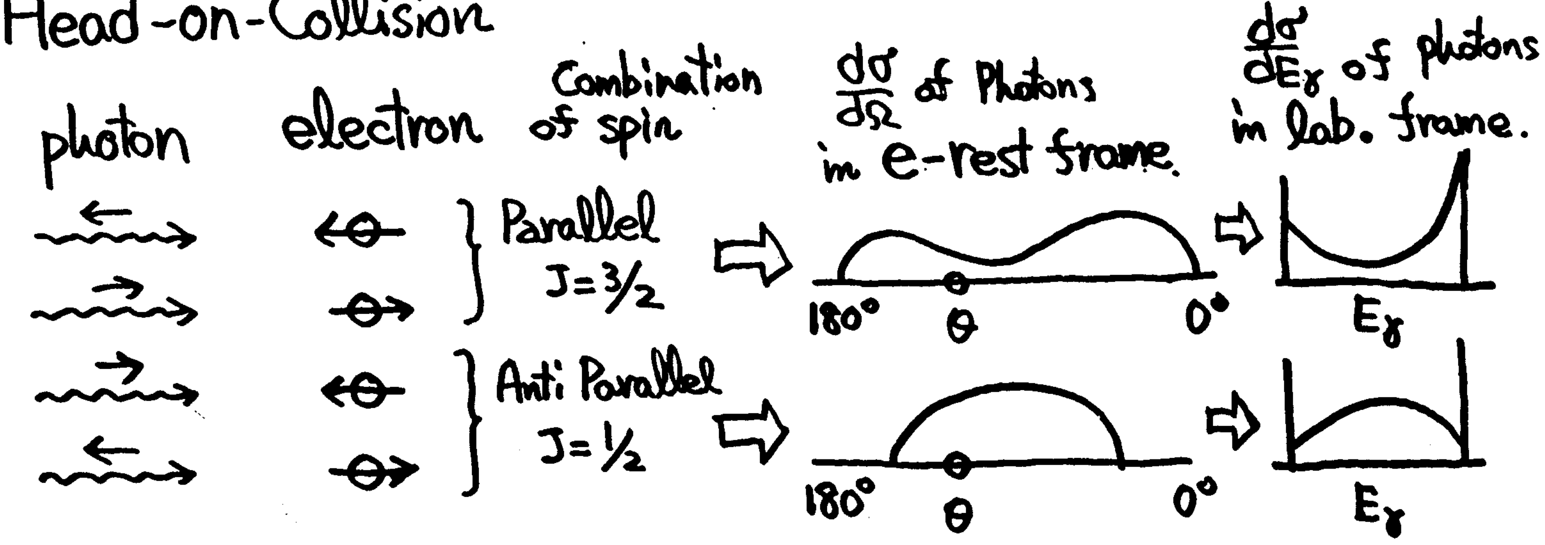

Non Head-on-Collision

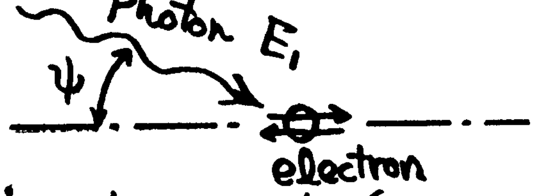

electron rest frame

integrated over azimuth angle

$$\frac{d\sigma}{d\theta} = \underbrace{\frac{d\sigma_0}{d\theta}}_{\text{spin independent}} \underbrace{- P_\gamma P_e \cos\psi \frac{d\sigma_1}{d\theta}}_{\text{spin dependent}}$$

when $\cos\psi = 0$ → analysing power $= 0$

$\sum_{\text{in a bunch}} E_\gamma$ Distribution $\left\{ \begin{array}{l} \text{1500 Linac Pulse} = \text{10 sec} \\ \text{select a bunch in a Pulse} \end{array} \right.$

a) $E_b = 50$ GeV

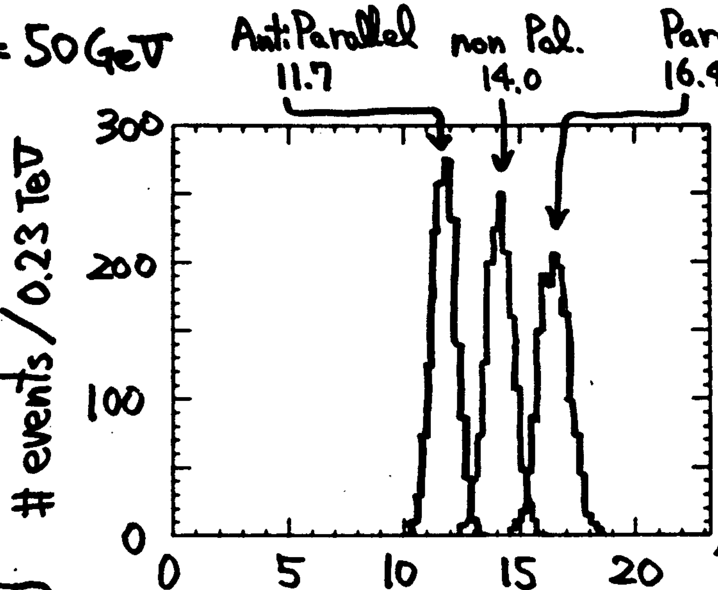

Laser
$E_0 = 4.66$ eV
100 MW

$\Delta P = 100\%$
$\updownarrow$
$\Delta(\sum E_\gamma) = 17\%$

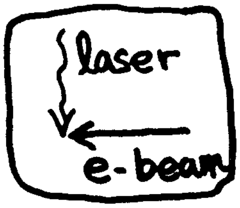

$\sum_{\text{in a bunch}} E_\gamma$ (TeV)

b) $E_b = 500$ GeV

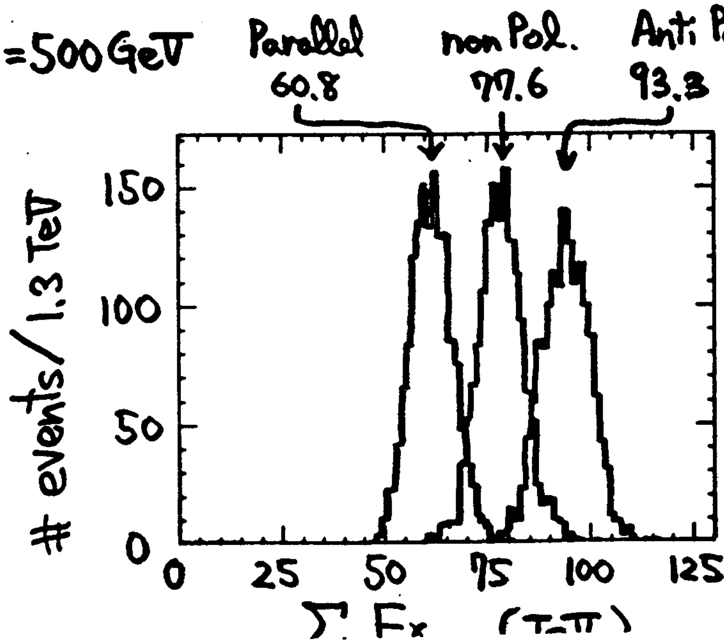

Laser
$E_0 = 4.66$ eV
100 MW

$\Delta P = 100\%$
$\updownarrow$
$\Delta(\sum E_\gamma) = 20\%$

Mirror Mover

put 2 Mirrors into the beam pipe

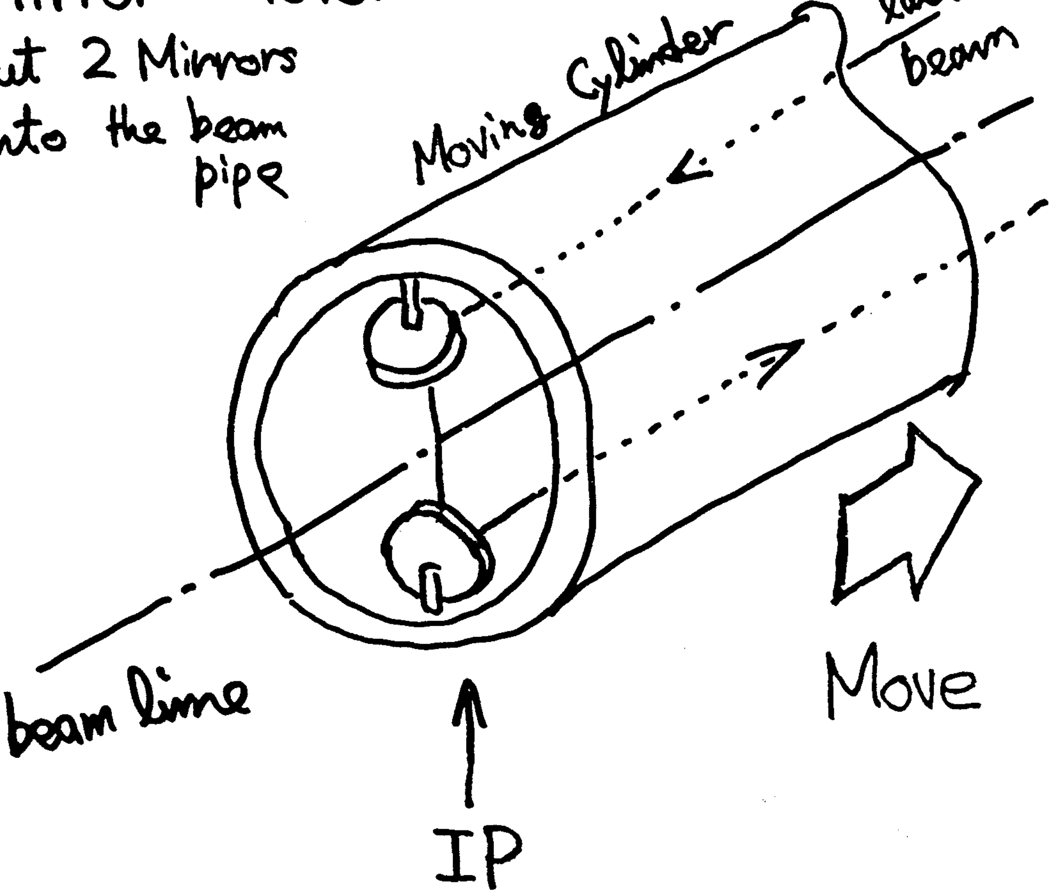

When taking Physics Data

⇩

Mirrors Go Away with a Cylinder

4) Need Move Study

(a) Responce of γ detector.

(b) Accuracy of Calibration.

(c) Optimization of Laser Power, related with (a), (b) & Beam Background.

(d) Other Calibration Method
Laser Wavelength Scan.

(e) Location of Mirror.

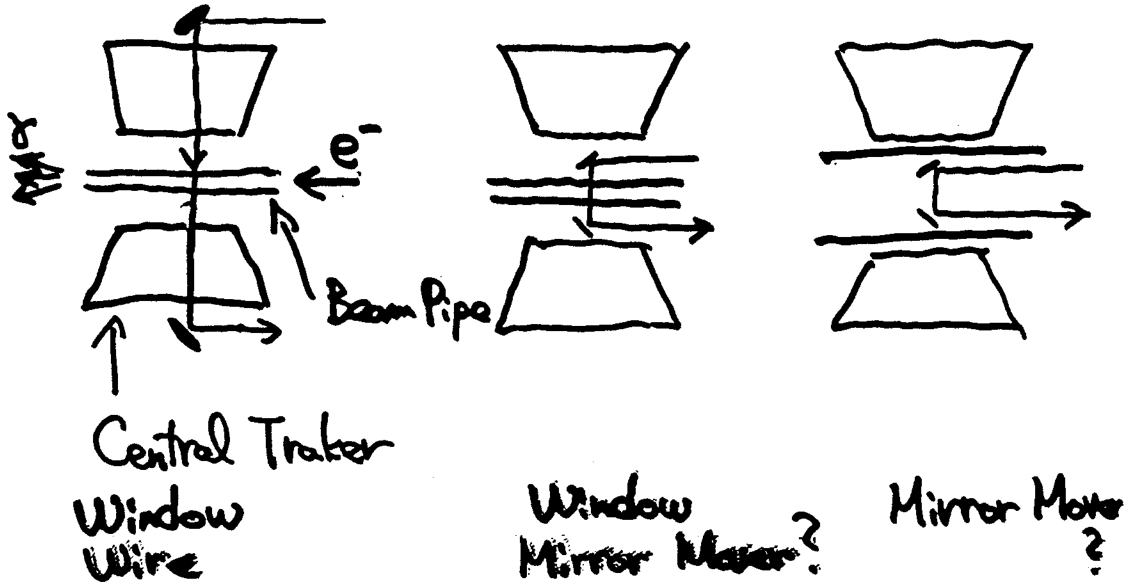

Beam Size Monitor

New method to measure transverse dimensions of a beam
down to 1 x 0.06 μm

Principle :
- low density gas target
- gas ionization by the beam
- space charge field $\vec{E}$ => transverse kick

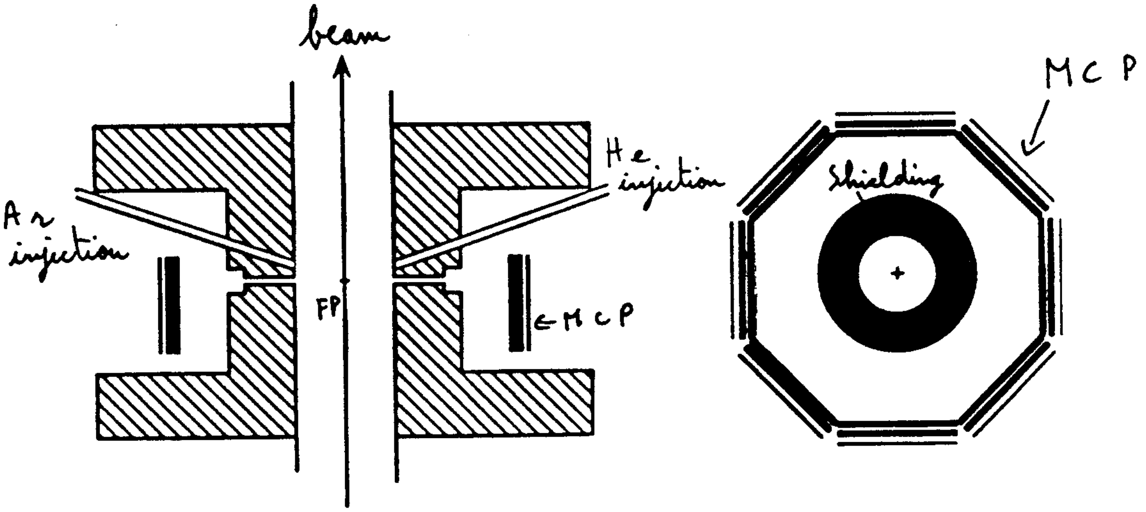

No sensitivity to the beam position

First measurement : aspect ratio

$$R = \frac{\sigma_x}{\sigma_y}$$

* Principle :

light ion : He^+

Electron beam potential well

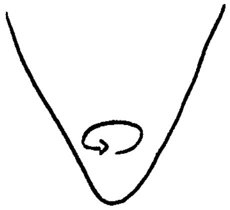

=> He^+ oscillations

=> Anisotropy of the angular distribution

$\sigma(He \rightsquigarrow He^+) \simeq 0.3$ Mb   no He^{2+}

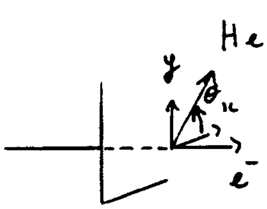

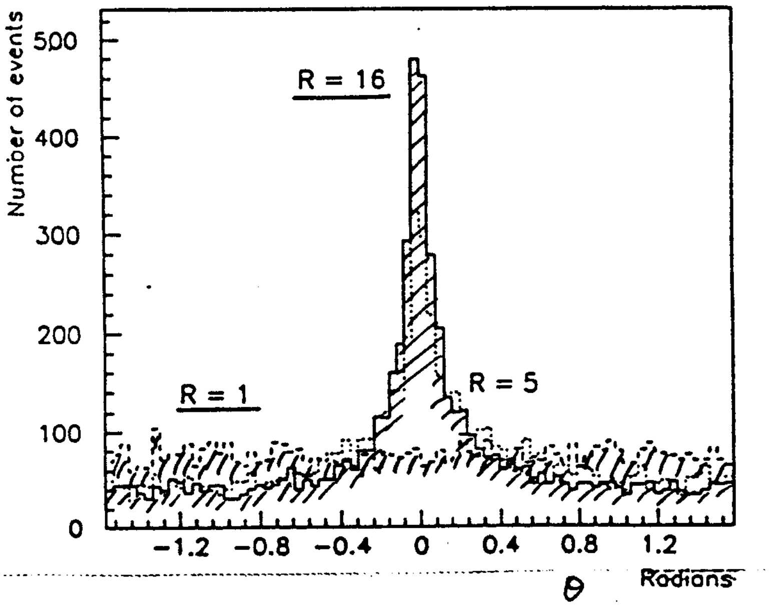

Second Measurement : σ_x

* Principle:

Heavy ions : Ar^+

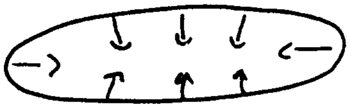

Maximum velocity : $V_{max} \propto E_{max} \propto \frac{1}{\sigma_x}$

$\Rightarrow \tau_{min} = F(\sigma_x ; \sigma_y)$

$\sigma(Ar \rightsquigarrow Ar^+) \simeq 2$ Mb

up to 20 % of Ar^{2+}

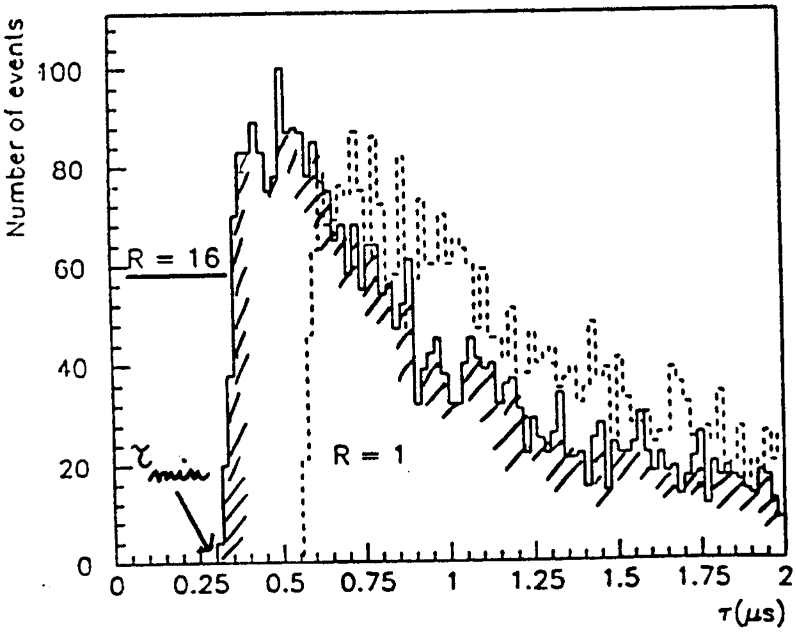

ENSEMBLE BSM

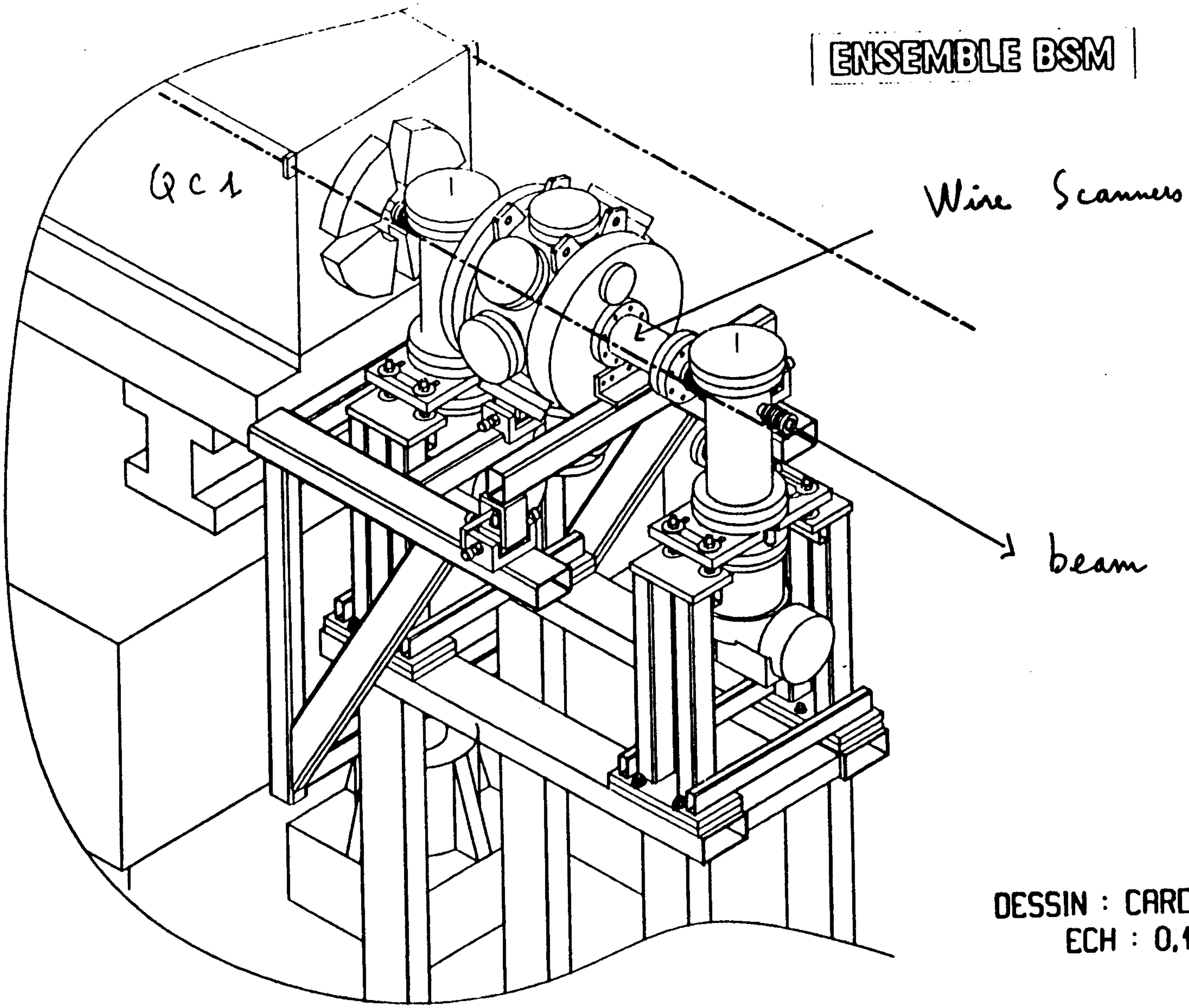

DESSIN : CARDUNER
ECH : 0.12

Beam Size and Position Monitors using liquid jets

F.Villa

SLAC

Wire scanners using carbon fibers have proven to be very useful in measuring beam profiles.

But, carbon fibers melt in high-brightness beams.

Liquid jet "fibers" may overcome this limitation.

Use low-melting-point eutectic alloys

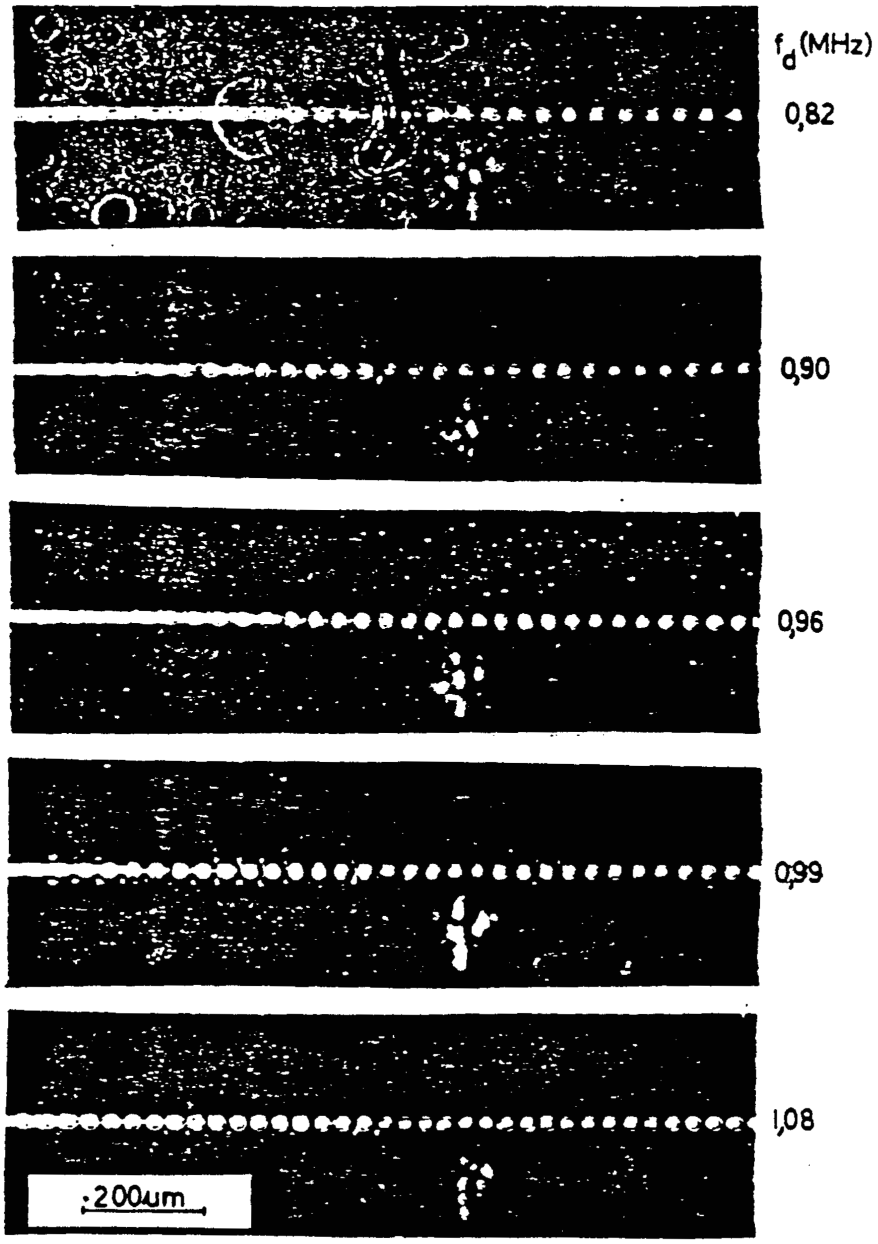

Fig. 2:6. Controlled drop formation of a 10 μm jet travelling at 40 m/s at different frequencies of the mechanical vibrations.

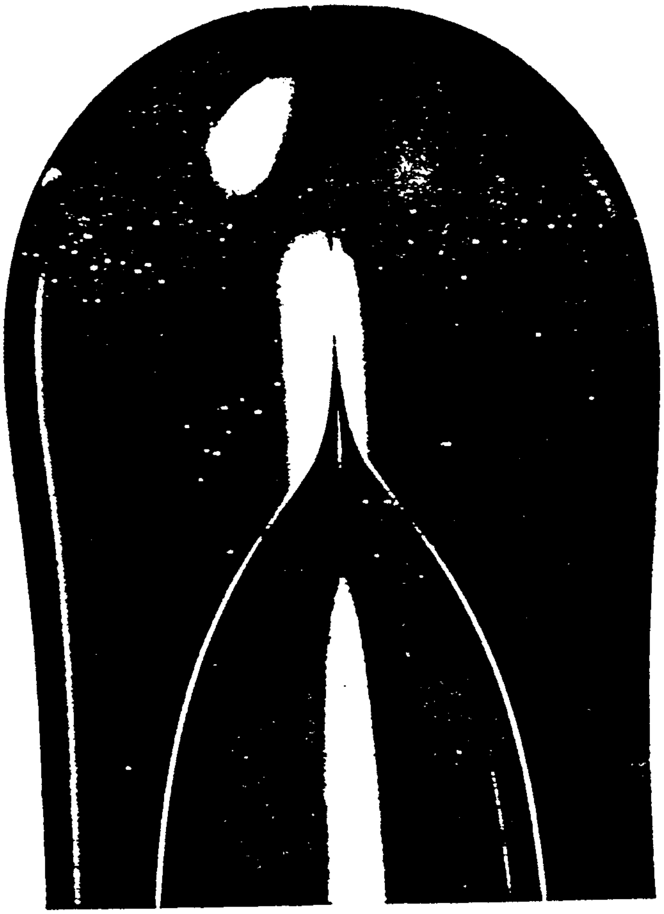

50×

Kim #1 2-25-92

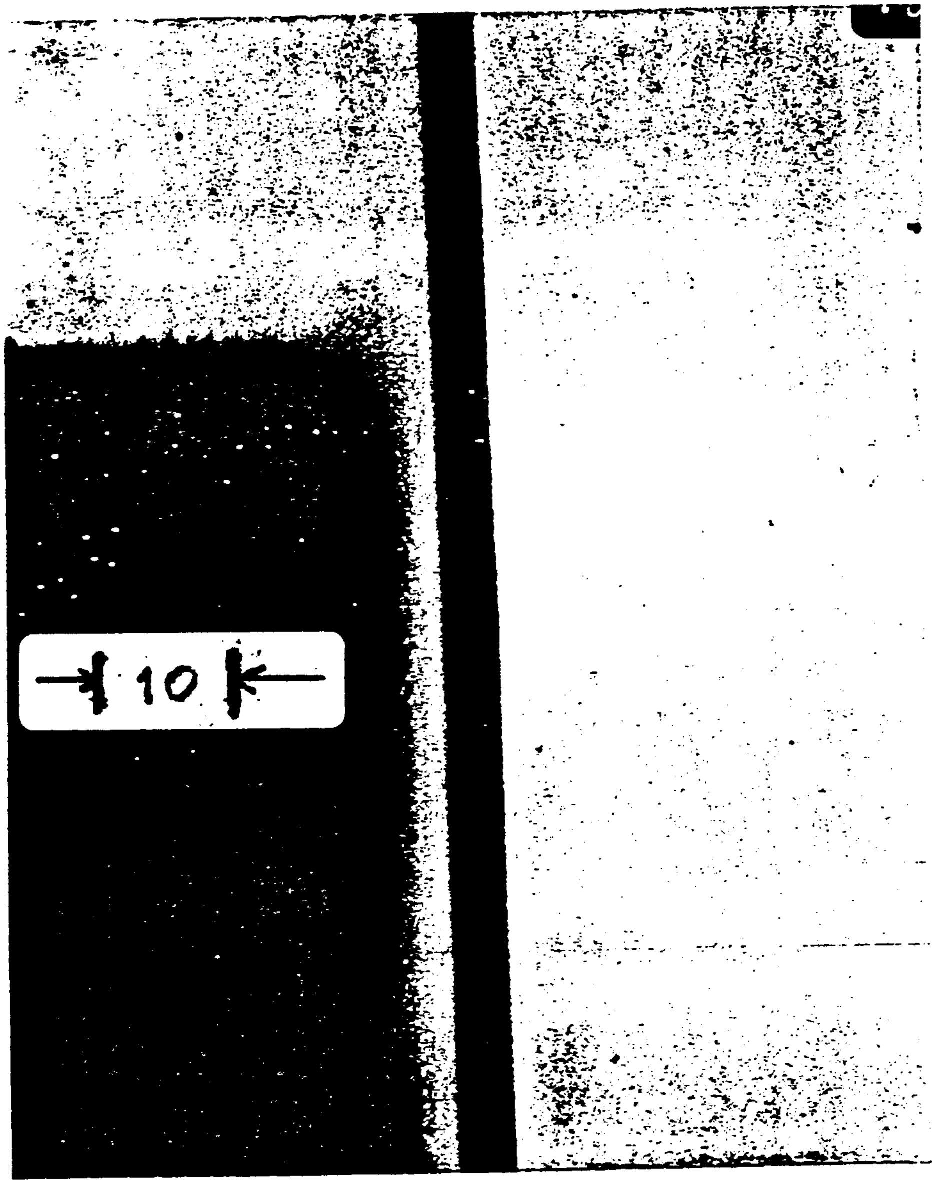

[illegible] TA 12/17/86
–4μ

→ Has made 4μ jets with ≈ 3000psi

→ New glass nossles under development.

→ 1μ possible in near future - raise temperature of jet to reduce viscosity and surface tension.

→ 0.1μ may be possible.

→ Possible future work in liquid metal ion sources (field-emission ions from tips of needles)

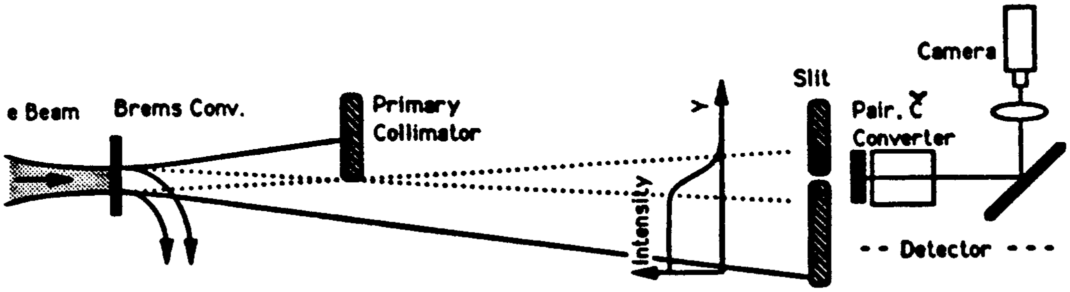

A Bremsstrahlung* Beam Profile Monitor for the FFTB at SLAC

J. Norem J. Dawson

HEP / Argonne

- Requirements / Desirable Features
- Design Issues
- Hardware
- Expts

* works with Laser targ Also

ANL SLAC/FFTB Bremssstrahlung Beam Profile Monitor

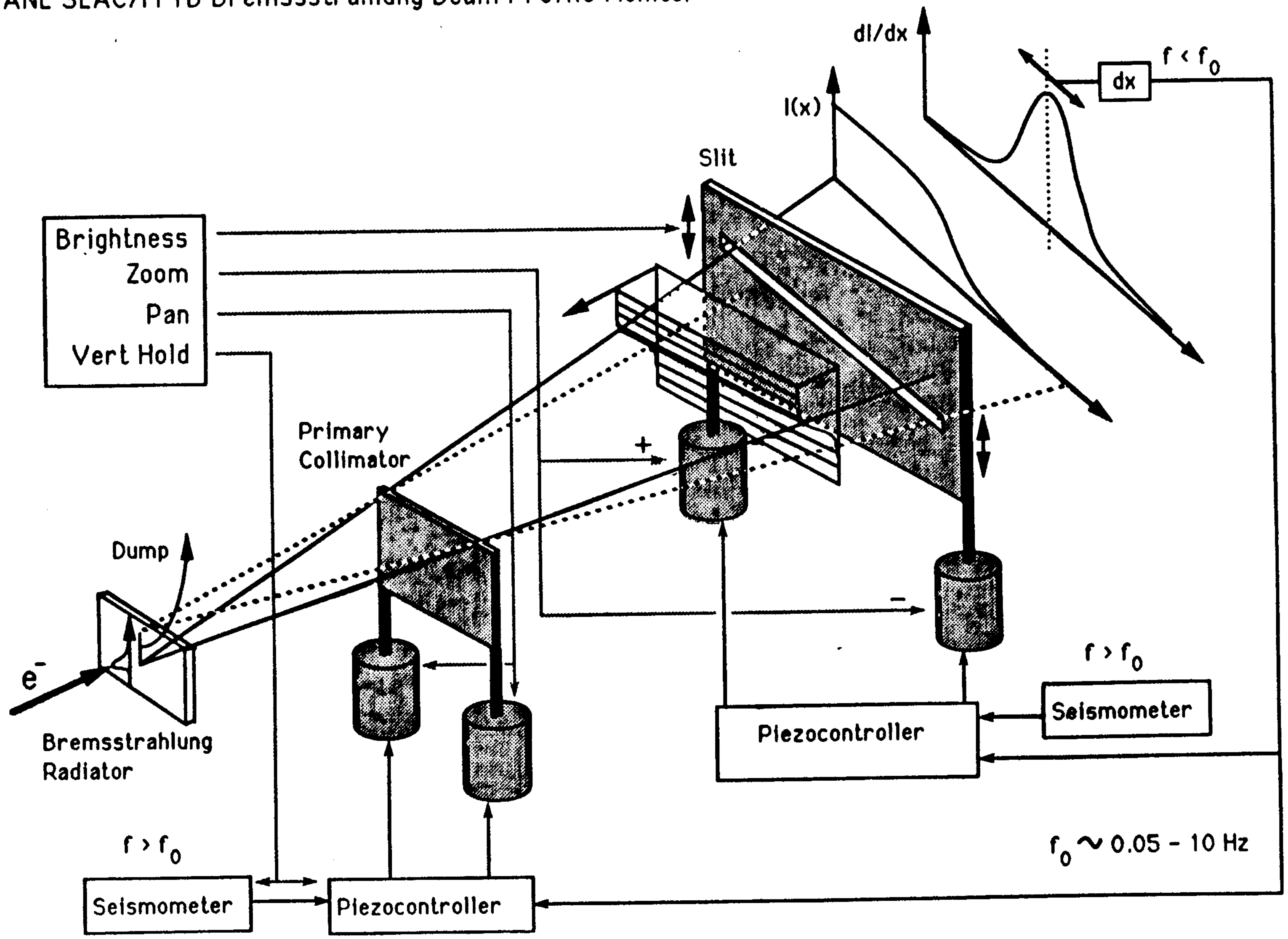

Slit / Collimator Assembly

Front view

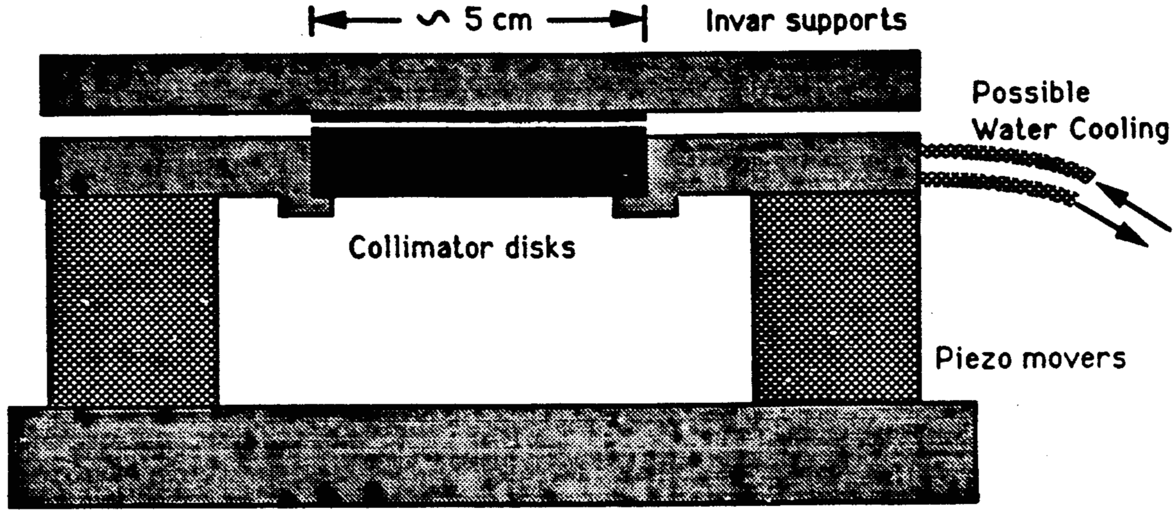

Collimator disks can be held in position by gravity, using silicon grease to conduct heat to the support frame.

Side View

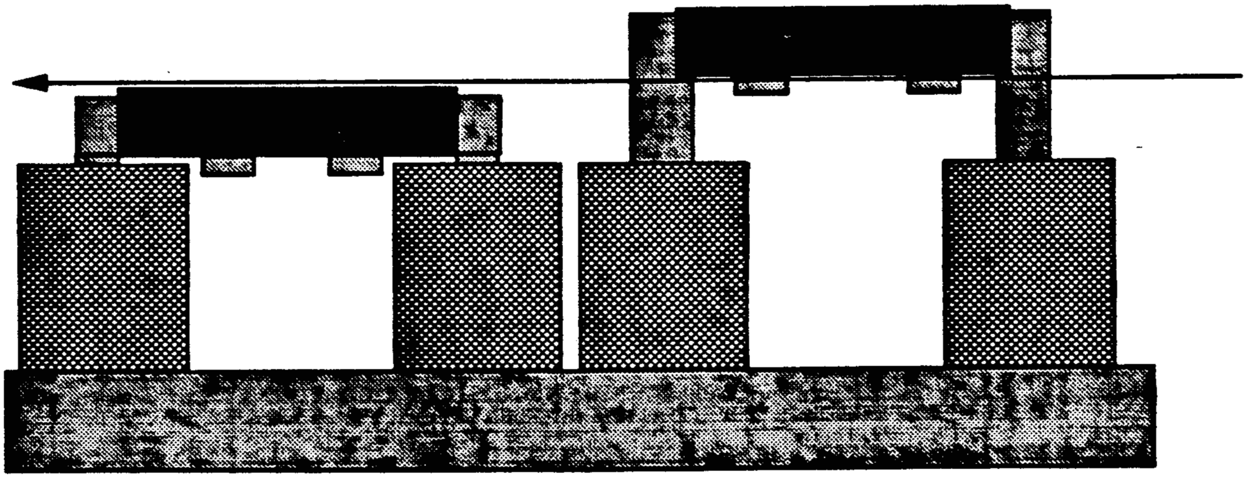

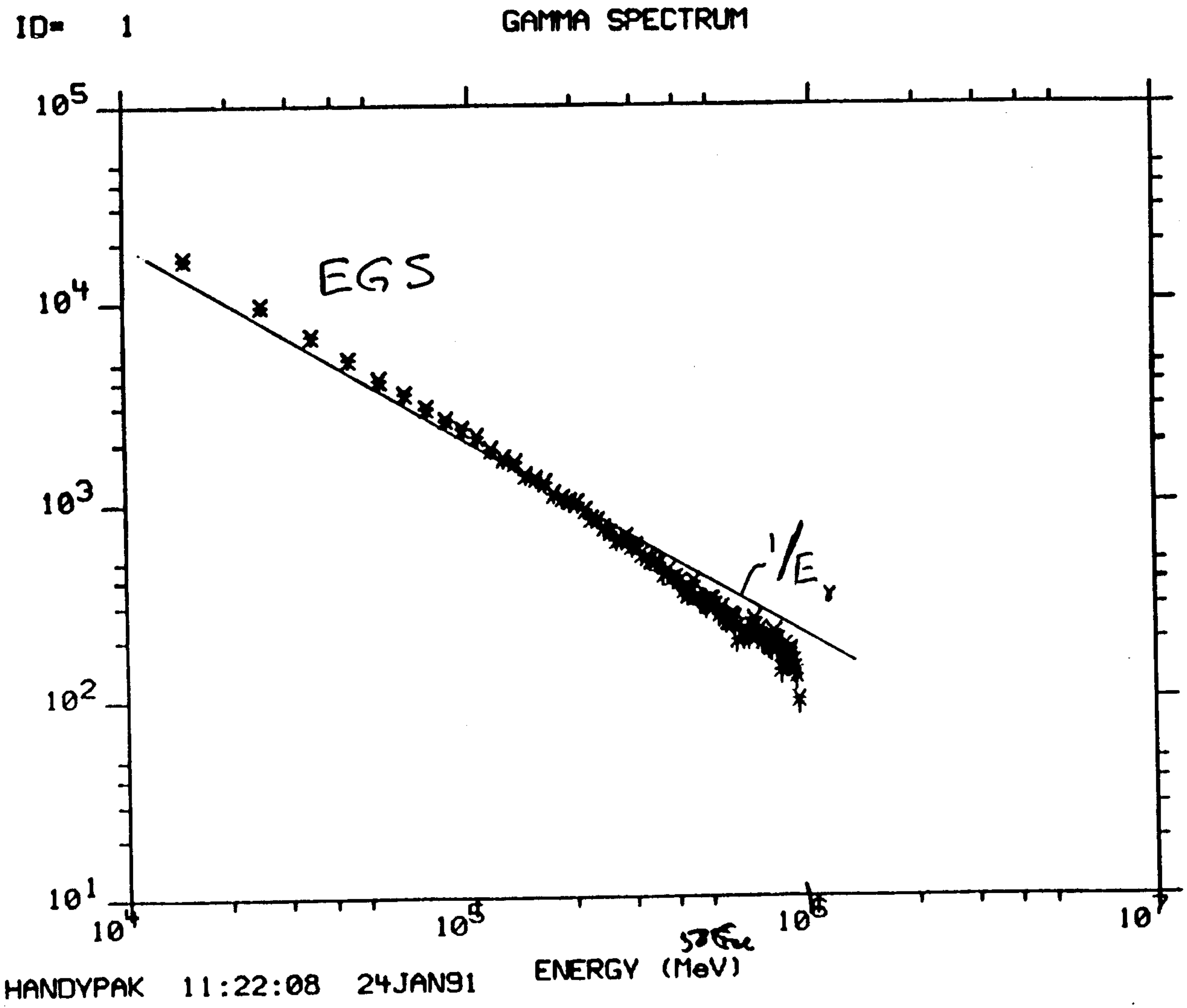ID= 1
GAMMA SPECTRUM
EGS
1/E_γ
10^5
10^4
10^3
10^2
10^1
10^4
10^5
500 GeV
10^6
10^7
ENERGY (MeV)
HANDYPAK 11:22:08 24JAN91

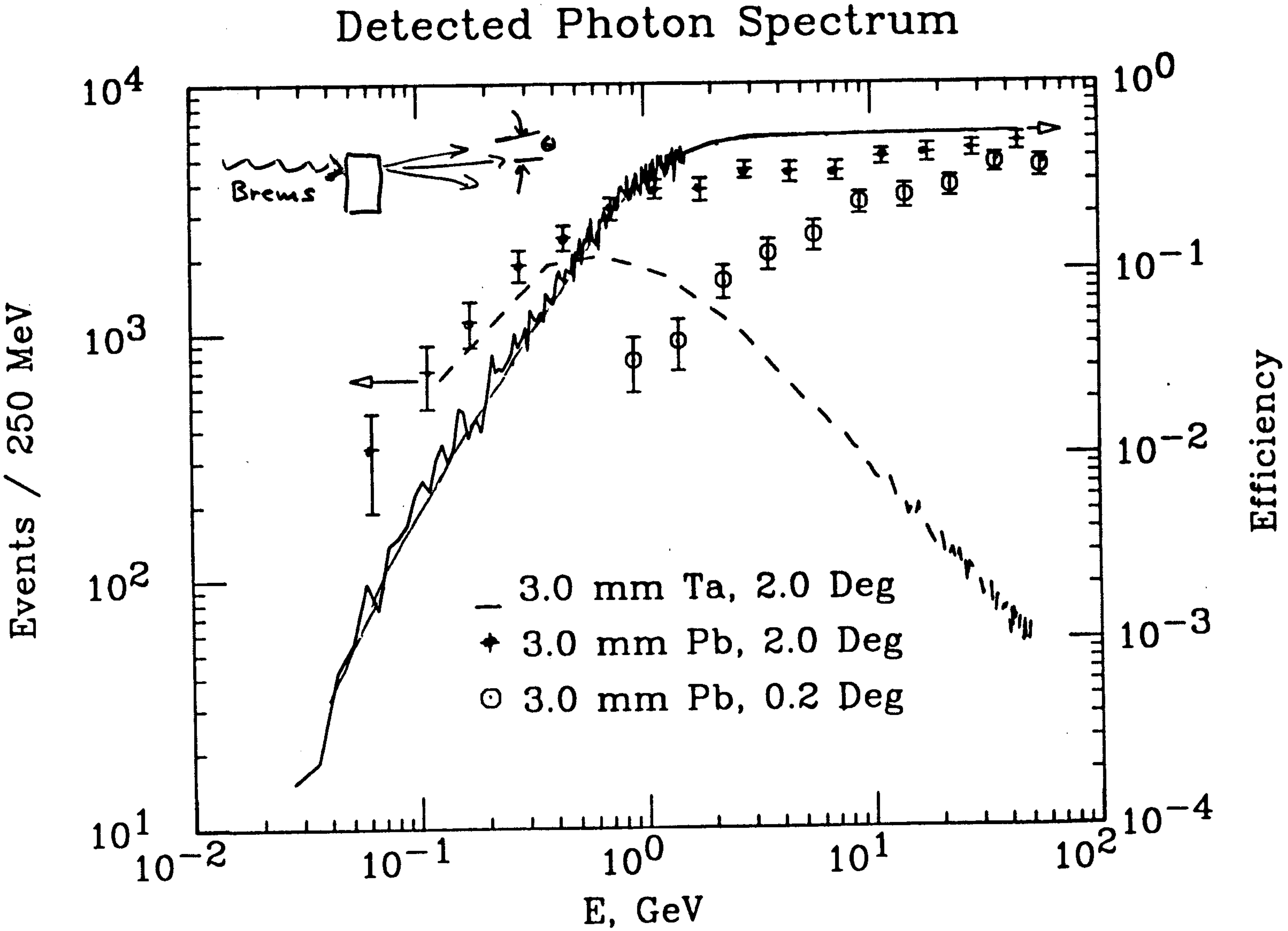
Detected Photon Spectrum
Brems
Events / 250 MeV
Efficiency
E, GeV
10^4
10^3
10^2
10^1
10^{-2}
10^{-1}
10^0
10^1
10^2
10^0
10^{-1}
10^{-2}
10^{-3}
10^{-4}
3.0 mm Ta, 2.0 Deg
3.0 mm Pb, 2.0 Deg
3.0 mm Pb, 0.2 Deg

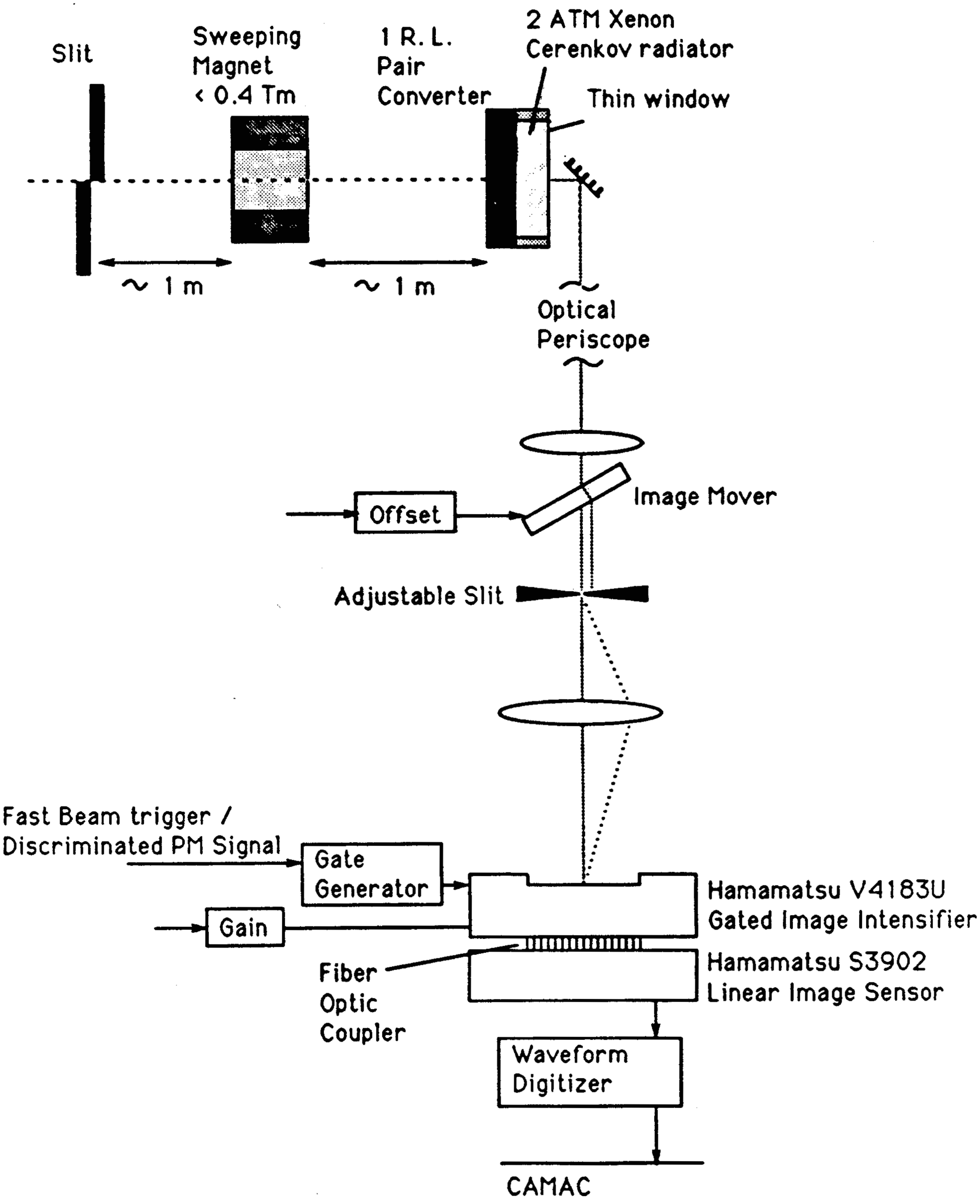
Slit
Sweeping Magnet < 0.4 Tm
1 R. L. Pair Converter
2 ATM Xenon Cerenkov radiator
Thin window
~ 1 m
~ 1 m
Optical Periscope
Image Mover
Offset
Adjustable Slit
Fast Beam trigger / Discriminated PM Signal
Gate Generator
Gain
Hamamatsu V4183U Gated Image Intensifier
Hamamatsu S3902 Linear Image Sensor
Fiber Optic Coupler
Waveform Digitizer
CAMAC

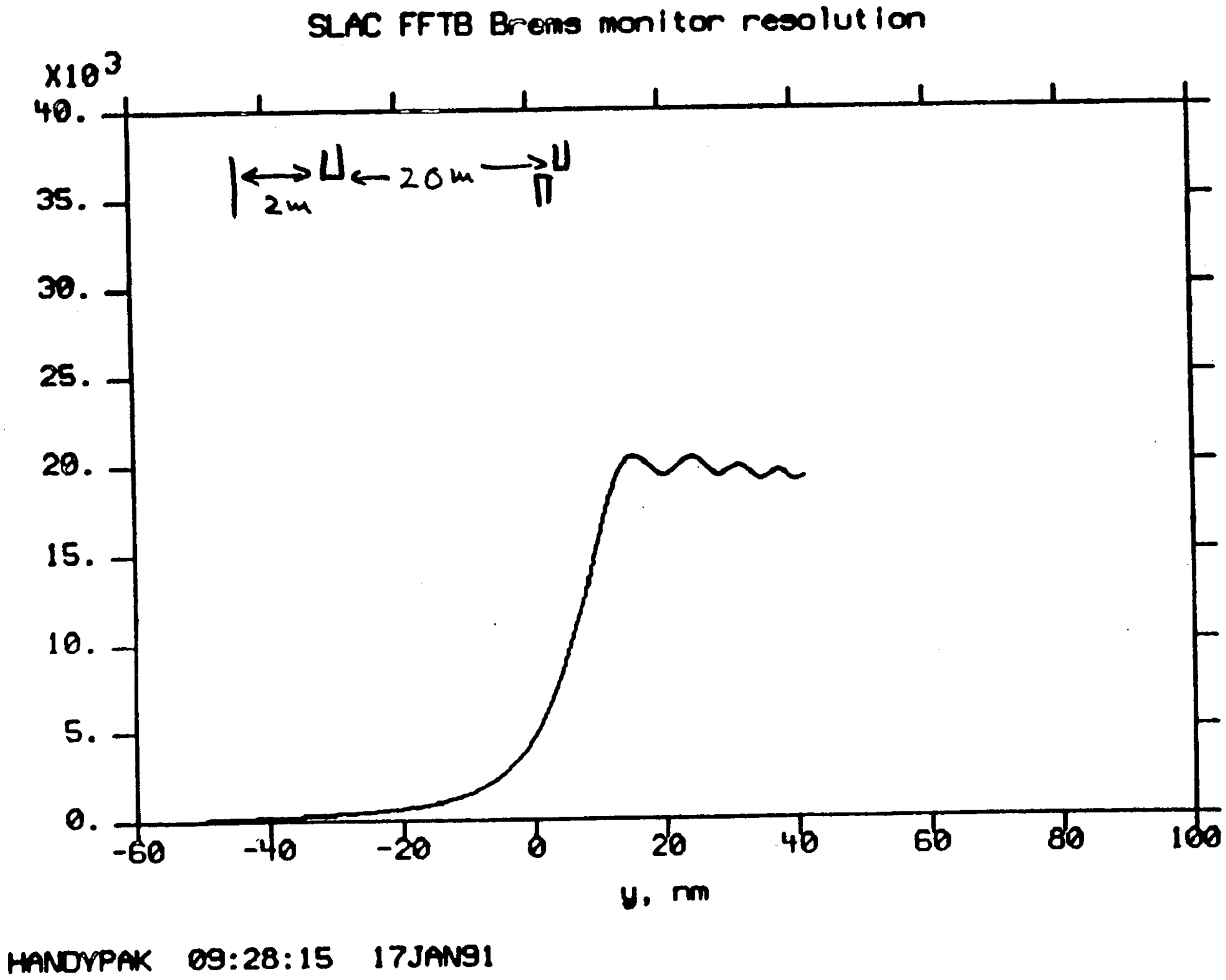
SLAC FFTB Brems monitor resolution
X10^3
40.
35.
30.
25.
20.
15.
10.
5.
0.
-60
-40
-20
0
20
40
60
80
100
y, nm
2m
20m
HANDYPAK 09:28:15 17JAN91

HARDWARE I : SUMMARY

TOPICS

1. FINAL FOCUS LAYOUT - GENERIC nm
2. DETECTOR LAYOUT - GENERIC
3. FINAL FOCUS MAGNETS (Fe, SC, PM)
4. SUPPORT & STABILIZATION - INNER EQUIP'T
5. TO BE DONE

FF MAGNET CHARACTERISTICS

✓ ID ~ 1.5 - 4 mm

✓ B_{Pole} ~ 1. - 1.5 T

✓ ℓ ~ 1 - 2 m

✓ g ~ 500 - 1000 T/m

✓ L^* ~ 1 - 3 m

TLCBF18 TLC FF Bx=10.0mm By=.10mm l*=1.0m 920211

QC1: L= 2.21 m, a = 2.0 mm, B(a) = 14.00 kGauss

QC2: L= 1.66 m, a = 2.5 mm, B(a) = 12.00 kGauss

QC3: L= 1.00 m, a = 5.0 mm, B(a) = 5.39 kGauss

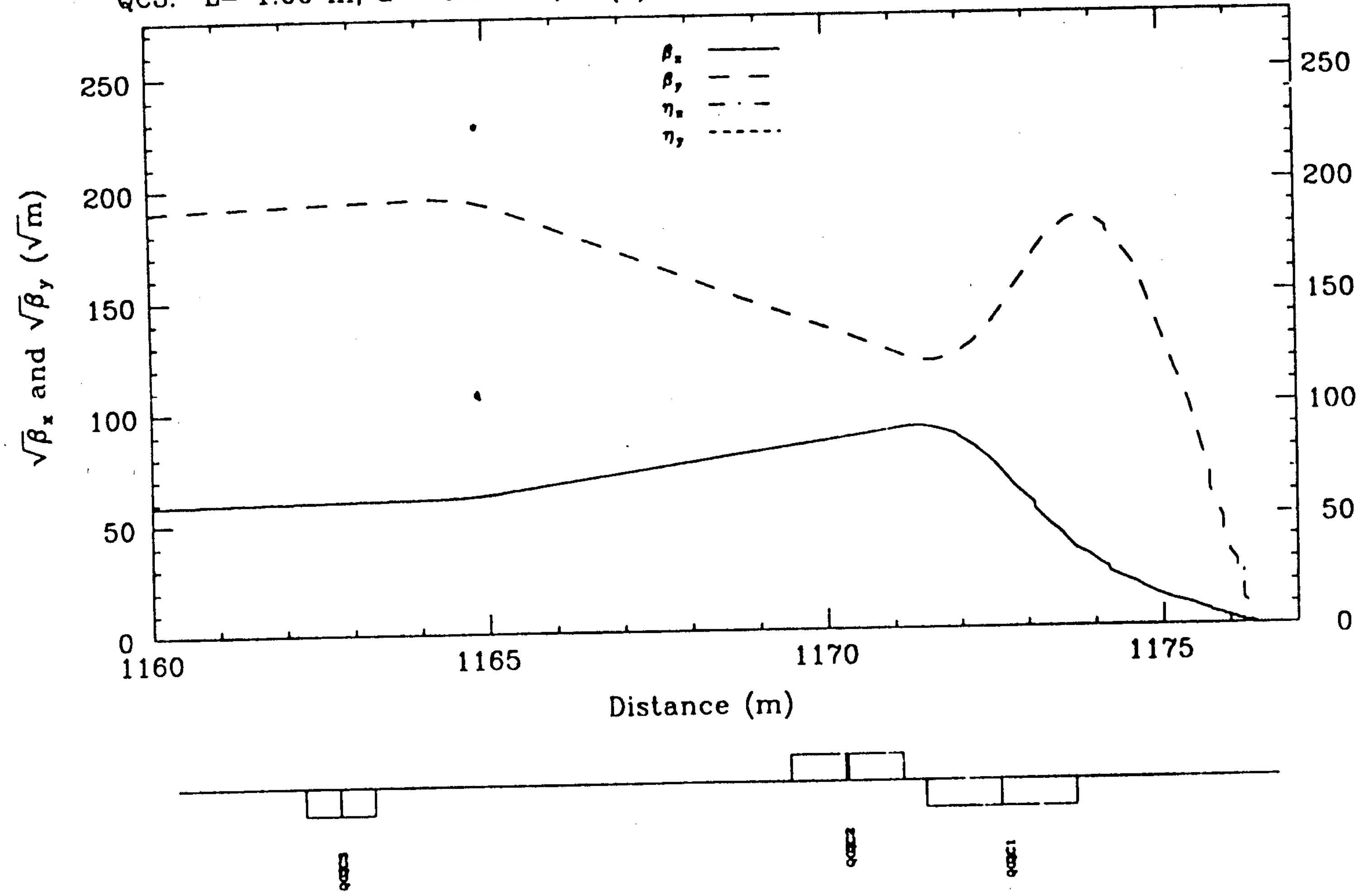

GENERIC OUTER DETECTOR

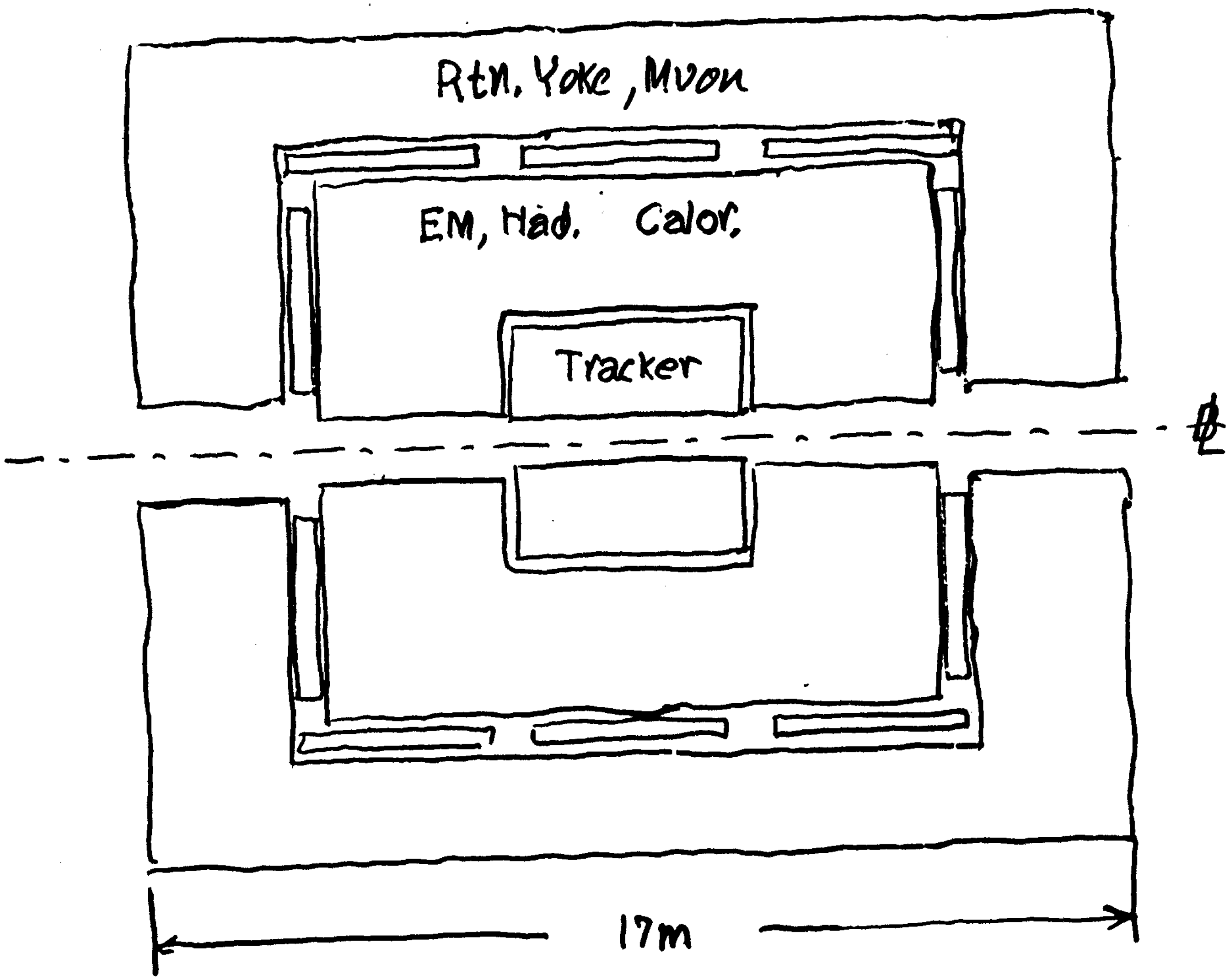

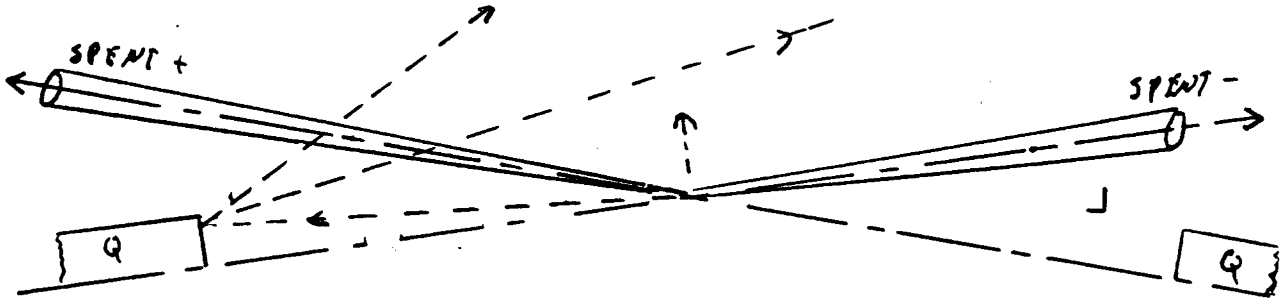

$\alpha \sim 30$ mr

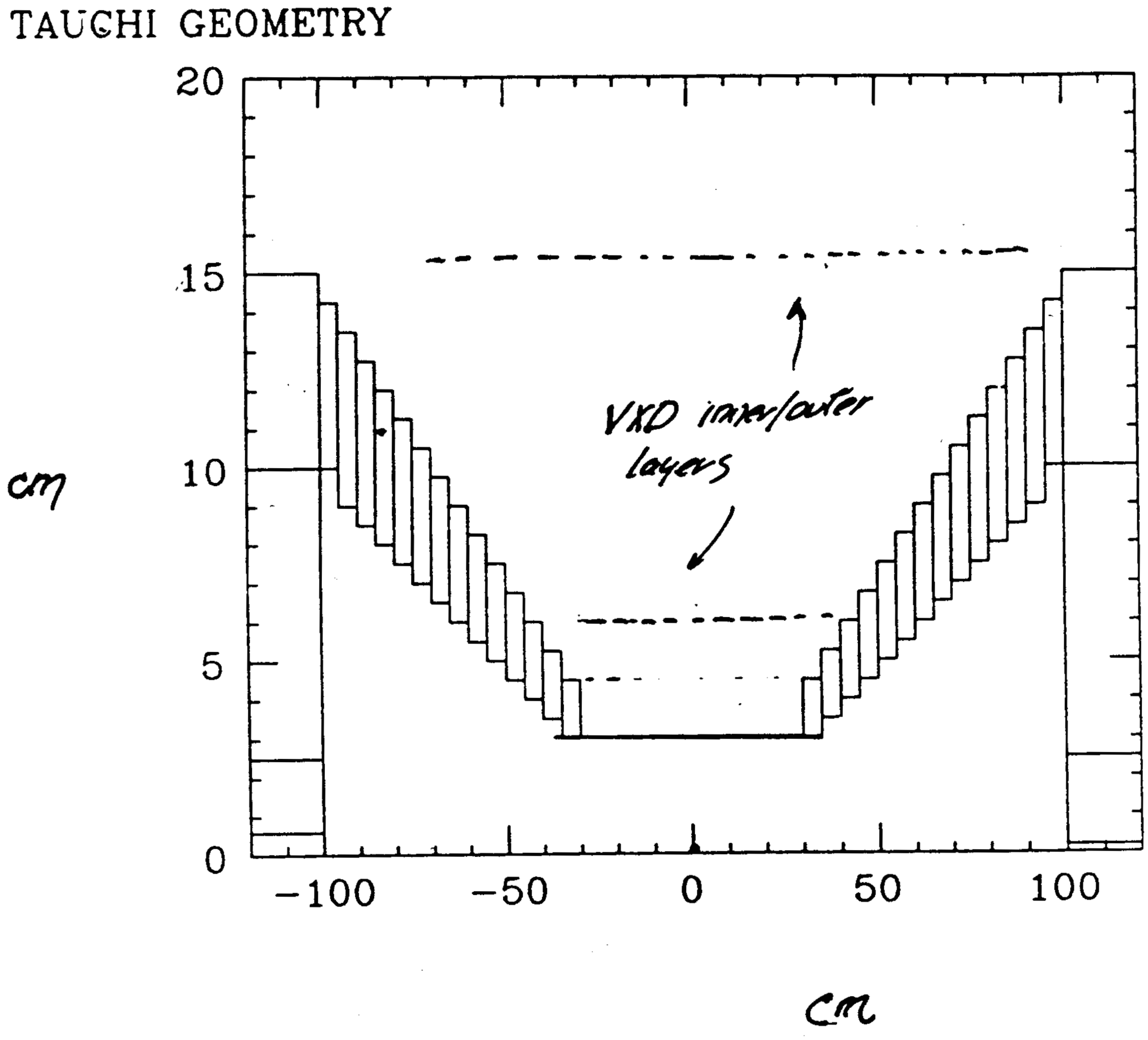
TAUCHI GEOMETRY
20
15
10
5
0
cm
−100
−50
0
50
100
cm
VXD inner/outer layers

KEK

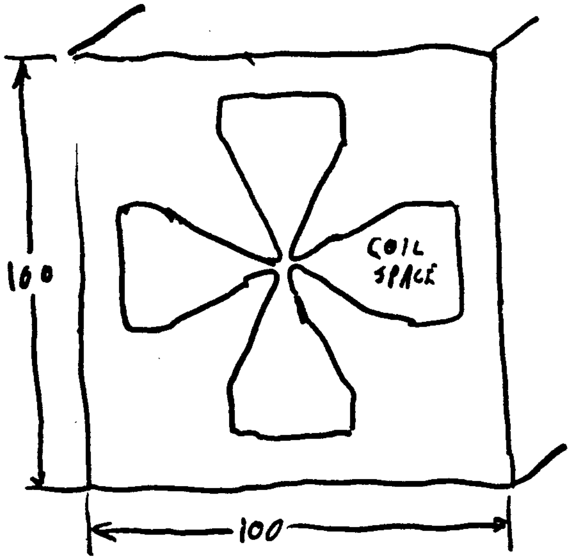

$\phi_{\ell} \sim 4$ mm

$I_{COIL} \sim 300$ A

$P \sim$ kW

F_e Alloy

PM

SLAC

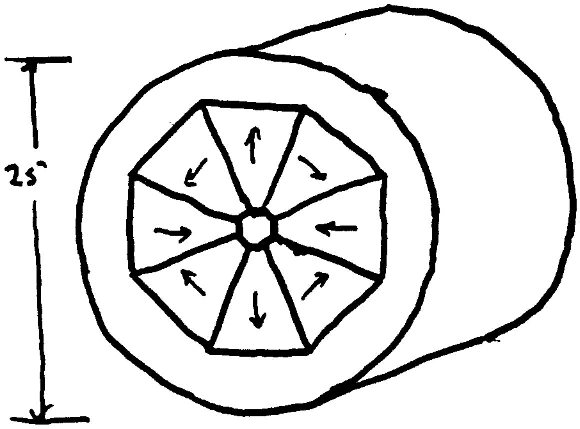

$\phi_{\ell} \sim 4$ mm

$I_{COIL} = 0$

$P = 0$

HELD IN RETAINING RING

S C

INP

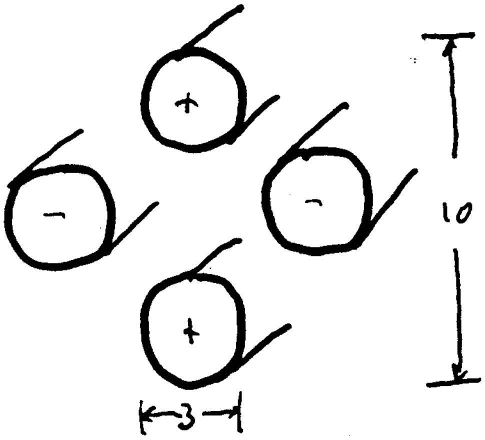

$\phi_{\ell} \sim 1.5$ mm

$I \sim 2 \times 10^{4}$ A

$P \sim 0$

SUPPORT & ALIGNMENT

$\Delta z < \beta^*$

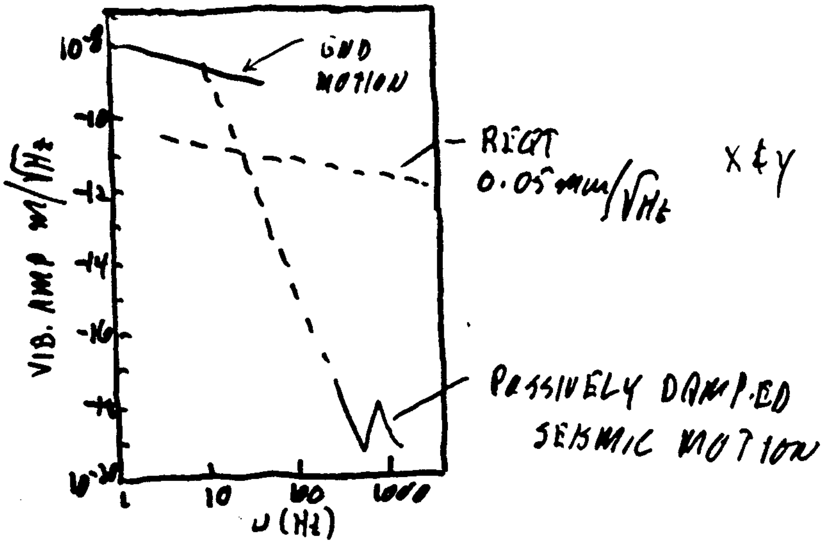

X & Y

PASSIVE DMP ~ OK > 100 Hz

ACTIVE STABILIZATION NEEDED < 100 Hz

COMB. OF "ABSOLUTE" POSITIONING
(wire, laser, accelerometer ...)
& (10 nm level DEMO ALREADY)
BEAM DERIVED SYSTEM

DISCUSSION ON SUPPORT SYSTEMS (THURSDAY)

1. SINGLE SUPPORT TUBE CONTAINING BOTH DOUBLETS MASKS, VXD.

2. MAY HAVE TO 'FLOAT' DOUBLETS WITHIN SUPPORT TUBE FOR HIGH-V ISOLATION

3. ACTIVE, (FAST FEEDBACK) SUPPORTS MAY BE DIFFICULT FOR THIS COMPOUND STRUCTURE; WORK FIRST ON PREVENTION & PASSIVE SUPPORTS

4. DECIDE BETWEEN ANCHORING SUPPORT TUBE
INSIDE DETECTOR (SHORTER) AND
OUTSIDE DETECTOR (QUIETER).

5. BUILD INTO THE SUPPORT TUBE PERMANENT, STRAIGHT-THROUGH ALIGNMENT CHANNELS.

INNER ASSY ~~TUBE~~ SUPPORT

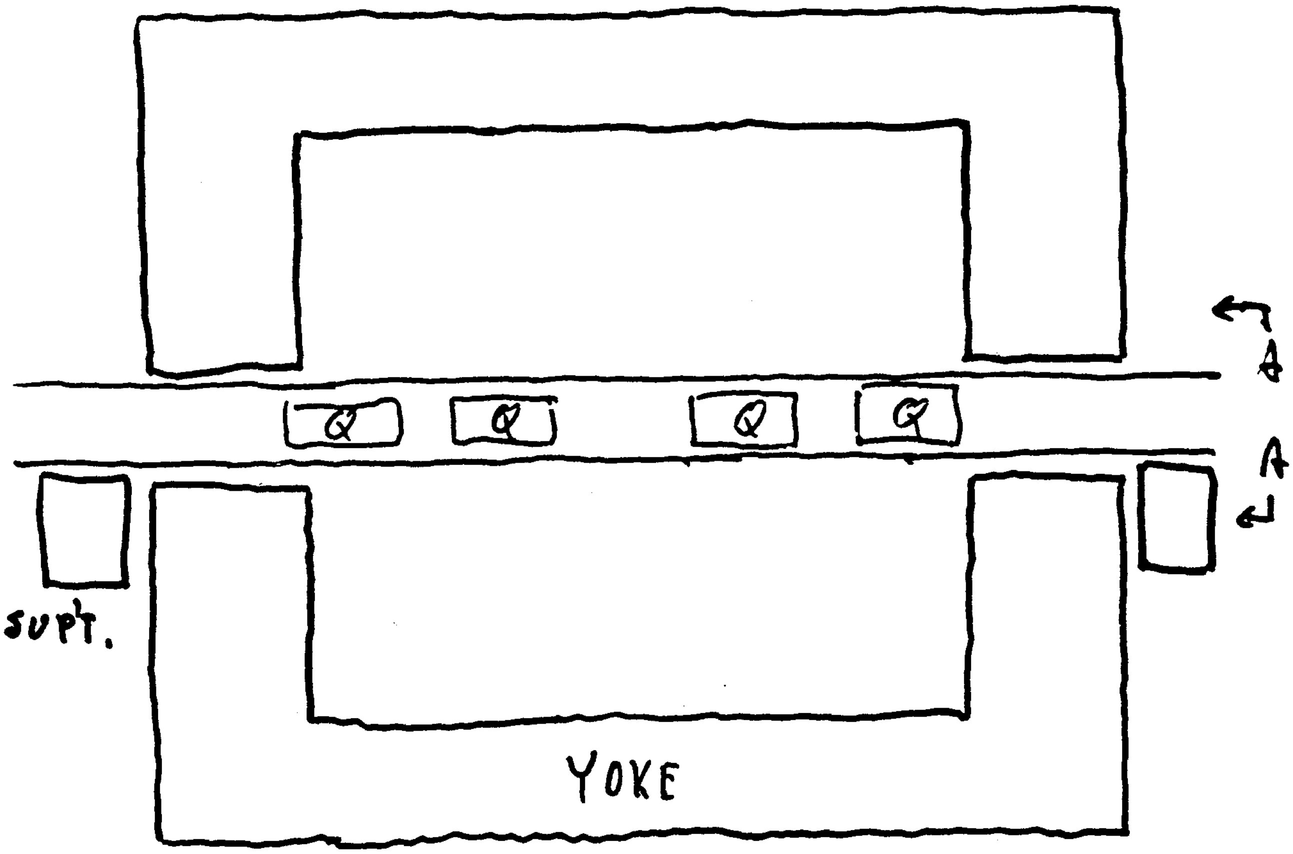

LEP
SLC

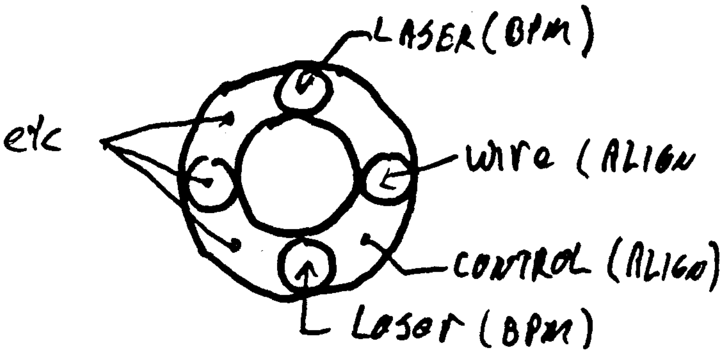

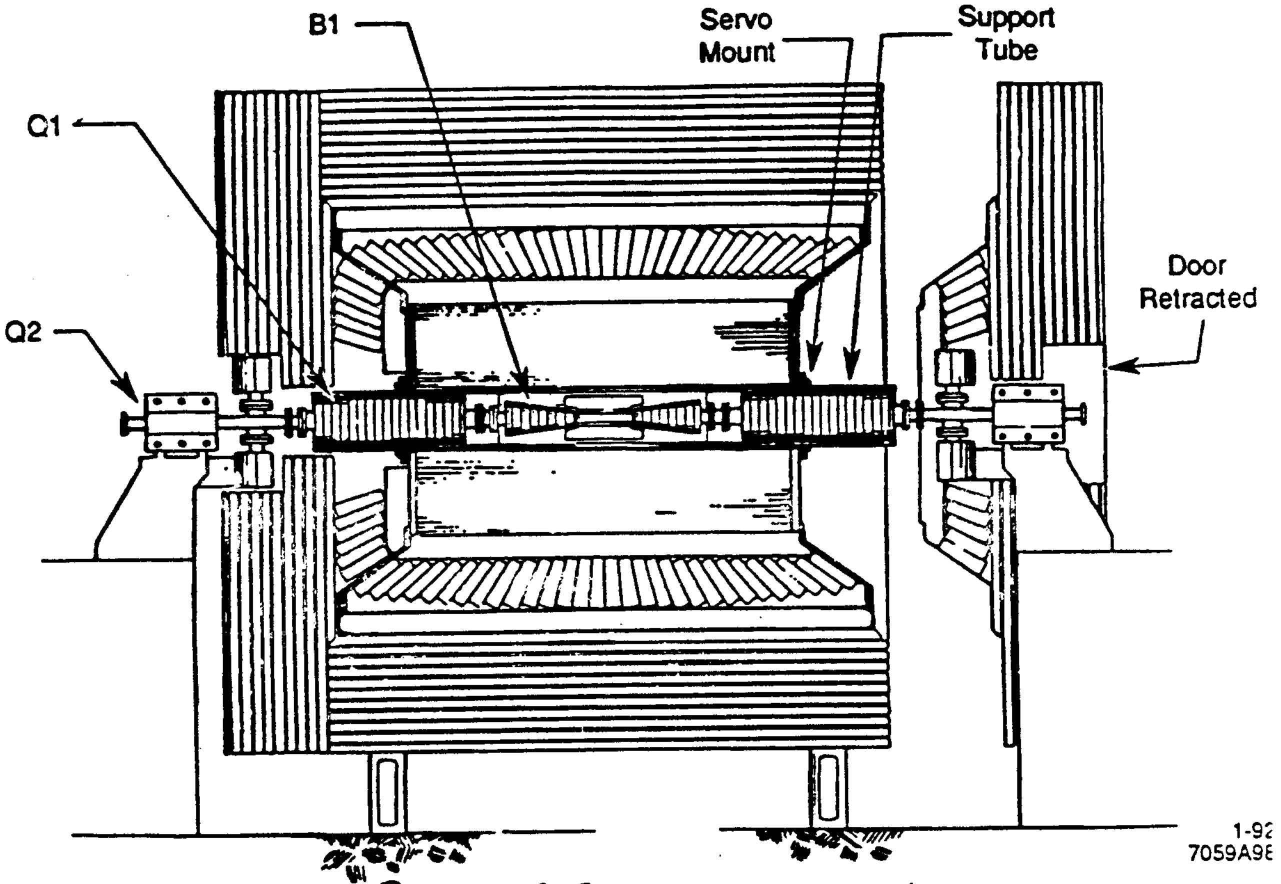

B FACTORY STUDY ↑

NLC FINAL QUAD SUPPORT ↓

GORDON BOWDEN

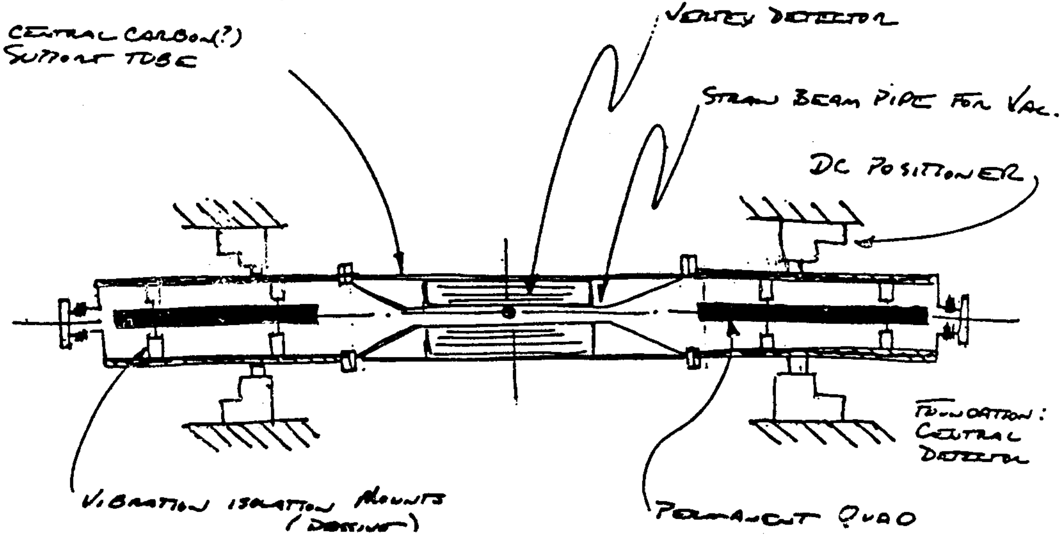

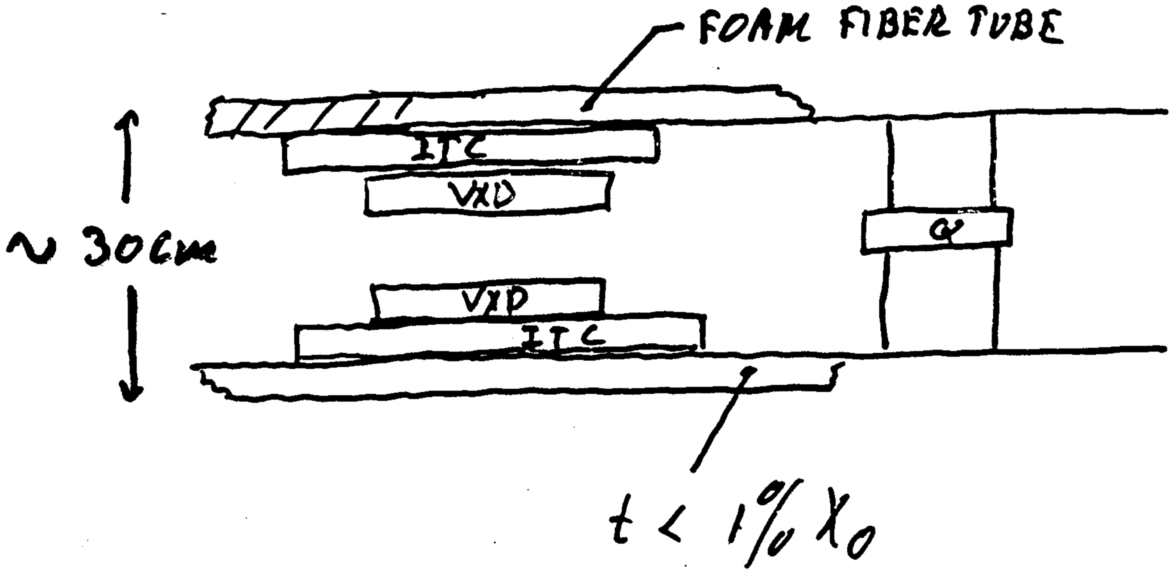

TO DO SOON

1. SYSTEM STUDIES TO FIND (IN PRINCIPLE)

✓ WORKABLE COMBINATIONS OF ELEMENTS THAT MEET ALL REQT'S - VIB, DRIFT, THERMAL STAB. (HOM, SR, I^2R, LOST PART.·) VACUUM, BKGND SHIELD···

2. MECHANICAL MODEL

DEMO. THAT MECH. REQTS CAN BE MET

MAYBE WE SHOULD HAVE :

"INNER TUBE" OLYMPIC @ LC 9?

OPTICS WORKING GROUP

Chairman: Katsunobu Oide

Members and Contributors

O. Napoly	CERN	J. Irwin	SLAC
R. Brinkmann	DESY	M. Lee	SLAC
B. Holzer	DESY	L. Merminga	SLAC
A. Sery	INP	P. Raimondi	SLAC
K. Oide	KEK	G. Roy	SLAC
N. Yamamoto	KEK	R. Ruth	SLAC
M. Ivancic	Sonoma	W. Spence	SLAC
S. Rajagopalan	UCLA	N. Walker	SLAC
P. Emma	SLAC	R. Warnock	SLAC
R. Helm	SLAC	V. Ziemann	SLAC

Summary of Optics Working Group Discussions

Katsunobu Oide

The optics subgroup was so organized to discuss all issues upstream of IP. These were design of optics, tolerance, tuning methods, beam diagnostics, collimators, and ground motion.

The basic design of the focusing optics has been more or less established in for years in all laboratories, but extensions and new ideas are still proposed. There were several presentations on the design of final focus optics: A. Sery on VLEPP final focus system with/without the travelling focus and also the SLC upgrade, O. Napoly on a semianalytic method for the calculation of luminosity, K. Oide on a wideband optics with "odd dispersion" scheme, R. Brinkmann on crab crossing and achromatic collision with dispersion at IP, and S. Rajagopalan on the plasma focus. On the design of the optics, more weight of the discussion was put on the tolerance problem. G. Roy talked on a detailed analysis of the tolerance and tuning of the FFTB optics. On the tolerance problem no comparison has been made for different designs with the same beam parameters and restrictions on the final lenses. The optics subgroup decided to do this comparison at the LC92 workshop using the following parameters:

$\varepsilon_{x,y} = 5 \times 10^{-6}, 5 \times 10^{-8}\mathrm{m}$, $\beta^*_{x,y} = 10, 0.1\mathrm{mm}$, $B_0 = 1.4\mathrm{T}$, $\ell^* = 1.5\mathrm{m}$, $a_1 = 2.5\mathrm{mm}$, $a_2 = \sqrt{2}a_1$, $D \geq 30\mathrm{cm}$, $\delta_{\mathrm{rms}} = 0.33\%$, $\sigma^*_{x,y} < 1.15\sqrt{\beta^*_{x,y}\varepsilon_{x,y}/\gamma}$, $L_{\mathrm{total}} \leq 600\mathrm{m}$, $\sqrt{\beta_x\beta_y}_{\mathrm{entrance}} = 10\mathrm{m}$.

The tuning of the future final focus is possible by applying the tuning methods and beam diagnostics done at SLC. Several ideas and experiences were introduced: V. Ziemann on a fast algorithm of sextupole alignment, P. Raimondi on the final triplet alignment, P. Emma on the matching of different sections, N. Walker on the tuning of final focus optics. These experiences tell that the beam diagnostic systems and also the beam-based alignment schemes basically work as expected and no essential difficulty was found on applying them on future machines.

A "complete" design of a collimation section with "big bend" was presented by J. Irwin and R. Helm, including wakefields, non-linear collimators, heating, and particle reflections. R. Warnock also gave a new method to calculate a wakefield of a smooth and non-periodic structure like a collimator.

N. Yamamoto introduced some results on the ground motion.

SUMMARY TALKS

Summary of Thursday Session	R. Brinkmann
1/2 Summary of Optics Group	A. Sery

PARALLEL SESSION TALKS

JLC Final Focus System	K. Oide
A Complete NLC Collimation System	J. Irwin/D. Helm/ L. Merminga/R. Nelson
A 10-mr "Big Bend" for 500 GeV NLC	R. Helm
Luminosity vs Errors	O. Napoly
Status of VLEPP FFS	A. Sery
FFTB Tuning	G. Roy
A Fast Sextupole Centering Algorithm	V. Ziemann
SLC Triplet Alignment	R. Raimondi
Integral Equation for Wake Field in a Tube With Smooth, Non-Periodic Variation of Radius	R. Warnock
Crab-crossing and Monochromatisation with D (IP)	R. Brinkmann
Using a Plasma as a Final Focus Lens	S. Rajagopalan
Upgraded Final Focus System for the SLC	A. Sery
Optics Matching in the SLC	P. Emma
Measurement of Optics in the SLC FFS	V. Ziemann
Analytic Solution for a Three Lens System	Y. Chao

OPTICS GROUP

SUMMARY OF THURSDAY SESSION

R. Brinkmann

- B. Warnock, Wakefield calculation
- R. Brinkmann, Crab-crossing & monochromatisation with D(IP)
- S. Rajagopalan, Plasma lens
- A. Sery, Travelling Focus, SLC upgrade
- P. Emma, Optics matching in the SLC
- V. Ziemann, measurement of optics in the SLC FFS.
- Discussion on K. Oide's large-bandwidth system
- Y. Chao, analytic solution for a three lens system

INTEGRAL EQUATION FOR WAKE FIELD IN A TUBE WITH SMOOTH, NON-PERIODIC VARIATION OF RADIUS

R. Warnock, SLAC

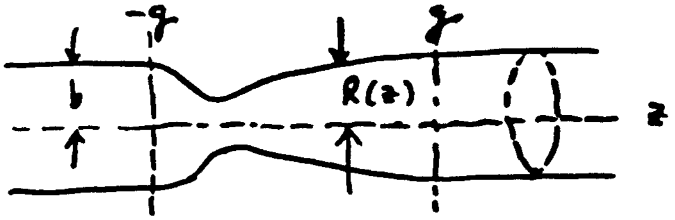

- Axially symmetric, $R(z) = b$, $|z| > g$
- Not necessarily symmetric under $z \to -z$

Similar method works for parallel plates, pinched together along infinite crease:

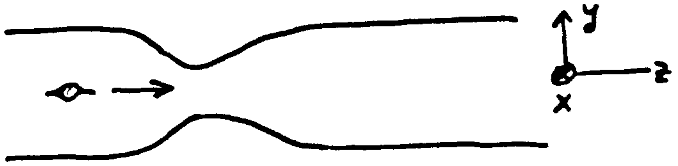

2D: translationally invariant in x - direction

Presently implemented for
- round tube
- longitudinal field, beam on axis
- perfectly conducting wall

Can be extended (I'll bet) to
- transverse fields
- resistive wall
- non-relativistic beams

} round tube or creased // plates

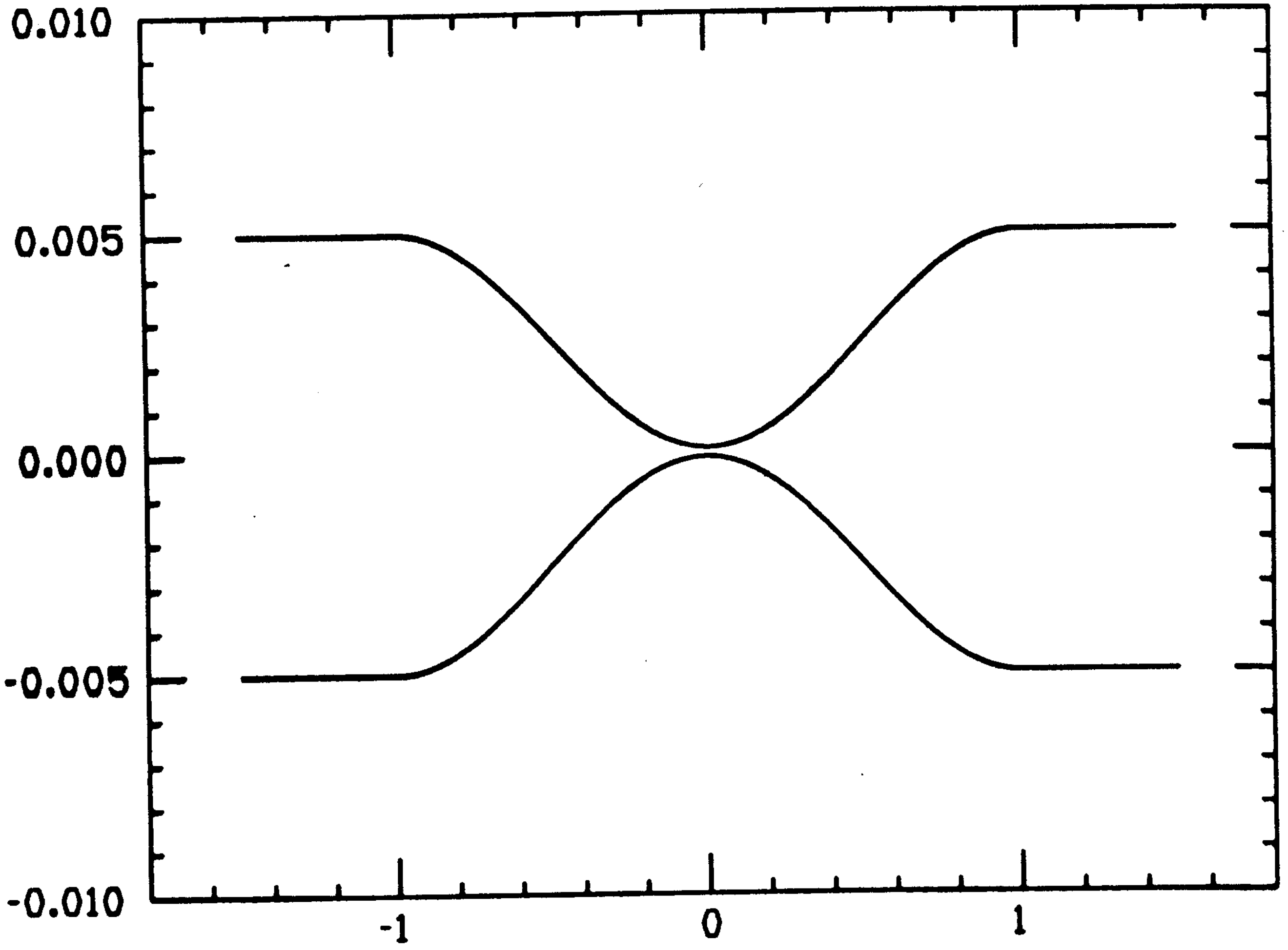

Scraper profile

Method uses Fourier Transform technique and integral equations, solved either analytically or numerically.

Calculates long. wakefield for typical NLC collimator with ≈ 1 min. CPU on IBM (TBCI fails for such a problem!)

Can be extended to transverse / res. wall wakefields

R. Brinkmann

GOOD REASONS FOR INCREASING σ_z :

IF, FOR GIVEN $N_b, \varepsilon_x, \varepsilon_y$, WE INCREASE σ_z
AND SCALE $\beta_y^* \sim \sigma_z$ BUT $\beta_y^* \beta_x^* = \text{const.}$ ($\mathcal{L} = \text{const.}$)
THEN:

- TIGHT TOLERANCES DUE TO EXTREMELY SMALL σ_y^* CAN BE LOOSENED
- WAKEFIELD EFFECTS (FIN. QUADS, COLLIMATORS) ARE REDUCED
- BEAMSTRAHLUNG PARM. $\Upsilon \sim \sigma_z^{-1/2}$
- $\langle \frac{\Delta E}{E} \rangle_{BS} \sim \text{const.}$ (slightly decreasing)
- $\theta_{MASK} \sim \sigma_z^{-1/2}$ (Yokoya)

<u>BUT</u>:

LARGER σ_z / σ_x^* REQUIRES SMALLER
θ_c OR CRAB CROSSING

(WHAT IS A REASONABLE LOWER LIMIT FOR θ_c?)

R. Brinkmann

"CRAB-CROSSING" WITH $D(IP) \neq 0$

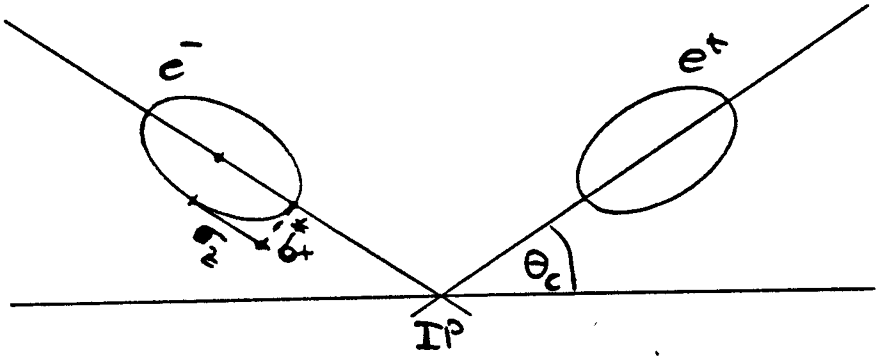

REDUCTION OF LUMINOSITY :

$$\mathcal{L} = \mathcal{L}_0 \times \frac{\sigma_x^*}{(\sigma_x^{*2} + (\theta_c \sigma_z)^2)^{1/2}}$$

$$\left(\mathcal{L}_0 = \frac{f_0 N_e^2}{4\pi \sigma_x^* \sigma_y^*}\right)$$

COMPENSATE θ_c BY CHOOSING $\overset{\pm}{D}(IP) = -\theta_c \sigma_z / \sigma_p$

IF MOM. SPREAD IS LINEAR :

$$\frac{\Delta p}{p}(z) \cong \left(\frac{z}{\sigma_z}\right)\sigma_p \Rightarrow \mathcal{L} \cong \mathcal{L}_0$$

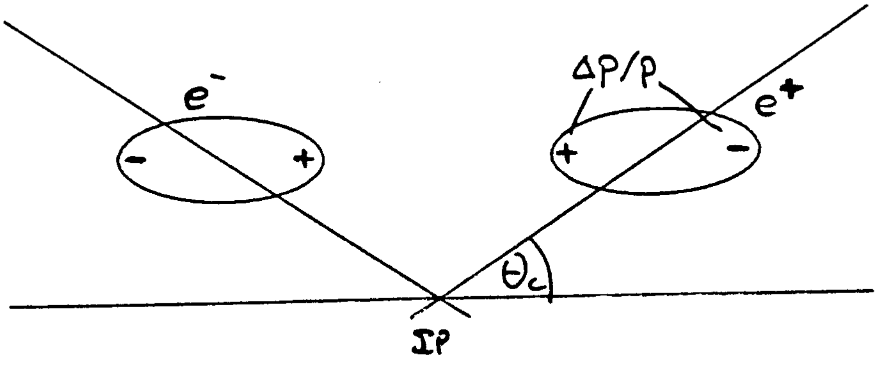

(<u>SAME</u> DISPERSION FOR e^+ AND e^- F.F. SYSTEMS)

FINAL FOCUS AND BEAM-BEAM PARAMETERS

	S-BAND	TESLA	
E_{CM}	500 GeV		
$\varepsilon_x / \varepsilon_y$	$10^{-11}/10^{-12}$	$4\times10^{-11}/2\times10^{-12}$	m
σ_x^* / σ_y^*	316 / 31.6	900 / 90	nm
σ_z	0.5	2.0	mm
N_e/bunch	2×10^{10}	5×10^{10}	
β_x^* / β_y^*	10 / 1	20/4	mm
D_x / D_y	1.0/10.5	1.3/12.9	
$-\langle\Delta E/E\rangle_{B.St.}$	5.4	1.1	%
Υ	0.10	0.03	
$\hat{u}_c(\gamma)$	45	10	GeV
$\hat{\Theta}_{x,y}$ (Disrupt.)	0.57/0.24	0.47/0.17	mrad
θ_c	±1.5	±1.5	mrad
$D^{\pm}$ (IP)	0.1	1.0	mm
$\frac{\Delta p}{p}$ $(\pm\sigma_z)$	±0.75	$\pm$ 0.3	%
H_D	1.6	1.8	
$\mathcal{L}$	4.1×10^{33}	3.6	$cm^{-2} s^{-1}$

(for $f_0 \times n_b$ = 8 kHz, incl. H_D)

OPERATION AT LOWER ENERGY/LUMINOSITY WITH HIGH ENERGY RESOLUTION

Assumption : CM- ENERGY SPREAD
DOMINATED BY BEAM - $\frac{\Delta p}{p}$,
BEAMSTRAHLUNG NEGLIGIBLE
$(\langle \frac{\Delta E}{E} \rangle_{rad} \sim \gamma^2 , N_\gamma \lesssim 1)$

How to reduce effective $\frac{\Delta E}{E}|_{CM}$?

REDUCE N/bunch : $\frac{\Delta E}{E}|_{CM} \sim \mathcal{L}^{1/2}$

"MONOCHROMATOR" WITH $D(IP) \neq 0$: $\frac{\Delta E}{E}|_{CM} \sim \mathcal{L}$

$$\sigma_x^* \longrightarrow (\sigma_x^{*2} + (D(IP)\,\sigma_p)^2)^{1/2}$$

$$\left(\frac{\Delta p}{p}\right)_{EFF.} \approx \left(\frac{\Delta p}{p}\right)_{BEAM} \times \sigma_x^* / (\sigma_x^{*2} + (D(IP)\,\sigma_p)^2)^{1/2}$$

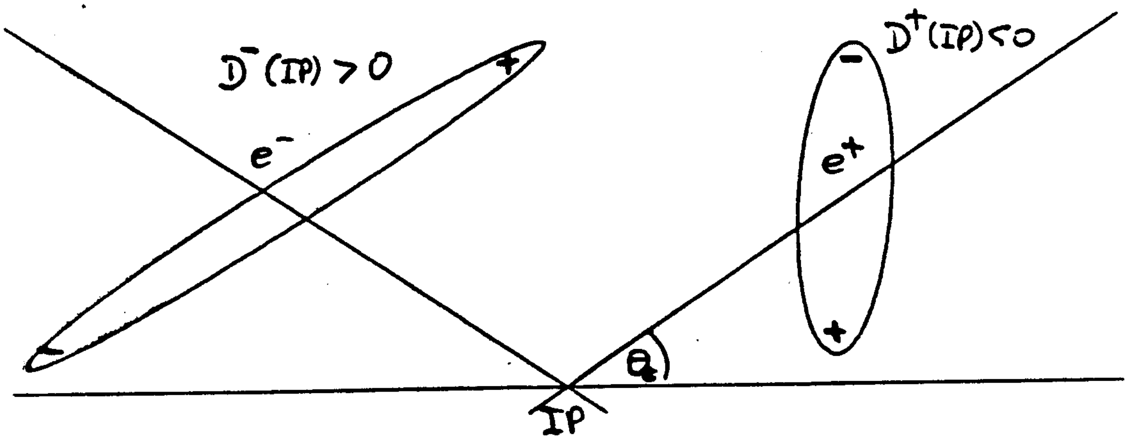

S. Rajagopalan:

Plasma as a final focus lens

beam-plasma interaction quite different
for e^--beam (plasma-e^- "kicked out" by beam)
and e^+-beam (plasma-oscillations excited)

strong focussing nevertheless for both cases.

Estimates for SLC:

round beam σ^*'s reduced by
≈ factor 3

seems even possible to ionize gas
by beam itself (depending on
particularities of long. distr. up to
factor 6 $\mathcal{L}$-enhancement expected)

Problems: alignment
background (mainly from synchr. rad.)

A. Sery :

1. Simulation of travelling focus ($\beta_y^* < \sigma_z$) to determine gain $\mathcal{L}/\mathcal{L}_0(\beta_y^* = \sigma_z)$ as a function of β_y^*/σ_z and Disruption parameter.

   maximum gain:

   $$\mathcal{L}/\mathcal{L}_0 \approx 1.8 \quad \text{for } 0.2 \lesssim \beta_y^*/\sigma_z \lesssim 0.5$$

2. new final focus system to upgrade SLC

One point of discussion:

for very flat beam ($\varepsilon_y/\varepsilon_x = 1‰$)
special correction of coupling in the arcs is required

with skew corrections, synchr. rad. emittance growth may be reduced

$$\Delta \varepsilon_y \cong 3\times10^{-11}\,\text{m} \longrightarrow 1\times10^{-12}\,\text{m}$$

- Table 1. Luminosity of SLC with new FF.

(A) corresp. to SLC param. of end of 1991 (Ecklund S, Status of SLC, LC91). Theoretical and achieved (in brackets).

(B-D) - new FF with $\ell^* = 2.2$ m

(E-G) - new FF with $\ell^* = 1$ m

$\varepsilon_x = 3 \cdot 10^{-8}$ cm (at 50 GeV), $f = 120$ Hz, $N = 3 \cdot 10^{10}$, $\sigma_z = 0.5$ mm, travell. focu..

Param. Set	ε_y 10^{-8} cm	$\beta_y^* \backslash \beta_x^*$ mm	$\sigma_y \backslash \sigma_x$ μm	R_0	$\frac{L}{L_0}$	L 10^{29} $cm^{-2} sec^{-1}$	$\frac{Z^0}{hr}$
A	3	4\4	1.1 (2.2)			7 (1.3)	75 (15)
B	3	0.2\2	0.3\1	0.23	1.1	24	250
C	0.3	—″—	0.09\0.9	0.43	1.5	110	1200
D	0.03	—″—	0.025\0.9	0.78	1.8	440	4800
E	3	0.2\0.5	0.35\0.5	0.31	1.2	50	500
F	0.3	—″—	0.085\0.5	0.55	1.6	230	2400
G	0.03	—″—	0.025\0.45	1.1	1.9	960	10000

beta - linear
sizes - with aberr. and SR
luminosity - with aberr., SR and beam-beam effects

P. Emma: Optics matching & ε-preservation

1. matching into SLC-linac

   e.g.: Dispersion match up to 3rd order was important (successfully done with octupoles)

2. wire scanners and measurement errors

   $\frac{\Delta\beta}{\beta}$ hard to separate from $\Delta\varepsilon$!

3. measurement of SLC-arcs transfer matrices is very important

4. Coupled matching of SLC Final Foci is performed

V. Ziemann:

Reconstruction of beam optics parameters in the FFS of SLC

method: change strengths of "well-suited" quads and observe change of spotsize with wire scanners downstream

allows reconstruction of σ-Matrix or (equivalently) β, α and coupling parameters.

Y. Chao:

Analytical solution of system with three thin lenses to yield a given transfer matrix

impressive MATHEMATICA output for the exact solution

Diskussion on Oide's "Odd dispersion"

FFS

Large bandwidth (1.5%) with only two pairs of sextupoles

is it particularly hard to tune?
(I don't think so)

tolerances need to be studied

$\frac{1}{2}$ Summary of Optics group

March 6, 1992
Sery A.

K. Oide	long l^* FF odd dispersion FF
J. Irwin	Complete collimation system
R. Helm	Big Bend
O. Napoly	Luminosity vs. errors.
A. Sery	Changes of VLEPP FFS
G. Roy	FFTB Tuning
V. Ziemann	Fast sextupole centering
R. Raimondi	SLC triplet alignment

• • •

• • •

K. Oide

- Long l^* design

  1m → 3m good for detector & backgrou

- „Odd dispersion" scheme

  Suppress −I breakdown aberrations

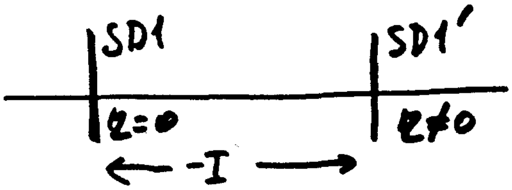

Chromo - geom. aberr. reduced.

Second order dispersion cancelled by SF SD sex. and quads. Third ord. dispersion cancelled by special bends.

- Simulation of FFS lifetime due to earth motio

  used $\delta y^2 \simeq A \cdot T \cdot L$, $A = 10^{-4} \frac{\mu m^2}{m \cdot sec}$

  ! $\underline{A}$ can be much smaller for case $L \sim$ size of rigid object (table, piece of concrete ...)

Chromo-geometric aberration

- Breakdown of $-I_y$

$$-I_y = \begin{pmatrix} -1 & a\chi\ell \\ \frac{a'\chi}{\ell} & -1 \end{pmatrix} + O(\chi^2)$$

$$(\chi = \Delta p/p)$$

$$\Delta y^* = \underbrace{\overset{\text{kick @ SD}}{k'xy} \cdot \overset{\text{breakdown of } -I_y}{a\chi\ell}}_{\substack{\text{chromatic displacement}\\ \text{@ SD'}}} \cdot \Big(\underset{①}{\underset{\substack{\uparrow \\ \text{chromaticity} \\ \text{between SD' and IP}}}{\chi \xi_y \sqrt{\frac{\beta_y^*}{\beta_y}}}} - \underset{②}{\underset{\substack{\uparrow \\ \text{chromatic kick} \\ \text{by SD'}}}{k'\eta_2 \chi \sqrt{\beta_y \beta_y^*}}} \Big)$$

$$k'\eta\beta_y \sim \xi_y$$

$$+ \overset{③}{\underset{\substack{\uparrow \\ \text{Chromatic kick @SD}}}{k'\eta_1 \chi y}} \cdot a\chi\ell \cdot \underset{\substack{\uparrow \\ \text{kick by SD'}}}{k'x\sqrt{\beta_y\beta_y^*}}$$

- Breakdown of $-I_x$

$$-I_x = \begin{pmatrix} -1 & b\chi\ell \\ \frac{b'\chi}{\ell} & -1 \end{pmatrix} + O(\chi^2)$$

$$\Delta y^* = \overset{④}{\underset{\substack{\uparrow \\ \text{chromatic kick} \\ \text{@ SD}}}{(\xi_x/\beta_x\, x\chi)}} \cdot \underset{\substack{\uparrow \\ \text{breakdown of } -I_x}}{b\chi\ell} \cdot \underset{\substack{\uparrow \\ \text{kick by SD'}}}{k'y\sqrt{\beta_y\beta_y^*}}$$

$\{ \eta_1 = \eta_2$ … ② and ③ cancel, ① and ④ remain.

$\beta_x^* = 15$ mm $\beta_y^* = 120$ μm $\Delta p/p$ < 1.5 %

Odd Dispersion

21:01:36.76 Tuesday 02/18/92

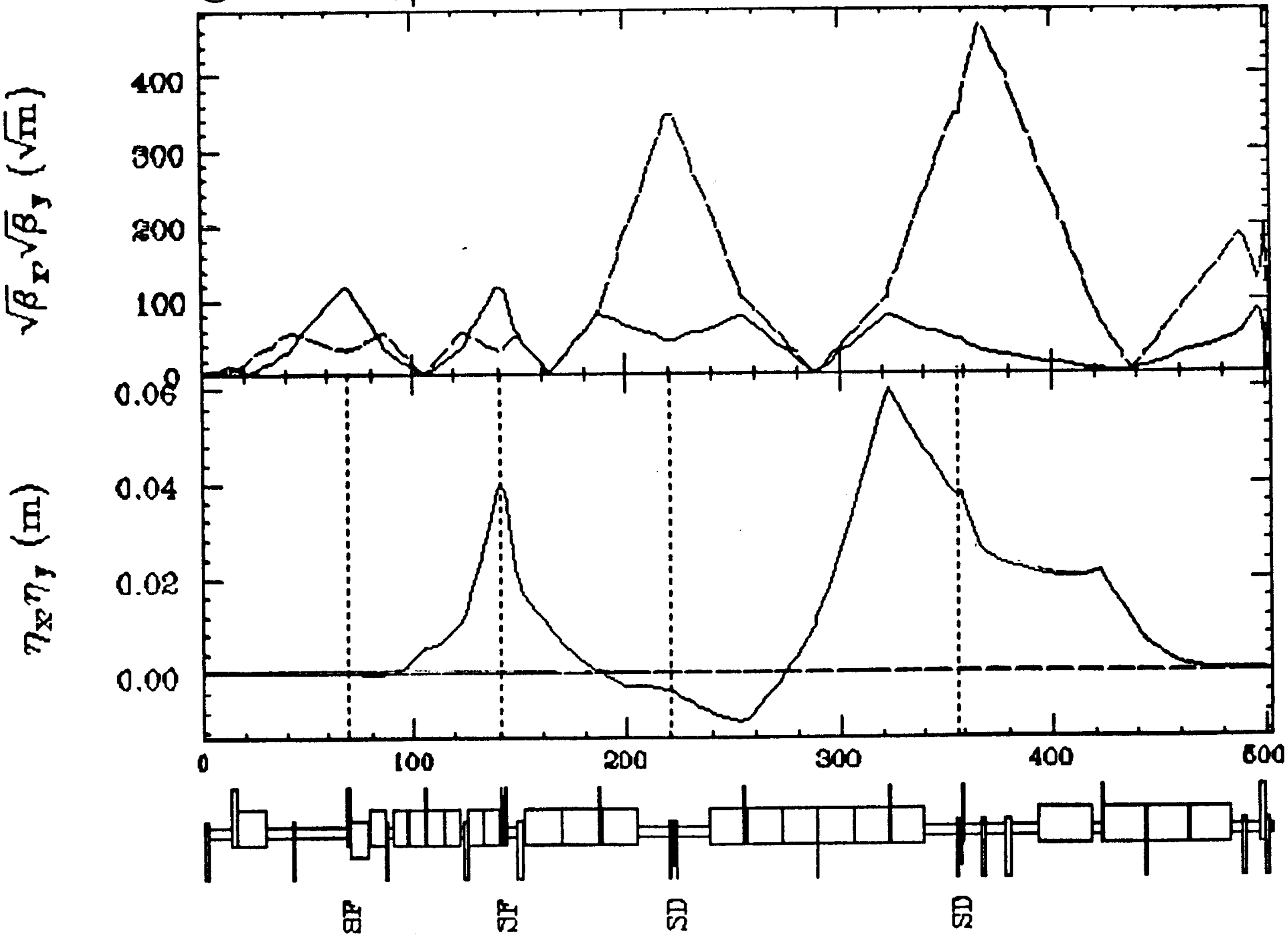

Irwin, Helm, Merminga, Nelson

- Complete NLC Collimation System

  collimate Both phases in poth planes and $\Delta P/p$

  in optimization geometric and resistive wakefields, Beam hit to collimator, position toleranses, 1σ of incoming Beam jitter ... were taken into account

  E=500 GeV, $5\sigma_x$, 4% $\Delta P/p$, $15\sigma_y$ (non-linear)

  length ≈ 1200 m ! possibly can be decrease.

- R. Helm Big Bend

  500 GeV, 10 mrad, ~160 m

A Complete NLC Collimation System

J. Irwin, D. Helm, L. Mergminga, and R. Nelson
SLAC

Abstract

We describe a collimation system that would be appropriate for a next linear collider with 500 GeV beam energy, a vertical beam emittance of 1/2 10^{-13} meter-radians and a horizontal beam emittance of 1/2 10^{-11} meter-radians. We have taken into account final focus system aperture requirements, transmission and edge-scattering properties of scrapers, wakefields, beam position tolerances at critical elements, an allowance for one sigma of incoming beam jitter, and an ability to collimate 1% of a 10^{11} particle beam. We first outline a system, without regard to length, that meets all criteria known to us, and then combine functional units where possible, to reduce system length. In the collimation of the final focus final doublet phase we incorporate a nonlinear collimation mechanism described in a previous paper.[1]

ε_y
ε_x

? × 2
< [illegible] × ε !

I. Introduction

Our primary purpose in this work is to provide an existence proof for an NLC collimation system that accomplishes all we now know to be required of a collimation system. We will i) identify all necessary functional units, ii) specify their parameters, iii) justify our choices for parameters with reference to collimation requirements or system tolerances, iv) identify relationships which exist between functionl units, v) identify all relevant physics for each unit, and vi) present lattice sub-systems that realize our choice of design parameters.

As a secondary objective we will discuss optimization with regard to total length. Shortening the length can degrade system tolerances and increase operational difficulty. On the other hand, a shorter system has less elements to maintain and align. The total length of a straightforward design, nearly 1.8 km, greatly motivates the search for shorter alternatives.

h/e or H/E

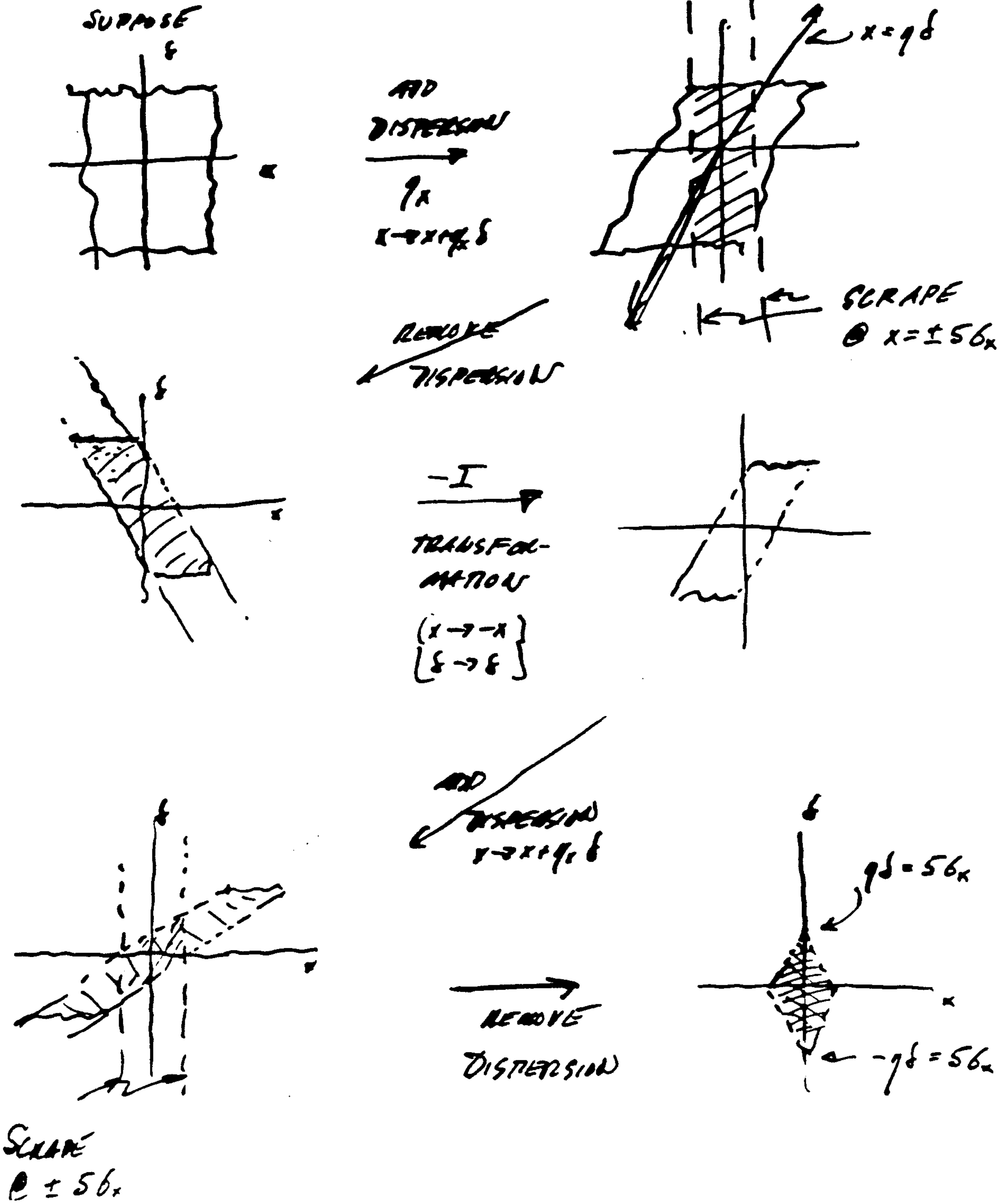
SUPPOSE
δ
x
ADD DISPERSION
η_x
x → x + η_x δ
x = ηδ
SCRAPE @ x = ±5σ_x
REMOVE DISPERSION
δ
x
−I TRANSFORMATION
(x → −x
δ → δ)
ADD DISPERSION
x → x + η_x δ
δ
x
ηδ = 5σ_x
x
−ηδ = 5σ_x
REMOVE DISPERSION
SCRAPE @ ±5σ_x

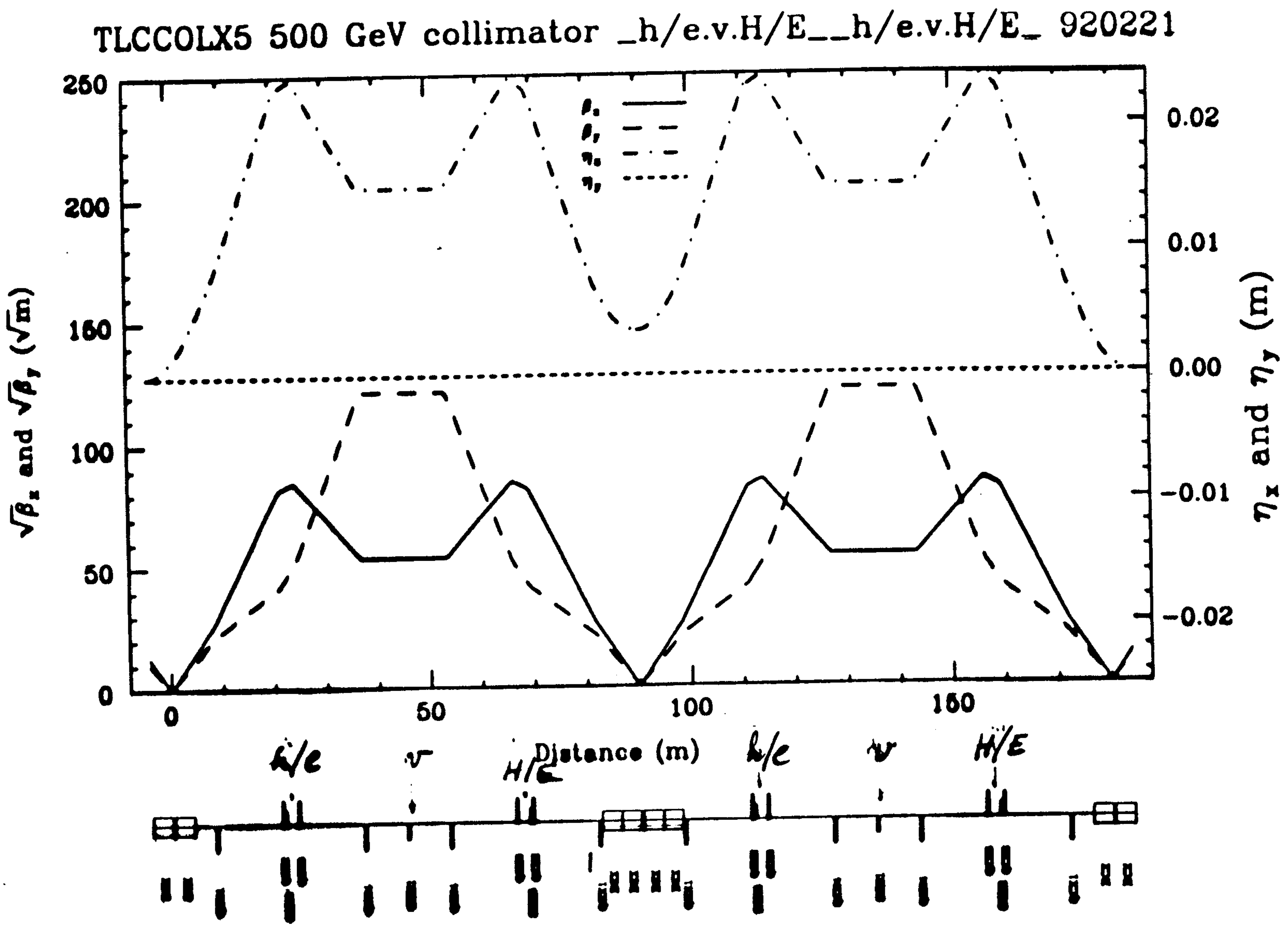
TLCCOLX5 500 GeV collimator _h/e.v.H/E__h/e.v.H/E_ 920221
β_x
β_y
η_x
η_y
$\sqrt{\beta_x}$ and $\sqrt{\beta_y}$ ($\sqrt{m}$)
η_x and η_y (m)
Distance (m)
0
50
100
150
200
250
0
50
100
150
0.02
0.01
0.00
−0.01
−0.02
h/e
v
H/E
h/e
v
H/E

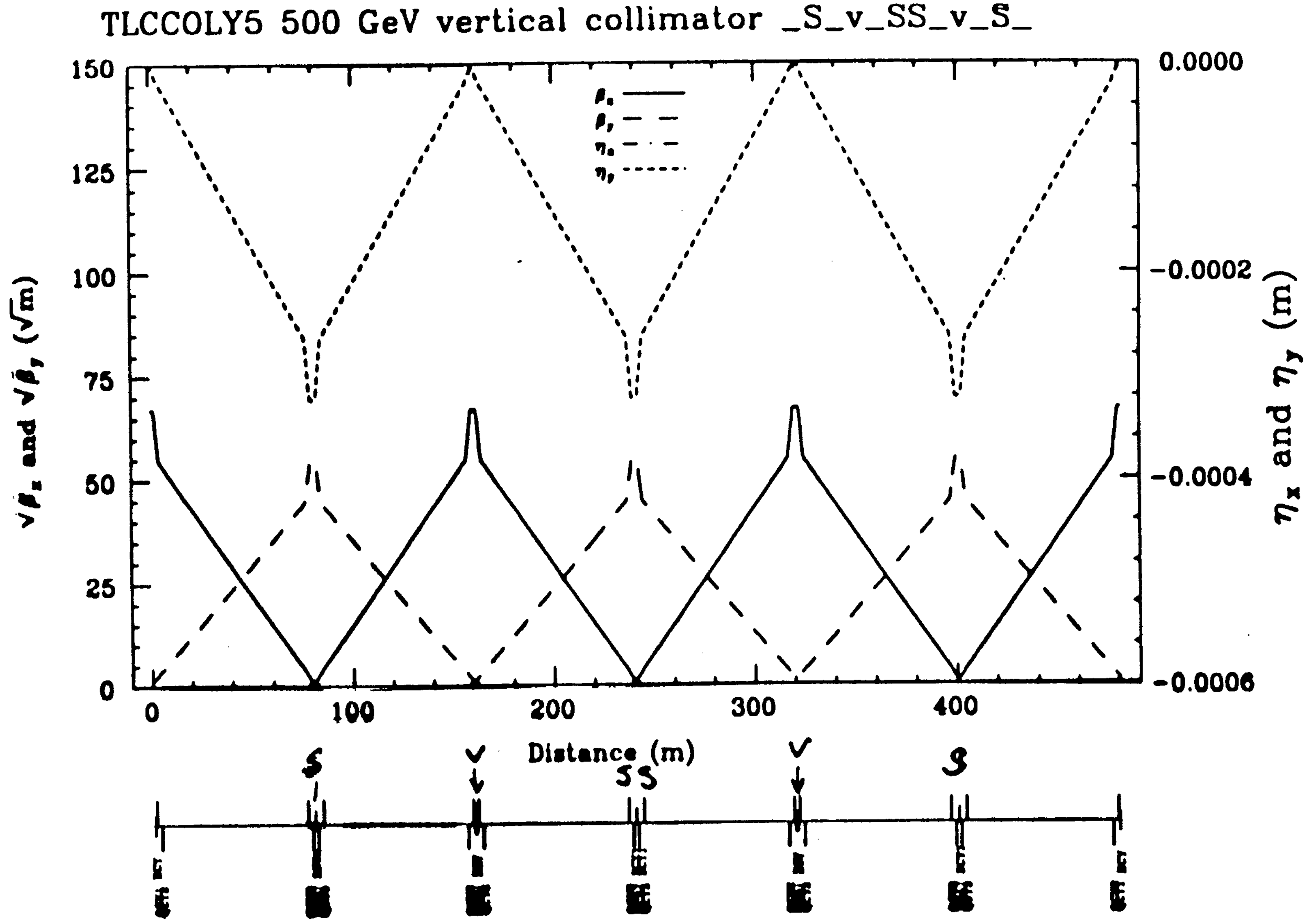
TLCCOLY5 500 GeV vertical collimator _S_v_SS_v_S_
$\sqrt{\beta_x}$ and $\sqrt{\beta_y}$ ($\sqrt{m}$)
150
125
100
75
50
25
0
η_x and η_y (m)
0.0000
-0.0002
-0.0004
-0.0006
β_x
β_y
η_x
η_y
0
100
200
300
400
Distance (m)
S
v
SS
v
S

Big Bend

R. Helm 92/03/04

500 GeV, 10 mrad, ~ 180 m

PARAMETERS FOR 10-mr ARC

Energy	500 GeV
Cell length	8 m
Number of cells	20
Total magnet length	136 m
Field at orbit	1.226 kG
Bending radius	13.6 km
Gradient:	
Focusing magnets	3281 kG/m
Defocusing magnets	3039 kG/m
Beam offset from quad axis:	
Focusing magnets	374 μm
Defocusing magnets	403 μm
β_{xmax}	12.20 m
β_{ymax}	12.77 m
μ_x	106deg
μ_y	90deg
ν_x	6
ν_y	5
σ_{xmax} (at $\epsilon_x = 5.0 \times 10^{-12}$ m)	7.6 μm (monochromatic)
σ_{ymax} (at $\epsilon_y = 5.0 \times 10^{-14}$ m)	0.77 μm
η_{max} (without matching)	3.86 mm
Emittance growth due to synchrotron excitation (DIMAD):	
Horizontal	1.007±.001
Vertical	~1.0
$\Delta p/p$	0.026 %

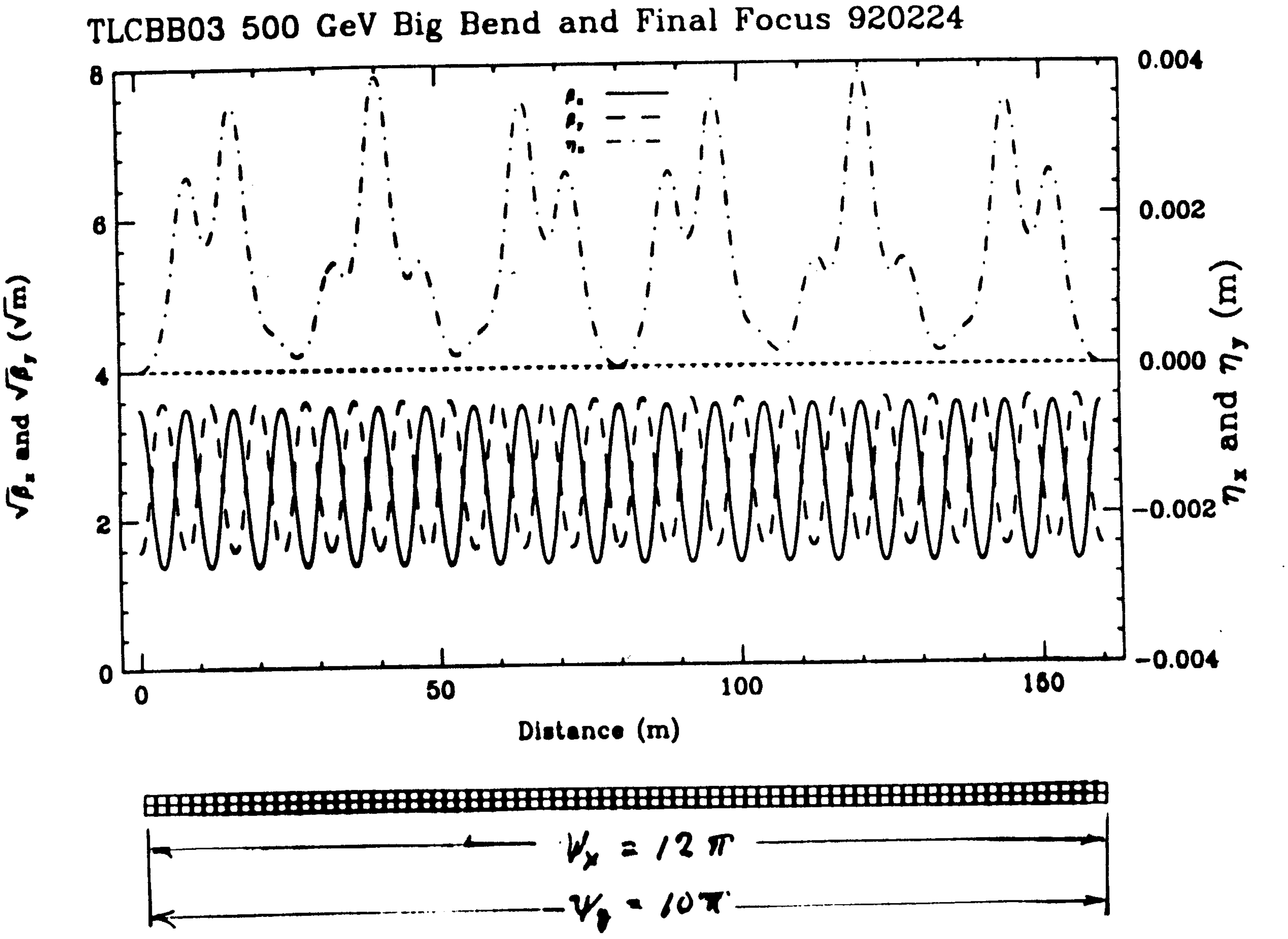
TLCBB03 500 GeV Big Bend and Final Focus 920224
$\sqrt{\beta_x}$ and $\sqrt{\beta_y}$ ($\sqrt{m}$)
0
2
4
6
8
η_x and η_y (m)
0.004
0.002
0.000
-0.002
-0.004
β_x
β_y
η_x
0
50
100
150
Distance (m)
$\psi_x = 12\pi$
$\psi_y = 10\pi$

Luminosity vs. Errors

O. Napoly

Calcul de $I_2(\lambda)$

$$-\lambda^T . P_z = (-\lambda_x, 0, -\lambda_y, 0, +\lambda_z, 0)$$

on déduit donc l'expression de $I_2(\lambda)$ de celle de I_1 en faisant $\lambda_{xy} \to -\lambda_{xy}$:

$$\cancel{I_2(\lambda) = \frac{1}{\sqrt{2\pi}\,\sigma_{z,2}}\, e^{+i\lambda_z(ct+z_{2,0}+\delta z_2)} \int dz_2\, e^{-z_2^2/2\sigma_{z,2}^2}\, e^{i\lambda_z z_2}}$$

$$I_2(\lambda) = \frac{1}{\sqrt{2\pi}\,\sigma_{z,2}}\, e^{-i(\lambda^T \mathbb{T}_t\, \delta X_2)_5}\, e^{i\lambda_z(\delta z_2 + ct + z_{2,0})} \int dz_2\, e^{-z_2^2/2\sigma_{z,2}^2}\, e^{i\lambda_z z_2}$$

$$\exp -i\left(\lambda^T \mathbb{T}_t\, R_2^* X_{2,0}\right)_5 \exp\left[-\frac{1}{2}\left(\lambda^T \mathbb{T}_t R_2^* S_2^{-1} R_2^{*T} \mathbb{T}_t^T \lambda\right)\Big|_5\right]$$

Reprise du calcul de $\bar{\mathcal{L}}$

$$\Rightarrow \bar{\mathcal{L}} = \frac{1}{(2\pi)^4}\left(\sigma_{z,1}\sigma_{z,2}\right)^{-1} \int c\,dt\, d\lambda_z\, dz_1 dz_2\; e^{i\lambda_z(2ct + \delta z_1 + \delta z_2 + z_{1,0} + z_{2,0})}\, e^{i\lambda_z(z_1+z_2)} \cdot e^{-z_1^2/2\sigma_{z,1}^2}\, e^{-z_2^2/2\sigma_{z,2}^2}$$

$$\cdot \int d\lambda_x d\lambda_y \exp\left(-\frac{1}{2}\lambda^T \left[\mathbb{T}_t\left(R_1^* S_1^{-1} R_1^{*T} + R_2 S_2^{-1} R_2^{*T}\right)\mathbb{T}_t^T\right]\Big|_{xy} \lambda\right)$$

$$\cdot \exp i\lambda^T . \left[\mathbb{T}_t\left(R_1^* X_{1,0} + \delta X_1 - R_2^* X_{2,0} - \delta X_2\right)\right]\Big|_{xy}$$

$$\left\|\begin{array}{l} A(t) = P_{xy}\left(\mathbb{T}_t\left(R_1^* S_1^{-1} R_1^{*T} + R_2 S_2^{-1} R_2^{*T}\right) \mathbb{T}_t^T\right) P_{xy} \quad \text{projecteur} \\ \Lambda(z,t) = P_{xy}\, \mathbb{T}_t\left(R_1^* X_{1,0}(z) + \delta X_1 - R_2^* X_{2,0}(z) - \delta X_2\right) \end{array}\right.$$

$$\boxed{\begin{array}{l} \bar{\mathcal{L}} = \frac{N_1 N_2}{(2\pi)^2}\left(\sigma_{z,1}\sigma_{z,2}\right)^{-1} \cdot \int c\,dt\, dz_1 dz_2\; \delta\left(z_1 + z_2 + 2ct + \delta z_1 + \delta z_2 + z_{1,0} + z_{2,0}\right) \\ \qquad \exp\left(-\frac{z_1^2}{2\sigma_{z,1}^2} - \frac{z_2^2}{2\sigma_{z,2}^2}\right) \exp\left(-\frac{1}{2}\Lambda^T(z,t) A(t)^{-1} \Lambda(z,t)\right) / \end{array}}$$

, R. Raimondi	presents experience of Q6/5/4 and triplet alignment in SLC-FF
V. Ziemann	Fast sextupole centering algorithm Beam-beam deflection as diagnostic tool Measurements of waist position and angular divergence Beamstrahlung as beam diagnostic
• G. Roy	presents many methods developed for FFTB tuning

FFTB
Tuning

TABLE 2: IMPORTANT FFTB STABILITY TOLERANCE

LARGE
MULTIPLIERS

Section	Element	Tolerance	Attribute	Aberration	Time
FD	Quads.	0.2μ†	Δx	Steering	τ_0
		12nm†	Δy	Steering	τ_0
		50μ	Δx	Dispersion	τ_1
	×17	4.7μ	Δy	Dispersion	τ_1
		$16\mu rad$	Tilt	Skew Quad	τ_2
		$2\ 10^{-5}$	$\Delta k_Q/k_Q$	Normal Quad	τ_3
	×3	$1\ 10^{-4}$	Bs/Bq at .7	N or Sk Sext	
FT	Mid Quad	1.5μ	Δx	Dispersion	τ_1
		1.2μ	Δy	Dispersion	τ_1
CCY	Sextupoles	0.9μ	Δx	Normal Quad	τ_2
		1.4μ	Δy	Skew Quad	τ_2
		$3\ 10^{-3}$	$\Delta k_S/k_S$	Sextupole	τ_3
	×5	$2mrad$	Tilt	Skew Sext.	
	End Quads	$2\ 10^{-4}$	$\Delta k_Q/k_Q$	Normal Quad	τ_3
		$.1mrad$	Tilt	Skew Quad	τ_2
	Center Quad	1.0μ	Δx	Normal Quad	τ_2
		0.3μ	Δy	Skew Quad	τ_2
	Dipole Bend	$1\ 10^{-5}$	$\Delta k_B/k_B$	Normal Quad	τ_2
BX	Mid Quad	4μ	Δy	Dispersion	τ_1
CCX	Sextupoles	3.5μ	Δx	Normal Quad	τ_2
		3.5μ	Δy	Skew Quad	τ_2
	End Quads	$.6\ 10^{-3}$	$\Delta k_Q/k_Q$	Normal Quad	τ_3
	×5	$.3mrad$	Tilt	Skew Quad	τ_2
	Center Quad	$.7\mu$	Δx	Normal Quad	τ_2
		4.0μ	Δy	Skew Quad	τ_2
	Dipole Bend	$2\ 10^{-5}$	$\Delta k_B/k_B$	Normal Quad	

† This steering tolerance, corresponding to an FP jitter of $.2\sigma$, need not be achieved for spot size measurement techniques insensitive to spot jitter.

TABLE 1: LOW ORDER ABERRATIONS AND GLOBAL CORRECTORS

Time Scale	Generator	Cause of loss of luminosity	# of knobs	Knob Name (Corrector)
τ_0	x', y'	horiz. and vert. steering	2	dipoles at FQ
τ_1	$x'\delta, y'\delta$	dispersion	2	dipoles in FT
τ_2	x'^2, y'^2	waist motion	2	trims on final doublet
	$x'y'$	coupling	1	skew quad. in FT
τ_3	$x'^2\delta, y'^2\delta$	chromaticity	2	main sextupoles
	$x'^3, x'y'^2$	sextupole	2	sextupoles in FT
	y'^3, x'^2y'	skew sext.	2	skew sext. in FT
variable (linac)	xx', x'^2, yy', y'^2 $x'\delta, y'\delta$	β and α mismatch incoming dispersion	6	quads in BM
	$xy', x'y'$	incoming coupling	2	skew quads in BM

Beam-based alignment recover up to 100 μm
+ knobs of initial errors.

BEAM-BASED SEGMENT (QUAD) ALIGNMENT

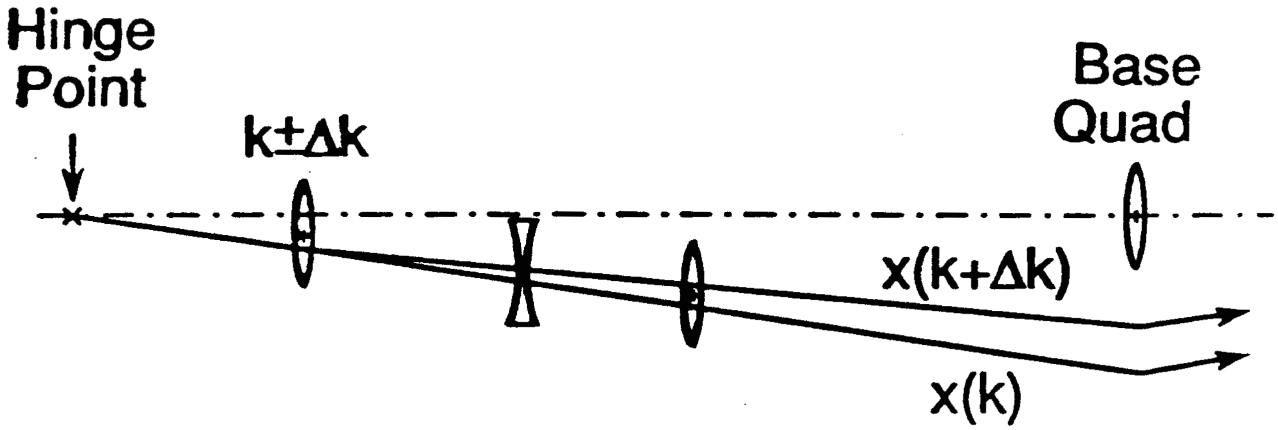

MODULATE Strength of each Quad and Move to Make Orbit Stationary

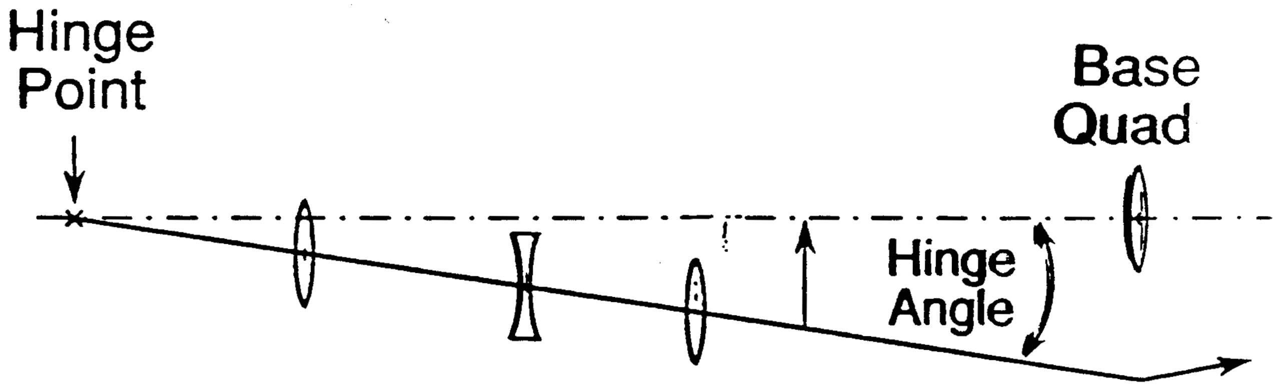

Hinge to put Beam through Base Quad

4-91 6869A2

TOOLS

1) BPMs 2-4μ S.S. Precision – 1μ MS Precision

2) Magnet Movers ± 1μ Every Quad

"LARGE" [10^4] BETA FUNCTION ADJUSTABILITY

(for β minima adjustments)

10)

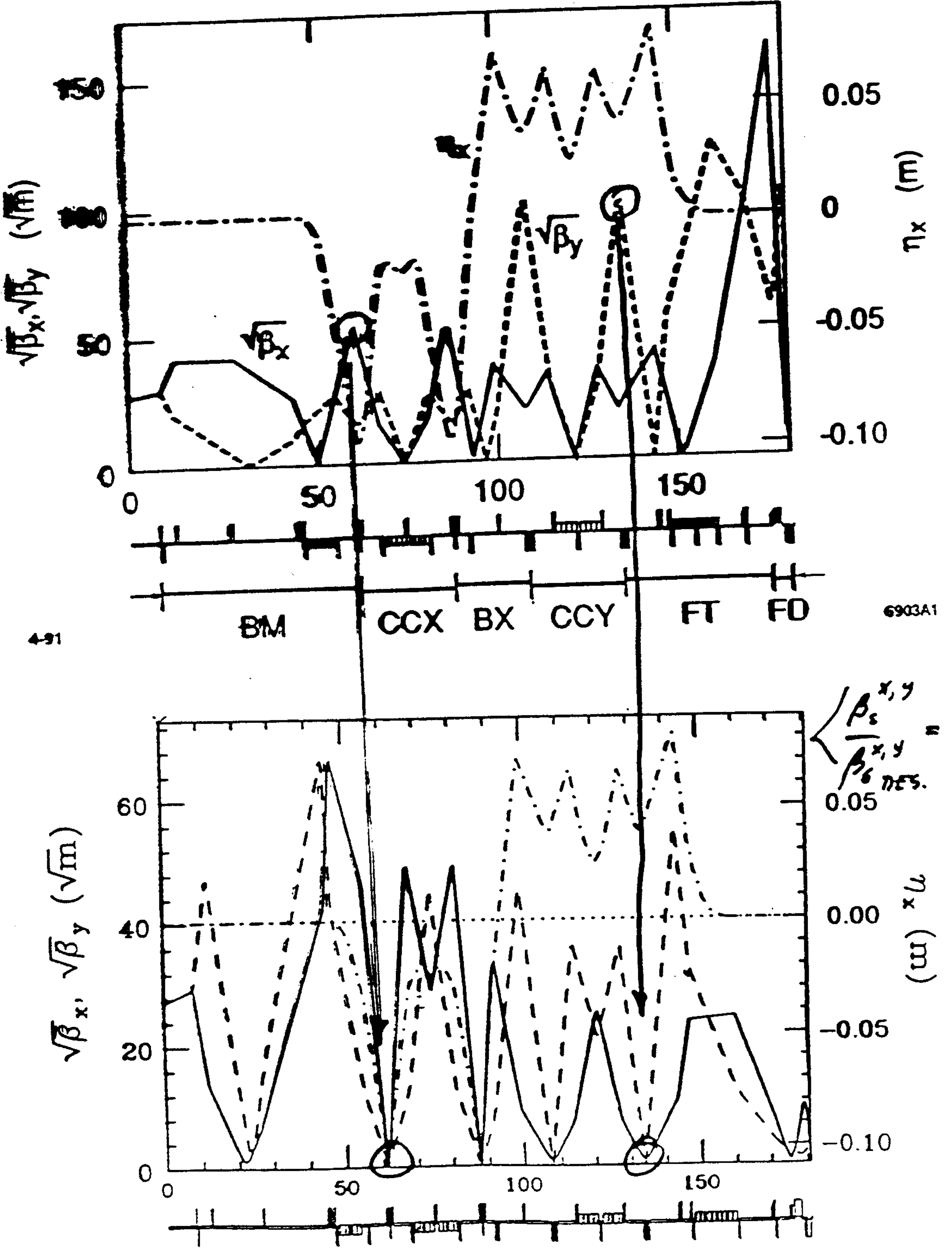

$\sqrt{\dfrac{\beta_s^{x,y}}{\beta_{0\ DES.}^{x,y}}} = 10^{-4}$

6/5/4 AND TRIPLET ALIGNAMENT IN SLC-FF

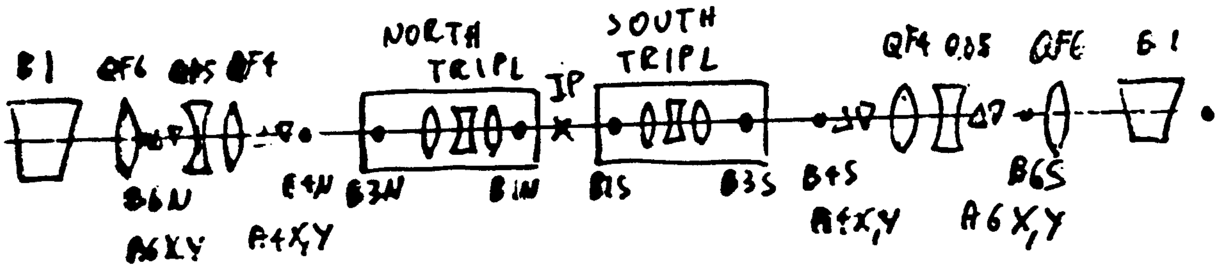

TURNED OFF QF6, QD5, QF4 N, S
TRIPLETS N, S

ESTABLISHED A GOOD REFERENCE TRAJ.
USING A7X,Y N
A6X,Y

TAKEN DATA MOVING A6X,Y N TO CALIBRATE THE BPMS DOWNSTREAM

) TAKEN DATA FOR <u>QF6, QD5, QF4 N, S</u>
<u>ALIGNAMENT</u> SCANNIG THEIR STRENGTHS

) TURNED <u>ON</u> QF6, QD5, QF4 N, S

) RESTEERED THE BEAM USING A7
A6
A4

N ORDER TO RESTORE THE <u>PREVIOUS</u>
EF. TRAJ IN THE TRIPLETS REGION [illegible]

A fast sextupole centering algorithm

V. Ziemann, SLAC

March, 3, 92

Objectives: (1) Maintain a given orbit through sextupoles, once a good one is established, and feedbackify procedure.
(2) find a good orbit (or: where are the sextupoles ?)

How to do it:

- Use experience from beam-beam deflections.
- use at least 3 BPMs to reconstruct x_0, x_0', Θ at the sextupole.

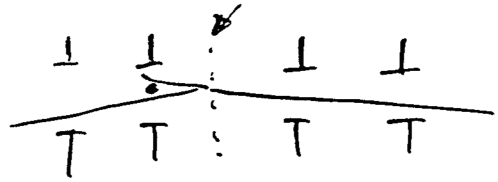

- Sweep the beam over the sextupole face (2D-GridScan™)
- Fit $\left\{ \begin{aligned} \Theta_x &= m[(x-\Delta_x)^2 - (y-\Delta_y)^2] + \Theta_{x_0} \\ \Theta_y &= 2m\,(x-\Delta_x)(y-\Delta_y) + \Theta_{y_0} \end{aligned} \right.$ to GridScan* data

$\Rightarrow$ sextupole offsets Δ_x, Δ_y

Spot size and Centering II

For stable fits use approximation for large aspect ratios of the Bassetti & Erskine Formula

$$\Delta = -\frac{2Nr_e}{\gamma \Sigma_x}\left\{\sqrt{\frac{\pi}{2}}\,\mathrm{erf}\left(\frac{y}{\sqrt{2}\Sigma_y}\right) - \frac{y}{\Sigma_x}\right\}$$

- Fit $\underbrace{A + B\left\{\sqrt{\frac{\pi}{2}}\,\mathrm{erf}\left(\frac{y-D}{\sqrt{2}C}\right) - \frac{y-D}{\Sigma_x}\right\}}$ to data

- Perform error analysis by changing a data point by

$$\left.\begin{array}{ll} \text{YERR :} & \sigma_y \text{ vertically} \\ \text{XERR :} & 1\,\text{nm horizontally} \\ \text{SERR :} & \Sigma_x \text{ by } +10\,\mu\text{m} \end{array}\right\} \text{and redo the fit}$$

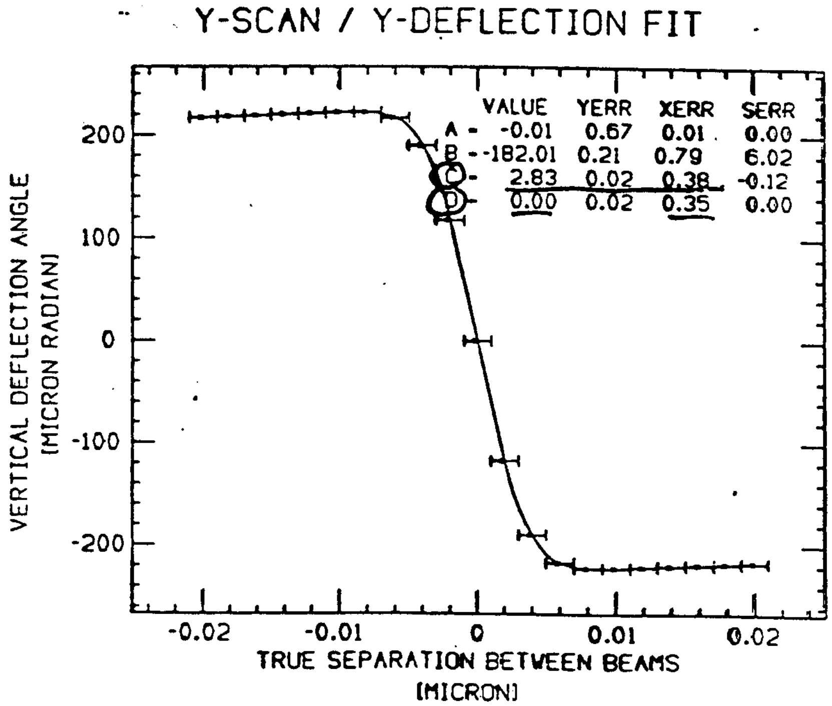

	VALUE	YERR	XERR	SERR
A -	-0.01	0.67	0.01	0.00
B -	-182.01	0.21	0.79	6.02
C -	2.83	0.02	0.38	-0.12
D -	0.00	0.02	0.35	0.00

Result: Spot size to better than 0,5 nm } dominated by
Centering to better than 0,5 nm } horizontal error.

Simulation Results

e^- : 5×5 onto e^+ 1×1 μm

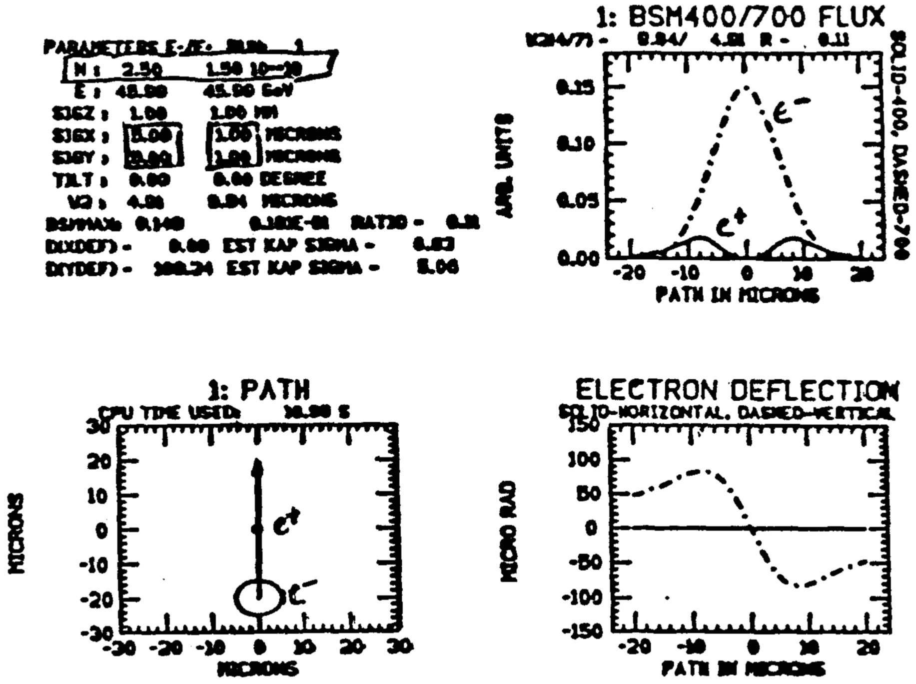

Figure 4: A typical output from the simulation code. In the upper left the input data are echoed. In the upper right the beamstrahlung fluxes are shown in arbitrary units. The solid curve is the flux from the radiating positrons on the north detector. In the lower left depicts the path on which the scan was taken and the lower right shows the electron deflection. Here the solid curve shows the horizontal deflection and the dashed curve the vertical.

- * radiation from the small (e^+) beam shows a dip
  - * large deflection angle ⇒ large BSM flux
- * radiation from the large (e^-) beam is almost gaussian
  - * small beam acts as a window through which the large beam can radiate.
- * W4/7 = truncated widths. (classify the scans)

R. Brinkmann $\eta \neq 0$ useful at IP

- „Crab- crossing with $\eta(IP) \neq 0$

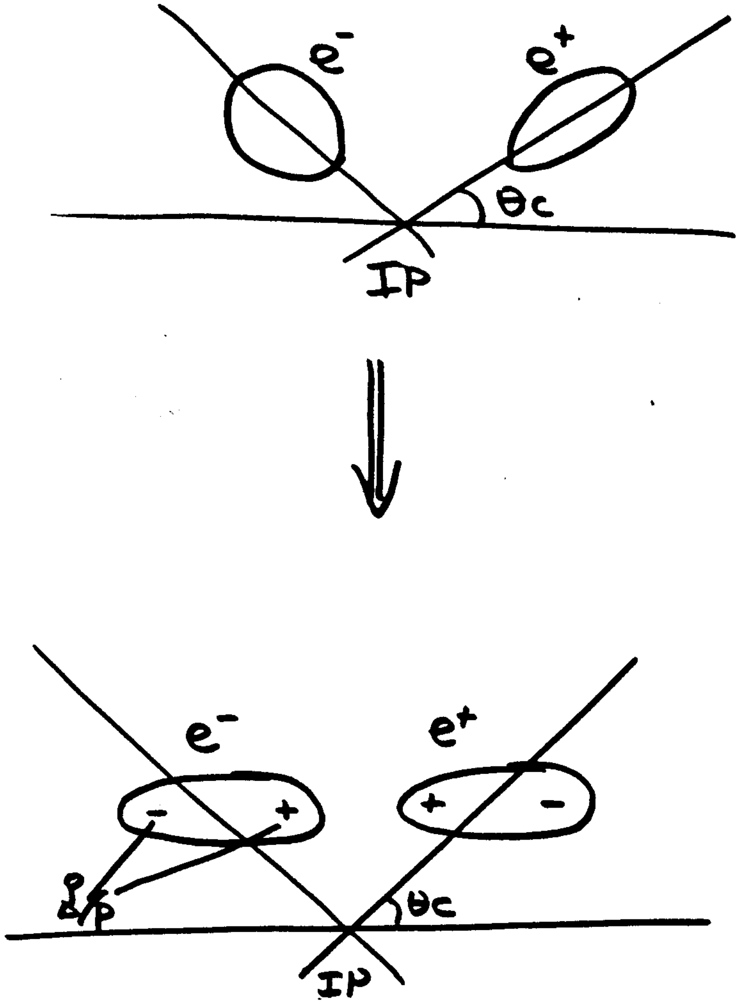

$$\eta^{\pm}(IP) = -\theta_c \frac{\sigma_z}{\sigma_p}$$

- Almost any FF can be designed
  (Big aperture, l^*, bandwidth...)

question is toleranses

? LC92 compare tolerances of different lattices with parameters:

$E = 500\ GeV$	$\sqrt{\beta_x \beta_y} = 10\,m$
$\varepsilon_y = \frac{1}{2} \cdot 10^{-13} m$	$\eta = 0$
$\varepsilon_x = \frac{1}{2} \cdot 10^{-11} m$	$L^* > 1.5\ m$
$\beta_y^* = 100\ \mu m$	$B \leq 1.4\ T$
$\beta_x^* = 10\ mm$	$a_1 \geq 2\,mm$
$\delta_{Rms} = \frac{1}{3} \cdot 10^{-2}$	$a_2 = \sqrt{2}\, a_1$
	$D \geq 30\ cm$
$\sigma/\sigma_0 \lessapprox 1.15$	$L_{tot} \leq 600\,m$

Progress in FF Optics since LC91

- Complete, 5 dimension phase space collimation syst
- FF schemes with big l^* (3 m)
- More perfect cancelation of aberrations with „odd dispersion" FF
- Usefulness of $\eta \neq 0$ at IP
- Further development of various tuning methods and diagnostics

- What we need: to continue

Optimization of tolerances

and Studying of tuning methods

• • •

LIST OF PARTICIPANTS - ALPHABETICALLY

Victor A. Alexandrov
Institute for High Energy Physics
142 284 Protvino (Moscow Region)
USSR

Bill Ash
Stanford Linear Accelerator Center
P. O. Box 4349, MS 96
Stanford, California 94309

Vladimir E. Balakin
Institute for High Energy Physics
142 284 Protvino (Moscow Region)
USSR

Henry Band
Stanford Linear Accelerator Center
P. O. Box 4349, MS 94
Stanford, California 94309

Tim Barklow
Stanford Linear Accelerator Center
P. O. Box 4349, MS 65
Stanford, California 94309

Karl Berkelman
CERN - SL Division
CH-1211 Geneva 23
Switzerland

Reinhard Brinkmann
DESY
Notkestrasse 85
D-2000, Hamburg 52
Germany

Gordon Bowden
Stanford Linear Accelerator Center
P. O. Box 4349, MS 95
Stanford, California 94309

Jean Buon
Lab. de l'Accelerateur Lineaire
Batiment 200, Centre d'Orsay
F-91405 Orsay, France

David Burke
Stanford Linear Accelerator Center
P. O. Box 4349, MS 65
Stanford, California 94309

Yu-Chiu Chao
Stanford Linear Accelerator Center
P. O. Box 4349, MS 66
Stanford, California 94309

Pisin Chen
Stanford Linear Accelerator Center
P. O. Box 4349, MS 26
Stanford, California 94309

Franz-Josef Decker
Stanford Linear Accelerator Center
P. O. Box 4349, MS 66
Stanford, California 94309

Paul Emma
Stanford Linear Accelerator Center
P. O. Box 4349, MS 66
Stanford, California 94309

Jim Ferrie
Stanford Linear Accelerator Center
P. O. Box 4349, MS 21
Stanford, California 94309

Gerard Fischer
Stanford Linear Accelerator Center
P. O. Box 4349, MS 66
Stanford, California 94309

Klaus Floettmann
DESY
Notkestrasse 85
D-2000, Hamburg 52
Germany

Sam Heifets
Stanford Linear Accelerator Center
P. O. Box 4349, MS 26
Stanford, California 94309

Richard Helm
Stanford Linear Accelerator Center
P. O. Box 4349, MS 26
Stanford, California 94309

Stanley S. Hertzbach
Stanford Linear Accelerator Center
P. O. Box 4349, MS 94
Stanford, California 94309

Bernhard Holzer
DESY
Notkestrasse 85
D-2000, Hamburg 52
Germany

Andrew Hutton
Stanford Linear Accelerator Center
P. O. Box 4349, MS 66
Stanford, California 94309

John Irwin
Stanford Linear Accelerator Center
P. O. Box 4349, MS 26
Stanford, California 94309

Monika Ivancic
170 Tioga Lane
Greenbrae, California 94904

Gerald P. Jackson
Fermilab
P. O. Box 500
Batavia, Illinois 60510

Vladimir I. Kalganov
Institute for High Energy Physics
142 284 Protvino (Moscow Region)
USSR

Lew Keller
Stanford Linear Accelerator Center
P. O. Box 4349, MS 20
Stanford, California 94309

Sam Kheifets
Stanford Linear Accelerator Center
P. O. Box 4349, MS 26
Stanford, California 94309

Patrick Krejcik
Stanford Linear Accelerator Center
P. O. Box 4349, MS 66
Stanford, California 94309

Evgeny A. Kushnirenko
Institute for High Energy Physics
142 284 Protvino (Moscow Region)
USSR

Martin Lee
Stanford Linear Accelerator Center
P. O. Box 4349, MS 26
Stanford, California 94309

Martin Leenen
DESY
Notkestrasse 85
D-2000, Hamburg 52
Germany

Sergey N. Lepshokov
Institute for High Energy Physics
142 284 Protvino (Moscow Region)
USSR

Torsten Limberg
Stanford Linear Accelerator Center
P. O. Box 4349, MS 66
Stanford, California 94309

Takayuki Matsui
National Laboratory for
High Energy Physics
1-1 Oho, Tsukuba-shi
Ibaraki-Ken, 305, Japan

Lia Merminga
Stanford Linear Accelerator Center
P. O. Box 4349, MS 26
Stanford, California 94309

Akiya Miyamoto
National Laboratory for
High Energy Physics
1-1 Oho, Tsukuba-shi
Ibaraki-Ken, 305, Japan

Phil Morton
Stanford Linear Accelerator Center
P. O. Box 4349, MS 26
Stanford, Califonria 94309

Hisayoshi Nakayama
National Laboratory for
High Energy Physics
1-1 Oho, Tsukuba-shi
Ibaraki-ken, 305, Japan

Yoshihito Namito
National Laboratory for
High Energy Physics
1-1 Oho, Tsukuba-shi
Ibaraki-ken, 305, Japan

Olivier Napoly
CERN - SL/AP Division
CH-1211, Geneva 23
Switzerland

Ralph Nelson
Stanford Linear Accelerator Center
P. O. Box 4349, MS 48
Stanford, California 94309

Cho-Kuen Ng
Stanford Linear Accelerator Center
P. O. Box 4349, MS 26
Stanford, California 94309

Jim Norem
Argonne National Laboratory
9700 S. Cass Ave., Bldg. 362
Argonne, Illinois 60439

Katsunobu Oide
National Laboratory for
High Energy Physics
1-1 Oho, Tsukuba-shi
Ibaraki-ken, 305, Japan

Tunehiko Omori
National Laboratory for
High Energy Physics
1-1 Oho, Tsukuba-shi
Ibaraki-ken, 305, Japan

James M. Paterson
Stanford Linear Accelerator Center
P. O. Box 4349, MS 26
Stanford, California 94309

Jean-Louis Pellegrin
Stanford Linear Accelerator Center
P. O. Box 4349, MS 50
Stanford, California 94309

Nan Phinney
Stanford Linear Accelerator Center
P. O. Box 4349, MS 66
Stanford, California 94309

Massimo Placidi
CERN
CH-1211 Geneva 23
Switzerland

Patrick Puzo
Lab. de l'Accelerateur Lineaire
Batiment 200, Centre d'Orsay
F-91405 Orsay, France

Tor Raubenheimer
Stanford Linear Accelerator Center
P. O. Box 4349, MS 26
Stanford, California 94309

Sayed Rokni
Stanford Linear Accelerator Center
P. O. Box 4349, MS 84
Stanford, California 94309

Mike Ronan
Lawrence Berkeley Laboratory
1 Cyclotron Road, MS 50b-5239
Berkeley, California 94720

James Rosenzweig
U.C.L.A.
Department of Physics
Los Angeles, California 90024

Marc Ross
Stanford Linear Accelerator Center
P. O. Box 4349, MS 66
Stanford, California 94305

Ghislain Roy
CERN SL/AP
01631 CERN Cedex
France

Ronald D. Ruth
Stanford Linear Accelerator Center
P. O. Box 4349, MS 26
Stanford, California 94309

Dan Schroeder
Grinnell College
Dept. of Physics
Grinnell, IA 50112

John Seeman
Stanford Linear Accelerator Center
P. O. Box 4349, MS 66
Stanford, California 94309

Andrey A. Sery
Institute for High Energy Physics
142 284 Protvino (Moscow Region)
USSR

Ron Settles
Max-Planck-Institute
Saupfercheckweg 1, Postfach 103980
D-W-6900 Heidelberg
Germany

Robert E. Shafer
Los Alamos National Laboratory
MS H808
Los Alamos, New Mexico 87545

Steve Smith
Stanford Linear Accelerator Center
P. O. Box 4349, MS 50
Stanford, California 94309

William L. Spence
Stanford Linear Accelerator Center
P. O. Box 4349, MS 66
Stanford, California 94309

Ryuhei Sugahara
National Laboratory for
High Energy Physics
1-1 Oho, Tsukuba-shi
Ibaraki-ken, 305, Japan

Toshiaki Tauchi
National Laboratory for
High Energy Physics
1-1 Oho, Tsukuba-shi
Ibaraki-ken, 305, Japan

Valery Telnov
Nuclear Physics Institute
USSR Academy of Sciences
Siberian Division
Novosibirsk 90, USSR

Kathleen Thompson
Stanford Linear Accelerator Center
P. O. Box 4349, MS 26
Stanford, California 94309

Maury Tigner
Newman Laboratory
Cornell University
Ithaca, New York 14853-5001

Nobu Toge
National Laboratory for
High Energy Physics
1-1 Oho, Tsukuba-shi
Ibaraki-ken, 305, Japan

Gustav-Adolf Voss
DESY
Notkestrasse 85
D-2000, Hamburg 52
Germany

Nick Walker
Stanford Linear Accelerator Center
P. O. Box 4349, Bin 66
Stanford, California 94309

Dieter Walz
Stanford Linear Accelerator Center
P. O. Box 4349, MS 24
Stanford, California 94309

Robert Warnock
Stanford Linear Accelerator Center
P. O. Box 4349, Bin 26
Stanford, California 94309

Bjorn Wiik
DESY
Notkestrasse 85
D-2000, Hamburg 52
Germany

Noboru Yamamoto
National Laboratory for
High Energy Physics
1-1 Oho, Tsukuba-shi
Ibaraki-ken, 305, Japan

Kaoru Yokoya
National Laboratory for
High Energy Physics
1-1 Oho, Tsukuba-shi
Ibaraki-ken, 305, Japan

Burton Richter
Stanford Linear Accelerator Center
P. O. Box 4349, MS 80
Stanford, California 94309

James Spencer
Stanford Linear Accelerator Center
P. O. Box 4349, MS 26
Stanford, California 94309

Volker Ziemann
Stanford Linear Accelerator Center
P. O. Box 4349, Bin 66
Stanford, California 94309